

UC Berkeley

UC Berkeley Electronic Theses and Dissertations

Title

Palladium-Mediated Formation of Alkyl-Nitrogen Bonds

Permalink

<https://escholarship.org/uc/item/43p4c0ng>

Author

Peacock, David Matthew

Publication Date

2017

Peer reviewed|Thesis/dissertation

PALLADIUM-MEDIATED FORMATION OF ALKYL–NITROGEN BONDS

by

David Matthew Peacock

A dissertation submitted in partial satisfaction of
the requirements for the degree of
Doctor in Philosophy
in
Chemistry
in the
Graduate Division
of the
University of California, Berkeley

Committee in charge:

Professor John F. Hartwig, Chair
Professor Richmond Sarpong
Professor Alexander Katz

Fall 2017

ABSTRACT

Palladium-Mediated Formation of Alkyl–Nitrogen Bonds

by

David Matthew Peacock

Doctor of Philosophy in Chemistry

University of California, Berkeley

Professor John F. Hartwig, Chair

The following dissertation discusses reactions of palladium complexes to form sp^3 carbon–nitrogen bonds. Both stoichiometric reductive elimination reactions to form alkylamines from characterized alkylpalladium(II) complexes and new palladium-catalyzed methods for the synthesis of *N*-alkylbenzophenone imines are reported.

Chapter 1 provides an overview of methods for the *N*-alkylation of nitrogen nucleophiles. Metal-catalyzed substitution reactions of nitrogen nucleophiles with alkyl electrophiles are discussed with a focus on the fundamental organometallic reactions that may form carbon–nitrogen bonds in these reactions. Examples of reductive elimination reactions from characterized alkylmetal complexes are covered in more detail because of their relevance to later chapters.

Chapter 2 discusses continued work in the Hartwig group studying the reductive elimination of norbornylamines from *syn*-2-methylnorbornylpalladium(II) amido complexes. This work focuses on the effects of phosphine ancillary ligands on the rate of reductive elimination and yield of alkylamine. These studies led to the design of bidentate P,O ligands that stabilize Pd(II) amido complexes while still enabling the reductive elimination of alkylamines to occur in good yield.

Chapter 3 presents the reductive elimination of *N*-neopentyl anilines and *N*-neopentyl imines from palladium(II) complexes. The P,O ligand structures developed as part of the work described in Chapter 2 proved particularly valuable to the study of neopentylpalladium(II) complexes and enabled the synthesis of stable, four-coordinate Pd(II) anilido and methyleneamido complexes that undergo reductive elimination to form *N*-neopentyl anilines and *N*-neopentyl imines in good yields.

Chapter 4 discusses the development of palladium catalysts for the cross-coupling of imines and primary alkyl bromides. The addition of fluorinated iminoquinolines as ancillary ligands was found to greatly increase the rate of the reaction. Mechanistic studies suggest that this reaction occurs through a two-electron pathway that may involve oxidative addition to a cyclometallated palladium(II) complex.

Chapter 5 expands the palladium-catalyzed cross-coupling of imines to include reactions with synthetically valuable secondary and tertiary alkyl halides. This method was applied to form a variety of imines bearing secondary and tertiary alkyl groups on nitrogen. Mechanistic studies suggest that this reaction occurs through single-electron transfer from a palladium(0) complex to form an alkyl radical intermediate. The intermediacy of this alkyl radical enabled this method to be expanded to include the intramolecular carboamination of unsaturated alkyl bromides.

TABLE OF CONTENTS

Chapter 1. The role of transition metals in the construction of sp^3 carbon–nitrogen bonds and catalytic <i>N</i> -alkylation reactions.....	1
1.1 Introduction	2
1.2 Uncatalyzed and radical-chain methods.....	3
1.3 Lewis acids	4
1.4 Reductive elimination to form sp^3 carbon–nitrogen bonds	5
1.5 Addition of alkyl radicals to anionic nitrogen ligands	10
1.6 Outlook and conclusions	11
1.7 References and notes	12
 Chapter 2. Reductive elimination of alkylamines from phosphine-ligated <i>syn</i> -2-methylnorbornylpalladium(II) complexes	15
2.1 Introduction	16
2.2 Results and discussion.....	17
2.3 Conclusions	33
2.4 Experimental	35
2.5 References and notes	81
 Chapter 3. Reductive elimination of <i>N</i> -neopentylamines and <i>N</i> -neopentylbenzophenone imines from neopentylpalladium(II) complexes.....	84
3.1 Introduction	85
3.2 Results and discussion.....	86
3.3 Conclusions	94
3.4 Experimental	95
3.5 References and notes	119
 Chapter 4. Pd-catalyzed <i>N</i> -alkylation of benzophenone imine with primary alkyl bromides ...	121
4.1 Introduction	122
4.2 Results and discussion.....	123
4.3 Conclusions	131
4.4 Experimental	132
4.5 References and notes	164

Chapter 5. Pd-catalyzed radical amination of secondary and tertiary alkyl bromides	166
5.1 Introduction	167
5.2 Results and discussion.....	168
5.3 Conclusions	176
5.4 Experimental	177
5.5 References and notes	211

ACKNOWLEDGEMENTS

I have difficulty remembering my thoughts from over five years ago when I first came to Berkeley, possibly due to how much the time here has changed me. It is still hard to believe that it is over. This easily could have gone differently at many points throughout the course of my academic life, and I am thankful to all the people who helped me along the way. They are too numerous to list, but I will try to mention the key figures here.

First, I would like to thank Dr. Kerim Samedov and Prof. Robert West with whom I worked at UW Madison. At that point in my life, I was soon to enter my senior year of undergraduate studies and was still in the process of deciding what I wanted to do after graduating or with my life generally. Research in the West group was a very valuable experience both in helping me decide to pursue a Ph.D. in chemistry and in preparing me for graduate school.

Naturally, I want to say thank you to my advisor Prof. John Hartwig for accepting me into his research group at Berkeley and teaching me everything I know about organometallics. Before joining the Hartwig group, I had never run a metal-catalyzed reaction, never synthesized a phosphine ligand, and never studied reaction kinetics. Between meetings and the infamous catalysis lunches, I learned a truly remarkable amount very quickly. Working with John has improved the way I write, the way I talk, and the way I think.

I would like to thank my qualifying exam committee Professors Bergman, Sarpong, Baranger, and Katz, as well as the chemistry department generally. Thank you also to Dr. Hasan Celik for an enormous amount of help with NMR experiments, Anneke Runtupalit for keeping the group running, and again to Prof. Bob Bergman for teaching the best class I've ever taken.

Research is best done in groups, and I appreciate all the help I have received from the entire Hartwig group over the years. In particular: thank you to my fume hood neighbor Chris Hill for the many enthusiastic conversations about science, to Dr. Allie Strom for always answering my questions and assuring me that I had not "broke science," and to Dr. Mike Mormino for forcing me to maintain some type of social life outside of lab. I am fortunate enough to have worked with a great undergraduate researcher, Casey Roos, and I wish her all the best in her graduate studies. I would also like to thank my computational collaborators Quan Jiang and Prof. Tom Cundari; both deserve special acknowledgement for their patience and hard work.

My family has been a great support through the stresses of graduate school. Despite being an artist by profession, my father is extremely enthusiastic about science and has always encouraged my continued study of chemistry. My mother places a great deal of value on education and has done her best to instill similar values in me since an early age, without which I doubt I would have ever gone to graduate school or made it this far.

Finally, I would like to thank Lauren and Andrew Corcoran for repeatedly offering their couch and always making me feel welcome whenever I needed a break from graduate school. My many visits to Pittsburgh have helped keep me sane the last five years. Lauren deserves some form of trophy for her amazing patience and continued faith in me over the twelve years of our friendship, but an acknowledgment in this dissertation will have to suffice for now.

CHAPTER 1

The role of transition metals in the construction of sp^3 carbon–nitrogen bonds
and catalytic *N*-alkylation reactions

1.1 Introduction

Alkylamines are ubiquitous in biologically active small molecules, and methods for the construction of sp^3 carbon–nitrogen bonds are therefore of particular importance in medicinal chemistry. Nine out of the eleven novel small molecule drugs approved by the FDA in 2016 contain at least one sp^3 carbon–nitrogen bond,¹ and aripiprazole (Abilify) – another alkylamine – was the highest selling drug in the United States before the patent expired in 2014. This prevalence is not unusual; a wider survey of functional group occurrence found that alkylamines (without including *N*-alkyl amides, sulfonamides, or heterocycles) are found in 43% of the biologically active molecules included in the survey.² Some widely known and historically important examples are shown below in Figure 1.1.

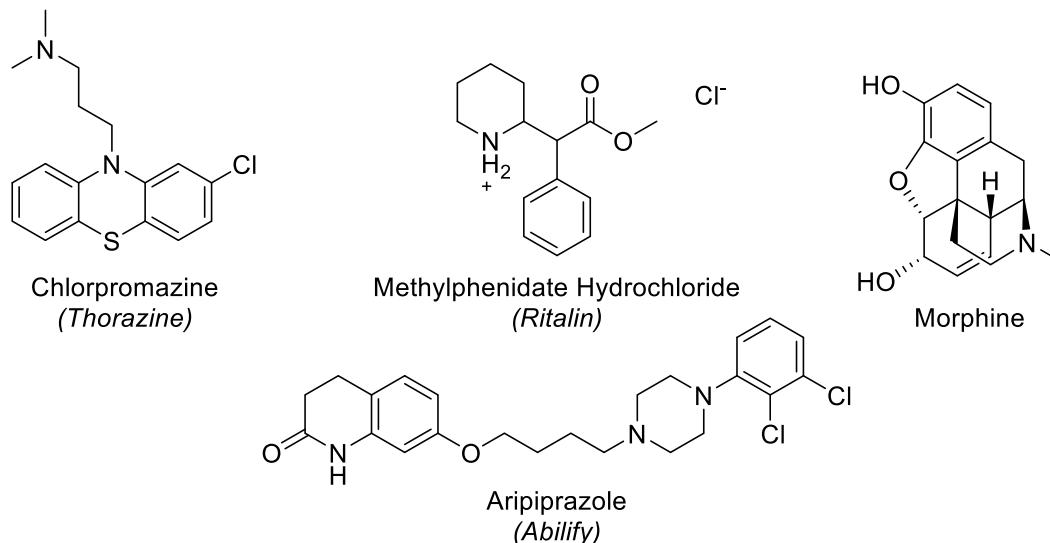


Figure 1.1. Examples of alkylamines in pharmaceuticals.

The frequency of reactions used in the construction of sp^3 carbon–nitrogen bonds in biologically active molecules has also been surveyed. Two traditional *N*-alkylations, substitution with alkyl electrophiles (S_N2) and reductive amination, are still widely used, and each accounts for over 20% of the reactions used to form sp^3 carbon–nitrogen bonds and over 5% of the total reported reactions.²⁻⁵ The widespread use of these methods in medicinal chemistry highlights their continued synthetic utility and the value of the alkylamine products formed from these reactions. Catalytic reactions have the potential to form similar products under milder conditions, expand the scope of nitrogen nucleophiles that participate in *N*-alkylation reactions, and to control the selectivity for reaction of one substrate over another.

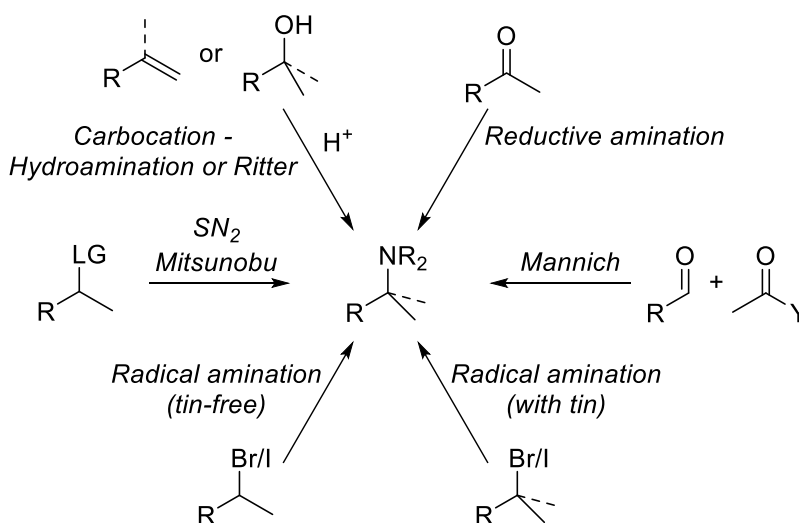
The projects presented in Chapters 2-5 of this dissertation cover two areas of research with the common goal of developing new methods for the synthesis of alkylamines. In this introductory chapter, traditional and radical-chain methods for the synthesis of alkylamines are summarized. Next, fundamental organometallic reactions relevant to the development of catalytic *N*-alkylation reactions with alkyl electrophiles are discussed. Examples of characterized complexes that undergo these fundamental reactions and examples of catalytic reactions that likely involve similar intermediates are presented. Reactions involving reductive elimination from transition

metals or involving the addition of alkyl radicals to nitrogen are discussed in more detail because these reactions are directly relevant to the research projects presented in Chapters 2-5. A comprehensive review of all transition metal-mediated reactions that form sp^3 carbon–nitrogen bonds is outside the scope of this dissertation.

1.2 Traditional and radical-chain methods

The preparations of alkylamines bearing primary alkyl groups are typically straight-forward. Direct substitutions with unhindered primary alkyl halides or pseudo halides are fast, and reductive amination reactions with aldehydes occur under mild conditions and in high yields.⁶⁻⁹ Therefore, this summary of traditional and uncatalyzed *N*-alkylation reactions will focus on the utility of these methods to produce amines bearing secondary and tertiary alkyl groups on nitrogen. The methods discussed in this section are summarized below in Scheme 1.1.

Scheme 1.1. Summary of traditional and radical-chain methods for the construction of sp^3 C–N bonds.



N-alkylation of nitrogen nucleophiles is traditionally achieved through substitution with alkyl halides or pseudohalides.¹⁰⁻¹⁴ Although reactions of unhindered primary or benzylic alkyl electrophiles are facile, reactions with secondary electrophiles typically require elevated temperatures, and tertiary electrophiles often undergo elimination in preference to substitution. Extremely hindered primary alkyl halides, such as neopentyl iodide or bromide, also generally require elevated temperatures to react. Early studies on the substitutions of alkyl halides found that, on average, rates of reactions with *iso*-propyl halides were approximately 40 times slower than the rates of reactions of ethyl halides. Neopentyl halides were even less reactive, with rates approximately 10^5 slower than those of ethyl halides. Furthermore, unactivated¹⁵ tertiary alkyl electrophiles often undergo elimination in preference to substitution.¹⁶ Mitsunobu reactions enable the use of unprotected alcohols as the alkyl electrophile, and many unhindered secondary alcohols react cleanly to form the corresponding amines.¹³ However, reactions of tertiary alcohols and hindered secondary alcohols suffer from competing elimination reactions that are similar to those observed from reactions of secondary and tertiary alkyl halides.

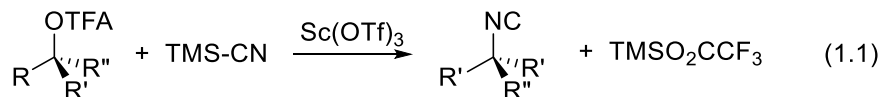
The acid-catalyzed hydroamination of olefins is a conceptually simple and atom-economical route for the addition of N–H bonds across olefins with Markovnikov selectivity. A particularly powerful related method is the Ritter reaction, in which 1,1-disubstituted olefins, secondary alcohols, or tertiary alcohols (or derivatives) undergo acid-promoted ionization to form carbocations.¹⁷ These carbocations are then trapped by nitriles and – after workup – yield secondary amides bearing secondary or tertiary alkyl groups on nitrogen. A similar reaction has been implicated in the biosynthesis of marine alkaloids.¹⁸ The significant limitation to these methods is the intermediacy of a highly reactive carbocation. Solvent-quantities of the nucleophile are typically required to form the product amide in high chemical yield, and rearrangements of the carbocation intermediate can lead to complicated mixtures of products in reactions of complex olefins or alcohols. The reactions of activated olefins are more controlled, and α,β -Unsaturated carbonyl compounds undergo hydroamination reactions (aza-Michael addition) to form the corresponding alkylamines without the generation of carbocation intermediates.¹⁹

Reductive amination reactions can accomplish the *N*-alkylation of primary and secondary amines with aldehydes and ketones.⁶⁻⁹ However, these reactions have two major limitations. First, these reactions cannot introduce tertiary alkyl groups on nitrogen. Second, combinations of ketones and amines for which condensation reactions are highly unfavored do not react in high yields. Mannich-type reactions offer an alternative, because the carbon–carbon bond is formed after a facile condensation reaction with an aldehyde. However, the classical Mannich reaction is limited in scope of carbon nucleophiles, and significant ongoing work – including the development of catalytic variants – has sought to address this limitation.²⁰

Recent work has shown the potential of carbon-centered radicals to participate in synthetically valuable amination reactions. Renaud has developed reactions of azides with alkyl halides or olefins to form *N*-alkyl azides.²¹⁻²⁵ Although both tin-mediated and tin-free methodologies have been developed, the scope of tin-mediated reactions is more general and includes examples of unactivated tertiary alkyl halides. Studer has reported the reaction of *N*-trimethylstannyl benzophenone imine with secondary and tertiary alkyl halides to form *N*-alkyl imines.²⁶ The role of radicals in modern chemistry and the similarities between radical-chain reactions and catalytic cycles have been reviewed.²⁷⁻²⁸ The relationships between these radical-chain aminations and the palladium-catalyzed radical amination reaction developed in the Hartwig group are discussed in Chapter 5 of this dissertation.

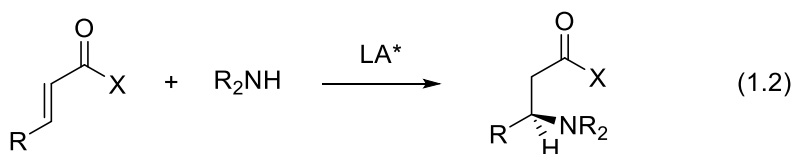
1.3 Lewis acids

As discussed in the preceding section of this chapter, Brønsted or Lewis acid-promoted *N*-alkylation reactions are widely used for the incorporation of tertiary alkyl groups on nitrogen. However, the harsh conditions required to generate carbocation intermediates and the rearrangement of carbocations limit the scope of alkyl groups that can be incorporated by these methods. Shenvi has reported rare examples in which metal-catalyzed alkylations of trimethylsilyl cyanide with activated alcohols formed the corresponding isonitriles with inversion of configuration at carbon (equation 1.1).^{16, 29}



The lack of racemization or rearrangements observed in these reactions suggests that either the carbocation exists as a contact ion pair with the scandium-coordinated trifluoroacetate leaving group, or that the reaction proceeds through a Lewis acid-catalyzed $\text{S}_{\text{N}}2$ mechanism. In either case, this example demonstrates the power of metal complexes to alter the reactivity and selectivity of traditional *N*-alkylation reactions, such as the Ritter amination.

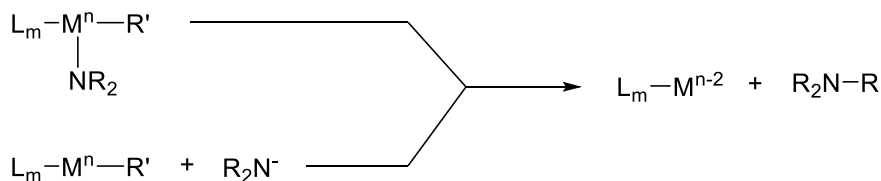
Conjugate additions of amines to α,β -unsaturated carbonyl compounds to form chiral β -amino acid derivatives can be also catalyzed by Lewis-acidic metals or by small-molecule organocatalysts.³⁰⁻³³ A particularly valuable application is to control the selectivity in reactions of β -substituted olefins (equation 1.2), and a variety of chiral Lewis acid-catalysts have been reported for these transformations.³⁴⁻⁴¹



1.4 Reductive elimination to form sp^3 carbon–nitrogen bonds

Perhaps the most conceptually simple reaction by which a transition metal complex can form a carbon–nitrogen bond is by reductive elimination. This reaction can occur either by a concerted mechanism or by nucleophilic attack of an alkyl ligand, as shown below in Scheme 1.2. Two classes of transition metal complexes undergo reductive elimination to form sp^3 carbon–nitrogen bonds: alkylmetal complexes and allylmetal complexes. Because the reactivity of these two classes of complexes are distinct from one another, they will be discussed separately.

Scheme 1.2. Two mechanisms of reductive elimination to form sp^3 C–N bonds.

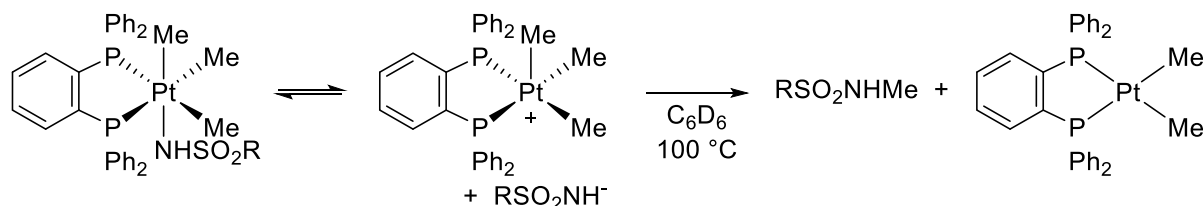


Reductive elimination from alkylmetal complexes. Despite the simplicity of this reaction, few examples of isolated and well-characterized alkylmetal complexes that undergo reductive elimination have been reported in the literature. Because they are particularly relevant to the research presented in Chapter 2 and Chapter 3 of this dissertation, these examples will be discussed individually.

The Goldberg group has reported the synthesis of 1,2-bis(diphenylphosphino)benzene (dppbz)-ligated trimethylplatinum(IV) sulfonamide complexes that undergo reductive elimination to form *N*-methyl sulfonamides (Scheme 1.3).⁴² Carbon–nitrogen bond-forming

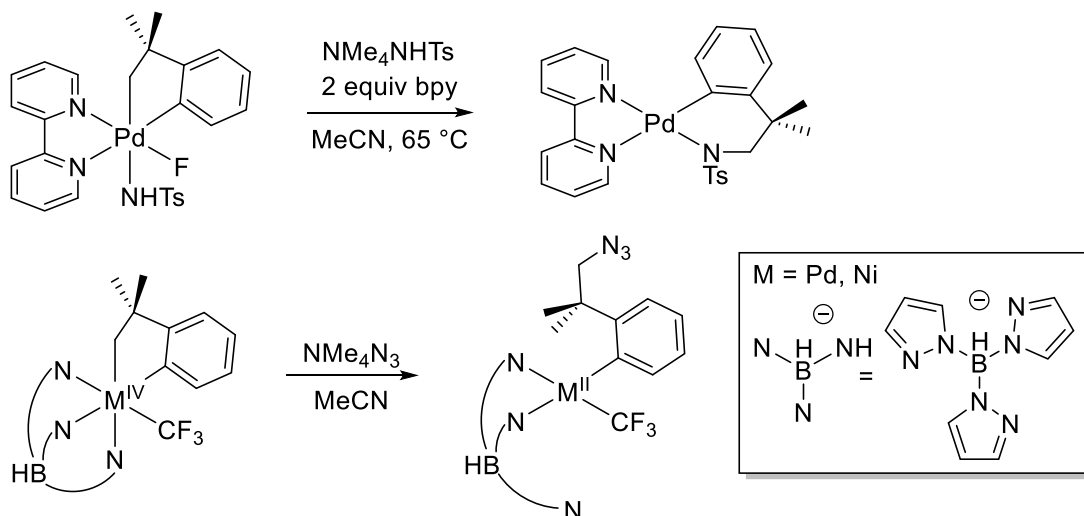
reductive elimination was found to be faster than carbon–carbon bond formation from these complexes, and kinetic experiments suggested that the reaction occurs by a two-step, nucleophilic attack mechanism. Key observations from these experiments were the zeroth order dependence on the concentration of RSO_2NHMe and the positive dependence on RSO_2NHMe . Similar mechanisms were proposed for carbon–oxygen and carbon–iodine bond-forming reductive eliminations from related trimethylPt(IV) carboxylate and iodide complexes.^{43–46}

Scheme 1.3. Reductive elimination of *N*-methyl sulfonamides from Pt(IV).



Sanford has demonstrated that the reductive elimination of *N*-alkyl sulfonamides also occurs from Pd(IV) metallacycles (Scheme 1.4, top).^{47–48} Competition between C–C, C–F, and C–N bond-forming reductive elimination reactions was investigated, and complexes that selectively react to form *N*-alkyl sulfonamides have been identified. More recently, this work has been expanded to include reductive elimination to form alkyl azides from Pd(IV) and Ni(IV) complexes (Scheme 1.4, bottom).⁴⁹ Kinetic experiments and computational studies suggest that these reactions occur through nucleophilic attack of the alkyl ligand.

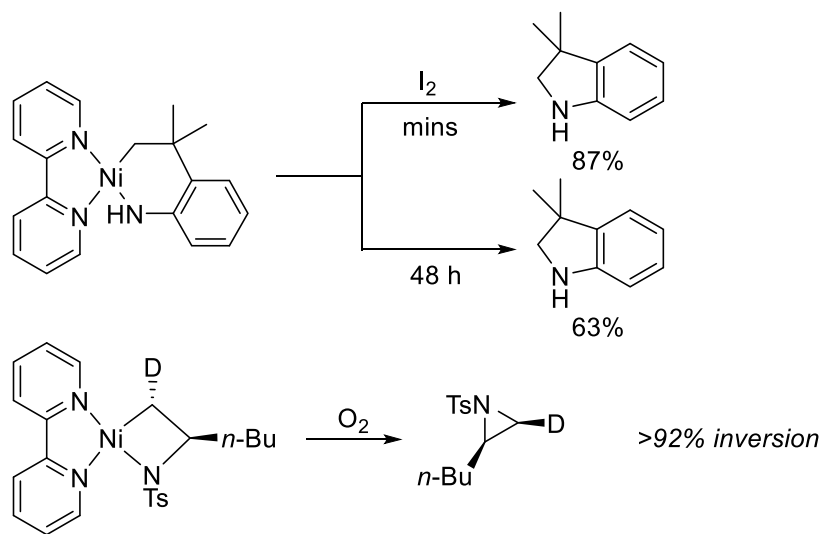
Scheme 1.4. Pd(IV) and Ni(IV) complexes that undergo reductive elimination to form sp^3 C–N bonds.



Hillhouse reported the synthesis of the azametallic Ni(II) complexes shown below in Scheme 1.5. These Ni(II) complexes were moderately stable at ambient temperature but underwent rapid reductive elimination in the presence of oxidants such as I_2 or O_2 . The authors proposed that single-electron oxidation to Ni(III) generates a complex active towards reductive elimination. Stereochemical studies (Scheme 1.5, bottom) determined that the reductive

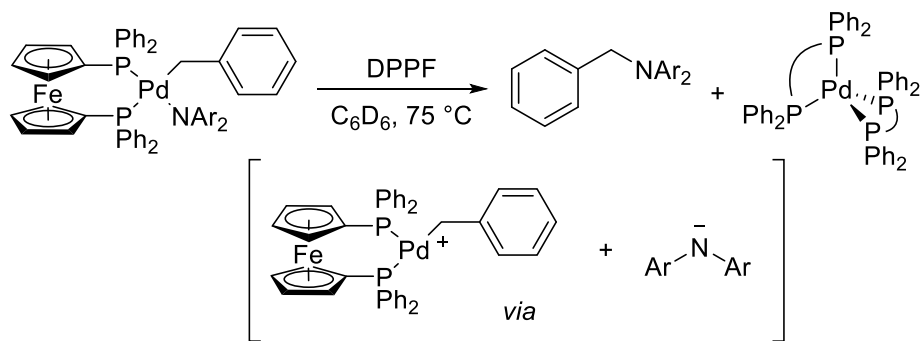
elimination to form aziridines occurs with inversion of configuration at the metal-bound carbon, and this result suggests that the reaction occurs by a stepwise mechanism involving dissociation and nucleophilic attack of the nitrogen on the palladium-bound carbon. However, these experiments were not sufficient to distinguish between Ni–N homolysis and heterolysis dissociation mechanisms.

Scheme 1.5. Ni(II) azametallacycles that undergo oxidatively induced reductive elimination.



The first example of a low-valent metal complex that undergoes reductive elimination to form sp^3 carbon–nitrogen bonds was reported by Hartwig in 2010.⁵⁰ The bis(diphenylphosphino)ferrocene-ligated benzylpalladium(II) amido complexes shown below in Scheme 1.6 underwent thermal reductive elimination to form benzylamines. This reaction occurred with inversion of configuration at the metal-bound carbon, which suggests a stepwise mechanism involving nucleophilic attack similar to those discussed above for high-valent group 10 metal centers. A similar reaction of analogous benzylpalladium(II) phenoxide complexes to form benzyl ethers has also been reported.⁵¹

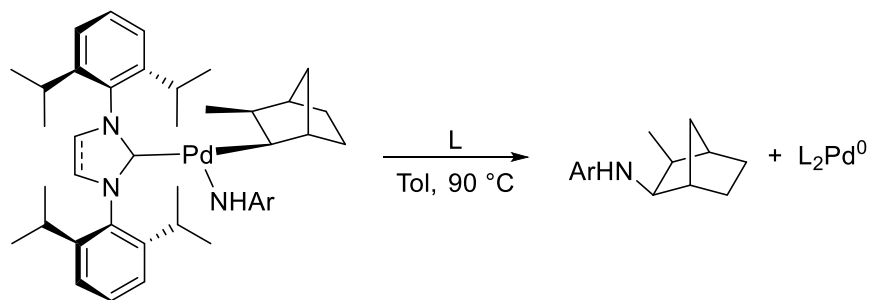
Scheme 1.6. Reductive elimination from Pd(II) to form benzylamines.



In 2012, Hartwig reported the synthesis of *syn*-2-methylnorbornylpalladium(II) complexes bearing bulky N-heterocyclic carbene ancillary ligands. These complexes underwent reductive

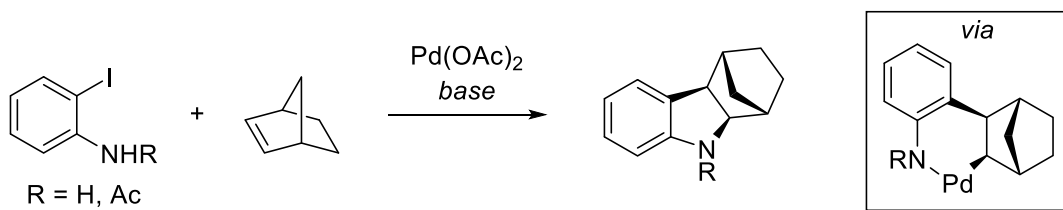
elimination to form norbornylamines with retention of configuration at the metal-bound carbon (Scheme 1.7).⁵² This stereochemical result suggests that reductive elimination occurs through a concerted mechanism, which contrasts the stepwise reductive elimination reactions presented above in this section. The proposed concerted mechanism was also supported by computations.

Scheme 1.7. Concerted reductive elimination from *syn*-2-methylnorbornylpalladium(II) complexes.

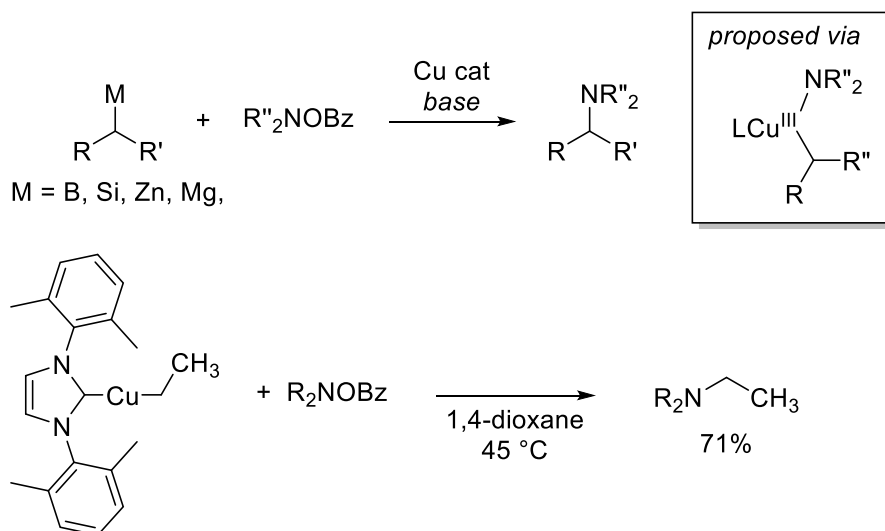


Despite the scarcity of characterized alkylpalladium complexes that react to form alkylamines, a number of palladium-catalyzed reactions have been developed that may involve sp^3 carbon–nitrogen bond-forming reductive elimination. A number of sp^3 C–H amination reactions have been proposed to involve reductive elimination of alkylamines from either Pd(II)^{53–55} or Pd(IV)⁵⁶ complexes. Lautens and Catellani have reported that 2-iodoaniline⁵⁷ and *N*-acetyl-2-iodoaniline⁵⁸ react with norbornene, a palladium-catalyst, and base to form the tricyclic structure shown below in Scheme 1.8. This result partially inspired the studies of norbornylpalladium(II) complexes in the Hartwig group, which are discussed above and further in Chapter 2 of this dissertation.^{52, 59}

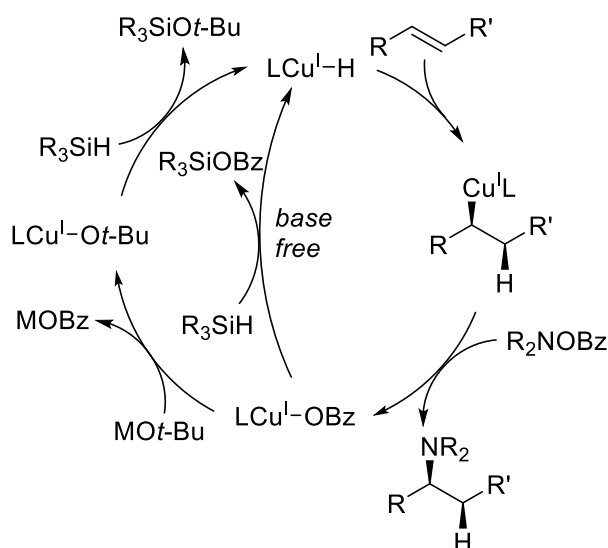
Scheme 1.8. Pd-catalyzed carboamination of norbornene.



The Johnson, Miura, and Lalic groups have reported copper-catalyzed electrophilic amination reactions with activated hydroxylamine derivatives (Scheme 1.9, top).^{60–63} These reactions constitute an “umpolung” strategy, in which a carbon nucleophile reacts with a nitrogen electrophile. Mechanistic studies implicated oxidative addition of the N–O bond to an alkylcopper(I) complex to form a transient Cu(III) intermediate that undergoes rapid reductive elimination.⁶¹ Although such an alkylcopper(III) amido complex has never been isolated and characterized, the NHC-ligated complex (IMes)Cu(Et) was prepared by Lalic. This complex was shown to react stoichiometrically with *O*-benzoyl hydroxylamines and to be a kinetically competent catalyst for electrophilic amination reactions (Scheme 1.9, bottom).

Scheme 1.9. Copper catalyzed electrophilic amination.

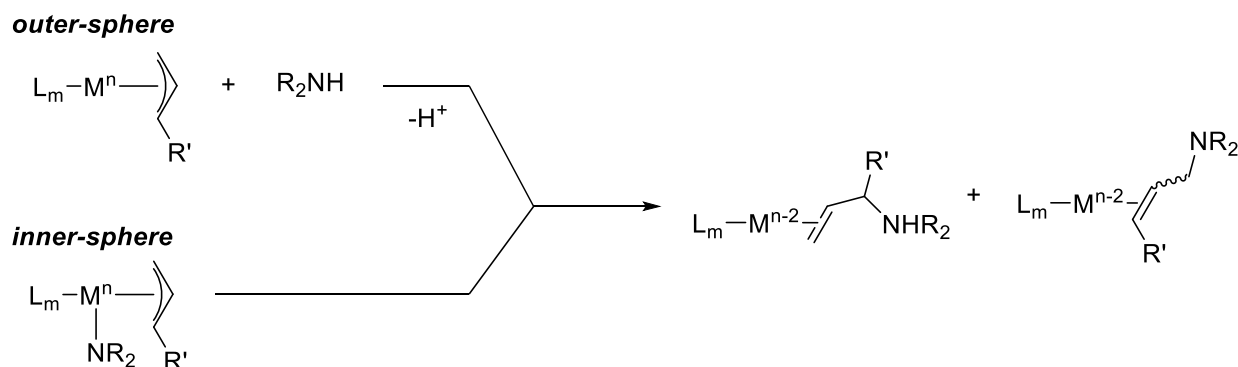
These copper-catalyzed electrophilic amination reactions have been expanded to include the aminoboration⁶⁴ and hydroamination⁶⁵ of olefins. These hydroaminations are mechanistically distinct from those occurring by insertion of olefins to metal–nitrogen bonds or by nucleophilic attack of coordinated olefins,⁶⁶ and a general mechanism is shown below in Scheme 1.10. The high enantioselectivity for the insertion of olefins to copper-hydride complexes bearing chiral phosphine ligands has enabled the development of copper-catalyzed asymmetric hydroamination reactions that occur by this general mechanism.⁶⁷⁻⁷⁶

Scheme 1.10. General mechanism for Cu-H catalyzed hydroamination.

Reductive elimination from allylmetal complexes. Metal complexes can also undergo reductive elimination to form the sp^3 carbon–nitrogen bonds in allylamines. In most examples, allyl ligands bind to the metal-center in an η^3 manner, and the carbon–nitrogen bond can form at

either the 1- or 3-position of the allyl group (Scheme 1.10).⁷⁷ Rare examples of attack at the central 2-position by carbon nucleophiles have also been reported.⁷⁸⁻⁸⁰

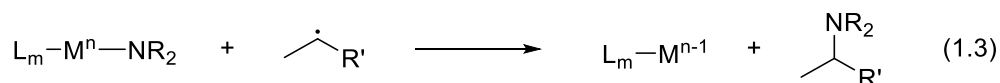
Scheme 1.10. Mechanisms of reductive elimination of allylamines.



Reductive elimination of allylamines has been most-commonly reported to occur by nucleophilic attack of an amine on an η^3 -allyl ligand bound to an electron-deficient metal center – often cationic Pd(II) (Scheme 1.10 top).^{77, 81-82} This mechanism is similar to that observed for the reductive elimination of benzylamines from palladium(II) complexes. This is logical because the cationic benzylpalladium(II) intermediate shown in Scheme 1.9 likely binds in an η^3 manner and is therefore a close analogy to the cationic η^3 -allylpalladium(II) complexes that react with amines to form *N*-allylamines. This reaction is favored with electrophilic (often cationic) metal centers and soft nucleophiles. Because nucleophilic attack can occur at either side of the allyl group to form the two constitutional isomers shown in Scheme 1.10, controlling the regioselectivity of this step is a key design feature in the development of catalytic reactions that involve this reaction.

1.5 Addition of alkyl radicals to anionic nitrogen ligands

No discrete, single-step examples of the addition of radicals to metal-amido complexes have been reported in the literature due to the unstable nature of alkyl radicals. However, mechanistic studies have implicated this reaction as the carbon–nitrogen bond-forming step in C–H amination and cross-coupling reactions. This reaction can be difficult to experimentally differentiate from reductive elimination; the key difference is that it occurs through single electron redox events at the metal center (equation 1.3), while reductive elimination occurs with a two-electron reduction of the metal center (Scheme 1.2).



Fu and Peters have reported a series of photochemical, copper-catalyzed cross-coupling reactions of amines, amides, carbamates, and nitrogen-containing heterocycles with alkyl halides.⁸³⁻⁸⁷ These reactions are proposed to occur through addition of alkyl radicals to Cu(II)-amido complexes, and a general mechanism is shown below in Scheme 1.11. Coordination of

[illegible]

Currently, examples of catalytic reactions which form sp^3 carbon–nitrogen bonds by reductive elimination are rare, and the key alkylmetal amido intermediates proposed in reported reactions have not been characterized. Examples of isolated alkylmetal amido complexes that undergo this reaction are also rare and are mostly limited to high-valent group 10 metals and complexes containing highly specialized or cyclometallated alkyl ligands (see section 1.4). Examples of reactions from isolated low-valent complexes are rarer still, and reductive eliminations that form amines bearing structurally simple, unfunctionalized primary alkyl groups on nitrogen are unknown. The following Chapters 2 and 3 of this dissertation present progress in the Hartwig group to discover new complexes that undergo this reaction.

11

1.7 References and notes

1. U.S. Food and Drug Administration: Novel Drug Approvals for 2016. <https://www.fda.gov/Drugs/DevelopmentApprovalProcess/DrugInnovation/ucm483775.htm>.
2. Roughley, S. D.; Jordan, A. M., *J. Med. Chem.* **2011**, *54* (10), 3451-3479.
3. Carey, J. S.; Laffan, D.; Thomson, C.; Williams, M. T., *Organic & Biomolecular Chemistry* **2006**, *4* (12), 2337-2347.
4. Dugger, R. W.; Ragan, J. A.; Ripin, D. H. B., *Organic Process Research & Development* **2005**, *9* (3), 253-258.
5. Philippidis, A.
6. Margaretha, P., *Science of Synthesis Knowledge Updates*. Thieme Chemistry: 2010; Vol. 4.
7. Abdel-Magid, A. F.; Mehrman, S. J., *Organic Process Research & Development* **2006**, *10* (5), 971-1031.
8. Baxter, E. W.; Reitz, A. B., Reductive Aminations of Carbonyl Compounds with Borohydride and Borane Reducing Agents. In *Organic Reactions*, al., L. E. O. e., Ed. John Wiley & Sons, Inc.: 2004; Vol. 59, pp 1-714.
9. Tripathi, R. P.; Verma, S. S.; Pandey, J.; Tiwari, V. K., *Curr. Org. Chem.* **2008**, *12* (13), 1093-1115.
10. Lawrence, S. A., *Science of Synthesis*. Thieme Chemistry: 2009; Vol. 40.
11. Boyd, G. V., Advances in the Chemistry of Amino and Nitro Compounds. In *Patai's Chemistry of Functional Groups*, John Wiley & Sons, Ltd: 2009.
12. Challis, B. C.; Butler, A. R., Substitution at an amino nitrogen. In *The Amino Group (1968)*, Patai, S., Ed. John Wiley & Sons, Ltd.: 2010; pp 277-347.
13. Mitsunobu, O., 1.3 - Synthesis of Amines and Ammonium Salts A2 - Fleming, Barry M. Trostlan. In *Comprehensive Organic Synthesis*, Trost, B. M.; Fleming, I., Eds. Pergamon: Oxford, 1991; Vol. 6, pp 65-101.
14. Scriven, E. F. V.; Turnbull, K., *Chem. Rev.* **1988**, *88* (2), 297-368.
15. By unactivated alkyl halides, we exclude those which possess a functional group (such as aryl, vinyl, or carbonyl) alpha to the halide.
16. Pronin, S. V.; Reiher, C. A.; Shenvi, R. A., *Nature* **2013**, *501* (7466), 195-199.
17. Jiang, D.; He, T.; Ma, L.; Wang, Z., *RSC Advances* **2014**, *4* (110), 64936-64946.
18. Garson, M. J.; Simpson, J. S., *Natural Product Reports* **2004**, *21* (1), 164-179.
19. Krishna, P. R.; Sreeshailam, A.; Srinivas, R., *Tetrahedron* **2009**, *65* (47), 9657-9672.
20. Arend, M.; Westermann, B.; Risch, N., *Angew. Chem. Int. Ed.* **1998**, *37* (8), 1044-1070.
21. Panchaud, P.; Renaud, P., *The Journal of Organic Chemistry* **2004**, *69* (9), 3205-3207.
22. Ollivier, C.; Renaud, P., *J. Am. Chem. Soc.* **2000**, *122* (27), 6496-6497.
23. Ollivier, C.; Renaud, P., *J. Am. Chem. Soc.* **2001**, *123* (20), 4717-4727.
24. Panchaud, P.; Chabaud, L.; Landais, Y.; Ollivier, C.; Renaud, P.; Zigmantas, S., *Chem. Eur. J.* **2004**, *10* (15), 3606-3614.
25. Renaud, P.; Ollivier, C.; Panchaud, P., *Angew. Chem. Int. Ed.* **2002**, *41* (18), 3460-3462.
26. Lamas, M.-C.; Vaillard, S. E.; Wibbeling, B.; Studer, A., *Org. Lett.* **2010**, *12* (9), 2072-2075.
27. Studer, A.; Curran, D. P., *Angew. Chem. Int. Ed.* **2016**, *55* (1), 58-102.
28. Studer, A.; Curran, D. P., *Nat Chem* **2014**, *6* (9), 765-773.

-
29. Pronin, S. V.; Shenvi, R. A., *J. Am. Chem. Soc.* **2012**, *134* (48), 19604-19606.
 30. Melchiorre, P., *Angew. Chem. Int. Ed.* **2012**, *51* (39), 9748-9770.
 31. Erkkilä, A.; Majander, I.; Pihko, P. M., *Chem. Rev.* **2007**, *107* (12), 5416-5470.
 32. Doyle, A. G.; Jacobsen, E. N., *Chem. Rev.* **2007**, *107* (12), 5713-5743.
 33. Enders, D.; Wang, C.; Liebich, J. X., *Chem. Eur. J.* **2009**, *15* (42), 11058-11076.
 34. Myers, J. K.; Jacobsen, E. N., *J. Am. Chem. Soc.* **1999**, *121* (38), 8959-8960.
 35. Kang, S. H.; Kang, Y. K.; Kim, D. Y., *Tetrahedron* **2009**, *65* (29), 5676-5679.
 36. Sibi, M. P.; Shay, J. J.; Liu, M.; Jasperse, C. P., *J. Am. Chem. Soc.* **1998**, *120* (26), 6615-6616.
 37. Doi, H.; Sakai, T.; Iguchi, M.; Yamada, K.-i.; Tomioka, K., *J. Am. Chem. Soc.* **2003**, *125* (10), 2886-2887.
 38. Sibi, M. P.; Liu, M., *Org. Lett.* **2001**, *3* (26), 4181-4184.
 39. Wang, L.; Chen, J.; Huang, Y., *Angew. Chem. Int. Ed.* **2015**, *54* (51), 15414-15418.
 40. Seijiro, M.; Masahito, Y.; Kiitiro, U., *Chem. Lett.* **1994**, *23* (5), 827-830.
 41. Yamagiwa, N.; Qin, H.; Matsunaga, S.; Shibasaki, M., *J. Am. Chem. Soc.* **2005**, *127* (38), 13419-13427.
 42. Pawlikowski, A. V.; Getty, A. D.; Goldberg, K. I., *J. Am. Chem. Soc.* **2007**, *129* (34), 10382-10393.
 43. Goldberg, K. I.; Yan, J.; Breitung, E. M., *J. Am. Chem. Soc.* **1995**, *117* (26), 6889-6896.
 44. Goldberg, K. I.; Yan, J. Y.; Winter, E. L., *J. Am. Chem. Soc.* **1994**, *116* (4), 1573-1574.
 45. Williams, B. S.; Goldberg, K. I., *J. Am. Chem. Soc.* **2001**, *123* (11), 2576-2587.
 46. Williams, B. S.; Holland, A. W.; Goldberg, K. I., *J. Am. Chem. Soc.* **1999**, *121* (1), 252-253.
 47. Pendleton, I. M.; Pérez-Temprano, M. H.; Sanford, M. S.; Zimmerman, P. M., *J. Am. Chem. Soc.* **2016**, *138* (18), 6049-6060.
 48. Pérez-Temprano, M. H.; Racowski, J. M.; Kampf, J. W.; Sanford, M. S., *J. Am. Chem. Soc.* **2014**, *136* (11), 4097-4100.
 49. Camasso, N. M.; Canty, A. J.; Ariafard, A.; Sanford, M. S., *Organometallics* **2017**, *36* (22), 4382-4393.
 50. Marquard, S. L.; Rosenfeld, D. C.; Hartwig, J. F., *Angew. Chem. Int. Ed.* **2010**, *49* (4), 793-796.
 51. Marquard, S. L.; Hartwig, J. F., *Angew. Chem. Int. Ed.* **2011**, *50* (31), 7119-7123.
 52. Hanley, P. S.; Marquard, S. L.; Cundari, T. R.; Hartwig, J. F., *J. Am. Chem. Soc.* **2012**, *134* (37), 15281-15284.
 53. Leal, R. A.; Bischof, C.; Lee, Y. V.; Sawano, S.; McAtee, C. C.; Latimer, L. N.; Russ, Z. N.; Dueber, J. E.; Yu, J.-Q.; Sarpong, R., *Angew. Chem. Int. Ed.* **2016**, *55* (39), 11824-11828.
 54. He, J.; Shigenari, T.; Yu, J.-Q., *Angew. Chem. Int. Ed.* **2015**, *54* (22), 6545-6549.
 55. Pan, J.; Su, M.; Buchwald, S. L., *Angew. Chem. Int. Ed. Engl.* **2011**, *50* (37), 8647-51.
 56. He, G.; Zhao, Y.; Zhang, S.; Lu, C.; Chen, G., *J. Am. Chem. Soc.* **2012**, *134* (1), 3-6.
 57. Catellani, M.; Del Rio, A., *Russ. Chem. Bull.* **1998**, *47* (5), 928-931.
 58. Lautens, M.; Paquin, J. F.; Piguel, S.; Dahlmann, M., *J. Org. Chem.* **2001**, *66* (24), 8127-34.
 59. Marquard, S. L. Reductive elimination of alkylamines and ethers: reactions of bisphosphine-ligated palladium(II) complexes. Dissertation, University of Illinois at Urbana-Champaign, 2012.

-
60. Berman, A. M.; Johnson, J. S., *J. Am. Chem. Soc.* **2004**, *126* (18), 5680-5681.
 61. Campbell, M. J.; Johnson, J. S., *Org. Lett.* **2007**, *9* (8), 1521-1524.
 62. Matsuda, N.; Hirano, K.; Satoh, T.; Miura, M., *Angew. Chem. Int. Ed.* **2012**, *51* (47), 11827-11831.
 63. Rucker, R. P.; Whittaker, A. M.; Dang, H.; Lalic, G., *J. Am. Chem. Soc.* **2012**, *134* (15), 6571-6574.
 64. Sakae, R.; Hirano, K.; Miura, M., *J. Am. Chem. Soc.* **2015**, *137* (20), 6460-6463.
 65. Miki, Y.; Hirano, K.; Satoh, T.; Miura, M., *Angew. Chem. Int. Ed.* **2013**, *52* (41), 10830-10834.
 66. Huang, L.; Arndt, M.; Gooßen, K.; Heydt, H.; Gooßen, L. J., *Chem. Rev.* **2015**, *115* (7), 2596-2697.
 67. Yang, Y.; Shi, S.-L.; Niu, D.; Liu, P.; Buchwald, S. L., *Science* **2015**, *349* (6243), 62.
 68. Miki, Y.; Hirano, K.; Satoh, T.; Miura, M., *Org. Lett.* **2014**, *16* (5), 1498-1501.
 69. Wang, H.; Yang, J. C.; Buchwald, S. L., *J. Am. Chem. Soc.* **2017**, *139* (25), 8428-8431.
 70. Niu, D.; Buchwald, S. L., *J. Am. Chem. Soc.* **2015**, *137* (30), 9716-9721.
 71. Zhu, S.; Niljianskul, N.; Buchwald, S. L., *Nature Chemistry* **2016**, *8*, 144.
 72. Zhu, S.; Niljianskul, N.; Buchwald, S. L., *J. Am. Chem. Soc.* **2013**, *135* (42), 15746-15749.
 73. Zhu, S.; Buchwald, S. L., *J. Am. Chem. Soc.* **2014**, *136* (45), 15913-15916.
 74. Niljianskul, N.; Zhu, S.; Buchwald, S. L., *Angew. Chem. Int. Ed.* **2015**, *54* (5), 1638-1641.
 75. Lu, G.; Liu, R. Y.; Yang, Y.; Fang, C.; Lambrecht, D. S.; Buchwald, S. L.; Liu, P., *J. Am. Chem. Soc.* **2017**, *139* (46), 16548-16555.
 76. Xi, Y.; Butcher, T. W.; Zhang, J.; Hartwig, J. F., *Angew. Chem. Int. Ed.* **2016**, *55* (2), 776-780.
 77. Hartwig, J. F., *Organotransition Metal Chemistry From Bonding to Catalysis*. 1 ed.; University Science Book: Mill Valley, CA, 2010.
 78. Ephritikhine, M.; Francis, B. R.; Green, M. L. H.; Mackenzie, R. E.; Smith, M. J., *J. Chem. Soc., Dalton Trans.* **1977**, (11), 1131-1135.
 79. Periana, R. A.; Bergman, R. G., *J. Am. Chem. Soc.* **1984**, *106* (23), 7272-7273.
 80. Stork, G.; Suh, H. S.; Kim, G., *J. Am. Chem. Soc.* **1991**, *113* (18), 7054-7056.
 81. Johannsen, M.; Jørgensen, K. A., *Chem. Rev.* **1998**, *98* (4), 1689-1708.
 82. Williams, J. M. J., *Synlett* **1996**, *1996* (08), 705-710.
 83. Ahn, J. M.; Peters, J. C.; Fu, G. C., *J. Am. Chem. Soc.* **2017**.
 84. Bissember, A. C.; Lundgren, R. J.; Creutz, S. E.; Peters, J. C.; Fu, G. C., *Angew. Chem. Int. Ed.* **2013**, *52* (19), 5129-5133.
 85. Do, H.-Q.; Bachman, S.; Bissember, A. C.; Peters, J. C.; Fu, G. C., *J. Am. Chem. Soc.* **2014**, *136* (5), 2162-2167.
 86. Kainz, Q. M.; Matier, C. D.; Bartoszewicz, A.; Zultanski, S. L.; Peters, J. C.; Fu, G. C., *Science* **2016**, *351* (6274), 681-684.
 87. Matier, C. D.; Schwaben, J.; Peters, J. C.; Fu, G. C., *J. Am. Chem. Soc.* **2017**.
 88. *Metal-Catalyzed Cross-Coupling Reactions*. 2 ed.; Wiley-VCH: 2004.
 89. Rudolph, A.; Lautens, M., *Angew. Chem. Int. Ed.* **2009**, *48* (15), 2656-2670.
 90. Frisch, A. C.; Beller, M., *Angew. Chem. Int. Ed.* **2005**, *44* (5), 674-688.

CHAPTER 2

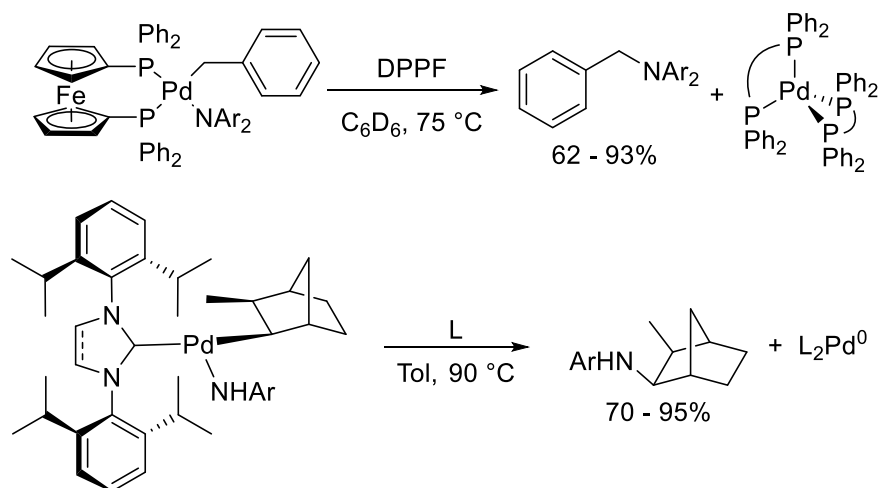
Reductive elimination of alkylamines from phosphine-ligated
syn-2-methylnorbornylpalladium(II) complexes

2.1 Introduction

Reductive eliminations to form carbon–nitrogen bonds are important steps in many reactions that produce amines catalyzed or mediated by transition-metal complexes. Reactions to form sp^2 carbon–nitrogen bonds from aryl- and heteroarylpalladium(II) complexes have been well studied.¹⁻² However, reductive eliminations to form the analogous sp^3 C–N bonds in alkylamines from alkylmetal amido complexes are rare, and the factors controlling the rates and scope of this elementary reaction are poorly defined. An increased understanding of this fundamental organometallic reaction could enable the development of new methods to construct sp^3 C–N bonds by catalytic reactions, such as C–H bond functionalization, olefin functionalization, or nucleophilic substitution.

Complexes of palladium(IV)³⁻⁵ and other high-valent metal centers⁶⁻⁹ have been reported to undergo reductive elimination to form sp^3 C–N bonds. However, examples of such reductive eliminations from low-valent metal complexes are more limited. Our group reported the first reductive eliminations from alkylpalladium(II) amido complexes (Scheme 2.1), in part motivated by reports of catalytic reactions that could occur through these intermediates.¹⁰⁻¹² Benzylpalladium(II) and alkylpalladium(II) complexes have been shown to react by two distinct mechanisms. Four-coordinate, bisphosphine-ligated benzylpalladium(II) amido complexes undergo reductive elimination by a stepwise mechanism involving initial dissociation of an anionic amido ligand, followed by nucleophilic attack of this anion on the coordinated benzyl ligand.¹³ This pathway results in inversion of configuration at the palladium-bound carbon atom. In contrast, three-coordinate, *N*-heterocyclic carbene (NHC)-ligated palladium(II) complexes bearing an unstabilized alkyl ligand (*syn*-2-methylnorbornyl) undergo reductive elimination by a concerted pathway, resulting in retention of configuration at the palladium-bound carbon atom.¹⁴

Scheme 2.1. Previous reports of reductive elimination of alkylamines from Pd(II) amido complexes.



The reported examples of reductive elimination from NHC-ligated (*syn*-2-methylnorbornyl)palladium(II) complexes occurred with high kinetic barriers (≥ 26 kcal/mol at $90\text{ }^\circ\text{C}$). Therefore, we have sought to understand the properties of the complexes and ligands that

control the rates of reaction and to identify complexes that undergo reductive elimination more rapidly. We have also sought to determine whether the rates of concerted reductive elimination to form sp^3 C–N bonds follow the trends previously reported for concerted reductive eliminations from d^8 transition metal centers that form sp^2 - sp^3 C–C, sp^3 - sp^3 C–C, and sp^2 C–N bonds.

In this chapter, we report the preparation of a series of phosphine-ligated palladium(II) amido complexes that undergo reductive elimination to form alkyl–nitrogen bonds. These studies reveal, by both experimental and computational methods, the effects controlling the structures of the Pd(II) anilido intermediates and the barriers to reductive elimination from these complexes. These results led to the discovery that the reductive elimination to form alkylamines from four-coordinate complexes containing particular P,O ligands is fast and depends on the ability of the Pd–O bond to lengthen or dissociate during reductive elimination.

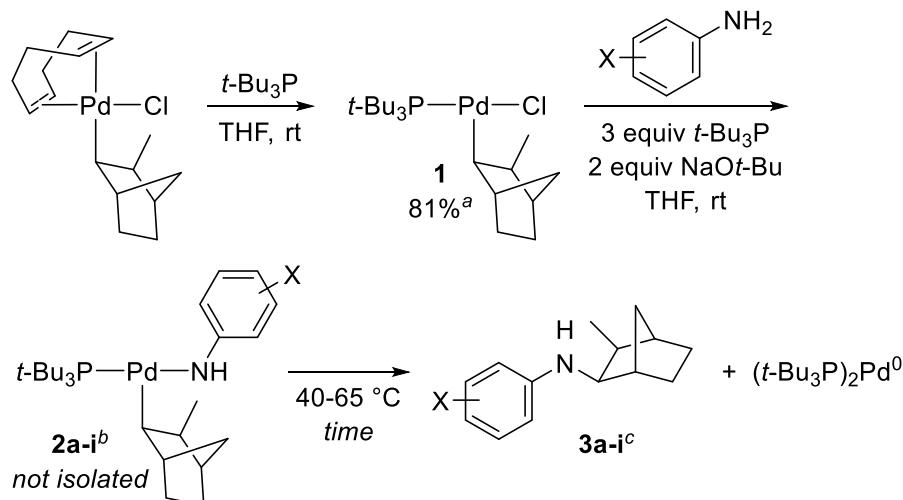
2.2 Results and Discussion

Palladium(II) complexes ligated by bulky monophosphines, such as tri-*tert*-butylphosphine (*t*-Bu₃P), undergo reductive elimination reactions that are slow or do not occur at all from analogous complexes containing less sterically demanding ligands.^{2, 15-16} Therefore, we investigated the potential of alkylpalladium complexes ligated by bulky monophosphines to undergo reductive elimination to form the sp^3 carbon–nitrogen bond in alkylamines.

Synthesis and reactions of monophosphine-ligated complexes. The preparation of *t*-Bu₃P-ligated alkylpalladium(II) anilido complexes was conducted in two steps from a known complex by the sequence shown in Scheme 2.2. Treatment of the olefin-ligated precursor 1,5-cyclooctadiene (*syn*-2-methylnorbornyl)palladium(II) chloride with *t*-Bu₃P at ambient temperature in THF generated the three-coordinate complex (*t*-Bu₃P)Pd(2-CH₃norbornyl)Cl (**1**). This complex was stable at ambient temperature and crystallized as red blocks in 81% yield (Scheme 2.2). The reaction of complex **1** with sodium *tert*-butoxide (NaOt-Bu), *t*-Bu₃P, and a series of arylamines at ambient temperature formed Pd(II) anilido complexes **2a-i** in 76-92% yield with (*t*-Bu₃P)₂Pd⁰ as a minor side product, as determined by NMR spectroscopy. Although *t*-Bu₃P is not consumed by the reaction, complexes bearing unhindered anilido ligands formed in lower yields when the reaction was performed without added *t*-Bu₃P.

The *t*-Bu₃P-ligated Pd(II) anilido complexes were typically unstable at ambient temperature and highly soluble in organic solvents, preventing recrystallization and isolation in pure form. However, the molecular weights (*M*) of **2g** and **2i** were approximated by ¹⁹F NMR diffusion ordered spectroscopy (DOSY) experiments, and these molecular weight-values agreed well with the expected values for monomeric, three-coordinate alkylpalladium(II) amido complexes (Table 2.1, entries 1 and 2). Furthermore, ¹H NMR nuclear Overhauser effect spectra (NOESY) of **2i** were consistent with a three-coordinate T-shaped or distorted T-shaped structure. Specifically, correlations were observed between the *endo* hydrogen on the palladium-bound carbon and the *tert*-butyl groups on the phosphine, as well as between the *exo* methyl group on the alkyl ligand and the NH proton of the anilido ligand (see the experimental section for spectra and assignments).

Scheme 2.2. Preparation of $(t\text{-Bu}_3\text{P})\text{Pd}(2\text{-CH}_3\text{norbornyl})\text{NHAr}$ **2a-i** and reductive elimination to form alkylamines **3a-i**.



	X	% yield 2a-i ^d	time /h	% yield 3a-i ^d
a	H	88	5	85 (75)
b	4-OMe	76	1	92 (70)
c	4-Me	89	2	88 (78)
d ^e	4-F	84	5	89 (75)
e	3-Me	92	5	93 (86)
f	3-OMe	85	6	91 (77)
g ^e	3-F	85	40	76 (65)
h ^f	2- <i>t</i> -Bu	86	6 (65 °C)	59 (51)
i ^e	4-F-2-OMe	91	4	quant (91)

^aIsolated yield after recrystallization. ^bConditions unless otherwise noted: Pd-Cl **1** (0.0399 mmol), $t\text{-Bu}_3\text{P}$ (0.12 mmol), arylamine (0.042 mmol), and NaO- $t\text{Bu}$ (0.080 mmol) in THF- d_8 (0.70 ml). ^cReactions were monitored by ^1H NMR spectroscopy while heating at 40 °C in a VT NMR probe for the noted time. ^dYield determined by ^1H NMR spectroscopy integration with 1,3,5-trimethoxybenzene (TMB) as internal standard; (values in parentheses are the overall yields of **3a-i** based on **1**); averages from two experiments. ^eReactions monitored by ^{19}F NMR spectroscopy in THF; 4-fluorotoluene (4-FTol) as internal standard. ^fReaction was heated at 65 °C.

Table 2.1. *In situ* molecular weight (M) estimation by DOSY.^a

entry	complex	$D \cdot 10^{10} / (\text{m}^2 \text{s}^{-1})$	expected M	DOSY M	error
1	2g	12.2	528	497	-31
2	2i	12.5	558	527	-31
3	6a	9.47	934	943	+9
4	8c	11.1	626	666	+40

^aDOSY experiments performed by ^{19}F NMR spectroscopy at 300 K in THF- d_8 /THF (~10%). See the experimental section for details on the calculations of diffusion constants and molecular weight estimates.

Due to the instability of $t\text{-Bu}_3\text{P}$ -ligated Pd(II) anilido complexes at room temperature, studies of the reductive elimination to form alkylamines were conducted with complexes prepared *in*

situ. Complexes **2a-i** underwent reductive elimination at 40-65 °C to form the corresponding norbornylamines **3a-i** in yields of 59 or higher% (Scheme 2.2). Excess *t*-Bu₃P (included during the formation of **2a-i**) served to trap the palladium-containing product as (*t*-Bu₃P)₂Pd⁰.

The reductive-elimination reactions were monitored by ¹H or ¹⁹F NMR spectroscopy at 40-65 °C in THF-*d*₈ or THF. All reactions of *t*-Bu₃P-ligated Pd(II) anilido complexes occurred with a first-order decay. The rate constants for reductive elimination (*k*_{RE}) and the corresponding free energies of activation (ΔG^\ddagger) are shown in Table 2.2.

Table 2.2. Effects of anilido substituents on the rate constants and free energies of activation for reductive eliminations to form alkyl–nitrogen bonds.^a

entry	Ar (complex)	<i>k</i> _{RE} ·10 ⁴ /s ⁻¹	ΔG_{RE}^\ddagger /(kcal·mol ⁻¹)
1	Ph (2a)	2.6	23.5
2	4-(OMe)C ₆ H ₄ (2b)	12	22.6
3	<i>p</i> -Tol (2c)	5.4	23.0
4	4-FC ₆ H ₄ (2d)	2.6	23.5
5	<i>m</i> -Tol (2e)	3.1	23.4
6	3-(OMe)C ₆ H ₄ (2f)	2.3	23.6
7 ^b	3-FC ₆ H ₄ (2g)	0.55	24.5
8 ^c	2-(<i>t</i> -Bu)C ₆ H ₄ (2h)	2.5	25.5
9	4-F-2-(OMe)C ₆ H ₃ (2i)	2.7	23.5

^aReactions performed as shown in Scheme 2.2; rate constants determined by fitting a plot of [2] vs time for 5 half-lives of data to the equation for an exponential decay; averages from two experiments; deviations were within 20% of the average value. ^bRate constant was determined from the linear fit of a ln[2g] vs time plot (1.3 half-lives). ^cThe reaction of **2h** was monitored at 338 K.

The kinetic data for reductive elimination from complexes bearing *meta*- and *para*-substituted anilido ligands (entries 1-7) were analyzed with a Hammett plot. A reasonable correlation ($R^2 = 0.95$) between Log *k*_X/*k*_H and σ was observed with a ρ value of -2.0 (Figure 2.1). This result suggests that complexes with less stabilization of a partial negative charge on nitrogen react faster than those with more stabilization of the charge, and the magnitude of ρ suggests that significant negative charge accumulates on nitrogen. The *ortho-tert*-butyl substituted **2h** underwent reductive elimination with the highest kinetic barrier of any *t*-Bu₃P-ligated complex that was investigated. Thus, reductive elimination generally occurred fastest from complexes bearing unhindered, electron-rich anilido ligands. Further studies were conducted primarily with 4-fluoro-2-methoxyaniline because the barrier for reductive elimination from the *ortho*-methoxy substituted **2i** was similar to that of the unsubstituted **2a**, but the reaction of **2i** could be followed by ¹⁹F NMR spectroscopy and occurred in high yield.

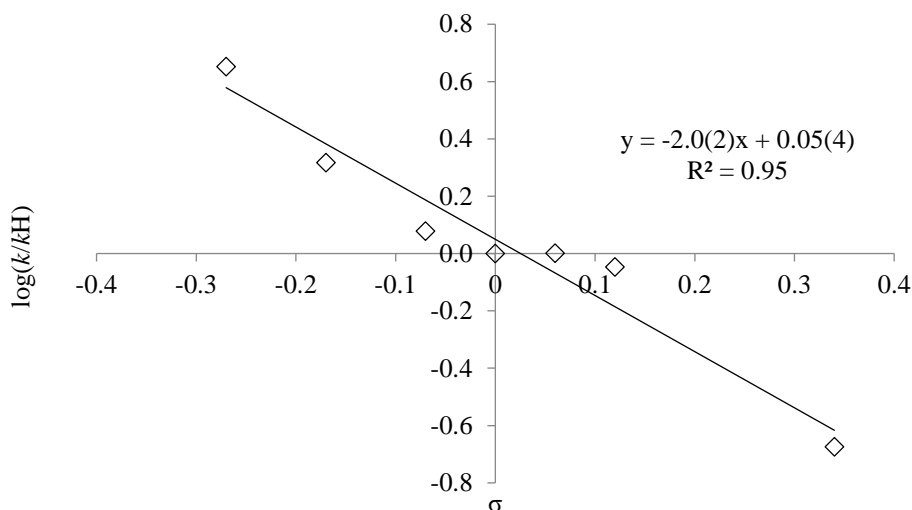


Figure 2.1. Hammett plot for substituent effects on the anilido ligand. Data from entries 1-7 of Table 2.2. Uncertainties in last digit of the slope and y-intercept are given in parentheses.

We sought to determine whether reductive elimination occurs directly from the three-coordinate complex observed in solution or from a different intermediate after association or dissociation of a ligand. The reaction of the *ortho*-methoxy substituted **2i** to form **3i** was determined to be zeroth-order in *t*-Bu₃P, and the yield of **3i** did not vary significantly with the concentration of *t*-Bu₃P (Figure 2.2a). These results suggest that the mechanism of reductive elimination does not involve either association or reversible dissociation of *t*-Bu₃P prior to the transition state.

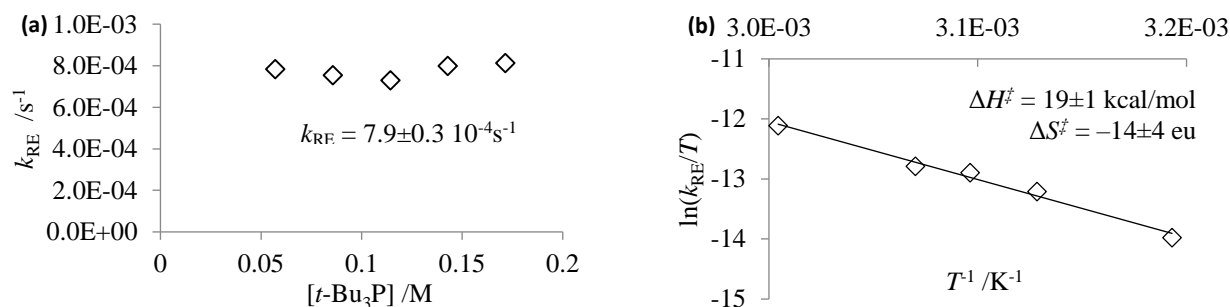


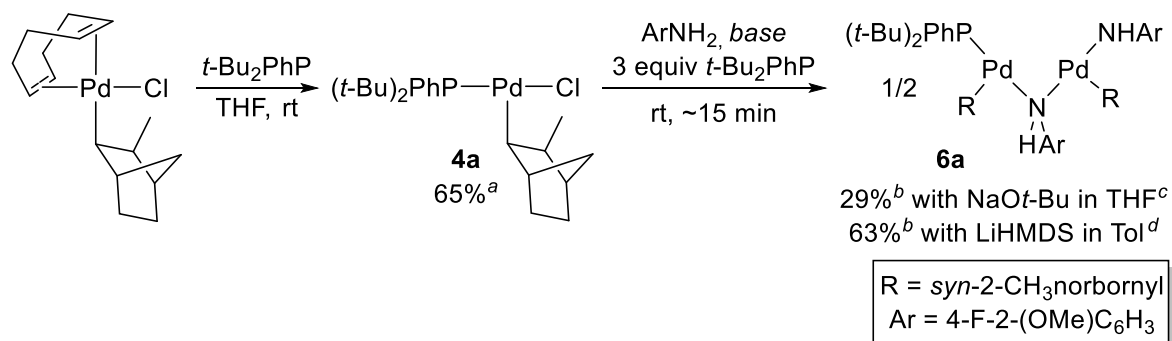
Figure 2.2. Determination of the order in $[t\text{-Bu}_3\text{P}]$ and activation parameters for reductive elimination from **2i**. Solutions of **2i** were prepared as described in Scheme 2.2. (a) Equivalents of *t*-Bu₃P were varied from 1 to 3 with $T = 323 \text{ K}$. (b) T was varied from 313 to 333 K with 3 equivalents of *t*-Bu₃P.

Further insight into the mechanism of reductive elimination was obtained by measuring the enthalpy and entropy of activation. An Eyring analysis (40-60 °C) of the reductive elimination from **2i** provided the parameters $\Delta H^\ddagger = 19 \pm 1 \text{ kcal/mol}$ and a $\Delta S^\ddagger = -14 \pm 4 \text{ eu}$ (Figure 2.2b). The negative value of ΔS^\ddagger is inconsistent with a pathway involving ligand dissociation prior to reductive elimination. The magnitude of ΔS^\ddagger is consistent with either an associative process or a unimolecular process in which the transition state is more ordered than the ground state. Because

the zeroth-order dependence on $[t\text{-Bu}_3\text{P}]$ rules out an associative pathway, these results support a mechanism for reductive elimination occurring directly from the three-coordinate complex observed in solution.

To dissect the steric and electronic effects on the reductive elimination to form the alkyl-nitrogen bond from phosphine-ligated palladium(II), we studied complexes containing di-*tert*-butylarylphosphines. Complexes of such ligands would enable the steric and electronic properties to be varied by substitution on the aryl group. The preparation of a $t\text{-Bu}_2\text{PhP}$ -ligated alkylpalladium(II) anilido complex was attempted by the same two step sequence described for complexes **2a-i**. Treatment of cyclooctadiene-ligated (*syn*-2-methylnorbornyl)palladium(II) chloride with $t\text{-Bu}_2\text{PhP}$ at ambient temperature in THF generated $(t\text{-Bu}_2\text{PhP})\text{Pd}(2\text{-CH}_3\text{norbornyl})\text{Cl}$ (**4a**), which was isolated as an off-white powder in 64% yield after recrystallization. Complex **4a** reacted with 4-fluoro-2-methoxyaniline and NaOt-Bu at ambient temperature with 3 equivalents of $t\text{-Bu}_2\text{PhP}$ in THF to produce a complicated mixture of palladium complexes (Scheme 2.3). The species formed in highest concentration in this mixture (as determined by ^{19}F or ^{31}P NMR spectroscopy) was assigned to be the bimetallic complex **6a**, which formed in approximately 29% yield (based on 2:1 stoichiometry of **4a** to **6a**). Complex **6a** formed in a higher yield of 63% when the same reaction was performed with LiHMDS as base in toluene.

Scheme 2.3. Formation of bimetallic alkylpalladium(II) amido complex **6a**.^a



^aIsolated yield after recrystallization. ^bYield determined by ^{19}F NMR spectroscopy integration against 4-FTol; average from two experiments. ^cConditions: Pd-Cl **4a** (0.020 mmol), $t\text{-Bu}_2\text{PhP}$ (0.060 mmol), 4-fluoro 2-methoxyaniline (0.020 mmol), and NaOt-Bu (0.040 mmol) in THF (2.0 ml). ^dConditions: **4a** (0.010 mmol), $t\text{-Bu}_2\text{PhP}$ (0.030 mmol), 4-fluoro 2-methoxyaniline (0.010 mmol), and LiHMDS (0.010 mmol) in Tol (1.0 ml).

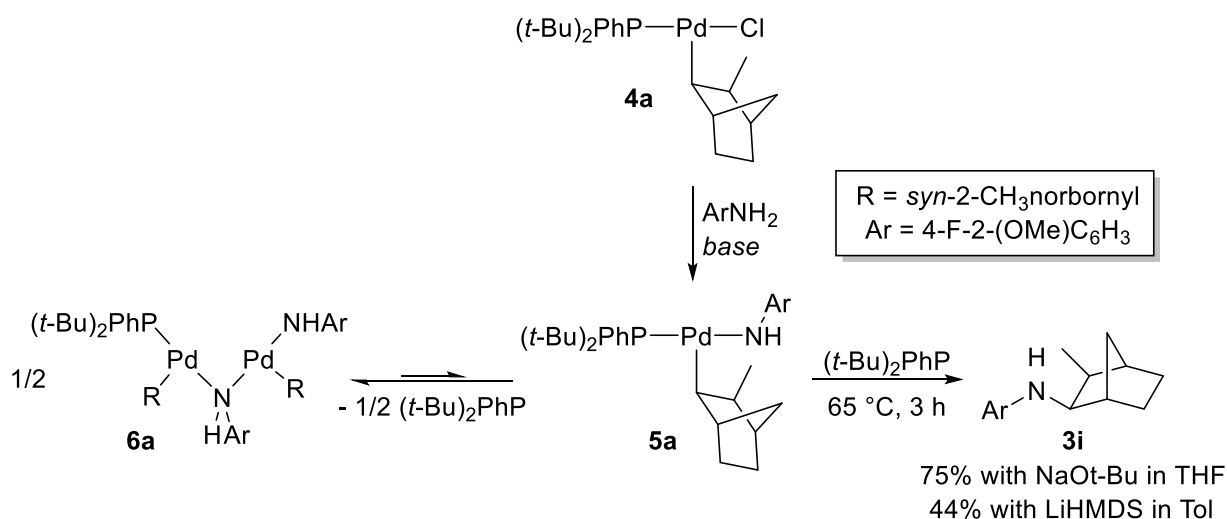
The identity of bimetallic amido complex **6a** was deduced by NMR spectroscopy using samples prepared *in situ* by the reaction of chloride complex **4a**, 4-fluoro-2-methoxyaniline, and LiHMDS in toluene.¹⁷ Complex **6a** contains one phosphine ligand, two inequivalent alkyl ligands, and two inequivalent anilido ligands. The formation of approximately one equivalent of free $t\text{-Bu}_2\text{PhP}$ per product was also observed, which accounts for the 1:2 ratio of phosphine to palladium in **6a**. Furthermore, the molecular weight of the complex, as determined by ^{19}F NMR DOSY experiments, was approximately 943 (Table 2.1, entry 3). These results are consistent with the assignment of **6a** as a bimetallic complex lacking one of the starting phosphine ligands (expected $M = 934$). ^1H NMR NOESY and ^1H - ^{31}P HMBC experiments suggested that the two

palladium centers are linked by a single bridging anilido ligand (see the experimental section for spectra). These experiments are consistent with the structure drawn in Scheme 2.3.

The observation of a monometallic complex with *t*-Bu₃P as ligand but a bimetallic complex with *t*-Bu₂PhP as ligand shows that increasing steric bulk at phosphorus leads to a decrease in relative concentration of the bimetallic complex. The greater electron donation by *t*-Bu₃P than by *t*-Bu₂PhP also would be expected favor the monometallic complex over the bimetallic complex. However, a mixture of Pd(II) anilido complexes was observed to form from reactions of (*t*-Bu₂CyP)Pd(2-CH₃norbornyl)Cl (**4b**), 4-fluoro-2-methoxyaniline, and base (see the experimental section for details). The electron-donating properties of *t*-Bu₃P and *t*-Bu₂CyP are similar.^{18, 19} Therefore, these results suggest that the steric properties of the ancillary ligand, not the electronic properties, primarily determine whether monometallic or bimetallic structures are favored.

Heating of the mixture of complexes described in Scheme 2.3 at 65 °C in THF for 3 h formed the norbornylamine product **3i** in 75% yield (based on **4a**) (Scheme 2.4). Under these conditions, the remainder of the mass balance (with respect to the amine) was 4-fluoro-2-methoxyaniline, as determined by ¹⁹F NMR spectroscopy. The yield of **3i** greatly exceeds the yield of any of the individual palladium complexes in the solution, indicating that multiple species undergo reductive elimination or that multiple species equilibrate prior to reductive elimination.

Scheme 2.4. Reductive elimination from bimetallic alkylpalladium(II) amido complex **6a**.^a



^aSamples prepared as described in Scheme 2.3; yields of **3i** (based on **4a**) determined by ¹⁹F NMR spectroscopy integration against 4-FTol; averages from two experiments.

To gain insight into the mechanism of reductive elimination from the *t*-Bu₂PhP-ligated bimetallic complex **6a**, the order in phosphine was measured. The initial rate (*r*) of formation of **3i** was measured for reactions conducted with 1, 4, or 9 equivalents of added *t*-Bu₂PhP (Table 2.3 and Figure 2.3). In contrast to the rate of reactions with *t*-Bu₃P, the rate of the reaction with *t*-Bu₂PhP was dependent on the concentration of phosphine. The approximately half-order dependence is consistent with a mechanism in which **6a** (or other bimetallic species lacking a phosphine ligand) undergoes fast reversible association of one *t*-Bu₂PhP to form two equivalents

of the monometallic intermediate prior to reductive elimination (Scheme 2.4). Due to its analogy with the *t*-Bu₃P-ligated complex **2i**, we proposed that complex **5a** is likely the intermediate that reductively eliminates the amine.

Table 2.3. Effect of [*t*-Bu₂PhP] on the rate of reductive elimination of **3i**.^a

entry	added equiv <i>t</i> -Bu ₂ PhP	theoretical initial [<i>t</i> -Bu ₂ PhP] /M	% yield 6a	initial rate (<i>r</i>) /10 ⁻⁶ M·s ⁻¹	% yield 3i (24 h)
1	1	0.0429	25	1.20	38
2	4	0.129	18	1.91	55
3	9	0.271	16	2.58	55

^aReactions monitored by ¹⁹F NMR.

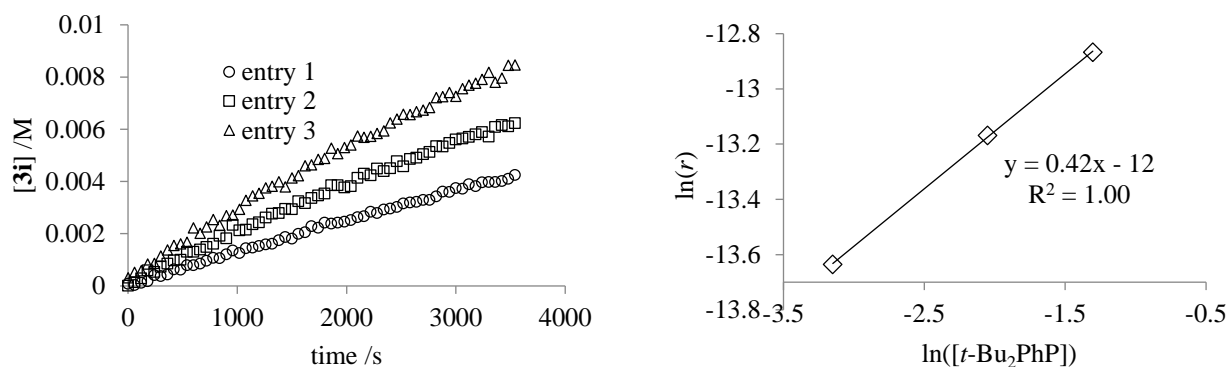
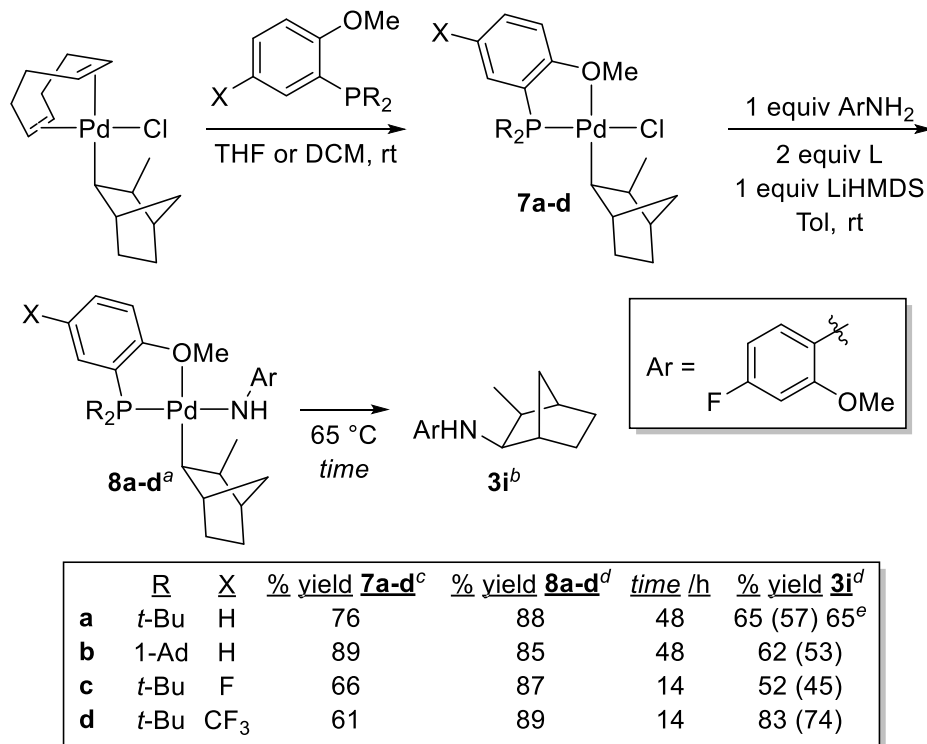


Figure 2.3. Effect of the concentration of *t*-Bu₂PhP on the rate of formation of **3i**. Entries are from Table 2.3. Experiments were performed at 50 °C in THF. Concentrations of **3i** were measured by ¹⁹F NMR integration against 4-fluorotoluene. Initial rates were measured as the slope of a linear fit of [**3i**] vs time plot for < 15% yield

Synthesis and reactions of four-coordinate complexes. Because reductive elimination from the *t*-Bu₂PhP-ligated complexes is a multi-step process involving multiple (likely equilibrating) Pd(II) anilido complexes, this system was not amenable to dissecting the effects of ancillary ligands on the rate of reductive elimination. Therefore, we sought to identify a class of complexes that was monometallic and contained a phosphine that could possess varied steric and electronic properties. We found that the formation of bimetallic species and the dissociation of the di-*tert*-butyl arylphosphine ligand could be prevented by introducing a second coordinating group at the *ortho*-position of the arylphosphine. The (*t*-Bu₂ArP)Pd(2-CH₃norbornyl)Cl complexes **7a-d** bearing 2-methoxyaryl groups on phosphorus were prepared from the reactions of (COD)Pd(2-CH₃norbornyl)Cl and the corresponding phosphines in THF or DCM (Scheme 2.5). All four complexes formed as single isomers, with the phosphine *cis* to the alkyl ligand and the ether oxygen *cis* to the chloride. This geometry was established by NOESY correlations between the alkyl ligand and the *tert*-butyl or adamantyl groups on phosphorus.

Scheme 2.5. Preparation of four-coordinate (*t*-Bu₂(2-(OMe)Ar)P-κ²P,O)Pd(2-CH₃norbornyl)NHAr complexes **8a-d** and reductive elimination to form **3i**.



^aConditions: Pd-Cl **7** (0.020 mmol), phosphine (0.040 mmol), 4-fluoro-2-methoxyaniline (0.020 mmol), and LiHMDS (0.020 mmol) in Tol (2.0 ml). ^bThe reaction mixture containing **8a-d** was heated at 65 °C with stirring in a Teflon-capped vial for the noted time. ^cIsolated yields after recrystallization. ^dYields determined by ¹⁹F NMR spectroscopy integration against 4-FTol; (values in parentheses are the overall yield of **3i** based on **7a-d**); averages from two experiments. ^eConditions: isolated **8a** (0.020 mmol) and *t*-Bu₂(*o*-anisyl)P (0.060 mmol) heated at 89 °C for 4 hours in Tol-*d*₈ (0.70 ml).

A comparison of the ¹³C NMR spectra of these complexes to those of the three-coordinate Pd(II) chloride complexes revealed a pronounced upfield shift of the resonance corresponding to the palladium-bound carbon: 40.8 to 44.3 ppm for the four-coordinate complexes **7a-d** versus 57.9 to 64.2 ppm for the three-coordinate complexes **1** and **4a-b**. This difference in chemical shift suggests that coordination of the ether to palladium causes a significant increase in electron density at the alkyl ligand.

The reactions of the Pd(II) chloride complexes **7a-d** with 4-fluoro-2-methoxyaniline and LiHMDS with excess phosphine at ambient temperature in toluene generated the corresponding Pd(II) anilido complexes **8a-d** in yields of 85-89% by NMR spectroscopy (Scheme 2.5). These four-coordinate complexes were moderately stable at ambient temperature, and samples suitable for analysis by X-ray diffraction were obtained from crystallization of **8a** and **8b** (Figure 2.4).

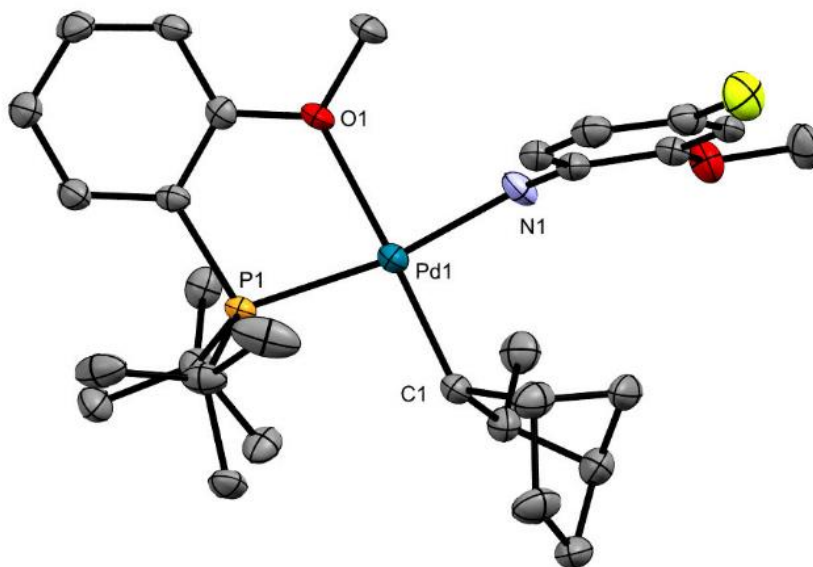


Figure 2.4. ORTEP drawing of $[t\text{-Bu}_2(o\text{-anisyl})\text{P-}\kappa^2\text{P,O}]\text{Pd}(2\text{-CH}_3\text{norbornyl})(\text{NHAr})$ **8a** with 50% probability ellipsoids. Hydrogen atoms are omitted for clarity. Selected bond lengths (Å) and angles (°) for **8a**: Pd1-O1 2.288(2), Pd1-P1 2.2881(8), Pd1-C1 2.057(3), Pd1-N1 2.053(3); O1-Pd1-P1 80.40(6), P1-Pd1-C1 97.38(9), C1-Pd1-N1 92.92(12), N1-Pd1-O1 89.32(9). For the analogous bonds in **8b**: Pd1-O1 2.297(2), Pd1-P1 2.2898(9), Pd1-C1 2.042(4), Pd1-N1 2.081(3); O1-Pd1-P1 81.79(6), P1-Pd1-C1 97.24(10), C1-Pd1-N1 92.98(13), N1-Pd1-O1 88.48(10).

The ^1H NMR signals corresponding to the alkyl ligand in complex **8a** containing di-*tert*-butyl(*o*-anisyl)phosphine were assigned by 2-dimensional NMR spectroscopy. An analysis of the ^1H NOESY correlations indicated that the alkyl ligand is positioned such that the *endo* face is close to the phosphine ligand, and the *exo* face is close to the anilido ligand. These results are consistent with the distorted square planar, solid-state structure obtained by X-ray diffraction. Therefore, any variation between the solid- and solution-state structures of this complex is small. Similar correlations were observed in the NOESY spectrum of the analogous three-coordinate, *t*-Bu₃P-ligated complex **2i**. This similarity suggests that the geometry at the metal and orientation of the ligands in **8a** are similar to those in **2i** (see the experimental section for spectra and assignments). Furthermore, ^{19}F NMR DOSY experiments with complex **8c** (which contains a second fluorine label on the ancillary ligand) confirmed that this complex, and presumably the other P-O ligated complexes, is monometallic in solution (Table 2.1, entry 4).

Complexes **8a-d** bearing 2-methoxyarylphosphine ligands on palladium underwent reductive elimination of norbornylamine **3i** in yields of 52-83% after 14 or 48 hours at 65 °C with 2 equivalents of added phosphine to trap the Pd(0) product (Scheme 2.5). The yields of these reactions depended on the substituents on the phosphine ligand; the highest yield of 83% was obtained from the reaction of complex **8d** containing a 5-CF₃-substituent on the phosphine aryl group.

The reductive eliminations from four-coordinate complexes **8a-d** were 12 to 120 times slower than that from the analogous three-coordinate, *t*-Bu₃P-ligated complex **2i** (Table 2.4). Previous studies on concerted reductive elimination reactions from d⁸ transition metal centers have led to

the conclusion that the rates of reductive elimination from four-coordinate, square planar complexes are typically slower than those from analogous three- or five-coordinate complexes.²⁰⁻²¹ Our observation that alkylpalladium amido complexes containing P,O ligands undergo reductive elimination more slowly than *t*-Bu₃P-ligated complexes is consistent with this general trend deduced from other classes of reductive eliminations. However, reductive elimination still occurs in moderate to good yield under mild conditions because the ether oxygen atom is a weak electron donor (*vide infra*).

Table 2.4. Effects of substituents on the ancillary ligand on the rate of reductive elimination.^a

entry	complex	$k_{\text{RE}} \cdot 10^5 / \text{s}^{-1}$	$\Delta G_{\text{RE}}^\ddagger / (\text{kcal} \cdot \text{mol}^{-1})$
1 ^b	2i	ca. 300	23.8
2 ^c	8a	2.7	26.9
3	8b	2.9	26.9
4 ^d	8c	25	25.4
5 ^e	8d	14	25.8
6	8e	18	25.7

^aConditions: Pd-NHAr **8a-e** (0.020 mmol) and phosphine (3 equiv) in THF (0.70 ml) at 65 °C in a VT NMR probe; concentrations were determined by ¹⁹F NMR spectroscopy integration against 4-FTol; rate constants and activation energies were determined from linear fits of ln[**8**] vs time plots (1 half-life). ^bThe k_{RE} and $\Delta G_{\text{RE}}^\ddagger$ for **2i** at 65 °C were extrapolated from the data in Figure 2.2b. ^cData averaged from two experiments. ^dComplex **8c** underwent significant (ca. 50%) unproductive decomposition during this experiment; the rate constant is approximate and an overestimation. ^eAttempts to isolate and purify **8d** were unsuccessful; a solution of **8d** in THF was generated by the method described in Scheme 2.2 for this experiment.

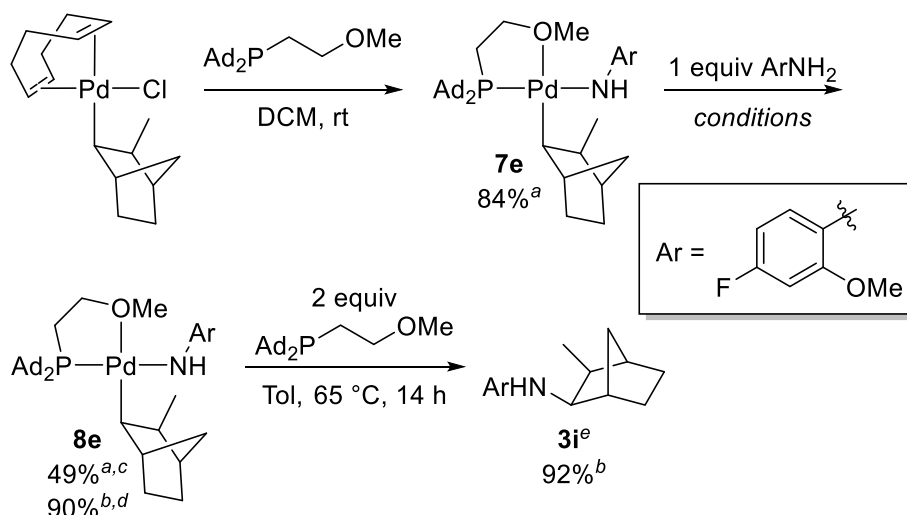
Small changes to the steric properties of the complexes did not significantly influence the rate of reductive elimination. The rate of reaction of the di-*tert*-butyl(*o*-anisyl)phosphine-ligated complex **8a** was similar to that of the di-adamantyl(*o*-anisyl)phosphine-ligated complex **8b** (Table 2.4, entries 2 and 3), and the solid-state structures of these two complexes (Figure 2.4) were similar, as expected. Attempts to synthesize and investigate the reactivity of complexes bearing less sterically-demanding P,O ligands were unsuccessful.

The effects of the electronic properties of the complexes on the rate of reductive elimination were more readily accessed and were significant. The rates of reductive elimination from the electron-deficient 5-F-substituted **8c** and 5-CF₃-substituted **8d** were 7 and 6 times faster, respectively, than that from **8a** (Table 2.4, entries 2 and 4). These results suggest that reductive elimination of alkylamines occurs faster from complexes bearing less electron-donating ancillary ligands than from complexes bearing more electron-donating ancillary ligands. This result is similar to that observed previously for other classes of reductive eliminations from palladium(II) complexes²² and is consistent with our observation that *t*-Bu₃P-ligated complexes are much more reactive than the previously reported complexes containing more electron-donating²³⁻²⁴ NHC ligands.

Computational studies on the mechanism of reductive elimination from complexes **8a-d** containing rigid 2-methoxyarylphosphine ligands suggested that the variation in the length of the Pd–O bond in the ground state and in the transition state would impact the rate of reaction (*vide infra*). To analyze this proposal experimentally, we prepared complexes with a more flexible linker between the phosphorus and oxygen donors. The Pd(II) chloride precursor

(Ad₂PCH₂CH₂OCH₃-κ²P,O)Pd(2-CH₃norbornyl)Cl **7e** bearing a chelating 2-methoxyethyl group on phosphorus was prepared by the same method as described previously for the preparation of complexes **7a-d** (Scheme 2.6). After recrystallization, the sample contained a single isomer in which the phosphine and alkyl ligands are mutually *cis*, as determined by NMR spectroscopy. The aliphatic linker in this methoxyethylphosphine is more flexible than the aryl linker in the 2-methoxyarylphosphines. The aliphatic ether unit in **7e** is also expected to be a stronger electron donor than the aryl ether units in **7a-d**. This assertion is consistent with the higher-field ¹³C NMR chemical shift of the palladium-bound alkyl carbon in **7e** than that of the alkyl carbon in **7a-d** (36.2 ppm for **7e** versus 40.8-44.3 ppm for **7a-d**).

Scheme 2.6. Preparation of the flexible (Ad₂PCH₂CH₂OCH₃-κ²P,O)Pd(2-CH₃norbornyl)NHAr (**8e**) and reductive elimination to form **3i**.



^aIsolated yield after recrystallization. ^bYield determined by ¹⁹F NMR spectroscopy integration against 4-FTol; average from two experiments. ^cConditions: Pd-Cl **7e** (0.134 mmol) and lithium (4-fluoro-2-methoxyphenyl)amide (0.136 mmol) in DCM. ^dConditions: Pd-Cl **7e** (0.020 mmol), phosphine (0.040 mmol), 4-fluoro-2-methoxyaniline (0.020 mmol), and LiHMDS (0.020 mmol) in Tol (2.0 ml). ^eThe reaction mixture containing **8e** and phosphine in toluene prepared as described above^d was heated at 65 °C with stirring in a Teflon-capped vial.

The reaction of the 2-methoxyethyl-ligated **7e** with 4-fluoro-2-methoxyaniline and LiHMDS in toluene produced the corresponding Pd(II) anilido complex **8e** in 90% yield by NMR spectroscopy (Scheme 2.6). Complex **8e** was isolated in a lower yield of 49% from a similar reaction of **7e** with amine and NaOt-Bu in THF. An analysis of the ¹H NMR NOE correlations for **8e** suggests that the 2-methoxyethyl group of the ligand is coordinated to palladium, despite the flexibility of the linker between oxygen and phosphorus (see the experimental section). A crystal suitable for X-ray diffraction was obtained, and the solid-state structure of **8e** was similar to those of **8a** and **8b** (Figure 2.5). The Pd-O bond length in **8e** was 2.297 Å, which is only slightly longer than the 2.288 and 2.283 Å Pd-O bond lengths in **8a** and **8b**, respectively. Each of the other bond distances to palladium varied by less than 0.04 Å between the three complexes, and the bond angles around palladium varied by less than 5°. These results suggest that the steric properties of the ligand in **8e** are similar to those of the ligands in **8a-d**.

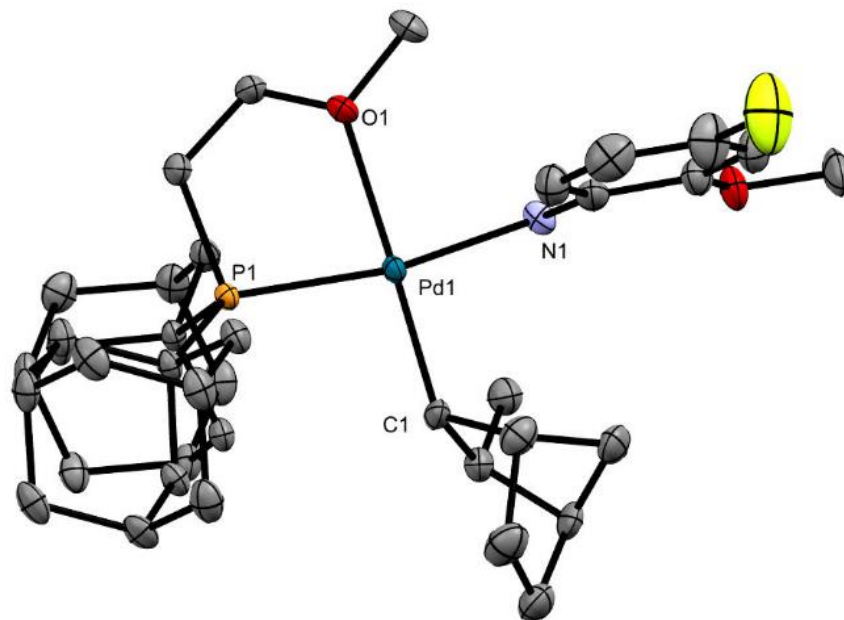
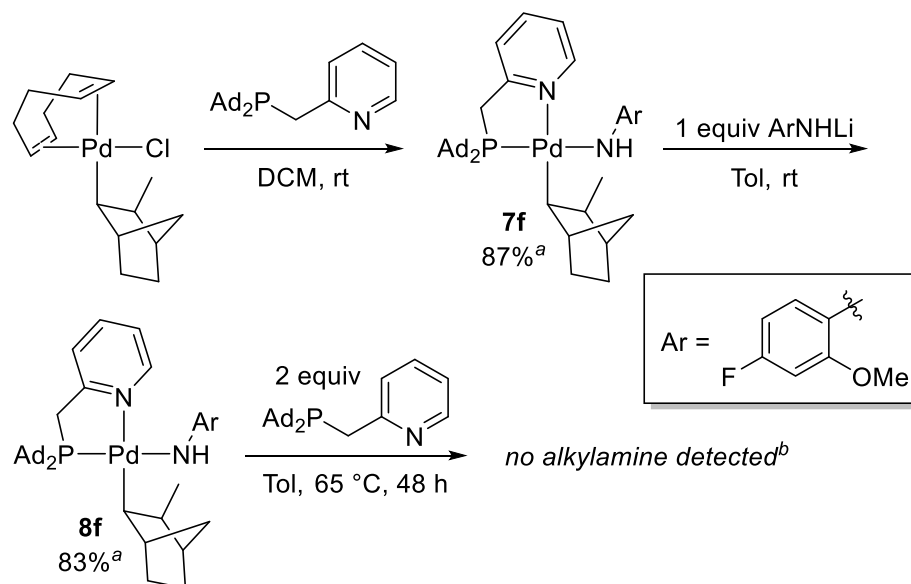


Figure 2.5. ORTEP drawing $[\text{Ad}_2\text{PCH}_2\text{CH}_2\text{OCH}_3\text{-}\kappa^2\text{P,O}]\text{Pd}(2\text{-CH}_3\text{norbornyl})(\text{NHAr})$ **8e** with 50% probability ellipsoids. Hydrogen atoms are omitted for clarity. Selected bond lengths (Å) and angles (°): Pd1-O1 2.297(2), Pd1-P1 2.2898(9), Pd1-C1 2.042(4), Pd1-N1 2.081(3); O1-Pd1-P1 81.79(6), P1-Pd1-C1 97.24(10), C1-Pd1-N1 92.98(13), N1-Pd1-O1 88.48(10).

Reductive elimination from complex **8e** containing the alkyl backbone was faster than that from complexes **8a-b** containing the more rigid aryl backbone. Complex **8e** underwent reductive elimination in the presence of 2 equivalents of ligand at 65 °C in toluene to form norbornylamine **3i** in 92% yield. This yield was higher than those from the reactions of 2-methoxyarylphosphine-ligated complexes (**8a-d**). The rate constant for reductive elimination from **8e** was 6 times larger than that for reductive elimination from **8b**, corresponding to a 1.2 kcal/mol lower barrier (Table 2.4, entry 4). We propose that this difference in reactivity is predominately due to the difference in flexibility between the aliphatic and aryl linkers, and this proposal was corroborated by computations (*vide infra*).

To investigate how the electron-donating property of the chelating group influences the rate of reductive elimination, we prepared $[\text{Ad}_2\text{PCH}_2(2\text{-C}_5\text{H}_4\text{N})\text{-}\kappa^2\text{P,N}]\text{Pd}(2\text{-CH}_3\text{norbornyl})(\text{NHAr})$ (**8f**) containing a picolinyl group on phosphorus by the methods previously described (Scheme 2.7). The ^1H NMR chemical shifts and NOE correlations observed for this complex are consistent the four-coordinate structure drawn. Complex **8f** underwent unproductive decomposition at 65 °C in either THF or toluene, with no detectable formation of norbornylamine **3i**. This result implies that the barrier to reductive elimination from a complex containing a strongly electron-donating fourth ligand (such as a pyridine) located *trans* to the alkyl ligand is significantly higher than that from a complex containing a weak donor (such as an ether).²⁵

Scheme 2.7. Preparation of the P,N-ligated [Ad₂PCH₂(2-C₅H₄N)-κ²P,N]Pd(2-CH₃norbornyl)NHAr (**8f**).



^aIsolated yield after recrystallization. ^bBy neither GCMS nor ¹⁹F NMR spectroscopy; **8e** was also not detected by ¹⁹F NMR spectroscopy after heating.

Computational Results (Quan Jiang). Computational studies were performed by the Cundari group to investigate the effects of ancillary ligands on reductive elimination from palladium(II) amido complexes. Density functional theory calculations were conducted using Gaussian09²⁶ with the hybrid exchange functional B3LYP.²⁷ The Pd atom was represented by the Stevens/Basch/Krauss effective core potential and associated triple- ξ valence basis set.²⁸⁻³⁰ The remaining main group atoms were represented by the 6-31+G(d) and 6-311++G(d,p) basis set for geometry optimizations in the gas phase and single point calculations, respectively. Solvent effects (THF, $\epsilon = 7.4257$) utilized the SMD³¹ continuum model via single point calculations on geometries optimized in the gas phase. Calculations of the free energies of activation for reductive elimination from palladium(II) amido complexes ligated by bulky *N*-heterocyclic carbene (NHC) ligands at the same level of theory matched the value measured experimentally.¹⁴ The ground states were determined to be minima on their potential energy surfaces by the absence of imaginary frequencies, while the transition states were determined to be saddle points by the presence of a single imaginary frequency.

Reactions of the Pd(II) anilido complexes **8a-e** containing P,O ligands were investigated computationally to understand how the structure of the bidentate ancillary ligands affects the rate of reductive elimination. The computed ground-state geometries were similar to those measured by X-ray diffraction (Table 2.5, Figure 2.4, and Figure 2.6). The computed free energy barrier of **8a** to reductive elimination was identical to the experimental result (26.9 kcal/mol). During the reductive elimination of norbornylamine **3i** from **8a**, the P–Pd–C bond angle is computed to increase from 101 to 127°, and the C–Pd–N bond angle to decrease from 95 to 57° (Figure 2.7). The Pd–C bond length is computed to increase from 2.09 to 2.46 Å, but the Pd–N distance

remains roughly constant (2.06 Å). Thus, the transition state for reductive elimination resembles a migration of the alkyl ligand to the anilide nitrogen.

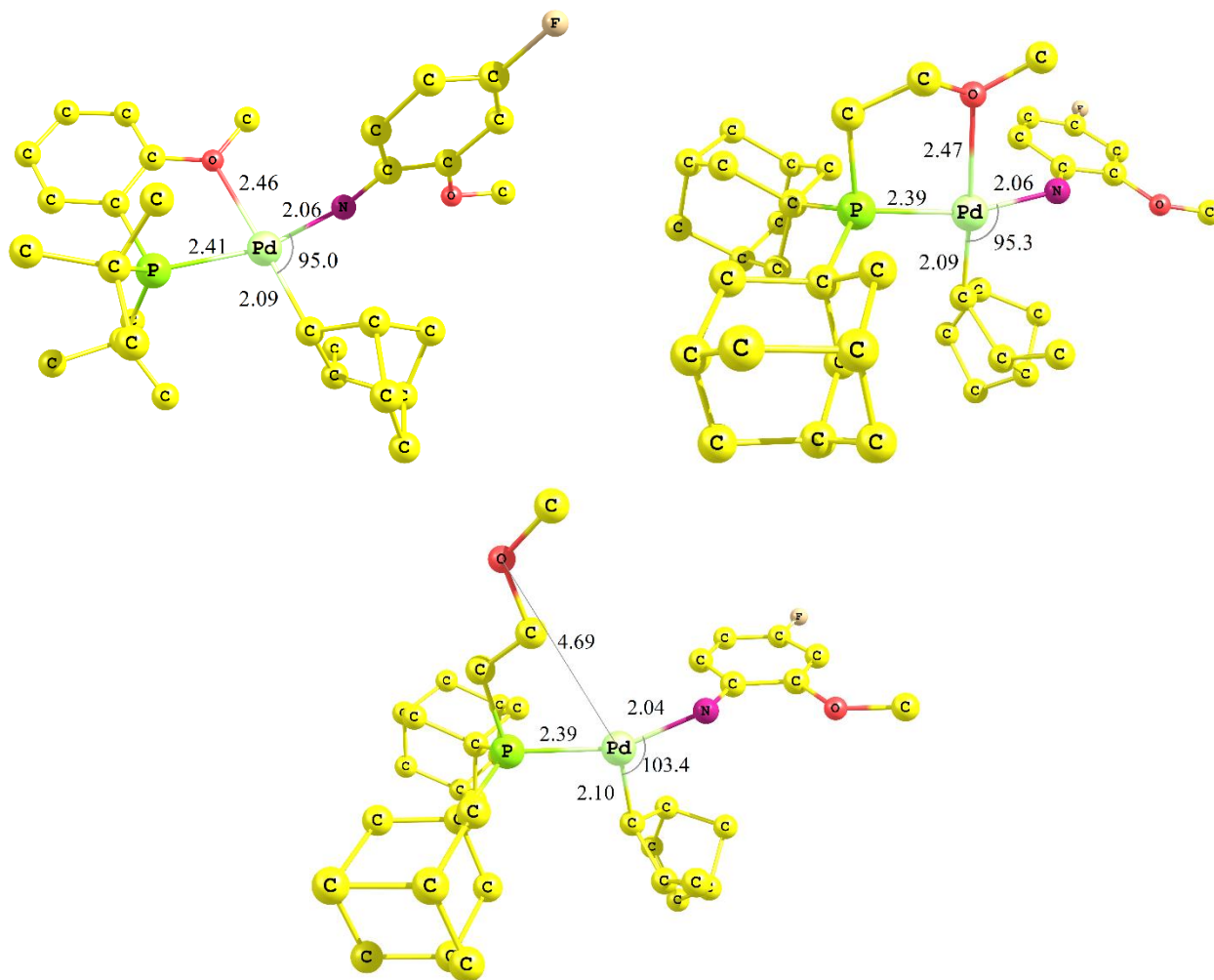


Figure 2.6. Computed ground state structures for [*t*-Bu₂(*o*-anisyl)P-κ²P,O]Pd(2-CH₃norbornyl)(NHAr) **8a** (top left) and [Ad₂PCH₂CH₂OCH₃-κ²P,O]Pd(2-CH₃norbornyl)(NHAr) **8e** (top right), and [Ad₂PCH₂CH₂OCH₃-κP]Pd(2-CH₃norbornyl)(NHAr) **9** (bottom). Bond lengths in Å, bond angles in degrees. Hydrogen atoms are omitted for clarity.

Table 2.5. Calculated effects of ancillary ligands on reductive elimination to form sp³ C–N bonds^a

entry	complex	Pd–O /Å	C–Pd–N /°	ΔG _{RE} [‡] /(kcal·mol ^{–1})
1	8a	2.46 (2.89)	95.0 (56.9)	26.9
2	8b	2.45 (2.87)	94.7 (56.5)	25.8
3	8d	2.48 (2.88)	95.4 (57.1)	25.5
4	8e	2.47(3.87)	95.3 (58.6)	23.1

^aPd–O and C–Pd–N values are from ground state calculations. Values in parentheses are from the corresponding optimized transition state structures. Barriers are calculated with temperatures at 338 K.

The distances from the palladium to the coordinated oxygen (Pd–O) are calculated to increase along the reaction coordinate from the ground states to the transition states (Figure 2.7, Table 2.5). The average increase in the Pd–O bond for the complexes **8a–d** containing rigid 2-methoxyaryl groups on the phosphine was only 17% of the starting bond length (Table 2.4, entries 1–3). These Pd–O distances are all significantly less than the sum of the van der Waals radii (1.63 and 1.52 Å for Pd and O, respectively).³² The calculated free-energy barriers for this pathway agreed well with those measured experimentally (Table 2.4 and Table 2.5). Therefore, computations suggest that reductive elimination occurs directly from the four-coordinate complexes and through a four-coordinate transition state (Figure 2.7).

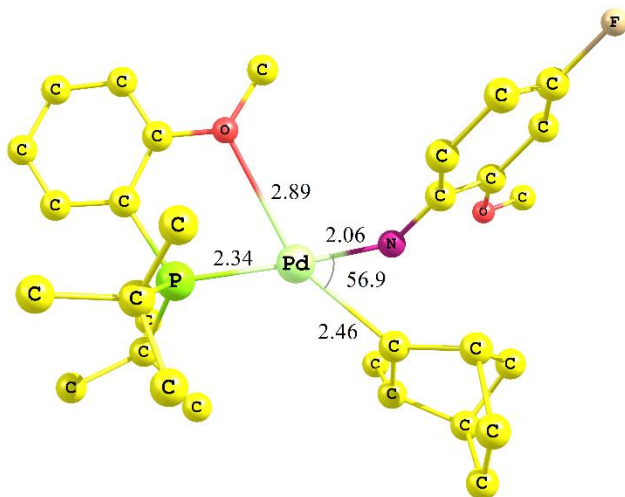


Figure 2.7. Computed transition state structure for reductive elimination of norbornylamine **3i** from [*t*-Bu₂(*o*-anisyl)P]Pd(2-CH₃norbornyl)(NHAr) **8a**. Bond lengths in Å, bond angles in degrees. Hydrogen atoms are omitted for clarity.

In contrast, the increase in the Pd–O distance during the reaction of complex **8e** containing the flexible 2-methoxyethyl group is approximately 57% of the starting bond length (Table 2.5, entry 4). The Pd–O distance in the transition state for reductive elimination from **8e** is longer than what can be considered a bond; the value of 3.87 Å is substantially greater than the sum of the van der Waals radii.³³ Furthermore, an isomeric three-coordinate ground state structure (**9**) was located in which the P,O ligand is bound only through phosphorus (Figure 2.6, bottom). The computed energy of complex **9** was 1.6 kcal/mol lower than the energy of **8e**; therefore, **8e** could potentially isomerize to **9** prior to reductive elimination. However, complex **9** was not observed by experiment. These computational results suggest that reductive elimination from **8e** occurs with dissociation of the oxygen from the palladium center, although it is still unclear whether this dissociation occurs prior to or in concert with the reductive elimination transition state.

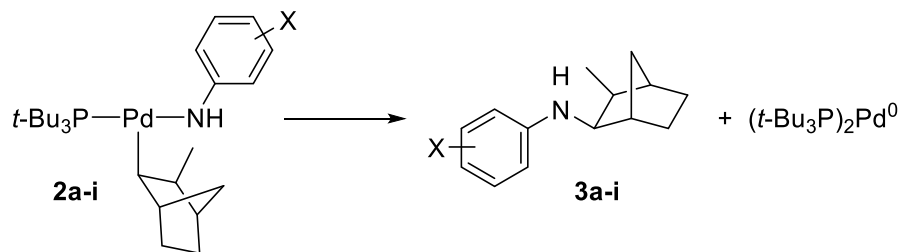
The computed and experimentally-measured barriers to reductive elimination from 2-methoxyethyl-ligated **8e** were lower than those from the analogous methoxyaryl-ligated **8b** (Table 2.4 and Table 2.5). This difference in reactivity is unlikely to result from differences in the steric or electronic properties of the phosphine because the differences in steric properties are small (Table 2.5, Figure 2.5, and Figure 2.6), and the greater electron donation by the ligand in

8e than by the ligands in **8a-b** should lead to an increase in the barrier to reductive elimination. Therefore, we propose that the higher reactivity of **8e** than of **8a** or **8b** is primarily a result of the smaller energy required for the flexible ether ligand in **8e** to dissociate from the metal center during reductive elimination.

The possibility that an interaction between the ether group in the anilido ligand and the palladium center affects the barrier to reductive elimination was evaluated. However, the distances from Pd to the oxygen in the anilido ligand were over 4.71 Å in the transition states for reductive elimination from **8a-e**. Therefore, the effect of these interactions on the kinetic barrier to reductive elimination is predicted to be small.

The *t*-Bu₃P-ligated complexes **2a-i** complexes were too unstable to isolate and characterize by X-ray diffraction. Therefore, the computed structure of the ground state of the three-coordinate, *t*-Bu₃P-ligated alkylpalladium(II) amido complex **2a** bearing a phenyl group on nitrogen was obtained by altering the structure of the four-coordinate, *t*-Bu₂(*o*-anisyl)P-ligated Pd(II) anilido complex **8a** (Figure 2.8). The *ortho*-anisyl group on phosphorus in this complex was replaced by a third *tert*-butyl group, and the 4-fluoro-2-methoxyphenyl group on nitrogen was replaced with a phenyl group. The energy of the resulting structure was then minimized, and the structures of the other *t*-Bu₃P-ligated complexes **2b-h** were obtained by introducing the appropriate substituents on the aryl group and minimizing the energy.

Table 2.6. Effects of anilido substituents on the calculated barrier to reductive elimination from **2a-i** to form **3a-i**.^a



entry	X	$\Delta G_{\text{RE}}^{\ddagger} / (\text{kcal} \cdot \text{mol}^{-1})^a$
1	H (2a)	21.9
2	4-OMe (2b)	22.7
3	4-Me (2c)	22.8
4	4-F (2d)	23.4
5	3-Me (2e)	21.6 (23.7)
6	3-OMe (2f)	22.6 (22.9)
7	3-F (2g)	22.7 (24.7)
8	2- <i>t</i> -Bu (2h)	25.2 (25.5)
9	2-OMe-4-F (2i)	23.4

^a ΔG^{\ddagger} values in parentheses are from isomers. Calculated temperatures at 313 K except for **2h** at 338 K.

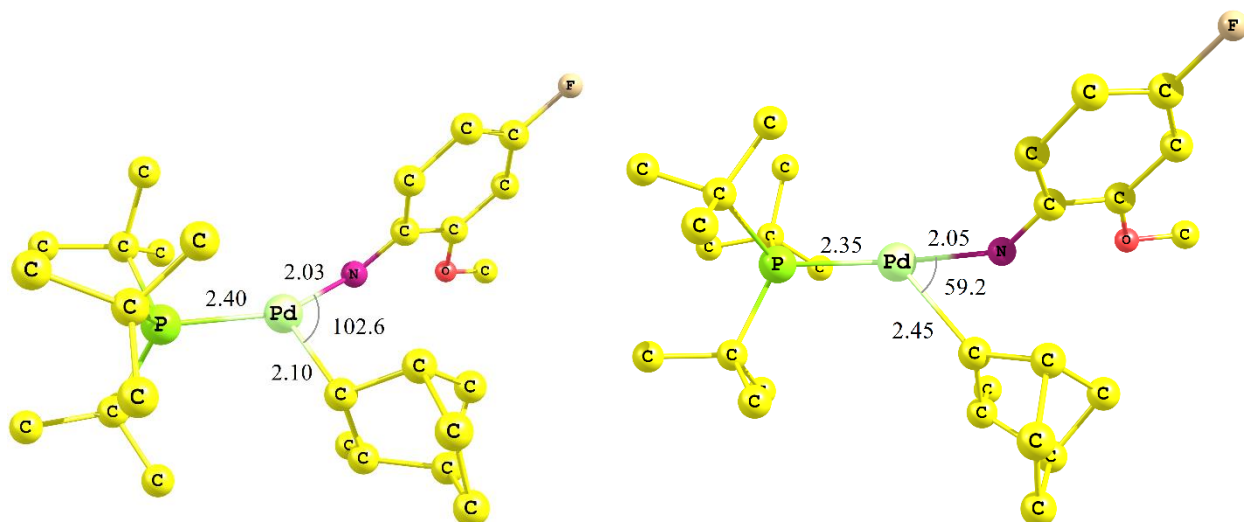


Figure 2.8. Computed ground state structure (left) and transition state structure (right) of $(t\text{-Bu}_3\text{P})\text{Pd}(2\text{-CH}_3\text{norbornyl})(\text{NHAr})$ **2i**. Bond lengths in Å, bond angles in degrees. Hydrogen atoms are omitted for clarity.

The average computed free-energy barrier for reductive elimination of alkylamines **3a-g** from $t\text{-Bu}_3\text{P}$ -ligated complexes containing *para*- and *meta*-substituted anilido ligands (**2a-g**, Table 2.6, entries 1-7) was 22.5 ± 0.6 kcal/mol. The average experimental free-energy barrier for reductive elimination from the same complexes was 23.4 ± 0.6 kcal/mol (Table 2.2, entries 1-7). These averages compare well between computations and experiments. However, the experimentally observed correlation between the electronic properties of the anilido ligand and the rate of reductive elimination from **2a-g** presented in Table 2.2 and Figure 2.1 was not well reproduced by DFT. The variations in computed barriers between these complexes are likely within the accuracy of the calculations. The barriers to reductive elimination from conformational isomers (by rotation of the C–N bond) of *meta*-substituted complexes **2e-h** were also computed, and this rotation was found to have a significant (up to 2.1 kcal/mol) effect on the barrier to reductive elimination. This result suggests that conformational effects may contribute substantially to the rate of reductive elimination. The computed free-energy barriers to reductive elimination from the more sterically encumbered, *ortho*-substituted **2h** and **2i** agreed exceptionally well with those measured experimentally. The agreement between the calculations and the experimental results for reductive elimination reactions from palladium(II) amido complexes containing a $t\text{-Bu}_3\text{P}$ ancillary ligand further support the conclusion of a concerted pathway for reductive elimination to form alkyl–nitrogen bonds.

4.3 Conclusions

We have shown that reductive elimination to form sp^3 C–N bonds by a concerted pathway can occur with low barriers from monomeric three-coordinate phosphine-ligated (*syn*-2-methylnorbornyl)palladium(II) complexes and from four-coordinate analogs containing chelating ligands with one phosphine and one weakly electron-donating ether. An analysis of the factors controlling the rate of reductive elimination revealed that the fastest reductive eliminations occurred from complexes bearing unhindered and electron-rich anilido ligands. This trend holds similarly for the $t\text{-Bu}_3\text{P}$ -ligated alkylpalladium(II) complexes reported herein, for the analogous

NHC-ligated complexes previously reported in communication form,¹⁴ and for arylpalladium(II) complexes which undergo reductive elimination of arylamines.^{1, 34}

Syn-2-methylnorbornylpalladium(II) anilido complexes containing monophosphines smaller than *t*-Bu₃P form bimetallic structures with one phosphine and one bridging anilide as the dominant species in solution. Kinetic experiments conducted with added phosphine suggest that reductive elimination from this bimetallic complex occurs *via* reversible formation of a three-coordinate monometallic species. Our results indicate that this reaction is reversible when phosphine is present in high concentrations. However, the unproductive formation of anilide-bridged bimetallic complexes would likely limit the utility of these complexes as catalysts in the development of new synthetic methods for the production of alkylamines.

Four-coordinate Pd(II) anilido complexes containing neutral bidentate 2-methoxyarylphosphine (P,O) ligands are monometallic and stable at ambient temperature but undergo reductive elimination at mild temperatures. The barriers to reductive elimination from these four-coordinate complexes are 1.6 to 3.2 kcal/mol higher than that for reductive elimination from the analogous three-coordinate, *t*-Bu₃P-ligated complex. Computations indicate that complexes of the rigid P,O ligands undergo reductive elimination directly from the four-coordinate complexes, but the palladium–oxygen bond lengthens significantly from the ground state to the transition state.

We observed that rates of reductive elimination from complexes ligated by 2-methoxyaryl phosphines bearing electron-withdrawing groups were faster than those from complexes ligated by unsubstituted, *o*-anisylphosphines. Furthermore, the rates of reductive elimination from the *t*-Bu₃P-ligated complexes are approximately 40 times faster than that from the analogous, more electron-rich NHC-ligated complexes,³⁵ corresponding to a difference in free energy of activation of approximately 3 kcal/mol. These results are consistent with the trend that reductive elimination occurs faster from more electron-deficient complexes, which is consistent with the trends reported for other classes of concerted reductive eliminations from Pd(II).²²

Flexibility in the backbone of chelating, bidentate ligands has been previously shown to lead to faster rates of reductive elimination. Goldberg and coworkers have reported that the rates of reaction to form sp³ C–C bonds from (P,P)Pt(IV)Me₄ complexes ligated by flexible bisphosphines are faster than the rates of the same reaction from complexes containing containing ligands with equal bite angles but more rigid linkers.³⁶⁻³⁷ The authors proposed that reductive elimination occurs *via* initial dissociation of one phosphine donor to form a penta-coordinate intermediate, and that the energy difference between hexa- and penta-coordinate structures is smaller for complexes ligated by flexible bisphosphine ligands than for complexes ligated by more rigid bisphosphines.³⁸⁻³⁹

We have shown that this trend can be taken even further by combining the effects of flexibility in the linker with weak donation by an ether. The four-coordinate (κ^2 P,O) and three-coordinate (κ P) isomers of an alkylpalladium(II) anilido complex bearing the flexible P,O ligand Ad₂PCH₂CH₂OCH₃ are computed to be similar in energy, and the reductive elimination reaction from this complex is faster and higher yielding than that from the analogous complex containing a rigid linker. Computations suggest that the rigid, aryl backbones in *ortho*-anisyl phosphines do not allow for dissociation of the ether to form the three-coordinate isomer. We suggest that the

effects of weak chelation on the mechanism of reductive elimination could be elements of design for catalysts reacting by reductive elimination to form alkyl–nitrogen bonds.

The trends revealed by the current work suggest strategies to increase the rate of reductive elimination and to prevent unproductive decomposition pathways. Specifically, we have shown that coordination by P,O bidentate ligands can stabilize reactive Pd(II) anilido intermediates without significantly decreasing the yields from reductive elimination. The square planar structures of these complexes are expected to lead to higher barriers to unproductive decomposition pathways, such as β -hydride elimination. Furthermore, chelation should disfavor decomposition pathways involving phosphine dissociation or formation of bimetallic, anilide-bridged complexes. Therefore, the ligand structures like those in Scheme 2.5 and Scheme 2.6 can enable an expansion of the scope of alkyl and amido groups that undergo reductive elimination. The following chapter discusses these advancements.

2.4 Experimental

General Experimental Details

Solvents referred to as “dry” were collected from a solvent purification system containing a 0.33 m column of activated alumina under nitrogen and then stored over molecular sieves under nitrogen. Solvents referred to as “dry and deoxygenated” were collected from a solvent system as described above, degassed by the freeze-pump-thaw method, and stored over molecular sieves under nitrogen. All NMR solvents used in the characterization of phosphines or phosphine-ligated palladium complexes were deoxygenated by either the freeze-pump-thaw method or distillation from sodium benzophenone ketyl. All other solvents, reagents, and starting materials were purchased from commercial suppliers and used as received unless otherwise noted.

Column chromatography was performed with 230–400 mesh silica gel from Fisher Scientific. TLC plates with fluorescent indicators were purchased from Silicycle or EMD and visualized under a 254 nm UV lamp unless otherwise noted. Column chromatography of phosphine ligands was performed inside a nitrogen-filled glovebox to prevent oxidation.

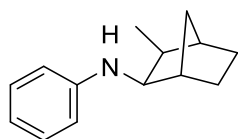
Gas chromatography was performed on an Agilent 7890 GC system equipped with an HP-5 column (25 m x 0.20 mm x 0.33 μ m film) and an FID detector. NMR spectra were obtained on 500 MHz or 600 MHz Bruker Avance series instruments at the University of California, Berkeley NMR facility. Chemical shifts are reported relative to the residual solvent signals (CDCl_3 7.26 ppm for ^1H , 77.16 ppm for ^{13}C ; C_6D_6 7.16 ppm for ^1H , 128.06 ppm for ^{13}C ; Tol- d_8 7.09 for ^1H , 137.34 for ^{13}C). For ^{19}F or ^{31}P NMR spectra, chemical shifts are corrected based on the ^2H lock signal. ESI and APCI high resolution mass spectrometry (HRMS) was performed at the LBNL Catalysis Center. EIMS (positive ionization) was performed on an Agilent 7890A/5975C GC-MS. Elemental analysis was performed by the UC Berkeley Microanalytical Laboratory. X-ray diffraction analysis, including solution, was performed by Dr. Antonio DiPasquale at the UC Berkeley CheXray facility.

Preparation of *N*-Arylnorbornylamines

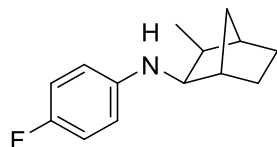
Syn-exo-3-methylbicyclo[2.2.1]heptan-2-amine was prepared according to procedures reported in the literature.⁴⁰⁻⁴¹ The preparations of and characterization data for *syn-exo*-3-methyl-2-(4-methoxyanilino)norbornane (**3b**) and *syn-exo*-3-methyl-2-(4-methylanilino)norbornane (**3c**) were reported in the previous publication.¹⁴

The following compounds were prepared from *syn-exo*-3-methylbicyclo[2.2.1]heptan-2-amine and the corresponding bromoarenes by a modification of the procedure reported in the previous publication:

General procedure. Inside an N₂-filled glovebox, 1-dram vial was charged with *syn-exo*-3-methylbicyclo[2.2.1]heptan-2-amine (0.500 mmol), bromoarene (0.50 mmol, 1.0 equiv), Pd(OAc)₂ (3 mg, 0.01 mmol, 3 mol%), CyPF-^{*t*}Bu Josiphos (7 mg, 0.01 mmol, 3 mol%), and dimethoxyethane (0.50 ml). LiHMDS (170 mg, 1.0 mmol, 2.0 equiv) was added portion-wise with stirring. The vial was sealed with a PTFE-lined cap and PTFE tape and heated with stirring at 80 °C in an aluminum block for the noted time (full conversion of the bromoarene was determined by GC/MS prior to workup). The reaction mixture was quenched with NH₄Cl_(aq) (~1 ml), and the organic products were extracted with ethyl acetate (3x~2 ml). Purification details are noted for each compound.



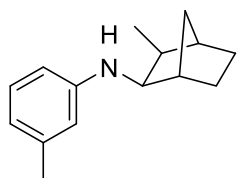
***Syn-exo*-3-methyl-2-(anilino)norbornane (3a).** Prepared according to the general procedure above with bromobenzene (79 mg, 0.50 mmol) and a reaction time of 2 h. The crude product was purified by column chromatography (0 to 10% ethyl acetate gradient in hexanes) to give the title compound as a yellow oil (62.9 mg, 0.312 mmol, 62% yield). ¹H NMR (400 MHz, CDCl₃) δ 7.16 (dd, *J* = 8.5, 7.4 Hz, 2H), 6.65 (tt, *J* = 7.3, 1.1 Hz, 1H), 6.56 (d, *J* = 8.6 Hz, 2H), 3.72 (br, 1H), 3.31 (d, *J* = 7.7 Hz, 1H), 2.18 (br, 1H), 2.02 – 1.94 (m, 1H), 1.91 (s, 1H), 1.62 – 1.48 (m, 3H), 1.35 – 1.21 (m, 2H), 1.09 (dp, *J* = 10.2, 1.6 Hz, 1H), 0.92 (t, *J* = 8.6, 7.4 Hz, 3H). ¹³C NMR (101 MHz, CDCl₃) δ 148.6, 129.3, 116.6, 112.6, 59.5, 43.8, 43.1, 42.4, 33.0, 29.2, 27.1, 14.8. APCI calc'd (M+H⁺) 202.1590, found 202.1590.



***Syn-exo*-3-methyl-2-(4-fluoroanilino)norbornane (3d).** Prepared according to the general procedure above with 4-fluoro-1-bromobenzene (88 mg, 0.50 mmol) and a reaction time of 12 h. The crude product was purified by column chromatography (0 to 5% ethyl acetate gradient in hexanes), precipitation of the ammonium chloride salt from ether with ethereal HCl, recrystallization from DCM and hexanes, basification with NaOH_(aq), and extraction with ether to give the title compound as a yellow oil (38.4 mg, 0.175 mmol, 35% yield; 33% yield corrected for impurity). ¹H NMR (400 MHz, CDCl₃) δ 6.90 – 6.81 (m, 2H), 6.51 – 6.43 (m, 2H), 3.60 (br, 1H), 3.24 (d, *J* = 7.7 Hz, 1H), 2.15 (s, 1H), 2.00 – 1.92 (m, 1H), 1.92 – 1.88 (m, 1H), 1.61 – 1.47 (m, 3H), 1.31 – 1.19 (m, 2H), 1.08 (dp, *J* = 10.1, 1.5 Hz, 1H), 0.90 (d, *J* = 7.4 Hz, 3H). ¹³C NMR (101 MHz, CDCl₃) δ 155.4 (d, *J* = 233.8 Hz), 145.0, 115.7

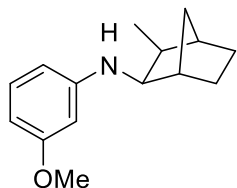
(d, $J = 22.2$ Hz), 113.3 (d, $J = 7.3$ Hz), 60.1, 43.9, 43.0, 42.3, 32.9, 29.2, 27.1, 14.8. ^{19}F NMR (565 MHz, CDCl_3) δ -130.5. APCI calc'd ($\text{M}+\text{H}^+$) 220.1496, found 220.1498.

Note: This reaction formed *syn-exo*-3-methyl-2-(anilino)norbornane (**3a**) as a minor side product. Neither column chromatography nor recrystallization of the ammonium chloride were successful in separating this impurity from the title compound. The small peaks in the ^1H NMR spectrum (~7 mol%) match those of the independently prepared sample of **3a**.



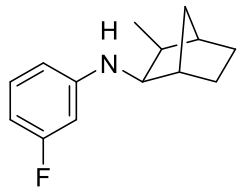
Syn-exo-3-methyl-2-(3-methylanilino)norbornane (3e). Prepared according to the general procedure above with 3-bromotoluene (86 mg, 0.50 mmol) and a reaction time of 12 h. The crude product was purified by column chromatography (0 to 5% ethyl acetate gradient in hexanes), precipitation of the ammonium chloride salt from ether with ethereal HCl, recrystallization from DCM and hexanes, basification with $\text{NaOH}_{(\text{aq})}$, and

extraction with ether to give the title compound as a pale yellow oil (42.0 mg, 0.195 mmol, 39% yield). ^1H NMR (400 MHz, CDCl_3) δ 7.05 (t, $J = 7.8$ Hz, 1H), 6.48 (d, $J = 7.3$ Hz, 1H), 6.42 – 6.34 (m, 2H), 3.67 (br, 1H), 3.30 (d, $J = 7.6$ Hz, 1H), 2.27 (s, 3H), 2.17 (s, 1H), 2.01 – 1.92 (m, 1H), 1.92 – 1.88 (m, 1H), 1.60 – 1.47 (m, 3H), 1.35 – 1.20 (m, 2H), 1.08 (dp, $J = 10.3, 1.6$ Hz, 1H), 0.91 (d, $J = 7.4$ Hz, 3H). ^{13}C NMR (101 MHz, CDCl_3) δ 148.6, 139.0, 129.2, 117.5, 113.5, 109.7, 59.5, 43.8, 43.2, 42.4, 33.0, 29.3, 27.1, 21.8, 14.9. APCI calc'd ($\text{M}+\text{H}^+$) 216.1747, found 216.1749.



Syn-exo-3-methyl-2-(3-methoxyanilino)norbornane (3f). Prepared according to the general procedure above with 3-bromoanisole (xx mg, 0.50 mmol) and a reaction time of 4 h. The crude product was purified by column chromatography (0 to 10% ethyl acetate gradient in hexanes), precipitation of the ammonium chloride salt from ether with ethereal HCl, recrystallization from methanol and ether, basification with $\text{NaOH}_{(\text{aq})}$, and

extraction with ether to give the title compound as a yellow oil (46.6 mg, 0.201 mmol, 40% yield). ^1H NMR (400 MHz, CDCl_3) δ 7.05 (t, $J = 8.1$ Hz, 1H), 6.20 (ddd, $J = 13.6, 8.1, 2.0$ Hz, 2H), 6.11 (t, $J = 2.2$ Hz, 1H), 3.77 (s, 3H), 3.74 (s, 1H), 3.29 (d, $J = 7.7$ Hz, 1H), 2.17 (s, 1H), 2.01 – 1.92 (m, 1H), 1.92 – 1.85 (m, 1H), 1.61 – 1.46 (m, 3H), 1.33 – 1.19 (m, 2H), 1.08 (dp, $J = 10.3, 1.6$ Hz, 1H), 0.91 (d, $J = 7.4$ Hz, 3H). ^{13}C NMR (101 MHz, CDCl_3) δ 161.0, 150.0, 130.0, 106.0, 101.6, 98.6, 59.5, 55.2, 43.8, 43.1, 42.4, 33.0, 29.2, 27.1, 14.8. APCI calc'd ($\text{M}+\text{H}^+$) 232.1696, found 232.1697.

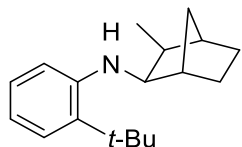


Syn-exo-3-methyl-2-(3-fluoroanilino)norbornane (3g). Prepared according to the general procedure above with 3-fluoro-1-bromobenzene (88 mg, 0.50 mmol) and a reaction time of 2 h. The crude product was purified by column chromatography (0 to 10% ethyl acetate gradient in hexanes) and kugelrohr distillation (~0.5 mTorr, set temp 94 °C) to give the title compound as a clear and colorless oil (26.3 mg, 0.120 mmol, 24% yield). ^1H

NMR (400 MHz, CDCl_3) δ 7.05 (td, $J = 8.1, 6.8$ Hz, 1H), 6.35 – 6.28 (m, 2H), 6.23 (dt, $J = 11.9, 2.3$ Hz, 1H), 3.83 (br, 1H), 3.26 (d, $J = 7.9$ Hz, 1H), 2.16 (br, 1H), 2.01 – 1.93 (m, 1H), 1.91 (br,

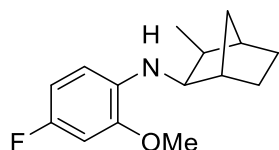
1H), 1.63 – 1.47 (m, 3H), 1.32 – 1.21 (m, 2H), 1.09 (dp, $J = 10.2, 1.5$ Hz, 1H), 0.89 (d, $J = 7.4$ Hz, 3H). ^{13}C NMR (101 MHz, CDCl_3) δ 164.4 (d, $J = 242.1$ Hz), 150.4 (d, $J = 10.8$ Hz), 130.2 (d, $J = 10.4$ Hz), 108.6 (d, $J = 2.0$ Hz), 102.9 (d, $J = 21.7$ Hz), 99.1 (d, $J = 25.4$ Hz), 59.5, 43.8, 43.1, 42.3, 33.0, 29.2, 27.1, 14.8. ^{19}F NMR (565 MHz, CDCl_3) δ -114.1 (ddd, $J = 11.9, 8.6, 6.9$ Hz). APCI calc'd ($\text{M}+\text{H}^+$) 220.1496, found 220.1496.

The following compounds were isolated from the reaction mixtures described in Scheme 2.2:



Syn-exo-3-methyl-2-(2-tert-butylanilino)norbornane (3h). The reaction mixtures from Scheme 2.2, entry 8 were combined and filtered through a plug of Celite, which was rinsed with ethyl acetate (3x1 ml). The volatile materials were removed at reduced pressure, and a sample of the title compound for characterization was isolated by column chromatography

(ethyl acetate gradient in hexanes). ^1H NMR (400 MHz, CDCl_3) δ 7.22 (dd, $J = 7.8, 1.5$ Hz, 1H), 7.10 (ddd, $J = 8.6, 7.3, 1.5$ Hz, 1H), 6.63 (td, $J = 7.6, 1.3$ Hz, 1H), 6.59 (d, $J = 8.1$ Hz, 1H), 3.97 (d, $J = 5.7$ Hz, 1H), 3.41 (t, $J = 6.9$ Hz, 1H), 2.25 (s, 1H), 2.01 (p, $J = 7.3$ Hz, 1H), 1.94 (s, 1H), 1.63 – 1.49 (m, 3H), 1.42 (s, 9H), 1.29 (dddt, $J = 13.8, 9.6, 5.1, 1.9$ Hz, 2H), 1.11 (dp, $J = 10.2, 1.6$ Hz, 1H), 0.96 (d, $J = 7.3$ Hz, 3H). ^{13}C NMR (101 MHz, CDCl_3) δ 146.2, 132.3, 127.2, 126.2, 115.9, 111.5, 59.7, 44.0, 42.8, 42.5, 34.2, 33.3, 30.0, 29.3, 27.0, 15.6. APCI calc'd ($\text{M}+\text{H}^+$) 258.2216, found 258.2212.



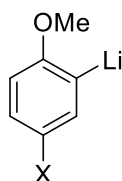
Syn-exo-3-methyl-2-(4-fluoro-2-methoxyanilino)norbornane (3i). The reaction mixtures from Figure 2.2a were combined and filtered through a plug of Celite, the volatile materials were evaporated at reduced pressure, and a sample of the title compound for characterization was isolated by column chromatography (ethyl acetate gradient in hexanes). ^1H NMR

(500 MHz, CDCl_3) δ 6.57 – 6.51 (m, 2H), 6.41 (dd, $J = 8.5, 5.6$ Hz, 1H), 4.15 – 4.06 (br, 1H), 3.83 (s, 3H), 3.24 (t, $J = 6.7$ Hz, 1H), 2.20 – 2.15 (br, 1H), 1.95 (p, $J = 8.0$ Hz, 1H), 1.92 – 1.89 (br, 1H), 1.63 – 1.48 (m, 3H), 1.31 – 1.21 (m, 2H), 1.08 (dp, $J = 10.3, 1.6$ Hz, 1H), 0.91 (d, $J = 7.3$ Hz, 3H). ^{13}C NMR (126 MHz, CDCl_3) δ 154.9 (d, $J = 233.1$ Hz), 146.9 (d, $J = 9.3$ Hz), 135.0 (d, $J = 2.2$ Hz), 109.2 (d, $J = 9.1$ Hz), 106.2 (d, $J = 21.2$ Hz), 98.4 (d, $J = 27.2$ Hz), 59.8, 55.8, 43.9, 43.0, 42.3, 33.0, 29.2, 27.1, 14.6. ^{19}F NMR (470 MHz, CDCl_3) δ -127.9 (ddd, $J = 10.1, 8.5, 5.5$ Hz). APCI calc'd ($\text{M}+\text{H}^+$) 250.1602, 250.1609.

Preparation of Phosphine Ligands

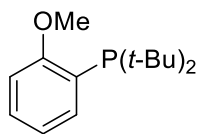
General notes. All reactions and manipulations of these compounds were performed with dry and deoxygenated solvents in dry glassware (oven or flame and vacuum) unless otherwise noted. The *n*-butyllithium solution used in these reactions was determined to be 1.6 M (consistent with label) by titration. 2-Methylpyridine and *N,N,N',N'*-tetramethylethylenediamine (TMEDA) were dried by distilling off of CaH under 1 atm of argon prior to use, and di-*iso*-propylamine was dried by distilling off of NaOH under 1 atm of argon prior to use. The following compounds were prepared with minor modifications from published procedures: di-1-adamantylphosphine

(Ad₂PH),⁴² di-1-adamantylchlorophosphine (Ad₂PCl),⁴³ and 2-bromo-1-methoxy-4-(trifluoromethyl)benzene.⁴⁴



2-Methoxyphenyllithium, 2-methoxy-5-(trifluoromethyl)phenyllithium, and 5-fluoro-2-methoxyphenyllithium. The corresponding aryl bromide was dissolved in pentane (~20% v/v) under nitrogen and cooled to 0 °C. An equimolar amount of *n*-BuLi (1.6 M in hexanes) was added dropwise with stirring. The reaction mixture was allowed to warm to ambient temperature and transferred to an N₂-filled glovebox.

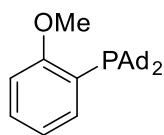
The precipitate was collected by filtration, washed thrice with pentane, and dried under vacuum to give the title compound as a bright white powder. These aryl lithium reagents were used in the subsequent reactions without characterization or further purification.



Di-tert-butyl(ortho-anisyl)phosphine. In an N₂-filled glovebox, di-tert-butylchlorophosphine (0.95 ml, 0.90 g, 5.0 mmol) was dissolved in ether (10 ml) in a 20 ml vial. (2-Methoxyphenyl)lithium (856 mg, 7.50 mmol, 1.50 equiv) was dissolved in ether (5 ml) and added dropwise with stirring to the reaction vial.

The vial was sealed with a Teflon-lined cap, and the reaction mixture was stirred at ambient temperature for 5 days. The reaction mixture was filtered through a pad of silica (~20 ml), which was rinsed with ether (~50 ml). The volatile materials were evaporated *in vacuo*. The crude product was purified by column chromatography (10% ether/pentane) and then filtered through a plug of glass wool with pentane to give the title compound as a clear and colorless oil (1.10 g, 4.36 mmol, 87% yield). The ¹H and ³¹P NMR spectra were consistent with those reported in the literature.⁴⁵

Note: This compound exists as a mixture (52:48 in C₆D₆; 76:24 in CDCl₃) of two rotamers (P–C(sp²) rotation).

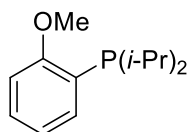


Di(1-adamantyl)(ortho-anisyl)phosphine. In an N₂-filled glovebox, di(1-adamantyl)chlorophosphine (674 mg, 2.00 mmol) was suspended in ether (5 ml) in a 20 ml vial. (2-Methoxyphenyl)lithium (251 mg, 2.20 mmol, 1.10 equiv) was dissolved in ether (2 ml + 1 ml rinse) and added dropwise with stirring to the reaction vial.

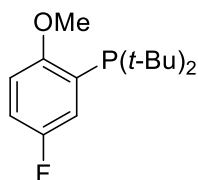
The vial was sealed with a Teflon-lined cap, and the reaction mixture was stirred at ambient temperature for 40 h. The reaction mixture was diluted with pentane (8 ml) and filtered through a pad of silica (~10 ml), which was rinsed with 1:1 pentane/ether (~25 ml). The volatile materials were evaporated *in vacuo* to give the title compound as a white powder (749 mg, 1.83 mmol, 92% yield). ¹H NMR (600 MHz, CDCl₃) δ 7.69 (dt, *J* = 7.5, 1.8 Hz, 1H major), 7.59 (ddd, *J* = 14.3, 7.4, 1.8 Hz, 1H minor), 7.38 – 7.31 (m, 1H major+minor), 6.97 – 6.89 (m, 2H major + 1H minor), 6.87 (d, *J* = 7.9 Hz, 1H minor), 3.84 (s, 3H minor), 3.82 (s, 3H major), 2.02 – 1.85 (m, 18H major+minor), 1.67 (s, 12H major+minor). ¹³C NMR (151 MHz, CDCl₃) Major: δ 164.4 (d, *J* = 18.8 Hz), 137.2 (d, *J* = 2.9 Hz), 130.2, 122.5 (d, *J* = 24.4 Hz), 119.4, 111.3 (d, *J* = 3.1 Hz), 56.0 (d, *J* = 1.1 Hz), 41.8 (d, *J* = 12.7 Hz), 37.2, 36.9 (d, *J* = 23.0 Hz), 29.0 (d, *J* = 8.6

Hz). Minor: δ 161.2 (d, $J = 5.8$ Hz), 142.9 (d, $J = 53.5$ Hz), 131.1, 122.6 (d, $J = 32.0$ Hz), 120.0 (d, $J = 17.9$ Hz), 110.1, 54.1, 41.8 (d, $J = 12.2$ Hz), 37.2, 36.9 (d, $J = 21.6$ Hz), 29.2 (d, $J = 8.9$ Hz). ^{31}P NMR (243 MHz, CDCl_3) δ 57.4 (minor), 10.9 (major). ESI^+ calc'd ($\text{M}+\text{H}^+$) 409.2655, found 409.2656.

Note: This compound exists as a mixture (51:49 in C_6D_6 , 72:28 in CDCl_3) of two rotamers ($\text{P}-\text{C}(\text{sp}^2)$ rotation). NMR signals were assigned to either the major or minor isomer by their integrations when possible.



Di-*iso*-propyl(*ortho*-anisyl)phosphine. In an N_2 -filled glovebox, di(*iso*-propyl)chlorophosphine (304 mg, 1.99 mmol) was dissolved in ether (3 ml) in a 20 ml vial. (2-Methoxyphenyl)lithium (249 mg, 2.18 mmol, 1.10 equiv) was dissolved in ether (1 ml + 1 ml rinse) and added dropwise with stirring to the reaction vial. The vial was sealed with a Teflon-lined cap, and the reaction mixture was stirred at ambient temperature for 2 d. The reaction mixture was diluted with THF (~5 ml) and filtered through a plug of silica (~1 ml), which was rinsed with THF (3x2 ml). The volatile materials were evaporated removed *in vacuo*, and the crude product was purified by column chromatography (5% ether/pentane) to give the title compound as a clear and colorless oil (408 mg, 1.82 mmol, 91% yield). ^1H NMR (600 MHz, CDCl_3) δ 7.36 (ddd, $J = 7.2, 5.4, 1.7$ Hz, 1H), 7.32 (td, $J = 7.8, 1.7$ Hz, 1H), 6.95 (t, $J = 7.4$ Hz, 1H), 6.87 (dd, $J = 8.3, 3.4$ Hz, 1H), 3.82 (s, 3H), 2.19 (heptd, $J = 7.0, 1.9$ Hz, 2H), 1.11 (dd, $J = 15.0, 7.0$ Hz, 6H), 0.91 (dd, $J = 11.8, 6.9$ Hz, 6H). ^{13}C NMR (151 MHz, CDCl_3) δ 162.8 (d, $J = 10.7$ Hz), 134.9 (d, $J = 9.4$ Hz), 130.2, 123.4 (d, $J = 20.7$ Hz), 120.3 (d, $J = 3.9$ Hz), 110.4 (d, $J = 1.7$ Hz), 55.4, 22.9 (d, $J = 11.8$ Hz), 20.4 (d, $J = 19.2$ Hz), 19.6 (d, $J = 9.8$ Hz). ^{31}P NMR (243 MHz, CDCl_3) δ -0.3. ESI^+ calc'd ($\text{M}+\text{H}^+$) 225.1403, found 225.1399.



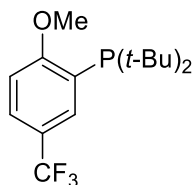
Di-*tert*-butyl(5-fluoro-2-methoxyphenyl)phosphine. In an N_2 -filled glovebox, di-*tert*-butylchlorophosphine (360 mg, 2.0 mmol) was dissolved in ether (2 ml) in a 1 dram vial. (5-Fluoro-2-methoxyphenyl)lithium (290 mg, 2.20 mmol, 1.10 equiv) was dissolved in ether (2 ml) and added dropwise with stirring to the reaction vial. The vial was sealed with a Teflon-lined cap, and the reaction mixture was stirred at ambient temperature for 24 h. The reaction mixture was filtered through a plug of silica, which was rinsed with ether (~20 ml). The volatile materials were evaporated *in vacuo*. The crude product was purified by column chromatography (10% ether/pentane) to give the title compound as a pale yellow oil (430 mg, 1.59 mmol, 80% yield). ^1H NMR (600 MHz, CDCl_3) δ 7.41 – 7.33 (m, 1H major+minor), 7.01 (ddd, $J = 9.0, 7.7, 3.1$ Hz, 1H major+minor), 6.84 (dt, $J = 9.2, 4.7$ Hz, 1H major), 6.77 (dd, $J = 8.9, 4.2$ Hz, 1H minor), 3.81 (s, 3H major), 3.77 (s, 3H minor), 1.21 (d, $J = 11.9$ Hz, 18H major), 1.19 (d, $J = 11.8$ Hz, 18H minor). ^{13}C NMR (151 MHz, CDCl_3) Major: δ 156.0 (dd, $J = 18.4, 1.8$ Hz), 156.1 (dd, $J = 240.3, 1.6$ Hz), 127.1 (dd, $J = 29.3, 4.2$ Hz), 121.9 (dd, $J = 21.3, 3.2$ Hz), 116.5 (d, $J = 22.8$ Hz), 112.0 (dd, $J = 7.7, 2.8$ Hz), 56.5 (d, $J = 1.1$ Hz), 32.4 (d, $J = 23.0$ Hz), 30.5 (d, $J = 15.3$ Hz). Minor: δ 116.8 (d, $J = 23.0$ Hz), 110.8 (d, $J = 8.2$ Hz), 54.6, 32.8 (d, $J = 21.9$ Hz), 30.7. ^{19}F

NMR (565 MHz, CDCl₃) δ -125.3 (major), -126.3 (minor). **³¹P NMR** ³¹P NMR (243 MHz, CDCl₃) δ 57.3 (minor), 10.6 (major). **ESI⁺** calc'd (M+H⁺) 271.1622, found 271.1619.

Note: The free phosphine appears to decompose partially during chromatography, generating an impurity with lower R_f (fluorescent). No decomposition was observed during the purification of any other 2-methoxyarylphosphines. The material prepared as described above contained this impurity in approximately 3 mol%. The downfield aryl ¹H NMR signals of the impurity suggest a P(V) compound. This impurity was reduced to approximately 1 mol% by converting the phosphine to the hydrochloride salt (precipitates from pentane with ethereal HCl) and then back to the free phosphine (KOH in degassed, slightly wet MeOH). The solid hydrochloride salt is air stable but highly hygroscopic. The free phosphine decomposes rapidly under air.

Note: This compound exists as a mixture (61:39 in C₆D₆, 80:20 in CDCl₃) of two rotamers (P–C(sp²) rotation). NMR signals were assigned to either the major or minor isomer by their integrations when possible.

Note: 4 aryl ¹³C resonances of the minor rotamer were not located.



Di-tert-butyl(2-methoxy-5-(trifluoromethyl)phenyl)phosphine. In an N₂-filled glovebox, di-tert-butylchlorophosphine (361 mg, 2.00 mmol) was dissolved in ether (2 ml) in a 1 dram vial. 2-Methoxy-5-(trifluoromethyl)phenyllithium (400 mg, 2.20 mmol, 1.10 equiv) was dissolved in ether (1 ml + 1 ml rinse) and added dropwise with stirring to the reaction vial. The vial was sealed with a Teflon-lined cap, and the reaction mixture was

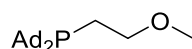
stirred at ambient temperature for 24 h. The reaction mixture was filtered through a plug of silica, which was rinsed with ether (6 ml). The volatile materials were evaporated *in vacuo* (30 mTorr). The crude product was purified by column chromatography (5 to 15% ether/pentane gradient) to give the title compound as a clear and colorless oil (500 mg, 1.56 mmol, 78% yield).

¹H NMR (600 MHz, CDCl₃) δ 7.95 – 7.88 (m, 1H major+minor), 7.64 – 7.55 (m, 1H major+minor), 6.96 (dd, *J* = 8.5, 4.5 Hz, 1H major), 6.92 (d, *J* = 8.5 Hz, 1H minor), 3.88 (s, 3H major) 3.85 (s, 3H minor), 1.20 (d, *J* = 12.0 Hz, 18H major) 1.19 (d, *J* = 12.2 Hz, 18H minor).

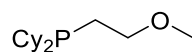
¹³C NMR (151 MHz CDCl₃) Major: δ 166.0 (d, *J* = 18.4 Hz), 132.9 (p, *J* = 3.2 Hz), 127.9 – 127.3 (m), 126.1 (d, *J* = 29.1 Hz), 124.7 (q, *J* = 271.5 Hz), 121.9 (q, *J* = 32.2 Hz), 110.6 (d, *J* = 2.5 Hz), 56.0, 32.5 (d, *J* = 22.8 Hz), 30.5 (d, *J* = 15.2 Hz). Minor: δ 163.7 (d, *J* = 5.4 Hz), 139.3, 139.0, 128.6, 125.7 (d, *J* = 37.3 Hz), 124.5 (q, *J* = 271.0 Hz), 54.6, 32.8 (d, *J* = 22.1 Hz), 30.6 (d, *J* = 14.9 Hz). **¹⁹F NMR** (565 MHz, CDCl₃) δ -62.5 (minor), -62.6 (major). **³¹P NMR** (243 MHz, CDCl₃) δ 56.5 (minor), 9.6 (major). **ESI⁺** calc'd (M+H⁺) 321.1590, 321.1577.

Note: This compound exists as a mixture (60:40 in C₆D₆, 75:25 in CDCl₃) of two rotamers (P–C(sp²) rotation). NMR signals were assigned to either the major or minor isomer by their integrations when possible. The two sets of ¹H NMR resonances were coalesced at 90 °C in C₆D₆.

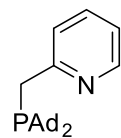
Note: The ¹³C-CF₃ resonance of the minor rotamer was not located.



Di(1-adamantyl)(2-methoxyethyl)phosphine. A 25 ml Schlenk flask under argon was charged with Ad_2PH (605 mg, 2.00 mmol), TMEDA (0.36 ml, 0.28 g, 2.4 mmol, 1.2 equiv), and ether (10 ml). The reaction mixture was cooled to 0 °C, and *n*-BuLi (1.5 ml, 1.6 M in hexanes, 2.4 mmol, 1.2 equiv) was added dropwise with stirring. The ice bath was then removed, and the reaction mixture was stirred for 30 minutes at ambient temperature. During this time, a white solid precipitated. The reaction mixture was then cooled to 0 °C, and 2-chloroethyl methyl ether (0.28 ml, 0.29 g, 3.1 mmol, 1.5 equiv) was added dropwise with stirring. The ice bath was then removed, and the reaction mixture was stirred for 5 h at ambient temperature. The reaction was quenched at 0 °C with H_2O (10 ml, N_2 -sparged). The organic layer was removed by syringe and transferred to a flask containing Na_2SO_4 under argon. The aqueous layer was extracted again with ether (10 ml). The combined organic layers were moved to an N_2 -filled glovebox, and then filtered through a plug of silica, which was rinsed with ether (3x4 ml). The volatile materials were evaporated *in vacuo*. The crude product was purified by column chromatography (10 to 20% ether gradient in pentane) to give the title compound as a white solid (509 mg, 1.41 mmol, 71% yield). ^1H NMR (500 MHz, CDCl_3) δ 3.48 – 3.39 (m, 2H), 3.36 (s, 3H), 1.98 – 1.90 (m, 6H), 1.89 – 1.78 (m, 12H), 1.73 – 1.67 (m, 14H). ^{13}C NMR (126 MHz, CDCl_3) δ 74.6 (d, J = 42.8 Hz), 58.7, 40.9 (d, J = 10.7 Hz), 37.1, 35.8 (d, J = 19.4 Hz), 28.7 (d, J = 8.1 Hz), 17.6 (d, J = 18.4 Hz). ^{31}P NMR (202 MHz, CDCl_3) δ 16.0. ESI⁺ calc'd ($\text{M}+\text{H}^+$) 361.2655, found 361.2654.

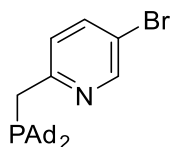


Dicyclohexyl(2-methoxyethyl)phosphine. A 25 ml Schlenk flask under argon was charged with dicyclohexylphosphine (399 mg, 2.01 mmol), TMEDA (0.36 ml, 0.28 g, 2.4 mmol, 1.2 equiv), and ether (10 ml). The reaction mixture was cooled to 0 °C, and *n*-BuLi (1.5 ml, 1.6 M in hexanes, 2.4 mmol, 1.2 equiv) was added dropwise with stirring. The ice bath was then removed, and the reaction mixture was stirred for 30 minutes at ambient temperature. During this time, a white solid precipitated. The reaction mixture was then cooled to 0 °C, and 2-chloroethyl methyl ether (0.28 ml, 0.29 g, 3.1 mmol, 1.5 equiv) was added dropwise with stirring. The ice bath was then removed, and the reaction mixture was stirred for 3 h at ambient temperature. The reaction was quenched at 0 °C with H_2O (10 ml, N_2 -sparged). The organic layer was removed by syringe and transferred to a flask containing Na_2SO_4 under argon. The aqueous layer was extracted again with ether (10 ml). The combined organic layers were moved to an N_2 -filled glovebox, and then filtered through a plug of silica, which was rinsed with ether (3x4 ml). The volatile materials were removed evaporated *in vacuo*. The crude product was purified by column chromatography (10 to 20% ether gradient in pentane) to give the title compound as a clear and colorless oil (351 mg, 1.37 mmol, 68% yield). The ^1H and ^{31}P NMR spectra were consistent with those reported in the literature.⁴⁶



2-((Di(1-adamantyl)phosphino)methyl)pyridine. A 25 ml Schlenk flask under argon was charged with 2-methylpyridine (140 μl , 132 mg, 1.42 mmol, 1.42 equiv), *N,N,N',N'*-tetramethylethylenediamine (210 μl , 163 mg, 1.40 mmol, 1.40 equiv), and THF (5 ml). The mixture was cooled to -78 °C, and *n*-BuLi (0.88 ml, 1.6 M in hexanes, 1.4 mmol, 1.4 equiv) was added dropwise with stirring. The resulting bright orange

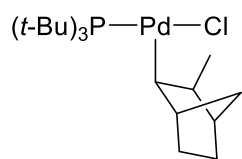
solution was stirred for an additional 30 min at $-78\text{ }^{\circ}\text{C}$. Ad_2PCl (337 mg, 1.00 mmol) was dissolved in THF (5 ml) and added dropwise to the reaction mixture with stirring. The reaction mixture was stirred for an additional 2 h at $-78\text{ }^{\circ}\text{C}$. The cooling bath was then removed, and the reaction mixture was stirred for 12 h at ambient temperature. The volatile materials were evaporated *in vacuo*. Ether (10 ml) and H_2O (15 ml, N_2 -sparged) were added to the reaction flask and mixed. The organic layer was removed with a syringe and passed through a PTFE filter into a clean flask under argon. The aqueous layer was extracted further with ether (2x10 ml). The volatile materials were evaporated from the combined organic layers under a stream of argon. Methanol (~10 ml, degassed, slightly wet) was added to the flask. The mixture was transferred to an N_2 -filled glovebox and cooled to $-30\text{ }^{\circ}\text{C}$. The solid was collected by filtration and rinse with chilled methanol (2x4 ml) to give the title product as a pale yellow powder (274 mg, 0.696 mmol, 70% yield). $^1\text{H NMR}$ (600 MHz, CDCl_3) δ 8.47 – 8.43 (m, 1H), 7.54 (td, $J = 7.7, 1.9$ Hz, 1H), 7.44 (dd, $J = 8.0, 1.2$ Hz, 1H), 7.05 – 7.00 (m, 1H), 3.04 (d, $J = 3.6$ Hz, 2H), 1.96 – 1.84 (m, 18H), 1.77 – 1.66 (m, 12H). $^{13}\text{C NMR}$ (151 MHz, CDCl_3) δ 162.9 (d, $J = 15.1$ Hz), 148.9, 136.0, 124.2 (d, $J = 10.2$ Hz), 120.5 (d, $J = 1.3$ Hz), 41.0 (d, $J = 10.5$ Hz), 37.1, 36.7 (d, $J = 22.1$ Hz), 28.8 (d, $J = 7.9$ Hz), 27.7 (d, $J = 22.8$ Hz). $^{31}\text{P NMR}$ (243 MHz, CDCl_3) δ 32.9. ESI^+ calc'd ($\text{M}+\text{H}^+$) 394.2658, found 394.2647.



5-Bromo-2-((di(1-adamantyl)phosphino)methyl)pyridine. A 25 ml Schlenk flask under argon was charged with 5-bromo-2-picoline (481 mg, 2.80 mmol, 1.40 equiv), N,N,N',N' -tetramethylethylenediamine (0.42 ml, 0.33 g, 2.8 mmol, 1.4 equiv), and ether (4 ml). The mixture was cooled to $-78\text{ }^{\circ}\text{C}$, and LDA (2.8 mmol in 5 ml of ether) was added dropwise *via* syringe with stirring, and the syringe was rinsed with ether (4 ml). The resulting dark red solution was stirred for an additional 30 min at $-78\text{ }^{\circ}\text{C}$. Di(1-adamantyl)chlorophosphine (673 mg, 2.00 mmol) was dissolved in THF (6 ml) and added dropwise to the reaction mixture with stirring. The reaction mixture was stirred for an additional 10 min at $-78\text{ }^{\circ}\text{C}$. The cooling bath was then removed, and the reaction mixture was stirred for 3 h at ambient temperature. The reaction mixture was cooled to $0\text{ }^{\circ}\text{C}$ and quenched with H_2O (6 ml, N_2 -sparged). The organic layer was removed with a syringe and transferred to a clean flask under argon. The aqueous layer was extracted further with ether (10 ml). The volatile materials were evaporated removed *in vacuo*. Methanol (~15 ml, degassed, slightly wet) was added to the flask. The mixture was transferred to an N_2 -filled glovebox and cooled to $-30\text{ }^{\circ}\text{C}$. The solid was collected by filtration and rinse with chilled methanol (2x4 ml). The crude product was recrystallized from hot ether (2 crops) to give the title compound as a pale yellow powder (546 mg, 1.16 mmol, 58% yield). $^1\text{H NMR}$ (600 MHz, CDCl_3) δ 8.50 (d, $J = 2.4$ Hz, 1H), 7.66 (dd, $J = 8.4, 2.5$ Hz, 1H), 7.35 (d, $J = 8.4$ Hz, 1H), 2.98 (d, $J = 3.5$ Hz, 2H), 1.95 – 1.91 (m, 6H), 1.89 – 1.86 (m, 12H), 1.72 – 1.69 (m, 12H). $^{13}\text{C NMR}$ (151 MHz, CDCl_3) δ 161.8 (d, $J = 15.7$ Hz), 149.7, 138.7, 125.6 (d, $J = 10.2$ Hz), 117.3 (d, $J = 2.0$ Hz), 41.0 (d, $J = 10.5$ Hz), 37.1, 36.8 (d, $J = 22.1$ Hz), 28.8 (d, $J = 7.9$ Hz), 27.2 (d, $J = 23.3$ Hz). $^{31}\text{P NMR}$ (243 MHz, CDCl_3) δ 33.8. ESI^+ calc'd ($\text{M}+\text{H}^+$, ^{79}Br) 472.1763, found 472.1776.

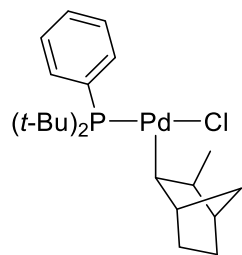
Preparation of Alkylpalladium(II) Complexes

General notes. All reactions and recrystallizations of these compounds were performed inside a nitrogen- or an argon-filled glovebox with dry and deoxygenated solvents. The alkylpalladium(II) anilido complexes are thermally unstable, highly moisture sensitive, and oxygen sensitive in solution. The isolated yields of alkylpalladium(II) amido complexes reported in this section do not reflect the chemical yields of the reactions and are typically low due to the challenges associated with recrystallization. Recrystallization of Pd(II) chloride and Pd(II) amido complexes was usually necessary to remove L_2Pd^0 . (COD)Pd(*syn*-2-CH₃norbornyl)Cl was prepared according to the previously published procedure.¹⁴



(*t*-Bu₃P)Pd(*syn*-2-CH₃norbornyl)Cl (1). (COD)Pd(*syn*-2-CH₃norbornyl)Cl (405 mg, 1.13 mmol) was dissolved in THF (2 ml) in a 20 ml scintillation vial. Tri-*tert*-butylphosphine (251 mg, 1.24 mmol, 1.10 equiv) was dissolved in THF (2 ml + 2 ml rinse) and added to the reaction vessel dropwise with stirring. The reaction mixture was stirred for approximately

10 min at ambient temperature, and then the solvent was evaporated under vacuum. The crude solid was dissolved in approximately 14 ml of warm ether and filtered through a plug of Celite. The product crystallized after layering with pentane and cooling to -40 °C. The solvent was decanted, and the crystals were rinsed with chilled pentane (3x2 ml) to give the title compound as red-orange blocks (416 mg, 0.918 mmol, 81% yield). ¹H NMR (600 MHz, CDCl₃) δ 4.25 (ddd, *J* = 17.2, 7.2, 1.9 Hz, 1H), 2.60 – 2.49 (m, 2H), 1.85 (d, *J* = 3.4 Hz, 1H), 1.65 (d, *J* = 7.3 Hz, 3H), 1.58 – 1.45 (m, 28H), 1.40 – 1.33 (m, 1H), 1.18 – 1.11 (m, 1H), 1.08 – 1.00 (m, 2H), 1.00 – 0.93 (m, 1H). ¹³C NMR (151 MHz, CDCl₃) δ 57.9 (d, *J* = 5.7 Hz), 49.2 (d, *J* = 3.0 Hz), 46.7, 45.9 (d, *J* = 3.0 Hz), 39.5 (d, *J* = 9.2 Hz), 35.0, 32.4, 29.3 (d, *J* = 6.3 Hz), 29.1, 24.2 (d, *J* = 7.5 Hz). ³¹P NMR (243 MHz, CDCl₃) δ 72.1. **Analysis** calc'd C 52.98, H 8.89; found C 53.26, H 8.75.



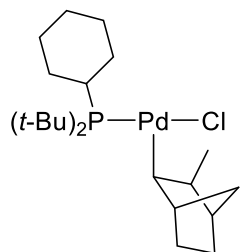
(*t*-Bu₂PhP)Pd(*syn*-2-CH₃norbornyl)Cl (4). (COD)Pd(*syn*-2-CH₃norbornyl)Cl (180 mg, 0.501 mmol) was dissolved in THF (2 ml) in a 20 ml scintillation vial. Di-(*tert*-butyl)phenylphosphine (114 mg, 0.513 mmol, 1.02 equiv) was dissolved in THF (1 ml + 1 ml rinse) and added to the reaction vessel dropwise with stirring. The reaction mixture was stirred for approximately 10 min at ambient temperature, and then the solvent was evaporated *in vacuo*. The solid was dissolved in ether (~5 ml) and filtered

through a plug of Celite, and then the solvent was evaporated *in vacuo*. The crude product was dissolved in a minimal amount of ether (~0.5 ml) and layered with pentane (5 ml). The mixture was allowed to sit at ambient temperature until solid began to form and then left overnight at -30 °C. The solid was collected by filtration and rinsed with chilled pentane (4x1 ml) to give the title compound as a pale yellow powder. (155 mg, 0.327 mmol, 65% yield). ¹H NMR (600 MHz, CDCl₃) δ 7.89 (t, *J* = 8.2 Hz, 2H), 7.54 – 7.48 (m, 1H), 7.50 – 7.44 (m, 2H), 3.14 (d, *J* = 12.7 Hz, 1H), 2.67 (s, 1H), 2.49 (dt, *J* = 10.3, 2.1 Hz, 1H), 1.85 (br d, *J* = 2.9 Hz, 1H), 1.74 (d, *J* = 7.5 Hz, 3H), 1.47 (d, *J* = 11.2 Hz, 9H), 1.44 (d, *J* = 11.3 Hz, 10H), 1.36 – 1.28 (m, 1H), 1.15 (ddt, *J* =

11.7, 7.5, 3.9 Hz, 1H), 1.10 (d, $J = 10.3$ Hz, 1H), 0.95 – 0.87 (m, 1H), 0.78 (t, $J = 10.3$ Hz, 1H). ^{13}C NMR (151 MHz, CDCl_3) δ 136.0 (d, $J = 10.3$ Hz), 131.1 (d, $J = 2.3$ Hz), 128.3 (d, $J = 9.6$ Hz), 48.7 (d, $J = 3.3$ Hz), 46.8, 45.2 (d, $J = 2.6$ Hz), 37.2 (d, $J = 17.3$ Hz), 36.7 (d, $J = 16.7$ Hz), 35.3, 31.1 (d, $J = 4.7$ Hz), 30.9 (d, $J = 5.1$ Hz), 29.4 (d, $J = 7.6$ Hz), 28.7, 22.1 (d, $J = 9.3$ Hz). ^{31}P NMR (243 MHz, CDCl_3) δ 76.7. **Analysis** calc'd C 55.82, H 7.67; found C 55.68, H 7.69.

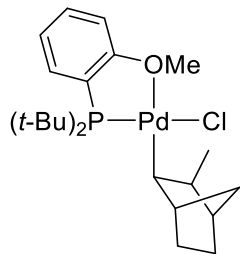
Note: Two carbon resonances (C1 of the alkyl ligand and the *ipso* carbon of the phosphine ligand) were not located in the ^{13}C NMR spectrum. These resonances are likely broadened by the same dynamic process that broadens some resonances in the ^1H NMR spectrum. The C1 carbon of the alkyl ligand was located at 64.2 ppm by HSQC and HMBC.

Note: The sample of complex **4a** prepared as described above contains (*t*-Bu₂PhP)₂Pd⁰ as a ~2 mol% impurity by ^1H or ^{31}P NMR spectroscopy.



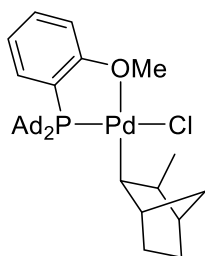
(*t*-Bu₂CyP)Pd(*syn*-2-CH₃norbornyl)Cl (4b**).** (COD)Pd(*syn*-2-CH₃norbornyl)Cl (53.9 mg, 0.150 mmol) was dissolved in THF (1 ml) in a 20 ml scintillation vial. Di-(*tert*-butyl)cyclohexylphosphine (68.5 mg, 0.300 mmol, 2.00 equiv) was dissolved in THF (~0.5 ml + ~0.5 ml rinse) and added to the reaction vessel dropwise with stirring. The reaction mixture was stirred for approximately 15 min at ambient temperature, and then the solvent was evaporated *in vacuo*. Pentane (2 ml) was added to the residue

with stirring to precipitate a yellow solid. The mixture was cooled to -30 °C, and the solvent was decanted. The crude product was recrystallized by dissolving in warm ether, filtering through a plug of Celite, and layering with pentane at -30 °C. The solvent was decanted and the solid was rinsed with cold pentane (2x1ml) to give the title compound as a yellow powder (44.2 mg, 0.0922 mmol, 61% yield). ^1H NMR (600 MHz, CDCl_3) δ 3.37 (ddd, $J = 16.5, 7.0, 1.5$ Hz, 1H), 2.59 (s, 1H), 2.48 (dt, $J = 10.4, 2.0$ Hz, 1H), 2.33 – 2.19 (m, 2H), 2.11 – 2.01 (m, 1H), 1.93 – 1.82 (m, 3H), 1.80 – 1.67 (m, 3H), 1.63 (d, $J = 7.4$ Hz, 3H), 1.51 – 1.40 (m, 19H), 1.39 – 1.32 (m, 1H), 1.32 – 1.24 (m, 3H), 1.22 – 1.16 (m, 1H), 1.09 – 1.02 (m, 2H), 0.98 (ddt, $J = 12.0, 8.9, 2.9$ Hz, 1H). ^{13}C NMR (151 MHz, CDCl_3) δ 62.2 (d, $J = 6.5$ Hz), 49.2 (d, $J = 3.0$ Hz), 46.6, 45.7 (d, $J = 2.6$ Hz), 38.0 (d, $J = 14.4$ Hz), 37.6 (d, $J = 14.0$ Hz), 37.0 (d, $J = 12.6$ Hz), 35.0, 32.3, 31.8 (d, $J = 3.7$ Hz, 2C overlap), 31.5 (d, $J = 3.9$ Hz), 29.6 (d, $J = 6.9$ Hz), 29.0, 28.7 (d, $J = 10.5$ Hz), 28.5 (d, $J = 9.5$ Hz), 26.5 (d, $J = 1.2$ Hz), 23.0 (d, $J = 8.1$ Hz). ^{31}P NMR (243 MHz, CDCl_3) δ 69.5. **Analysis** calc'd C 55.12, H 8.83; found C 55.35, H 8.96.



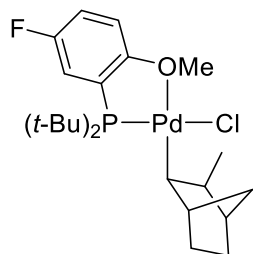
[*t*-Bu₂(*o*-anisyl)P- κ^2 P,O]Pd(*syn*-2-CH₃norbornyl)Cl (7a**).** (COD)Pd(*syn*-2-CH₃norbornyl)Cl (359 mg, 0.999 mmol) was dissolved 3 ml of THF in a 20 ml scintillation vial. Di-*tert*-butyl(*ortho*-anisyl)phosphine (280 mg, 1.11 mmol, 1.11 equiv) was dissolved in THF (2 ml + 2 ml rinse) and added to the reaction vessel dropwise with stirring. The reaction mixture was stirred for approximately 10 min at ambient temperature. After this time, the solvent was evaporated *in vacuo*. The crude solid was dissolved in a warm mixture of DCM and ether, filtered through a plug of Celite, crystallized by

layering with pentane at 0 °C, then -40 °C, and rinsed with chilled pentane (2x4 ml) to give the title compound as bright yellow flakes (381 mg, 0.757 mmol, 76% yield). **¹H NMR** (600 MHz, CDCl₃) δ 7.79 (t, *J* = 7.1 Hz, 1H), 7.45 (t, *J* = 7.8 Hz, 1H), 7.11 – 6.99 (m, 2H), 4.21 (s, 3H), 4.02 (dd, *J* = 16.8, 7.0 Hz, 1H), 2.81 (d, *J* = 9.7 Hz, 1H), 2.46 (s, 1H), 1.84 (d, *J* = 4.0 Hz, 1H), 1.59 – 1.49 (m, 5H), 1.46 (d, *J* = 14.1 Hz, 9H), 1.42 (d, *J* = 14.3 Hz, 9H), 1.21 – 1.14 (m, 1H), 1.09 – 0.95 (m, 3H). **¹³C NMR** (151 MHz, CDCl₃) δ 163.1 (d, *J* = 9.5 Hz), 134.9, 132.9 (d, *J* = 1.4 Hz), 121.2 (d, *J* = 4.8 Hz), 117.9 (d, *J* = 29.5 Hz), 113.6 (d, *J* = 4.9 Hz), 58.9, 48.6 (d, *J* = 2.4 Hz), 45.8, 45.6 (d, *J* = 2.5 Hz), 42.1 (d, *J* = 3.5 Hz), 37.9 (d, *J* = 14.2 Hz), 37.3 (d, *J* = 12.8 Hz), 36.2, 31.0 (d, *J* = 5.5 Hz), 30.9 (d, *J* = 4.6 Hz), 30.7 (d, *J* = 5.9 Hz), 29.7, 24.3 (d, *J* = 5.8 Hz). **³¹P NMR** (243 MHz, CDCl₃) δ 49.6. **Analysis** calc'd C 54.88, H 7.61; found C 55.09, H 7.46.



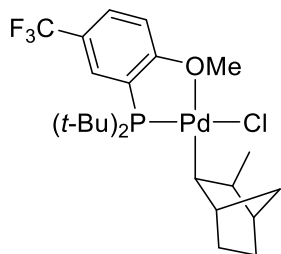
[(1-Ad)₂(*o*-anisyl)P-κ²P,O]Pd(*syn*-2-CH₃norbornyl)Cl (7b**). (COD)Pd(*syn*-2-CH₃norbornyl)Cl (120 mg, 0.334 mmol) was dissolved in DCM (2 ml) in a 20 ml scintillation vial. Di(1-adamantyl)(*ortho*-anisyl)phosphine (137 mg, 0.335 mmol, 1.01 equiv) was dissolved in DCM (1 ml + 1 ml rinse) and added to the reaction vessel dropwise with stirring. The reaction mixture was stirred for approximately 10 min at ambient temperature, then diluted with ether (4 ml), and then filtered through a plug of Celite. The volatile materials were evaporated *in vacuo*. The crude product was recrystallized by dissolving in DCM (~4 ml), mixing in pentane (~10 ml), and letting sit at ambient temperature until crystals began to form. The mixture was then moved to a freezer at -30 °C. The solid was collected by filtration and rinsed with pentane (2x3 ml) to give the title compound as a yellow powder (196 mg, 0.297 mmol, 89% yield). **¹H NMR** (600 MHz, CDCl₃) δ 7.79 (ddd, *J* = 7.7, 5.9, 1.6 Hz, 1H), 7.45 (t, *J* = 7.8 Hz, 1H), 7.09 – 7.04 (m, 2H), 4.20 (s, 3H), 4.19 (dd, *J* = 15.2, 7.7 Hz, 1H), 2.87 (d, *J* = 9.7 Hz, 1H), 2.51 (s, 1H), 2.45 – 2.38 (m, 3H), 2.38 – 2.29 (m, 3H), 2.14 – 2.08 (m, 3H), 2.08 – 2.03 (m, 3H), 2.01 (br, 6H), 1.86 (d, *J* = 3.6 Hz, 1H), 1.71 (br, 12H), 1.62 – 1.59 (m, 3H), 1.59 – 1.51 (m, 2H), 1.24 – 1.17 (m, 1H), 1.12 – 1.06 (m, 1H), 1.06 – 1.00 (m, 2H). **¹³C NMR** (151 MHz, CDCl₃) δ 163.6 (d, *J* = 9.2 Hz), 135.8 (d, *J* = 2.4 Hz), 132.6 (d, *J* = 1.5 Hz), 120.8 (d, *J* = 4.4 Hz), 115.6 (d, *J* = 28.1 Hz), 113.7 (d, *J* = 5.0 Hz), 58.9, 48.9 (d, *J* = 2.2 Hz), 45.8, 45.7 (d, *J* = 2.3 Hz), 42.9 (d, *J* = 11.9 Hz), 42.3 (d, *J* = 10.8 Hz), 41.7 (d, *J* = 1.8 Hz), 41.1 (d, *J* = 2.4 Hz), 40.8 (d, *J* = 4.7 Hz), 36.5 (two signals overlap), 36.3, 30.9 (d, *J* = 4.8 Hz), 29.8, 28.9 (d, *J* = 8.9 Hz), 28.8 (d, *J* = 9.1 Hz), 24.3 (d, *J* = 5.3 Hz). **³¹P NMR** (243 MHz, CDCl₃) δ 51.7. **Analysis** calc'd C 63.73, H 7.64; found C 63.38, H 7.67.**

Note: The sample of complex **7b** prepared as described above contained [Ad₂(*o*-anisyl)P]₂Pd⁰ as a 1 mol% impurity by ¹H or ³¹P NMR spectroscopy.



[*t*-Bu₂(5-F-2-(CH₃O)C₆H₃)P-κ²P,O]Pd(*syn*-2-CH₃norbornyl)Cl (7c). (COD)Pd(*syn*-2-CH₃norbornyl)Cl (180 mg, 0.501 mmol) was dissolved THF (3 ml) in a 20 ml scintillation vial. Di-*tert*-butyl(5-fluoro-2-methoxyphenyl)phosphine (142 mg, 0.525 mmol, 1.05 equiv) was dissolved in THF (1 ml + 1 ml rinse) and added to the reaction vessel dropwise with stirring. The reaction mixture was stirred for approximately 15 min at ambient temperature and then filtered through a plug of Celite.

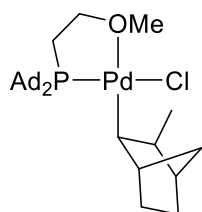
The solvent was evaporated *in vacuo*. The crude solid was dissolved in ether (~5 ml) and filtered through a plug of Celite. The solution was layered with pentane (~15 ml) and let sit until crystals began to form. The vial was then left overnight at -40 °C. The solid was collected by filtration and rinsed with chilled pentane (2x2 ml). Two further crops were grown from the mother liquor in a similar manner with lower volumes. The three crops were combined to give the title compound as a yellow powder (173 mg, 0.332 mmol, 66% yield). ¹H NMR (600 MHz, CDCl₃) δ 7.55 – 7.44 (m, 1H), 7.17 (ddd, *J* = 9.6, 7.5, 2.9 Hz, 1H), 7.02 (dt, *J* = 9.2, 4.6 Hz, 1H), 4.19 (s, 3H), 4.03 (dd, *J* = 17.4, 7.2 Hz, 1H), 2.81 (d, *J* = 9.4 Hz, 1H), 2.46 (s, 1H), 1.85 (d, *J* = 3.2 Hz, 1H), 1.60 – 1.40 (m, 24H), 1.22 – 1.15 (m, 1H), 1.09 – 1.01 (m, 2H), 0.98 (t, *J* = 10.3 Hz, 1H). ¹³C NMR (151 MHz, CDCl₃) δ 159.3 (d, *J* = 9.1 Hz), 156.4 (dd, *J* = 243.2, 5.8 Hz), 121.0 (d, *J* = 23.4 Hz), 119.7 (d, *J* = 26.7 Hz), 119.3 (dd, *J* = 23.2, 1.2 Hz), 114.6 – 114.3 (m), 59.6, 48.7 (d, *J* = 2.4 Hz), 45.8, 45.7 (d, *J* = 2.5 Hz), 43.0, 38.0 (d, *J* = 13.4 Hz), 37.4 (d, *J* = 11.9 Hz), 36.2, 31.0 – 30.9 (m, two overlapping signals), 30.7 (d, *J* = 6.0 Hz), 29.6, 24.3 (d, *J* = 6.0 Hz). ³¹P NMR (243 MHz, CDCl₃) δ 50.0. ¹⁹F NMR (565 MHz, CDCl₃) δ -122.2. **Analysis** calc'd C 52.98, H 7.15; found C 53.05, H 7.18.



[*t*-Bu₂(2-OCH₃O-5-(CF₃)C₆H₃)P-κ²P,O]Pd(*syn*-2-CH₃norbornyl)Cl (7d). (COD)Pd(*syn*-2-CH₃norbornyl)Cl (180 mg, 0.501 mmol) was dissolved THF (3 ml) in a 20 ml scintillation vial. Di-*tert*-butyl(5-(trifluoromethyl)-2-methoxyphenyl)phosphine (176 mg, 0.549 mmol, 1.10 equiv) was dissolved in THF (2 ml + 1 ml rinse) and added to the reaction vessel dropwise with stirring. The reaction mixture was stirred for approximately 15 min at ambient temperature, and then the solvent was evaporated *in vacuo*. The crude solid was dissolved in ether (6 ml)

and filtered through a plug of Celite. After filtration, the Celite was rinsed with ether (4 ml). The solution was layered with pentane (~7 ml) and let sit until crystals began to form. The vial was then left overnight at -30 °C. The solvent was decanted, and the solid was rinsed with chilled pentane (2x3 ml). This solid was recrystallized again from warm ether (12 ml) layered with pentane (8 ml) at ambient temperature. A second crop was grown from the mother liquor in a similar manner with lower volumes at -30 °C. The two crops were combined to give the title compound as a bright yellow powder. (174 mg, 0.305 mmol, 61% yield). ¹H NMR (600 MHz, CDCl₃) δ 8.07 (d, *J* = 6.1 Hz, 1H), 7.72 (dd, *J* = 8.9, 2.2 Hz, 1H), 7.15 (dd, *J* = 8.9, 4.0 Hz, 1H), 4.26 (s, 3H), 4.10 (dd, *J* = 17.3, 6.3 Hz, 1H), 2.80 (d, *J* = 9.4 Hz, 1H), 2.47 (s, 1H), 1.86 (d, *J* = 3.4 Hz, 1H), 1.60 – 1.50 (m, 5H), 1.47 (d, *J* = 14.3 Hz, 9H), 1.43 (d, *J* = 14.5 Hz, 9H), 1.22 – 1.14 (m, 1H), 1.10 – 1.02 (m, 2H), 1.01 – 0.94 (m, 1H). ¹³C NMR (151 MHz, CDCl₃) δ 165.1 (d, *J* = 8.7 Hz), 132.2, 130.0, 123.9 (q, *J* = 271.8 Hz), 123.9 – 123.1 (m), 119.1 (d, *J* = 27.9 Hz,

113.4 (d, $J = 3.8$ Hz), 59.0, 48.7 (d, $J = 2.4$ Hz), 45.9, 45.8 (d, $J = 2.5$ Hz), 44.3, 38.1 (d, $J = 13.3$ Hz), 37.5 (d, $J = 11.7$ Hz), 36.1, 30.9 (d, $J = 5.6$ Hz), 30.8 (d, $J = 4.2$ Hz), 30.7 (d, $J = 6.0$ Hz), 29.6, 24.3 (d, $J = 5.7$ Hz). ^{19}F NMR (565 MHz, CDCl_3) δ -62.9. ^{31}P NMR (243 MHz, CDCl_3) δ 49.2. **Analysis** calc'd C 50.45, H 6.53; found C 50.47, H 6.38.

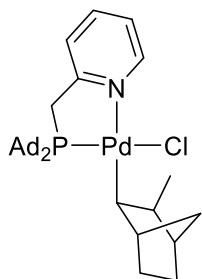


[(1-Ad)₂(CH₃OCH₂CH₂)P- κ^2 P,O]Pd(syn-2-CH₃norbornyl)Cl (7e).

(COD)Pd(syn-2-CH₃norbornyl)Cl (120 mg, 0.334 mmol) was dissolved in DCM (1 ml) in a 20 ml scintillation vial. Di(1-adamantyl)(2-methoxyethyl)phosphine (132 mg, 0.366 mmol, 1.11 equiv) was dissolved in DCM (1 ml + 1 ml rinse) and added dropwise to the reaction vial with stirring. The reaction mixture was stirred at ambient temperature for approximately 10 minutes, then diluted with pentane (6 ml), and then filtered through a plug of Celite. After filtration, the Celite was rinsed with 5:1 pentane/DCM (2 ml). The volatile materials were evaporated *in vacuo*. The crude product was recrystallized from DCM/pentane (2 crops) to give the title compound as yellow crystals (172 mg, 0.281 mmol, 84%). ^1H NMR (600 MHz, CDCl_3) δ 3.87 (dd, $J = 16.7, 7.4$ Hz, 1H), 3.60 – 3.48 (m, 5H), 2.78 (d, $J = 9.7$ Hz, 1H), 2.45 (s, 1H), 2.33 – 2.26 (m, 3H), 2.23 – 2.16 (m, 3H), 2.16 – 2.10 (m, 3H), 2.08 – 2.02 (m, 9H), 1.94 – 1.83 (m, 2H), 1.81 (d, $J = 3.9$ Hz, 1H), 1.79 – 1.73 (m, 12H), 1.54 (d, $J = 7.1$ Hz, 3H), 1.52 – 1.44 (m, 2H), 1.24 – 1.16 (m, 1H), 1.08 – 1.02 (m, 1H), 1.02 – 0.95 (m, 2H). ^{13}C NMR (151 MHz, CDCl_3) δ 72.5, 60.6, 48.5 (d, $J = 2.1$ Hz), 45.6, 45.2 (d, $J = 2.3$ Hz), 40.8, 40.7 (d, $J = 22.9$ Hz), 40.6 (d, $J = 21.6$ Hz), 40.0, 36.7 (two overlapping res), 36.2 (d, $J = 2.6$ Hz), 35.9, 31.2 (d, $J = 4.6$ Hz), 29.8, 28.7 (d, $J = 8.4$ Hz), 28.5 (d, $J = 8.4$ Hz), 24.7 (d, $J = 5.5$ Hz), 19.1 (d, $J = 17.8$ Hz). ^{31}P NMR (243 MHz, CDCl_3) δ 52.1. **Analysis** calc'd C 60.88, H 8.24; found C 60.45, H 8.45.

Note: The crude sample (without recrystallization) of complex **7e** contained a minor (~1:20) side product by ^1H NMR, which appeared to be a different (possibly isomeric) alkylpalladium complex. This minor complex was removed during recrystallization.

Note: There is some ambiguity about which ^{13}C NMR peaks belong to which doublet. Peaks were assigned such that the ^{31}P - ^{13}C J values were similar to those of the free ligand.



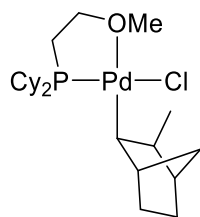
[2-(((1-Ad)₂P)CH₂)C₅H₅N- κ^2 P,N]Pd(syn-2-CH₃norbornyl)Cl (7f).

(COD)Pd(syn-2-CH₃norbornyl)Cl (120 mg, 0.334 mmol) was dissolved in DCM (2 ml) in a 20 ml scintillation vial. 2-((Di(1-adamantyl)phosphino)methyl)pyridine (131 mg, 0.333 mmol, 1.00 equiv) dissolved in DCM (1 ml + 1 ml rinse) was added to the reaction vial dropwise with stirring. The reaction mixture was stirred at ambient temperature for approximately 15 minutes, then diluted with pentane (7 ml), and then filtered through a plug of Celite. After filtration, the Celite was rinsed with 2:1 pentane/DCM (3 ml). The volume was reduced to approximately 1 ml *in vacuo*. The mixture was diluted with DCM (2 ml), and the product was precipitated by adding pentane (8 ml). The mixture was cooled to -30 °C, and the solid was collected by filtration and rinsed with pentane (3x3 ml) to give the title compound as a white powder (186 mg, 0.289 mmol, 87% yield). ^1H

NMR (600 MHz, CDCl₃) δ 9.62 (d, J = 5.4 Hz, 1H), 7.64 (t, J = 7.6 Hz, 1H), 7.29 (d, J = 7.7 Hz, 1H), 7.21 (t, J = 6.4 Hz, 1H), 3.54 (dd, J = 16.4, 8.1 Hz, 1H), 3.31 (dd, J = 16.7, 9.8 Hz, 1H), 3.25 (dd, J = 16.7, 9.9 Hz, 1H), 2.82 (d, J = 9.4 Hz, 1H), 2.48 (s, 1H), 2.27 – 2.19 (m, 3H), 2.19 – 2.07 (m, 6H), 2.05 – 1.95 (m, 9H), 1.86 (d, J = 4.2 Hz, 1H), 1.80 – 1.68 (m, 12H), 1.68 – 1.60 (m, 1H), 1.55 (tdd, J = 11.0, 4.9, 2.6 Hz, 1H), 1.51 (d, J = 7.2 Hz, 3H), 1.32 – 1.24 (m, 1H), 1.13 – 1.00 (m, 3H). **¹³C NMR** (151 MHz, CDCl₃) δ 159.6 (d, J = 3.5 Hz), 151.0, 137.8, 122.4, 122.0 (d, J = 7.0 Hz), 48.4 (d, J = 2.2 Hz), 45.2, 44.7 (d, J = 2.5 Hz), 40.6, 40.5 (expect d, left peak overlaps), 40.2 (d, J = 11.9 Hz), 39.9, 36.7, 36.6, 36.3, 32.7 (d, J = 4.8 Hz), 31.4 (d, J = 21.1 Hz), 30.0, 29.9 (d, J = 4.2 Hz), 28.6 (d, J = 8.4 Hz), 28.5 (d, J = 8.6 Hz), 24.6 (d, J = 5.4 Hz). **³¹P NMR** (243 MHz, CDCl₃) δ 60.6. **Analysis** calc'd (+CH₂Cl₂) C 57.62, H 7.05, N 1.92; found C 57.77, H 7.01, N 2.19.

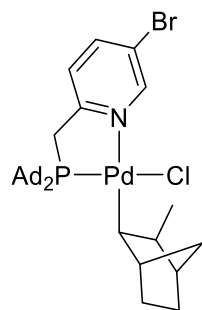
Note: The crude sample (without recrystallization) of complex **7f** contained a minor (~1:20) side product, as determined by ¹H NMR spectroscopy. This side product appeared to be a different (possibly isomeric) alkylpalladium complex and was removed by recrystallization.

Note: The recrystallized sample of **7f** contains residual DCM in a 1:1 molar ratio. Placing the sample under vacuum (~30 mTorr) for multiple hours did not remove this residual solvent. The molecular weight (used for yield and subsequent experiments) and calc'd CHN values are corrected to include DCM in the molecular formula.



[Cy₂(2-methoxyethyl)P- κ^2 P,O]Pd(*syn*-2-CH₃-norbornyl)Cl (7g**).**

(COD)Pd(*syn*-2-CH₃-norbornyl)Cl (120 mg, 0.334 mmol, 1.00 equiv) was dissolved in DCM (1 ml) in a 20 ml scintillation vial. Dicyclohexyl(2-methoxyethyl)phosphine (85.5 mg, 0.334 mmol, 1.00 equiv) was dissolved in DCM (1 ml + 1 ml rinse) and added dropwise to the reaction vial with stirring. The reaction mixture was stirred at ambient temperature for approximately 10 minutes, then the volatile materials were removed *in vacuo*. The oily residue was dissolved in methanol (2 ml) and filtered through a plug of Celite, which was rinsed with methanol (3x1 ml). The volatile materials were removed *in vacuo*. The residue was dissolved in pentane (2 ml) and filtered through a plug of Celite, which was rinsed with pentane (3x1 ml). The volatile materials were removed *in vacuo*, and then the residue was dissolved in pentane (2 ml). The last step was repeated twice more. The volatile materials were removed again, and the solid dried under vacuum (<50 mTorr for ~2 hours) to give the title compound as a light tan powder (161 mg, 0.317 mmol, 95% yield). Due to the high solubility of this complex in organic solvents, attempts to purify it further by recrystallization were abandoned. **¹H NMR** (500 MHz, CDCl₃) δ 3.68 – 3.56 (m, 2H), 3.52 (s, 3H), 2.73 – 2.54 (m, 2H), 2.46 (s, 1H), 2.31 – 2.20 (m, 1H), 2.05 – 1.94 (m, 3H), 1.94 – 1.71 (m, 12H), 1.72 – 1.58 (m, 1H), 1.55 – 1.44 (m, 6H), 1.43 – 1.20 (m, 8H), 1.12 – 1.01 (m, 1H), 0.97 (d, J = 10.0 Hz, 1H), 0.93 – 0.82 (m, 1H). **³¹P NMR** (243 MHz, CDCl₃) δ 44.7 (br). **Analysis** calc'd C 54.44, H 8.34; found C 54.70, H 8.30.

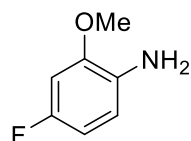


[2-(((1-Ad)₂P)CH₂)5-BrC₅H₅N-κ²P,N]Pd(*syn*-2-CH₃-norbornyl)Cl (7h**).**

(COD)Pd(*syn*-2-CH₃-norbornyl)Cl (71.7 mg, 0.200 mmol, 1.00 equiv) was dissolved in DCM (3 ml) in a 20 ml scintillation vial. 2-((Di(1-adamantyl)phosphino)methyl)5-bromopyridine (94.5 mg, 0.200 mmol, 1.00 equiv) was dissolved in DCM (~0.5 ml + ~0.5 ml rinse) was added to the reaction vial dropwise with stirring. The reaction mixture was stirred at ambient temperature for approximately 10 minutes, then diluted with pentane (2 ml), and then filtered through a plug of Celite, which was rinsed with 1:1 pentane/DCM (2 ml). The volume was reduced to approximately 1 ml *in vacuo*, and the product was precipitated by adding pentane (6 ml). The solid was collected by filtration and rinsed with pentane and ether (2 ml each). The crude product was recrystallized from DCM/ether (1 crop) to give the title compound as a white powder (101 mg, 0.140 mmol, 70% yield). ¹H NMR (600 MHz, CDCl₃) δ 9.73 (d, *J* = 2.3 Hz, 1H), 7.77 (dd, *J* = 8.2, 2.1 Hz, 1H), 7.21 (d, *J* = 8.3 Hz, 1H), 3.60 (dd, *J* = 17.0, 8.1 Hz, 1H), 3.25 (dd, *J* = 16.9, 9.8 Hz, 1H), 3.19 (dd, *J* = 16.9, 9.7 Hz, 1H), 2.81 (d, *J* = 9.4 Hz, 1H), 2.47 (s, 1H), 2.26 – 2.18 (m, 3H), 2.18 – 2.12 (m, 3H), 2.11 – 2.06 (m, 3H), 2.04 – 1.96 (m, 9H), 1.86 (d, *J* = 4.6 Hz, 1H), 1.80 – 1.69 (m, 12H), 1.68 – 1.60 (m, 1H), 1.59 – 1.52 (m, 1H), 1.50 (d, *J* = 7.2 Hz, 3H), 1.32 – 1.23 (m, 1H), 1.12 – 0.99 (m, 3H). ¹³C NMR (151 MHz, CDCl₃) δ 158.3 (d, *J* = 3.5 Hz), 152.1, 140.7, 123.3 (d, *J* = 6.8 Hz), 119.4, 48.4 (d, *J* = 2.2 Hz), 45.3, 44.8 (d, *J* = 2.5 Hz), 40.6 (d, *J* = 12.9 Hz), 40.6, 40.3 (d, *J* = 11.8 Hz), 40.0, 36.6, 36.6, 36.2, 32.5 (d, *J* = 4.7 Hz), 31.3 (d, *J* = 4.2 Hz), 30.7 (d, *J* = 20.7 Hz), 29.9, 28.6 (d, *J* = 8.3 Hz), 28.5 (d, *J* = 8.5 Hz), 24.7 (d, *J* = 5.4 Hz). ³¹P NMR (243 MHz, CDCl₃) δ 60.0. **Analysis** calc'd C 56.44, H 6.69, N 1.94; found C 56.78, H 6.60, N 1.81.

Table 2.7. Comparison of key NMR chemical shifts for Pd(II) chloride complexes in CDCl₃.

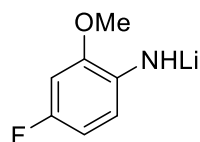
Complex	(¹ H) C ₁ -H	(¹³ C) C ₁	³¹ P	Complex	(¹ H) C ₁ -H	(¹³ C) C ₁	³¹ P
1	4.25	57.9	72.1	7d	4.10	44.3	49.2
4a	3.14	64.2	76.7	7e	3.87	36.2	52.1
4b	3.37	62.2	69.5	7f	3.54	29.8	60.5
7a	4.02	42.1	49.6	7g	nd	nd	44.7
7b	4.19	40.8	51.7	7h	3.25	31.3	60.0
7c	4.03	43.0	50.0				



4-Fluoro-2-methoxyaniline. 4-Fluoro-2-methoxynitrobenzene (3.4 g, 20.0

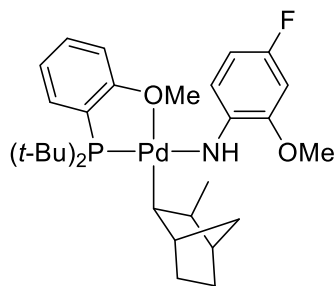
mmol), EtOH (60 ml), and H₂O (30 ml) were mixed in a 250 ml round bottom flask. The mixture was frozen, the pressure was reduced to approximately 50 mTorr, and then the mixture was allowed to thaw. The atmosphere was refilled with argon. HCl_{aq} (18 ml, 37%, 210 mmol, 10 equiv) and Fe⁰ (5.59 g, 100 mmol, 5.00 equiv) were added to the flask. The mixture was heated at reflux until the nitroarene was no longer detected by TLC (~12 h). The reaction was quenched with solid KOH until basic, and the mixture was extracted with ethyl acetate (4x100 ml). The crude amine was purified by acid-base extraction (HCl/KOH), column chromatography (0 to 25% ethyl acetate gradient in hexanes),

and kugelrohr distillation (60 °C, ~0.5 Torr) to give the title compound as a clear and colorless oil (1.60 g, 11.3 mmol, 57% yield). **¹H NMR** (500 MHz, CDCl₃) δ 6.62 (dd, *J* = 8.5, 5.8 Hz, 1H), 6.56 (dd, *J* = 10.3, 2.7 Hz, 1H), 6.50 (td, *J* = 8.5, 2.8 Hz, 1H), 3.83 (s, 3H), 3.62 (s, 2H). **¹⁹F NMR** (470 MHz, CDCl₃) δ -124.2 (td, *J* = 9.3, 6.1 Hz).



Lithium (4-fluoro-2-methoxyphenyl)amide. 4-Fluoro-2-methoxyaniline (282 mg, 2.00 mmol) was dissolved in toluene (8 ml) in a 20 ml vial. Lithium hexamethyldisilazide (335 mg, 2.00 mmol) was added slowly with stirring. The reaction mixture was stirred at ambient temperature for 2 h and then cooled to 0 °C to precipitate a solid. Pentane (~8 ml) was added to precipitate more solid.

The precipitate was isolated by filtration and rinsed with pentane (2x4 ml) to give the title compound as a white powder (268 mg, 1.82 mmol, 91% yield). This reagent was used in subsequent reactions without characterization or further purification.



[*t*-Bu₂(*o*-anisyl)P-κ²P,O]Pd(*syn*-2-CH₃norbornyl)NH(4-F-2-(OMe)C₆H₃) (8a). [*t*-Bu₂(*o*-anisyl)P]Pd(*syn*-2-CH₃norbornyl)Cl (101 mg, 0.201 mmol) was suspended in ether (1 ml) in a 1 dram vial and briefly chilled. A suspension of lithium (4-fluoro-2-methoxyphenyl)amide (30.4 mg, 0.207 mmol, 1.03 equiv) in ether (1 ml + 1 ml rinse) was slowly added to the vial with stirring by pipet. The reaction mixture was stirred until all solid disappeared (~30 min). The reaction mixture was then filtered through a plug of

Celite. After filtration, the Celite was rinsed with ether (2 ml). The solvent was evaporated *in vacuo*. The crude product was dissolved in pentane (14 ml), and the solution was filtered through a pad of Celite. The solvent was allowed to slowly evaporate through a loose cap overnight at 0 °C, until crystals began to form (volume ~8 ml). The cap was then tightened, and the mixture was left at -40 °C overnight. The solvent was decanted and the crystals were rinsed with chilled pentane (2x1 ml) to give the title compound as reddish-yellow crystals (44.5 mg, 0.0732 mmol, 36% yield). A crystal suitable for X-ray diffraction was selected directly from this sample. **¹H NMR** (500 MHz, C₆D₆) δ 7.48 (td, *J* = 7.7, 5.8, 1.7 Hz, 1H), 7.31 (dd, *J* = 8.6, 5.9 Hz, 1H), 6.97 – 6.87 (m, 2H), 6.72 – 6.63 (m, 2H), 6.33 (dd, *J* = 8.4, 4.4 Hz, 1H), 4.14 (s, 1H), 3.94 (dd, *J* = 17.4, 7.3 Hz, 1H), 3.74 (s, 3H), 3.50 (s, 3H), 2.57 (d, *J* = 3.7 Hz, 1H), 2.40 (d, *J* = 9.6 Hz, 1H), 2.00 (d, *J* = 3.9 Hz, 1H), 1.86 – 1.78 (m, 1H), 1.76 (d, *J* = 6.7 Hz, 3H), 1.67 – 1.59 (m, 1H), 1.43 – 1.32 (m, 1H), 1.27 – 1.14 (m, 20H), 1.10 (d, *J* = 9.4 Hz, 1H). **¹⁹F NMR** (376 MHz, C₆D₆) δ -133.8. **³¹P NMR** (203 MHz, C₆D₆) δ 42.8. **Analysis** calc'd C 59.26, H 7.46, N 2.30; found C 59.42, H 7.32, N 2.25

The ¹H NMR resonances were assigned as follows:

- The *tert*-butyl signals are clear.
- The aryl signals based on shift, multiplicity, and ¹H NOESY. Overlapping resonances were not assigned.
- The NH signal is clear by ¹H-¹³C HSQC.

- The methoxy signals based on integration and ^1H - ^{13}C HSQC. The two methoxy signals were differentiated based on the ^1H - ^{31}P HMBC spectrum.
- The C1 alkyl signal (m) based on multiplicity and ^1H - ^{31}P HMBC spectra.
- The remaining alkyl signals were categorized as CH and CH_2 groups based on the ^1H - ^{13}C HSQC spectrum and assigned based on their ^1H NOE correlations to each other. Due to the rigid structure of this alkyl group, some $^4J_{\text{HH}}$ values are larger than some $^3J_{\text{HH}}$ values. Therefore, the NOE correlations are more informative than J coupling correlations (COSY).

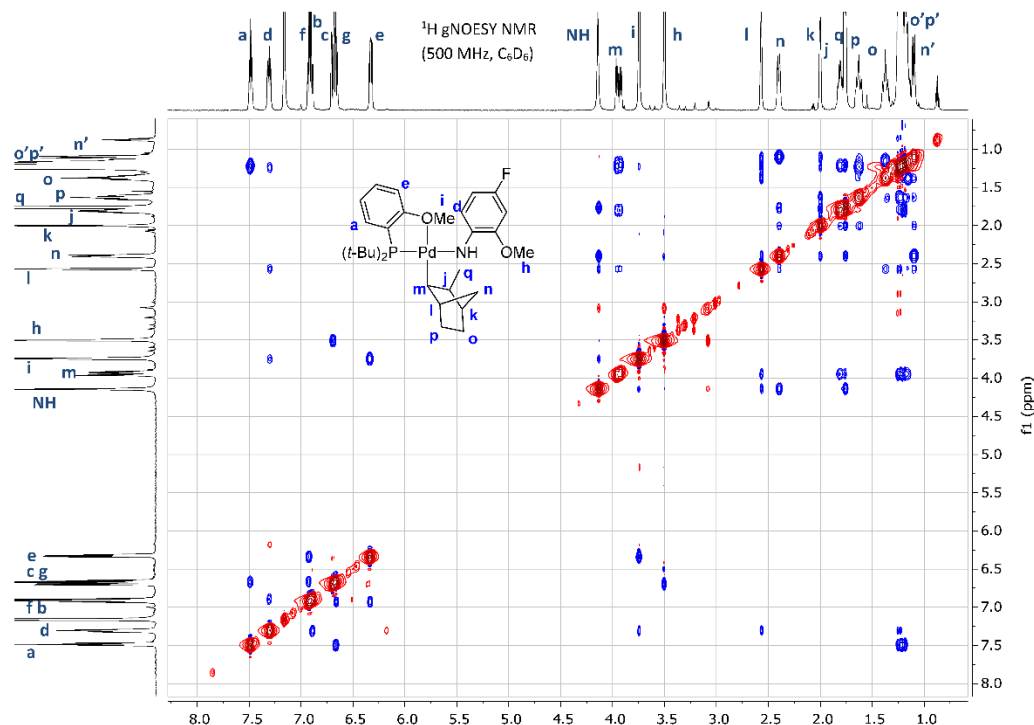
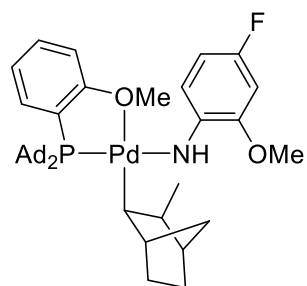


Figure 2.9. 2-Dimensional ^1H - ^1H gradient-enhanced NOE spectrum of **8a**.

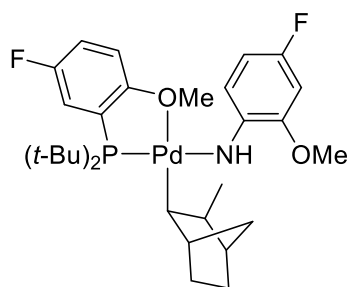


[(1-Ad) $_2$ (*o*-anisyl)P- κ^2 P,O]Pd(*syn*-2-CH $_3$ norbornyl)NH(4-F-2-(OMe)C $_6$ H $_3$) (8b**).** [(1-Ad) $_2$ (*o*-anisyl)P]Pd(*syn*-2-CH $_3$ norbornyl)Cl (98.8 mg, 0.150 mmol) was dissolved in DCM (3 ml) in a 20 ml scintillation vial and briefly chilled. A solution of lithium (4-fluoro-2-methoxyphenyl)amide (23.3 mg, 0.158 mmol, 1.05 equiv) in DCM (1 ml + 1 ml rinse) was slowly added to the vial with stirring by pipet. The reaction mixture was stirred for approximately 10 minutes at ambient temp. The reaction mixture was then filtered through a plug of

Celite. After filtration, the Celite was rinsed with DCM (1 ml). The volume was reduced to approximately 1 ml *in vacuo*. The crude product was precipitated by adding ether (6 ml), mixing, reducing the volume to approximately 2 ml, diluting again with ether (6 ml), and cooling to -30 $^\circ\text{C}$. The orange powder was collected by filtration and rinsed with chilled ether (2x1 ml) and chilled pentane (2x2 ml). The crude product was recrystallized from THF layered with ether at -

30 °C to give the title compound as an orange powder (42.8 mg, 0.0560 mmol, 37% yield). Crystals suitable for X-ray diffraction were grown from a solution of **8b** in DCM layered with pentane at ambient temperature. **¹H NMR** (500 MHz, C₆D₆) δ 7.60 (t, *J* = 6.4 Hz, 1H), 7.40 (t, *J* = 6.2 Hz, 1H), 6.96 (t, *J* = 7.8 Hz, 1H), 6.91 (td, *J* = 8.6, 2.7 Hz, 1H), 6.75 (t, *J* = 7.5 Hz, 1H), 6.71 (dd, *J* = 10.5, 2.6 Hz, 1H), 6.40 (dd, *J* = 8.2, 4.1 Hz, 1H), 4.26 – 4.13 (m, 2H), 3.80 (s, 3H), 3.52 (s, 3H), 2.68 – 2.56 (m, 1H), 2.53 – 2.40 (m, 4H), 2.38 – 2.28 (m, 3H), 2.22 – 2.11 (m, 3H), 2.11 – 1.99 (m, 4H), 1.87 (s, 4H), 1.84 – 1.77 (m, 6H), 1.69 – 1.48 (m, 13H), 1.46 – 1.35 (m, 1H), 1.33 – 1.19 (m, 2H), 1.16 – 1.09 (m, 1H). **¹⁹F NMR** (470 MHz, C₆D₆) δ -134.8. **³¹P NMR** (202 MHz, C₆D₆) δ 44.5. **Analysis** calc'd C 66.00, H 7.52, N 1.83; found C 64.29, H 7.95, N 1.66.

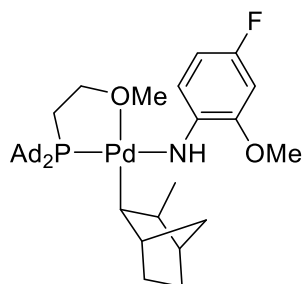
Note: The ¹H NMR spectrum of the bulk sample of **8b** prepared as described above contains multiple signals corresponding to minor impurities. These impurities likely cause the poor agreement between calculated and experimental microanalytical data.



[*t*-Bu₂(5-F-2-(OMe)C₆H₃)P-κ²P,O]Pd(*syn*-2-CH₃norbornyl)NH(4-F-2-(OMe)C₆H₃) (8c**). [*t*-Bu₂(5-F-2-(OMe)C₆H₃)P]Pd(*syn*-2-CH₃norbornyl)Cl (104 mg, 0.199 mmol) was dissolved in THF (3 ml) in a 20 ml scintillation vial and briefly chilled. 4-Fluoro-2-methoxyaniline (0.52 ml, 0.40 M, 0.21 mmol, 1.0 equiv) and NaO*t*-Bu (0.55 ml, 0.40 M, 0.22 mmol, 1.1 equiv) were slowly added to the vial in that order with stirring. The reaction mixture was stirred at ambient temperature for**

approximately 10 minutes. The solvent was evaporated *in vacuo*. The residue was dissolved in ether (~3 ml) and filtered through a plug of Celite. After filtration, the Celite was rinsed with ether (2x1 ml). The solution was layered with pentane (~6 ml) and cooled to -30 °C to precipitate the product. The solid was collected by filtration and rinsed with chilled pentane (2x1 ml) to give the title compound as a yellow-orange powder (56.3 mg, 0.0899 mmol, 45% yield). **¹H NMR** (500 MHz, C₆D₆) δ 7.41 – 7.34 (m, 1H), 7.28 (t, *J* = 7.3 Hz, 1H), 6.91 (td, *J* = 8.6, 3.0 Hz, 1H), 6.69 (dd, *J* = 10.4, 2.8 Hz, 1H), 6.66 – 6.60 (m, 1H), 6.11 – 6.03 (m, 1H), 4.16 (s, 1H), 3.89 (dd, *J* = 17.6, 7.0 Hz, 1H), 3.65 (s, 3H), 3.49 (s, 3H), 2.53 (s, 1H), 2.36 (d, *J* = 9.4 Hz, 1H), 1.98 (s, 1H), 1.81 – 1.70 (m, 4H), 1.66 – 1.57 (m, 1H), 1.35 (ddd, *J* = 14.8, 10.2, 3.7 Hz, 1H), 1.25 – 1.05 (m, 21H). **¹⁹F NMR** (470 MHz, C₆D₆) δ -122.5, -134.3. **³¹P NMR** (202 MHz, C₆D₆) δ 43.2.

Analysis calc'd C 57.55, H 7.08, N 2.24; found C 57.11, H 7.06, N 2.10.



[(1-Ad)₂(CH₃OCH₂CH₂)P-κ²P,O]Pd(*syn*-2-CH₃norbornyl)NH(4-F-2-(OMe)C₆H₃) (8e**). [(1-Ad)₂(CH₃OCH₂CH₂)P]Pd(*syn*-2-CH₃norbornyl)Cl (81.8 mg, 0.134 mmol) was dissolved in DCM (3 ml) in a 20 ml scintillation vial and briefly chilled. A solution of lithium (4-fluoro-2-methoxyphenyl)amide (20.0 mg, 0.136 mmol, 1.01 equiv) in DCM (1 ml + 1 ml rinse) was slowly added to the vial with stirring by pipet. The reaction mixture was stirred for approximately 10 minutes at ambient temp. The solvent was evaporated *in vacuo*. The residue was**

dissolved in ether (3 ml) and filtered through a plug of Celite. After filtration, the Celite was rinsed with ether (2 ml). The solvent was evaporated *in vacuo*, more ether (6 ml) was added, and a yellow solid precipitated. The mixture was cooled to -30 °C to complete precipitation. The solid was collected by filtration and rinsed with chilled pentane (3x1 ml). The crude product was recrystallized from a solution in DCM layered with pentane at -30 °C (2 crops). The solid was collected by filtration and rinsed with chilled pentane (3x1 ml) to give the title compound as a yellow powder (47.0 mg, 0.0656 mmol, 49% yield). Crystals suitable for x-ray diffraction were grown from a solution of **8e** in DCM layered with pentane at ambient temperature. **¹H NMR** (600 MHz, C₆D₆) δ 7.36 (dd, *J* = 8.5, 6.1 Hz, 1H), 6.96 (td, *J* = 8.4, 1.8 Hz, 1H), 6.69 (d, *J* = 10.0 Hz, 1H), 3.96 (s, 1H), 3.86 (dd, *J* = 17.6, 7.0 Hz, 1H), 3.50 (s, 3H), 3.25 (s, 3H), 2.95 (dt, *J* = 12.9, 6.2 Hz, 2H), 2.61 (s, 1H), 2.43 (d, *J* = 9.0 Hz, 1H), 2.16 (d, *J* = 11.8 Hz, 3H), 2.01 (dd, *J* = 20.6, 7.3 Hz, 7H), 1.92 – 1.81 (m, 9H), 1.76 (d, *J* = 6.3 Hz, 4H), 1.68 – 1.57 (m, 13H), 1.43 – 1.34 (m, 1H), 1.33 – 1.13 (m, 4H), 1.09 (d, *J* = 9.6 Hz, 1H). **¹⁹F NMR** (565 MHz, C₆D₆) δ -137.0. **³¹P NMR** (243 MHz, C₆D₆) δ 44.2. **Analysis** calc'd C 63.72, H 8.02, N 1.96; calc'd corrected for residual solvent C 62.21, H 7.92, N 1.87; found C 61.56, H 8.16, N 1.66.

Note: The sample prepared as described above contained residual pentane and DCM in 12 and 31 mol %, respectively. The CHN values corrected for residual solvent are also reported below, and these values agree better with the experimental values. However, the experimental carbon content is still lower than calculated.

The ¹H NMR spectrum was partially assigned based on coupling constants, chemical shifts, and ¹H-¹³C HMBC correlations.

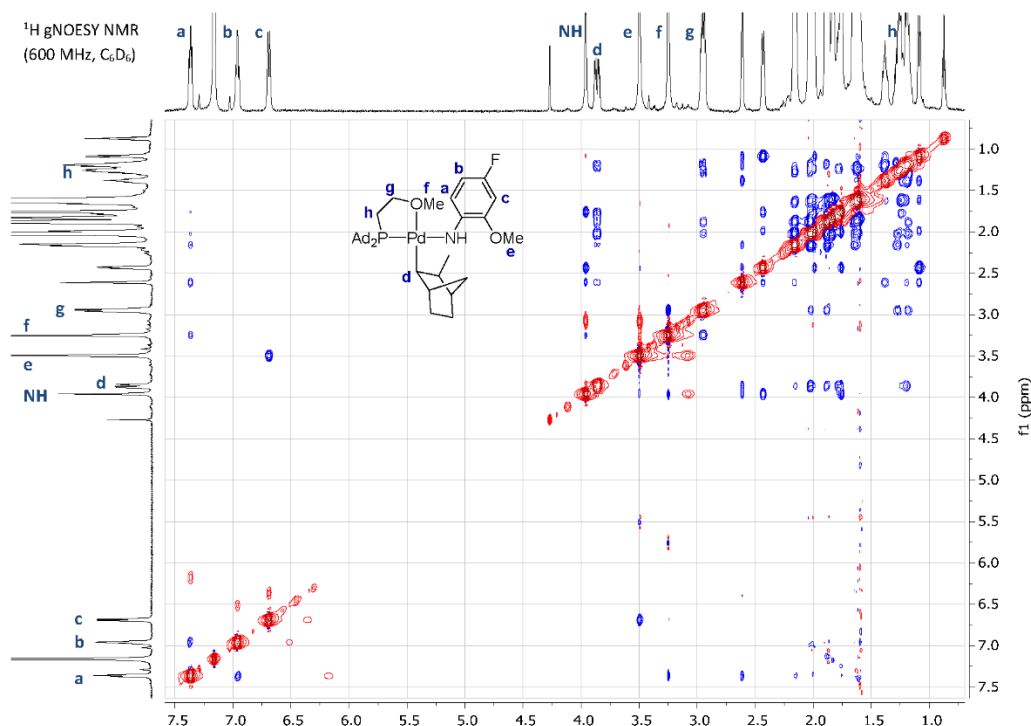
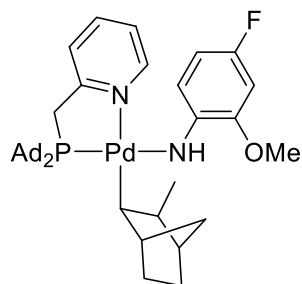


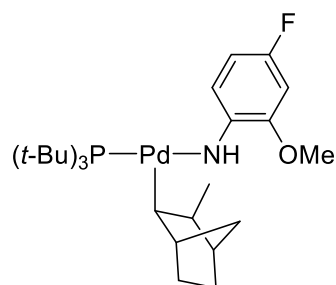
Figure 2.10. 2-Dimensional ¹H-¹H gradient-enhanced NOE spectrum of **8e**.



[2-(((1-Ad)₂P)CH₂)C₅H₅N-κ²P,N]Pd(syn-2-CH₃norbornyl)NH(4-F-2-(OMe)C₆H₃) (8f). [2-(((1-Ad)₂P)CH₂)C₅H₅N]Pd(syn-2-CH₃norbornyl)Cl (+DCM) (33.3 mg, 0.456 mmol) was dissolved in toluene (2 ml) in a 20 ml scintillation vial. A solution of lithium (4-fluoro-2-methoxyphenyl)amide (6.8 mg, 0.046 mmol, 1.0 equiv) in toluene (1 ml + 1 ml rinse) was slowly added to the vial with stirring by pipet. The reaction mixture was stirred for approximately 10 minutes at ambient temp. The volume was reduced to approximately 2 ml *in vacuo*. The mixture was diluted with pentane (2 ml) and filtered through a plug of Celite. After filtration, the Celite was rinsed with 1:1 pentane/Tol (2 ml). The solvent was evaporated *in vacuo*. The crude product was recrystallized from a solution in DCM layered with pentane at -30 °C to give the title compound as yellow-orange crystals (30.2 mg, 0.0379 mmol, 83% yield). ¹H NMR (600 MHz, C₆D₆) δ 9.46 (s, 1H), 7.34 – 6.96 (br, 1H), 6.87 (br, 1H), 6.78 (t, *J* = 7.6 Hz, 1H), 6.74 (dd, *J* = 10.6, 2.6 Hz, 1H), 6.58 (d, *J* = 7.7 Hz, 1H), 6.29 (t, *J* = 6.5 Hz, 1H), 4.22 (s, 1H), 3.62 – 3.55 (m, 4H), 2.77 – 2.53 (m, 4H), 2.18 – 1.69 (m, 24H), 1.58 (s, 13H), 1.41 – 1.33 (m, 1H), 1.33 – 1.22 (m, 2H). ¹⁹F NMR (565 MHz, C₆D₆) δ -138.0 (br and asymmetrical). ³¹P NMR (243 MHz, C₆D₆) δ 53.0. **Analysis** calc'd (+2/3 pentane) C 66.78, H 8.09, N 3.51; found C 66.44, H 8.08, N 3.48.

Note: The recrystallized sample of **8f** was determined to be a 3:2 molar ratio of **8f** and pentane by ¹H NMR. The calculated yield and CHN values are corrected to account for this residual solvent.

Repeated attempts to isolate and recrystallize the following compounds were unsuccessful. Therefore, they were characterized *in situ* by NMR spectroscopy:



(*t*-Bu₃P)Pd(syn-2-CH₃norbornyl)NH(4-F-2-(OMe)C₆H₃) (2i). (*t*-Bu₃P)Pd(syn-2-CH₃norbornyl)Cl (13.7 mg, 0.0300 mmol) was dissolved in toluene-*d*₈ (0.5 ml) in a 1 dram vial and briefly chilled. A suspension of lithium (4-fluoro-2-methoxyphenyl)amide (4.6 mg, 0.0315 mmol, 1.05 equiv) in toluene-*d*₈ (0.50 ml) was slowly added to the vial with stirring. The reaction mixture was briefly stirred at ambient temperature then transferred to a J-Young NMR tube. The sample was kept in a -20 °C bath until injection into the

spectrometer. All spectra were acquired at 263 K to prevent decomposition. ¹H NMR (600 MHz, Tol-*d*₈) δ 7.51 (t, *J* = 7.4 Hz, 1H), 6.83 (td, *J* = 8.6, 2.8 Hz, 1H), 6.48 (dd, *J* = 10.4, 2.8 Hz, 1H), 4.91 (s, 1H), 4.03 (dd, *J* = 18.4, 7.3 Hz, 1H), 3.30 (s, 3H), 2.42 (s, 1H), 1.85 (d, *J* = 9.8 Hz, 1H), 1.75 (d, *J* = 4.2 Hz, 1H), 1.68 (d, *J* = 7.1 Hz, 3H), 1.52 – 1.45 (m, 1H), 1.45 – 1.37 (m, 1H), 1.25 – 1.21 (m, 1H), 1.15 (d, *J* = 11.7 Hz, 27H), 1.08 – 1.00 (m, 2H), 0.77 (d, *J* = 9.7 Hz, 1H). ¹⁹F NMR (565 MHz, Tol-*d*₈) δ -131.8. ³¹P NMR (243 MHz, Tol-*d*₈) δ 66.1.

The ¹H NMR resonances were assigned as follows:

- The *tert*-butyl signals are clear

- The aryl signals based on shift and multiplicity.
- The methoxy and NH signals based on the ^1H - ^{13}C HSQC spectrum.
- The C1 alkyl signal (e) based on multiplicity and ^1H - ^{31}P HMBC.
- The remaining alkyl signals were categorized as CH and CH_2 groups based on the ^1H - ^{13}C HSQC spectrum, and assigned based on their ^1H NOESY correlations to each other. Due to the rigid structure of this alkyl group, some $^4J_{\text{HH}}$ values are larger than some $^3J_{\text{HH}}$ values. Therefore, the NOESY spectrum is more informative than the COSY spectrum.

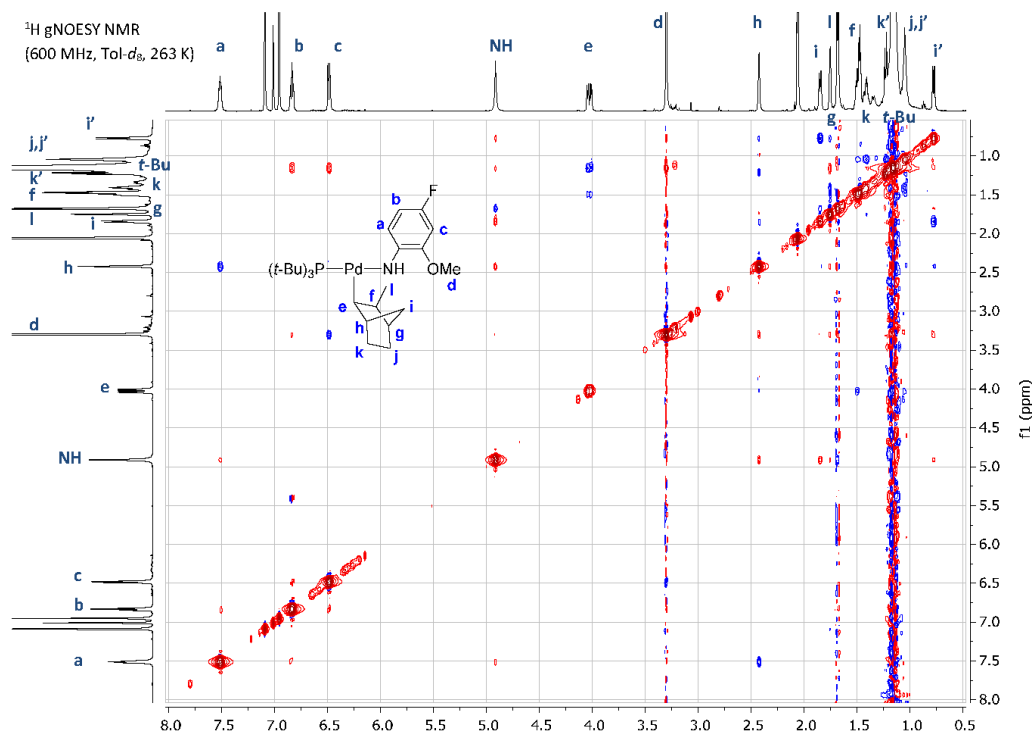
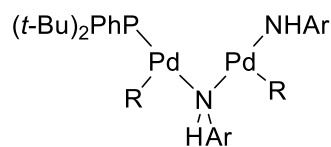


Figure 2.11. 2-Dimensional ^1H - ^1H gradient-enhanced NOE spectrum of **2i**.



R = *syn*-2- CH_3 norbornyl

Ar = 4-F-2-(OMe) C_6H_3

Bimetallic complex 6a: procedure 1. (*t*-Bu $_2$ PhP)Pd(*syn*-2- CH_3 norbornyl)Cl (**4a**) (14.2 mg, 0.0300 mmol) was dissolved in toluene- d_8 (0.5 ml) in a 1 dram vial and briefly chilled. A suspension of lithium (4-fluoro-2-methoxyphenyl)amide (4.6 mg, 0.0315 mmol, 1.05 equiv) in toluene- d_8 (0.50 ml) was slowly added to the vial with stirring. The reaction mixture was briefly stirred at ambient temperature then transferred to a J-Young NMR tube. The sample

was kept in a $-20\text{ }^\circ\text{C}$ bath until injection into the spectrometer. All spectra were acquired at 263 K to prevent decomposition.

Procedure 2. **4a** (14.2 mg, 0.0300 mmol) was dissolved in toluene- d_8 (0.5 ml) in a 1 dram vial. A solution of 4-fluoro-2-methoxyaniline (75 μl , 0.40 M, 0.030 mmol, 1.0 equiv) in toluene- d_8

was added to the vial with stirring. The reaction mixture was briefly chilled, then a solution of LiHMDS (78 μ l, 0.40 M, 0.031 mmol, 1.0 equiv) in toluene- d_8 was added with stirring. The reaction mixture was briefly stirred at ambient temperature then transferred to a J-Young NMR tube. The sample was kept in a -20 $^{\circ}$ C bath until injection into the spectrometer. All spectra were acquired at 263 K to prevent decomposition.

Note: The presence of at least two isomers of **6a** and impurities from decomposition complicates the analysis of these spectra. See the spectra below for partial assignments.

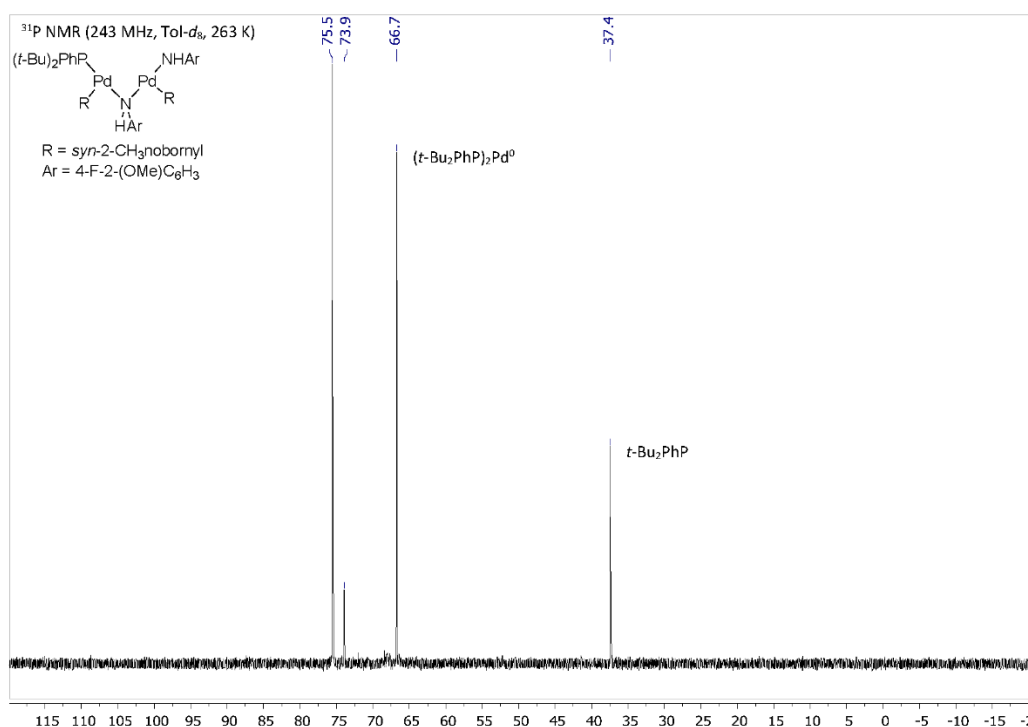


Figure 2.12. ^{31}P NMR spectrum of **6a**.

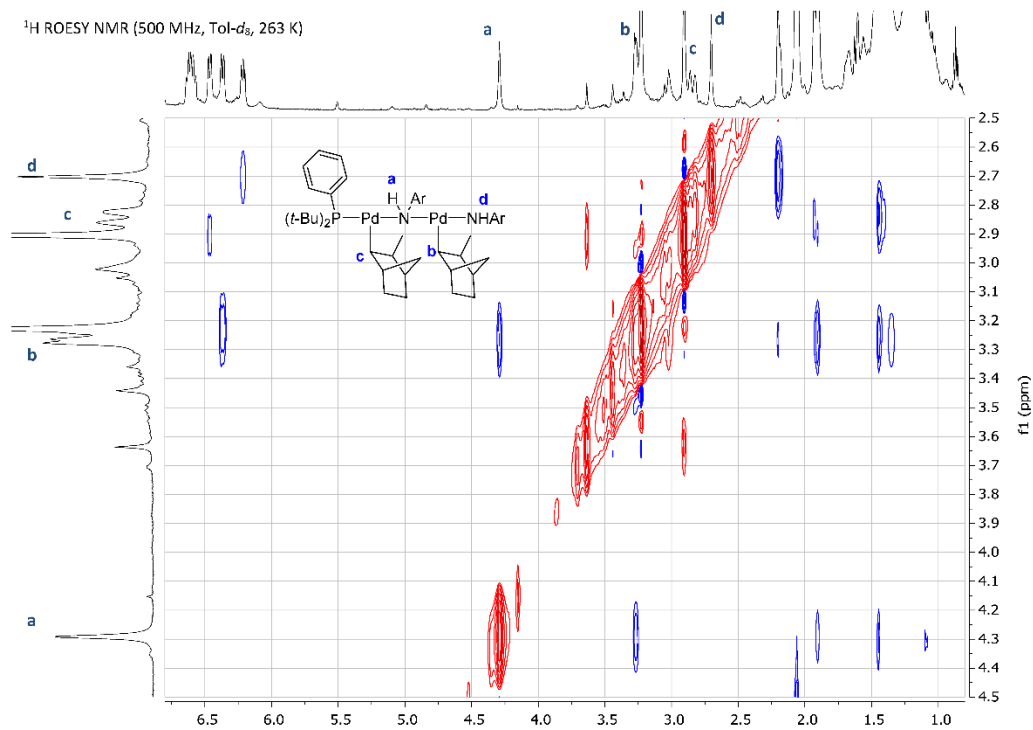


Figure 2.13. 2-Dimensional ^1H - ^1H rotating frame NOE spectrum of **6a**.

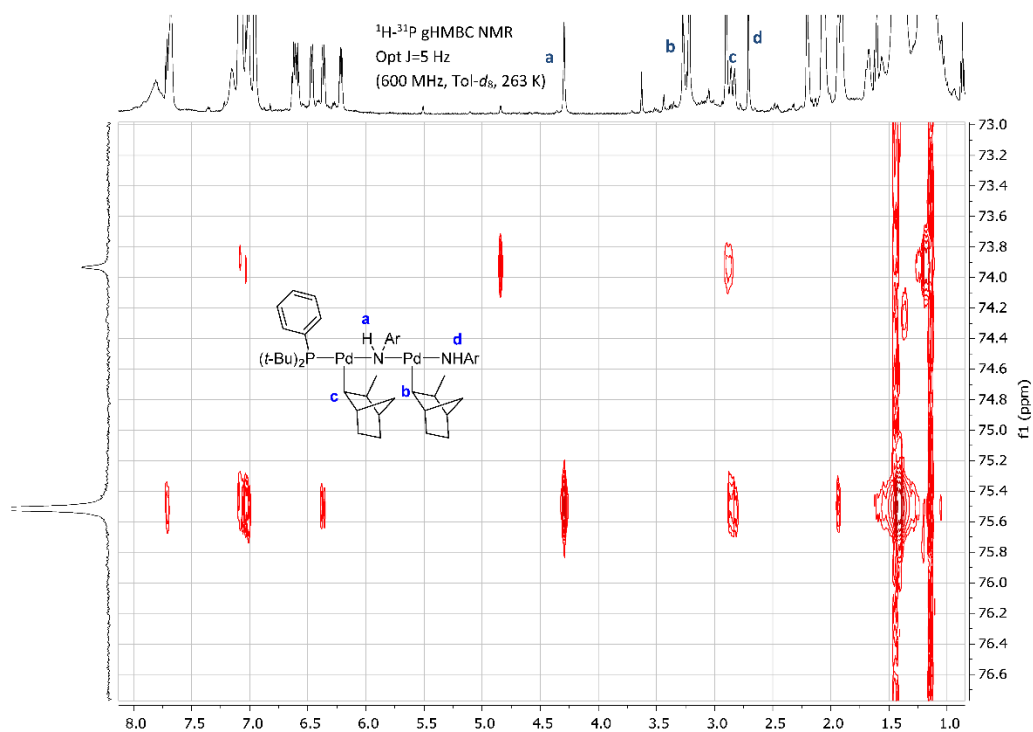
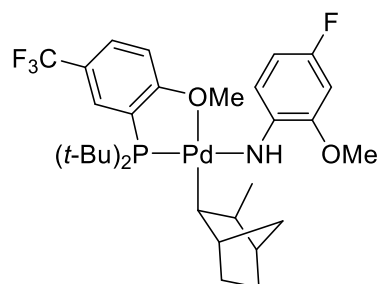


Figure 2.14. 2-Dimensional ^1H - ^{31}P gradient-enhanced HMBC spectrum of **6a**.



[*t*-Bu₂(2-OCH₃-5-(CF₃)C₆H₃)P-κ²P,O]Pd(*syn*-2-CH₃norbornyl)NH(4-F-2-(OMe)C₆H₃) (8d**).** [*t*-Bu₂(2-(CH₃O)-5-(CF₃)C₆H₃)P]Pd(*syn*-2-CH₃norbornyl)Cl (11.4 mg, 0.0200 mmol) was dissolved in toluene-*d*₈ (0.6 ml) in a 1 dram vial. A solution of 4-fluoro-2-methoxyaniline (50 μl, 0.40 M, 0.020 mmol, 1.0 equiv) in toluene-*d*₈ was added to the vial with stirring. The reaction mixture was briefly chilled, then a solution of LiHMDS (50 μl, 0.40 M, 0.020 mmol, 1.0 equiv) in toluene-*d*₈

was added with stirring. The reaction mixture was briefly stirred at ambient temperature then transferred to a J-Young NMR tube. Spectra were acquired at ambient temperature. **¹H NMR** (600 MHz, Tol-*d*₈) δ 8.02 (d, *J* = 3.9 Hz, 1H), 7.17 (d, *J* = 8.7 Hz, 1H), 7.16 – 7.10 (m, 1H), 6.76 (td, *J* = 8.6, 2.7 Hz, 1H), 6.56 (d, *J* = 10.2 Hz, 1H), 6.19 (dd, *J* = 8.6, 3.7 Hz, 1H), 4.03 (s, 1H), 3.86 (dd, *J* = 17.7, 7.5 Hz, 1H), 3.65 (s, 3H), 3.49 (s, 3H), 2.39 (s, 1H), 2.21 (d, *J* = 9.8 Hz, 1H), 1.90 (s, 1H), 1.72 – 1.67 (m, 1H), 1.66 – 1.60 (m, 3H), 1.60 – 1.52 (m, 1H), 1.52 – 1.44 (m, 1H), 1.27 (dd, *J* = 10.8, 5.9 Hz, 1H), 1.21 – 1.11 (m, 18H), 1.05 (t, *J* = 9.8 Hz, 2H), 0.96 (d, *J* = 9.3 Hz, 1H). **¹⁹F NMR** (565 MHz, Tol-*d*₈) δ -62.6 (3F), -134.7 (br, 1F). **³¹P NMR** (243 MHz, Tol-*d*₈) δ 42.5.

Experimental Details for Table 2.1

Notes on compound selection, sample preparation, and corrections. Compounds designated as “controls” are various fluorine-containing arenes, phosphines, amines, and the Pd(II) chloride complex **7c**. Due to the excellent resolution of ¹⁹F NMR experiments, there were no complications involved with analyzing mixtures of compounds. Samples were prepared in dry and deoxygenated THF-*d*₈/THF mixtures (~10%). Samples of Pd(II) anilido complexes were prepared by the same reaction with 4-fluoro-2-methoxyaniline and NaOt-Bu described above for kinetic experiments, except the sample of **8c**, which was prepared by dissolving isolated **8c** in THF-*d*₈/THF. Complex **8c** was chosen for these experiments because the resonance from the fluorine atom in the ancillary P,O ligand of this complex is sharp, while the resonances from the fluorine atoms in the anilido ligands of **8a-d** are broad.

We observed that the linearity of the log*D* vs log*M* plot could be improved by correcting *M* to “*M**,” the molecular weight of the analogous compound with all fluorine atoms replaced by hydrogen atoms. This is logical because fluorination of organic compounds greatly increases the molecular weight without significantly altering the volume of the molecule.

Data acquisition parameters. Spectra were collected at 300 K (calibrated with an ethylene glycol/DMSO-*d*₆ standard) on a 500 MHz Bruker spectrometer. The DOSY experiment was performed with a gradient ramp from 1 to 95% in 16 exponentially spaced steps of 8-32 scans each (delay time 1.5 s), with 8 dummy scans. The Δ parameter d20 was 0.050 s for all experiments, and the δ/2 parameter p30 was varied from 0.0010 (low *M*) to 0.0030 s (high *M*) to account for the range of diffusion constants measured. In each case, p30 was set such that the signal was mostly attenuated by ~20 G·cm⁻¹.

Data analysis notes. Diffusion constants ($D/\text{m}^2\text{s}^{-1}$) were calculated by fitting the resulting integral (I) and gradient data ($G/\text{g}\cdot\text{cm}^{-1}$) to the function $f(t) = I = I_0 \exp(-DG^2\Delta^2g^2k^2(\Delta-\delta)/3)$ with $g = 25162.33/\text{G}^{-1}\text{s}^{-1}$, $k = 1$. The stock G values of the spectrometer were used without calibration. The fit was performed using the solver function in Microsoft Excel to vary I_0 and D to minimize the sum of squared residuals. Examples of experimental integral vs G and the data calculated from the fit are included for 4-fluoro-2-methoxyaniline, **2g**, **2i**, and **6** (Figure 2.15). In the case of **6**, the integrals of the two major ^{19}F NMR resonances were added together.

The resulting $\log D$ and $\log M^*$ data from control compounds was fit to a linear formula by the LINEST function in Microsoft Excel. The molecular weight of each compound was then calculated by applying this linear formula and adding $18 \times \text{\#fluorine}$, and “error” is defined as calculated M – expected M . The full set of data used for this analysis and the resulting calculated M vs expected M plot are included below in Table 2.8 and Figure 2.16.

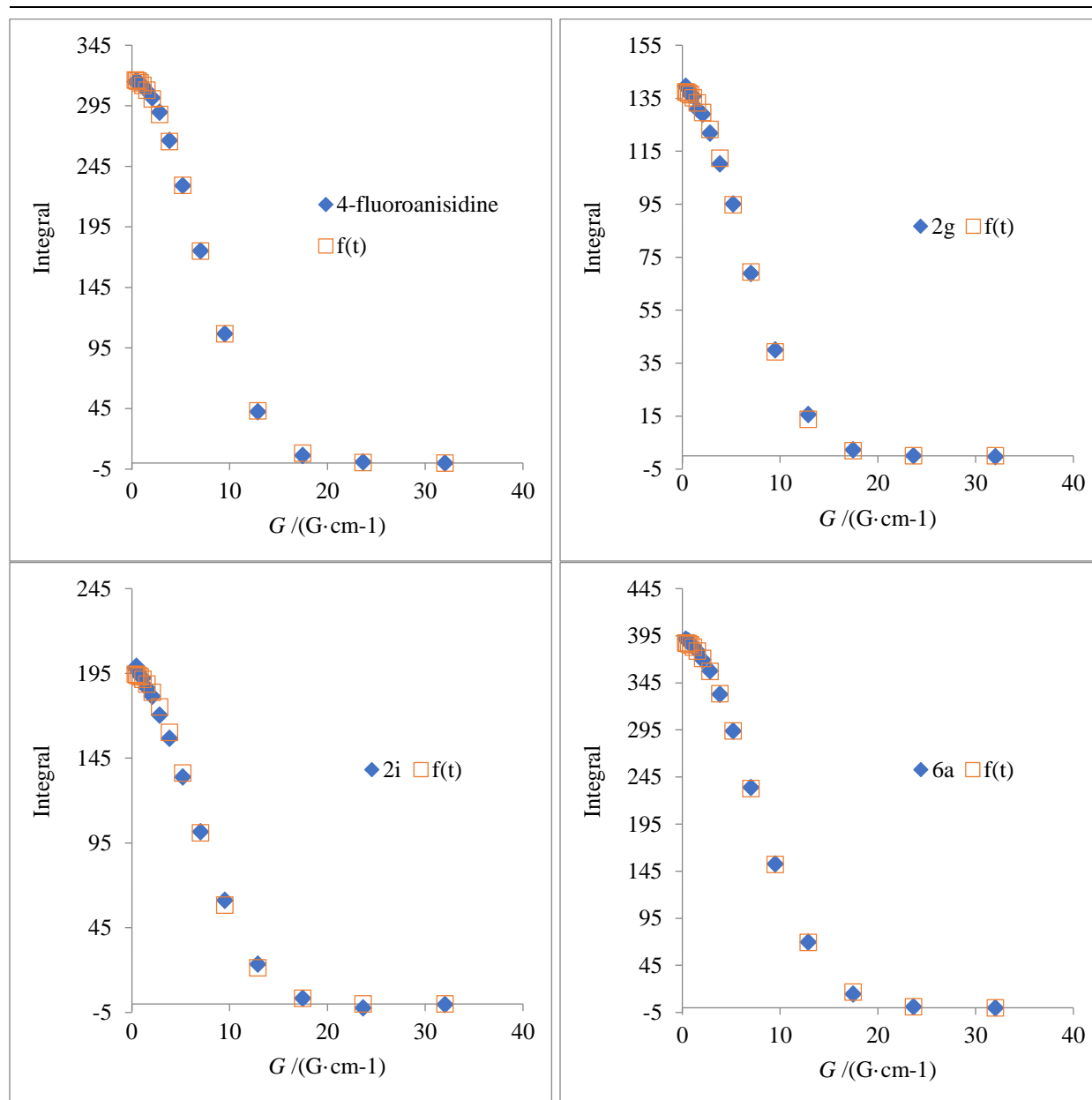


Figure 2.15. Example integral vs gradient (G) plots (DOSY).

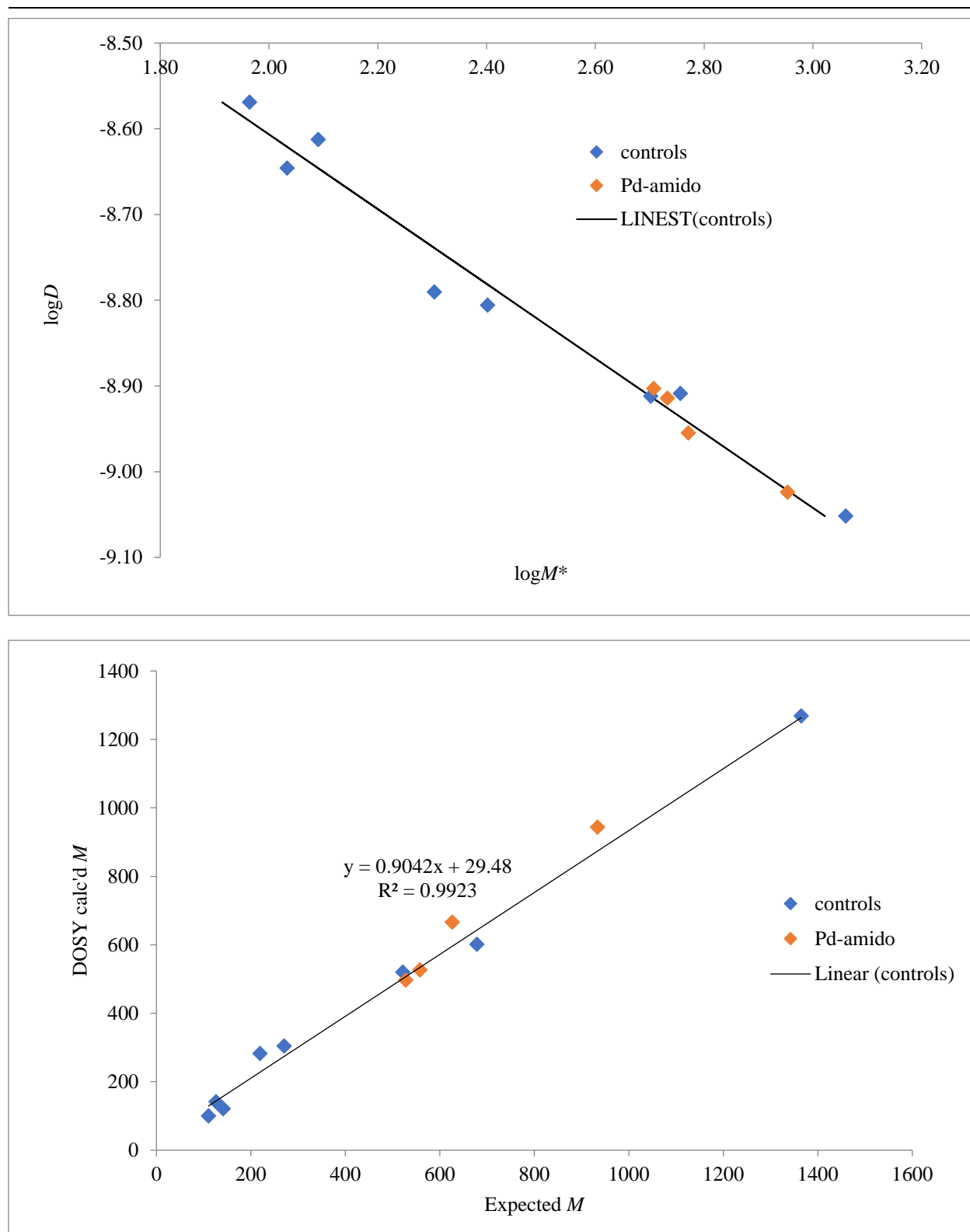


Figure 2.16. $\log(D)$ vs $\log(M^*)$ plot and comparison of expected and calculated molecular weights (DOSY).

Table 2.8. Full data for Table 2.1.

entry	compound	expected M	M^*	$D \cdot 10^9 / \text{m}^2\text{s}^{-1}$	calc'd M	error
1	4-fluoro-2-methoxyaniline	141	123	2.44	121	-20
2	di- <i>tert</i> -butyl(5-fluoro-2-methoxyphenyl)phosphine	270	252	1.56	304	+34
3	BTFM MandyPhos	1365	1149	0.887	1268	-96
4	PTFM JosiPhos	678	570	1.23	601	-77
5	7c	521	503	1.22	520	-1
6	4-fluorotoluene	110	92	2.70	100	-10
7	3g	219	201	1.62	282	+63
8	3-fluoroaniline	126	108	2.26	141	+15
9	2i	558	540	1.22	527	-31
10	6	934	898	0.947	943	+9
11	2g	528	510	1.25	497	-31
12	8c	626	590	1.11	666	+40

Entries 1-8 are “controls”

Entries 9-12 are “Pd-amido” complexes

Controls LINEST(log D , log M^*): $m = -2.30(16)$, $b = -17.8(15)$

Note: Because $D = kT/(6\pi\eta r_s)$ and $M \propto r_s^3$ (for a sphere of constant density), the slope of a log D vs log M plot is expected to be -3. Considering that these molecules are not spherical, and molecular weight is only approximately proportional to volume, the slope of -2.3 from the experimental data is reasonable.

Experimental Details for Scheme 2.2, Table 2.2, Figure 2.1, and Figure 2.2

Reagent notes. All organic compounds were used as stock solutions in the reaction solvent. The internal standard and amine solutions were measured with a glass micro syringe; the ligand and base solutions were measured with an adjustable-volume pipettor.

General procedure for sample preparation (1H**).** In an N₂-filled glovebox, (*t*-Bu₃P)Pd(*syn*-2-CH₃norbornyl)(Cl) (**1**) (18.1 mg, 0.0399 mmol), arylamine (100 μ l, 0.42 M in THF-*d*₈, 0.042 mmol, 1.0 equiv), 1,3,5-trimethoxybenzene (100 μ l, 0.40 M in THF-*d*₈, 0.040 mmol, 1.0 equiv), and *t*-Bu₃P (300 μ l, 0.40 M in THF-*d*₈, 0.12 mmol, 3.0 equiv) were mixed in a 1 dram vial. The reaction mixture was briefly chilled in a 0 °C cold well, after which time NaOt-Bu (200 μ l, 0.40 M in THF-*d*₈, 0.080 mmol, 2.0 equiv) was added slowly with stirring. The mixture was then transferred to a J-Young NMR tube, which was sealed and kept in an ice bath until injection into the spectrometer.

Data acquisition notes. Spectra were acquired in a 500 or 600 MHz Avance series Bruker NMR spectrometer set to maintain a constant temperature. The noted reaction temperature refers to that calibrated with an ethylene glycol sample within one week of the experiment (either neat or 80% in dms-*d*₆). NMR spectrometer acquired spectra with a 90° pulse and 1-4 scans per timepoint at set intervals of 1-4 minutes (varied depending on the signal-to-noise ratio and half-life).

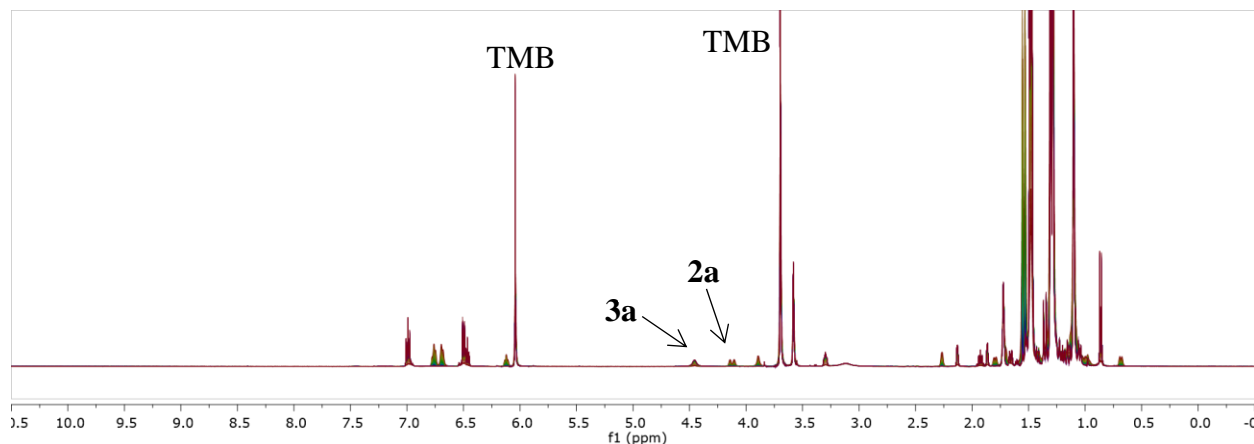
Data analysis notes. Concentrations of Pd(II)-anilide complexes were determined by integration against the internal standard. First-order rate constants were calculated by fitting the plotted data to the formula $f(t) = A \cdot \exp(-k_{\text{RE}} \cdot t) + C$ using the solver function in Microsoft Excel to vary A , k_{RE} , and C to minimize the sum of squared residuals. The constant “ C ” term was included in analysis of ^1H NMR spectra due to overlapping impurities and imperfect baseline corrections. The data from five half-lives were used in the fit. The values of A , k_{RE} , and C are noted for each experiment in Table 2.9 and Table 2.11. The free energy of activation was calculated as $\Delta G^\ddagger = -RT \cdot \ln(k_{\text{RE}} \cdot h / (k_{\text{B}} \cdot T))$. These experiments were replicated, and the results were averaged.

Modifications for ^{19}F NMR spectroscopy kinetic experiments. In cases where the anilide ligand contains a fluorine atom (**2d**, **2g**, and **2i**), the reaction was monitored by ^{19}F NMR spectroscopy. THF was substituted for THF- d_8 , and 4-fluorotoluene was substituted for 1,3,5-trimethoxybenzene as the internal standard in these experiments. Spectra were acquired with the lock off. If necessary, the spectra were aligned during processing to remove drift. The constant “ C ” term in the fit was set to 0 as the ^{19}F NMR spectra do not contain significant overlapping peaks, and the quality of the baselines were good.

Modifications for compound **2i (Figure 2.2, Table 2.11).** Reaction mixtures were prepared with **1** (18.1 mg, 0.0399 mmol), 4-fluoro-2-methoxyaniline (100 μL , 0.40 M, 0.040 mmol, 1.0 equiv), $t\text{-Bu}_3\text{P}$ (x μL , 0.40 M), 4-fluorotoluene (100 μL , 0.40 M or 0.50 M, 0.040 mmol or 0.050 mmol, 1.0 equiv or 1.25 equiv), THF (300- x μL), and NaOt-Bu (200 μL , 0.40 M, 0.080 mmol, 2.0 equiv).

Identification of intermediates and products. For **2a**, **2b**, **2c**, **2e**, **2f**, and **2h**: ^1H , ^{31}P , and ^1H - ^{13}C HSQC NMR spectra were acquired at ambient temperature from the samples prepared as described above prior to heating, and ^1H and ^{31}P spectra were also acquired at ambient temperature after the kinetic experiment was completed. For **2d** and **2g**: ^1H , ^{19}F , ^{31}P , and ^1H - ^{13}C HSQC NMR spectra were acquired from separate samples prepared in THF- d_8 (similar procedure at 0.010 mmol scale). For **2i**: this compound was characterized more extensively at 263 K in Tol- d_8 to fully assign the ^1H NMR spectrum (*vide supra*).

Examples of superimposed NMR spectra, concentration vs time plots, and fitting to exponential decay are included below in Figure 2.17 and 18.



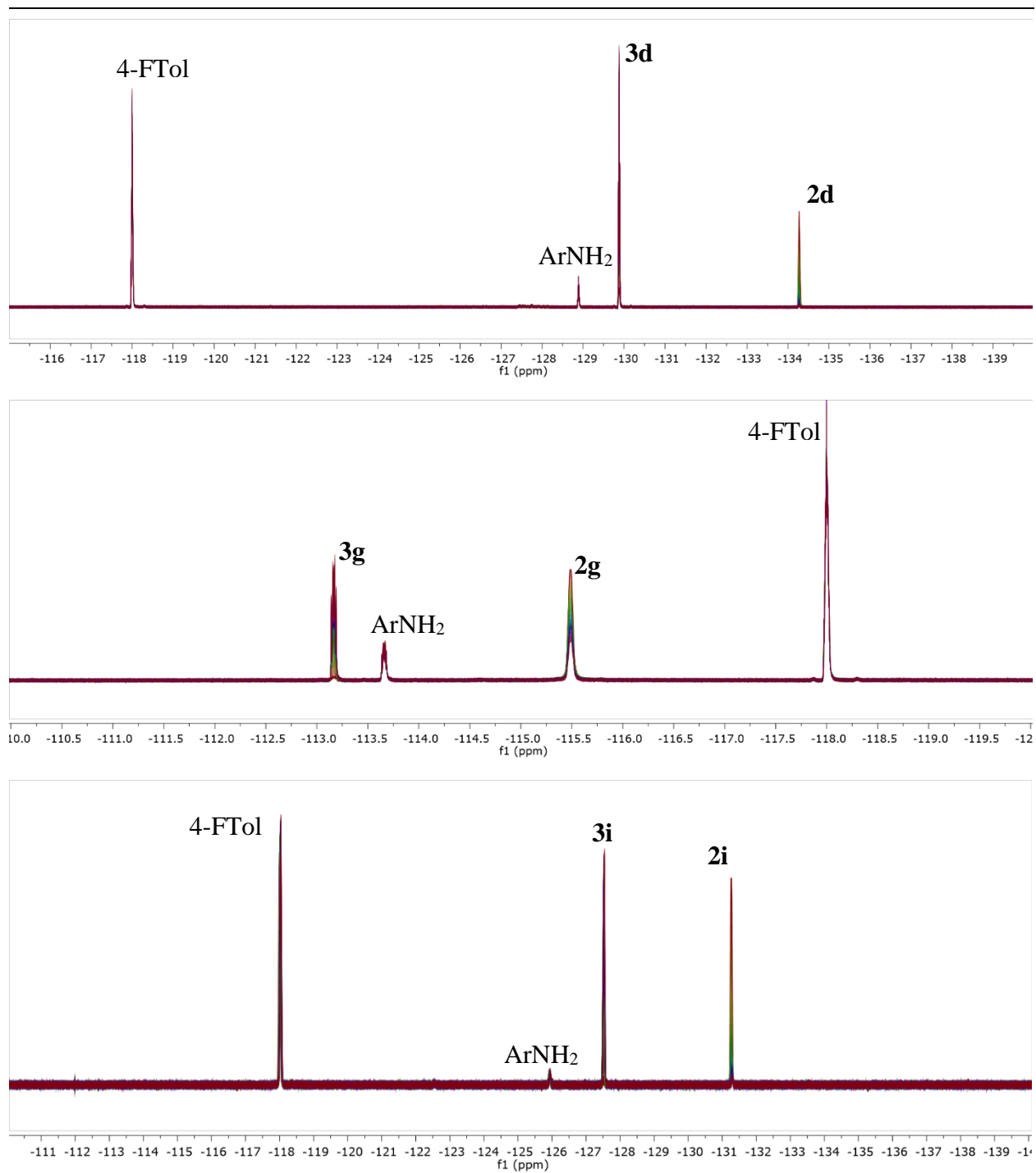


Figure 2.17. Superimposed ^1H NMR spectra for the decay of **2a** and superimposed ^{19}F NMR spectra for the decay of **2d**, **2g**, and (referenced to 4-FTol at -118.0 ppm).

Table 2.9. Full data for Table 2.2 and Figure 2.1.

entry	X (complex)	time /h	% yield 2a-h	% yield 3a-h ^a	A /M	k_{RE} /10 ⁻⁴ s ⁻¹	C /M	ΔG^\ddagger /kcalmol ⁻¹
1	H (2a)	5	85	74 (63)	0.0485	2.45	0.0019	23.5
			91	97 (88)	0.0493	2.74	-0.0004	23.5
			72	99 (71)	0.0400	10.5	0.0040	22.6
2	4-OMe (2b)	1	70	100 (70)	0.0429	11.6	0.0013	22.6
			85	82 (70)	0.0411	12.8	0.0017	22.5
3	4-Me (2c)	2	89	83 (74)	0.0513	4.72	0.0044	23.1
			89	93 (83)	0.0426	6.02	0.0021	23.0
4	4-F (2d)	5	78	92 (72)	0.0428	2.62	-	23.5
			90	88 (79)	0.0425	2.57	-	23.5
5	3-Me (2e)	5	91	90 (82)	0.0467	2.80	0.00074	23.5
			93	97 (90)	0.0473	3.41	0.0019	23.3
6	3-OMe (2f)	6	79	84 (66)	0.0445	2.09	0.0013	23.6
			92	97 (89)	0.0420	2.56	0.014	23.5
7	3-F (2g)	40	83	76 (63)	-	0.512	-	24.5
			88	77 (68)	-	0.586	-	24.4
8	2- <i>t</i> -Bu (2h)	6	88	60 (53)	0.0487	2.50	-0.0008	25.5
			84	58 (49)	0.0452	2.49	-0.0005	25.4

^aThe yields of **3a-h** reported are based on the initial concentrations of the corresponding intermediates **2a-h**; (the yields of **3a-h** based on **1** are in parentheses).

Table 2.10. Hammett parameters.⁴⁷

entry	X (complex)	ln($k_{RE}X/k_{RE}H$)	σ_p	σ_{p+}	σ_{p-}	σ_m
1	H (2a)	0	-	-	-	-
2	4-OMe (2b)	0.652	-0.27	-0.78	-0.26	
3	4-Me (2c)	0.317	-0.17	-0.31	-0.17	
4	4-F (2d)	0.001	0.06	-0.07	-0.03	
5	3-Me (2e)	0.079				-0.07
6	3-OMe (2f)	-0.047				0.12
7	3-F (2g)	-0.674				0.34

Entry 2. The % yield of **2b** is an underestimation due to the reaction beginning to occur before the first spectrum was acquired. The result for the third replicate (85% yield) is more accurate, because the first spectrum was acquired at 0 °C.

Entry 7. This complex reacted very slowly at 40 °C. The rate constant was calculated from a linear fit of ln([**2g**]) vs time using 5 hours (1.3 half-lives) of data. The tube was then heated in an oil bath at 40 °C for the remaining 35 hours, after which another ¹⁹F NMR spectrum was acquired to determine the yield of **3g**.

Entry 9. This complex did not significantly react at 40 °C. Therefore, the experiment was performed at 65 °C.

Table 2.11. Full data for Figure 2.2.

entry	[<i>t</i> -Bu ₃ P] /M	<i>T</i> /K	time /h	% yield 2i	% yield 3i ^a	<i>A</i> /M	<i>k</i> _{RE} /10 ⁻⁴ s ⁻¹	Δ <i>G</i> [‡] /kcal·mol ⁻¹
1	0.0571	323	1.5	88	97 (85)	0.0478	7.82	23.5
2	0.0857	“	“	87	100 (87)	0.0479	7.54	23.5
3	0.114	“	“	86	103 (89)	0.0486	7.28	23.5
4	0.143	“	“	88	103 (91)	0.0503	7.99	23.5
5	0.171	“	“	89	102 (91)	0.0492	8.12	23.5
6	“	313	4.0	91	100 (91)	0.0494	2.67	23.4
7	“	320	1.5	86	100 (86)	0.0485	5.88	23.5
8	“	326	1.25	85	106 (90)	0.0490	9.09	23.6
9	“	333	0.75	84	105 (88)	0.0508	18.3	23.7

^aThe yields of **3i** reported are based on the initial concentrations of the corresponding intermediate **2i**; (the yields of **3i** based on **1** are in parentheses).

For entries 1-5: average $k_{\text{RE}} = 7.9 \pm 0.3 \cdot 10^{-4} \text{ s}^{-1}$.

For entries 5-9: the slope, intercept, and uncertainties used for the calculations of activation parameters below were obtained by fitting the data to the linear function $\ln(k_{\text{RE}}/T) = m \cdot (1/T) + b$ with the LINEST function in Microsoft Excel.

$$m = -\Delta H^{\ddagger}/R = -9642(17) \text{ K}$$

$$\Delta H^{\ddagger} = 80(5) \text{ kJ/mol} = 19.2(12) \text{ kcal/mol}$$

$$b = \ln(k_{\text{B}}/h) + \Delta S^{\ddagger}/R = 16.9(19)$$

$$\Delta S^{\ddagger} = -57(16) \text{ J/(mol} \cdot \text{K)} = -14(4) \text{ eu}$$

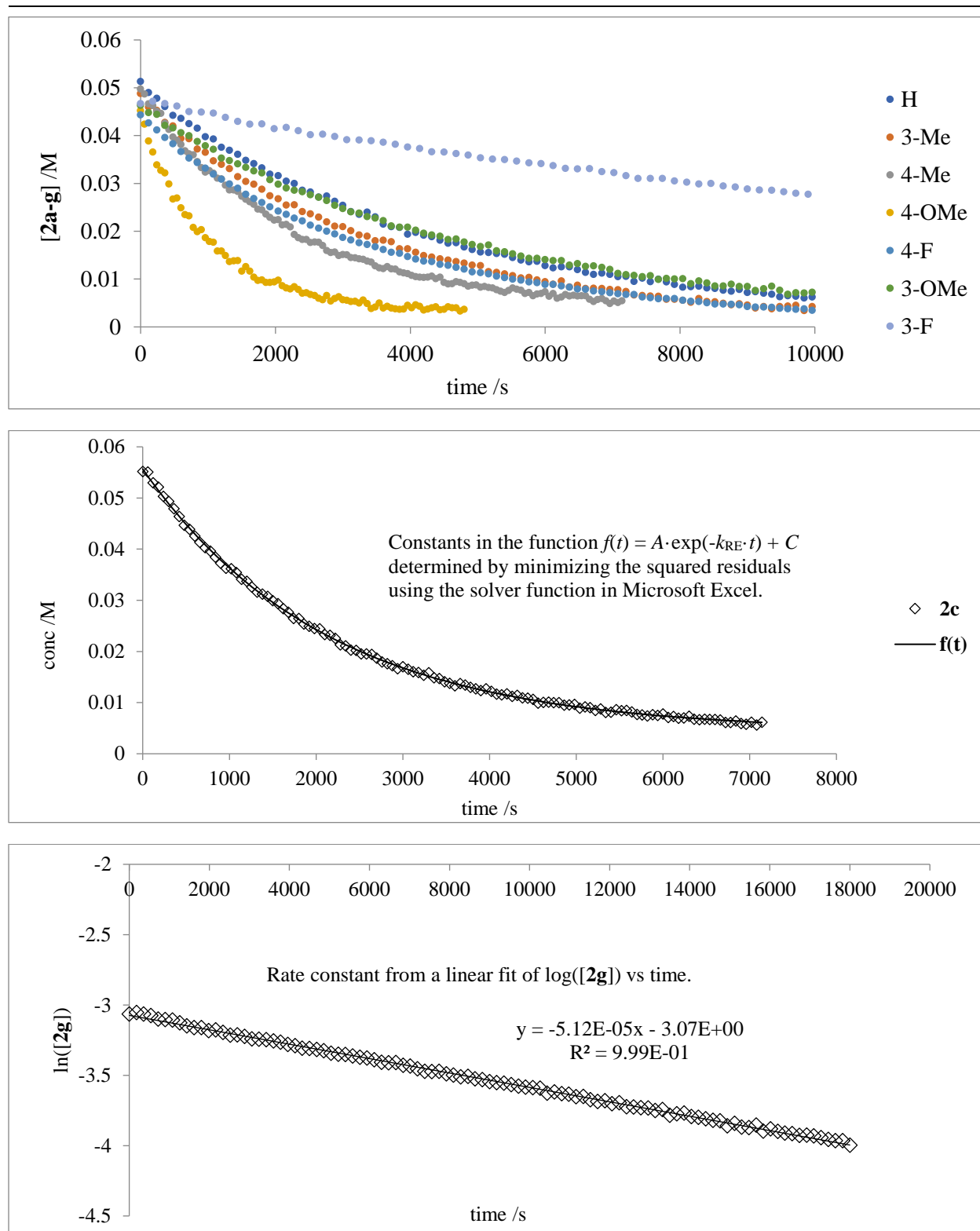


Figure 2.18. Concentration vs time plots for the decay of **2a-g** at 40 °C and examples of fitting methods to determine first-order rate constants (k_{RE}).

Experimental Details for Scheme 2.3 and Scheme 2.4

With NaOt-Bu in THF: In an N₂-filled glovebox, (*t*-Bu₂PhP)Pd(2-CH₃norbornyl)Cl **4a** (9.5 mg, 0.020 mmol), *t*-Bu₂PhP (150 μ l, 0.40 M, 0.060 mmol, 3.0 equiv), 4-fluoro-2-methoxyaniline + 4-fluorotoluene (50 μ l, 0.40 M in both, 0.020 mmol, 1.0 equiv), and THF (1.7 ml) were mixed in a 1 dram vial. NaOt-Bu (100 μ l, 0.40 M, 0.040 mmol, 2.0 equiv) was added slowly with stirring. An aliquot (~0.7 ml) was then transferred to an NMR tube, which was sealed with a cap and parafilm. ¹⁹F (90° pulse, delay time = 20 s) and ³¹P NMR spectra were acquired, and the yield of the major Pd-amido species **6** was determined by integration of the ¹⁹F resonances against 4-fluorotoluene. The vial containing the remainder of the sample was sealed with a PTFE-lined cap and PTFE tape and then heated at 65 °C in an aluminum block. After 3 h, the sample was removed from the heating block, and a second aliquot was taken for ¹⁹F and ³¹P NMR analysis. The yield of **3i** was determined by integrating against 4-fluorotoluene and is based on **4**.

This experiment was duplicated, and the yields were averaged: trial 1: 34% yield **6**, 74% yield **3i**; trial 2: 25% yield **6**, 76% yield **3i**.

With LiHMDS in Tol: In an N₂-filled glovebox, Pd-Cl **4** (300 μ l, 0.033 M, 0.010 mmol), *t*-Bu₂PhP (75 μ l, 0.40 M, 0.030 mmol, 3.0 equiv), 4-fluoro-2-methoxyaniline + 4-fluorotoluene (25 μ l, 0.40 M in both, 0.020 mmol, 1.0 equiv), and Tol (575 μ l) were mixed in a 1 dram vial. LiHMDS (25 μ l, 0.40 M, 0.010 mmol, 1.0 equiv) was added slowly with stirring. The solution was then transferred to a J-Young NMR tube, which was sealed. ¹⁹F (90° pulse, delay time = 60 s) and ³¹P NMR spectra were acquired, and the yield of the major Pd-amido species **6** was determined by integration of the ¹⁹F resonances against 4-fluorotoluene. The reaction mixture was then heated at 65 °C in an aluminum block. After 3 h, the sample was removed from the heating block, and a second set of ¹⁹F and ³¹P NMR spectra were acquired. The yield of **3i** was determined by integrating against 4-fluorotoluene and is based on **4**.

This experiment was duplicated, and the yields were averaged: trial 1: 63% yield **6**, 51% yield **3i**; trial 2: 64% yield **6**, 38% yield **3i**.

Experimental Details for Table 2.3 and Figure 2.3

Sample preparation. In an N₂-filled glovebox, (*t*-Bu₂PhP)Pd(2-CH₃norbornyl)Cl **4a** (47.3 mg, 0.0999 mmol), *t*-Bu₂PhP (22.3 mg, 0.100 mmol, 1.0 equiv), 4-fluoroanisidine (250 μ l, 0.40 M, 0.10 mmol, 1.0 equiv), 4-fluorotoluene (250 μ l, 0.40 M, 0.10 mmol, 1.0 equiv), were mixed in a 1 dram vial. NaOt-Bu (0.50 ml, 0.40 M, 0.20 mmol, 2.0 equiv) was added slowly with stirring. An aliquot (200 μ l, 0.020 mmol Pd) of this solution was transferred to a J-Young NMR tube. Additional *t*-Bu₂PhP (0, 150, or 400 μ l; 0.40 M; 0, 0.060, or 0.16 mmol; 0, 3, or 8 equiv) and THF (500, 350, or 100 μ l) were then added to the NMR tube. The samples were kept in an ice bath until injection into the spectrometer.

Data acquisition notes. Spectra were acquired in a 500 MHz Avance series Bruker NMR spectrometer set to maintain a constant temperature. The noted reaction temperature of 323 K was calibrated with an ethylene glycol sample (80% in DMSO-*d*₆). The NMR spectrometer acquired spectra with a 90° pulse and 4 scans per timepoint at set intervals of 1 minute. After 60 minutes of data had been collected, the sample was heated in an aluminum heating block at 50 °C for an

additional 23 h. Another ^{19}F NMR spectrum was then acquired, and the yield of **3i** was determined by integration against 4-fluorotoluene.

Data analysis notes. The concentrations of Pd-amido **6** and norbornylamine **3i** were determined by integration against 4-fluorotoluene. Plots of [**3i**] vs time were fit using the LINEST function in Microsoft Excel using the data from 0-15% yield (0.0040 M) of **3i**. Initial rates (R) were determined from the slopes of these plots, and the order in [$t\text{-Bu}_2\text{PhP}$] was calculated from the slope of a $\ln(R)$ vs $\ln([t\text{-Bu}_2\text{PhP}])$. The initial [$t\text{-Bu}_2\text{PhP}$] was approximated as $(1.5 + \text{additional equiv})(0.02/.7)$ M to account for the one equivalent added before the reaction to form **6** and the half equivalent which forms stoichiometrically with **6**. These are approximations, because unproductive decomposition to form $(t\text{-Bu}_2\text{PhP})_2\text{Pd}^0$ will reduce the concentration of available $t\text{-Bu}_2\text{PhP}$. These plots are shown below.

Reactions of (*t*-Bu₂CyP)Pd(2-CH₃norbornyl)Cl (**4b**)

Procedure. In an N₂-filled glovebox, (*t*-Bu₂CyP)Pd(2-CH₃norbornyl)Cl **4b** (20.1 mg, 0.0419 mmol, 1.04 equiv), 4-fluoro-2-methoxyaniline (100 μ l, 0.40 M, 0.040 mmol, 1.0 equiv), and THF (10% THF-*d*₈, 0.38 ml) were mixed in a 1 dram vial. NaOt-Bu (120 μ l, 0.40 M, 0.048 mmol, 1.2 equiv) was added slowly with stirring. The mixture was then transferred to an NMR tube, which was sealed with a cap and parafilm. The tube was kept in an ice bath until injection in the spectrometer. ¹⁹F NMR spectra (90° pulse) were acquired every 15 minutes for 1 hour.

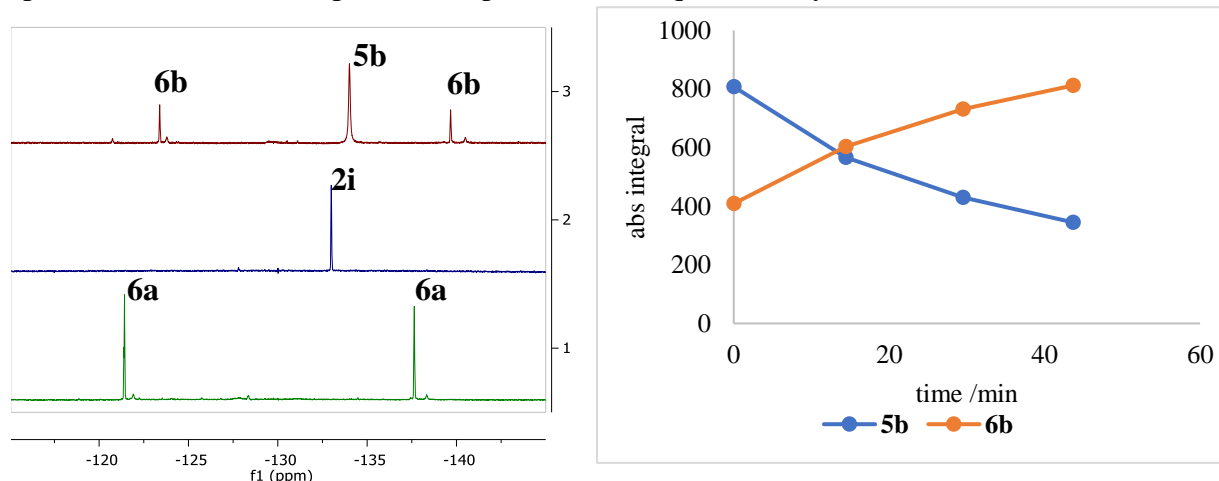
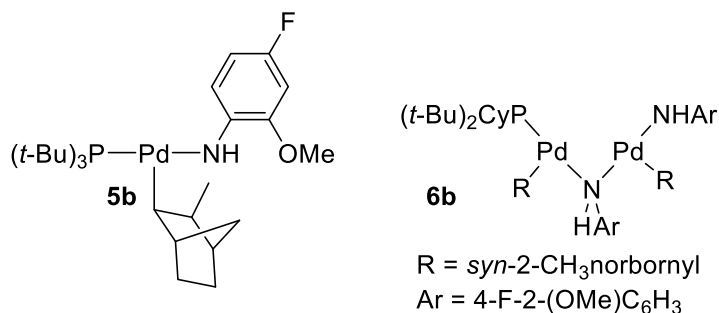


Figure 2.19. Formation of a mixture of *t*-Bu₂CyP-ligated Pd(I) anilido complexes. Left: ¹⁹F NMR spectrum (first time point) of the reaction mixture containing *t*-Bu₂CyP-ligated Pd(II) anilido complexes; ¹⁹F NMR spectra under similar conditions of **2i** and **6a** shown underneath for comparison. Right: Absolute integrals of peaks assigned as **5b** and **6b** vs time.



Proposed structures of complexes **5b** and **6b** by analogy to **2i** and **6a**.

Procedure. In an N₂-filled glovebox, (*t*-Bu₂CyP)Pd(2-CH₃norbonyl)Cl **4b** (19.2 mg, 0.0400 mmol), *t*-Bu₂CyP (28 mg, 0.12 mmol, 3.0 equiv), 4-fluoro-2-methoxyaniline (100 μ l, 0.40 M, 0.040 mmol, 1.0 equiv), 4-fluorotoluene (100 μ l, 0.40 M, 0.040 mmol, 1.0 equiv), and THF (0.27 ml) were mixed in a 1 dram vial. NaO*t*-Bu (200 μ l, 0.40 M, 0.080 mmol, 2.0 equiv) was added slowly with stirring. The mixture was then transferred to an NMR tube, which was sealed with a cap and parafilm. ¹⁹F NMR kinetic data was acquired at 60 °C as previously described (see details for Table 2.2).

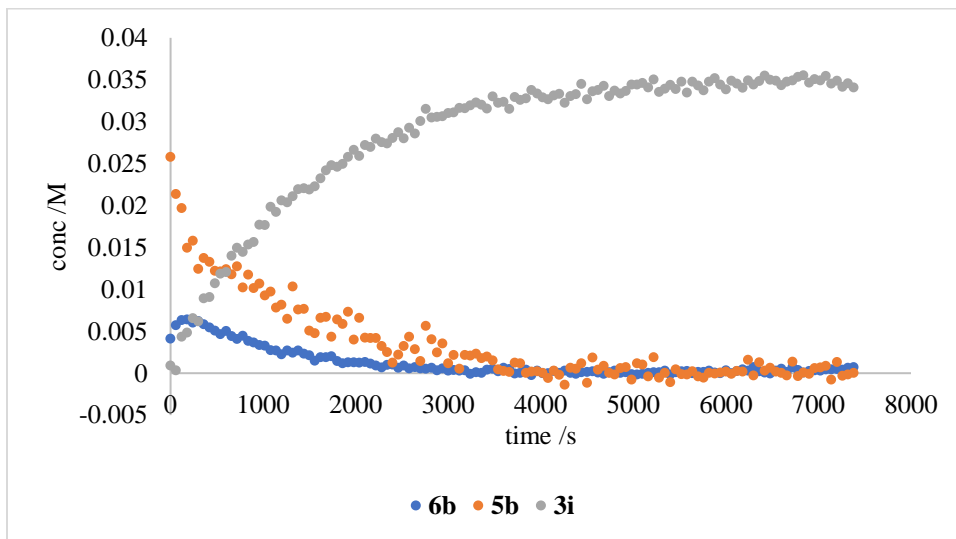


Figure 2.20. Reductive elimination of **3i** from a mixture of *t*-Bu₂CyP-ligated Pd(II) anilido complexes; 61% yield of **3i** after 2 h.

Experimental Details for Scheme 2.5

Procedure. In an N₂-filled glovebox, Pd-Cl **7a-e** (0.020 mmol), the corresponding phosphine (0.040 mmol, 2.0 equiv), 4-fluoroanisidine + 4-fluorotoluene (50 μ l, 0.40 M in both, 0.020 mmol, 1.0 equiv), and toluene (1.9 ml) were mixed in a 1 dram vial. LiHMDS (50 μ l, 0.40 M, 0.020 mmol, 1.0 equiv) was added slowly with stirring. After stirring for approximately 10 min at ambient temperature, an aliquot (~0.7 ml) was transferred to an NMR tube, which was sealed with a rubber septum and parafilm. ¹⁹F (90° pulse, delay time = 60 s) and ³¹P NMR spectra were acquired from this sample within an hour from adding LiHMDS, and the yield of **8a-e** was determined by integration of the ¹⁹F resonance against 4-fluorotoluene. The vial containing the remainder of the solution was sealed with a Teflon cap and tape and heated at 65 °C in an aluminum block. After the noted time, the sample was moved back inside an N₂-filled glovebox, and another aliquot was taken for a second NMR sample. The yield of **3i** was determined by integration of the ¹⁹F resonance against 4-fluorotoluene and is based on **8**. Each experiment was duplicated, and the yields were averaged.

Table 2.12. Full data for Scheme 2.5.

entry	complex	mass 7 /mg	mass phosphine /mg	time /h	% yield 8a-f trial 1, 2	% yield 3i trial 1, 2 (based on 7)
1	7a	10.1	10.1	48	89, 88	65 (58), 65 (57)
2	7b	13.2	16	48	85, 85	62 (53), 51 (43)
3	7c	10.4	11	14	87, 88	53 (46), 51 (45)
4	7d	11.4	13	14	88, 91	89 (78), 78 (71)
5	7e	12.2	15	14	89, 91	92 (82), 92 (84)
6	7f	14.6	16	48	~83, ~81	0, 0

Experimental Details for Table 2.4

Sample preparation. In an N₂-filled glovebox, Pd-amido **8a-e** (0.020 mmol), the corresponding phosphine (0.060 mmol, 3.0 equiv), 4-fluorotoluene (50 μ l, 0.40 M, 0.020 mmol, 1.0 equiv), and THF (0.65 ml) were mixed in a 1-dram vial. The mixture was then transferred to a J-Young NMR tube, which was sealed and kept in an ice bath until injection into the spectrometer.

Data acquisition notes. Spectra were acquired in a 500 MHz Avance series Bruker NMR spectrometer set to maintain a constant temperature. The noted reaction temperature of 338 K was calibrated with an ethylene glycol sample (80% in DMSO-*d*₆). The NMR spectrometer acquired spectra with a 90° pulse and 2-8 scans per timepoint at set intervals of 1-6 minutes (varied depending on the signal-to-noise ratio and half-life). After at least one half-life of data had been collected, the sample was heated in an aluminum heating block at 65 °C for the remainder of the reaction time (noted). Another ¹⁹F NMR spectrum was then acquired, and the yield of **3i** was determined by integration against 4-fluorotoluene.

Data analysis notes. Concentrations of Pd-amido complexes **8a-e** were determined by integration against 4-fluorotoluene. Plots of ln([**8**]) vs time were fit using the LINEST function in Microsoft Excel using one half-life of data. First order rate constants were determined from

the slopes of these plots, and the free energy of activation was calculated as $\Delta G^\ddagger = -RT \cdot \ln(k_{\text{RE}} \cdot h / (k_{\text{B}} \cdot T))$. The **[8]** and $\ln(\text{[8]})$ vs times plots and the results of LINEST fits are included below. The uncertainty in k_{RE} (from LINEST) is reported in parentheses; however, this value is an underestimation. The experiment from entry 1 was replicated 9 months later using a different spectrometer (entry 2), and the difference between these two experiments provides a better indication of the error in k_{RE} .

Modification for entry 5. Because we were unable to obtain crystalline samples of complex **8d**, this complex was prepared *in situ* from **7d** (11.4 mg, 0.0200 mmol), di-*tert*-butyl(5-(trifluoromethyl)-2-methoxyphenyl)phosphine (19.0 mg, 0.0593 mmol, 2.97 equiv), 4-fluoroanisidine (50 μl , 0.40 M, 0.020 mmol, 1.0 equiv), NaOt-Bu (100 μl , 0.40 M, 0.040 mmol, 2.0 equiv), and 4-fluorotoluene (50 μl , 0.40 M, 0.020 mmol, 1.0 equiv).

Table 2.13. Full data for Table 2.4.

entry	complex	mass Pd /mg	mass L /mg	$k_{\text{RE}} \cdot 10^{-5} (\sigma) / \text{s}^{-1}$	ΔG^\ddagger /kcal·mol ⁻¹	time /h	% yield
1	8a	12.2	15.1	2.52(1), 2.90(2)	27.0, 26.9	40	47, 39
3	8b	15.3	24.4	2.853(6)	26.9	40	53
4	8c	12.5	16	25.2(8)	25.4	8	31
5	7d	11.4	19.0	14.35(14)	25.8	10	69
6	8e	14.3	21.6	17.96(10)	25.7	10	67

Note: The data from entry 4 were also fit to an exponential function $f(t) = A \cdot \exp(-k_{\text{RE}} \cdot t) + C$ by minimizing the sum of squared residuals (five half-lives of data, see the analysis of data for Table 2.1). This alternative analysis gave the following parameters: $A = 0.0193 \text{ M}$, $k_{\text{RE}} = 1.46 \cdot 10^{-4} \text{ s}^{-1}$, $C = 0.00065 \text{ M}$, and $\Delta G^\ddagger = 25.8 \text{ kcal/mol}$. These values agree well with those determined from the linear fit of $\ln(\text{[8d]})$ vs time.

Note: The yields of **3i** from these reactions of isolated samples of **8a-e** in THF are lower than the yields of **3i** from reactions of samples of **8a-e** prepared *in situ* in Tol (Scheme 2.5, Table 2.12). The majority of this unproductive decomposition appears to occur during the initial preparation of the samples and at later reaction times (possibly due to small leaks in the seals of the NMR tubes). However, this unproductive decomposition appears to be minimal during the timeframe used for determination of k_{RE} ($[\text{3i}] \approx [\text{8}]_0 - [\text{8}]$, see Figure 2.S-7) for all complexes except for **8c**.

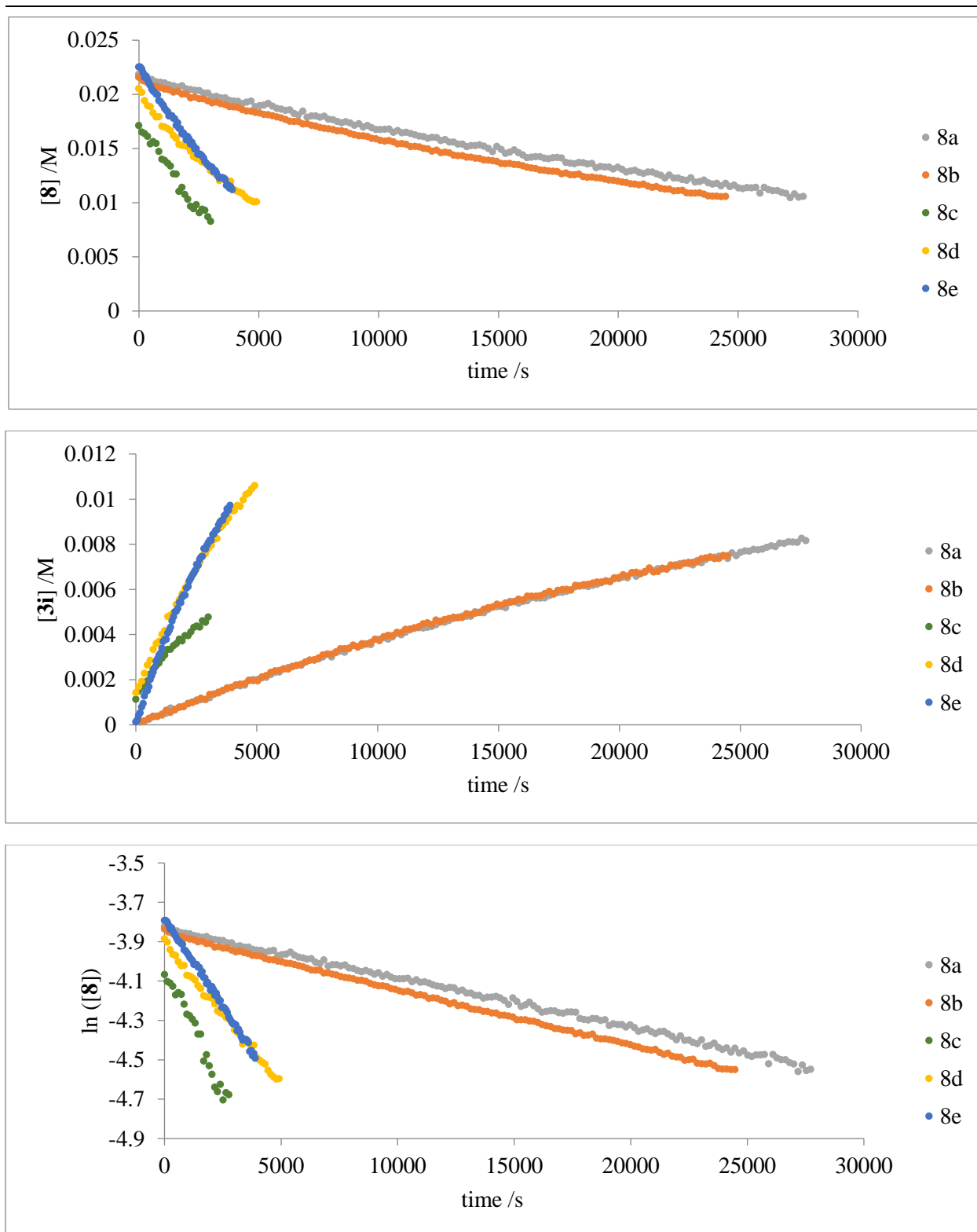


Figure 2.21. Concentration vs time and $\ln([8])$ vs time plots for the reductive elimination of **3i** from **8a-e** (Table 2.3).

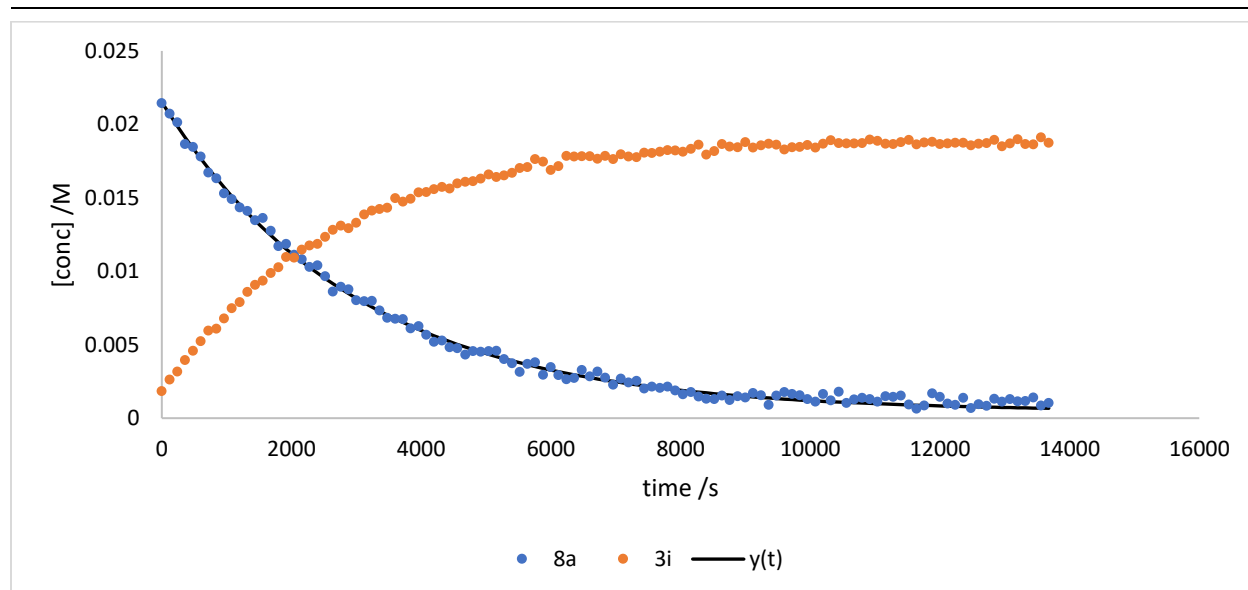


Figure 2.22. Reaction of **8a** in Tol-*d*₈. Same procedure as above (Table 2.11, entry 1), except at 89 °C in Tol-*d*₈, rate constant determined by fitting 5 half-lives of data to the exponential decay function $y(t) = A \cdot \exp(-k_{\text{RE}} \cdot t) + C$ by minimizing the squared residuals using the solver function in Microsoft Excel. $A = 0.0210$, $k_{\text{RE}} = 3.3 \cdot 10^{-4} \text{ s}^{-1}$, $C = 0.00046$, $\Delta G_{\text{RE}}^\ddagger = 27.1 \text{ kcal/mol}$. 65% yield of **3i** at 4 h

X-ray Data

A single crystal was mounted on a Cryoloop with Paratone oil. Data were collected in a nitrogen gas stream at 100(2) K. The data were integrated using the Bruker SAINT software program and scaled using the SADABS software program. Solution by iterative methods (SHELXT-2014) produced a complete heavy-atom phasing model consistent with the proposed structure. All non-hydrogen atoms were refined anisotropically by full-matrix least-squares (SHELXL-2014). All hydrogen atoms were placed using a riding model. Their positions were constrained relative to their parent atom using the appropriate HFIX command in SHELXL-2014.

[*t*-Bu₂(*o*-anisyl)P- κ^2 P,O]Pd(*syn*-2-CH₃norbornyl)NH(4-F-2-(OMe)C₆H₃) (8a**)** (yellow prism). Crystal-to-detector distance was 50 mm and exposure time was 10 seconds per frame using a scan width of 2.0°. Data collection was 100.0% complete to 25.000° in θ . A total of 96975 reflections were collected covering the indices, $-9 \leq h \leq 9$, $-20 \leq k \leq 20$, $-25 \leq l \leq 25$. 5328 reflections were found to be symmetry independent, with an R_{int} of 0.0472. Indexing and unit cell refinement indicated a primitive, monoclinic lattice. The space group was found to be P 21/c (No. 14).

[(1-Ad)₂(*o*-anisyl)P- κ^2 P,O]Pd(*syn*-2-CH₃norbornyl)NH(4-F-2-(OMe)C₆H₃) (8b**)** (yellow prism). Crystal-to-detector distance was 40 mm and exposure time was 10 seconds per frame using a scan width of 2.0°. Data collection was 100.0% complete to 25.000° in θ . A total of 63247 reflections were collected covering the indices, $-12 \leq h \leq 12$, $-14 \leq k \leq 14$, $-17 \leq l \leq 17$. 6562 reflections were found to be symmetry independent, with an R_{int} of 0.0262. Indexing and unit cell refinement indicated a primitive, triclinic lattice. The space group was found to be P -1 (No. 2). Solution and refinement with SHELXL-2016.

[(1-Ad)₂(CH₃OCH₂CH₂)P- κ^2 P,O]Pd(*syn*-2-CH₃norbornyl)NH(4-F-2-(OMe)C₆H₃) (8e)
(yellow prism). Crystal-to-detector distance was 50 mm and exposure time was 20 seconds per frame using a scan width of 1.0°. Data collection was 100.0% complete to 25.000° in θ . A total of 57935 reflections were collected covering the indices, $-13 \leq h \leq 13$, $-14 \leq k \leq 14$, $-17 \leq l \leq 17$. 6182 reflections were found to be symmetry independent, with an R_{int} of 0.0667. Solution and refinement with SHELXL-2016.

Table 2.13. Crystal structure data.

Compound	8a	8b	8c
Empirical formula	C30 H45 F N O2 P Pd	C42 H57 F N O2 P Pd	C38 H57 F N O2 P Pd
Formula weight	608.04	764.25	716.21
Temperature (K)	100(2)	100(2)	100(2)
Wavelength (Å)	0.71073	0.71073	0.71073
Crystal system	Monoclinic	Triclinic	Triclinic
Space group	P 21/c	P -1	P -1
Unit cell lengths (Å)	a = 8.2454(7) b = 16.8060(14) c = 21.3582(18)	a = 10.5660(7) b = 12.3759(9) c = 14.7842(10)	a = 11.1182(13) b = 11.9143(14) c = 14.2549(16)
Unit cell angles (°)	α = 90 β = 99.868(2) γ = 90	α = 107.368(3) β = 101.454(3) γ = 94.717(4)	α = 70.103(2) β = 73.800(2) γ = 77.068(2)
Volume (Å ³)	2915.9(4)	1787.5(2)	1687.6(3)
Z	4	2	2
Density (calculated) (Mg/m ³)	1.385	1.420	1.409
Absorption coefficient (mm ⁻¹)	0.724	0.607	0.637
F(000)	1272	804	756
Crystal size (mm ³)	0.140 x 0.120 x 0.080	0.060 x 0.050 x 0.040	0.050 x 0.040 x 0.030
Theta range for data collection (°)	1.551 to 25.366	1.485 to 25.393	1.558 to 25.346
Index ranges	$-9 \leq h \leq 9$, $-20 \leq k \leq 20$, $-25 \leq l \leq 25$	$-12 \leq h \leq 12$, $-14 \leq k \leq 14$, $-17 \leq l \leq 17$	$-13 \leq h \leq 13$, $-14 \leq k \leq 14$, $-17 \leq l \leq 17$
Reflections collected	96975	63247	57935
Independent reflections	5328 [R(int) = 0.0472]	6562 [R(int) = 0.0262]	6182 [R(int) = 0.0667]
Completeness to theta = 25.000°	100.0%	100.0%	100.0%
Absorption correction	Semi-empirical from equivalents	Semi-empirical from equivalents	Semi-empirical from equivalents
Max. and min. transmission	0.862 and 0.759	0.745 and 0.708	0.928 and 0.832
Refinement method	Full-matrix least-squares on F ²	Full-matrix least-squares on F ²	Full-matrix least-squares on F ²
Data / restraints / parameters	5328 / 0 / 334	6562 / 0 / 436	6182 / 0 / 400
Goodness-of-fit on F ²	1.098	1.116	1.068
Final R indices [I > 2 σ (I)]	R1 = 0.0394, wR2 = 0.0886	R1 = 0.0291, wR2 = 0.0648	R1 = 0.0421, wR2 = 0.1020
R indices (all data)	R1 = 0.0449, wR2 = 0.0924	R1 = 0.0336, wR2 = 0.0687	R1 = 0.0525, wR2 = 0.1087
Extinction coefficient	n/a	n/a	n/a
Largest diff. peak and hole (e.Å ⁻³)	1.654 and -0.785	0.942 and -0.557	1.267 and -0.389

Table 2.14. Atomic coordinates ($\times 10^4$) and equivalent isotropic displacement parameters ($\text{\AA}^2 \times 10^3$) for **8a**. $U(\text{eq})$ is defined as one third of the trace of the orthogonalized U_{ij} tensor.

	x	y	z	$U(\text{eq})$
C(1)	4890(4)	7750(2)	4460(2)	24(1)
C(2)	4141(5)	7726(2)	3749(2)	35(1)
C(3)	4539(5)	8535(2)	3468(2)	40(1)
C(4)	6439(5)	8502(2)	3514(2)	36(1)
C(5)	6872(5)	7650(2)	3755(2)	35(1)
C(6)	5308(5)	7191(2)	3456(2)	39(1)
C(7)	6764(4)	7600(2)	4470(2)	28(1)
C(8)	7512(5)	6835(2)	4780(2)	36(1)
C(9)	2571(4)	5906(2)	3908(2)	25(1)
C(10)	952(4)	6187(2)	3805(2)	27(1)
C(11)	-186(4)	5996(2)	3261(2)	30(1)
C(12)	321(4)	5524(2)	2809(2)	29(1)
C(13)	1893(4)	5220(2)	2874(2)	26(1)
C(14)	3002(4)	5402(2)	3419(2)	25(1)
C(15)	5096(5)	4622(2)	3078(2)	35(1)
C(16)	2169(4)	7473(2)	6292(2)	20(1)
C(17)	1773(4)	7809(2)	6848(2)	27(1)
C(18)	861(4)	7401(2)	7233(2)	30(1)
C(19)	302(4)	6644(2)	7057(2)	29(1)
C(20)	656(4)	6294(2)	6513(2)	26(1)
C(21)	1616(4)	6699(2)	6138(1)	21(1)
C(22)	1541(5)	5555(2)	5450(2)	35(1)
C(23)	2126(4)	8887(2)	5470(2)	29(1)
C(24)	1212(5)	9283(2)	5953(2)	43(1)
C(25)	863(5)	8550(2)	4921(2)	52(1)
C(26)	3157(4)	9527(2)	5208(2)	28(1)
C(27)	5358(4)	8279(2)	6328(2)	23(1)
C(28)	5978(4)	7518(2)	6682(2)	29(1)
C(29)	6658(4)	8538(2)	5935(2)	30(1)
C(30)	5198(4)	8946(2)	6808(2)	31(1)
N(1)	3681(4)	6077(2)	4441(1)	27(1)
O(1)	2093(3)	6356(1)	5614(1)	26(1)
O(2)	4596(3)	5130(1)	3540(1)	31(1)
F(1)	-771(3)	5326(1)	2269(1)	41(1)
P(1)	3423(1)	7989(1)	5775(1)	17(1)
Pd(1)	3673(1)	7051(1)	5021(1)	22(1)

Table 2.15. Atomic coordinates ($\times 10^4$) and equivalent isotropic displacement parameters ($\text{\AA}^2 \times 10^3$) for **8b**. $U(\text{eq})$ is defined as one third of the trace of the orthogonalized U^{ij} tensor.

	x	y	z	U(eq)
C(1)	4104(2)	5771(2)	7291(2)	19(1)
C(2)	5490(2)	6501(2)	7737(2)	24(1)
C(3)	5291(2)	7576(2)	7430(2)	26(1)
C(4)	4970(3)	7246(2)	6321(2)	31(1)
C(5)	3521(3)	6669(3)	6006(2)	32(1)
C(6)	3245(2)	6616(2)	6973(2)	25(1)
C(7)	6049(2)	6783(2)	8831(2)	31(1)
C(8)	3958(2)	7797(2)	7651(2)	28(1)
C(9)	2146(2)	2625(2)	5893(2)	17(1)
C(10)	1683(2)	1330(2)	5364(2)	21(1)
C(11)	718(2)	1139(2)	4380(2)	23(1)
C(12)	1356(2)	1650(2)	3729(2)	24(1)
C(13)	1775(2)	2935(2)	4244(2)	24(1)
C(14)	592(2)	3514(2)	4445(2)	30(1)
C(15)	-51(2)	2991(2)	5089(2)	28(1)
C(16)	924(2)	3199(2)	6065(2)	23(1)
C(17)	2760(2)	3122(2)	5214(2)	21(1)
C(18)	-479(2)	1707(2)	4569(2)	27(1)
C(19)	4945(2)	2576(2)	7087(2)	19(1)
C(20)	5611(2)	2646(2)	8140(2)	25(1)
C(21)	7028(3)	2397(3)	8192(2)	31(1)
C(22)	6996(3)	1186(3)	7506(2)	36(1)
C(23)	6380(3)	1122(2)	6458(2)	32(1)
C(24)	7168(3)	1996(3)	6171(2)	33(1)
C(25)	7183(2)	3198(2)	6857(2)	28(1)
C(26)	5776(2)	3464(2)	6811(2)	25(1)
C(27)	4959(2)	1371(2)	6383(2)	27(1)
C(28)	7823(2)	3266(3)	7893(2)	32(1)
C(29)	2489(2)	2198(2)	7753(2)	18(1)
C(30)	2354(2)	1008(2)	7489(2)	23(1)
C(31)	1629(3)	394(2)	7907(2)	25(1)
C(32)	974(3)	974(2)	8582(2)	26(1)
C(33)	1117(2)	2149(2)	8880(2)	22(1)
C(34)	1893(2)	2760(2)	8495(2)	19(1)
C(35)	1583(3)	4518(2)	9620(2)	25(1)
C(36)	1988(2)	6924(2)	8950(2)	20(1)
C(37)	748(2)	6364(2)	8379(2)	22(1)
C(38)	-343(2)	6920(2)	8330(2)	24(1)
C(39)	-197(2)	8056(2)	8870(2)	23(1)
C(40)	994(2)	8661(2)	9449(2)	22(1)
C(41)	2074(2)	8110(2)	9472(2)	22(1)

C(42)	3503(3)	9847(2)	10435(2)	35(1)
N(1)	3064(2)	6401(2)	9045(1)	21(1)
O(1)	2108(2)	3938(1)	8808(1)	21(1)
O(2)	3317(2)	8633(1)	10001(1)	28(1)
F(1)	-1251(1)	8631(1)	8832(1)	33(1)
P(1)	3302(1)	3051(1)	7134(1)	16(1)
Pd(1)	3277(1)	4898(1)	8067(1)	17(1)

Table 2.16. Atomic coordinates ($\times 10^4$) and equivalent isotropic displacement parameters ($\text{\AA}^2 \times 10^3$) for **8e**. $U(\text{eq})$ is defined as one third of the trace of the orthogonalized U^{ij} tensor.

	x	y	z	$U(\text{eq})$
C(1)	5967(3)	6997(3)	6247(3)	19(1)
C(2)	5201(4)	5937(3)	6542(3)	21(1)
C(3)	4136(4)	6515(4)	5955(3)	25(1)
C(4)	3287(4)	7520(4)	6374(3)	31(1)
C(5)	4101(4)	8557(4)	5942(4)	35(1)
C(6)	5359(4)	7986(4)	5398(3)	28(1)
C(7)	5921(4)	4779(4)	6315(3)	27(1)
C(8)	4861(4)	7238(4)	4927(3)	28(1)
C(9)	8044(3)	5319(3)	8438(3)	15(1)
C(10)	8389(4)	5301(3)	9421(3)	19(1)
C(11)	8217(4)	4072(3)	10236(3)	23(1)
C(12)	6830(4)	3885(3)	10494(3)	23(1)
C(13)	6475(4)	3897(3)	9529(3)	21(1)
C(14)	7310(4)	2875(3)	9127(3)	26(1)
C(15)	8697(4)	3046(3)	8880(3)	24(1)
C(16)	8892(4)	4270(3)	8059(3)	20(1)
C(17)	6656(3)	5104(3)	8701(3)	17(1)
C(18)	9063(4)	3049(4)	9840(3)	26(1)
C(19)	7673(3)	8148(3)	7729(3)	16(1)
C(20)	7737(4)	9175(3)	6702(3)	20(1)
C(21)	7247(4)	10410(3)	6898(3)	24(1)
C(22)	8061(4)	10613(3)	7521(3)	27(1)
C(23)	7965(4)	9612(3)	8553(3)	25(1)
C(24)	6585(4)	9646(3)	9136(3)	26(1)
C(25)	5787(4)	9432(3)	8512(3)	23(1)
C(26)	6287(3)	8194(3)	8331(3)	19(1)
C(27)	8465(4)	8383(3)	8359(3)	21(1)
C(28)	5872(4)	10429(4)	7481(3)	27(1)
C(29)	10012(3)	6730(3)	6988(3)	20(1)
C(30)	10667(3)	6203(4)	6109(3)	21(1)
C(31)	10756(4)	6550(4)	4366(3)	23(1)

C(32)	7940(4)	7564(4)	3547(3)	23(1)
C(33)	8222(4)	8704(4)	3437(3)	28(1)
C(34)	8296(4)	9632(4)	2518(4)	37(1)
C(35)	8077(5)	9419(4)	1701(3)	40(1)
C(36)	7793(4)	8325(4)	1747(3)	31(1)
C(37)	7720(4)	7426(4)	2651(3)	24(1)
C(38)	7201(5)	6111(4)	1927(3)	37(1)
N(1)	7902(3)	6649(3)	4396(2)	17(1)
O(1)	10036(2)	6809(2)	5292(2)	19(1)
O(2)	7443(3)	6302(3)	2783(2)	29(1)
F(1)	8150(4)	10309(3)	784(2)	70(1)
P(1)	8276(1)	6727(1)	7332(1)	14(1)
Pd(1)	7896(1)	6746(1)	5828(1)	14(1)

2.5 References and notes

Contributions:

Experimental results – D. Matthew Peacock

Computational results – Quan Jiang advised by Professor Thomas R. Cundari, University of North Texas

1. Driver, M. S.; Hartwig, J. F., *J. Am. Chem. Soc.* **1997**, *119* (35), 8232-8245.
2. Yamashita, M.; Hartwig, J. F., *J. Am. Chem. Soc.* **2004**, *126* (17), 5344-5345.
3. Pendleton, I. M.; Pérez-Temprano, M. H.; Sanford, M. S.; Zimmerman, P. M., *J. Am. Chem. Soc.* **2016**, *138* (18), 6049-6060.
4. Pérez-Temprano, M. H.; Racowski, J. M.; Kampf, J. W.; Sanford, M. S., *J. Am. Chem. Soc.* **2014**, *136* (11), 4097-4100.
5. Camasso, N. M.; Canty, A. J.; Ariafield, A.; Sanford, M. S., *Organometallics* **2017**, *36* (22), 4382-4393.
6. Koo, K.; Hillhouse, G. L., *Organometallics* **1995**, *14* (9), 4421-4423.
7. Pawlikowski, A. V.; Getty, A. D.; Goldberg, K. I., *J. Am. Chem. Soc.* **2007**, *129* (34), 10382-10393.
8. Rucker, R. P.; Whittaker, A. M.; Dang, H.; Lalic, G., *J. Am. Chem. Soc.* **2012**, *134* (15), 6571-6574.
9. Lin, B. L.; Clough, C. R.; Hillhouse, G. L., *J. Am. Chem. Soc.* **2002**, *124* (12), 2890-2891.
10. Catellani, M.; Del Rio, A., *Russ. Chem. Bull.* **1998**, *47* (5), 928-931.
11. Lautens, M.; Paquin, J. F.; Piguel, S.; Dahlmann, M., *J. Org. Chem.* **2001**, *66* (24), 8127-34.
12. Pan, J.; Su, M.; Buchwald, S. L., *Angew Chem Int Ed Engl* **2011**, *50* (37), 8647-51.
13. Marquard, S. L.; Rosenfeld, D. C.; Hartwig, J. F., *Angew. Chem.* **2010**, *122* (4), 805-808.
14. Hanley, P. S.; Marquard, S. L.; Cundari, T. R.; Hartwig, J. F., *J. Am. Chem. Soc.* **2012**, *134* (37), 15281-15284.
15. Low, J. J.; Goddard, W. A., *J. Am. Chem. Soc.* **1986**, *108* (20), 6115-6128.
16. Mann, G.; Shelby, Q.; Roy, A. H.; Hartwig, J. F., *Organometallics* **2003**, *22* (13), 2775-2789.
17. Attempts to isolate a crystalline sample of complex 6 were unsuccessful.

18. Tolman, C. A., *Chem. Rev.* **1977**, 77 (3), 313-348.
19. The substituent contributions to the Tolman electronic parameter are 0, 4.3, and, 0.1 for *t*-Bu, Ph, and Cy, respectively.
20. DiCosimo, R.; Whitesides, G. M., *J. Am. Chem. Soc.* **1982**, 104 (13), 3601-3607.
21. Tatsumi, K.; Nakamura, A.; Komiya, S.; Yamamoto, A.; Yamamoto, T., *J. Am. Chem. Soc.* **1984**, 106 (26), 8181-8188.
22. Hartwig, J. F., *Inorg. Chem.* **2007**, 46 (6), 1936-1947.
23. Gusev, D. G., *Organometallics* **2009**, 28 (22), 6458-6461.
24. Kelly III, R. A.; Clavier, H.; Giudice, S.; Scott, N. M.; Stevens, E. D.; Bordner, J.; Samardjiev, I.; Hoff, C. D.; Cavallo, L.; Nolan, S. P., *Organometallics* **2008**, 27 (2), 202-210.
25. We also synthesized the complex [Ad₂PCH₂(2-(5-BrC₅H₃N))][Pd(2-CH₃norbornyl)(Cl)] to test whether decreasing the basicity of the pyridine donor would enable reductive elimination to occur. However, only trace formation of **3i** was detected in reactions of this complex (see the experimental section for details).
26. Gaussian 09, Revision D.01, M.J. Frisch, G.W. Trucks, H.B. Schlegel, G.E. Scuseria, M.A. Robb, J.R. Cheeseman, G. Scalmani, V. Barone, B. Mennucci, G.A. Petersson, H. Nakatsuji, M. Caricato, X. Li, H.P. Hratchian, A.F. Izmaylov, J. Bloino, G. Zheng, J.L. Sonnenberg, M. Hada, M. Ehara, K. Toyota, R. Fukuda, J. Hasegawa, M. Ishida, T. Nakajima, Y. Honda, O. Kitao, H. Nakai, T. Vreven, J.A. Montgomery, Jr., J.E. Peralta, F. Ogliaro, M. Bearpark, J.J. Heyd, E. Brothers, K.N. Kudin, V.N. Staroverov, R. Kobayashi, J. Normand, K. Raghavachari, A. Rendell, J. C. Burant, S.S. Iyengar, J. Tomasi, M. Cossi, N. Rega, J.M. Millam, M. Klene, J.E. Knox, J.B. Cross, V. Bakken, C. Adamo, J. Jaramillo, R. Gomperts, R.E. Stratmann, O. Yazyev, A.J. Austin, R. Cammi, C. Pomelli, J.W. Ochterski, R.L. Martin, K. Morokuma, V.G. Zakrzewski, G.A. Voth, P. Salvador, J.J. Dannenberg, S. Dapprich, A.D. Daniels, O. Farkas, J.B. Foresman, J.V. Ortiz, J. Cioslowski, D.J. Fox, Gaussian, Inc., Wallingford CT, 2013.
27. Becke, A. D., *J. Chem. Phys.* **1993**, 98 (7), 5648-5652.
28. Cundari, T. R.; Stevens, W. J., *J. Chem. Phys.* **1993**, 98 (7), 5555-5565.
29. Stevens, W. J.; Basch, H.; Krauss, M., *J. Chem. Phys.* **1984**, 81 (12), 6026-6033.
30. Stevens, W. J.; Krauss, M.; Basch, H.; Jasien, P. G., *Can. J. Chem.* **1992**, 70 (2), 612-630.
31. Marenich, A. V.; Cramer, C. J.; Truhlar, D. G., *J. Phys. Chem. B* **2009**, 113 (18), 6378-6396.
32. Bondi, A., *J. Phys. Chem.* **1964**, 68 (3), 441-451.
33. Attempts to locate a transition state structure in which the Pd-O distance is within the sum of the VdW radii were unsuccessful.
34. Yamashita, M.; Cuevas Vicario, J. V.; Hartwig, J. F., *J. Am. Chem. Soc.* **2003**, 125 (52), 16347-16360.
35. The rate constants for reductive elimination for **2b** and **2c** were calculated at 263 K, assuming an entropy of activation of -14 eu. Solvent effects are expected to be small.
36. Arthur, K. L.; Wang, Q. L.; Bregel, D. M.; Smythe, N. A.; O'Neil, B. A.; Goldberg, K. I.; Moloy, K. G., *Organometallics* **2005**, 24 (19), 4624-4628.
37. Crumpton-Bregel, D. M.; Goldberg, K. I., *J. Am. Chem. Soc.* **2003**, 125 (31), 9442-9456.
38. Brown, M. P.; Puddephatt, R. J.; Upton, C. E. E., *J. Chem. Soc., Dalton Trans.* **1974**, (22), 2457-2465.
39. Roy, S.; Puddephatt, R. J.; Scott, J. D., *J. Chem. Soc., Dalton Trans.* **1989**, (11), 2121-2125.

-
40. Kirmse, W.; Hartmann, M.; Siegfried, R.; Wroblowsky, H.-J.; Zang, B.; Zellmer, V., *Chem. Ber.* **1981**, *114* (5), 1793-1808.
 41. Moriconi, E. J.; Crawford, W. C., *J. Org. Chem.* **1968**, *33* (1), 370-378.
 42. Goerlich, J. R.; Schmutzler, R., *Phosphorus, Sulfur Silicon Relat. Elem.* **1995**, *102* (1-4), 211-215.
 43. Köllhofer, A.; Plenio, H., *Chem. Eur. J.* **2003**, *9* (6), 1416-1425.
 44. Romines, K. R.; Freeman, G. A.; Schaller, L. T.; Cowan, J. R.; Gonzales, S. S.; Tidwell, J. H.; Andrews, C. W., 3rd; Stammers, D. K.; Hazen, R. J.; Ferris, R. G.; Short, S. A.; Chan, J. H.; Boone, L. R., *J. Med. Chem.* **2006**, *49* (2), 727-39.
 45. Bornand, M.; Chen, P., *Angew. Chem. Int. Ed.* **2005**, *44* (48), 7909-7911.
 46. Lindner, E.; Meyer, S.; Wegner, P.; Karle, B.; Sickinger, A.; Steger, B., *J. Organomet. Chem.* **1987**, *335* (1), 59-70.
 47. Hansch, C.; Leo, A.; Taft, R. W., *Chem. Rev.* **1991**, *91* (2), 165-195.

CHAPTER 3

Reductive elimination of *N*-neopentylamines and *N*-neopentylbenzophenone
imines from neopentylpalladium(II) complexes

3.1 Introduction

As discussed in the previous chapter of this dissertation, reductive elimination to form sp^3 carbon–nitrogen bonds from alkylmetal complexes is a potentially important but poorly understood fundamental organometallic reaction. All previously published examples of this reaction have been limited to those occurring from high-valent metal centers¹⁻⁷ or the highly specialized benzylpalladium(II)⁸ and *syn*-2-methylnorbornylpalladium(II)⁹ complexes investigated by the Hartwig group (Figure 3.1). There are no reported examples of isolated low-valent metal complexes that undergo reductive elimination of alkylamines bearing unstabilized,¹⁰ primary alkyl groups on nitrogen. Furthermore, the examples of well characterized, high-valent, primary alkylmetal complexes that undergo this reaction are limited to metallacycles.^{1-2, 5, 7} Reductive elimination of alkylamines from complexes containing non-chelating primary alkyl ligands (excluding methyl) has not been reported.

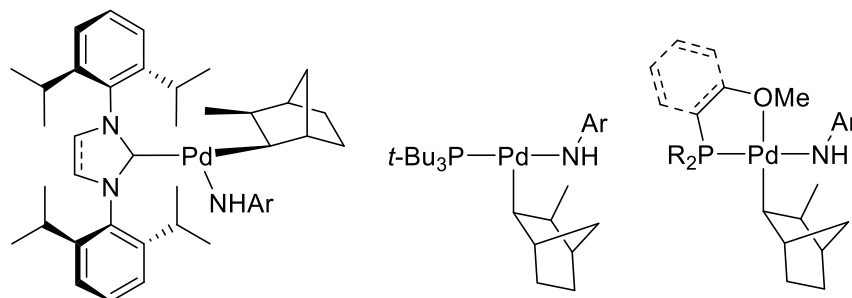
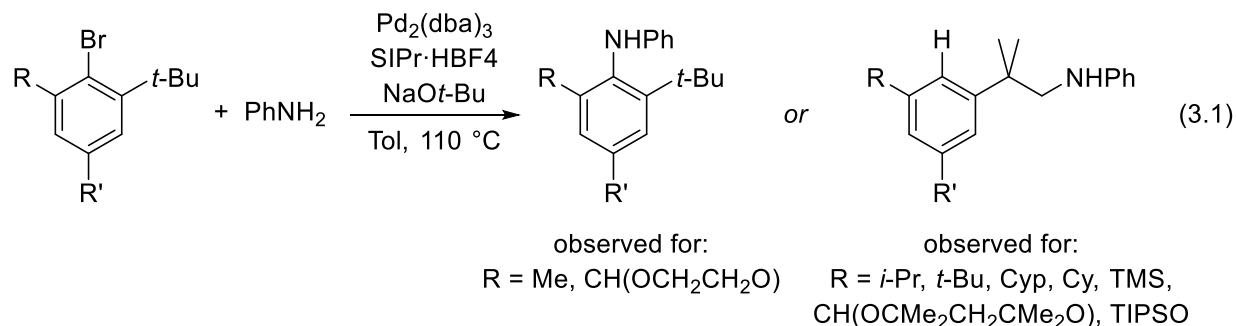


Figure 3.1. *Syn*-2-methylnorbornylpalladium(II) amido complexes that undergo reductive elimination to form sp^3 C–N bonds.

Despite the rarity of this reaction, reductive elimination from primary alkylpalladium complexes to form alkylamines could be a key bond-forming step in synthetically valuable catalytic reactions. Palladium-catalyzed C–H amination reactions have been proposed to involve reductive elimination from either Pd(II)¹¹⁻¹³ or Pd(IV)¹⁴ intermediates, and an improved understanding of this fundamental organometallic reaction should enable the further development of palladium-catalyzed reactions.

Primary alkylpalladium(II) complexes can undergo rapid β -hydride elimination reactions, and this decomposition pathway complicates their synthesis and limits their utility in catalytic reactions.¹⁵⁻¹⁷ The simplest primary alkyl group lacking β -hydrogens is the neopentyl group ($-\text{CH}_2-t\text{-Bu}$). Published, isolated neopentylpalladium(II) complexes have not undergone reductive elimination of amines,¹⁸⁻¹⁹ but some reported synthetic methods suggest that this reaction might occur as part of the mechanism of catalytic reactions. Buchwald et al. reported that 2-*tert*-butylaryl bromides undergo palladium-catalyzed cross coupling with anilines to form *N*-alkyl anilines (Equation 3.1).^{13, 20} This product could form by a formal migration of palladium from the aryl carbon to the neopentyl primary carbon and reductive elimination, but the proposed alkylpalladium(II) intermediate was not isolated or observed. Other reported catalytic reactions suggest that carbon–carbon,²¹⁻²⁵ carbon–boron,²⁶ and carbon–halogen²⁷⁻³⁵ bond-forming reductive elimination might occur from similar neopentylpalladium(II) intermediates. These examples demonstrate that neopentylpalladium(II) amido complexes would serve as a valuable model of intermediates in a variety of proposed catalytic reactions.



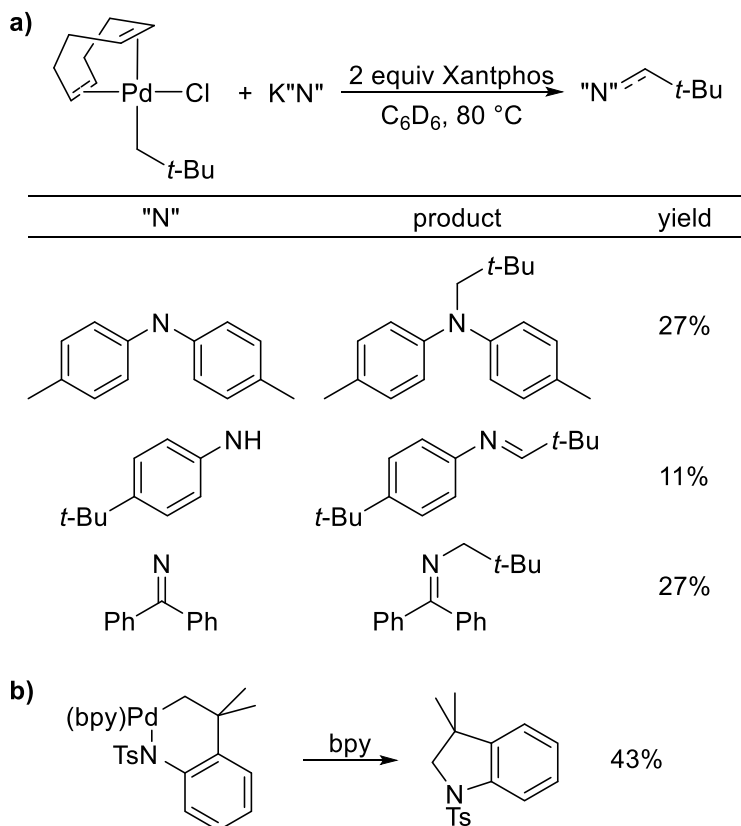
This chapter describes the synthesis and characterization of stable neopentylpalladium(II) anilido and methyleneamido complexes that undergo reductive elimination to form *N*-neopentyl amines and imines. The use of a weakly chelating P,O bidentate ligand simultaneously increased the yields of Pd(II) amido complexes, enabled the isolation of these complexes in pure, crystalline form, and allowed reductive elimination to occur under mild conditions.

3.2 Results and discussion

Previous, unpublished work in the Hartwig group explored the reactions of 1,5-cyclooctadiene (COD) neopentylpalladium(II) chloride with commercially available phosphine ligands and nitrogen nucleophiles, and *N*-neopentyl products were detected in reaction mixtures containing the bisphosphine ligand Xantphos (Scheme 3.1a).³⁶ However, the yields of the *N*-alkyl amine and imine products from these reactions did not exceed 30%. Reactions of azametallacyclic complexes were also explored (Scheme 3.1b); however, the yield of the *N*-alkylsulfonamide was still low, and the intermediate Pd(II) sulfonamidate complex was not fully characterized.³⁶

More recently, we sought to apply the understanding gained from studying reactions of *syn*-2-methylnorbornylpalladium(II) complexes to discover neopentylpalladium(II) complexes that undergo reductive elimination of alkylamines in good yields. As part of the work described in Chapter 2, we observed that tri-*tert*-butylphosphine (*t*-Bu₃P)-ligated complexes reacted at mild temperatures (40–65 °C) and that the yields of reactions with 2-methoxyanilines were higher than the yields of reactions with other aniline derivatives. Therefore, we attempted the synthesis of a *t*-Bu₃P-ligated neopentylpalladium(II) 2-methoxyanilido complex.

Scheme 3.1. Unpublished prior results of reductive elimination to form primary sp^3 C–N bonds from primary alkylpalladium(II) complexes.

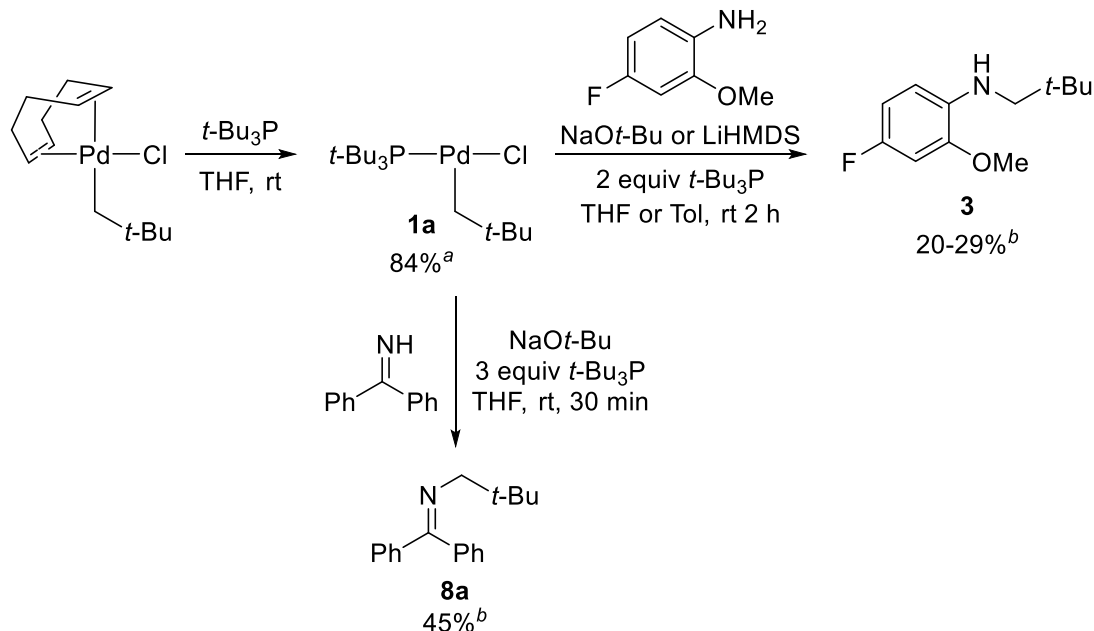


The known complex (COD)neopentylpalladium(II) chloride reacted with tri-*tert*-butylphosphine ($t\text{-Bu}_3\text{P}$) at ambient temperature in THF to form ($t\text{-Bu}_3\text{P}$)Pd(neopentyl)Cl **1a** (Scheme 3.2). Complex **1a** was stable and crystallized as red-orange needles in 84% yield. The *cis* relationship between the phosphine and the neopentyl group was confirmed by ^1H NMR nuclear Overhauser effect spectroscopy (NOESY). Complex **1a** reacted with 4-fluoro-2-methoxyaniline and base (NaOt-Bu or LiHMDS) in THF or toluene with 2 equivalents of $t\text{-Bu}_3\text{P}$ at ambient temperature to form *N*-neopentyl-2-methoxy-4-fluoroaniline (**3**), albeit in a modest 20-29% yield. Complex **1a** also reacted with benzophenone imine, NaOt-Bu , and $t\text{-Bu}_3\text{P}$ at ambient temperature to form *N*-neopentylbenzophenone imine (**8a**) in 45% yield.

The intermediate amido complexes in these reactions decomposed rapidly at ambient temperature and did not form cleanly from the Pd(II) chloride precursor **1a**. These factors complicated analyses of the structure and reactivity of these complexes. As part of the work described in Chapter 2, we synthesized the bidentate ligands $t\text{-Bu}_2(2\text{-OCH}_3\text{-5-(CF}_3\text{)C}_6\text{H}_3\text{)P}$ and $\text{Ad}_2\text{PCH}_2\text{CH}_2\text{OCH}_3$ (Figure 3.2), and we found that Pd(II) chloride complexes containing these ligands reacted to form stable, four-coordinate *syn*-2-methylnorbornylpalladium(II) amido complexes. Despite the stability of these complexes, they underwent reductive elimination to form alkylamines in good yields. These two ligands revealed two strategies to increase the rate and yield of reductive elimination from four-coordinate complexes: adding an electron-

withdrawing substituent (CF_3) to the ancillary ligand backbone or increasing the flexibility of the linker between P and O (aliphatic vs aryl). We envisioned that these ancillary ligands could enable the synthesis of stable neopentylpalladium(II) amido complexes that undergo reductive elimination of neopentylamines in good yields.

Scheme 3.2. Reductive elimination of *N*-neopentylamine **3** and *N*-neopentylbenzophenone imine **8a** from *t*-Bu₃P-ligated complexes.



^aIsolated yield. ^bYield determined by ¹H or ¹⁹F NMR spectroscopy with 1,3,5-trimethoxybenzene (TMB) or 4-fluorotoluene (4-FTol) as internal standard; average of two experiments.

The four-coordinate, palladium(II) anilido complexes (**L1**- $\kappa^2\text{P,O}$]Pd(neopentyl)(NHAr) (**2b**) and (**L2**- $\kappa^2\text{P,O}$]Pd(neopentyl)(NHAr) (**2c**) (with Ar=4-F-2-(OCH₃)C₆H₃) were synthesized from (COD)Pd(neopentyl)Cl by a two-step procedure that is similar to that described above (Scheme 3.3). Complex **2b**, bearing the more rigid ligand Ad₂(2-OCH₃-5-(CF₃)C₆H₃)P (**L1**)³⁷ containing an aryl linker, was stable for ca. 1 h at ambient temperature and was isolated in 73% yield. The geometry of **2b** in the solid state was determined by X-ray diffraction to be a slightly distorted square plane (Figure 3.3). The bond lengths and bond angles around the palladium center in **2b** were similar to those previously reported for (P,O)Pd(2-CH₃norbornyl)(NHAr) complexes (see Chapter 2). The correlations observed in the 2D ¹H NMR NOE spectrum of **2b** in C₆D₆ were consistent with this four-coordinate structure, implying that the solution-phase structure is similar to that in the solid state.

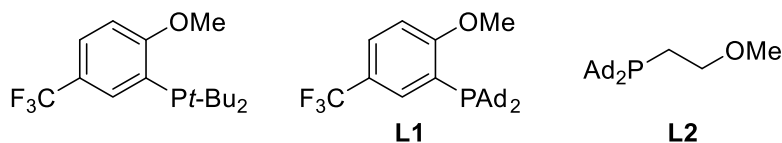
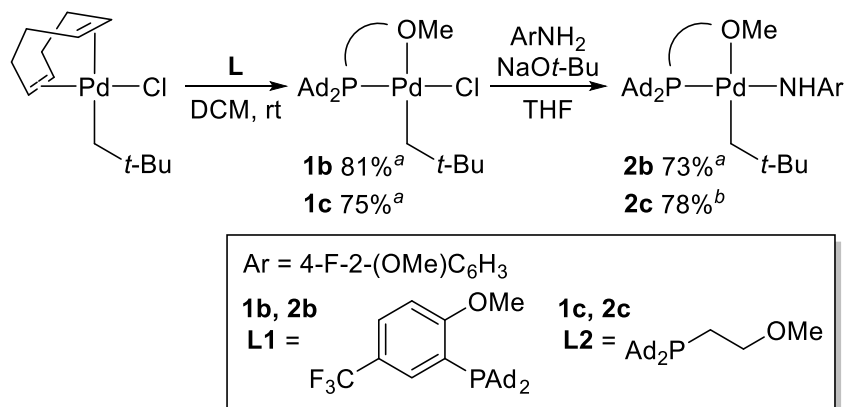


Figure 3.2. Ligand structures for reductive elimination of alkylamines from four-coordinate alkylPd(II) complexes

Scheme 3.3. Synthesis of (P,O)Pd(neopentyl)(NHAr) (**2b-c**).^a

^aIsolated yield; geometry determined by 2D ¹H NMR NOESY. ^bYield determined by ¹⁹F NMR spectroscopy with 4-FTol as internal standard.

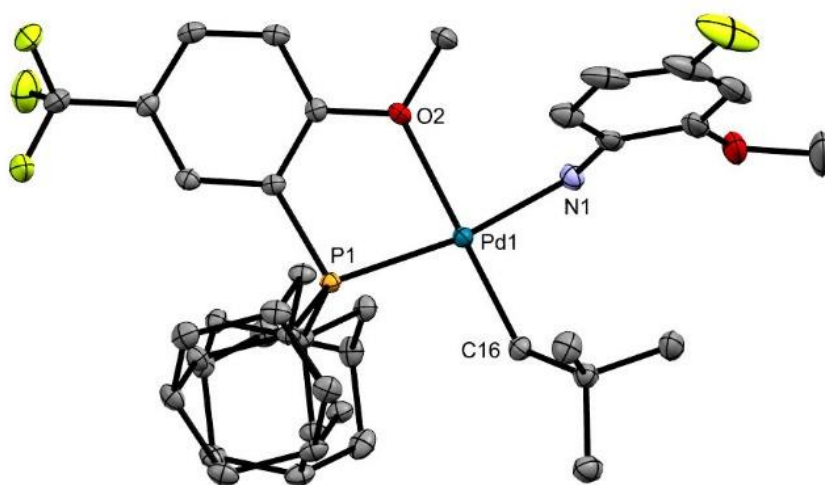


Figure 3.3. ORTEP drawing of (L1-κ²P,O)Pd(neopentyl)(NHAr) (**2b**) with 50% probability ellipsoids. Hydrogen atoms are omitted for clarity. Selected bond lengths (Å) and angles (°): Pd1-O2 2.2689(13), Pd1-P1 2.2958(5), Pd1-C16 2.0473(19), Pd1-N1 2.0418(16); O2-Pd1-P1 81.62, P1-Pd1-C16 98.22(5), C16-Pd1-N1 91.49(7), N1-Pd1-O2 88.24(6).

Complex **1c** bearing the flexible ligand Ad₂PCH₂CH₂OCH₃ (**L2**) reacted under the same conditions to form a Pd(II) amido complex in 78% yield, as determined by ¹⁹F NMR spectroscopy (Scheme 3.3). However, a mixture of two complexes was isolated from this reaction (Equation 3.2). The chemical shifts of the ¹H and ¹⁹F NMR signals for the major component (ca. 79%) were similar to those for **2b**; therefore, the structure of this complex was assigned as the monomeric, four-coordinate (κ²P,O) complex **2c**. Recrystallization of this mixture at -30 °C selectively formed crystals of the dimeric complex **4**; the structure of **4** was determined by single-crystal X-ray diffraction (Figure 3.4). Therefore, the second, minor

component in the isolated sample of **2c** was assigned as this dimer. Formation of **4** suggests that dissociation of the ether ligand occurs with a low barrier.

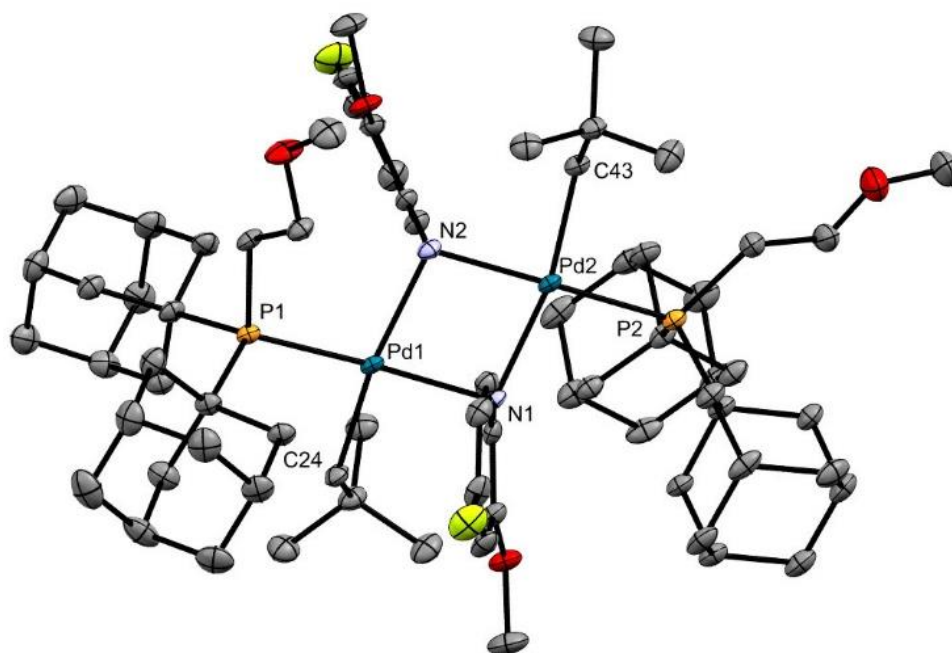
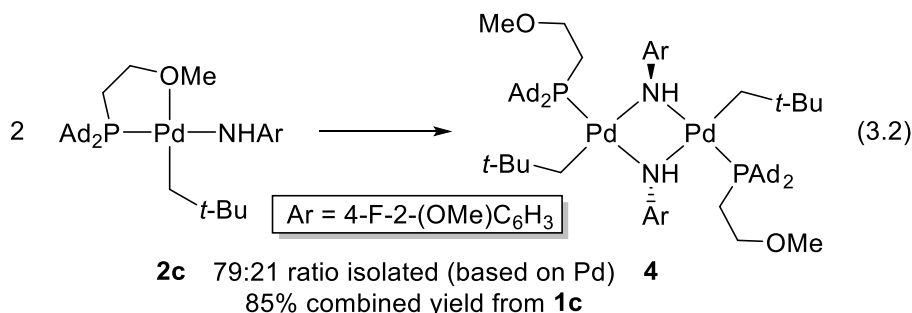
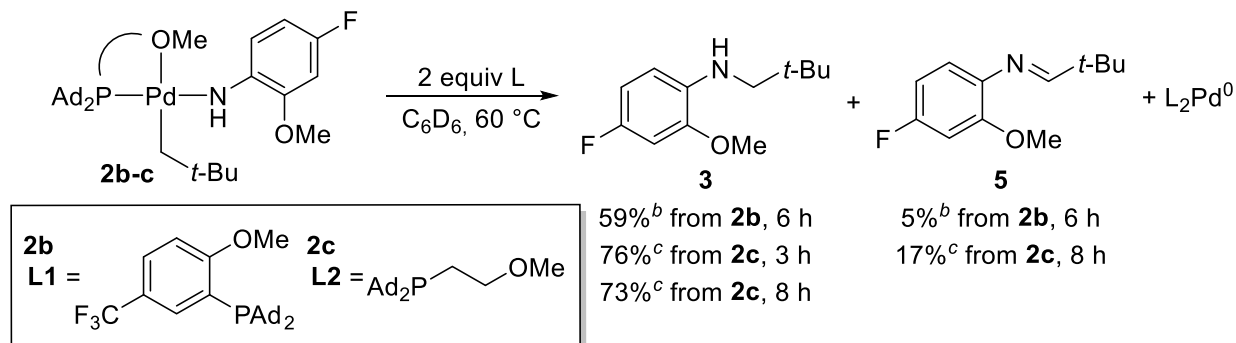


Figure 3.4. ORTEP drawing of $[(\text{L2-}\kappa\text{P})\text{Pd}(\text{neopentyl})(\text{NHAr})_2]$ (**4**) with 50% probability ellipsoids. Hydrogen atoms are omitted for clarity. Selected bond lengths (Å): Pd1-P1 2.2951(7), Pd1-C24 2.070(3), Pd1-N1 2.168(2), Pd1-N2 2.199(2), Pd2-P2 2.3279(7), Pd2-C43 2.074(3), Pd2-N1 2.208(2), Pd2-N2 2.141(2).

Neopentylpalladium(II) anilido complex **2b** containing the more rigid ligand **L1** underwent reductive elimination at 60 °C in the presence of 2 equivalents of **L1** in C_6D_6 to form neopentylamine **3** in 59% yield after 5 h (Scheme 3.4). The imine **5** was detected as a minor side product, which likely formed by substitution of the primary anilide by **3**, followed by β -hydrogen elimination. Under the same reaction conditions, the mixture of monomer **2c** and dimer **4** produced amine **3** in 76% yield after 3 h, with respect to the initial concentration of **2c** before heating (50% with respect to the combination of **2c** and **4**). The decay of the dimeric complex **4** was significantly slower than that of the monomeric **2c** (Figure 3.5), and 1-2% of **4** remained, even after 8 h at 60 °C (compared to ca. 9% at the beginning of the reaction). Furthermore, the combined yield of **3** and **5** did not significantly increase after **2c** had been consumed (ca. 3 h).

that formation of **4** from **2c** is irreversible, and that **4** does not undergo reductive elimination in significant yield.

Scheme 3.4. Reductive elimination from (P,O)Pd(neopentyl)(NHAr) (**2b-c**) to form *N*-neopentylamine **3**.^a



^aYield determined by ¹⁹F NMR spectroscopy with 4-FTol as internal standard; average from two experiments.

^bBased on the weighed mass of **2b**. ^cBased on the initial concentration of **2c**, as determined by ¹⁹F NMR spectroscopy prior to heating.

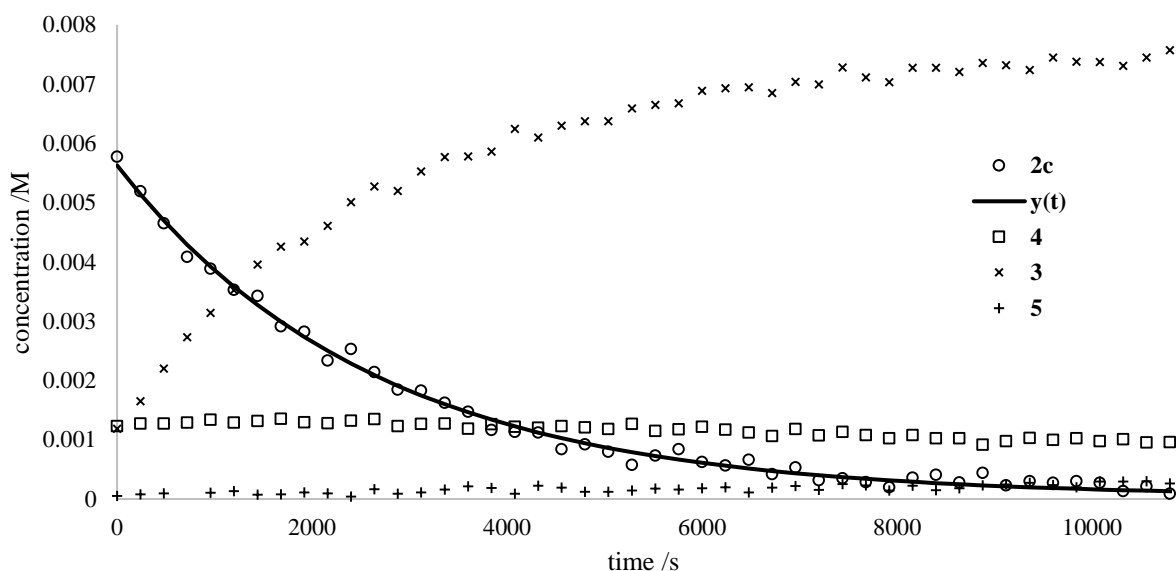


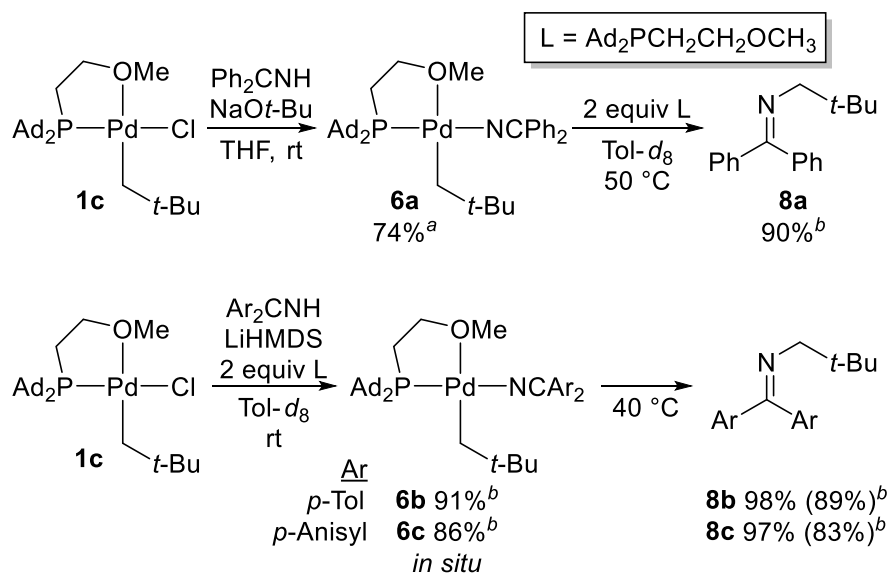
Figure 3.5. Concentration vs time plot for the reductive elimination from a mixture of **2c** and **4** (first 3 h); concentrations determined by ¹⁹F NMR integrations with 4-FTol as an internal standard.

We also sought to expand the scope of anionic nitrogen ligands that form palladium complexes that reductively eliminate primary sp³ carbon–nitrogen bonds. The pK_a values of benzophenone imines are similar to those of anilines, and the methyleneamido ligands formed from imines do not possess β-hydrogens. Furthermore, the anion of benzophenone imine has been shown to participate in reductive eliminations from arylpalladium(II) complexes.³⁸ Benzophenone imines are synthetic equivalents to ammonia; acidic hydrolysis of *N*-alkyl imines produces the corresponding primary

produces the corresponding primary alkylamines under mild conditions,³⁹ making them valuable synthetic targets for the development of new catalytic methods.

The four-coordinate Pd(II) chloride complex **1c**, which bears the flexible ligand **L2**, reacted with benzophenone imine and NaOt-Bu in THF to form the corresponding methyleneamido complex (**L2**- κ^2 P,O)Pd(neopentyl)(NCPh₂) (**6a**), which was isolated as a bright yellow powder in 74% yield (Scheme 3.5). Complex **6a** was stable at ambient temperature for ca. 1 h, and crystals suitable for X-ray diffraction were obtained by recrystallization at -30 °C (Figure 3.6). The bond distances and bond angles around the palladium center were similar to those of the other mononuclear P,O-ligated alkylpalladium(II) amido complexes. The correlations observed by ¹H NOESY of **6a** in C₆D₆ were consistent with this geometry and suggest that the ether oxygen atom is coordinated to the palladium center in solution.

Scheme 3.5. Synthesis of (**L2**- κ^2 P,O)Pd(neopentyl)(NCAr₂) (**6a-c**) and reductive elimination of *N*-neopentylimines **8a-c**.



^aIsolated yield. ^bYield determined by ¹H NMR spectroscopy with TMB as internal standard; (yield in parentheses is based on **1c**); average from two experiments.

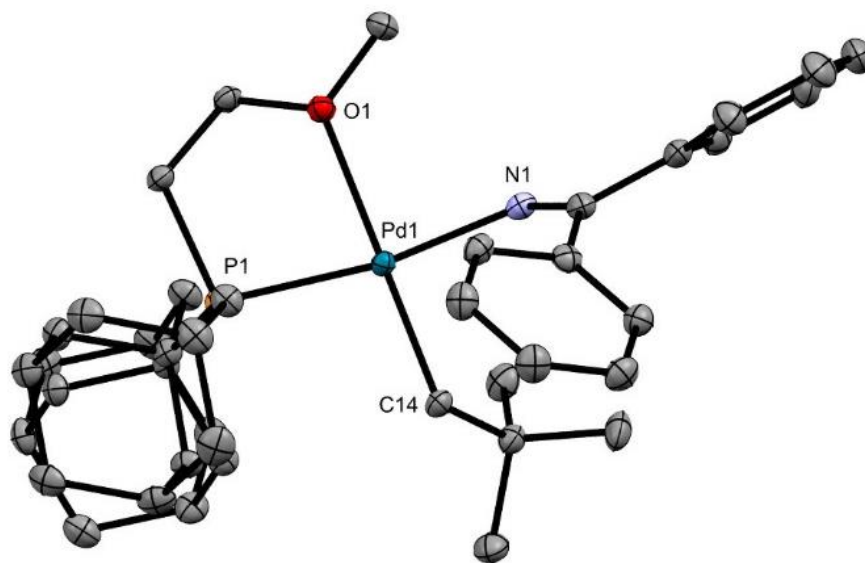
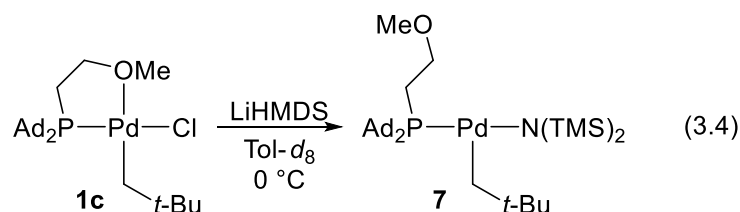


Figure 3.6. ORTEP drawing of $(\mathbf{L2}-\kappa^2\text{P,O})\text{Pd}(\text{neopentyl})(\text{NCPh}_2)$ (**6a**) with 50% probability ellipsoids. Hydrogen atoms are omitted for clarity. Selected bond lengths (Å) and angles (°): Pd1–O1 2.2701(11), Pd1–P1 2.3195(4), Pd1–C14 2.0571(15), Pd1–N1 2.0368(13); O1–Pd1–P1 81.18(3), P1–Pd1–C14 98.70(4), C14–Pd1–N1 90.87(6), N1–Pd1–O1 89.31(4).

To investigate the effects of substituents on the methyleneamido ligand on the reductive elimination reaction, complexes **6b** and **6c** bearing 4,4'-dimethyl and 4,4'-dimethoxy substituents were also studied. These complexes were unstable at ambient temperature and, therefore, were not isolated. However, the reaction of Pd(II) chloride **1c**, imine, 2 equivalents of phosphine, and LiHMDS in toluene produced **6b** and **6c** in yields of 91 and 86%, respectively, as determined by NMR spectroscopy (Scheme 3.5). $(\mathbf{L2})_2\text{Pd}^0$ (<2%) and $(\mathbf{L2}-\kappa\text{P})\text{Pd}(\text{neopentyl})[\text{N}(\text{TMS})_2]$ (**7**) (3-5%) were detected as minor side products in these reaction mixtures.



To confirm the identity of the minor complex **7**, the Pd(II) chloride precursor **1c** was allowed to react with LiHMDS in toluene- d_8 , and NMR spectra were obtained from the resulting mixture at 0 °C (Equation 3.4). The NMR spectra of Pd(II) hexamethyldisilazide complex **7** suggest that it exists predominantly as the three-coordinate (κP) structure drawn in Equation 3.4. Specifically, ^1H NMR NOE correlations between the resonance of the methylene group in the neopentyl ligand and the resonances of both the methoxyethyl group and the adamantyl groups in the ancillary ligand were observed by rotating frame nuclear Overhauser effect spectroscopy (ROESY). These correlations suggest that the phosphine and neopentyl ligands are mutually *cis*, and that rotation around the P–Pd bond is fast. Analogous NOE correlations were not observed in

the spectra of the other mononuclear **L2**-ligated Pd(II) complexes **1c**, **2c**, and **6a-c**, which exist predominately as four-coordinate ($\kappa^2\text{P,O}$) structures.

The diphenylmethyleneamido complex **6a** underwent reductive elimination at 50 °C in toluene to form *N*-neopentyl-benzophenone imine (**8a**) in 90% yield after 2 h, as determined by NMR spectroscopy (Scheme 3.5). The more reactive dimethyl- and dimethoxy-substituted **6b** and **6c** underwent reductive elimination at 40 °C in toluene to produce the corresponding *N*-neopentyl imines in yields of 98 and 97%, with respect to the initial concentration of **6b-c**.

The decays of neopentylpalladium(II) complexes **2b-c** and **6a-c** were monitored by ^1H or ^{19}F NMR spectroscopy, and first-order rate constants for reductive elimination (k_{RE}) were determined by fitting the decay of the palladium complex to first-order exponential decay functions. These rate constants and the free energies of activation calculated from them are reported in Table 3.1. Comparing the rates of reductive elimination leads to the following conclusions: the rates of reductive elimination from neopentylpalladium(II) complexes are faster than those from the analogous *syn*-2-methylnorbornylpalladium(II) complexes (ca. 1 kcal/mol lower barrier, see Chapter 2), and the rates of reductive eliminations from diarylmethyleneamido complexes are faster than those from anilido complexes (ca. 1 kcal/mol lower barrier). The trend of faster rates from reactions of complexes containing more electron-rich methyleneamido ligands parallels our previous observation that the *syn*-2-methylnorbornylpalladium(II) anilido complexes bearing electron-rich anilido ligands react faster than complexes bearing electron-deficient anilido ligands (see Chapter 2).

Table 3.1. Rates of reductive elimination to form neopentyl–nitrogen bonds.^a

entry	complex	<i>T</i> / °C	solvent	$k_{\text{RE}} \cdot 10^4$ / s ⁻¹	$\Delta G_{\text{RE}}^\ddagger$ / (kcal·mol ⁻¹)
1	2b	60	C ₆ D ₆	3.1	24.9
2	2c	60	C ₆ D ₆	4.4	24.7
3	6a	50	Tol- <i>d</i> ₈	5.3	23.8
4	6b	40	Tol- <i>d</i> ₈	2.5	23.5
5	6c	40	Tol- <i>d</i> ₈	4.0	23.2

^aReactions monitored by ^1H or ^{19}F NMR spectroscopy; rate constants (k_{RE}) determined by fitting the decay of **2a-c** or **6a-c** to first-order exponential decay; free-energy barriers ($\Delta G_{\text{RE}}^\ddagger$) calculated from $\ln(k_{\text{RE}})/RT$; all numbers averages from two experiments.

3.3 Conclusions

Despite multiple reported examples of catalytic reactions to form alkylamines that could involve reductive elimination from primary alkylpalladium(II) amido complexes,¹²⁻¹³ no example of a characterized, low-valent, primary alkylmetal complex that undergoes reductive elimination in good yield had yet been reported. We showed that weak chelation by the bidentate ligands Ad₂(2-OCH₃-5-(CF₃)C₆H₃)P (**L1**) and Ad₂PCH₂CH₂OCH₃ (**L2**) enables the synthesis of neopentylpalladium(II) anilido and methyleneamido complexes that are sufficiently stable to be isolated and characterized but undergo reductive elimination to form *N*-neopentyl anilines and *N*-neopentyl imines in moderate to high yields.

The formation of dimeric structures, such as **4**, with bridging anilido ligands, appears to be an unproductive decomposition pathway for these complexes. We propose that the chelation by P,O ligands can disfavor the formation of dinuclear complexes and other unproductive decomposition pathways, resulting in high yields of the Pd(II) amido intermediates from the Pd(II) chloride precursors. However, chelation from these ligands is weak, and reductive elimination still occurs with fast rates and in good yields of the neopentyl aniline and neopentyl imine products.

Kinetic experiments led us to conclude that the rates of reductive elimination from neopentylpalladium(II) complexes are faster than those from the analogous *syn*-2-methylnorbornylpalladium(II) complexes, and that the rates of reductive elimination from diarylmethyleneamido complexes are faster than those from anilido complexes. The electron-rich diarylmethyleneamido complexes **6b-c** form in high yields from the Pd(II) chloride precursor and undergo reductive elimination in near quantitative yields at mild temperatures (half-lives less than 1 h at 40 °C). We expect that these properties will make complexes like **6b-c** applicable to the development of catalytic reactions. Furthermore, we expect that the P,O ligand structures discussed in this and the preceding chapter could enable the synthesis of stable four-coordinate analogs to reactive three-coordinate palladium(II) intermediates without significantly altering the reactivity of those complexes.

3.4 Experimental

General Experimental Details. Solvents referred to as “dry” were collected from a solvent purification system containing a 0.33 m column of activated alumina under nitrogen and then stored over molecular sieves under nitrogen. Solvents referred to as “dry and deoxygenated” were collected from a solvent system as described above, degassed by the freeze-pump-thaw method, and stored over molecular sieves under nitrogen. CDCl₃ and C₆D₆ used in the characterization of phosphines or phosphine-ligated palladium complexes were degassed by the freeze-pump-thaw method and stored over molecular sieves under nitrogen. THF-*d*₈ and toluene-*d*₈ were distilled from sodium benzophenone ketyl prior to use. All other solvents, reagents, and starting materials were purchased from commercial suppliers and used as received unless otherwise specified.

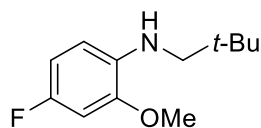
Column chromatography was performed with 230-400 mesh silica gel from Fisher Scientific. TLC plates with fluorescent indicators were purchased from Silicycle or EMD and visualized under a 254 nm UV lamp unless otherwise noted. Column chromatography of phosphine ligands was performed inside a nitrogen-filled glovebox to prevent oxidation.

GC spectra were obtained on an Agilent 7890 GC equipped with an HP-5 column (25 m x 0.20 mm x 0.33 μm film) and an FID detector. NMR spectra were obtained on 500 MHz or 600 MHz Bruker Avance series instruments at the University of California, Berkeley NMR facility. Chemical shifts are reported relative to the residual solvent signals (CDCl₃ 7.26 ppm for ¹H, 77.16 ppm for ¹³C; C₆D₆ 7.16 ppm for ¹H, 128.06 ppm for ¹³C; Tol-*d*₈ 7.09 ppm for ¹H, 137.5 ppm for ¹³C). For ¹⁹F or ³¹P NMR spectra, chemical shifts are corrected based on the ²H lock signal. ESI and APCI high resolution mass spectrometry (HRMS) was performed at the LBNL Catalysis Center at the University of California, Berkeley. EIMS (positive ionization) was performed on an Agilent 7890A/5976c GC-MS. Elemental analysis was performed by the UC

Berkeley Microanalytical Laboratory. X-ray diffraction analysis, including solution, was performed by Nicholas Settineri at the UC Berkeley CheXray facility.

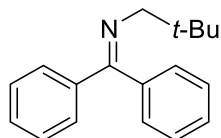
Preparation of authentic products 3 and 8a-c.

The preparations of 4-fluoro-2-methoxyaniline,(see Chapter 2) 4,4'-dimethylbenzophenone imine,⁴⁰ and 4,4'-dimethoxybenzophenone imine (see Chapter 4)⁴⁰ are reported in other chapters of this dissertation.



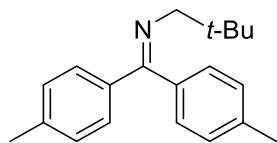
N-neopentyl-4-fluoro-2-methoxyaniline (3). 4-Fluoro-2-methoxyaniline (70.7 mg, 0.501 mmol), pivaldehyde (49 mg, 0.57 mmol, 1.1 equiv), and ammonium formate (315 mg, 5.00 mmol, 10 equiv) were dissolved in *i*-PrOH (3 ml) and H₂O (1 ml) in a 20 ml scintillation vial with a stir bar.

The reaction mixture was cooled to 0 °C, and Pd⁰ (53 mg, 10% on C, 0.050 mmol, 10%) was slowly added with stirring. The cooling bath was removed, and the mixture was stirred for 1 h at ambient temperature. A second portion of pivaldehyde (49 mg, 0.57 mmol, 1.1 equiv) was then added, and the reaction mixture was stirred for an additional 9 h. The mixture was diluted with ether (~10 ml) and washed with H₂O (~10 ml). The aqueous layer was extracted again with ether (~10 ml), and the combined organic layers were filtered through a plug of Celite and K₂CO₃. The volatile materials were removed at reduced pressure, and the crude product was purified by column chromatography (5% ethyl acetate in hexanes, R_f 0.35) to give the title compound as a clear and colorless oil (44.0 mg, 0.208 mmol, 42% yield). ¹H NMR (400 MHz, CDCl₃) δ 6.60 – 6.52 (m, 2H), 6.52 – 6.46 (m, 1H), 4.02 (s, 1H), 3.84 (s, 3H), 2.86 (s, 2H), 1.01 (s, 9H). ¹³C NMR (101 MHz, CDCl₃) δ 155.1 (d, *J* = 233.6 Hz), 147.3 (d, *J* = 9.4 Hz), 135.6 (d, *J* = 2.3 Hz), 109.3 (d, *J* = 9.0 Hz), 106.2 (d, *J* = 21.4 Hz), 98.6 (d, *J* = 27.2 Hz), 56.4, 55.8, 32.0, 27.9. ¹⁹F NMR (565 MHz, CDCl₃) δ -128.3. APCI calc'd (M+H⁺) 212.1445, found 212.1442.

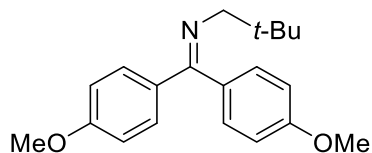


N-neopentylbenzophenone imine (8a). A 1-dram vial was charged with benzophenone imine (180 mg, 0.993 mmol), neopentylamine (104 mg, 1.23 mmol, 1.24 equiv), and dry DCM (1.0 ml). The vial was flushed with N₂ and sealed with a Teflon cap. The solution was stirred for 2 days at ambient

temperature. The solvent was evaporated at reduced pressure, and the crude product was purified by kugelrohr distillation followed by column chromatography (3% triethylamine in hexanes, R_f 0.77) to give the title compound as a clear and colorless oil (143 mg, 0.569 mmol, 57% yield). ¹H NMR (600 MHz, CDCl₃) δ 7.67 (d, *J* = 7.7 Hz, 2H), 7.47 (t, *J* = 7.3 Hz, 2H), 7.43 (t, *J* = 7.2 Hz, 1H), 7.39 (t, *J* = 7.1 Hz, 1H), 7.35 (t, *J* = 7.4 Hz, 2H), 7.17 (d, *J* = 7.5 Hz, 2H), 3.16 (s, 2H), 1.00 (s, 9H). ¹³C NMR (151 MHz, CDCl₃) δ 167.4, 140.4, 137.3, 129.8, 128.5, 128.4, 128.2, 128.2, 128.1, 65.7, 33.1, 28.2. EIMS 251.1 (M⁺), 91.0 (base peak). ESI⁺ calc'd (M+H⁺) 252.1747, found 252.1755.



***N*-neopentyl-4,4'-dimethylbenzophenone imine (8b).** A 1-dram vial was charged with 4,4'-dimethylbenzophenone imine (105 mg, 0.502 mmol), neopentylamine (52 mg, 0.60 mmol, 1.2 equiv), Na₂SO₄ (40 mg), and dry DCM (0.50 ml). The vial was flushed with N₂ and sealed with a Teflon cap. The solution was stirred for 2 days at ambient temperature. The solvent was evaporated at reduced pressure, and the crude product was purified by column chromatography (5% triethylamine and 0 to 10% ethyl acetate gradient in hexanes on dry silica) to give the title compounds as a viscous, clear, and colorless oil (71.5 mg, 0.256 mmol, 51% yield). ¹H NMR (500 MHz, CDCl₃) δ 7.51 (d, *J* = 8.2 Hz, 2H), 7.24 (d, *J* = 7.8 Hz, 2H), 7.12 (d, *J* = 8.0 Hz, 2H), 7.02 (d, *J* = 7.9 Hz, 2H), 3.12 (s, 2H), 2.42 (s, 3H), 2.35 (s, 3H), 0.95 (s, 9H). ¹³C NMR (126 MHz, CDCl₃) δ 167.5, 139.8, 138.1, 137.9, 134.4, 129.1, 128.80, 128.5, 128.2, 65.5, 33.1, 28.2, 21.5, 21.5. ESI⁺ calc'd (M+H⁺) 280.2060, found 280.2058.

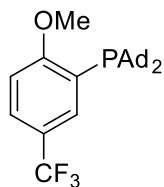


***N*-neopentyl-4,4'-dimethoxybenzophenone imine (8c).** A 1-dram vial was charged with 4,4'-dimethoxybenzophenone imine (121 mg, 0.501 mmol), neopentylamine (52 mg, 0.60 mmol, 1.2 equiv), Na₂SO₄ (40 mg), and dry DCM (0.50 ml). The vial was flushed with N₂ and sealed with a Teflon cap. The solution was stirred for 2 days at ambient temperature. The solvent was evaporated at reduced pressure, and the crude product was purified by column chromatography (5% triethylamine and 10% ethyl acetate in hexanes on dry silica) to give the title compound as a viscous, clear, and colorless oil (63.3 mg, 0.203 mmol, 41% yield). ¹H NMR (500 MHz, CDCl₃) δ 7.57 (d, *J* = 8.9 Hz, 2H), 7.07 (d, *J* = 8.7 Hz, 2H), 6.96 (d, *J* = 8.7 Hz, 2H), 6.84 (d, *J* = 8.9 Hz, 2H), 3.87 (s, 3H), 3.81 (s, 3H), 3.13 (s, 2H), 0.94 (s, 10H). ¹³C NMR (126 MHz, CDCl₃) δ 166.7, 161.0, 159.4, 133.9, 130.0, 129.8, 129.6, 113.7, 113.4, 65.5, 55.5, 55.4, 33.1, 28.2. ESI⁺ calc'd (M+H⁺) 312.1958, 312.1944.

Preparation of phosphine ligands and phosphine-ligated neopentylpalladium(II) complexes.

Di(1-adamantyl)chlorophosphine (Ad₂PCl),⁴¹ di(1-adamantyl)(2-methoxyethyl)phosphine (**L2**) (see Chapter 2), (2-methoxy-5-(trifluoromethyl)phenyl)lithium (see Chapter 2), and (COD)Pd(neopentyl)Cl¹⁸ were prepared according to published procedures or procedures reported in other chapters of this dissertation.

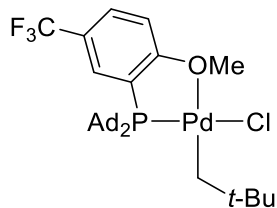
General notes. All reactions and purifications were performed with dry and deoxygenated solvents in dry glassware. All reactions and recrystallizations of neopentylpalladium(II) complexes were performed inside a nitrogen-filled glovebox.



Di-1-adamantyl(2-methoxy-5-(trifluoromethyl)phenyl)phosphine (L1). In an N_2 -filled glovebox, di(1-adamantyl)chlorophosphine (336 mg, 0.997 mmol) was suspended in ether (2 ml) in a 1 dram vial. (2-methoxy-5-(trifluoromethyl)phenyl)lithium (218 mg, 1.20 mmol, 1.20 equiv) was dissolved in ether (1 ml + 1 ml rinse) and added dropwise with stirring to the reaction vial. The vial was sealed with a Teflon-lined cap, and the reaction mixture was stirred at ambient temperature for 4 days. The reaction mixture was filtered through a pad of silica (~10 ml), which was rinsed with 1:1 ether/pentane (3x4 ml). The volatile materials were removed *in vacuo*. The residue was filtered through a second, smaller plug of silica (~2 ml) with pentane (2x2 ml) and then 20% ether/pentane (2x2 ml). The crude product was purified by column chromatography (5 to 15% ether/pentane gradient) to give the title compound as a white powder (323 mg, 0.678 mmol, 68% yield). ^1H NMR (600 MHz, CDCl_3) δ 7.95 (s, major 1H), 7.87 (dd, J = 13.3, 1.8 Hz, minor 1H), 7.61 (d, J = 8.6 Hz, minor 1H), 7.58 (dd, J = 8.7, 1.7 Hz, major 1H), 6.97 (dd, J = 8.6, 4.5 Hz, major 1H), 6.93 (d, J = 8.6 Hz, minor 1H), 3.90 (s, minor 3H), 3.87 (s, major 3H), 2.00 – 1.81 (m, major+minor 18H), 1.73 – 1.62 (m, major+minor 12H). ^{13}C NMR (151 MHz, CDCl_3) major: δ 166.5 (d, J = 18.7 Hz), 134.0 (p, J = 3.6 Hz), 127.5 (q, J = 3.7 Hz), 124.8 (q, J = 271.7 Hz), 123.5 (d, J = 28.8 Hz), 121.4 (q, J = 32.0 Hz), 110.7 (d, J = 2.8 Hz), 56.1 (d, J = 0.9 Hz), 41.8 (d, J = 12.6 Hz), 37.1, 37.1, 29.0 (d, J = 8.7 Hz); minor: δ 163.6 (d, J = 4.3 Hz), 140.0 – 139.3 (m), 128.5, 124.58 (q, J = 271.8 Hz), 124.0 (d, J = 36.4 Hz), 110.1, 54.6, 41.8 (d, J = 12.4 Hz), 37.2, 37.2, 29.1 (d, J = 8.9 Hz). ^{19}F NMR (565 MHz, CDCl_3) δ -62.3 (minor), -62.4 (major). ^{31}P NMR (243 MHz, CDCl_3) δ 58.0 (minor), 10.8 (major). ESI+ calc'd ($\text{M}+\text{H}^+$) 477.2529, found 477.2529.

Note: this compound exists as a mixture (52:48 in C_6D_6 , 70:30 in CDCl_3) of two rotamers ($\text{P}-\text{C}(\text{sp}^2)$ rotation). NMR signals were assigned to major/minor by their integrations, HSQC correlations, and HMBC correlations when possible. The $\underline{\text{C}}-\text{CF}_3$ resonance of the minor rotamer was not observed in the ^{13}C NMR spectrum; however, it was located at approximately 122 ppm by HMBC.

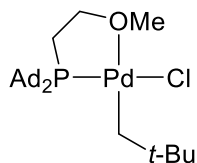
$(t\text{-Bu})_3\text{P}-\text{Pd}-\text{Cl}$ **(*t*-Bu₃P)Pd(neopentyl)Cl (1a).** (COD)Pd(neopentyl)Cl (96.4 mg, 0.300 mmol) was dissolved in THF (3 ml) in a 20 ml scintillation vial. Tri-*tert*-butylphosphine (63.7 mg, 0.315 mmol, 1.05 equiv) was dissolved in THF (1 ml + 2x1 ml rinse) and added to the reaction vessel dropwise with stirring. The reaction mixture was stirred for approximately 15 min at ambient temperature. The volatile materials were removed *in vacuo*. The residue was triturated with pentane (2x4 ml). The mixture was cooled (-30 °C) to complete precipitation. The crude product was recrystallized by dissolving in ether (~5 ml), filtering, through a plug of Celite, layering with pentane (~5 ml), and cooling to -30 °C. The supernatant was decanted, and the crystals rinsed with chilled pentane (2x2 ml) to give the title compound as red-orange needles (104 mg, 0.250 mmol, 84% yield). ^1H NMR (600 MHz, CDCl_3) δ 3.14 (d, J = 5.0 Hz, 2H), 1.53 (d, J = 12.4 Hz, 28H), 1.19 (s, 9H). ^{13}C NMR (151 MHz, CDCl_3) δ 40.24 (d, J = 4.3 Hz), 39.86 (d, J = 10.1 Hz), 35.05 (d, J = 3.1 Hz), 32.43 (d, J = 2.3 Hz), 31.48 (d, J = 2.7 Hz). ^{31}P NMR (243 MHz, CDCl_3) δ 71.1. Analysis calc'd C 49.16, H 9.22; found C 49.51, H 9.44.



[(1-Ad)₂(2-OCH₃-5-(CF₃)C₆H₃)P]Pd(neopentyl)Cl (1b).

(COD)Pd(neopentyl)Cl (96.4 mg, 0.300 mmol) was dissolved in DCM (4 ml) in a 20 ml scintillation vial. Di-1-adamantyl(2-methoxy-5-(trifluoromethyl)phenyl)phosphine (157 mg, 0.330 mmol, 1.10 equiv) was dissolved in DCM (1 ml + 1 ml rinse) and added to the reaction vessel dropwise with stirring. The reaction mixture was stirred for approximately 15 min at ambient temperature. The volume was reduced to approximately 1 ml *in vacuo*. Pentane (~5 ml) was added to precipitate the product. The mixture was cooled (-30 °C) to complete precipitation. The supernatant was decanted. The crude product was recrystallized by dissolving in DCM, filtering through a plug of Celite, and layering with pentane. After solid began to form, the vial was moved to a -30 °C freezer. The supernatant was decanted, and the solid rinsed with chilled pentane (2x2 ml). This material was then recrystallized again by dissolving in DCM (~2 ml), diluting with pentane until the solution turns cloudy (~5 ml), adding DCM dropwise until the solution nearly clears, filtering through a plug of Celite, and cooling to -30 °C. The solvent was decanted, and the yellow crystals were rinsed with chilled pentane (2x1 ml). A second crop was grown from the mother liquor by the same method with lower volumes. ¹H NMR (600 MHz, CDCl₃) δ 8.06 (dd, *J* = 5.8, 2.2 Hz, 1H), 7.73 (dd, *J* = 8.9, 2.1 Hz, 1H), 7.17 (dd, *J* = 8.9, 3.8 Hz, 1H), 4.31 (s, 3H), 2.93 (d, *J* = 4.2 Hz, 2H), 2.36 – 2.27 (m, 6H), 2.10 – 1.98 (m, 12H), 1.75 – 1.67 (m, 12H), 1.31 (s, 9H). ¹³C NMR (151 MHz, CDCl₃) δ 165.50 (d, *J* = 9.3 Hz), 132.8 (p, *J* = 3.5 Hz), 129.9 – 129.8 (m), 123.9 (q, *J* = 271.8 Hz), 123.7 – 123.0 (m), 117.1 (d, *J* = 24.8 Hz), 113.4 (d, *J* = 4.8 Hz), 59.2, 43.2 (d, *J* = 10.9 Hz), 41.2 (d, *J* = 1.8 Hz), 36.4 (d, *J* = 1.1 Hz), 34.8 (d, *J* = 2.0 Hz), 33.6 (d, *J* = 2.0 Hz), 28.7 (d, *J* = 9.2 Hz), 26.9 (d, *J* = 3.0 Hz). ¹⁹F NMR (565 MHz, CDCl₃) δ -62.8. ³¹P NMR (243 MHz, CDCl₃) δ 51.2. **Analysis** calc'd (+1/2 CH₂Cl₂ + 1/2 C₆H₁₄) C 56.29, H 7.09; found C 55.75, H 6.97.

Note: the recrystallized sample contains **1c**, DCM, and pentane in a 2:1:1 molar ratio. Placing the sample under vacuum (< 50 mTorr) for multiple hours did not remove this residual solvent. The molecular weight (used for yield and subsequent experiments) and calc'd CHN values are corrected to account for this.

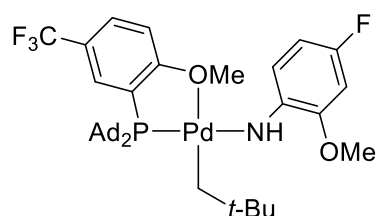


[(1-Ad)₂(CH₃OCH₂CH₂)P]Pd(neopentyl)Cl (1c).

(COD)Pd(neopentyl)Cl (96.4 mg, 0.300 mmol) was dissolved in DCM (4 ml) in a 20 ml scintillation vial. di(1-adamantyl)(2-methoxyethyl)phosphine (119 mg, 0.330 mmol, 1.10 equiv) was dissolved in DCM (1 ml + 1 ml rinse) and added to the reaction vessel dropwise with stirring. The reaction mixture was stirred for approximately 15 min at ambient temperature. The volume was reduced to approximately 1 ml *in vacuo*. Pentane (~5 ml) was added to precipitate the product. The mixture was cooled (-30 °C) to complete precipitation. The supernatant was decanted. The crude product was recrystallized by dissolving in warm 5:1 pentane/DCM (~5 ml), and filtering through a plug of Celite, which was rinsed with 5:1 pentane/DCM (1 ml). After crystals began to form, the vial was moved to a -30 °C freezer. The supernatant was decanted, and the crystals rinsed with chilled pentane (2x2 ml) to give the title compound as pale yellow blocks (162 mg, 0.246 mmol, 82% yield). ¹H NMR (600 MHz, CDCl₃) δ 3.60 (s, 3H), 3.56 (dt, *J* = 15.0, 6.2 Hz, 2H), 2.57 (d, *J* = 4.6 Hz, 2H), 2.23 (d, *J* = 11.9 Hz, 6H), 2.09 (d, *J* = 12.2 Hz, 6H), 2.05 (broad s, 6H), 1.86 (dt, *J* = 8.5, 6.3 Hz, 2H), 1.76

(broad s, 12H), 1.25 (s, 9H). ^{13}C NMR (151 MHz, CDCl_3) δ 73.0, 60.8, 41.1 (d, $J = 13.4$ Hz), 40.3, 36.8 – 36.4 (m), 34.2 (d, $J = 1.9$ Hz), 33.7 (d, $J = 1.9$ Hz), 28.5 (d, $J = 8.5$ Hz), 21.0, 19.0 (d, $J = 18.2$ Hz). ^{31}P NMR (243 MHz, CDCl_3) δ 51.3. **Analysis** calc'd (+ CH_2Cl_2) C 52.90, H 7.65; found C 53.08, 7.68.

Note: the recrystallized sample contains **1c** and DCM in a 1:1 molar ratio. Placing the sample under vacuum (~30 mTorr) for multiple hours did not remove this residual solvent. The molecular weight (used for yield and subsequent experiments) and calc'd CHN values are corrected to account for this.



[(1-Ad)₂(2-OCH₃-5-(CF₃)C₆H₃)P]Pd(neopentyl)NH(4-F-2-(OMe)C₆H₃) (2b). [(1-Ad)₂(2-OCH₃-5-(CF₃)C₆H₃)P]-Pd(neopentyl)Cl·½DCM·½C₅H₁₂ (**1c**) (65.3 mg, 0.0850 mmol) and 4-fluoro-2-methoxyaniline (215 μl , 0.40 M, 0.0850 mmol, 1.0 equiv) were dissolved in THF (5 ml) in a 20 ml scintillation vial. The solution was chilled, and then NaOt-Bu (245 μl , 0.40 M,

0.098 mmol, 1.2 equiv) was added slowly with stirring. The solvent was evaporated *in vacuo* with stirring. Ether (2 ml) was added and then evaporated *in vacuo* to give an orange solid. The residue was dissolved in ether (16 ml) and filtered through a syringe filter (0.2 μm PTFE), which was rinsed with ether (2 ml). The volume was reduced until an orange powder began to precipitate (~4 ml). The mixture was left in a freezer (-30 °C) for 2 days. The solid was collected by filtration while still cold and rinsed with cold pentane (2x1 ml) to give the title compound as a bright yellow-orange powder (49.1 mg, 0.0618 mmol, 73% yield). ^1H NMR (600 MHz, C_6D_6) δ 8.22 (d, $J = 4.5$ Hz, 1H), 7.49 (dd, $J = 8.6, 5.9$ Hz, 1H), 7.21 (d, $J = 8.6$ Hz, 1H), 6.91 (td, $J = 8.6, 2.9$ Hz, 1H), 6.67 (dd, $J = 10.4, 2.9$ Hz, 1H), 6.18 (dd, $J = 8.9, 3.9$ Hz, 1H), 4.29 (s, 1H), 3.74 (s, 3H), 3.48 (s, 3H), 2.95 (d, $J = 5.9$ Hz, 2H), 2.37 (d, $J = 12.3$ Hz, 6H), 2.08 (d, $J = 12.3$ Hz, 6H), 1.78 (s, 6H), 1.54 (d, $J = 12.2$ Hz, 6H), 1.48 (d, $J = 11.7$ Hz, 6H), 1.45 (s, 9H). ^{19}F NMR (565 MHz, C_6D_6) δ -62.5 (s, 3F), -134.9 (ddd, $J = 10.2, 8.8, 6.0$ Hz, 1F). ^{31}P NMR (243 MHz, C_6D_6) δ 44.2. **Analysis** calc'd C 60.49, H 6.85, N 1.76; found C 60.74, H 6.68, N 1.84.

A crystal suitable for X-ray diffraction was grown from a solution of **2b** in DCM layered with pentane at -30 °C.

The ^1H NMR resonances were assigned as follows:

- The adamantyl signals based on integration and ^1H - ^{13}C HSQC. The two CH_2 groups were differentiated based on ^1H NOESY.
- The aryl signals based on shift, multiplicity, and COSY correlations.
- The NH signal based on ^1H - ^{13}C HSQC (no ^{13}C correlation).
- The methoxy signals based on integration and HSQC (downfield ^{13}C shift). The two methoxy signals were differentiated by HMBC.
- The remaining neopentyl signals are clear based on integration.

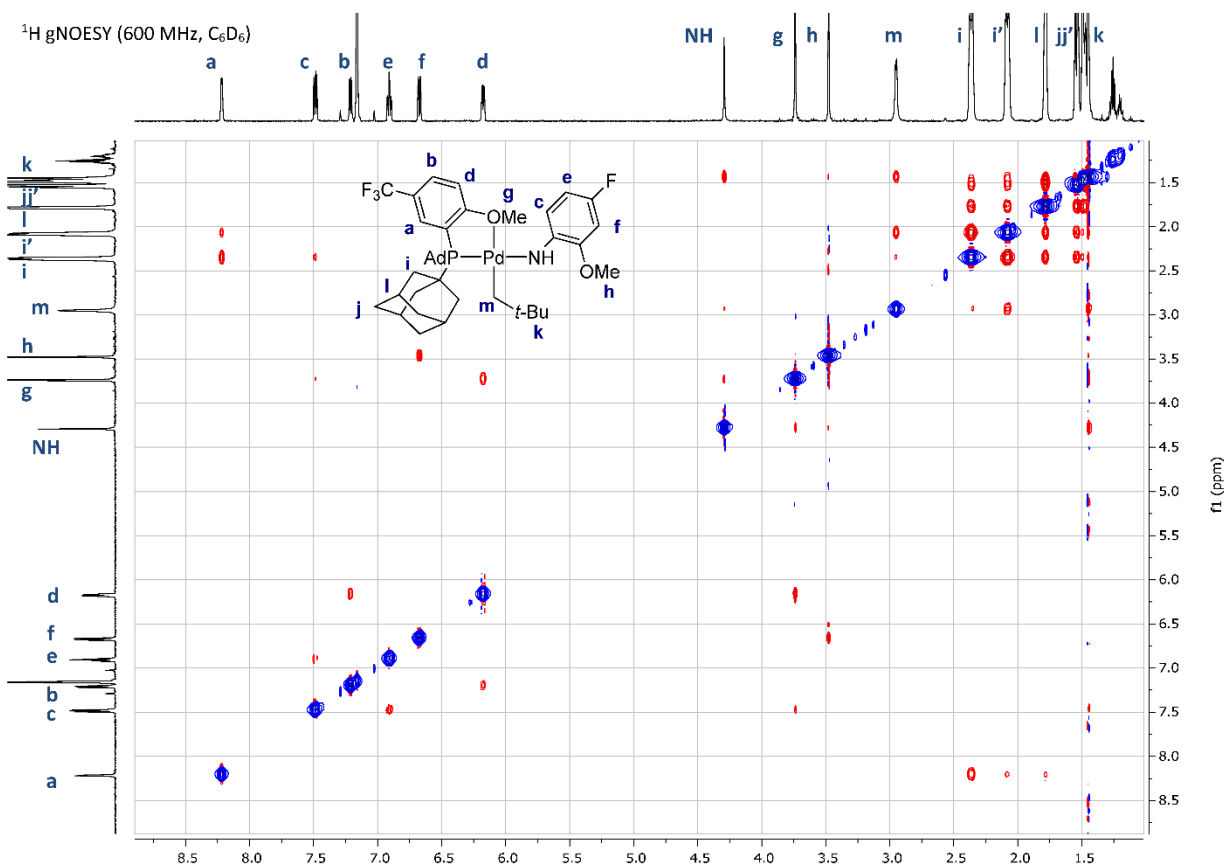
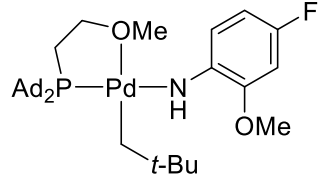


Figure 3.7. 2-Dimensional ^1H - ^1H gradient-enhanced NOE spectrum of **2b**.


[(1-Ad)₂(CH₃OCH₂CH₂)P]Pd(neopentyl)NH(4-F-2-(OMe)C₆H₃) (2c). [1-Ad)₂(CH₃OCH₂CH₂)P]Pd(neopentyl)Cl·DCM (**1c**) (98.8 mg, 0.150 mmol) and 4-fluoro-2-methoxyaniline (375 μl , 0.40 M, 0.150 mmol, 1.0 equiv) were dissolved in THF (14 ml) in a 20 ml scintillation vial. The solution was chilled, and then NaO*t*-Bu (450 μl , 0.40 M, 0.180 mmol, 1.2 equiv) was added in 3 portions with stirring, with the solution chilled after each portion. The reaction mixture was filtered by syringe (0.2 μm PTFE), which was rinsed with cold THF (2x1 ml), into a cold 100 ml round-bottom flask. The solvent was evaporated *in vacuo* with stirring. Cold ether (2 ml) was added to the flask and then removed *in vacuo*. The solid residue was suspended in cold 1:1 ether/pentane (12 ml), and the mixture was left in a freezer (-30 $^{\circ}\text{C}$) for 4 h. The solid was collected by filtration while still cold and rinsed with cold pentane (2x1 ml) to give the title compound as a bright yellow powder (86.4 mg, 0.127 mmol, 85% yield). **Analysis** calc'd C 61.98, H 8.17, N 2.07; found C 61.63, H 8.17, N 1.74.

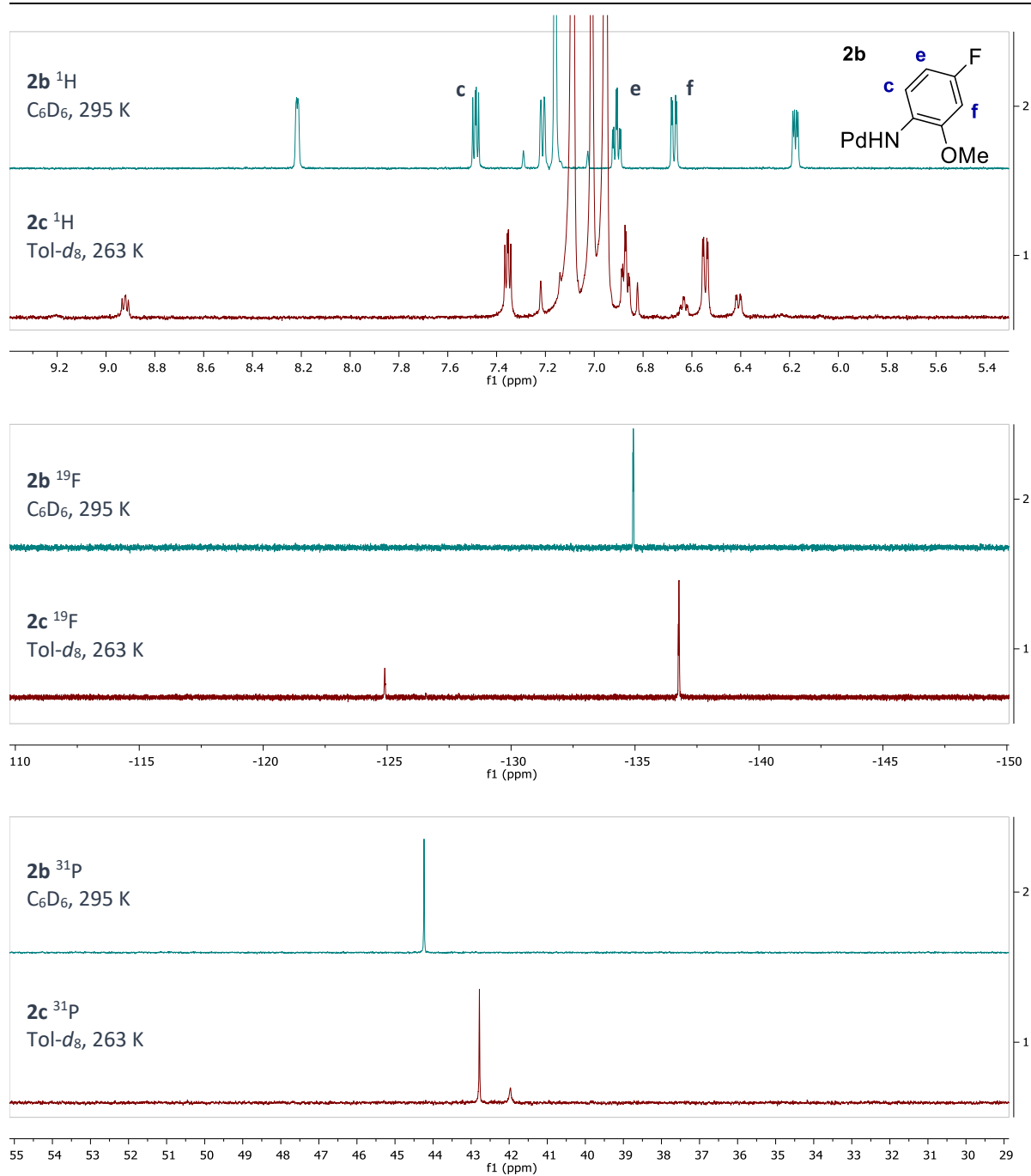
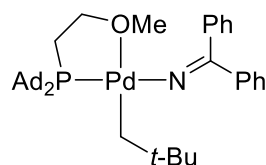


Figure 3.8. Stacked ^1H (aryl region), ^{19}F , and ^{31}P NMR spectra of **2b** in C_6D_6 at 295 K (top, green) and **2c** in $\text{Tol-}d_8$ at 263 K (bottom, red).

Note: compound **2c** decomposed rapidly at ambient temperature when no phosphine ligand is present in solution. Therefore, all solutions and glassware were chilled in a freezer prior to use in the preparation of **2c**, and the reaction mixture was not allowed to fully warm to ambient temperature at any point during the procedure.

The isolated sample was found to be a mixture of the monomer **2c** and the dimer **4** by NMR spectroscopy. NMR spectroscopy characterization was performed at 263 K to prevent decomposition of **2c**. Due to the complexity of this mixture, 2-dimensional NMR spectra were more informative than was the 1-dimensional ^1H NMR spectrum. Multiple attempts to isolate a pure sample of complex **2c** by recrystallization were unsuccessful.

A crystal suitable for X-ray diffraction was grown from a solution of this mixture in DCM layered with pentane at $-30\text{ }^\circ\text{C}$; however, the crystal obtained in this manner contained only the dimer **4** and co-crystallized solvent.



[(1-Ad)₂(CH₃OCH₂CH₂)P]Pd(neopentyl)NCPPh₂ (6a**).**

[1-Ad)₂(CH₃OCH₂CH₂)P]Pd(neopentyl)Cl·DCM (**1c**) (65.8 mg, 0.0999 mmol) and benzophenone imine (250 μl , 0.40 M, 0.100 mmol, 1.0 equiv) were dissolved in THF (9 ml) in a 20 ml scintillation vial. The solution was chilled, and then NaOt-Bu (300 μl , 0.40 M, 0.12 mmol, 1.2 equiv) was added slowly with stirring. The solvent was evaporated *in vacuo* with stirring. The residue was dissolved in ether (10 ml) and filtered through a syringe filter (0.2 μm PTFE), which was rinsed with ether (2x1 ml). The volume was reduced until an orange powder began to precipitate (~2 ml). Pentane (3 ml) was added to the vial, and the mixture was left in a freezer ($-30\text{ }^\circ\text{C}$) overnight (~14 h). The solid was collected by filtration while still cold and rinsed with cold pentane (2x1 ml) to give the title compound as a yellow powder (53.2 mg, 0.0741 mmol, 74% yield). ^1H NMR (500 MHz, C₆D₆) δ 8.06 (d, J = 6.7 Hz, 4H), 7.34 – 7.27 (m, 4H), 7.21 (tt, J = 7.3, 1.3 Hz, 2H), 2.97 (s, 3H), 2.85 (dt, J = 13.8, 6.1 Hz, 2H), 2.17 (br, 2H), 2.07 – 2.00 (m, 6H), 1.92 – 1.84 (m, 12H), 1.68 – 1.59 (m, 12H), 1.50 (s, 9H), 1.15 – 1.08 (m, 2H). ^{31}P NMR (203 MHz, C₆D₆) δ 36.4. **Analysis** calc'd C 68.56, H 8.14, 1.95; found C 68.38, H 8.13, N 2.10.

A crystal suitable for X-ray diffraction was grown from a solution of **6a** in 1:7 DCM/pentane layered with pentane at $-30\text{ }^\circ\text{C}$.

The ^1H NMR resonances were assigned as follows:

- The adamantyl signals based on integration and ^1H - ^{13}C HSQC. The two CH₂ groups were differentiated based on ^1H NOESY.
- The aryl signals based on integration and multiplicity.
- The CH₂O and OCH₃ signals based on integration and ^1H - ^{13}C HSQC (downfield ^{13}C shift).
- The PCH₂ signal based on integration and multiplicity.
- The remaining neopentyl signals are clear based on integration.

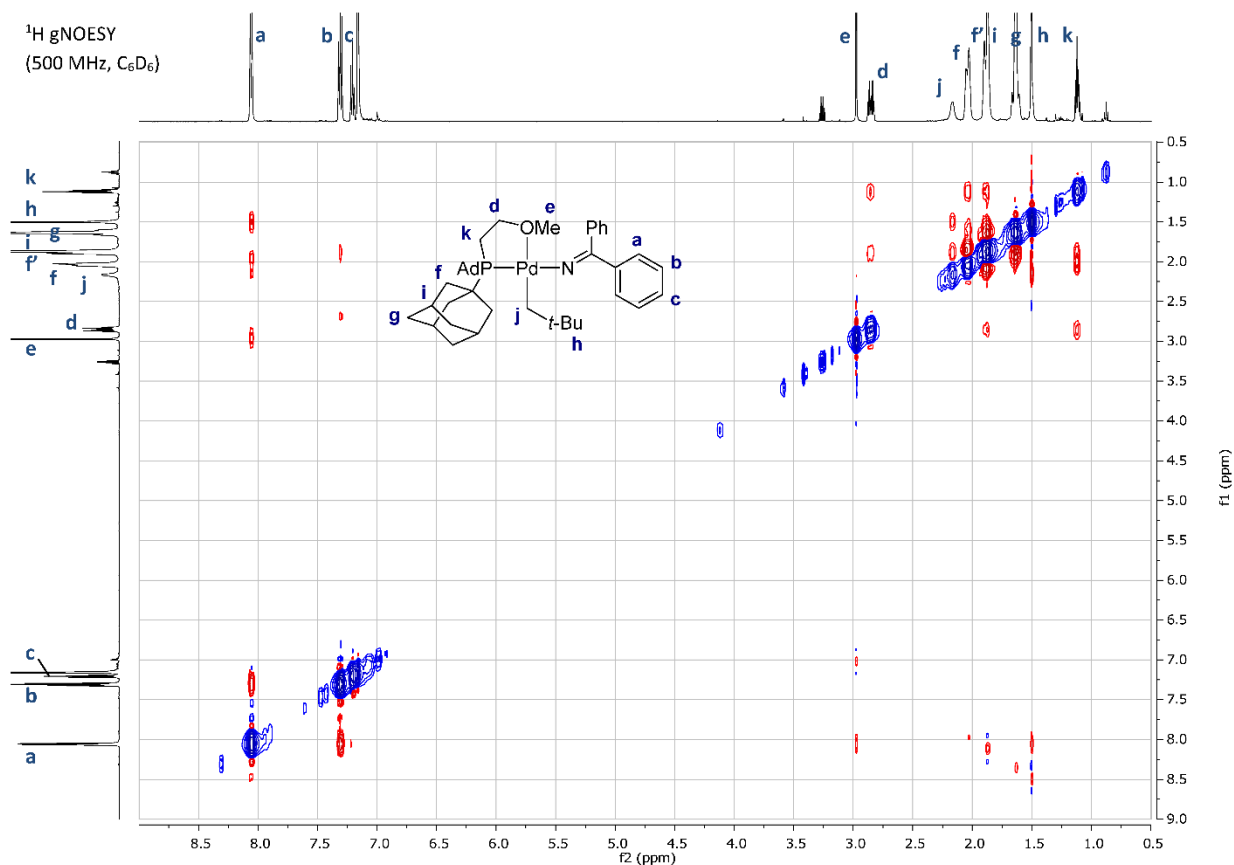
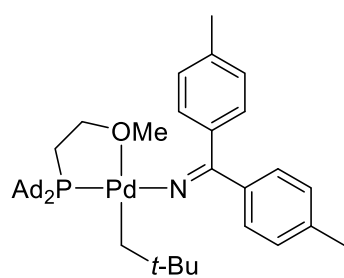


Figure 3.9. 2-Dimensional ^1H - ^1H gradient-enhanced NOE spectrum of **6a**.

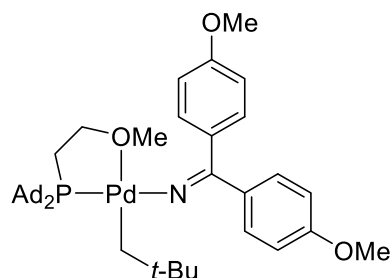
***In situ* characterization of unstable complexes **6b**, **6c**, and **7** by NMR spectroscopy.**



(Ad₂PCH₂CH₂OCH₃-κ²P,O)Pd(neopentyl)[NC(*p*-Tol)₂] (6b**).**

[1-Ad]₂(CH₃OCH₂CH₂P)Pd(neopentyl)Cl·DCM (**1c**) (375 μl, 0.016 M, 0.0060 mmol), 4,4'-dimethylbenzophenone imine (15 μl, 0.40 M, 0.060 mmol, 1.0 equiv), and Tol-*d*₈ (0.30 ml) were mixed in a 1-dram vial. The solution was briefly chilled in a freezer (-30 °C), and then LiHMDS (15 μl, 0.40 M, 0.0060 mmol, 1.0 equiv) was added slowly with stirring while the solution was still cold. The mixture was transferred to a cold J-Young NMR tube, which was kept in an ice bath until injection into an NMR probe at 273 K. All spectra were acquired at 273 K to prevent decomposition. **¹H NMR** (500 MHz, Tol-*d*₈) δ 7.90 (br d, *J* = 6.9 Hz, 4H), 7.09 – 7.05 (overlaps with Tol-*d*₇, 4H), 2.98 (s, 3H), 2.86 (dt, *J* = 14.1, 6.1 Hz, 2H), 2.22 (s, 6H), 2.10 – 2.00 (overlaps with Tol-*d*₇, 8H), 1.92 – 1.83 (m, 12H), 1.67 – 1.59 (m, 12H), 1.46 (s, 9H), 1.12 (q, *J* = 6.3 Hz, 2H). **³¹P NMR** (203 MHz, Tol-*d*₈) δ 36.0.

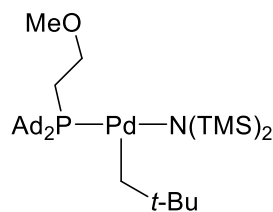
Note: (Ad₂PCH₂CH₂OCH₃-κP)Pd(neopentyl)[N(TMS)₂] (**7**) was detected as an impurity in this sample (~14 mol%).



(**Ad₂PCH₂CH₂OCH₃-κ²P,O**)Pd(neopentyl)[NC(*p*-Anisyl)₂] (**6c**). [1-Ad)₂(CH₃OCH₂CH₂)P]Pd(neopentyl)Cl·DCM (**1c**) (375 μl, 0.016 M, 0.0060 mmol), 4,4'-dimethoxybenzophenone imine (60 μl, 0.10 M, 0.060 mmol, 1.0 equiv), and Tol-*d*₈ (0.25 ml) were mixed in a 1-dram vial. The solution was briefly chilled in a freezer (-30 °C), and then LiHMDS (15 μl, 0.40 M, 0.0060 mmol, 1.0 equiv) was added slowly with stirring while the solution was still cold. The mixture was transferred to a cold J-

Young NMR tube, which was kept in an ice bath until injection into an NMR probe at 273 K. All spectra were acquired at 273 K to prevent decomposition. ¹H NMR (500 MHz, Tol-*d*₈) δ 7.97 (d, *J* = 8.2 Hz, 4H), 6.84 (d, *J* = 8.7 Hz, 4H), 3.38 (s, 6H), 3.00 (s, 3H), 2.88 (dt, *J* = 13.9, 6.1 Hz, 2H), 2.08 – 2.02 (m, 8H), 1.93 – 1.85 (m, 12H), 1.70 – 1.58 (m, 12H), 1.48 (s, 9H), 1.13 (q, *J* = 6.4 Hz, 2H). ³¹P NMR (203 MHz, Tol-*d*₈) δ 35.9.

Note: (Ad₂PCH₂CH₂OCH₃-κP)Pd(neopentyl)[N(TMS)₂] (**7**) was detected as an impurity in this sample (~7 mol%).



(**Ad₂PCH₂CH₂OCH₃-κP**)Pd(neopentyl)[N(TMS)₂] (**7**).

[1-Ad)₂(CH₃OCH₂CH₂)P]Pd(neopentyl)Cl·DCM (**1c**) (375 μl, 0.016 M, 0.0060 mmol) was mixed with Tol-*d*₈ (0.30 ml) in a 1-dram vial. The solution was briefly chilled in a freezer (-30 °C), and then LiHMDS (15 μl, 0.40 M, 0.0060 mmol, 1.0 equiv) was added slowly with stirring while the solution was still cold. The mixture was transferred to a cold J-

Young NMR tube, which was kept in an ice bath until injection into an NMR probe at 273 K. All spectra were acquired at 273 K. ¹H NMR (500 MHz, Tol-*d*₈) δ 3.62 (q, *J* = 7.2 Hz, 2H), 3.15 (s, 3H), 2.71 (d, *J* = 7.7 Hz, 2H), 2.06 – 2.01 (m, 6H), 2.01 – 1.91 (m, 6H), 1.80 (s, 6H), 1.75 (dt, *J* = 10.0, 7.4 Hz, 2H), 1.63 – 1.56 (m, 6H), 1.56 – 1.49 (m, 6H), 1.34 (s, 9H), 0.59 (s, 18H). ³¹P NMR (203 MHz, Tol-*d*₈) δ 46.8.

The ¹H NMR resonances were assigned as follows:

- The adamantyl signals based on integration and ¹H-¹³C HSQC. The two CH₂ groups were differentiated based on ¹H NOESY.
- The TMS signal based on integration and ¹H-¹³C HSQC (upfield ¹³C shift).
- The CH₂O and OCH₃ signals based on integration and ¹H-¹³C HSQC (downfield ¹³C shift).
- The PCH₂ signal based on integration, multiplicity, and strong ¹H-³¹P HMBC correlation.
- The neopentyl signals are clear based on integration.

Note: the NOE correlation from the neopentyl group (resonance **d**) to both the methoxyethyl group (resonances **a** and **h**) and to the adamantyl groups (resonances **c** and **c'**) are not consistent with a four-coordinate (κ²P,O) structure. Therefore, the three-coordinate (κP) structure is proposed.

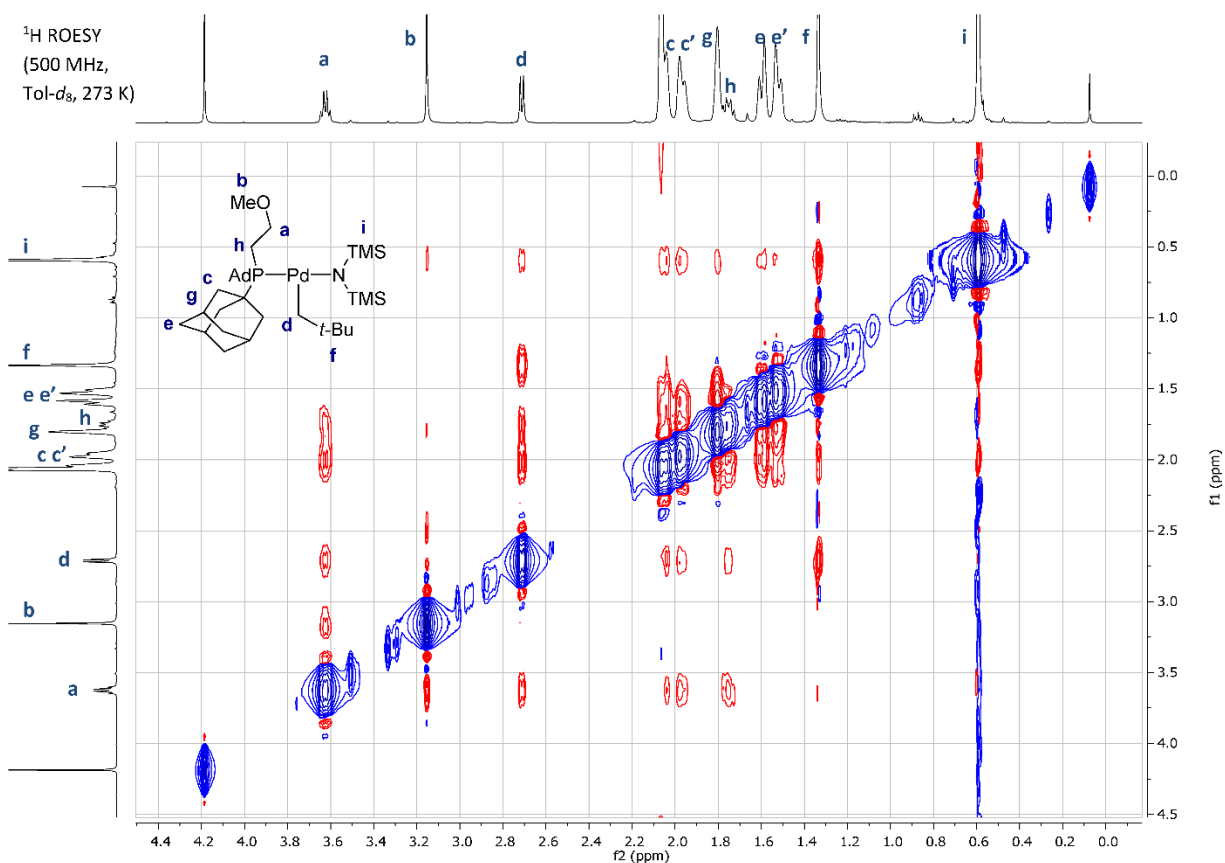


Figure 3.10. 2-Dimensional ¹H-¹H rotating frame NOE spectrum of **7**.

Table 3.2. Key NMR chemical shifts of Ad₂CH₂CH₂OCH₃-ligated complexes.

nucleus	position	1c , C ₆ D ₆ 295 K	6a , C ₆ D ₆ 295 K	6b , Tol- <i>d</i> ₈ 273 K	6c , Tol- <i>d</i> ₈ 273 K	7 , Tol- <i>d</i> ₈ 273 K
³¹ P	-	-	36.4	35.9	35.9	46.8
¹ H	PdCH ₂	2.97	2.17	~2.1	~2.1	2.71
"	PCH ₂	1.14	1.11	1.12	1.13	1.75
"	CH ₂ O	2.88 <i>J</i> _{P-H} =14.9 Hz	2.85 <i>J</i> _{P-H} =13.8 Hz	2.86 <i>J</i> _{P-H} =14.1 Hz	2.88 <i>J</i> _{P-H} =13.9 Hz	3.62 <i>J</i> _{P-H} =7.2 Hz
"	OCH ₃	3.56	2.97	2.98	3.00	3.15

Experimental details for reductive elimination of *N*-neopentylamine **3 from complexes **2b-c** and *N*-neopentylimines **8a-c** from complexes **6a-c** (Scheme 3.4, Scheme 3.5, and Table 3.1).**

Procedure for **2b-c.** In an N₂-filled glovebox, **2b** or **2c** (0.010 mmol), phosphine (0.020 mmol, 2.0 equiv), 4-fluorotoluene (25 μ l, 0.40 M, 0.010 mmol, 1.0 equiv), and C₆D₆ (0.67 ml) were mixed in a 1-dram vial. This mixture was then transferred to a J-Young NMR tube, and the sample was injected into a VT NMR probe at 60 °C. After heating for the noted time in the spectrometer, the probe and sample were cooled to ambient temperature, and the yield of the product was determined by integrating against the internal standard.

For **2b** 8.0 mg **2b**, 9.5 mg Ad₂(2-OCH₃-5-(CF₃)C₆H₃)P, 6 h reaction time.

For **2c**: 6.8 mg **2c**, 7.2 mg Ad₂PCH₂CH₂OCH₃, 8 h reaction time. The initial concentration of **2c** in the mixture was determined by ¹⁹F NMR spectroscopy at ambient temperature prior to heating.

Procedure for **6a.** In an N₂-filled glovebox, **6a** (7.2 mg, 0.010 mmol), Ad₂PCH₂CH₂OCH₃ (7.2 mg, 0.020 mmol, 2.0 equiv), 1,3,5-trimethoxybenzene (25 μ l, 0.133 M, 0.0033 mmol, 0.33 equiv), and Tol-*d*₈ (1.0 ml) were mixed in a 1-dram vial. Approximately 0.7 ml of this mixture was then transferred to a J-Young NMR tube, and the sample was injected into a VT NMR probe at 50 °C. After heating for 2 h in the spectrometer, the probe and sample were cooled to ambient temperature, and the yield of the product was determined by integrating a well-resolved peak (NCH₂*t*-Bu) against the internal standard.

Note: The impurities of the corresponding ketones in samples of 4,4'-dimethylbenzophenone imine and 4,4'-dimethoxybenzophenone were reduced to <1 mol% by column chromatography (5% triethylamine, ethyl acetate gradient in hexanes) with dry silica (150 °C, ~50 mTorr) prior to use in these experiments.

Procedure for **6b.** In an N₂-filled glovebox, **1c** (625 μ l, 0.016 M, 0.010 mmol), 4,4'-dimethylbenzophenone imine (25 μ l, 0.40 M, 0.010 mmol, 1.0 equiv), Ad₂PCH₂CH₂OCH₃ (7.2 mg, 0.020 mmol, 2.0 equiv), 1,3,5-trimethoxybenzene (25 μ l, 0.133 M, 0.0033 mmol, 0.33 equiv), and Tol-*d*₈ (0.30 ml) were mixed in a 1-dram vial. LiHMDS (25 μ l, 0.40 M, 0.010 mmol, 1.0 equiv) was then added slowly to the reaction mixture with stirring. Approximately 0.7 ml of this mixture was then transferred to a J-Young NMR tube, which was kept in an ice bath until injection into the spectrometer. ¹H (90° pulse, 50 s dwell time) and ³¹P NMR spectra were acquired at ambient temperature, the sample was removed, the probe was warmed to 40 °C, and the sample reinjected. After heating for 5 h in the spectrometer, the probe and sample were cooled to ambient temperature, and the yield of the product was determined by integrating a well-resolved peak against the internal standard.

Procedure for **6c.** As described for complex **6b** except with 4,4'-dimethoxybenzophenone imine (100 μ l, 0.10 M, 0.010 mmol, 1.0 equiv). ¹H and ³¹P NMR spectra were acquired at 273 K prior to heating.

Data acquisition notes. Spectra were acquired in a 500 or 600 MHz Avance series Bruker NMR spectrometer set to maintain a constant temperature. The noted reaction temperature was determined by calibration with an ethylene glycol sample (80% in DMSO-*d*₆).

Pulse program for kinetic experiments. The NMR spectrometer acquired spectra at set intervals with a calibrated 90° pulse. For ^1H NMR spectra in Tol-*d*₈: 2 scans, 120 s dwell time, 6 minute intervals. For ^{19}F NMR spectra in C₆D₆: 6 scans, 50 s dwell time, 6 minute intervals.

Data analysis notes. Concentrations were determined by integration against the internal standard. First-order rate constants were calculated by fitting the plotted data to the formula $y(t)=A\cdot\exp(-k_{\text{RE}}\cdot t)+C$ using the solver function in Microsoft Excel to vary A , k_{RE} , and C to minimize the sum of squared residuals. The constant “ C ” term was included to account for overlapping impurities and imperfect baseline corrections. The data from five half-lives were used in the fit. The free energy of activation was calculated as $\Delta G^\ddagger=-RT\cdot\ln(k_{\text{RE}}\cdot h/(k_{\text{B}}\cdot T))$. Experiments were replicated, and the results from each trial and the average are reported.

Kinetic data and analysis for reductive elimination reactions.

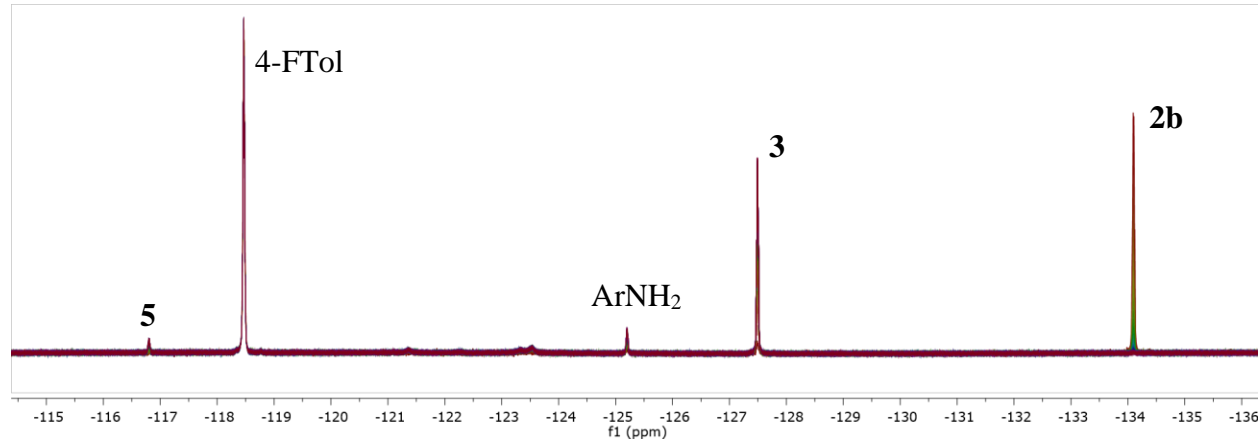


Figure 3.11. Superimposed ^{19}F NMR spectra for the reductive elimination of **3** from **2b**.

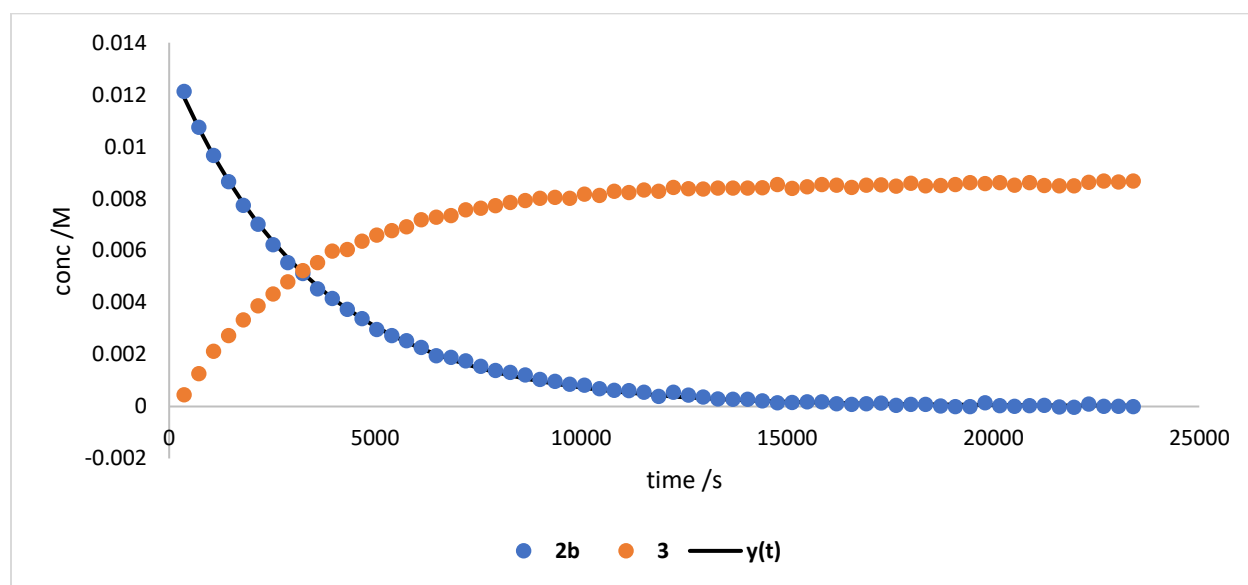


Figure 3.12. Concentration vs time plot for the reductive elimination of **3** from **2b**.

Table 3.3. Reductive elimination of **3** from **2b**.

Trial	% yield 3	% yield 5	$k_{\text{RE}} \cdot 10^4 / \text{s}^{-1}$	$\Delta G^\ddagger / (\text{kcal} \cdot \text{mol}^{-1})$
1	62	4	2.93	24.97
2	56	6	3.24	3.24
avg	59	5	3.1	24.9

Note: compound **5** was identified by the characteristic $\text{N}=\text{CH}$ ^1H NMR spectroscopy signal of the imine and by the detection of a compound with $m/z=209$ ($m/z=211$ for **3**) as the only other significant organic product.

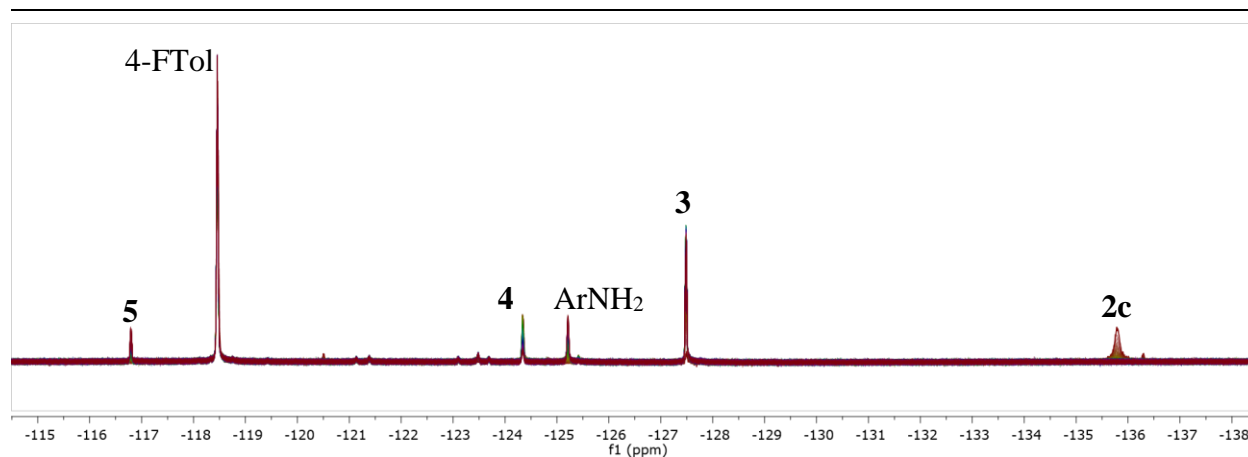


Figure 3.13. Superimposed ^{19}F NMR spectra for the reductive elimination of **3** from **2c+4** mixture.

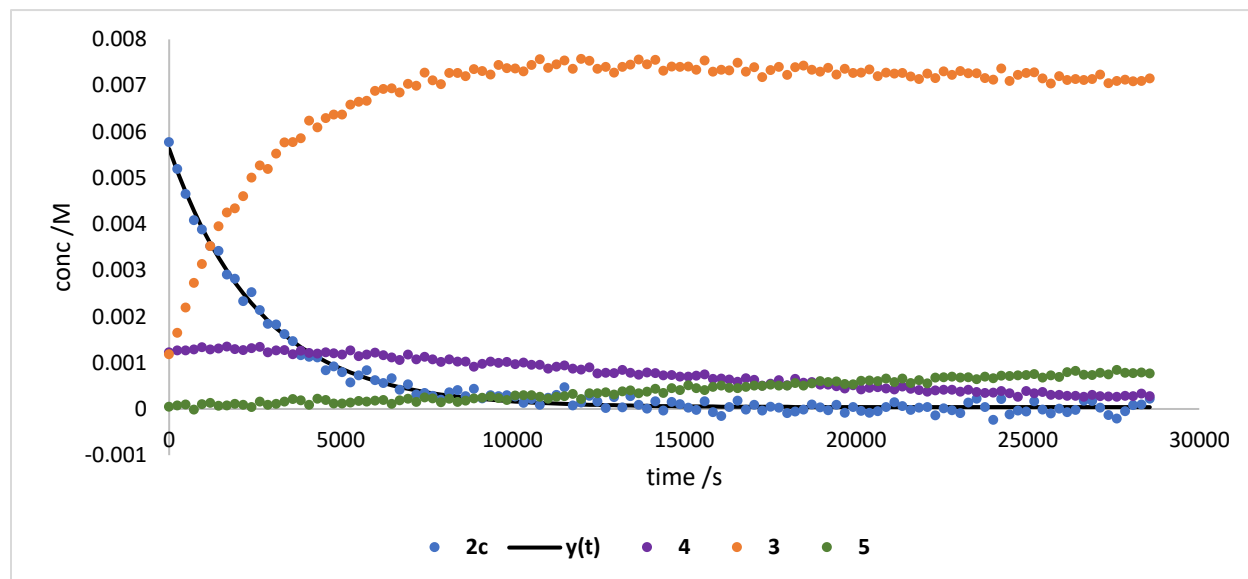


Figure 3.14. Concentration vs time plot for the reductive elimination of **3** from **2c+4** mixture; the concentration of **4** is corrected to account for the dimeric structure (2F per molecule).

Table 3.4. Reductive elimination of **3** from **2c+4** mixture.

Trial	% yield 3 after 3h (after 8 h)	% yield 5 after 8 h	$k_{\text{RE}} \cdot 10^4 / \text{s}^{-1}$	$\Delta G^\ddagger / (\text{kcal} \cdot \text{mol}^{-1})$
1 ^a	47 (47)	12	5.04	24.61
2 ^a	53 (50)	11	3.79	24.80
avg ^a	50 (48)	11		
avg based on initial concentration of 2c ^b	76 (73)	17	4.4	24.7

^aBased on weighed mass of **2c+4** solid. ^bDetermined by ^{19}F NMR spectroscopy at ambient temperature prior to heating; the initial concentration was 0.0094 M (66%) for both trials.

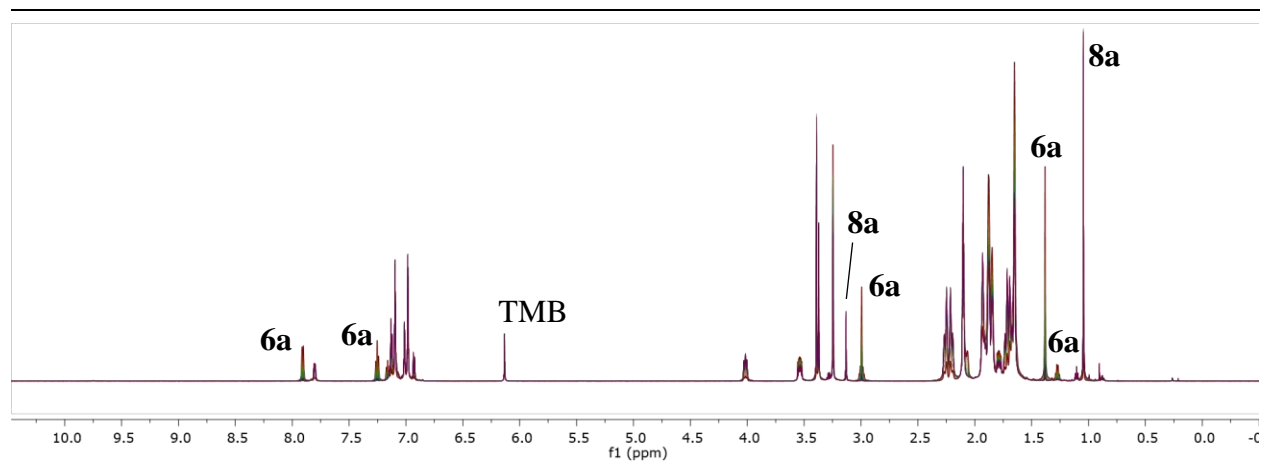


Figure 3.15. Superimposed ^1H NMR spectra for the reductive elimination of **8a** from **6a**.

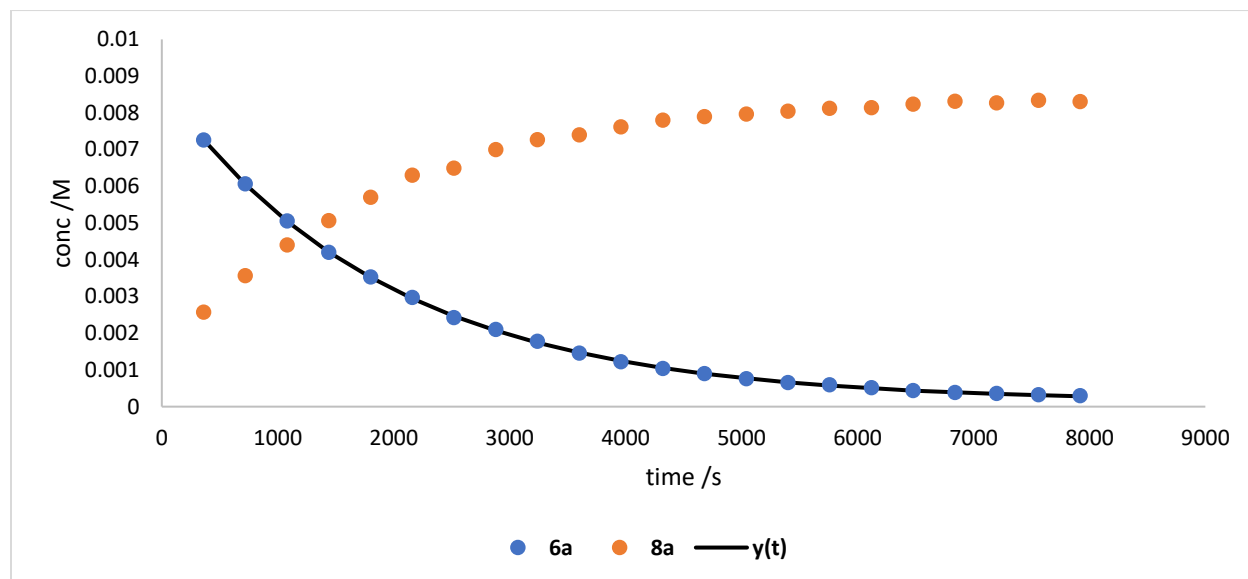


Figure 3.16. Concentration vs time plot for the reductive elimination of **8a** from **6a**.

Trial 1: 90% yield **8a**, $k_{\text{RE}}=5.41 \cdot 10^{-4} \text{s}^{-1}$, $\Delta G^\ddagger=23.80 \text{ kcal/mol}$.

Trial 2: 91% yield **8a**, $k_{\text{RE}}=5.18 \cdot 10^{-4} \text{s}^{-1}$, $\Delta G^\ddagger=23.83 \text{ kcal/mol}$.

Avg: 90% yield **8a**, $k_{\text{RE}}=5.3 \cdot 10^{-4} \text{s}^{-1}$, $\Delta G^\ddagger=23.8 \text{ kcal/mol}$.

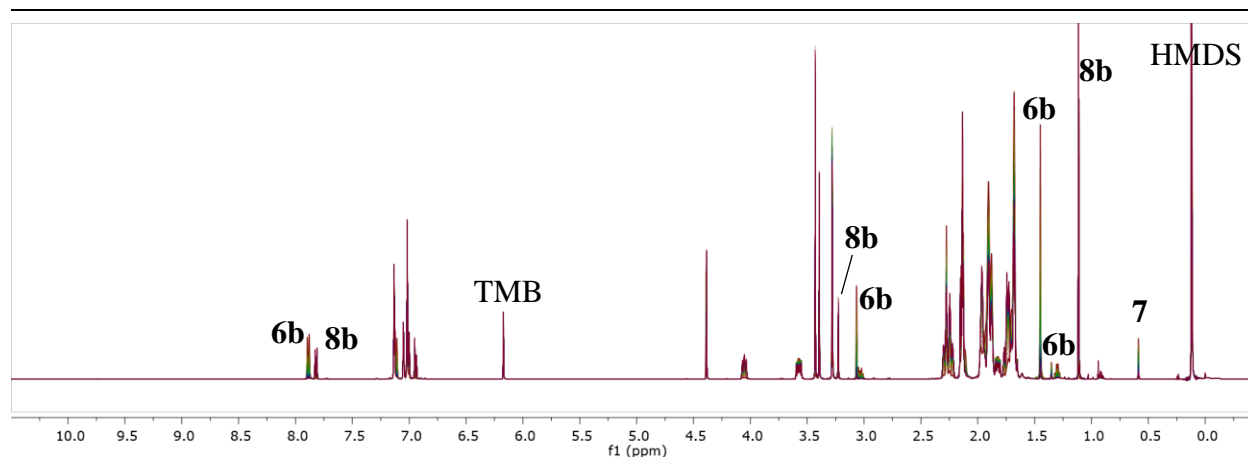


Figure 3.17. Superimposed ^1H NMR spectra for the reductive elimination of **8b** from **6b**.

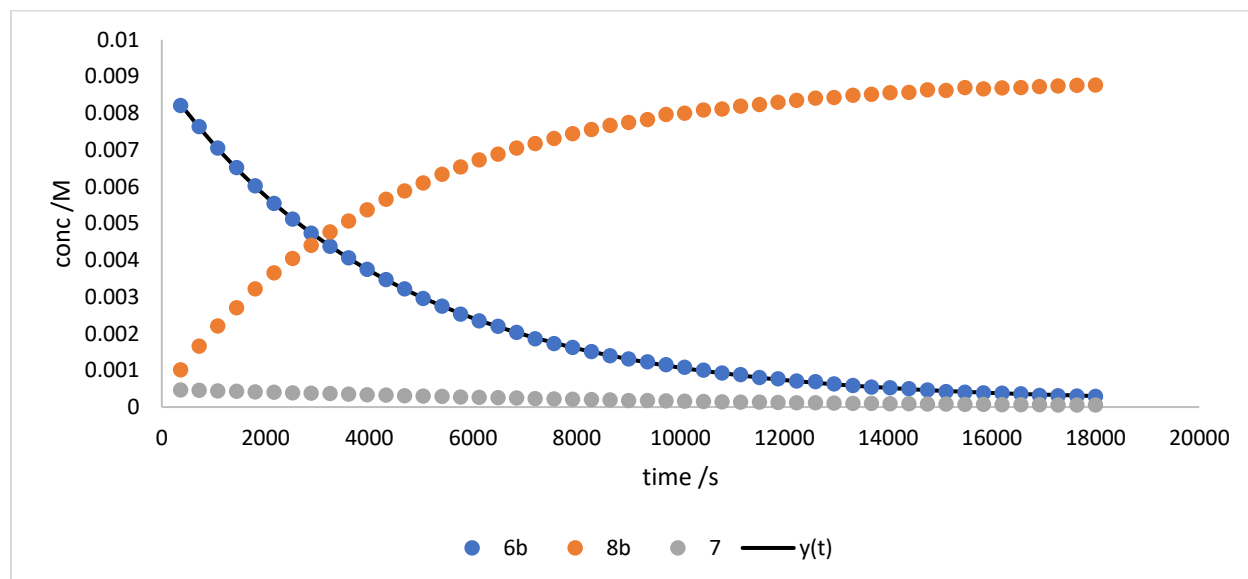


Figure 3.18. Concentration vs time plot for the reductive elimination of **8a** from **6a**.

Trial 1: 91% yield **6b**, 99% yield **8b** (90% based on **1c**), $k_{\text{RE}}=2.72 \cdot 10^{-4} \text{s}^{-1}$, $\Delta G^\ddagger=23.47 \text{ kcal/mol}$.
 Trial 2: 91% yield **6b**, 98% yield **8b** (89% based on **1c**), $k_{\text{RE}}=2.25 \cdot 10^{-4} \text{s}^{-1}$, $\Delta G^\ddagger=23.59 \text{ kcal/mol}$.
 Avg: 91% yield **6b**, 98% yield **8b** (89% based on **1c**), $k_{\text{RE}}=2.5 \cdot 10^{-4} \text{s}^{-1}$, $\Delta G^\ddagger=23.5 \text{ kcal/mol}$.

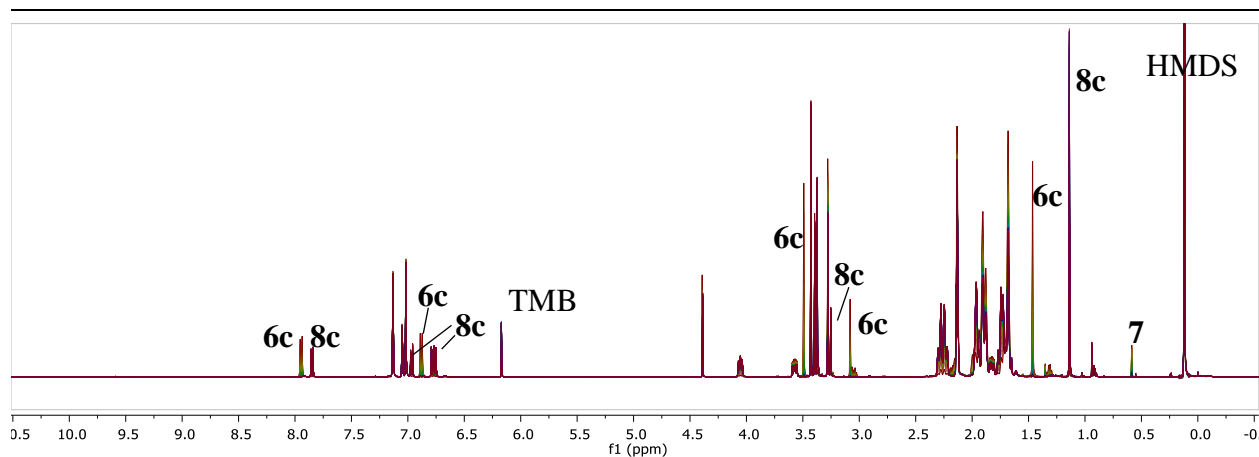


Figure 3.19. Superimposed ^1H NMR spectra for the reductive elimination of **8c** from **6c**.

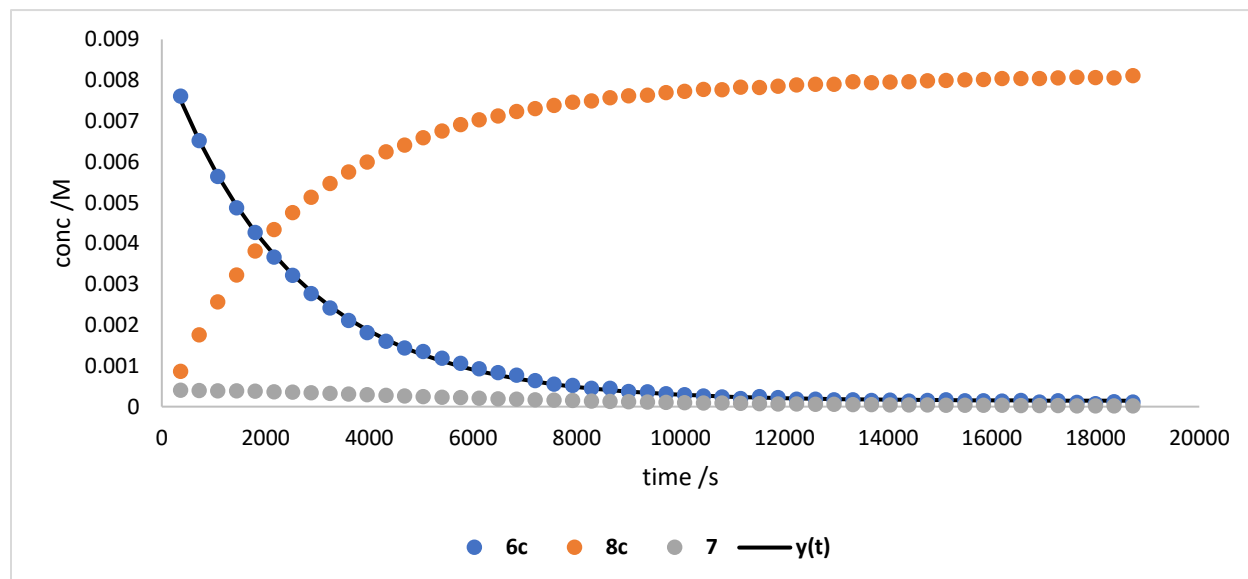


Figure 3.20. Concentration vs time plot for the reductive elimination of **8c** from **6c**.

Trial 1: 85% yield **6c**, 99% yield **8c** (84% based on **1c**), $k_{\text{RE}}=4.02 \cdot 10^{-4} \text{s}^{-1}$, $\Delta G^\ddagger=23.23 \text{ kcal/mol}$.
 Trial 2: 87% yield **6c**, 95% yield **8c** (83% based on **1c**), $k_{\text{RE}}=4.03 \cdot 10^{-4} \text{s}^{-1}$, $\Delta G^\ddagger=23.23 \text{ kcal/mol}$.
 Avg: 86% yield **6c**, 97% yield **8c** (83% based on **1c**), $k_{\text{RE}}=4.0 \cdot 10^{-4} \text{s}^{-1}$, $\Delta G^\ddagger=23.2 \text{ kcal/mol}$.

Table 3.5. Crystal structure data.

Compound	2b	4	6a
Empirical formula	C42.50 H60 F4 N O2 P Pd	C37.50 H61 F N O2 P Pd	C41 H58 N O P Pd
Formula weight	830.28	714.24	718.25
Temperature (K)	100(2)	100(2)	100(2)
Wavelength (Å)	0.71073	0.71073	0.71073
Crystal system	Monoclinic	Triclinic	Monoclinic
Space group	C 2/c	P -1	P 21/n
Unit cell lengths (Å)	a = 32.318(2) b = 14.3174(10) c = 19.7465(14)	a = 10.9155(10) b = 18.2623(18) c = 21.474(2)	a = 11.1621(11) b = 14.1050(14) c = 22.743(2)
Unit cell angles (°)	α = 90 β = 117.761(3) γ = 90	α = 102.755(5) β = 98.270(5) γ = 97.943(5)	α = 90 β = 99.820(4) γ = 90
Volume (Å ³)	8085.3(10)	4067.1(7)	3528.2(6)
Z	8	4	4
Density (calculated) (Mg/m ³)	1.364	1.166	1.352
Absorption coefficient (mm ⁻¹)	0.553	0.529	0.604
F(000)	3480	1516	1520
Crystal size (mm ³)	0.200 x 0.150 x 0.100	0.200 x 0.140 x 0.100	0.270 x 0.180 x 0.150
Theta range for data collection (°)	1.424 to 28.315	1.161 to 28.525	1.706 to 28.389
Index ranges	-43 ≤ h ≤ 42 -19 ≤ k ≤ 19 -25 ≤ l ≤ 26	-14 ≤ h ≤ 14 -24 ≤ k ≤ 24 -28 ≤ l ≤ 28	-14 ≤ h ≤ 14 -18 ≤ k ≤ 18 -29 ≤ l ≤ 30
Reflections collected	125816	185405	80939
Independent reflections	10021 [R(int) = 0.0506]	20179 [R(int) = 0.0490]	8787 [R(int) = 0.0346]
Completeness to theta=28.000°	99.9%	99.0 %	100.0 %
Absorption correction	Semi-empirical from equivalents	Semi-empirical from equivalents	Semi-empirical from equivalents
Max. and min. transmission	0.263 and 0.230	0.647 and 0.606	0.563 and 0.533
Refinement method	Full-matrix least-squares on F ²	Full-matrix least-squares on F ²	Full-matrix least-squares on F ²
Data / restraints / parameters	10021 / 0 / 475	20179 / 0 / 804	8787 / 0 / 410
Goodness-of-fit on F ²	1.064	1.070	1.086
Final R indices [I > 2σ(I)]	R1 = 0.0338 wR2 = 0.0823	R1 = 0.0453 wR2 = 0.1107	R1 = 0.0266 wR2 = 0.0672
R indices (all data)	R1 = 0.0420 wR2 = 0.0862	R1 = 0.0634 wR2 = 0.1210	R1 = 0.0304 wR2 = 0.0688
Extinction coefficient	n/a	n/a	n/a
Largest diff. peak and hole (e.Å ⁻³)	1.330 and -0.473	2.230 and -0.610	0.999 and -0.282

Table 3.6. Atomic coordinates (x 10⁴) and equivalent isotropic displacement parameters (Å²x 10³) for **2b**. U(eq) is defined as one third of the trace of the orthogonalized U^{ij} tensor.

	<u>x</u>	<u>y</u>	<u>z</u>	<u>U(eq)</u>
C(1)	9531(1)	3394(2)	8178(2)	57(1)
C(2)	8852(1)	3756(2)	6997(1)	27(1)
C(3)	9100(1)	3776(2)	6581(2)	40(1)
C(4)	8874(1)	4059(2)	5824(2)	43(1)
C(5)	8415(1)	4306(2)	5465(2)	35(1)
C(6)	8168(1)	4305(1)	5891(1)	24(1)
C(7)	8376(1)	4042(1)	6663(1)	20(1)
C(8)	7332(1)	2874(1)	5841(1)	21(1)
C(9)	6647(1)	3802(1)	5546(1)	14(1)

C(10)	6380(1)	3144(1)	4997(1)	16(1)
C(11)	5901(1)	3243(1)	4597(1)	17(1)
C(12)	5689(1)	4000(1)	4742(1)	15(1)
C(13)	5171(1)	4106(2)	4294(1)	21(1)
C(14)	5955(1)	4648(1)	5296(1)	14(1)
C(15)	6443(1)	4574(1)	5716(1)	13(1)
C(16)	7923(1)	5738(1)	7690(1)	16(1)
C(17)	8297(1)	6586(2)	6961(1)	24(1)
C(18)	8353(1)	6277(1)	7741(1)	17(1)
C(19)	8807(1)	5711(2)	8152(1)	24(1)
C(20)	8410(1)	7139(2)	8236(1)	24(1)
C(21)	6620(1)	5400(1)	7211(1)	13(1)
C(22)	6911(1)	4617(1)	7768(1)	16(1)
C(23)	6795(1)	4537(2)	8438(1)	19(1)
C(24)	6911(1)	5465(2)	8878(1)	21(1)
C(25)	6618(1)	6243(1)	8337(1)	19(1)
C(26)	6730(1)	6329(1)	7662(1)	16(1)
C(27)	6098(1)	6023(1)	8028(1)	19(1)
C(28)	5985(1)	5101(1)	7589(1)	16(1)
C(29)	6274(1)	4317(1)	8125(1)	18(1)
C(30)	6098(1)	5178(1)	6915(1)	15(1)
C(31)	6676(1)	6579(1)	5911(1)	13(1)
C(32)	6169(1)	6938(1)	5604(1)	16(1)
C(33)	6105(1)	7855(1)	5159(1)	18(1)
C(34)	6442(1)	8595(1)	5685(1)	19(1)
C(35)	6946(1)	8254(1)	5972(1)	18(1)
C(36)	7016(1)	7340(1)	6424(1)	16(1)
C(37)	7042(1)	8081(1)	5292(1)	19(1)
C(38)	6702(1)	7337(1)	4771(1)	18(1)
C(39)	6774(1)	6425(1)	5222(1)	16(1)
C(40)	6198(1)	7681(1)	4477(1)	20(1)
C(41)	4818(1)	7238(3)	3631(2)	73(1)
C(42)	4893(1)	7809(2)	3033(2)	59(1)
C(43)	5000	7226(3)	2500	55(1)
N(1)	8133(1)	4043(1)	7076(1)	18(1)
O(1)	9034(1)	3470(1)	7745(1)	34(1)
O(2)	7125(1)	3718(1)	5948(1)	16(1)
F(1)	9129(1)	4066(1)	5430(1)	67(1)
F(2)	5009(1)	3821(1)	3569(1)	34(1)
F(3)	4938(1)	3597(1)	4580(1)	37(1)
F(4)	5027(1)	4986(1)	4268(1)	30(1)
P(1)	6818(1)	5434(1)	6446(1)	12(1)
Pd(1)	7549(1)	4820(1)	6822(1)	13(1)

Table 3.7. Atomic coordinates ($\times 10^4$) and equivalent isotropic displacement parameters ($\text{\AA}^2 \times 10^3$) for **4**. $U(\text{eq})$ is defined as one third of the trace of the orthogonalized U^{ij} tensor.

	x	y	z	U(eq)
C(1)	3732(2)	7530(2)	5110(1)	17(1)
C(2)	2928(3)	6814(2)	5226(1)	20(1)
C(3)	1659(3)	6596(2)	4765(2)	26(1)
C(4)	914(3)	7252(2)	4879(2)	27(1)
C(5)	1677(3)	7960(2)	4751(2)	24(1)
C(6)	1898(3)	7786(2)	4052(2)	28(1)
C(7)	2630(3)	7124(2)	3937(2)	27(1)
C(8)	1869(3)	6421(2)	4063(2)	29(1)
C(9)	3915(3)	7361(2)	4400(1)	20(1)
C(10)	2948(2)	8176(2)	5218(1)	20(1)
C(11)	6424(2)	8543(2)	5575(1)	17(1)
C(12)	7098(3)	8222(2)	5013(1)	23(1)
C(13)	8165(3)	8832(2)	4949(2)	28(1)
C(14)	7618(3)	9511(2)	4799(2)	35(1)
C(15)	6958(3)	9844(2)	5351(2)	31(1)
C(16)	5889(3)	9230(2)	5412(2)	24(1)
C(17)	7401(2)	8838(2)	6212(1)	18(1)
C(18)	8469(3)	9440(2)	6137(2)	24(1)
C(19)	7909(3)	10114(2)	5985(2)	31(1)
C(20)	9120(3)	9094(2)	5587(2)	28(1)
C(21)	5906(2)	6914(2)	5501(1)	17(1)
C(22)	7183(3)	6850(2)	5850(1)	19(1)
C(23)	8629(3)	5999(2)	5793(2)	33(1)
C(24)	4496(3)	9026(2)	6820(1)	18(1)
C(25)	3211(3)	9161(2)	7030(1)	21(1)
C(26)	2275(3)	8418(2)	6949(2)	26(1)
C(27)	3416(3)	9601(2)	7742(2)	26(1)
C(28)	2591(3)	9653(2)	6624(2)	27(1)
C(29)	6818(2)	8642(2)	7898(1)	16(1)
C(30)	7744(3)	8235(2)	7714(1)	19(1)
C(31)	8961(3)	8581(2)	7698(1)	22(1)
C(32)	9233(3)	9361(2)	7879(1)	23(1)
C(33)	8381(3)	9805(2)	8085(1)	22(1)
C(34)	7182(3)	9449(2)	8110(1)	18(1)
C(35)	6606(3)	10637(2)	8560(2)	33(1)
C(36)	4011(3)	6312(2)	6691(1)	17(1)
C(37)	2870(3)	6455(2)	6856(1)	19(1)
C(38)	1742(3)	5958(2)	6576(2)	25(1)
C(39)	1779(3)	5309(2)	6123(2)	26(1)
C(40)	2877(3)	5123(2)	5943(2)	24(1)
C(41)	3997(3)	5622(2)	6236(1)	19(1)

C(42)	5243(3)	4750(2)	5762(2)	31(1)
C(43)	5473(2)	5948(2)	7932(1)	16(1)
C(44)	6737(3)	5658(2)	7933(1)	20(1)
C(45)	7467(3)	5919(2)	7436(2)	24(1)
C(46)	6454(3)	4779(2)	7745(2)	28(1)
C(47)	7601(3)	5924(2)	8596(2)	28(1)
C(48)	3527(2)	7408(2)	9085(1)	18(1)
C(49)	2790(3)	6588(2)	8758(2)	21(1)
C(50)	1365(3)	6587(2)	8685(2)	26(1)
C(51)	986(3)	7109(2)	8253(2)	28(1)
C(52)	1712(3)	7924(2)	8563(2)	23(1)
C(53)	3135(2)	7930(2)	8645(1)	19(1)
C(54)	3152(3)	7693(2)	9749(1)	22(1)
C(55)	1717(3)	7680(2)	9661(2)	27(1)
C(56)	1352(3)	8198(2)	9228(2)	26(1)
C(57)	1027(3)	6861(2)	9355(2)	29(1)
C(58)	6307(2)	8215(2)	9673(1)	17(1)
C(59)	5931(3)	8964(2)	9547(1)	18(1)
C(60)	6883(3)	9663(2)	9964(1)	20(1)
C(61)	8195(3)	9610(2)	9813(2)	24(1)
C(62)	8584(3)	8883(2)	9955(1)	24(1)
C(63)	8605(3)	8899(2)	10672(2)	27(1)
C(64)	7291(3)	8959(2)	10822(1)	24(1)
C(65)	6894(3)	9683(2)	10681(1)	24(1)
C(66)	6362(3)	8245(2)	10400(1)	20(1)
C(67)	7647(3)	8183(2)	9525(1)	21(1)
C(68)	5560(3)	6593(2)	9526(1)	21(1)
C(69)	4990(3)	6442(2)	10106(2)	28(1)
C(70)	5275(4)	5716(2)	10878(2)	45(1)
C(71)	-8(4)	4388(3)	7757(2)	62(1)
C(72)	1371(4)	4350(2)	7735(2)	51(1)
C(73)	1575(3)	3855(2)	7120(2)	39(1)
C(74)	2939(4)	3813(3)	7093(2)	50(1)
C(75)	3105(5)	3279(3)	6485(2)	58(1)
N(1)	5581(2)	8260(1)	7858(1)	15(1)
N(2)	5140(2)	6837(1)	6974(1)	14(1)
O(1)	7447(2)	6139(1)	5520(1)	30(1)
O(2)	6277(2)	9829(1)	8337(1)	21(1)
O(3)	5150(2)	5496(1)	6102(1)	23(1)
O(4)	5704(2)	5937(1)	10342(1)	37(1)
F(1)	10402(2)	9726(1)	7853(1)	33(1)
F(2)	684(2)	4815(1)	5834(1)	37(1)
P(1)	5216(1)	7779(1)	5744(1)	13(1)
P(2)	5246(1)	7346(1)	9100(1)	14(1)

Pd(1)	4999(1)	7973(1)	6813(1)	13(1)
Pd(2)	5450(1)	7098(1)	8013(1)	13(1)

Table 3.8. Atomic coordinates ($\times 10^4$) and equivalent isotropic displacement parameters ($\text{\AA}^2 \times 10^3$) for **6a**. $U(\text{eq})$ is defined as one third of the trace of the orthogonalized U^{ij} tensor.

	x	y	z	U(eq)
C(1)	8655(1)	4519(1)	4229(1)	21(1)
C(2)	9705(2)	3979(1)	4395(1)	24(1)
C(3)	10032(2)	3308(1)	4008(1)	28(1)
C(4)	9302(2)	3171(1)	3458(1)	29(1)
C(5)	8252(2)	3706(1)	3294(1)	24(1)
C(6)	7919(1)	4392(1)	3677(1)	18(1)
C(7)	6787(1)	4990(1)	3514(1)	16(1)
C(8)	6376(1)	5138(1)	2855(1)	16(1)
C(9)	7184(1)	5427(1)	2486(1)	19(1)
C(10)	6780(2)	5634(1)	1890(1)	22(1)
C(11)	5560(2)	5523(1)	1648(1)	22(1)
C(12)	4753(2)	5218(1)	2005(1)	21(1)
C(13)	5154(1)	5036(1)	2605(1)	18(1)
C(14)	5503(1)	7206(1)	3453(1)	15(1)
C(15)	6662(1)	7674(1)	3814(1)	17(1)
C(16)	6788(2)	7525(1)	4488(1)	23(1)
C(17)	7814(1)	7294(1)	3613(1)	26(1)
C(18)	6598(2)	8741(1)	3682(1)	24(1)
C(19)	4466(2)	4036(1)	4432(1)	18(1)
C(20)	2777(1)	5042(1)	4443(1)	15(1)
C(21)	1939(1)	5716(1)	4048(1)	15(1)
C(22)	2552(1)	7744(1)	4245(1)	13(1)
C(23)	2971(1)	7396(1)	4892(1)	18(1)
C(24)	2943(2)	8211(1)	5337(1)	21(1)
C(25)	1643(2)	8591(1)	5277(1)	23(1)
C(26)	1225(2)	8954(1)	4644(1)	19(1)
C(27)	1253(1)	8143(1)	4191(1)	16(1)
C(28)	2077(2)	9753(1)	4520(1)	20(1)
C(29)	3374(1)	9370(1)	4575(1)	19(1)
C(30)	3797(2)	9000(1)	5209(1)	22(1)
C(31)	3403(1)	8556(1)	4127(1)	16(1)
C(32)	1851(1)	6830(1)	2978(1)	14(1)
C(33)	455(1)	6795(1)	2940(1)	17(1)
C(34)	-177(1)	6806(1)	2283(1)	19(1)
C(35)	160(2)	7714(1)	1985(1)	21(1)
C(36)	1538(2)	7760(1)	2011(1)	20(1)
C(37)	2178(1)	7746(1)	2669(1)	16(1)
C(38)	1941(2)	6901(1)	1680(1)	24(1)

C(39)	1596(2)	5996(1)	1976(1)	21(1)
C(40)	2251(2)	5981(1)	2629(1)	17(1)
C(41)	218(2)	5947(1)	1955(1)	21(1)
N(1)	6284(1)	5339(1)	3921(1)	15(1)
O(1)	3766(1)	4803(1)	4139(1)	15(1)
P(1)	2759(1)	6708(1)	3753(1)	12(1)
Pd(1)	4694(1)	6079(1)	3806(1)	11(1)

3.5 References and notes

1. Koo, K.; Hillhouse, G. L., *Organometallics* **1995**, *14* (9), 4421-4423.
2. Lin, B. L.; Clough, C. R.; Hillhouse, G. L., *J. Am. Chem. Soc.* **2002**, *124* (12), 2890-2891.
3. Pawlikowski, A. V.; Getty, A. D.; Goldberg, K. I., *J. Am. Chem. Soc.* **2007**, *129* (34), 10382-10393.
4. Pendleton, I. M.; Pérez-Temprano, M. H.; Sanford, M. S.; Zimmerman, P. M., *J. Am. Chem. Soc.* **2016**, *138* (18), 6049-6060.
5. Pérez-Temprano, M. H.; Racowski, J. M.; Kampf, J. W.; Sanford, M. S., *J. Am. Chem. Soc.* **2014**, *136* (11), 4097-4100.
6. Rucker, R. P.; Whittaker, A. M.; Dang, H.; Lalic, G., *J. Am. Chem. Soc.* **2012**, *134* (15), 6571-6574.
7. Camasso, N. M.; Canty, A. J.; Ariafard, A.; Sanford, M. S., *Organometallics* **2017**, *36* (22), 4382-4393.
8. Marquard, S. L.; Rosenfeld, D. C.; Hartwig, J. F., *Angew. Chem. Int. Ed.* **2010**, *49* (4), 793-796.
9. Hanley, P. S.; Marquard, S. L.; Cundari, T. R.; Hartwig, J. F., *J. Am. Chem. Soc.* **2012**, *134* (37), 15281-15284.
10. By "unstabilized," we exclude benzyl, allyl, enolate, and other ligands containing a stabilizing group on carbon.
11. Leal, R. A.; Bischof, C.; Lee, Y. V.; Sawano, S.; McAtee, C. C.; Latimer, L. N.; Russ, Z. N.; Dueber, J. E.; Yu, J.-Q.; Sarpong, R., *Angew. Chem. Int. Ed.* **2016**, *55* (39), 11824-11828.
12. He, J.; Shigenari, T.; Yu, J.-Q., *Angew. Chem. Int. Ed.* **2015**, *54* (22), 6545-6549.
13. Pan, J.; Su, M.; Buchwald, S. L., *Angew Chem Int Ed Engl* **2011**, *50* (37), 8647-51.
14. He, G.; Zhao, Y.; Zhang, S.; Lu, C.; Chen, G., *J. Am. Chem. Soc.* **2012**, *134* (1), 3-6.
15. Ozawa, F.; Ito, T.; Yamamoto, A., *J. Am. Chem. Soc.* **1980**, *102* (21), 6457-6463.
16. Fumiyuki, O.; Takashi, I.; Yoshiyuki, N.; Akio, Y., *Bull. Chem. Soc. Jpn.* **1981**, *54* (6), 1868-1880.
17. Hartwig, J. F., *Organotransition Metal Chemistry From Bonding to Catalysis*. 1 ed.; University Science Book: Mill Valley, CA, 2010.
18. Esposito, O.; Gois, P. M. P.; de K. Lewis, A. K.; Caddick, S.; Cloke, F. G. N.; Hitchcock, P. B., *Organometallics* **2008**, *27* (24), 6411-6418.
19. Esposito, O.; Lewis, A. K. d. K.; Hitchcock, P. B.; Caddick, S.; Cloke, F. G. N., *Chem. Commun.* **2007**, (11), 1157-1159.
20. Pan, J.; Su, M.; Buchwald, S. L., *Angew. Chem. Int. Ed.* **2011**, *50* (37), 8647-8651.
21. Tatsuo, I.; Shigeru, A.; Norio, M.; Akira, S., *Chem. Lett.* **1992**, *21* (4), 691-694.

-
22. Kurandina, D.; Parasram, M.; Gevorgyan, V., *Angew. Chem. Int. Ed.* **2017**, *56* (45), 14212-14216.
 23. Zou, Y.; Zhou, J., *Chem. Commun.* **2014**, *50* (28), 3725-3728.
 24. Ziadi, A.; Correa, A.; Martin, R., *Chem. Commun.* **2013**, *49* (39), 4286-4288.
 25. Yoon, H.; Petrone, D. A.; Lautens, M., *Org. Lett.* **2014**, *16* (24), 6420-6423.
 26. Yoon, H.; Jang, Y. J.; Lautens, M., *Synthesis* **2016**, *48* (10), 1483-1490.
 27. Jia, X.; Petrone, D. A.; Lautens, M., *Angew Chem Int Ed Engl* **2012**, *51* (39), 9870-2.
 28. Lan, Y.; Liu, P.; Newman, S. G.; Lautens, M.; Houk, K. N., *Chemical Science* **2012**, *3* (6), 1987-1995.
 29. Newman, S. G.; Howell, J. K.; Nicolaus, N.; Lautens, M., *J. Am. Chem. Soc.* **2011**, *133* (38), 14916-14919.
 30. Newman, S. G.; Lautens, M., *J. Am. Chem. Soc.* **2011**, *133* (6), 1778-1780.
 31. Petrone, D. A.; Franzoni, I.; Ye, J.; Rodríguez, J. F.; Poblador-Bahamonde, A. I.; Lautens, M., *J. Am. Chem. Soc.* **2017**, *139* (9), 3546-3557.
 32. Petrone, D. A.; Lischka, M.; Lautens, M., *Angew. Chem. Int. Ed.* **2013**, *52* (40), 10635-10638.
 33. Petrone, D. A.; Malik, H. A.; Clemenceau, A.; Lautens, M., *Org. Lett.* **2012**, *14* (18), 4806-4809.
 34. Petrone, D. A.; Yoon, H.; Weinstabl, H.; Lautens, M., *Angew. Chem. Int. Ed.* **2014**, *53* (30), 7908-7912.
 35. Sickert, M.; Weinstabl, H.; Peters, B.; Hou, X.; Lautens, M., *Angew. Chem. Int. Ed.* **2014**, *53* (20), 5147-5151.
 36. Marquard, S. L. Reductive elimination of alkylamines and ethers: reactions of bisphosphine-ligated palladium(II) complexes. Dissertation, University of Illinois at Urbana-Champaign, 2012.
 37. Complexes containing the di-tert-butyl-substituted analog of this ligand discussed in Chapter 2 are highly soluble in organic solvents. The di-adamantyl-substituted L1 was synthesized to simplify the isolation and purification of the corresponding palladium complexes.
 38. Mann, G.; Hartwig, J. F.; Driver, M. S.; Fernández-Rivas, C., *J. Am. Chem. Soc.* **1998**, *120* (4), 827-828.
 39. Protection for the Amino Group. In *Greene's Protective Groups in Organic Synthesis*, 5 ed.; Wuts, P. G. M., Ed. John Wiley & Sons, Inc.: 2014; pp 895-1193.
 40. Peacock, D. M.; Roos, C. B.; Hartwig, J. F., *ACS Cent. Sci.* **2016**, *2* (9), 647-652.
 41. Köllhofer, A.; Plenio, H., *Chem. Eur. J.* **2003**, *9* (6), 1416-1425.

CHAPTER 4

Palladium-catalyzed *N*-alkylation of benzophenone imine with
primary alkyl bromides

4.1 Introduction

Transition metal-catalyzed cross coupling reactions are now common methods for the construction of sp^2 carbon–carbon and carbon–heteroatom bonds. Metal-catalyzed methods for the construction of sp^3 carbon–carbon bonds have recently undergone much development, and efficient catalysts for the coupling of alkyl halides with a wide variety of carbon nucleophiles have been reported.¹⁻⁵ However, catalysts for the analogous coupling reactions of alkyl halides with nitrogen nucleophiles are much less developed. Yet, such reactions could create a means to control the selectivity for substitution vs elimination, to control the site selectivity for reaction at one carbon–halogen bond over another, to create dynamic kinetic transformations at racemic electrophiles, or to expand the scope of nitrogen reagents to encompass those that are weakly nucleophilic.

We recently reported that palladium complexes containing bulky tri-alkylphosphine ligands catalyze the thermal cross coupling of secondary and tertiary alkyl halides with benzophenone imines (see Chapter 5).⁶ In addition, Fu and Peters reported photoinduced, copper-catalyzed alkylation reactions of carbazoles,⁷ amides,⁸⁻⁹ heterocycles,¹⁰ and amines¹¹ with alkyl halides. Both of these reactions occur *via* alkyl radical intermediates. However, the potential of transition-metal complexes to catalyze *N*-alkylation reactions through traditional, two-electron pathways has not yet been demonstrated.

We envisioned that this reaction could occur by a palladium-catalyzed pathway involving oxidative addition and reductive elimination as the key bond-breaking and bond-forming steps. The oxidative addition of alkyl halides has been reported to occur to palladium(0) complexes with low kinetic barriers.¹² A variety of palladium(II) complexes have been reported to react with methyl halides and – albeit less commonly – larger alkyl halides.¹³ Furthermore, mechanistic studies have implicated the oxidative additions of alkyl halides to Pd(II) complexes in a number of catalytic reactions.¹⁴ Our group has investigated reductive elimination reactions from alkylpalladium(II) amido complexes.¹⁵⁻¹⁶ As part of this work, we observed that reductive elimination from neopentylpalladium(II) amido complexes can occur with exceptionally low barriers (see Chapter 3). Sanford has reported examples of alkylpalladium(IV) amido complexes that undergo reductive elimination with low barriers. We therefore expected that both key steps in this proposed reaction would be feasible in either Pd^0 - Pd^{II} or Pd^{II} - Pd^{IV} catalytic cycles.

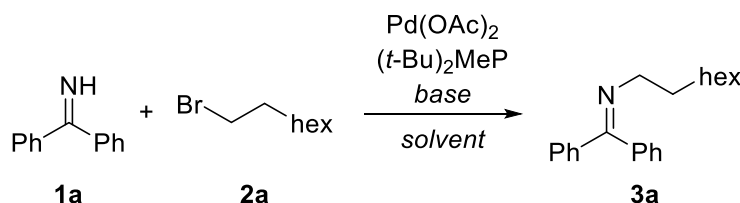
However, such a catalytic process could be complicated by competitive formation of alkenes by an E2 process or by β -hydride elimination from the proposed alkylpalladium intermediate. To avoid the competing E2 process, the alkyl bromide must react faster with the palladium catalyst than with the strong base required to form a palladium-amido complex. Similarly, the proposed alkylpalladium intermediate must undergo reductive elimination to form the C–N bond faster than it undergoes β -hydride elimination.

We report that palladium complexes containing iminoquinoline ligands catalyze the thermal coupling of primary alkyl bromides with benzophenone imine. Our studies focused on the reactions of imines because benzophenone imine can participate in reductive elimination reactions from Pd(II) (see Chapter 3), does not undergo traditional S_N2 processes with unactivated alkyl halides,¹⁷⁻²⁷ and can serve as a synthetic equivalent to ammonia.

4.2 Results and discussion

We evaluated reactions of benzophenone imine (**1a**) with 1-bromooctane (**2a**) and alkoxide bases catalyzed by palladium complexes and tri-*tert*-butylphosphine because reductive elimination appeared to occur from the alkylpalladium methyleneimido complex of this ligand. We also evaluated reactions catalyzed by palladium and the less bulky ligand di-(*tert*-butyl)methylphosphine because of the precedent of Pd(0) complexes of this ligand undergoing oxidative addition of alkyl halides at 0 °C (Table 4.1).²⁸ The reaction of **1a** with **2a** and NaOt-Bu in THF catalyzed by 10 mol % (*t*-Bu)₃Pd⁰ at ambient temperature gave no detectable *N*-octylbenzophenone imine (**3a**) after 18 h. The same reaction catalyzed by Pd(OAc)₂ and *t*-Bu₂MeP produced **3a** in less than one turnover after 5 d (entry 1). However, the reaction run in DMF with LiOt-Bu as the base gave 53% yield of **3a** after 24 h (entry 6). Only trace amounts of **3a** were detected when the palladium catalyst was omitted (entry 5). Surprisingly, the reaction run with no added phosphine ligand produced **3a** in a higher yield of 65% after 24 h (entry 7). The reaction occurred identically in room light or in the dark, indicating that it is a thermal process. The reactivity in the absence of added ligand suggests that the imine might act as both a reagent and an ancillary ligand for the palladium catalyst.

Table 4.1. Pd(OAc)₂ catalyzed *N*-alkylation of benzophenone imine with 1-bromooctane.



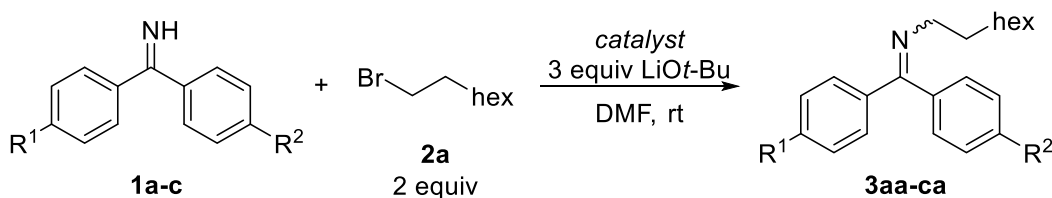
entry	mol% Pd/L	base	solvent	time	yield ^a
1 ^b	10/20	NaOt-Bu	THF	5 days	~5%
2 ^c	10/20	NaOt-Bu	DMF	15 h	23%
3 ^c	10/20	KOt-Bu	DMF	15 h	<1%
4 ^c	10/20	LiOt-Bu	DMF	15 h	59%
5 ^c	-	LiOt-Bu	DMF	24 h	~1%
6 ^c	5/10	LiOt-Bu	DMF	24 h	53%
7 ^c	5/-	LiOt-Bu	DMF	24 h	65%
8 ^{c,d}	5/-	LiOt-Bu	DMF	24 h	63%

^aYield determined by corrected GC integration against TMB. ^bConditions: 1 equiv **2a**, 2 equiv base. ^cConditions: 1.2 equiv **2a**, 3 equiv base. ^dReaction performed in the dark.

To investigate further the role of the imine in the reaction, we studied the alkylation of fluorine-labelled 4,4'-difluorobenzophenone imine (**1b**) with 1-bromooctane (**2a**) catalyzed by Pd(OAc)₂. Although we were unable to identify the resting state, monitoring of this reaction by ¹⁹F NMR spectroscopy with varying amounts of Pd(OAc)₂ showed that the combined concentration of **1b** and *N*-octyl-4,4'-difluorobenzophenone imine (**3ba**) was lower than the expected total concentration of imine, based on the amount of **1b** added to the reaction. When the reaction was performed with varying amounts of Pd(OAc)₂, we found that this difference increased concomitantly with the catalyst loading (2-3 imines per palladium; see the experimental section).

This result suggests that multiple imine molecules are bound to the palladium catalyst. In addition, we observed that the alkylation of 4,4'-difluorobenzophenone imine (**1b**) was faster than the same reaction of either benzophenone imine (**1a**) or 4-methylbenzophenone imine (**1c**) (Table 4.2, entries 1-3). We considered that the faster rates for reactions of the fluorinated **1b** result, predominantly, from the electronic effect on this imine when acting as ancillary ligand.

Table 4.2. Relative rates of the *N*-alkylation of substituted benzophenone imines catalyzed by Pd(OAc)₂ and by Pd(OAc)₂ and **L3**.

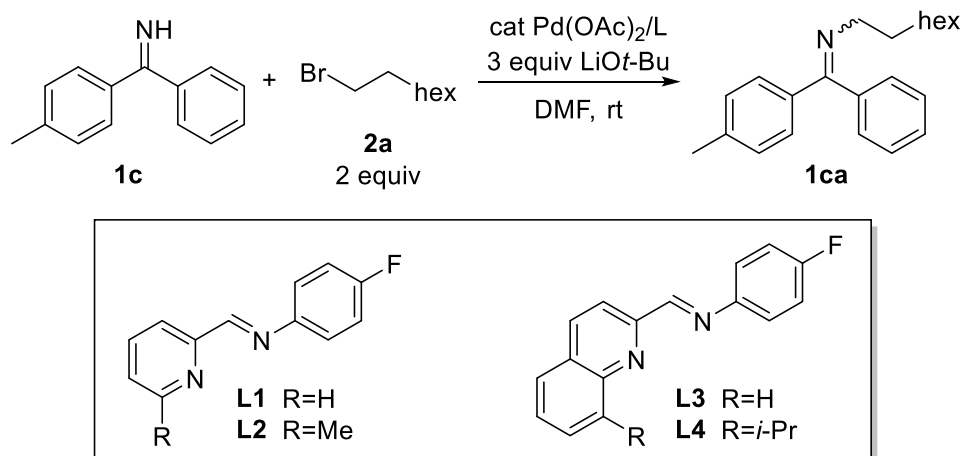


entry	catalyst	R ¹	R ²		conversion at 40 min ^a	conversion at 80 min ^a
1	4% Pd(OAc) ₂	H	H	(1a)	23	39
2		F	F	(1b)	39	57
3		CH ₃	H	(1c)	26	39
4	2% Pd(OAc) ₂ , 2% L3	H	H	(1a)	88	>99
5		F	F	(1b)	40	63
6		CH ₃	H	(1c)	56	93

^aConversion determined by corrected GC integration of **1a-c** against TMB.

On the basis of this hypothesis, we investigated the potential of chelating ancillary ligands containing imine donors to create more active catalysts (Table 4.3). After exploring a variety of N,N and P,N ligands, we found that the combination of Pd(OAc)₂ and (E)-*N*-(4-fluorophenyl)-2-pyridinecarboxaldehyde imine (**L1**) formed a more active catalyst than Pd(OAc)₂ alone. Reaction mixtures containing more sterically bulky ancillary ligands, such as **L2** and **L3**, consumed **1c** in higher conversion (entry 3), at faster rates (entries 4 and 5), or with lower catalyst loadings (entry 6). However, the 8-*iso*-propyl substituted **L4** is likely too bulky to coordinate to the palladium center, and does not form an effective catalyst when combined with Pd(OAc)₂ (entry 7).

The reaction of 4,4'-difluorobenzophenone imine (**1b**) with 1-bromooctane (**2a**) catalyzed by Pd(OAc)₂ and **L3** was slower than the same reaction of the unsubstituted benzophenone imine (Table 4.2, entries 4 and 5). These relative rates contrast those of reactions catalyzed by Pd(OAc)₂ alone (entries 1 and 2). This difference in relative rates in the presence and absence of added ligand supports our proposal that the relative rates of the reactions catalyzed by Pd(OAc)₂ are due predominantly to the effect of the electronic properties of the benzophenone imine derivatives on their ability to serve as ancillary ligands.

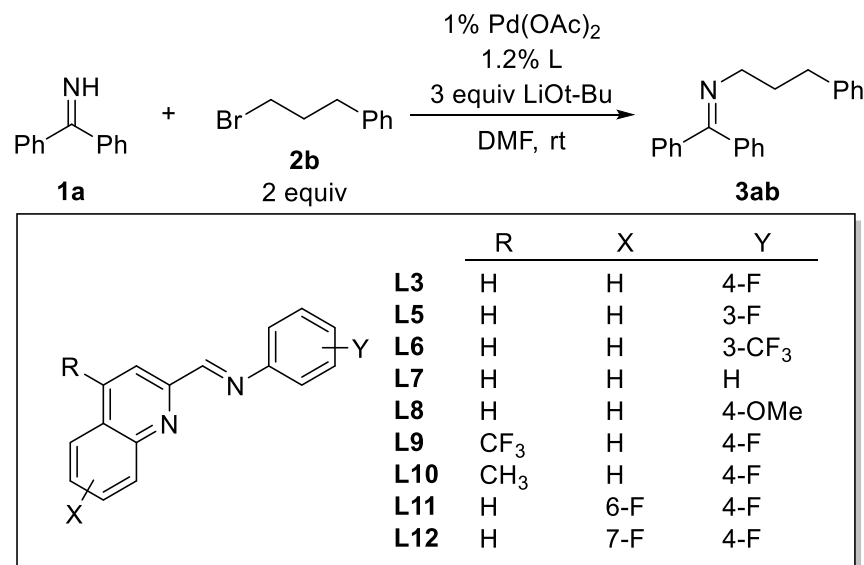
Table 4.3. Effect of iminopyridine and iminoquinoline ancillary ligands on the *N*-alkylation of 4-methylbenzophenone imine (**1c**).

entry	L	mol% Pd(OAc) ₂ /L	time / h	conversion 1c ^a
1	None	4	8	56
2	L1	4	8	78
3	L2	4	8	>99
4	L2	4	3	79
5	L3	4	1	>99
6	L3	2	3	97
7	L4	2	3	32

^aConversion determined by corrected GC integration of 4-methylbenzophenone imine against TMB.

To increase the activity of the catalyst further, we explored the reaction of benzophenone imine (**1a**) with 1-bromo-3-phenylpropane (**2b**) in the presence of 1 mol % of Pd(OAc)₂ as the metal precursor and 1.2 mol % of derivatives of **L3** bearing various aryl groups on the imine nitrogen donor (Table 4.4). Reactions catalyzed by Pd(OAc)₂ and **L7** or **L8** containing unsubstituted or *p*-methoxyphenyl groups on the imine occurred to less than 30% conversion after 100 min (entries 5 and 6), while reactions with **L3** or **L5** containing fluoroaryl groups on nitrogen both occurred to greater than 90% conversion in the same time (entries 1, 2, and 3). The same reaction catalyzed by Pd(OAc)₂ and **L6**, which contains the more strongly withdrawing 3-CF₃ group, occurred to 61% conversion after 100 min (entry 7). These results suggest that catalysts bound by ancillary ligands containing mildly σ -withdrawing groups are more active than catalysts bound by ancillary ligands containing electron-donating or strongly σ -withdrawing groups.

We also investigated the effect of substituents on the quinoline ring of the ancillary ligand. The reactions catalyzed by Pd(OAc)₂ and **L9**, **L11**, or **L12** containing electron-withdrawing groups on the quinoline all occurred to greater than 90% conversion of **1a** after 100 min (Table 4.4, entries 7, 9, and 10). However, the reaction with **L10**, which contains the σ -donating 4-methyl substituent, occurred to only 76% conversion in the same time (entry 8). These results further support the proposal that the mildly electron-deficient character of the ancillary ligand increases catalyst activity. Subsequent studies were conducted primarily with **L3** because preparation of this ligand is simpler and less expensive than the preparations of **L11** or **L12**.

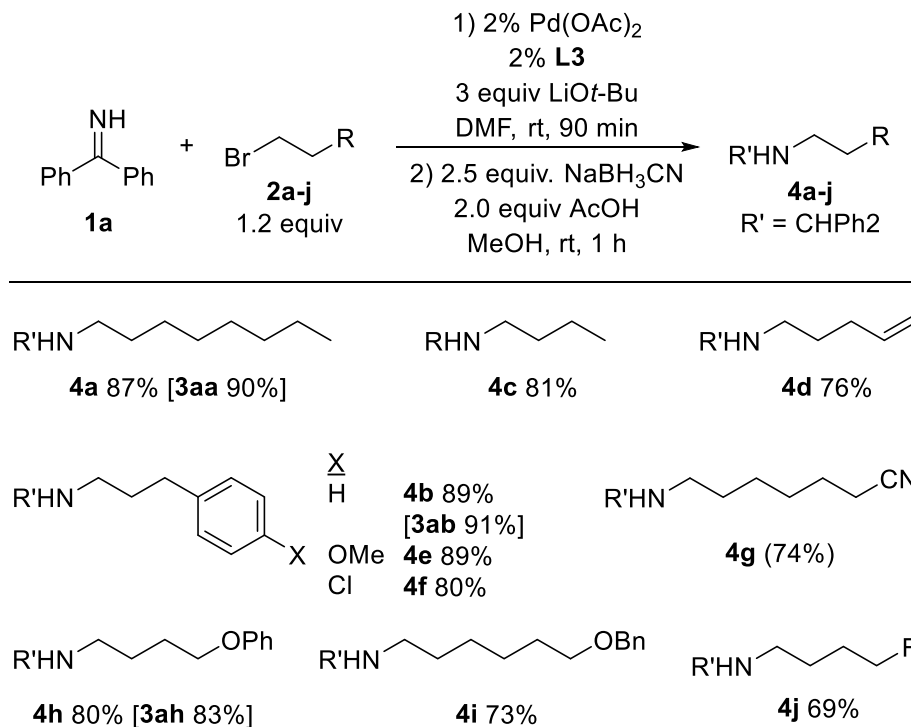
Table 4.4. Effect of ancillary ligand electronic properties on the rate of *N*-alkylation.

entry	L	% conversion 1a at 60 min ^a	% conversion 1a at 100 min ^a
1 ^b	L3	84	>99
2 ^b	L3	76	97
3	L5	77	96
4	L6	48	61
5	L7	24	28
6	L8	21	29
7	L9	73	92
8	L10	59	76
9	L11	84	>99
10	L12	90	>99

^aConversion determined by corrected GC integration of **1a** against TMB. ^bTo account for variations in ambient temperature, entries 1, 3, 4, 5, and 6 were run in parallel, and entries 2, 7, 8, 9, and 10 were run in parallel.

The scope of alkyl bromides that participated in this coupling reaction catalyzed by Pd(OAc)₂ and **L3** is summarized in Scheme 4.1. A variety of *N*-alkyl benzophenone imine derivatives were prepared by allowing benzophenone imine to react with 1.2 equivalents alkyl bromide, 3 equivalents of LiOt-Bu, and 2 mol % of Pd(OAc)₂ and **L3** at ambient temperature for 90 minutes. The reduction of the *N*-alkyl benzophenone imine products to the corresponding benzhydramines (**4a-c**) was conducted on the crude reaction mixtures to simplify purification and characterization. Primary alkyl bromides containing fluoride, alkene, aryl, phenoxy, benzyloxy, and cyano groups reacted with benzophenone imine under these conditions to give good to excellent yields of the coupled products.

Scheme 4.1. Scope of alkyl bromides for the *N*-alkylation of benzophenone imine catalyzed by Pd(OAc)₂ and **L3**.^a



^aIsolated yield of *N*-alkyl benzhydramine **4**; [yield of *N*-alkyl benzophenone imine **3** intermediate after step 1 determined by ¹H NMR spectroscopy integration against TMB]; (yield of *N*-alkyl benzhydramine **4** determined by ¹H NMR spectroscopy integration against TMB).

Attempts to observe and characterize the resting state of this coupling reaction did not lead to the identification of a well-defined complex. However, we designed a series of mechanistic experiments to rule out some of the plausible mechanisms. Specifically, we sought to determine whether the cleavage of the carbon–bromine bond is a single- or double-electron process, whether the palladium catalyst is involved in the carbon–bromine bond-cleaving step, and whether Pd(0) complexes are intermediates on the catalytic cycle.

The dependence of the rate (*r*) on each reagent was measured (Figure 4.1). The reaction of 4,4'-difluorobenzophenone imine (**1b**) and 1-bromooctane (**2a**) catalyzed by Pd(OAc)₂ with LiOt-Bu as base was found to be first-order in catalyst and zeroth-order in **1b** and LiOt-Bu. A partial-order dependence of the reaction on the concentration of the alkyl bromide **2a** was observed, and this dependence approached zero when the reactions were run with 0.25 M or greater concentration of **2a**. At this concentration, the rate was zeroth-order in all reagents except for the catalyst, which suggests that the rate determining step is a unimolecular reaction of a palladium complex.

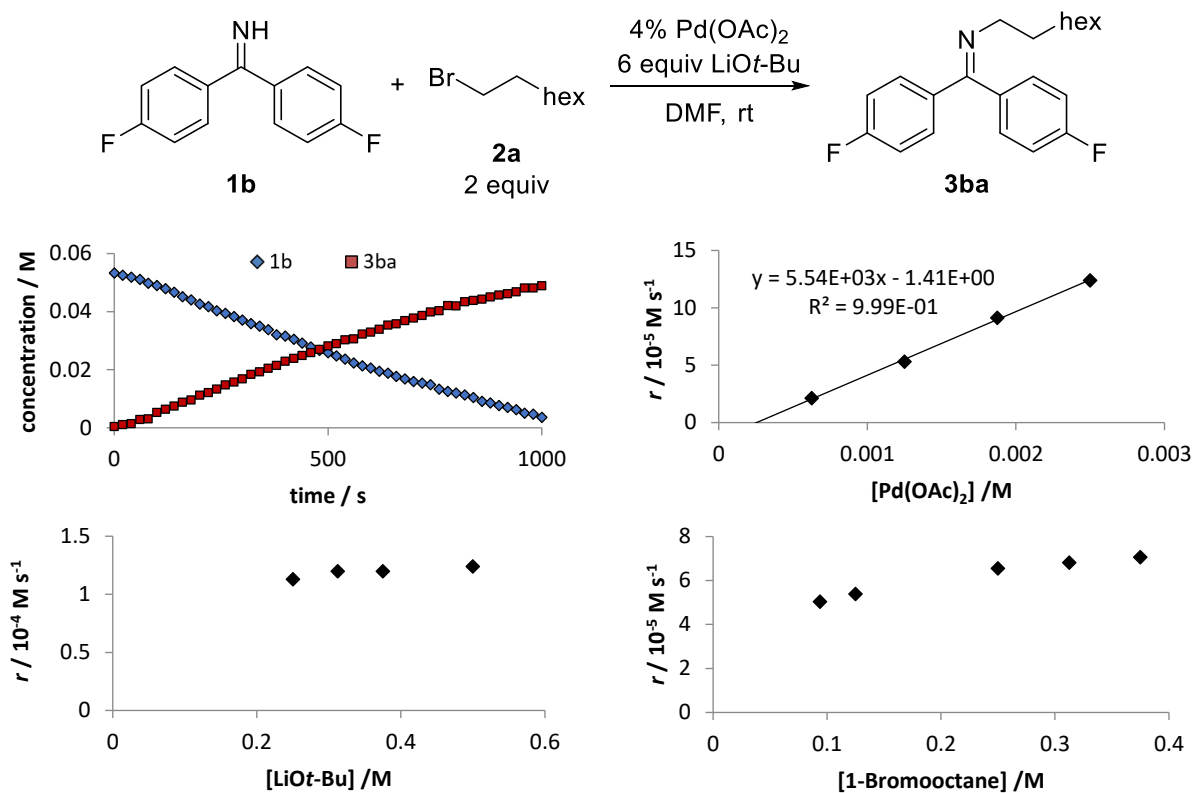
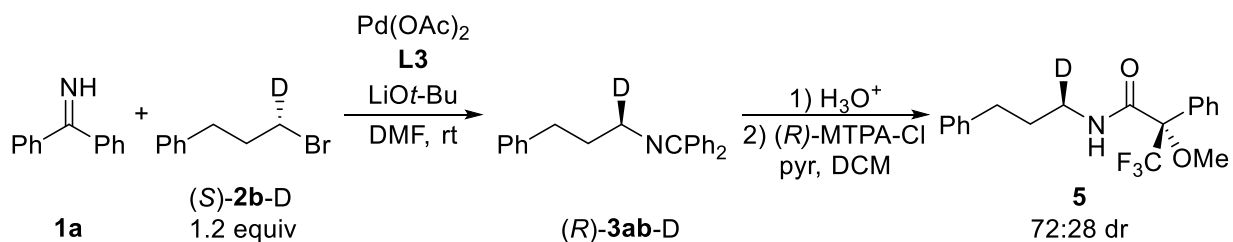


Figure 4.1. Kinetic studies on the *N*-alkylation of 4,4'-difluorobenzophenone imine. Standard conditions shown in the equation (above). Rates (r) were determined from linear fits of [**1b**] vs time. The experiments presented in each plot were performed with the same stock solutions and consecutively.

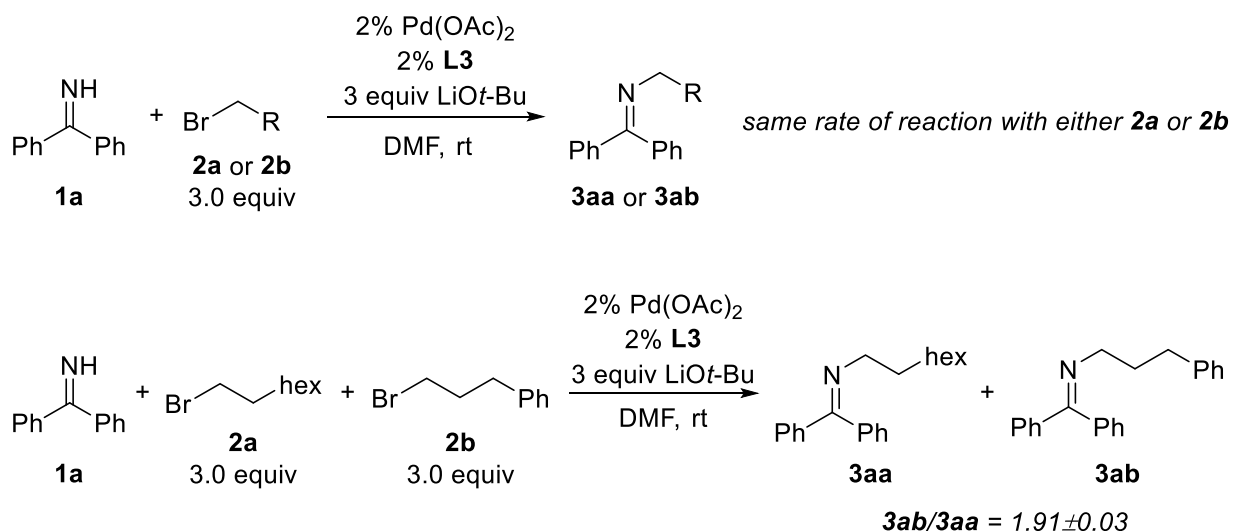
To determine the stereochemical outcome of this reaction, an enantioenriched mono-deuterated alkyl bromide (*S*)-**2b-D** was prepared. The palladium-catalyzed coupling reaction produced the corresponding *N*-alkyl imine (*R*)-**3ab-D** (Scheme 4.2). The configuration of the stereogenic carbon was determined by hydrolysis of the imine and protection with (*R*)-MTPA-Cl to give the corresponding Mosher amide **5** in 72:28 d.r.. The same alkyl bromide was converted by the sequence of sodium azide substitution, Staudinger reduction, and MTPA protection to give to the same configuration of the Mosher amide in 80:20 d.r.. This result shows that the palladium-catalyzed coupling reaction proceeds predominately with inversion of configuration, and, therefore, that a mechanism occurring through an alkyl radical is unlikely.

Scheme 4.2. Inversion of configuration in the reaction of an enantioenriched primary alkyl bromide.



To determine whether the palladium catalyst is involved in cleavage of the carbon–bromine bond, we performed competition experiments with mixtures of alkyl bromides. When performed in separate vials, the reactions of benzophenone imine (**1a**) and either 3 equivalents of 1-bromooctane (**2a**) or 1-bromo-3-phenylpropane (**2b**) with LiOt-Bu in DMF occurred at essentially identical rates (Scheme 4.3 top). This result is consistent with our previous observation that the rate of reaction is zeroth-order in the concentration of the alkyl bromide and that cleavage of the carbon–bromine bond is not likely involved in the rate-determining step. However, when the same reactions were performed in a competitive fashion (same vial), the reaction formed predominately the *N*-(3-phenyl)propyl imine product **3ab** (Scheme 4.3 bottom). A similar result (ratio of 1.65) was observed for the alkylation of potassium phthalimide in DMF with a mixture of the same two alkyl bromides.

Scheme 4.3. Relative rates of alkylation with **2a** or **2b**, and competitive reaction of **2a** and **2b**.



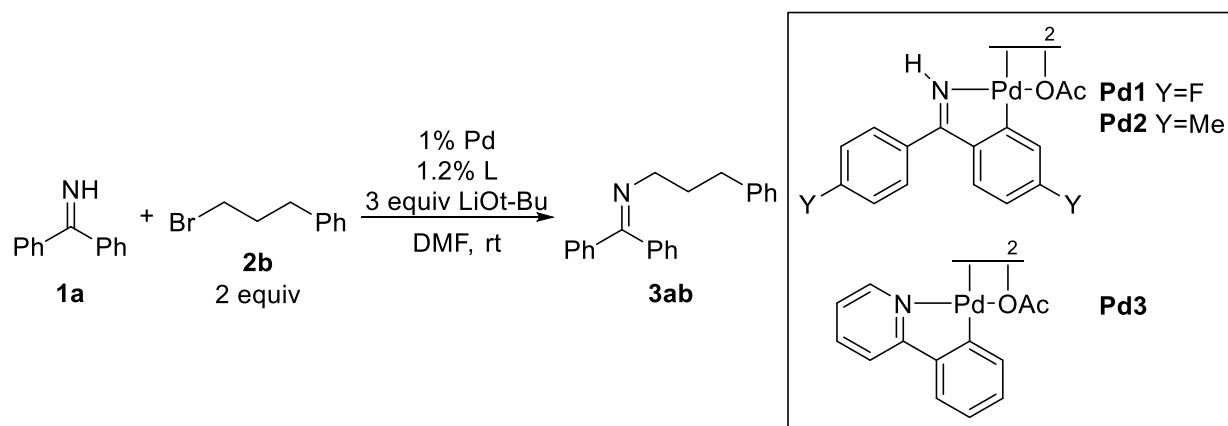
The choice of ancillary ligand was found to affect the ratio of products observed in these competition experiments (Table 4.5). The competitive reactions of **1a** with **2a** and **2b** (electronically differentiated) gave product mixtures consisting of **2ab** to **2aa** in ratios ranging from 1.70 to 2.16. Similar competitive reactions of **1a** with **2a** and **2k** (sterically differentiated) gave product mixtures consisting of **3aa** to **3ak** in ratios ranging from 4.1 to 5.5. Although the differences in these ratios between reactions with different catalysts are small, they are significantly greater than the uncertainty in their measurements. These results suggest that an iminoquinoline-ligated complex is involved in the product-determining step, which is likely cleavage of the carbon–bromine bond.

Table 4.5. Effect of ancillary ligand on selectivity in competition experiments.

$ \begin{array}{c} \text{NH} \\ \parallel \\ \text{Ph}-\text{C}=\text{Ph} \\ \mathbf{1a} \end{array} + \text{Br}-\text{CH}_2\text{CH}_2\text{CH}_2\text{CH}_2\text{CH}_3 \quad \mathbf{2a} \quad 3.0 \text{ equiv} + \text{Br}-\text{CH}_2\text{CH}_2\text{R} \quad \mathbf{2b} \text{ R=Bn} \quad \mathbf{2k} \text{ R}=i\text{-Pr} \quad 3.0 \text{ equiv} \xrightarrow[\text{DMF, rt}]{\text{catalyst, 3 equiv LiOt-Bu}} \begin{array}{c} \text{N-CH}_2\text{CH}_2\text{CH}_2\text{CH}_2\text{CH}_3 \\ \parallel \\ \text{Ph}-\text{C}=\text{Ph} \\ \mathbf{3aa} \end{array} + \begin{array}{c} \text{N-CH}_2\text{CH}_2\text{R} \\ \parallel \\ \text{Ph}-\text{C}=\text{Ph} \\ \mathbf{3ab \text{ or } 3ak} \end{array} $			
entry	alkyl bromide	catalyst	ratio ^a (3ab/3aa or 3aa/3ak)
1	2b	4% Pd(OAc) ₂	2.16±0.05
2	“	2% Pd(OAc) ₂ 2% L3	1.91±0.03
3	“	2% Pd(OAc) ₂ 2% L6	1.699±0.007
4	2k	4% Pd(OAc) ₂	4.2±0.1
5	“	2% Pd(OAc) ₂ 2% L2	4.09±0.04
6	“	2% Pd(OAc) ₂ 2% L3	4.80±0.07
7	“	2% Pd(OAc) ₂ 2% L9	5.5±0.1

^aRatio determined by corrected GC integration; reported numbers are averages and standard deviations from four experiments.

We considered that the active catalyst could form from cyclopalladation of benzophenone imine. To test this proposal, the cyclopalladated imines **Pd1** and **Pd2** were prepared. We observed that the reactions catalyzed by **Pd1** or **Pd2** occurred at very similar rates to that of the reaction catalyzed by Pd(OAc)₂ (Table 4.6, entries 1-3). Furthermore, no 4,4'-difluorobenzophenone imine (**2b**) or the corresponding *N*-alkyl product **3bb** was detected by ¹⁹F NMR in the reaction catalyzed by **Pd1** until after **1a** was almost entirely consumed, even when the reaction was performed with 8 mol % of **Pd1**. To determine whether other palladacycles would also catalyze this reaction, we prepared the cyclopalladated 2-phenylpyridine complex **Pd3**. However, the reaction catalyzed by **Pd3** occurred to low conversion of **1a** (entry 4). These results suggest that the complexes containing a cyclopalladated imine do not simply decompose to Pd⁰ and the corresponding imine. Instead, the metallacycle appears to remain intact throughout the course of the reaction. Therefore, a mechanism involving interconversion between Pd(0) and Pd(II) species is not a likely mechanism for this reaction.

Table 4.6. Comparison of cyclopalladated imines as precatalysts.

entry	Pd	% conversion 1a at 10 min ^a	% conversion 1a at 30 min ^a	% conversion 1a at 60 min ^a
1	Pd(OAc) ₂	20	56	87
2 ^b	Pd1	22±1	53±3	86±6
3	Pd2	24	57	>99
4	Pd3	7	18	18

^aConversion determined by corrected GC integration against TMB. ^bReported numbers for this entry are averages with standard deviations from three experiments.

4.3 Conclusions

We have developed a palladium-catalyzed coupling of benzophenone imines with primary alkyl bromides to form diphenylmethylen- or benzyldryl-protected primary alkylamines. The reaction catalyzed by the combination of Pd(OAc)₂ and an iminoquinoline ligand occurs faster than the reaction catalyzed by Pd(OAc)₂ alone, and catalyst activity depends strongly on the electronic and steric properties of this ligand. This reaction affords the *N*-alkyl benzophenone imine products in good to excellent yields under mild conditions and short reaction times.

Mechanistic studies have revealed that the reaction occurs with inversion of configuration, that the structure of the catalyst controls the distribution of products in competition experiments, and that the active catalyst is likely a cyclopalladated species or forms from a reaction of a cyclopalladated complex. Taken together, these results argue against mechanisms involving alkyl radical or Pd(0) intermediates, leaving a Pd(II)-Pd(IV) cycle as the most likely mechanism. However, significant work remains before the mechanism of this reaction can be conclusively established.

The scope of imine products presented in this work is limited to those containing primary alkyl groups on nitrogen. Because the majority of the corresponding primary amines could be readily prepared by traditional substitution or reductive amination reactions with ammonia surrogates (sodium azide, potassium phthalimide, PMB, etc), this palladium-catalyzed reaction is not yet valuable as a synthetic method. Attempts to expand the scope of substrates for this catalytic system to include the more synthetically valuable secondary and tertiary alkyl electrophiles have not led

to the identification of conditions under which formation of the *N*-alkyl imine product outcompetes formation of olefins by elimination. Under these reaction conditions, background (E2) and palladium-catalyzed elimination reaction are both fast. However, we discovered that phosphine-ligated palladium complexes can successfully catalyze the cross-coupling of secondary and tertiary alkyl bromides with benzophenone imine derivatives by an alternative mechanism involving alkyl radical intermediates under more-weakly basic conditions in less polar solvents. The development of catalysts for the cross-coupling of these more valuable substrates has been published⁶ and is described in Chapter 5.

4.4 Experimental

General experimental details. All reactions were performed under a nitrogen atmosphere unless otherwise specified. The following compounds were synthesized from literature procedures: 8-isopropylquinoline-2-carboxaldehyde,²⁹ and (4-methylquinolin-2-yl)methanol.³⁰ DMF over molecular sieves was purchased from Acros Organics and used as received. THF, diethyl ether, hexane, pentane, ethyl acetate, methanol, and triethylamine were purchased from Fisher Scientific. THF, pentane, and diethyl ether were collected from a solvent purification system containing a 0.33 m column of activated alumina under nitrogen prior to use in reactions. Benzophenone imine (97%) purchased from Acros Organics was used in coupling reactions. Benzophenone imine (95%) purchased from Sigma Aldrich was used for the preparation of authentic imines by condensation reactions. Palladium(II) acetate was donated by Johnson Matthey. All other compounds were purchased from commercial suppliers and used as received. Many reagents were used as solutions to allow for accurate addition of small quantities. All such solutions were prepared by dilution with the reaction solvent in a nitrogen-filled drybox.

Column chromatography was performed with 230-400 mesh silica gel from Fisher Scientific. TLC plates with fluorescent indicators were purchased from Silicycle or EMD and visualized under a 254 nm UV lamp. The inclusion of triethylamine (noted for each compound) in the mobile phase was found to improve resolution of amines and decrease hydrolysis of imines. In these cases, both silica gel and TLC plates were pretreated with 3 or 4% triethylamine in hexanes. R_f values reported for these products were measured on these pretreated TLC plates and are generally significantly higher than R_f values measured on non-pretreated plates.

GC spectra were obtained on an Agilent 7890 GC equipped with an HP-5 column (25 m x 0.20 mm x 0.33 μ m film) and an FID detector. NMR spectra were obtained on 500 MHz or 600 MHz Bruker Avance series instruments at the University of California, Berkeley NMR facility. Chemical shifts are reported relative to the residual solvent signal (CDCl₃ = 7.26 ppm for ¹H and 77.16 ppm for ¹³C). High resolution ESI high resolution mass spectrometry (HRMS) was performed by the QB3 Mass Spectrometry Facility at the University of California, Berkeley. EIMS was performed on an Agilent 7890A/5975C GC-MS. Elemental analysis was performed by the UC Berkeley Microanalytical Laboratory.

Preparation of benzophenone imine derivatives

4,4'-Difluorobenzophenone imine (2b).³¹ Under an N₂ atmosphere, a solution of 4-fluorophenylmagnesium bromide (17 ml, 1.0 M in THF, 17 mmol, 1.2 equiv) was cooled to 0 °C in a three-necked flask equipped with a reflux condenser and addition funnel. 4-Fluorobenzonitrile (1.75 g, 14.5 mmol) was dissolved in 10 ml of dry THF and added dropwise with stirring via the addition funnel over 20 minutes. The addition funnel and ice bath were removed, and the solution was heated at reflux for 5 hours. The reaction mixture was cooled to 0 °C, and 5 ml of dry MeOH was added slowly. The white solid was removed by filtration through Celite, and the solvent was evaporated under reduced pressure. The crude product was purified by kugelrohr distillation to give the title compound as a yellow oil (2.67 g, 12.3 mmol, 85%, 95% imine). ¹H NMR (600 MHz, CDCl₃) δ 9.62 (broad, NH), 7.52 (broad, 4H), 7.06 (t, *J* = 8.6 Hz, 4H). ¹³C NMR (151 MHz, CDCl₃) δ 175.9, 164.1 (d, *J* = 250.9 Hz), 135.4 (broad), 130.4 (broad), 115.4 (d, *J* = 21.7 Hz). ¹⁹F NMR (565 MHz, CDCl₃) δ -110.8. EIMS 217.1 (M⁺), 216.1 (base peak).

4-Methylbenzophenone imine (2c).³² Under an N₂ atmosphere, a solution of phenylmagnesium bromide (17.1 ml, 1.0 M in THF, 17.1 mmol) was cooled to 0 °C in a three-neck flask equipped with a reflux condenser and addition funnel. *p*-Tolunitrile (2.00 g, 17.1 mmol) was dissolved in 10 ml of dry THF in the addition funnel and added dropwise with stirring via the addition funnel. The ice bath was replaced with an oil bath, and the reaction mixture was heated at reflux overnight (approximately 14 h). The reaction mixture was cooled to 0 °C, and 15 ml of dry MeOH was added slowly. The solvent was evaporated under reduced pressure. Hexanes (100 ml) was added, and the solution was filtered through Celite followed by filter paper. The solvent was evaporated under reduced pressure, and the residue dried under vacuum to give the title compound as a yellow oil (3.18 g, 16.3 mmol, 95%). No further purification was performed. ¹H NMR (400 MHz, CDCl₃) δ 9.38 (broad, NH), 7.57 (d, *J* = 7.1 Hz, 2H), 7.51 – 7.38 (m, 5H), 7.23 (d, *J* = 7.9 Hz, 2H), 2.41 (s, 3H). ¹³C NMR (101 MHz, CDCl₃) δ 178.2, 140.6, 139.6, 136.4, 130.1, 129.0, 128.4, 128.4, 128.2, 21.4. EIMS 195.1 (M⁺), 180.1 (base peak).

Preparation of authentic *N*-alkyl benzophenone imines by condensation

General procedure. A 1 dram vial was charged with benzophenone imine (181 mg, 1.00 mmol), amine (1.20 mmol, 1.2 equiv), and 1.0 ml of dry DCM. The vial was flushed with N₂ and sealed with a Teflon cap. The solution was stirred for 2 days at ambient temperature. The solvent was evaporated under reduced pressure, and the product was purified by kugelrohr distillation or column chromatography as stated. All imines prepared in this manner contained the corresponding ketone as a minor impurity. The % imine was determined by NMR spectroscopy when possible are reported.

***N*-Octylbenzophenone imine (3aa).**³³ Prepared by the general procedure above with 160 mg 1-octylamine. Kugelrohr distillation resulted in partial decomposition of the imine product. The title compound was isolated as a pale yellow oil (92.4 mg, 0.315 mmol, 32%, >99% imine). ¹H NMR (500 MHz, CDCl₃) δ 7.62 (d, *J* = 7.1 Hz, 2H), 7.49 – 7.40 (m, 3H), 7.40 – 7.30 (m, 3H), 7.18 (d,

$J = 6.7$ Hz, 2H), 3.39 (t, $J = 7.1$ Hz, 2H), 1.70 (p, $J = 7.1$ Hz, 2H), 1.37 – 1.20 (m, 10H), 0.89 (t, $J = 6.9$ Hz, 3H). The NMR spectrum matched that reported previously.³³ **EIMS** 293.1 (M^+), 91.0 (base peak).

***N*-(3-Phenylpropyl)benzophenone imine (3ab).** Prepared by the general procedure above with 163 mg 3-phenyl-1-aminopropane to give the title compound as a clear oil after kugelrohr distillation (216 mg, 0.721 mmol, 72%, >99% imine). **¹H NMR** (600 MHz, CDCl₃) δ 7.67 (d, $J = 7.8$ Hz, 2H), 7.50 – 7.39 (m, 4H), 7.37 (t, $J = 7.5$ Hz, 2H), 7.29 (t, $J = 7.5$ Hz, 2H), 7.23 – 7.17 (m, 5H), 3.46 (t, $J = 6.8$ Hz, 2H), 2.76 – 2.71 (m, 2H), 2.06 (p, $J = 7.1$ Hz, 2H). **¹³C NMR** (151 MHz, CDCl₃) δ 168.2, 142.4, 140.1, 137.1, 129.9, 128.6, 128.5, 128.4, 128.3 (2C), 128.2, 127.9, 125.7, 53.3, 33.8, 32.9. **EIMS** 299.1 (M^+), 194.0 (base peak).

***N*-Octyl-4,4'-difluorobenzophenone imine (3ba).** 4,4'-Difluorobenzophenone (3.27 g, 15.0 mmol) and tosic acid monohydrate (32 mg, 0.17 mmol, 1%) were dissolved in 50 ml of toluene. A Dean-Stark trap and condenser were attached, and the system was flushed with nitrogen. 1-Octylamine (1.96 g, 15.1 mmol, 1 equiv) was added to the flask, and the mixture was heated at reflux for 8 days. Toluene was evaporated under reduced pressure. The crude product was purified by column chromatography (30% ethyl acetate in hexanes) and kugelrohr distillation to give the title compound as a yellow oil (2.53 g, 7.68 mmol, 51%, 99% imine). **¹H NMR** (600 MHz, CDCl₃) δ 7.58 (dd, $J = 8.5, 5.7$ Hz, 2H), 7.20 – 7.10 (m, 4H), 7.00 (t, $J = 8.6$ Hz, 2H), 3.35 (t, $J = 7.1$ Hz, 2H), 1.67 (p, $J = 7.1$ Hz, 2H), 1.36 – 1.19 (m, 10H), 0.87 (t, $J = 6.9$ Hz, 3H). **¹³C NMR** (151 MHz, CDCl₃) δ 165.5, 164.1 (d, $J = 250.1$ Hz), 162.6 (d, $J = 248.2$ Hz), 136.3 (d, $J = 2.9$ Hz), 132.7 (d, $J = 3.5$ Hz), 130.3 (d, $J = 8.5$ Hz), 129.8 (d, $J = 8.0$ Hz), 115.7 (d, $J = 21.5$ Hz), 115.1 (d, $J = 21.6$ Hz), 54.1, 32.0, 31.3, 29.5, 29.4, 27.6, 22.8, 14.2. **¹⁹F NMR** (565 MHz, CDCl₃) δ -112.3, -113.4. **EIMS** 329.1 (M^+), 109.0 (base peak).

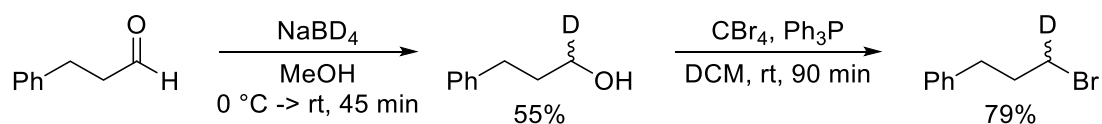
***N*-(4-Phenylbutan-2-yl)benzophenone imine.** Prepared by the general procedure above with 179 mg 3-amino-1-phenylbutane. The reaction time was increased to 4 d. The pale yellow oil was isolated by kugelrohr distillation and became a white solid after standing overnight (286 mg, 0.912 mmol, 91%, 98% imine). **¹H NMR** (600 MHz, CDCl₃) δ 7.62 (d, $J = 7.4$ Hz, 2H), 7.45 – 7.40 (m, 3H), 7.40 – 7.35 (m, 1H), 7.33 (t, $J = 7.4$ Hz, 2H), 7.24 (t, $J = 7.5$ Hz, 2H), 7.17 – 7.10 (m, 5H), 3.52 – 3.41 (m, 1H), 2.60 (ddd, $J = 13.7, 11.2, 5.4$ Hz, 1H), 2.44 (ddd, $J = 13.8, 11.1, 5.6$ Hz, 1H), 2.03 – 1.91 (m, 1H), 1.87 – 1.74 (m, 1H), 1.20 (d, $J = 6.2$ Hz, 3H). **¹³C NMR** (151 MHz, CDCl₃) δ 166.5, 142.7, 140.4, 137.6, 129.8, 128.5, 128.5, 128.4, 128.2, 128.2, 127.9, 125.7, 57.3, 40.2, 33.2, 22.4. **EIMS** M^+ not observed, 208.1 (base peak).

Preparation of alkyl bromides

The following compounds were prepared with minor modifications from published procedures: 1-bromo-4-(3-bromopropyl)benzene³⁴ and 1-benzyloxy-6-bromohexane.³⁵

1-Bromo-3-(4-chlorophenyl)propane (2f).³⁶ Prepared by modification of a literature procedure.³⁴ 3-(4-chlorophenyl)-1-propanol (498 mg, 2.92 mmol) was dissolved in 10 ml of dry THF under N₂ and cooled to 0 °C. Ph₃P (965 mg, 3.68 mmol, 1.25 equiv) and CBr₄ (1.21 g, 3.65 mmol, 1.25 equiv) were added in that order. The reaction mixture was stirred at 0 °C for approximately 15 min, then the ice bath was removed, and the reaction mixture was stirred at ambient temperature for 8 h. The solvent volume was lowered at reduced pressure, and the crude product was purified by column chromatography (5% ethyl acetate in hexanes). The title compound was isolated as a pale yellow oil (491 mg, 2.10 mmol, 72%). ¹H NMR (600 MHz, CDCl₃) δ 7.27 (d, *J* = 8.2 Hz, 2H), 7.14 (d, *J* = 8.2 Hz, 2H), 3.38 (t, *J* = 6.5 Hz, 2H), 2.76 (t, *J* = 7.4 Hz, 2H), 2.14 (p, *J* = 6.8 Hz, 2H). ¹³C NMR (151 MHz, CDCl₃) δ 139.1, 132.1, 130.0, 128.7, 34.1, 33.4, 32.9.

(*rac*)-1-Bromo-3-phenylpropane-1-*d*₁ ((*rac*)-2b-D).

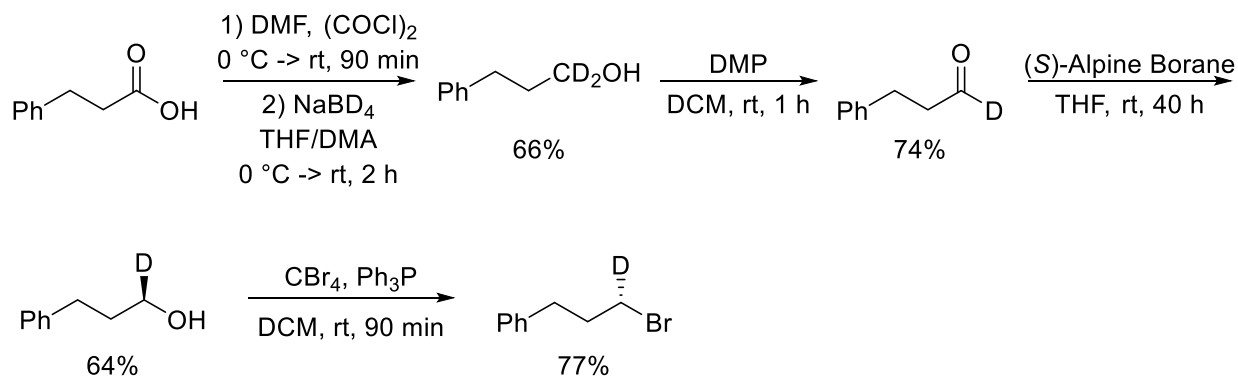


Step 1. Hydrocinnamaldehyde (tech. grade ~90%, distilled prior to use, 632 mg, 4.71 mg) was dissolved in MeOH (9 ml) in a 20 ml scintillation vial. The solution was cooled to 0 °C, and the vial was flushed with N₂. Sodium borodeuteride (50.5 mg, 1.21 mmol, 0.26 equiv) was dissolved in MeOH (1 ml) and slowly added to the reaction vial with stirring. After the bubbling stopped (~15 min), the cooling bath was removed, and the reaction mixture was stirred at ambient temperature until the aldehyde could no longer be detected by TLC (~45 min). The reaction mixture was quenched with HCl_(aq) (0.5 M, 10 ml) and transferred to a separatory funnel. Ether (20 ml) and additional HCl_(aq) (0.5 M, 10 ml) were added and mixed. The layers were separated, and the aqueous layer was extracted twice more with ether (20 ml). The combined organic layers were dried (MgSO₄), and the volatile materials were evaporated at reduced pressure. The crude product was purified by column chromatography (25% ethyl acetate in hexanes, R_f 0.33) to give (*rac*)-3-phenylpropan-1-*d*₁-1-ol as a clear and colorless oil (358 mg, 2.61 mmol, 55% yield). The ¹H NMR spectrum was consistent with that reported in the literature.³⁷ Quantitative ¹H NMR spectroscopy indicated that the product was 98.5% D at C1.

Step 2. (*rac*)-3-Phenylpropan-1-*d*₁-1-ol (274 mg, 2.00 mmol) was dissolved in dry DCM (15 ml) in a 100 ml round-bottom flask. The solution was cooled to 0 °C, and then Ph₃P (656 mg, 2.50 mmol, 1.25 equiv) and CBr₄ (829 mg, 2.50 mmol, 1.25 equiv) were added in that order with stirring. The flask was flushed with N₂, the cooling bath was removed, and the reaction mixture was stirred at ambient temperature until only trace amounts of the alcohol could be detected by

TLC (~90 min). H₂O (~100 ml) and additional DCM (~100 ml) were added, and the organic layer was separated. The aqueous layer was acidified (4 ml 3 M HCl_(aq)) to clear the emulsion, and extracted again with DCM (~100 ml). The combined organic layers were dried (MgSO₄), and the volatile materials were evaporated at reduced pressure. The crude product was purified by column chromatography (hexanes) to give the title compound as a clear and colorless oil (318 mg, 1.59 mmol, 79% yield). Quantitative ¹H NMR spectroscopy indicated that the product was >97% D at C1. ¹H NMR (500 MHz, CDCl₃) δ 7.30 (t, J = 7.6 Hz, 2H), 7.24 – 7.18 (m, 3H), 3.39 (t, J = 7.0 Hz, 1H), 2.78 (t, J = 7.4 Hz, 2H), 2.17 (q, J = 7.0 Hz, 2H). ¹³C NMR (151 MHz, CDCl₃) δ 140.7, 128.7, 128.7, 126.3, 34.2, 34.1, 33.0 (1:1:1 t, J = 23.2 Hz).

(S)-1-Bromo-3-phenylpropane-1-*d*₁ ((S)-2b-D).



Step 1. Hydrocinnamic acid (2.25 g, 15.0 mmol) was dissolved in dry DCM (~150 ml) in a 250 ml round-bottom flask. DMF (0.14 ml, 0.13 g, 1.8 mmol, 12%) was added, and the mixture was cooled to 0 °C. Oxalyl chloride (1.4 ml, 2.1 g, 17 mmol, 1.1 equiv) was added slowly with stirring. The reaction mixture was stirred at 0 °C for ~15 min, then the cooling bath was removed and the mixture was stirred at ambient temperature until the bubbling stopped (~90 min). The volatile materials were evaporated at reduced pressure to give the crude acid chloride as a viscous oil, which was reduced in the subsequent step without purification.

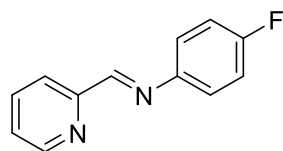
Step 2. Sodium borodeuteride (420 mg, 10.0 mmol, 0.666 equiv relative to starting hydrocinnamic acid) was dissolved in THF and DMA (10 ml each) in a 100 ml round-bottom flask, the solution was cooled to 0 °C, and the flask was flushed with N₂. The crude acid chloride from step 1 was also dissolved in THF and DMA (10 ml each), and this solution was slowly added to the flask containing NaBD₄ with stirring. The cooling bath was removed, and the mixture was stirred at ambient temperature for 2 h. The reaction was quenched at 0 °C with 0.5 M HCl_(aq) (~20 ml), and the mixture was transferred to a separatory funnel. The mixture was extracted thrice with ether (~80 ml each). The combine organic layers were dried (MgSO₄), and the volatile materials were removed at reduced pressure. The crude product was purified by column chromatography (25% ethyl acetate in hexanes) to give 3-phenylpropan-1,1-*d*₂-1-ol as a clear and colorless oil (1.37 g, 9.91 mmol, 66% yield). The ¹H and ¹³C NMR spectra were consistent with those reported in the literature.³⁸ Quantitative ¹H NMR spectroscopy indicated that the product was ~195% D at C1.

Step 3 was performed according to a published procedure to obtain 3-phenylpropanal-1-*d*.³⁸ Quantitative ¹H NMR spectroscopy indicated that the product was ~99% D at C1.

Step 4 was performed with minor modifications from a procedure reported in the literature for similar 1-*d*-aldehydes:³⁹ 3-phenylpropanal-1-*d* (1.22 g, 9.03 mmol) was dissolved in dry THF (~20 ml) in a nitrogen-flushed flask. A solution of (*S*)-Alipine borane (27 ml, 0.50 M, 13.5 mmol, 1.5 equiv) was added slowly with stirring. The reaction mixture was stirred at ambient temperature for 40 h, and then quenched excess borane was quenched with acetaldehyde (1 ml). The volatile materials were evaporated at reduced pressure (ca. 200-300 mTorr). Dry ether (30 ml) was added, the mixture was cooled to 0 °C, and ethanolamine (0.82 ml) was added dropwise. The mixture was stirred for 1 h at 0 °C, and then the cooling bath was removed. After allowing the mixture to warm to ambient temperature, the white precipitate was removed by filtering through a pad of Celite, which was rinsed thrice with ether (~10 ml each). The solution was transferred to a separatory funnel and washed with 0.5 M HCl_(aq) (~60 ml). The layers were separated, and the aqueous layer was extracted thrice more with ether (~60 ml each). The combined organic layers were dried (MgSO₄), and the volatile materials were evaporated at reduced pressure. The crude product was purified by column chromatography (25% ethyl acetate in hexanes, R_f 0.33) and kugelrohr distillation (85 °C, 0.5-1 Torr) to give (*R*)-3-phenylpropan-1-*d*₁-1-ol as a clear and colorless oil (797 mg, 5.81 mmol, 64% yield). The ¹H and ¹³C NMR spectra matched those of the racemate. Quantitative ¹H NMR spectroscopy indicated that the product was >98% D at C1.

Step 5 was performed with (*R*)-3-phenylpropan-1-*d*₁-1-ol (412 mg, 3.00 mmol) by the same procedure reported for the racemate to give the title compound as a clear and colorless oil (463 mg, 2.31 mmol, 77% yield). The ¹H NMR spectrum matched that of the racemate. Quantitative ¹H NMR spectroscopy indicated that the product was >98% D at C1.

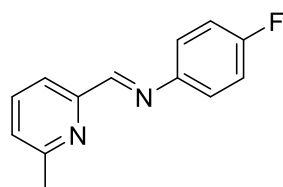
3-Bromo-1-phenylbutane.⁴⁰ 1-Phenyl-3-butanol (1.50 g, 10.0 mmol) was dissolved in 30 ml of dry THF under N₂ and cooled to 0 °C. Ph₃P (3.28 g, 12.5 mmol, 1.25 equiv) and CBr₄ (4.15 g, 12.5 mmol, 1.25 equiv) were added in that order. The reaction mixture was stirred at 0 °C for approximately 30 min, then the ice bath was removed, and the reaction mixture was stirred at ambient temperature for 20 h. The solvent was evaporated at reduced pressure. The residue was extracted thrice with 20 ml of hexanes, and the resulting solution was filtered through paper. The solvent was evaporated under reduced pressure, and the crude product was purified by two successive column chromatography procedures (5% ethyl acetate in hexanes, then 2% ethyl acetate in hexanes) followed by Kugelrohr distillation (80 °C, approximately 500 mTorr) to give the title compound as a clear oil (1.34 g, 6.29 mmol, 63%). The ¹H NMR spectrum matched that reported previously.⁴⁰ ¹H NMR (400 MHz, CDCl₃) δ 7.34 – 7.28 (m, 1H), 7.25 – 7.19 (m, 1H), 4.09 (dq, *J* = 8.9, 6.7, 4.5 Hz, 1H), 2.88 (ddd, *J* = 14.1, 8.9, 5.3 Hz, 1H), 2.76 (ddd, *J* = 13.8, 8.7, 7.3 Hz, 1H), 2.15 (dtd, *J* = 14.2, 8.9, 5.3 Hz, 1H), 2.06 (dddd, *J* = 14.4, 8.9, 7.2, 4.4 Hz, 1H), 1.74 (d, *J* = 6.7 Hz, 2H).

Preparation of iminoquinoline ligands

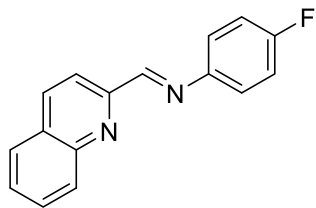
(E)-N-(4-Fluorophenyl)-2-pyridinecarboxaldehyde imine (L1).⁴¹ 2-Pyridinecarboxaldehyde (210 mg, 2.0 mmol) and tosic acid monohydrate (40 mg, 0.21 mmol, 10%) were mixed in 10 ml of toluene in a boiling flask fitted with a Dean-Stark condenser. 4-Fluoroaniline (210 μ l, 250 mg, 2.2 mmol, 1.1 equiv) was added, and the system was heated at reflux for 2 days. The volume was lowered at reduced pressure, and the reaction mixture was purified by column chromatography (0.2% NH_4OH and 25% MeOH in DCM) followed by kugelrohr distillation to give the title compound as a yellow-brown solid (251 mg, 1.25 mmol, 63%). This product contained approximately 1% 2-pyridinecarboxaldehyde as an impurity. **^1H NMR** (500 MHz, CDCl_3) δ 8.73 (d, J = 4.8 Hz, 1H), 8.61 (s, 1H), 8.20 (d, J = 7.9 Hz, 1H), 7.83 (t, J = 7.7 Hz, 1H), 7.42 – 7.36 (m, 1H), 7.34 – 7.27 (m, 2H), 7.12 (t, J = 8.6 Hz, 2H). **^{13}C NMR** (126 MHz, CDCl_3) δ 161.8 (d, J = 245.9 Hz), 160.4, 154.5, 149.8, 147.0 (d, J = 2.8 Hz), 136.8, 125.3, 122.8 (d, J = 8.3 Hz), 122.0, 116.1 (d, J = 22.6 Hz). **^{19}F NMR** (470 MHz, CDCl_3) δ -115.9. **HRMS** (ESI) calc'd (+H⁺) 201.0823, found 201.0824.

General procedure A. The 2-pyridinecarboxaldehyde or 2-quinolinecarboxaldehyde was mixed with the corresponding aniline in methanol in a boiling flask. The flask was equipped with a reflux condenser and flushed with N_2 . The reaction was heated at reflux until the aldehyde was consumed, as determined by TLC or GC. The solvent was evaporated under reduced pressure, and the crude products were purified by recrystallization or kugelrohr distillation.

General procedure B. 2-Quinolinecarboxaldehyde was mixed with the corresponding aniline in methanol in a 1 dram vial, and the vial was flushed with N_2 and sealed with a Teflon-lined cap. The reaction was heated at 65 $^\circ\text{C}$ in an aluminum heating block. The solvent was evaporated under reduced pressure, and the crude products were purified by recrystallization or kugelrohr distillation.

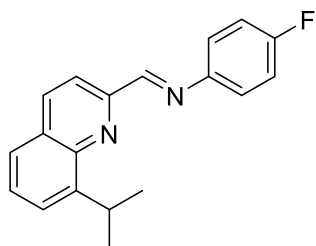


(E)-N-(4-Fluorophenyl)-6-methylpyridine-2-carboxaldehyde imine (L2). Prepared by general procedure A with 6-methylpyridine-2-carboxaldehyde (302 mg, 2.49 mmol) and 4-fluoroaniline (300 mg, 2.7 mmol, 1.1 equiv) in 5 ml of MeOH for 2 h. Purified by recrystallization from 6 ml of hexanes to give the title compound as a white powder (420 mg, 2.10 mmol, 79%). This product contained approximately 1% 6-methylpyridine-2-carboxaldehyde as an impurity. **^1H NMR** (500 MHz, CDCl_3) δ 8.58 (s, 1H), 8.00 (d, J = 7.5 Hz, 1H), 7.70 (t, J = 7.5 Hz, 1H), 7.36 – 7.26 (m, 2H), 7.24 (d, J = 7.4 Hz, 1H), 7.10 (t, J = 8.1 Hz, 2H), 2.64 (s, 3H). **^{13}C NMR** (126 MHz, CDCl_3) δ 161.7 (d, J = 245.8 Hz), 160.7, 158.6, 153.9, 147.1 (d, J = 2.9 Hz), 137.0, 125.0, 122.8 (d, J = 8.4 Hz), 119.1, 116.1 (d, J = 22.5 Hz), 24.5. **^{19}F NMR** (470 MHz, CDCl_3) δ -116.1. **HRMS** (ESI) calc'd (+H⁺) 215.0979, found 215.0980.



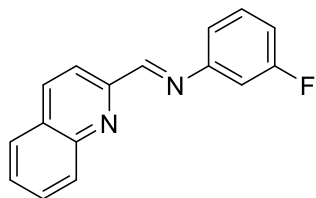
(E)-N-(4-Fluorophenyl)-2-quinolinecarboxaldehyde imine (L3). Prepared by general procedure A with 2-quinolinecarboxaldehyde (393 mg, 2.50 mmol) and 4-fluoroaniline (300 mg, 2.7 mmol, 1.1 equiv) in 5 ml of MeOH for 2 h. Purified by recrystallization from 5/3 ml of MeOH (2 crops) to give the title compound as a yellow powder (262 mg, 1.05 mmol, 42%). This product contained approximately 2% 2-quinolinecarboxaldehyde as an impurity. $^1\text{H NMR}$ (600 MHz, CDCl_3) δ 8.78 (s, 1H), 8.35 (d, $J = 8.5$ Hz, 1H), 8.27 (d, $J = 8.5$ Hz, 1H), 8.17 (d, $J = 8.4$ Hz, 1H), 7.89 (d, $J = 8.1$ Hz, 1H), 7.78 (t, $J = 7.4$ Hz, 1H), 7.62 (t, $J = 7.5$ Hz, 1H), 7.40 – 7.34 (m, 2H), 7.13 (t, $J = 8.6$ Hz, 2H). $^{13}\text{C NMR}$ (151 MHz, CDCl_3) δ 162.0 (d, $J = 246.4$ Hz), 160.5, 154.8, 148.0, 146.8 (d, $J = 2.9$ Hz), 136.8, 130.1, 129.8, 129.0, 127.9 (2C, overlap), 123.0 (d, $J = 8.4$ Hz), 118.6, 116.2 (d, $J = 22.6$ Hz). $^{19}\text{F NMR}$ (470 MHz, DMF) δ -116.8. **HRMS** (ESI) calc'd ($+\text{H}^+$) 251.0979, found 251.0979.

8-*Iso*-propylquinoline-2-carboxaldehyde was prepared according to a published procedure.²⁹



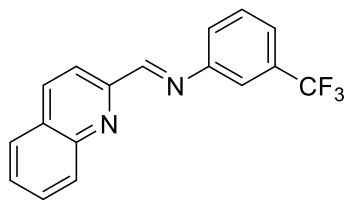
(E)-N-(4-Fluorophenyl)-8-*iso*-propylquinoline-2-carboxaldehyde imine (L4). Prepared by the general procedure A with 8-*iso*-propylquinoline-2-carboxaldehyde (185 mg, 0.928 mmol) and 4-fluoroaniline (110 mg, 0.98 mmol, 1.1 equiv) in 3 ml of MeOH for 90 min. Purified by kugelrohr distillation to give the title compound as a yellow oil which solidifies to a yellow glass on standing under N_2 (261 mg, 0.893 mmol, 87%). *Note:* the starting material, 8-*iso*-propylquinoline-2-carboxaldehyde, was not separated from 10% of the 2-methyl-8-isopropylquinoline precursor.

The 185 mg listed here is corrected from the 206 mg weighed mass. The imine product contained approximately 2% 8-isopropylquinoline-2-carboxaldehyde as an impurity. $^1\text{H NMR}$ (400 MHz, CDCl_3) δ 8.80 (s, 1H), 8.33 (d, $J = 8.5$ Hz, 1H), 8.21 (d, $J = 8.5$ Hz, 1H), 7.71 – 7.65 (m, 2H), 7.57 (t, $J = 7.6$ Hz, 1H), 7.40 – 7.34 (m, 2H), 7.14 (t, $J = 8.6$ Hz, 2H), 4.48 (hept, $J = 6.9$ Hz, 1H), 1.45 (d, $J = 7.0$ Hz, 6H). $^{13}\text{C NMR}$ (101 MHz, CDCl_3) δ 161.8 (d, $J = 245.7$ Hz), 161.8, 153.6, 148.2, 147.2 (d, $J = 2.8$ Hz), 145.9, 137.0, 129.0, 127.9, 125.7, 125.5, 122.9 (d, $J = 8.3$ Hz), 118.0, 116.1 (d, $J = 22.6$ Hz), 27.4, 23.7. $^{19}\text{F NMR}$ (565 MHz, CDCl_3) δ -117.1. **EIMS** 292.1 (M^+ , base peak), 154.0 (2nd most intense peak).

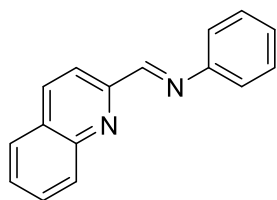


(E)-N-(3-Fluorophenyl)-2-quinolinecarboxaldehyde imine (L5). Prepared by general procedure B with 2-quinolinecarboxaldehyde (157 mg, 1.00 mmol) and 3-fluoroaniline (121 mg, 1.10 mmol, 1.1 equiv) in 2 ml of MeOH for 2 h. Purified by column chromatography (4% ethyl acetate and 3% TEA in hexanes, R_f 0.39). The yellow oil was recrystallized to give the title compound as pale yellow crystals (139 mg, 0.555 mmol, 56%). This product contained <1% 2-quinolinecarboxaldehyde as an impurity. $^1\text{H NMR}$ (600 MHz, CDCl_3) δ 8.76 (s, 1H), 8.34 (d, $J = 8.5$ Hz, 1H), 8.27 (d, $J = 8.5$ Hz, 1H), 8.17 (d, $J = 8.4$ Hz, 1H), 7.89 (d, $J = 8.0$ Hz, 1H), 7.78 (t, $J = 7.6$ Hz, 1H), 7.63 (t, $J = 7.4$ Hz, 1H), 7.39 (q, $J = 7.3$ Hz, 1H), 7.13 (d, $J = 7.8$ Hz, 1H), 7.07 (d, $J = 9.9$ Hz, 1H), 7.00 (t, $J = 8.2$ Hz, 1H). $^{13}\text{C NMR}$ (151 MHz, CDCl_3) δ 163.4 (d, $J = 246.8$ Hz), 162.1, 154.6, 152.9, 148.2, 136.9,

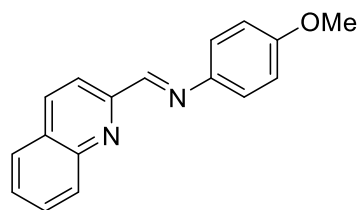
130.5 (d, $J = 9.1$ Hz), 130.2, 123.0, 129.1, 128.1, 127.9, 118.8, 117.0 (d, $J = 2.8$ Hz), 113.7 (d, $J = 21.4$ Hz), 108.7 (d, $J = 22.6$ Hz). ^{19}F NMR (565 MHz, CDCl_3) δ -113.3. EIMS 250.0 (M^+), 222.0 (base peak).



(E)-N-(3-(Trifluoromethyl)phenyl)-2-quinolinecarboxaldehyde imine (L6). Prepared by general procedure B with 2-quinolinecarboxaldehyde (157 mg, 1.00 mmol) and 3-(trifluoromethyl)aniline (178 mg, 1.10 mmol, 1.1 equiv) in 2 ml of MeOH for 2 h. Purified by recrystallization from hexanes (3 crops) to give the title compound as a yellow powder (159 mg, 0.530 mmol, 53%). No aldehyde impurity was detected in this product. ^1H NMR (600 MHz, CDCl_3) δ 8.80 (s, 1H), 8.35 (d, $J = 8.5$ Hz, 1H), 8.29 (d, $J = 8.5$ Hz, 1H), 8.18 (d, $J = 8.4$ Hz, 1H), 7.90 (d, $J = 8.1$ Hz, 1H), 7.79 (t, $J = 7.5$ Hz, 1H), 7.64 (t, $J = 7.5$ Hz, 1H), 7.61 (s, 1H), 7.56 (broad, 2H), 7.51 (broad, 1H). ^{13}C NMR (151 MHz, CDCl_3) δ 162.7, 154.5, 151.5, 148.2, 136.9, 131.9 (q, $J = 31.9$ Hz), 130.2, 130.0, 130.0, 129.2, 128.2, 127.9, 124.4, 124.1 (q, $J = 273.0$ Hz), 123.5 (q, $J = 3.9$ Hz), 118.7, 118.5 (q, $J = 3.6$ Hz). ^{19}F NMR (565 MHz, CDCl_3) δ -63.6. EIMS 300.0 (M^+), 272.0 (base peak).

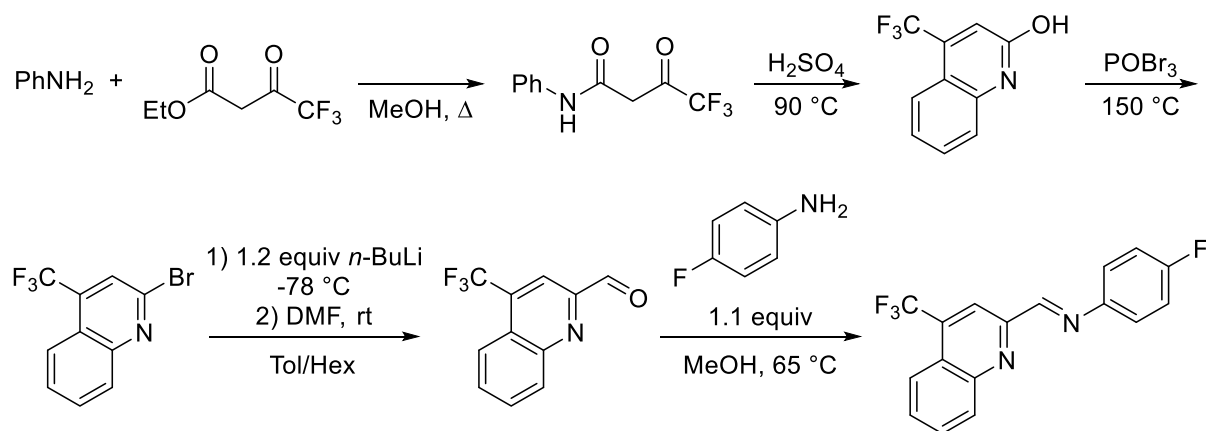


(E)-N-Phenyl-2-quinolinecarboxaldehyde imine (L7).⁴² Prepared by general procedure B with 2-quinolinecarboxaldehyde (157 mg, 1.00 mmol) and aniline (102 mg, 1.10 mmol, 1.1 equiv) in 2 ml of MeOH for 2 h. The solvent was evaporated under reduced pressure to give a red residue. The red color was removed by dissolving the residue in 1:3 Et_2O /Hexanes and filtering through a short plug of silica. The fractions eluting prior to the red band were combined, the solvent evaporated under reduced pressure, and the yellow residue recrystallized from 1 ml of hexanes to give the title compound as a pale yellow solid. The fractions containing the red material were combined, the solvent was evaporated under reduced pressure, and the residue was redissolved in hexanes containing 4% ethyl acetate and 3% triethylamine. This solution was filtered through another plug of silica, and the plug was rinsed with 2 ml of hexanes. The solvent was evaporated under reduced pressure, and the yellow residue was recrystallized from 1 ml of hexanes to give a second crop of the title compound as a pale yellow solid. The two crops were combined (125 mg, 0.538 mmol, 54%). This product contained approximately 2% 2-quinolinecarboxaldehyde as an impurity. ^1H NMR (600 MHz, CDCl_3) δ 8.80 (s, 1H), 8.38 (d, $J = 8.5$ Hz, 1H), 8.27 (d, $J = 8.5$ Hz, 1H), 8.18 (d, $J = 8.4$ Hz, 1H), 7.88 (d, $J = 8.1$ Hz, 1H), 7.78 (t, $J = 7.6$ Hz, 1H), 7.61 (t, $J = 7.5$ Hz, 1H), 7.45 (t, $J = 7.6$ Hz, 2H), 7.37 (d, $J = 7.8$ Hz, 2H), 7.31 (t, $J = 7.3$ Hz, 1H). ^{13}C NMR (151 MHz, CDCl_3) δ 161.0, 155.0, 151.0, 148.1, 136.7, 130.0, 129.9, 129.4, 129.0, 127.9, 127.8, 127.1, 121.4, 118.8. EIMS 232.0 (M^+), 204.0 (base peak).



(E)-N-(4-Methoxyphenyl)-2-quinolinecarboxaldehyde imine (L8)⁴³ Prepared by the general procedure B with 2-quinolinecarboxaldehyde (157 mg, 1.00 mmol) and *p*-anisidine (135 mg, 1.10 mmol, 1.1 equiv) in 2 ml of MeOH for 2 h. Purified by recrystallization from 10 ml of hexanes to give the title compound as a yellow solid (200 mg, 0.762 mmol, 76%). No aldehyde impurity was detected in this product. ¹H NMR (600 MHz, CDCl₃) δ 8.82 (s, 1H), 8.36 (d, *J* = 8.5 Hz, 1H), 8.23 (d, *J* = 8.5 Hz, 1H), 8.16 (d, *J* = 8.4 Hz, 1H), 7.86 (d, *J* = 8.0 Hz, 1H), 7.76 (t, *J* = 8.2 Hz, 1H), 7.59 (t, *J* = 7.4 Hz, 1H), 7.41 (d, *J* = 8.8 Hz, 2H), 6.97 (d, *J* = 8.8 Hz, 2H), 3.85 (s, 3H). ¹³C NMR (151 MHz, CDCl₃) δ 159.31, 158.53, 155.35, 148.15, 143.69, 136.65, 129.98, 129.77, 128.94, 127.88, 127.64, 123.02, 118.73, 114.64, 55.64. EIMS 262.0 (M⁺, base peak), 129.0 (2nd most intense peak).

(E)-N-(4-Fluorophenyl)-4-(trifluoromethyl)quinoline-2-carboxaldehyde imine (L9).

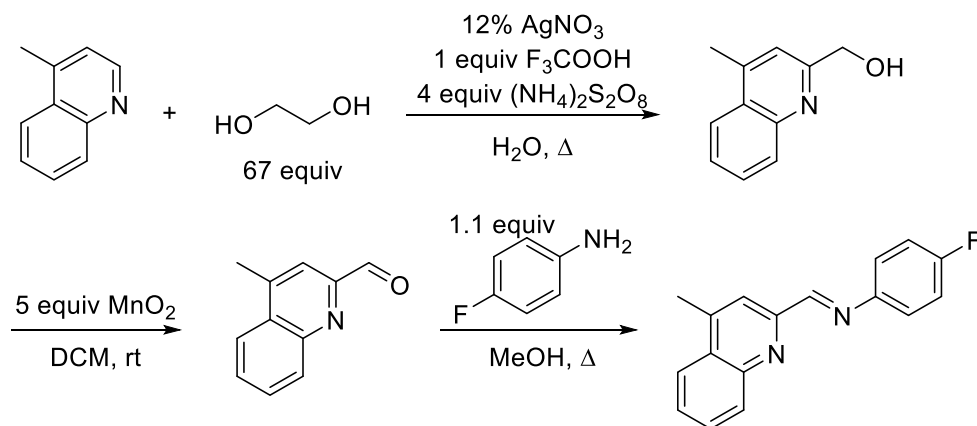


Steps 1-3 were performed according to published synthetic sequence to prepare 2-bromo-4-(trifluoromethyl)quinoline.⁴⁴

Step 4. 2-Bromo-4-(trifluoromethyl)quinoline (657 mg, 2.38 mmol) was added to a flame-dried 25 ml flask under N₂ with 6 ml of toluene and cooled to -78 °C in a dry ice/acetone bath. *n*-BuLi (1.80 ml, 1.6 M in hexanes, 2.88 mmol, 1.2 equiv) was added dropwise with stirring, and the reaction mixture turned deep red in color. After stirring an additional 2 hours, DMF (0.28 ml, 3.6 mmol, 1.5 equiv) was added dropwise. The dry ice/acetone bath was removed, and the reaction mixture was stirred 18 h at ambient temperature. The reaction was quenched by addition of 1 ml of saturated NH₄Cl_(aq), and the organic solvent was evaporated at reduced pressure. The aqueous layer was diluted with 30 ml of H₂O, and the mixture was extracted with ethyl acetate (3x 20 ml). The combined organic layers were dried with MgSO₄, the solvent was evaporated under reduced pressure, and the residue was purified by column chromatography (5% ethyl acetate in hexanes) to give an impure mixture (54 mg) containing 4-(trifluoromethyl)quinoline-2-carboxaldehyde (0.24 mmol, 10%, uncorrected) as a red solid.

Step 5. The product from step 1 was added to a 1 dram vial containing 4-fluoroaniline (29 mg, 0.26 mmol, 1.1 equiv) in 1 ml of MeOH. The vial was flushed with N₂, sealed with a Teflon-lined cap, and heated at 65 °C with stirring for 2 h. The reaction mixture solidified upon cooling. A further 1 ml of MeOH was added to the vial, the mixture was reheated until the solid dissolved, and the solution was allowed to cool. The off-white solid was collected by filtration. Two further crops were obtained from the mother liquor and combined with this material. The crude product was purified by column chromatography (3% TEA and 16% ethyl acetate in hexanes, R_f 0.58) followed by recrystallization from 1 ml of hexanes to give the title compound as white needles (25.7 mg, 0.081 mmol, 34%). This product contained <2% of 4-(trifluoromethyl)quinoline-2-carboxaldehyde as an impurity. ¹H NMR (500 MHz, CDCl₃) δ 8.78 (s, 1H), 8.65 (s, 1H), 8.25 (d, *J* = 8.4 Hz, 1H), 8.18 (d, *J* = 8.5 Hz, 1H), 7.86 (t, *J* = 7.7 Hz, 1H), 7.73 (t, *J* = 7.7 Hz, 1H), 7.42 – 7.34 (m, 2H), 7.14 (t, *J* = 8.6 Hz, 2H). ¹³C NMR (126 MHz, CDCl₃) δ 162.3 (d, *J* = 247.2 Hz), 159.1 (d, *J* = 1.3 Hz), 154.4, 148.8, 146.3 (d, *J* = 3.1 Hz), 135.1 (q, *J* = 32.0 Hz), 130.8 (d, *J* = 2.1 Hz), 129.5, 124.4 (d, *J* = 2.0 Hz), 123.6, 123.5 (q, *J* = 274.9 Hz), 123.2 (d, *J* = 8.4 Hz), 116.4, 116.3, 116.1 (q, *J* = 5.6 Hz). ¹⁹F NMR (470 MHz, CDCl₃) δ -61.5 (3F), -114.6 (1F). EIMS 318.0 (M⁺), 290.0 (base peak).

(E)-N-(4-Fluorophenyl)-4-methylquinoline-2-carboxaldehyde imine (L10).



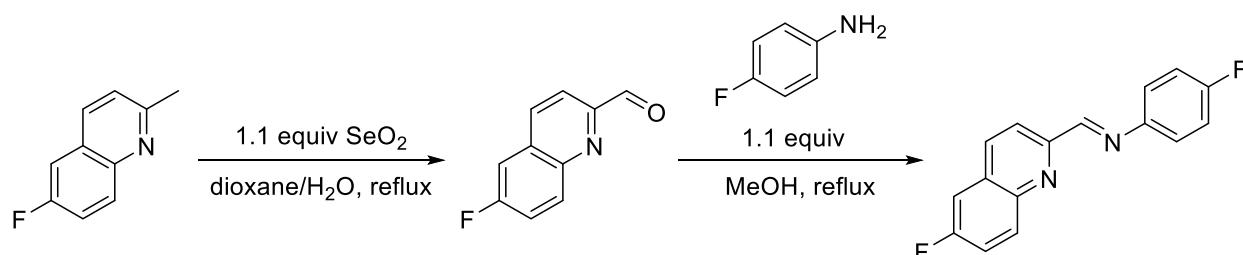
Step 1 was performed according to a published procedure³⁰ to prepare (4-methylquinolin-2-yl)methanol.

Step 2. (4-Methylquinolin-2-yl)methanol (101 mg, 0.583 mmol) was dissolved in 5 ml of dry DCM in a 20 ml vial. MnO₂ (253 mg, 2.91 mmol, 5 equiv) was added, and the reaction mixture was stirred for 90 minutes. The reaction mixture was filtered through a plug of Celite, after which the Celite was rinsed twice with 2 ml of DCM. The solvent was evaporated under reduced pressure, and the crude product was purified by column chromatography (50% ethyl acetate in hexanes) to give 4-methylquinoline-2-carboxaldehyde as an off-white powder (66.5 mg, 0.388 mmol, 67%).

Step 3. 4-Methylquinoline-2-carboxaldehyde (63.1 mg, 0.369 mmol) and 4-fluoroaniline (43 mg, 0.39 mmol, 1.1 equiv) were mixed in 1.5 ml of MeOH, and the reaction mixture was heated at reflux for 90 min. The solvent was evaporated at reduced pressure, and the yellow residue was

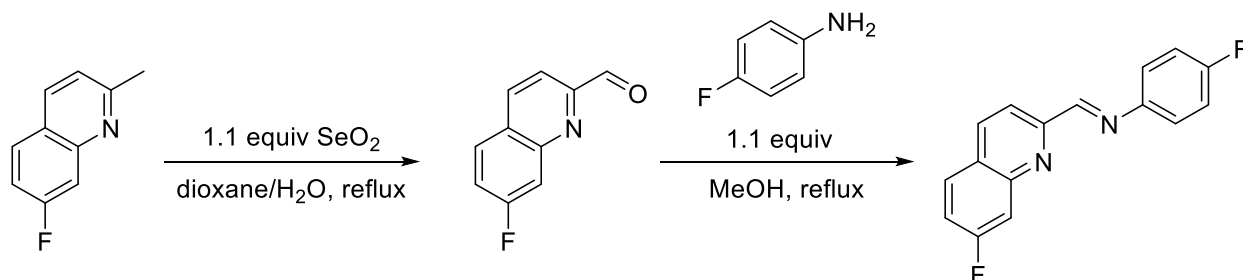
purified by Kugelrohr distillation to give the title compound as an off-white powder (79.8 mg, 0.302 mmol, 82%). This product contained approximately 3% 4-methylquinoline-2-carboxaldehyde as an impurity. $^1\text{H NMR}$ (400 MHz, CDCl_3) δ 8.72 (s, 1H), 8.19 – 8.12 (m, 2H), 8.00 (d, $J = 8.3$ Hz, 1H), 7.74 (t, $J = 7.6$ Hz, 1H), 7.60 (t, $J = 7.6$ Hz, 1H), 7.34 (dd, $J = 8.4, 5.0$ Hz, 2H), 7.11 (t, $J = 8.4$ Hz, 2H), 2.75 (s, 3H). $^{13}\text{C NMR}$ (101 MHz, CDCl_3) δ 161.9 (d, $J = 246.2$ Hz), 160.9, 154.2, 147.8, 146.9 (d, $J = 3.0$ Hz), 145.2, 130.3, 129.8, 129.1, 127.7, 124.0, 123.0 (d, $J = 8.4$ Hz), 119.0, 116.2 (d, $J = 22.6$ Hz), 19.0. $^{19}\text{F NMR}$ (376 MHz, CDCl_3) δ -115.5. **EIMS** 264.0 (M^+), 236.1 (base peak).

(E)-N-(4-Fluorophenyl)-6-fluoroquinoline-2-carboxaldehyde imine (L11).



Step 1. 6-Fluoro-2-methylquinoline (323 mg, 2.00 mmol) was mixed with SeO_2 (244 mg, 2.20 mmol, 1.1 equiv) in 2 ml of dioxane and 0.20 ml of deionized water in a pear flask. The reaction mixture was heated at reflux for 2 h. After allowing it to cool to room temperature, the reaction mixture was loaded directly onto a column of silica gel, and 6-fluoroquinoline-2-carboxaldehyde was isolated by column chromatography (15% ethyl acetate in hexanes, R_f 0.75) as a white solid (248 mg, 1.42 mmol, 71%).

Step 2. 6-Fluoroquinoline-2-carboxaldehyde (123 mg, 0.702 mmol) and 4-fluoroaniline (85 mg, 0.77 mmol, 1.1 equiv) were mixed in 4 ml of MeOH, and the reaction mixture was heated at reflux for 2 h. White needles formed as the reaction mixture was allowed to cool to room temperature, were collected by vacuum filtration, and rinsed twice with 2 ml of MeOH. A second crop of crystals was obtained by reducing the filtrate volume to 3 ml. The second crop was rinsed with 1 ml of MeOH and combined with the first crop. The combined material was recrystallized from 10 ml of hexanes to give the title compound as thin white needles (143 mg, 0.533 mmol, 76%). This product contained approximately 2% 6-fluoroquinoline-2-carbaldehyde as an impurity. $^1\text{H NMR}$ (500 MHz, CDCl_3) δ 8.71 (s, 1H), 8.33 (d, $J = 8.5$ Hz, 1H), 8.20 – 8.07 (m, 2H), 7.55 – 7.48 (m, 1H), 7.48 – 7.42 (m, 1H), 7.34 (dd, $J = 8.2, 5.0$ Hz, 2H), 7.11 (t, $J = 8.4$ Hz, 2H). $^{13}\text{C NMR}$ (126 MHz, CDCl_3) δ 161.9 (d, $J = 246.4$ Hz), 161.2 (d, $J = 250.7$ Hz), 160.2, 154.3 (d, $J = 2.7$ Hz), 146.7 (d, $J = 2.9$ Hz), 145.1, 136.1 (d, $J = 5.4$ Hz), 132.3 (d, $J = 9.3$ Hz), 129.7 (d, $J = 10.3$ Hz), 123.0 (d, $J = 8.5$ Hz), 120.4 (d, $J = 25.8$ Hz), 119.4, 116.2 (d, $J = 22.6$ Hz), 111.1 (d, $J = 21.9$ Hz). $^{19}\text{F NMR}$ (470 MHz, CDCl_3) δ -111.0, -115.3. **EIMS** 268.0 (M^+ , base peak), 240.0 (2nd most intense peak).

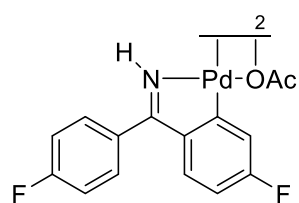
(E)-N-(4-Fluorophenyl)-7-fluoroquinoline-2-carboxaldehyde imine (L12).

Step 1. 7-Fluoro-2-methylquinoline (323 mg, 2.00 mmol) was mixed with SeO₂ (244 mg, 2.20 mmol, 1.1 equiv) in 2 ml of dioxane and 0.20 ml of deionized water in a pear flask. The reaction mixture was heated at reflux for 2 h. After allowing it to cool to room temperature, the reaction mixture was loaded directly onto a column of silica gel, and 6-fluoroquinoline-2-carboxaldehyde was isolated by column chromatography (15% ethyl acetate in hexanes) as a white solid (244 mg, 1.39 mmol, 70%).

Step 2. 7-Fluoroquinoline-2-carboxaldehyde (123 mg, 0.702 mmol) and 4-fluoroaniline (85 mg, 0.77 mmol, 1.1 equiv) were mixed in 2 ml of MeOH, and the reaction mixture was heated at reflux for 2 h. The reaction mixture solidified as it was allowed to cool to room temperature. An additional 2 ml of MeOH was added, and the reaction mixture was reheated to reflux then allowed to cool to room temperature. The title compound precipitated as a white solid, which turned yellow after standing overnight (132 mg, 0.492 mmol, 70%). This product contained approximately 2% 7-fluoroquinoline-2-carboxaldehyde as an impurity. ¹H NMR (600 MHz, CDCl₃) δ 8.75 (s, 1H), 8.31 (d, *J* = 8.5 Hz, 1H), 8.25 (d, *J* = 8.4 Hz, 1H), 7.87 (dd, *J* = 8.8, 6.1 Hz, 1H), 7.79 (d, *J* = 9.7 Hz, 1H), 7.40 (td, *J* = 8.6, 2.0 Hz, 1H), 7.37 (dd, *J* = 8.2, 5.1 Hz, 2H), 7.13 (t, *J* = 8.4 Hz, 2H). ¹³C NMR (151 MHz, CDCl₃) δ 163.4 (d, *J* = 250.7 Hz), 162.1 (d, *J* = 246.6 Hz), 160.3, 155.8, 149.1 (d, *J* = 12.6 Hz), 146.8, 136.7, 129.9 (d, *J* = 9.8 Hz), 126.0, 123.1 (d, *J* = 8.5 Hz), 118.3 (d, *J* = 25.4 Hz), 118.1 (d, *J* = 2.4 Hz), 116.3 (d, *J* = 22.7 Hz), 113.5 (d, *J* = 20.4 Hz). ¹⁹F NMR (565 MHz, CDCl₃) δ -109.7, -116.2. EIMS 268.0 (M⁺), 240.0 (base peak).

Preparation of cyclopalladated complexes.

[(2-phenylpyridine)Pd(μ-OAc)]₂ (**Pd3**) was prepared according to a published procedure.⁴⁵



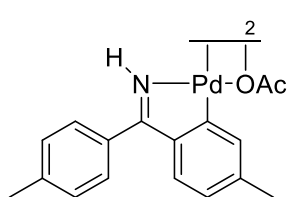
[[((4-FC₆H₄)(4-FC₆H₃)CNH)Pd(μ-OAc)]₂ (**Pd1**). Palladium acetate trimer (112 mg, 0.499 mmol Pd) and 4,4'-difluorobenzophenone imine (114 mg, 0.525 mmol, 1.05 equiv) were mixed in glacial acetic acid (4 ml) in a 20 ml scintillation vial. The vial was flushed with N₂ and sealed with a PTFE-lined cap. The mixture was heated at 65 °C with stirring for 12 h. The volatile materials were then evaporated under reduced pressure.

Acetone (~5 ml) was added and then evaporated under reduced pressure thrice to give the crude product as a red-orange solid. The solid was washed thrice with cold ether (~4 ml each), then thrice with DI H₂O (~2 ml each), and then thrice with ether (~2 ml each) to give the title compound as a

bright orange solid (134 mg, 0.351 mmol Pd, 70% yield). **¹H NMR** (600 MHz, DMF-*d*₇) δ 10.46 (br, 2H), 7.25 (br, 4H), 7.00 (br, 4H), 6.90 (4H), 6.83 (br, 2H) 2.05 (s, 6H). **¹³C NMR** (151 MHz, DMF-*d*₇) δ 184.2, 181.5, 164.9 (d, *J* = 244.1 Hz), 163.2 (d, *J* = 251.4 Hz), 161.6 (d, *J* = 5.5 Hz), 144.0, 131.2, 131.7 (d, *J* = 3.3 Hz), 131.4 (d, *J* = 8.9 Hz), 120.2 (d, *J* = 18.7 Hz), 116.4 (d, *J* = 22.0 Hz), 111.5 (d, *J* = 23.3 Hz), 24.7. **¹⁹F NMR** (565 MHz, DMF-*d*₇) δ -108.6, -111.7. **Analysis** calc'd C 47.20, H 2.91, N 3.67; found C 46.88, H 2.98, N 3.50.

Note: there is some ambiguity to the assignment of specific aryl peaks ¹³C NMR spectrum to each double. Doublets were assigned such that the *J*_{C-F} values were consistent with other 4,4'-difluorobenzophenone imine derivatives.

Note: a minor, likely isomeric complex (~17%) was also observed by NMR spectroscopy.



[[[(4-(CH₃)C₆H₄)(4-(CH₃)C₆H₃)CNH)Pd(μ-OAc)]₂ (Pd₂). Palladium acetate trimer (224 mg, 0.998 mmol Pd) and 4,4'-dimethylbenzophenone imine (220 mg, 1.05 mmol, 1.05 equiv) were mixed in glacial acetic acid (12 ml) in a 20 ml scintillation vial. The vial was flushed with N₂ and sealed with a PTFE-lined cap. The mixture was heated at 65 °C with stirring for 12 h. The volatile materials were then evaporated under reduced pressure. Acetone (~10 ml) was added and then evaporated under reduced pressure thrice to give the crude product as a red-orange solid. The crude product was purified by column chromatography (1:1 DCM/ether, collected red-orange band) followed by precipitation from ether and pentane (2 crops) to give the title compound as a bright orange solid (277 mg, 0.741 mmol Pd, 74% yield). **¹H NMR** (600 MHz, CDCl₃) δ 7.70 (br, 2H), 7.04 (d, *J* = 7.9 Hz, 4H), 6.98 (s, 2H), 6.72 (d, *J* = 7.8 Hz, 2H), 6.68 (d, *J* = 7.4 Hz, 2H), 6.59 (d, *J* = 8.0 Hz, 4H), 2.34 (s, 6H), 2.30 (s, 6H), 2.22 (s, 6H). **¹³C NMR** (151 MHz, CDCl₃) δ 185.5, 181.4, 156.7, 142.6, 141.6, 141.2, 133.1, 132.2, 129.9, 129.2, 127.2, 124.3, 24.7, 22.2, 21.6. **Analysis** calc'd C 54.63, H 4.58, N 3.75; found C 54.67, H 4.77, N 3.71.

Note: the ¹H and ¹³C NMR spectra indicate that the two acetate groups are equivalent, which is consistent with a highly-symmetric dimer. A minor complex (~10% was also observed by ¹H NMR spectroscopy with four inequivalent methyl groups (6:3:6:3 integration ratios) which is consistent with a dimer of lower symmetry.

Preparation of *N*-alkyl benzhydrylamines by palladium-catalyzed *N*-alkylation

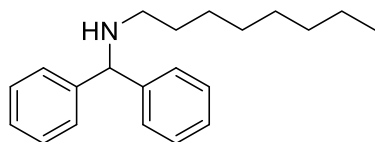
Step 1. In a nitrogen-filled glovebox, benzophenone imine (90.7 mg, 0.501 mmol) and the alkyl bromide (0.60 mmol, 1.2 equiv) were added to an oven-dried 20 ml scintillation vial. **L3** (250 μl, 0.040M, 0.010 mmol, 2%) and Pd(OAc)₂ (250 μl, 0.040M, 0.010 mmol, 2%) were added, and the solution was diluted to 3.0 ml with DMF. LiOt-Bu (120 mg, 1.50 mmol, 3.0 equiv) was dissolved in 2.0 ml of DMF and transferred to the reaction vial with stirring. The vial was sealed with a Teflon-lined cap, and the reaction mixture was stirred for 90 min at ambient temperature (approximately 25 °C). In most examples, the reaction mixture color transitioned from dark purple to dark green as benzophenone imine was consumed. After completion of the reaction, the

resulting mixture was diluted with 10 ml of Et₂O and washed with 10 ml of deionized water in a separatory funnel. The aqueous layer was extracted with 10 ml of Et₂O. The organic layers were dried with MgSO₄ and combined. The solvent was evaporated under reduced pressure.

Step 2. The residue from step 1 was dissolved in 2.0 ml of MeOH. NaBH₃CN (79 mg, 1.3 mmol, 2.5 equiv) and AcOH (57 μ l, 60 mg, 1.0 mmol, 2.0 equiv) were added in that order with stirring. The solution was stirred for 60 minutes at ambient temperature under air. The reaction mixture was then diluted with 10 ml of Et₂O and washed with 10 ml of 5% NaOH_(aq). The solvent was evaporated under reduced pressure, and the crude products were purified by column chromatography, acid/base extraction, or both. Purification method(s) and any deviations from the general procedure are noted for each compound.

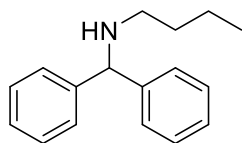
Acid/Base Extraction Procedure. For compounds noted “purified by acid/base extraction,” the following procedure was followed. The Et₂O solution from step 2 was extracted twice with 4 ml of 0.5 M HCl_(aq) in a separatory funnel. The aqueous layers were combined, basified with 3 NaOH pellets (approximately 600 mg), and extracted twice with 10 ml of Et₂O. The organic layers were combined and dried with MgSO₄. The solvent was evaporated under reduced pressure, and the resulting residue was dried under vacuum.

Procedure for ¹H NMR spectroscopy yields. Samples were prepared by the general procedure above, with the modification that no column chromatography or acid/base extraction was performed. Instead, the solution of the crude product in ether was transferred to a vial containing 84.1 mg (0.500 mmol) 1,3,5-trimethoxybenzene (TMB). The solvent was evaporated under reduced pressure, and a ¹H NMR spectrum was obtained with d1 > 8 s. Yield was determined by integration of non-overlapping product signals against the aryl ¹H signal of TMB, corrected by relative hydrogen number.



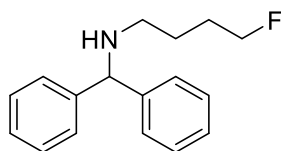
N-Benzhydryloctan-1-amine (4a).³³ Prepared by the general procedure above with 115 of mg 1-bromooctane. The crude product was purified by column chromatography (3% TEA in hexanes, R_f 0.54) to give the title compound as a clear oil (129 mg, 87%). ¹H NMR (600 MHz, CDCl₃) δ 7.44 (d, J = 7.4 Hz, 4H), 7.33 (t, J = 7.7 Hz, 4H), 7.24 (t, J = 7.3 Hz, 2H), 4.86 (s, 1H), 2.61 (t, J = 7.1 Hz, 2H), 1.56 (p, J = 7.1 Hz, 2H), 1.50 (broad, NH), 1.39 – 1.27 (m, 10H), 0.93 (t, J = 7.0 Hz, 3H). ¹³C NMR (151 MHz, CDCl₃) δ 144.6, 128.5, 127.4, 127.0, 67.8, 48.5, 32.0, 30.4, 29.7, 29.4, 27.5, 22.8, 14.2. HRMS (ESI) calc'd (+H⁺) 296.2373, found 296.2373.

¹H NMR spectroscopy yield for 3aa (Step 1): prepared by the general procedure above with 115 mg 1-bromooctane; 90% yield.

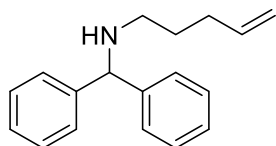


N-Benzhydrylbutan-1-amine (4c).⁴⁶ Prepared by the general procedure above with 82 mg of 1-bromobutane. The crude product was purified by acid/base extraction to give the title compound as a pale yellow oil (97.3 mg, 81%). ¹H NMR (600 MHz, CDCl₃) δ 7.43 (d, J = 7.2 Hz, 4H), 7.32 (t, J =

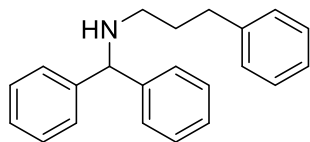
7.5 Hz, 4H), 7.23 (t, $J = 7.2$ Hz, 2H), 4.85 (s, 1H), 2.61 (t, $J = 7.0$ Hz, 2H), 1.58 – 1.48 (m, 3H, CH₂ + NH), 1.43 – 1.35 (m, 2H), 0.93 (t, $J = 7.3$ Hz, 3H). ¹³C NMR (151 MHz, CDCl₃) δ 144.6, 128.5, 127.4, 127.0, 67.8, 48.2, 32.6, 20.6, 14.2. HRMS (ESI) calc'd (+H⁺) 240.1747, found 240.1747.



N-Benzhydryl-4-fluorobutan-1-amine (4d). Prepared by the general procedure above with 93 mg of 1-bromo-4-fluorobutane. The crude product was purified by acid/base extraction, followed by column chromatography (3% TEA in hexanes, R_f 0.42) to give the title compound as a clear oil (89.9 mg, 69%). ¹H NMR (600 MHz, CDCl₃) δ 7.44 (d, $J = 7.4$ Hz, 4H), 7.34 (t, $J = 7.6$ Hz, 4H), 7.25 (t, $J = 7.3$ Hz, 2H), 4.86 (s, 1H), 4.47 (dt, $J = 47.3$, 6.1 Hz, 2H), 2.66 (t, $J = 7.0$ Hz, 2H), 1.85 – 1.75 (m, 2H), 1.66 (p, $J = 7.0$ Hz, 2H), 1.50 (broad, NH). ¹³C NMR (151 MHz, CDCl₃) δ 144.4, 128.6, 127.3, 127.1, 84.1 (d, $J = 164.5$ Hz), 67.7, 47.8, 28.4 (d, $J = 19.7$ Hz), 26.1 (d, $J = 5.2$ Hz). HRMS (ESI) calc'd (+H⁺) 258.1653, found 258.1652.



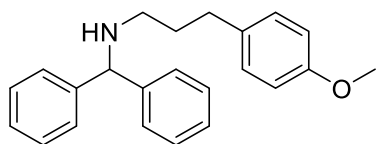
N-Benzhydryl-4-en-1-amine (4e). Prepared by the general procedure above with 91 mg of 5-bromo-1-pentene. Modification to workup of step 2: the reaction mixture was then diluted with 10 ml of Et₂O and washed with 10 ml of 5% NaOH_(aq). The aqueous layer was extracted with 10 ml of Et₂O, and the organic layers were combined. The solvent was evaporated under reduced pressure, and the crude product was purified by column chromatography (2% TEA in hexanes, R_f 0.58) to give the title compound as a clear oil (95.9 mg, 76%). ¹H NMR (600 MHz, CDCl₃) δ 7.47 (d, $J = 7.0$ Hz, 4H), 7.35 (t, $J = 7.6$ Hz, 4H), 7.26 (t, $J = 7.3$ Hz, 2H), 5.91 – 5.83 (m, 1H), 5.07 (d, $J = 17.1$ Hz, 1H), 5.01 (d, $J = 10.2$ Hz, 1H), 4.88 (s, 1H), 2.66 (t, $J = 7.0$ Hz, 2H), 2.18 (q, $J = 7.1$ Hz, 2H), 1.69 (p, $J = 7.2$ Hz, 2H), 1.53 (broad, NH). ¹³C NMR (151 MHz, CDCl₃) δ 144.5, 138.7, 128.5, 127.4, 127.0, 114.7, 67.7, 47.8, 31.7, 29.6. HRMS (ESI) calc'd (+H⁺) 252.1747, found 252.1747.



N-Benzhydryl-3-phenylpropan-1-amine (4b). Prepared by the general procedure above with 120 mg of 1-bromo-3-phenylpropane. The crude product was purified by acid/base extraction to give the title compound as a pale yellow oil (135 mg, 89%). The acid/base extraction procedure was modified as follows: after acid extraction, white crystals formed in the ether layer on standing overnight. The solvent was decanted, and the crystals were rinsed twice with approximately 2 ml of Et₂O. NaOH_(aq) (10 ml, 5% by weight) was added to the vial containing the crystals, and the resulting mixture was extracted thrice with 4 ml of Et₂O. The combined organic extracts were dried with MgSO₄. The original acid extracts were basified with 3 NaOH pellets, extracted twice with 10 ml of Et₂O, and dried with MgSO₄. The two batches of product were combined for the reported yield and characterization. ¹H NMR (600 MHz, CDCl₃) δ 7.53 (d, $J = 7.2$ Hz, 4H), 7.44 – 7.37 (m, 6H), 7.35 – 7.28 (m, 5H), 4.94 (s, 1H), 2.81 – 2.78 (m, 2H), 2.75 (t, $J = 7.0$ Hz, 2H), 2.01 – 1.94 (m, 2H), 1.63 (broad, NH). ¹³C NMR (151 MHz, CDCl₃) δ 144.4,

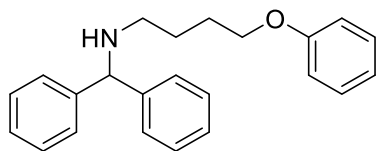
142.3, 128.5, 128.5, 128.4, 127.4, 127.0, 125.8, 67.6, 47.8, 33.7, 32.0. **HRMS** (ESI) calc'd (+H⁺) 302.1903, found 302.1903.

¹H NMR spectroscopy yield for 3ab (Step 1): prepared by the general procedure above with 119 mg 1-bromo-3-phenylpropane; 91% yield.



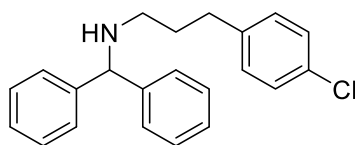
***N*-Benzhydryl-3-(4-methoxyphenyl)propan-1-amine (4f).**

Prepared by the general procedure above with 138 mg of 1-(3-bromopropyl)-4-methoxybenzene. The crude product was purified by column chromatography (1.5% TEA in hexanes, R_f 0.14) to give the title compound as a clear oil (148 mg, 89%). **¹H NMR** (600 MHz, CDCl₃) δ 7.46 (d, *J* = 6.9 Hz, 4H), 7.35 (t, *J* = 7.4 Hz, 4H), 7.26 (t, *J* = 7.1 Hz, 2H), 7.14 (d, *J* = 8.1 Hz, 2H), 6.87 (d, *J* = 8.3 Hz, 2H), 4.87 (s, 1H), 3.82 (s, 3H), 2.71 – 2.65 (m, 4H), 1.92 – 1.85 (m, 2H), 1.56 (broad, NH). **¹³C NMR** (151 MHz, CDCl₃) δ 157.8, 144.4, 134.4, 129.3, 128.5, 127.4, 127.0, 113.8, 67.6, 55.3, 47.8, 32.8, 32.3. **HRMS** (ESI) calc'd (+H⁺) 332.2009, found 332.2009.



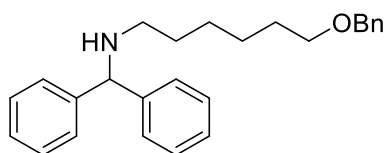
***N*-Benzhydryl-4-phenoxybutan-1-amine (4g).**

Prepared by the general procedure above with 137 mg of (4-bromobutoxy)benzene. The crude product was purified by column chromatography (1.5% TEA in hexanes, R_f 0.17) to give the title compound as a white powder (132 mg, 80%). **¹H NMR** (600 MHz, CDCl₃) δ 7.42 (d, *J* = 7.7 Hz, 4H), 7.34 – 7.26 (m, 6H), 7.21 (t, *J* = 7.1 Hz, 2H), 6.94 (t, *J* = 7.3 Hz, 1H), 6.89 (d, *J* = 8.3 Hz, 2H), 4.84 (s, 1H), 3.96 (t, *J* = 6.4 Hz, 2H), 2.66 (t, *J* = 7.0 Hz, 2H), 1.86 (p, *J* = 6.6 Hz, 2H), 1.71 (p, *J* = 7.1 Hz, 2H), 1.54 (broad, NH). **¹³C NMR** (151 MHz, CDCl₃) δ 159.1, 144.4, 129.5, 128.6, 127.4, 127.1, 120.7, 114.6, 67.8, 67.7, 48.0, 27.3, 26.9. **HRMS** (ESI) calc'd (+H⁺) 332.2009, found 332.2008.

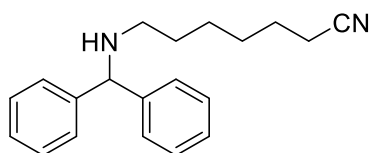


***N*-Benzhydryl-3-(4-chlorophenyl)propan-1-amine (4h).**

Prepared by the general procedure above with 140 mg of 1-(3-bromopropyl)-4-chlorobenzene. The crude product was purified by column chromatography (1.5% TEA in hexanes, R_f 0.23) to give the title compound as a clear oil (135 mg, 80%). **¹H NMR** (600 MHz, CDCl₃) δ 7.49 (d, *J* = 7.3 Hz, 4H), 7.38 (t, *J* = 7.7 Hz, 4H), 7.32 – 7.27 (m, 4H), 7.15 (d, *J* = 8.4 Hz, 2H), 4.89 (s, 1H), 2.75 – 2.65 (m, 4H), 1.93 – 1.85 (m, 2H), 1.55 (broad, NH). **¹³C NMR** (151 MHz, CDCl₃) δ 144.3, 140.8, 131.5, 129.8, 128.5, 128.4, 127.3, 127.1, 67.6, 47.6, 33.0, 31.9. **HRMS** (ESI) calc'd (³⁵Cl, +H⁺) 336.1515, found 336.1514.

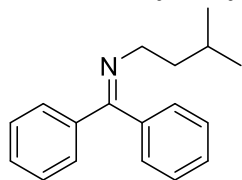


N-Benzhydryl-6-(benzyloxy)hexan-1-amine (4i). Prepared by the general procedure above with 163 mg of 1-benzyloxy-6-bromohexane. The crude product was purified by column chromatography (1.5% TEA in hexanes, R_f 0.16) to give the title compound as a clear oil (136 mg, 73%). This procedure was duplicated on a separate day (137 mg, 73%). **^1H NMR** (600 MHz, CDCl_3) δ 7.43 (d, J = 7.6 Hz, 4H), 7.36 (d, J = 4.0 Hz, 4H), 7.34 – 7.29 (m, 5H), 7.23 (t, J = 7.3 Hz, 2H), 4.84 (s, 1H), 4.52 (s, 2H), 3.48 (t, J = 6.6 Hz, 2H), 2.60 (t, J = 7.0 Hz, 2H), 1.68 – 1.61 (m, 2H), 1.59 – 1.49 (m, 3H), 1.44 – 1.34 (m, 4H). **^{13}C NMR** (151 MHz, CDCl_3) δ 144.5, 138.8, 128.5, 128.4, 127.7, 127.6, 127.4, 127.0, 73.0, 70.5, 67.8, 48.4, 30.4, 29.8, 27.3, 26.3. **HRMS** (ESI) calc'd ($+\text{H}^+$) 274.2478, found 274.2478.



7-(Benzhydrylamino)heptanenitrile (4j). Prepared by the general procedure above with 113 mg of 7-bromoheptanenitrile. Modification to workup of step 2: the reaction mixture was then diluted with 10 ml of Et_2O and washed with 10 ml of 5% $\text{NaOH}_{(\text{aq})}$. The aqueous layer was extracted with 10 ml of Et_2O , and the organic layers were combined. The solvent was evaporated under reduced pressure, and the crude product was purified by two successive column chromatography procedures: 5% ethyl acetate and 6% TEA in hexanes; changed to 10% ethyl acetate and 5% TEA in hexanes after elution of benzophenone; then 10% TEA in hexanes to give the title compound as a clear oil (109 mg). Title compound R_f : 0.21 (5% ethyl acetate, 6% TEA in hexanes), 0.33 (10% ethyl acetate, 5% TEA in hexanes), and 0.23 (10% TEA in hexanes). This product contained approximately 7 mol% 1-bromoheptanenitrile as an impurity. When corrected for this impurity, the yield of the title compound is 71% (104 mg, 0.356 mmol).

A duplicate reaction was performed with 114 mg 7-bromoheptanenitrile. Modification to workup of step 2: the solvent was evaporated at reduced pressure, and 4 ml of ethyl ether was added to the reaction vial. The mixture was filtered through a plug of Celite, and the Celite was rinsed twice with 2 ml of ether. The crude product was adsorbed onto silica and purified by column chromatography (3% TEA in hexanes – ethyl acetate gradient). A single analytically pure fraction was collected and used for characterization (21.9 mg, clear oil). **^1H NMR** (600 MHz, CDCl_3) δ 7.40 (d, J = 7.5 Hz, 4H), 7.30 (t, J = 7.6 Hz, 4H), 7.21 (t, J = 7.3 Hz, 2H), 4.81 (s, 1H), 2.58 (t, J = 7.1 Hz, 2H), 2.31 (t, J = 7.1 Hz, 2H), 1.64 (p, J = 7.2 Hz, 2H), 1.55 (broad, NH), 1.54 (p, J = 7.2 Hz, 2H), 1.47 – 1.41 (m, 2H), 1.41 – 1.34 (m, 2H). **^{13}C NMR** (151 MHz, CDCl_3) δ 144.3, 128.6, 127.3, 127.1, 119.9, 67.8, 48.1, 30.1, 28.7, 26.6, 25.4, 17.2. **HMRS** (ESI) calc'd ($+\text{H}^+$) 293.2012, found 293.2013. **^1H NMR spectroscopy yield (Step 2):** prepared by the general procedure above with 114 mg 7-bromoheptanenitrile; 74% yield.

***N*-(3-Methylbutyl)benzophenone Imine (3ak).**

benzophenone imine (182 mg, 1.00 mmol), 1-bromo-3-methylbutane (305 mg, 2.02 mmol, 2.0 equiv), Pd(OAc)₂ (0.50 ml, 0.040 M, 0.020 mmol, 2 mol%), and **L3** (0.50 ml, 0.040 M, 0.020 mmol, 2 mol%) were mixed in an oven-dried 20 ml vial, and the mixture was diluted to 7 ml with DMF. LiOt-Bu (240 mg, 3.00 mmol, 3.0 equiv) was dissolved in 3 ml DMF, and this solution was slowly added to the reaction mixture with stirring. The vial was sealed with a Teflon-lined cap, and the reaction mixture

was stirred at ambient temperature. After 150 min, the reaction mixture was diluted with 20 ml of Et₂O and washed with 10 ml of deionized water. The organic layer was dried with MgSO₄ and filtered through paper. The solvent was evaporated at reduced pressure, and the crude product purified by column chromatography (4% TEA in hexanes) to give the title compound as a pale yellow oil (186 mg, 0.740 mmol, 74%). This product contained <1% of benzophenone as an impurity. ¹H NMR (600 MHz, CDCl₃) δ 7.60 (d, *J* = 7.1 Hz, 2H), 7.48 – 7.44 (m, 2H), 7.42 (tt, *J* = 7.1, 1.7 Hz, 1H), 7.36 (tt, *J* = 7.2, 1.6 Hz, 1H), 7.34 – 7.30 (m, 2H), 7.20 – 7.14 (m, 2H), 3.39 (t, *J* = 7.4 Hz, 2H), 1.65 (“nonet”, *J* = 6.6 Hz, 1H), 1.57 (q, *J* = 7.0 Hz, 2H), 0.84 (d, *J* = 6.6 Hz, 6H). ¹³C NMR (151 MHz, CDCl₃) δ 167.8, 140.2, 137.2, 129.8, 128.5, 128.4, 128.4, 128.1, 128.0, 52.3, 40.4, 26.3, 22.7. EIMS 251.1 (M⁺), 194.0 (base peak).

Experimental details for Table 4.1

Procedure. A 4 ml vial was charged with benzophenone imine, bromooctane, Pd(OAc)₂, *t*-Bu₂MeP, DMF, and one equivalent of 1,3,5-trimethoxybenzene (TMB) as an internal standard. A solution of LiOt-Bu was added with stirring. The vial was sealed with a Teflon-lined cap and stirred for the noted reaction time. A small aliquot was then diluted with ethyl acetate or THF and analyzed by gas chromatography. GC integration against TMB was calibrated with a response factor of 0.37 (entry 1) or 0.297 (entries 2-8) determined with independently prepared *N*-octylbenzophenone imine.

Entry 1 was performed with benzophenone imine (37 mg, 0.20 mmol), 1-bromooctane (39 mg, 0.20 mmol, 1 equiv), Pd(OAc)₂ (4.5 mg, 0.020 mmol, 10%), *t*-Bu₂MeP (6.4 mg, 0.040 mmol, 20%), NaOt-Bu (38 mg, 0.40 mmol, 2 equiv), TMB (200 μl, 1.0 M, 0.20 mmol, 1 equiv), and a total of 2.0 ml of THF ([benzophenone imine] = 0.10 M).

Entries 2-8 were performed with benzophenone imine (50 μl, 1.0 M, 0.050 mmol), 1-bromooctane (60 μl, 1.0 M, 0.060 mmol, 1.2 equiv), Pd(OAc)₂ (125 or 62.5 μl, 0.040 M, 0.0050 or 0.0025 mmol, 10 or 5%), *t*-Bu₂MeP (125 or 62.5 μl, 0.080 M, 0.010 or 0.0050 mmol, 20 or 10%), base (75 μl, 2.0 M, 0.15 mmol, 3 equiv), TMB (50 μl, 1.0 M, 0.050 mmol, 1 equiv), and diluted to a total of 0.50 ml of DMF ([benzophenone imine] = 0.10 M).

For entry 3, KOt-Bu was added as a solid (16.8 mg, 0.150 mmol, 3 equiv).

For entry 8, the reaction vial was covered in a layer of electrical tape to block room light.

Experimental details for Table 4.2

Entries 1-3: the benzophenone imine derivative (100 μ l, 1.0 M, 0.10 mmol), 1-bromooctane (200 μ l, 1.0 M, 0.20 mmol, 2.0 equiv), 1,3,5-trimethoxybenzene (100 μ l, 1.0 M, 0.10 mmol, 1.0 equiv), Pd(OAc)₂ (100 μ l, 0.040 M, 0.0040 mmol, 4%), and 350 μ l DMF were mixed in an oven-dried 1 dram vial. LiOt-Bu (150 μ l, 2.0 M, .30 mmol, 3.0 equiv) was added with stirring. The vial was sealed with a Teflon-lined cap, and the reaction mixture was stirred at ambient temperature. 40 μ l aliquots were taken and diluted with THF at various times to measure conversion of the imine starting material by GC. Response factors of 0.589, 0.573, and 0.546 were used for integration of 4,4'-difluorobenzophenone imine, benzophenone imine, and 4-methylbenzophenone imine against TMB, respectively.

Entries 4-6: the benzophenone imine derivative (100 μ l, 1.0 M, 0.10 mmol), 1-bromooctane (200 μ l, 1.0 M, 0.20 mmol, 2.0 equiv), 1,3,5-trimethoxybenzene (100 μ l, 1.0 M, 0.10 mmol, 1.0 equiv), Pd(OAc)₂ (50 μ l, 0.040 M, 0.0020 mmol, 2%), **L3** (50 μ l, 0.040 M, 0.0020 mmol, 2%), and 350 μ l DMF were mixed in an oven-dried 1 dram vial. LiOt-Bu (150 μ l, 2.0 M, .30 mmol, 3.0 equiv) was added with stirring. The vial was sealed with a Teflon-lined cap, and the reaction mixture was stirred at ambient temperature. 40 μ l aliquots were taken and diluted with THF at various times to measure conversion of the imine starting material by GC. Response factors of 0.589, 0.573, and 0.546 were used for integration of 4,4'-difluorobenzophenone imine, benzophenone imine, and 4-methylbenzophenone imine against TMB, respectively.

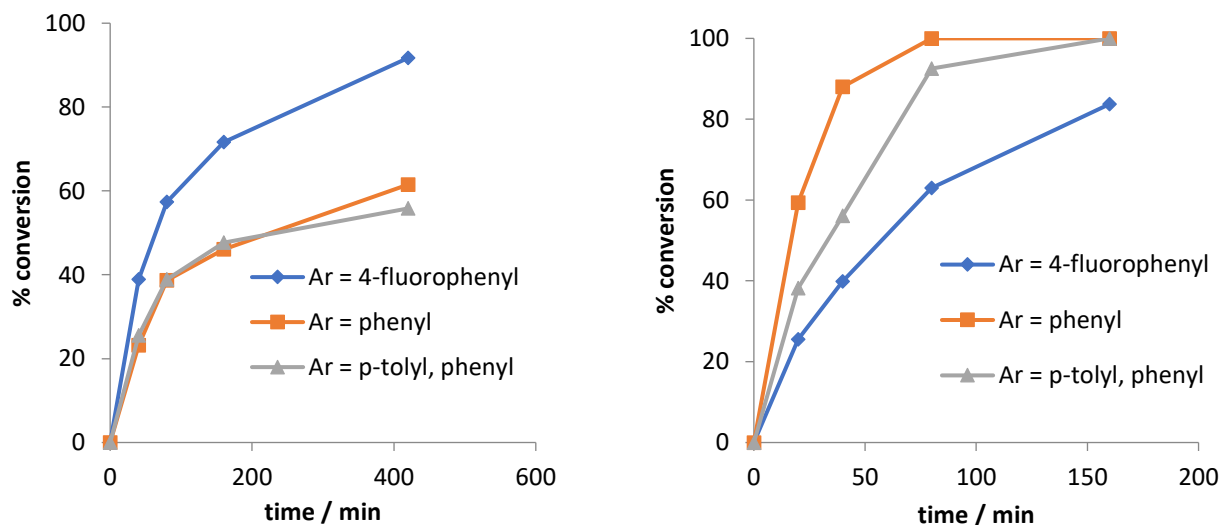


Figure 4.2. Conversion vs time plots for reactions of substituted imines **1a-c** catalyzed by 4% Pd(OAc)₂ (left) or 2% Pd(OAc)₂ + 2% **L3** (right).

Experimental details for Table 4.3

4-Methylbenzophenone imine (50 μ l, 1.0 M, 0.050 mmol), 1-bromooctane (19 mg, 0.10 mmol, 2.0 equiv), durene (50 μ l, 1.0 M, 0.050 mmol, 1.0 equiv), Pd(OAc)₂ (50 μ l, 0.040 M, 0.0020 mmol, 4%), L (50 μ l, 0.040 M, 0.0020 mmol, 4%), and 200 μ l DMF were mixed in an oven-dried 1 dram vial. LiOt-Bu (75 μ l, 2.0 M, 1.5 mmol, 3.0 equiv) was added with stirring. For entries 6 and 7, only 25 μ l Pd(OAc)₂ was used, and an additional 25 μ l DMF was added to maintain the same reaction volume and concentration. The vial was sealed with a Teflon-lined cap, and the reaction mixture was stirred at ambient temperature. Aliquots (40 μ l) were taken and diluted with THF at various times to measure the conversion of 4-methylbenzophenone imine by GC. A response factor of 0.676 was used for integration of 4-methylbenzophenone imine against durene.

Experimental details for Table 4.4.

Benzophenone imine (50 μ l, 1.0 M, 0.050 mmol), 1-bromo-3-phenylpropane (100 μ l, 1.0 M, 0.10 mmol, 2.0 equiv), 1,3,5-trimethoxybenzene (50 μ l, 1.0 M, 0.050 mmol, 1.0 equiv), Pd(OAc)₂ (12.5 μ l, 0.040 M, 0.00050 mmol, 1%), L (15 μ l, 0.040 M, 0.00060 mmol, 1.2%), and 200 μ l DMF were mixed in an oven-dried 1 dram vial. LiOt-Bu (75 μ l, 2.0 M, 1.5 mmol, 3.0 equiv) was added with stirring. The vial was sealed with a Teflon-lined cap, and the reaction mixture was stirred at ambient temperature. 40 μ l aliquots were taken and diluted with THF at various times to measure conversion of benzophenone imine by GC. A response factor of 0.52 was used for integration of benzophenone imine against TMB.

Experimental details for Figure 4.1

Kinetic experiments were performed on a 500 MHz Bruker NMR spectrometer programmed to record ¹⁹F NMR spectra every 20 seconds with the following parameters T = 323 K, NS = 1, d7 = 20 s, and O1P = -116 ppm. Concentrations were determined by ¹⁹F integration against an internal standard (4-fluorotoluene). Rates were measured by linear fits of 4,4'-difluorobenzophenone imine consumption as shown.

Procedure. A 20 ml vial was charged with 4,4'-difluorobenzophenone imine (250 μ l, 1.0 M, 0.25 mmol), Pd(OAc)₂ (250 μ l, 0.040 M, 0.010 mmol, 4%), 4-fluorotoluene (250 μ l, 1.0 M, 0.25 mmol, 1.0 equiv), and 2.25 ml of DMF. LiOt-Bu (750 μ l, 2.0 M, 1.5 mmol, 6.0 equiv) was added with stirring. A 750 μ l (0.050 mmol imine) sample of this solution was then transferred to an NMR tube containing 50- x μ l of DMF. The tube was sealed with a septum and Parafilm. The sample was then heated at 50 °C for 5 minutes. x (13.0/17.3/26/35) μ l (1.5, 2.0, 3.0, 4.0 equiv) of 1-bromooctane was then added through the septum, the sample was mixed by shaking, and data acquisition was initiated.

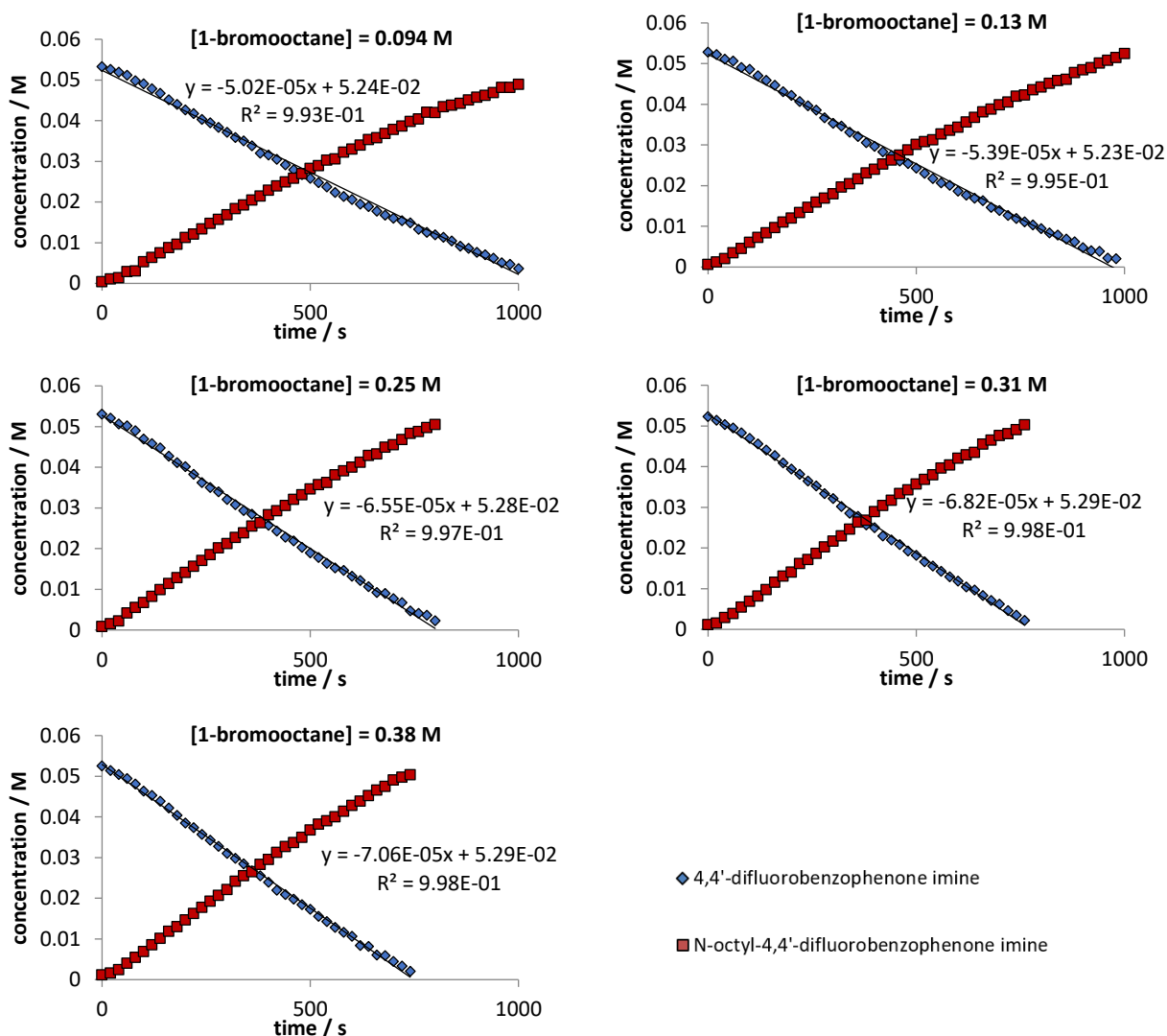


Figure 4.3. Concentration vs time plots for reactions of 4,4'-difluorobenzophenone imine (1b) catalyzed by 4% Pd(OAc)₂ with varying equivalents of 1-bromooctane (2a).

Procedure. A 20 ml vial was charged with 4,4'-difluorobenzophenone imine (250 μ l, 1.0 M, 0.25 mmol), Pd(OAc)₂ (250 μ l, 0.040 M, 0.010 mmol, 4%), 4-fluorotoluene (250 μ l, 1.0 M, 0.25 mmol, 1.0 equiv), and 2.00 ml of DMF. LiOt-Bu (500 μ l, 2.0 M, 1.0 mmol, 4.0 equiv) was added with stirring. A 650 μ l (0.050 mmol imine) sample of this solution was then transferred to an NMR tube containing x (0/25/50/100) μ l of LiOt-Bu (2.0 M) and 133- x μ l DMF. The tube was sealed with a septum and Parafilm. The sample was then heated at 50 °C for 5 minutes. 1-bromooctane (17.3 μ l, 0.10 mmol, 2.0 equiv) was added through the septum, the sample was mixed by shaking, and data acquisition was initiated.

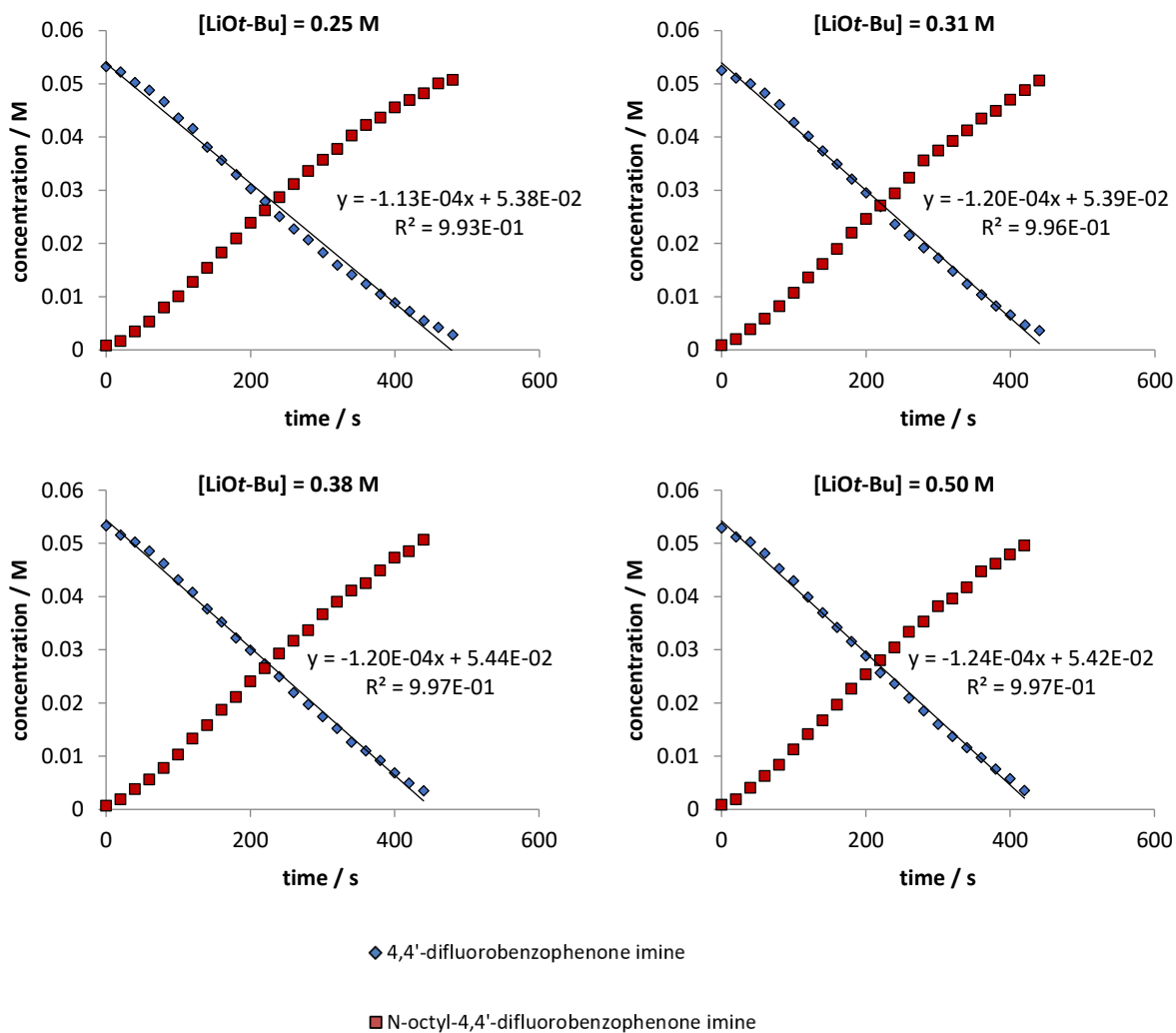


Figure 4.4. Concentration vs time plots for reactions of 4,4'-difluorobenzophenone imine (1b) catalyzed by 4% Pd(OAc)₂ with varying equivalents of LiOt-Bu.

Procedure. An NMR tube was charged with 4,4'-difluorobenzophenone imine (50 μl , 1.0 M, 0.050 mmol), x (25/50/75/100) μl $\text{Pd}(\text{OAc})_2$ (0.040 M), 4-fluorotoluene (50 μl , 1.0 M, 0.050 mmol, 1.0 equiv), 533- x μl DMF, and LiOt-Bu (150 μl , 2.0 M, 0.30 mmol, 6.0 equiv). The tube was sealed with a septum and Parafilm. The sample was then heated at 50 $^{\circ}\text{C}$ for 5 minutes. 1-Bromooctane (17.3 μl , 0.10 mmol, 2.0 equiv) was added through the septum, the sample was mixed by shaking, and data acquisition was begun. Initial rates were measured until the concentration of 4,4'-difluorobenzophenone imine was reduced to 0.030 M (0.040M for $[\text{Pd}(\text{OAc})_2] = 0.63$ mM (1 mol%)). Initial rates were used due to significant deactivation observed with low catalyst loadings.

The catalyst concentration was found to affect the mass balance of the reaction (mass balance = [4,4'-difluorobenzophenone imine] + [*N*-octyl-4,4'-difluorobenzophenone imine]). When the difference between the mass balance and the intended starting concentration of 4,4'-difluorobenzophenone imine (0.0625 M) was calculated, this number was found to correspond to the concentration of palladium with a ratio of 2.1 imines to 1 palladium. Note: the y-intercept of this plot is not zero, this is likely due to impurities in the 4,4'-difluorobenzophenone imine; the dominant impurity is 4,4'-difluorobenzophenone (~3%).

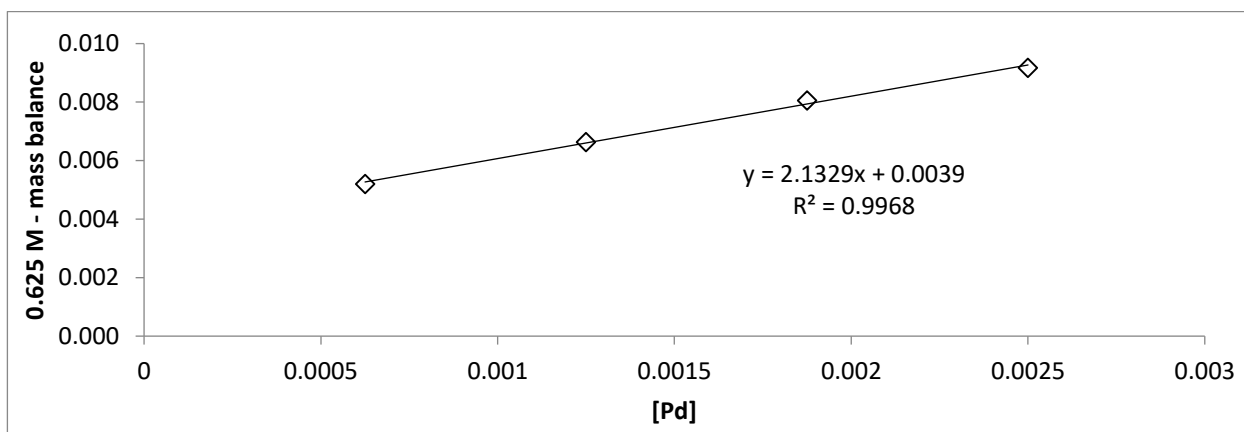
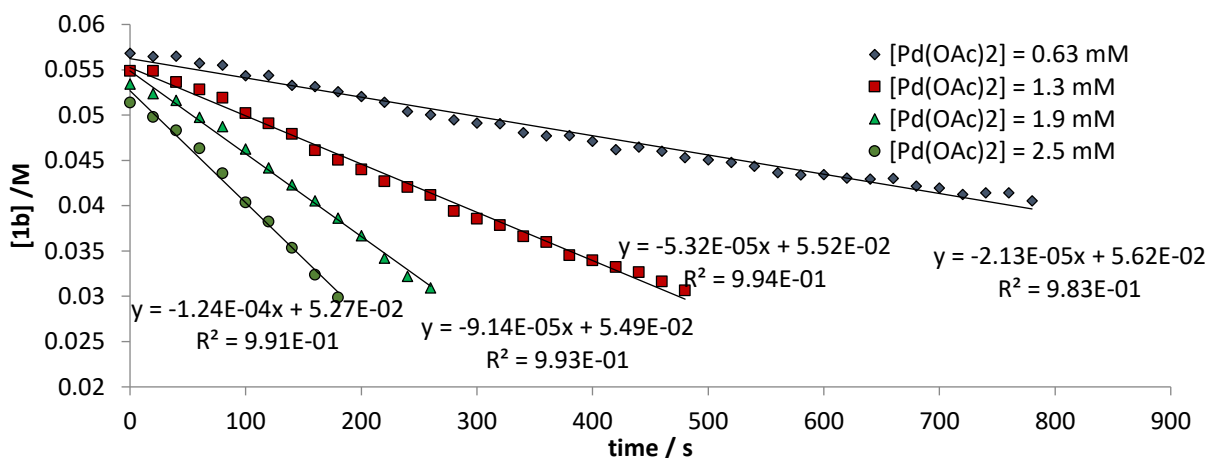
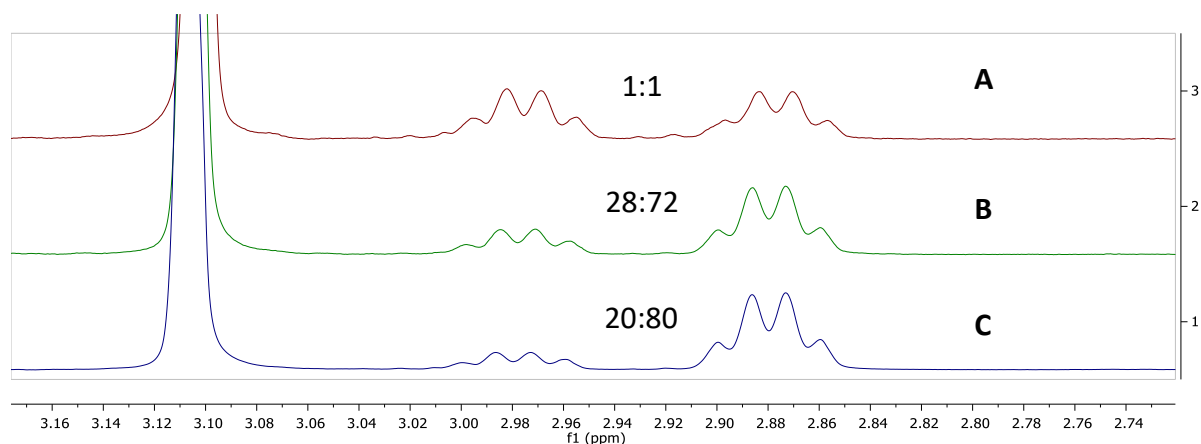
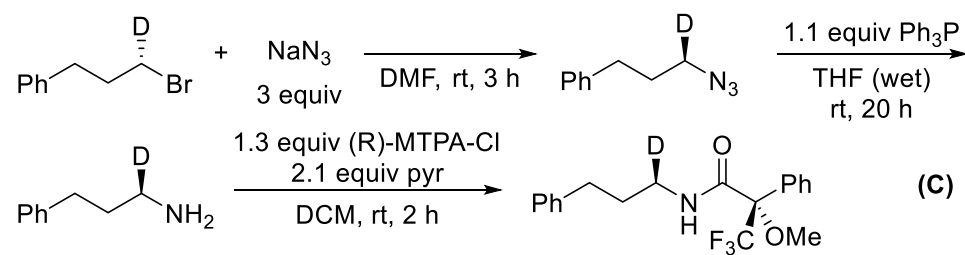
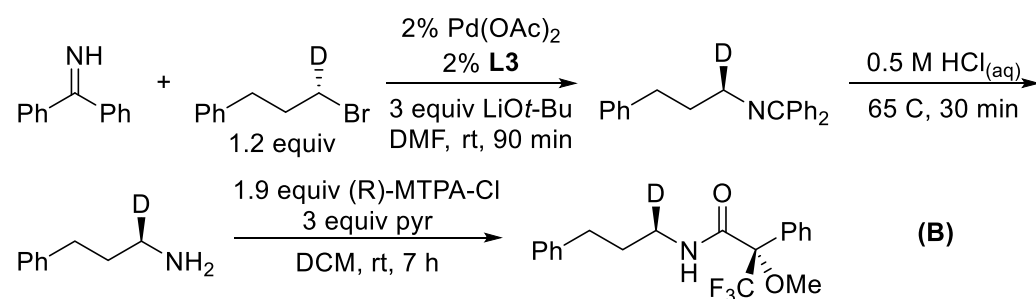
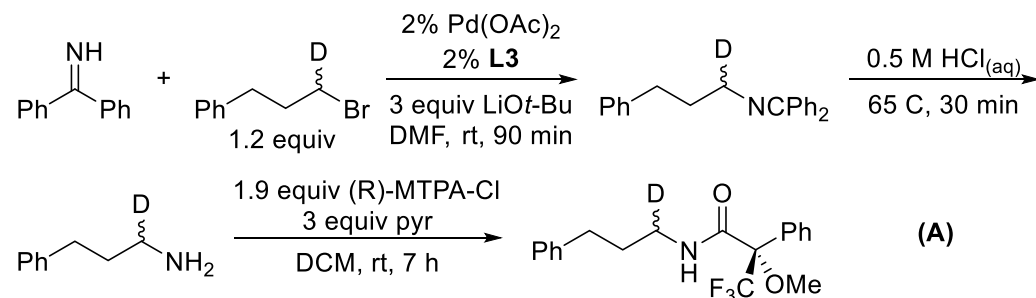


Figure 4.5. Concentration vs time and “missing imine” vs catalyst loading plots for reactions of 4,4'-difluorobenzophenone imine (**1b**) catalyzed by varying amounts of $\text{Pd}(\text{OAc})_2$.

Experimental details for Scheme 4.2**(2S)-3,3,3-trifluoro-2-methoxy-2-phenyl-N-(3-phenylpropyl-1-d)propenamide (5).****Figure 4.6.** ¹H NMR spectra showing the C1 resonance of the MTP-amide **5** for samples A-C.

Procedure A: step 1. In a nitrogen-filled glovebox, benzophenone imine (50 μ l, 1.0 M, 0.050 mmol) and (*rac*)-1-bromo-3-phenylpropane-1-*d*₁ (12.0 mg, 0.0600 mmol, 1.20 equiv) were added to an oven-dried 1 dram vial. **L3** (25 μ l, 0.040M, 0.0010 mmol, 2%) and Pd(OAc)₂ (25 μ l, 0.040M, 0.0010 mmol, 2%) were added, and the solution was diluted to 0.5 ml with DMF. LiOt-Bu (75 μ l, 2.0 M, 0.150 mmol, 3.0 equiv) was added to the reaction vial with stirring. The vial was sealed with a Teflon-lined cap, and the reaction mixture was stirred for 90 min at ambient temperature (approximately 25 °C). The reaction was quenched with H₂O (1 ml), and the resulting mixture was extracted thrice with ether (2 ml each). The combined organic layers were dried (MgSO₄), and the volatile materials were evaporated under reduced pressure. The residue was dissolved in a minimal amount of 5% triethylamine/hexanes and filtered through a plug of silica with 5% triethylamine/hexanes (~10 ml) into a 20 ml scintillation vial. The volatile materials were evaporated under reduced pressure to give the crude imine product, which was carried on to the next step without further purification.

Step 2. HCl_(aq) (0.5 M, 1.0 ml) and a magnetic stir bar were added to the vial containing the crude imine. The vial was flushed with N₂ and sealed with a PTFE-lined cap. The mixture was heated for 30 min at 65 °C with stirring in an aluminum heating block. The mixture was allowed to cool to ambient temperature, and then washed thrice with ether (~2 ml each). The aqueous layer was basified with a single pellet of NaOH and then extracted four times with ether (~2 ml each). The combined organic layers (after basification) were combined and filtered through a plug of Na₂SO₄. The volatile materials were evaporated under reduced pressure to give the crude primary amine product (~5 mg, ~0.034 mmol, ~70% yield), which was carried on to the next step without further purification.

Step 3 was adapted with minor modifications from a published protocol for MTPA analysis.⁴⁷ The crude amine from step 2 was dissolved in 1 ml dry DCM (ethanol-free). Pyridine (7.9 μ l, 7.8 mg, 0.10 mmol, 3.0 equiv) and (*R*)-MTPA-Cl (12 μ l, 16 mg, 0.064 mmol, 1.9 equiv) were added with stirring. The reaction mixture was stirred for 7 h at ambient temperature. The reaction was quenched with H₂O (1 ml) and extracted four time with ether (~2 ml each). The combined organic layers were dried (MgSO₄), and the volatile materials were evaporated under reduced pressure. The crude product was purified by column chromatography (0 to 25% ethyl acetate gradient in hexanes, R_f 0.48 in 25% EtOAc/hex) to give the title compound as a clear and colorless oil (4.5 mg, 0.013 mmol, 38% yield).

Procedure B. Performed similarly to procedure **A** except with (*S*)-1-bromo-3-phenylpropane-1-*d*₁ to give the title compound (8.0 mg, 0.023 mmol, 80:20 d.r.).

Procedure C: step 1. (*S*)-1-Bromo-3-phenylpropane-1-*d*₁ (100 mg, 0.500 mmol) was dissolved in DMF (2 ml) in a 20 ml scintillation vial. Sodium azide (97.3 mg, 1.50 mmol, 3.0 equiv) was added with stirring. The vial was flushed with N₂ and sealed with a PTFE-lined cap, and the mixture was stirred for 3 h at ambient temperature. Ether (10 ml) was then added, and the mixture was transferred to a separatory funnel and washed twice with H₂O (~15 ml each). The organic layer was filtered through a plug of MgSO₄ into a 20 ml scintillation vial, and the volatile materials were removed under reduced pressure to give the crude alkyl azide product, which was carried on to the next step without purification.

Step 2. The crude azide was dissolved in wet THF (3 ml with 10 drops of H₂O), and Ph₃P (144 mg, 0.549 mmol, 1.1 equiv) was added with stirring. The reaction mixture was stirred for 20 h at ambient temperature, and then the volatile materials were removed under reduced pressure. HCl_(aq) (0.5 M, 6 ml) was added, and the mixture was washed thrice with ether (~6 ml each). The aqueous layer was basified with three NaOH pellets and extracted thrice with ether (~6 ml each). The combined organic layers (after basification) were filtered through a plug of Na₂SO₄ and the volatile materials were removed under reduced pressure. The crude product was purified by column chromatography (5% triethylamine and 5% methanol in DCM, R_f 0.33) followed by the same acid/base extraction procedure as above to give (*R*)-3-phenylpropan-1-*d*₁-1-amine as a pale yellow oil (23.0 mg, 0.169 mmol, 34% yield).

Step 3. As described for procedures **A** and **B** except with 13.5 mg (0.0991 mmol) (*R*)-3-phenylpropan-1-*d*₁-1-amine, 24 μ l (32 mg, 0.128 mmol, 1.3 equiv) (*R*)-MTPA-Cl, and 16 μ l (16 mg, 0.212 mmol, 2.1 equiv) pyridine in 2 ml DCM to give the title compound as a clear and colorless oil (23.0 mg, 0.0653 mmol, 66% yield, 80:20 d.r.).

Experimental details for Scheme 4.3 top

Procedure. Benzophenone imine (92 mg, 0.50 mmol), durene (67 mg, 0.50 mmol, 1.0 equiv), Pd(OAc)₂ (250 μ l, 0.040 M, 0.010 mmol, 2%), **L3** (250 μ l, 0.040 M, 0.010 mmol, 2%), were mixed in 2.50 ml of DMF. LiOt-Bu (120 mg, 1.50 mmol, 3.0 equiv) was dissolved in 2.0 ml of DMF and added slowly to the reaction mixture with stirring. A 1.0 ml sample of this reaction mixture was transferred to a vial containing 1-bromooctane (20.6 μ l, 23.1 mg, 0.119 mmol, 1.2 equiv) or 1-bromo-3-phenylpropane (18.2 μ l, 23.8 mg, 1.20 mmol, 1.2 equiv) and a stir bar. 40 μ l aliquots were taken at various times and diluted with THF. A response factor of 0.766 was used for integration of benzophenone imine against durene.

Procedure. Benzophenone imine (100 μ l, 1.0 M, 0.10 mmol), 1-bromo-3-phenylpropane (60 mg, 0.30 mmol, 3.0 equiv) or 1-bromooctane (58 mg, 0.30 mmol, 3.0 equiv), 1,3,5-trimethoxybenzene (100 μ l, 1.0 M, 0.10 mmol, 1.0 equiv), Pd(OAc)₂ (50 μ l, 0.040 M, 0.0020 mmol, 2%), **L3** (50 μ l, 0.040 M, 0.0020 mmol, 2%), and 500 μ l DMF were mixed in an oven-dried 1 dram vial. LiOt-Bu (150 μ l, 2.0 M, 3.0 mmol, 3.0 equiv) was added with stirring. The vial was sealed with a Teflon-lined cap, and the reaction mixture was stirred at ambient temperature. 40 μ l aliquots were taken and diluted with THF at various times to measure conversion of benzophenone imine by GC. A response factor of 0.52 was used for integration of benzophenone imine against TMB.

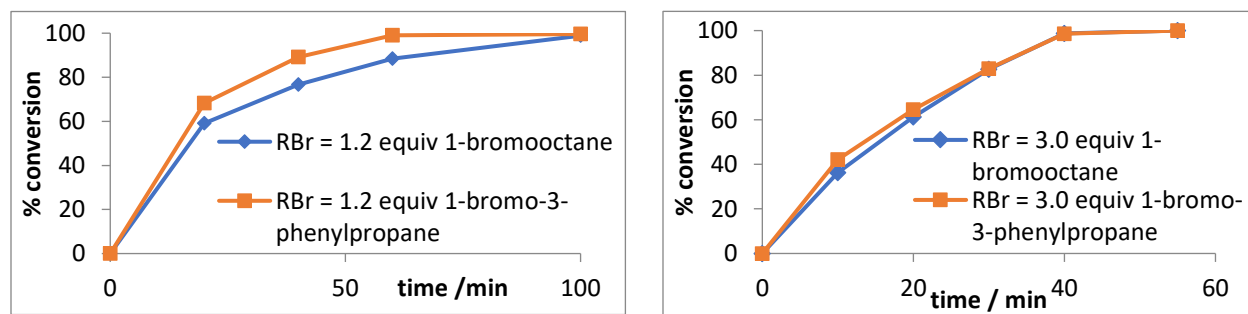


Figure 4.7. Conversion of **1a** vs time plots with 1.2 equivalents (left) or 3.0 equivalents (right) of alkyl bromides.

Experimental details for Scheme 4.3 bottom and Table 4.5

Procedure. For each trial a fresh 1:1 molar solution of 1-bromooctane and 1-bromo-3-phenylpropane was prepared by weighing 290 mg 1-bromooctane and 299 mg 1-bromo-3-phenylpropane into a 2.0 ml volumetric flask and diluting with DMF. Benzophenone imine (50 μ l, 1.0 M, 0.050 mmol), the solution of alkyl bromides (200 μ l, 0.75 M in each, 0.15 mmol each, 3.0 equiv each), 1,3,5-trimethoxybenzene (50 μ l, 1.0 M, 0.050 mmol, 1.0 equiv), Pd(OAc)₂ (25 μ l, 0.040 M, 0.0010 mmol, 2%), L (25 μ l, 0.040 M, 0.0010 mmol, 2%), and 75 μ l of DMF were mixed in an oven-dried 1 dram vial. LiOt-Bu (75 μ l, 2.0 M, 1.5 mmol, 3.0 equiv) was added with stirring. For entry 1, 50 μ l of Pd(OAc)₂ was used. For entry 3, 100 μ l of **L3** was used, and no additional DMF was added. The vial was sealed with a Teflon-lined cap, and the reaction mixture was stirred at ambient temperature. 40 μ l aliquots were taken and diluted with THF at 5 h. A response factor of 0.945 was used for integration of **3ab** against **3aa**

entry	L	mol% Pd(OAc) ₂ /L	trial 1	trial 2	trial 3	trial 4	average	std dev
1	None	4/-	2.099	2.145	2.195	2.198	2.16	0.05
2	L3	2/2	1.879	1.894	1.918	1.946	1.91	0.03
3	L3	2/8	1.817	1.854	1.839	1.858	1.84	0.02
4	L6	2/2	1.697	1.693	1.694	1.709	1.699	0.007

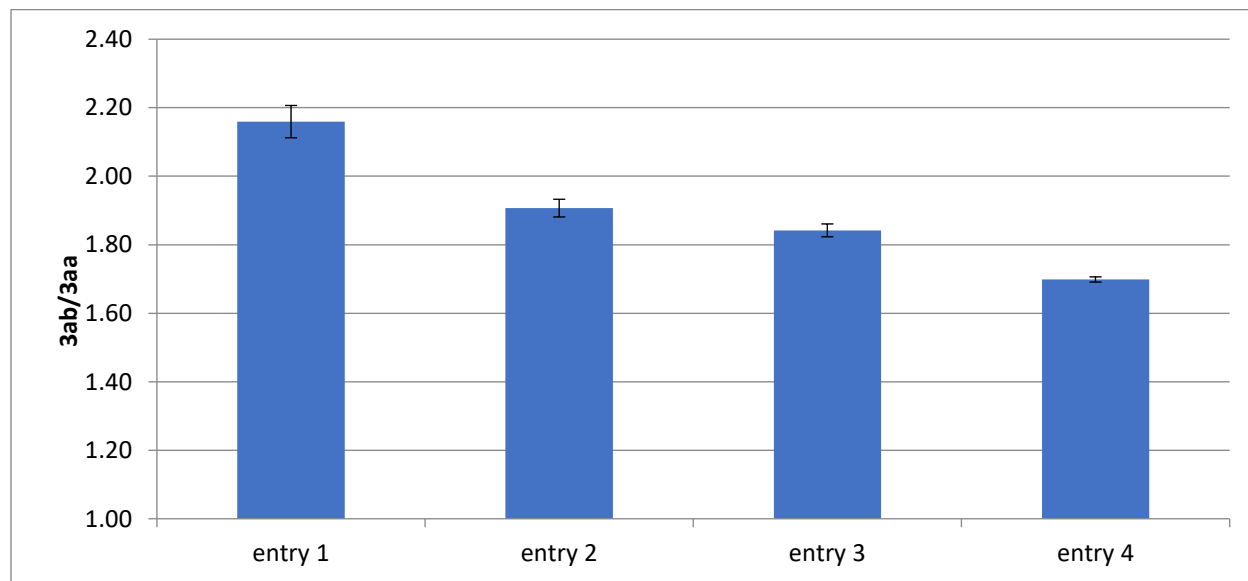


Figure 4.8. Full data for Table 4.5 entries 1-3.

Procedure. for each trial a fresh 1:1 molar solution of 1-bromooctane and 1-bromo-3-methylbutane was prepared by weighing 290 mg 1-bromooctane and 227 mg 1-bromo-3-methylbutane into a 2.0 ml volumetric flask and diluting with DMF. Benzophenone imine (50 μ l, 1.0 M, 0.050 mmol), the solution of alkyl bromides (200 μ l, 0.75 M in each, 0.15 mmol each, 3.0 equiv each), 1,3,5-trimethoxybenzene (50 μ l, 1.0 M, 0.050 mmol, 1.0 equiv), Pd(OAc)₂ (25 μ l, 0.040 M, 0.0010 mmol, 2%), L (25 μ l, 0.040 M, 0.0010 mmol, 2%), and 75 μ l of DMF were mixed in an oven-dried 1 dram vial. LiOt-Bu (75 μ l, 2.0 M, 1.5 mmol, 3.0 equiv) was added with stirring. For entry 1, 50 μ l of Pd(OAc)₂ was used. For entries 5 and 6, 100 μ l of L was used and no additional DMF was added. The vial was sealed with a Teflon-lined cap, and the reaction mixture was stirred at ambient temperature. 40 μ l aliquots were taken and diluted with THF at 8 h. A response factor of 0.874 was used for integration of **3aa** against **3ak**.

entry	L	mol% Pd(OAc) ₂ /L	trial 1	trial 2	trial 3	trial 4	average	std dev
1	None	4/-	4.365	4.377	4.162	4.091	4.2	0.1
2	L2	2/2	4.141	4.109	4.054	4.056	4.09	0.04
3	L3	2/2	4.734	4.757	4.884	4.832	4.80	0.07
4	L9	2/2	5.420	5.395	5.541	5.679	5.5	0.1
5	L3	2/8	4.914	4.865			4.9	n/a
6	L9	2/8	5.437	5.433			5.4	n/a

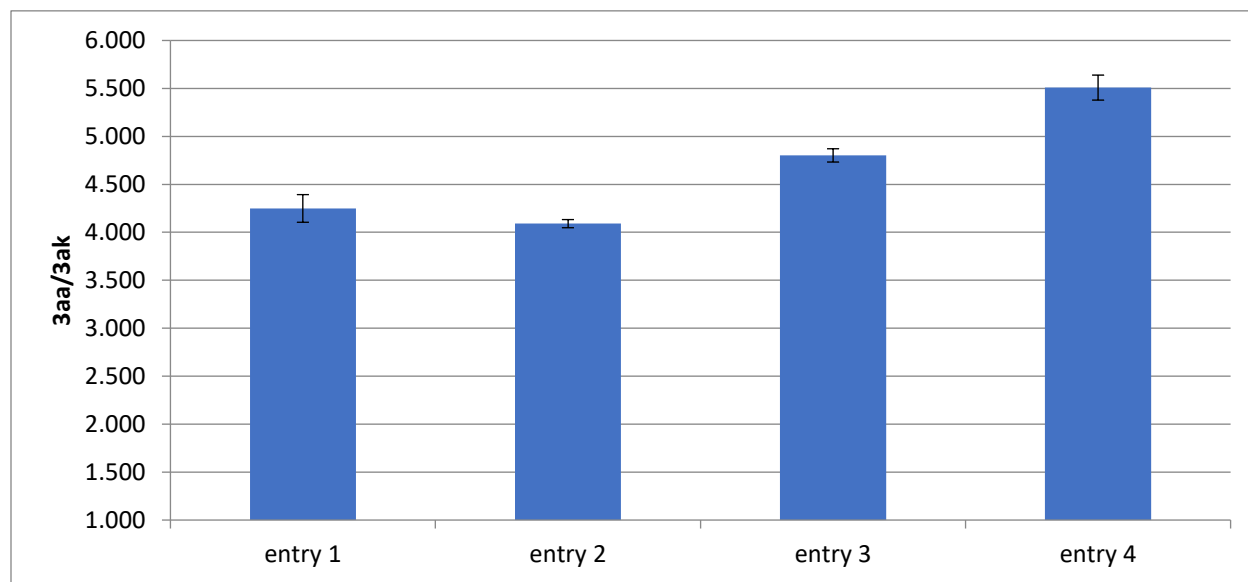


Figure 4.9. Full data for Table 4.5 entries 4-7.

Competition experiments with potassium phthalimide

Procedure. Potassium phthalimide (18.5 mg, 0.0999 mmol), the solution of alkyl bromides (400 μ l, 0.75 M in each, 0.30 mmol each, 3.0 equiv each) 1,3,5-Trimethoxybenzene (100 μ l, 1.0 M, 0.10 mmol, 1.0 equiv) were added to an oven-dried 1 dram vial equipped with a stir bar. The reaction mixture was diluted to a total volume of 1.0 ml with DMF. The vial was sealed with a Teflon-lined cap, and the reaction mixture was heated in an aluminum heating block at 100 °C for 1 hour. A 40 μ l aliquot for GC analysis was removed, diluted with ethyl acetate, and passed through a plug of Celite. A response factor of 0.915 was used for integration of *N*-(3-phenylpropyl)phthalimide against *N*-octylphthalimide. This experiment was duplicated and the results averaged.

Ratio of *N*-(3-phenylpropyl)phthalimide to *N*-octylphthalimide.

Trial 1: 1.37; trial 2: 1.39; average: 1.38.

Procedure. Potassium phthalimide (18.5 mg, 0.0999 mmol), the solution of alkyl bromides (400 μ l, 0.75 M in each, 0.30 mmol each, 3.0 equiv each) 1,3,5-Trimethoxybenzene (100 μ l, 1.0 M, 0.10 mmol, 1.0 equiv) were added to an oven-dried 1 dram vial equipped with a stir bar. The reaction mixture was diluted to a total volume of 1.0 ml with DMF. The vial was sealed with a Teflon-lined cap, and the reaction mixture was heated in an aluminum heating block at 100 °C for 1 hour. A 40 μ l aliquot for GC analysis was removed, diluted with ethyl acetate, and passed through a plug of Celite. A response factor of 0.764 was used for integration of *N*-octylphthalimide against *N*-(3-methylbutyl)phthalimide. This experiment was duplicated, and the results were averaged.

Ratio of *N*-octylphthalimide. to *N*-(3-methylbutyl)phthalimide

Trial 1: 1.65; trial 2: 1.64, average; 1.65.

Experimental details for Table 4.6

Benzophenone imine (50 μ l, 1.0 M, 0.050 mmol), 1-bromo-3-phenylpropane (100 μ l, 1.0 M, 0.10 mmol, 2.0 equiv), 1,3,5-trimethoxybenzene (50 μ l, 1.0 M, 0.050 mmol, 1.0 equiv), the palladium precatalyst (12.5 μ l, 0.040 M, 0.00050 mmol, 1%), **L3** (15 μ l, 0.040 M, 0.00060 mmol, 1.2%), and 200 μ l DMF were mixed in an oven-dried 1 dram vial. LiOt-Bu (75 μ l, 2.0 M, 1.5 mmol, 3.0 equiv) was added with stirring. The vial was sealed with a Teflon-lined cap, and the reaction mixture was stirred at ambient temperature. 40 μ l aliquots were taken and diluted with THF at various times to measure conversion of benzophenone imine by GC. A response factor of 0.52 was used for integration of benzophenone imine against TMB.

Alkylation of Benzophenone Imine with 3-Bromo-1-phenylbutane

Benzophenone imine (50 μ l, 1.0 M, 0.050 mmol), 3-bromo-1-phenylbutane (200 μ l, 1.0 M, 4.0 equiv), 1,3,5-trimethoxybenzene (50 μ l, 1.0 M, 0.050 mmol, 1.0 equiv), Pd(OAc)₂ (50 μ l, 0.040 M, 0.0010 mmol, 2%), **L3** (50 μ l, 0.040 M, 0.0010 mmol, 2%), and 25 μ l DMF were mixed in an oven-dried 1 dram vial. LiOt-Bu (75 μ l, 2.0 M, 1.5 mmol, 3.0 equiv) was added with stirring. After 28 h a 40 μ l aliquot was removed and diluted with THF for GC analysis. A response factor of 0.277 was used for integration of *N*-(4-phenylbutan-2-yl)benzophenone imine against TMB.

Table 4.7. Analysis of Elimination Products from 3-Bromo-1-phenylbutane.

$ \begin{array}{c} \text{cat Pd/L} \\ 20\% \text{ benzophenone imine} \\ 3 \text{ equiv LiOt-Bu} \\ \text{Ph-CH}_2\text{-CH}_2\text{-CH(Br)-CH}_3 \xrightarrow{\text{DMF, rt, 2 h}} \text{Ph-CH}_2\text{-CH=CH}_2 + \text{Ph-CH=CH-CH}_3 \\ \text{terminal} \qquad \qquad \text{internal} \end{array} $					
entry	Pd/L	4-phenyl-1-butene	1-phenyl-2-butene	total olefin	terminal/internal
1	None	22	35	58	0.64
2	4% Pd(OAc) ₂	36	32	68	1.15
3	4% Pd(OAc) ₂ / L3	32	38	70	0.84
4	4% Pd(OAc) ₂ / L6	25	35	60	0.71

Procedure. 3-Bromo-1-phenylbutane (50 μ l, 1.0 M, 0.050 mmol), benzophenone imine (10 μ l, 1.0 M, 0.010 mmol, 10%), Pd(OAc)₂ (50 μ l, 0.040 M, 0.0020 mmol, 4%), L (50 μ l, 0.040 M, 0.0020 mmol, 4%), 1,3,5-trimethoxybenzene (50 μ l, 1.0 M, 0.050 mmol, 1.0 equiv), and 215 μ l DMF were mixed in an oven-dried 1 dram vial. LiOt-Bu (75 μ l, 2.0 M, 1.5 mmol, 3.0 equiv) was added with stirring. For entry 1, no Pd(OAc)₂ or L was added, and an additional 100 μ l DMF was added. For entry 2, no L was added, and an additional 50 μ l DMF was added. The vial was sealed with a Teflon-lined cap, and the reaction mixture was stirred at ambient temperature. 40 μ l aliquots were taken and diluted with THF at 2 h for GC analysis. A response factor of 0.75 was used for integration of olefins against TMB. Note that this response factor was determined with commercially available 4-phenyl-1-butene and was assumed to apply equally to all isomers. 1-Phenyl-2-butene was identified by the EIMS spectrum.

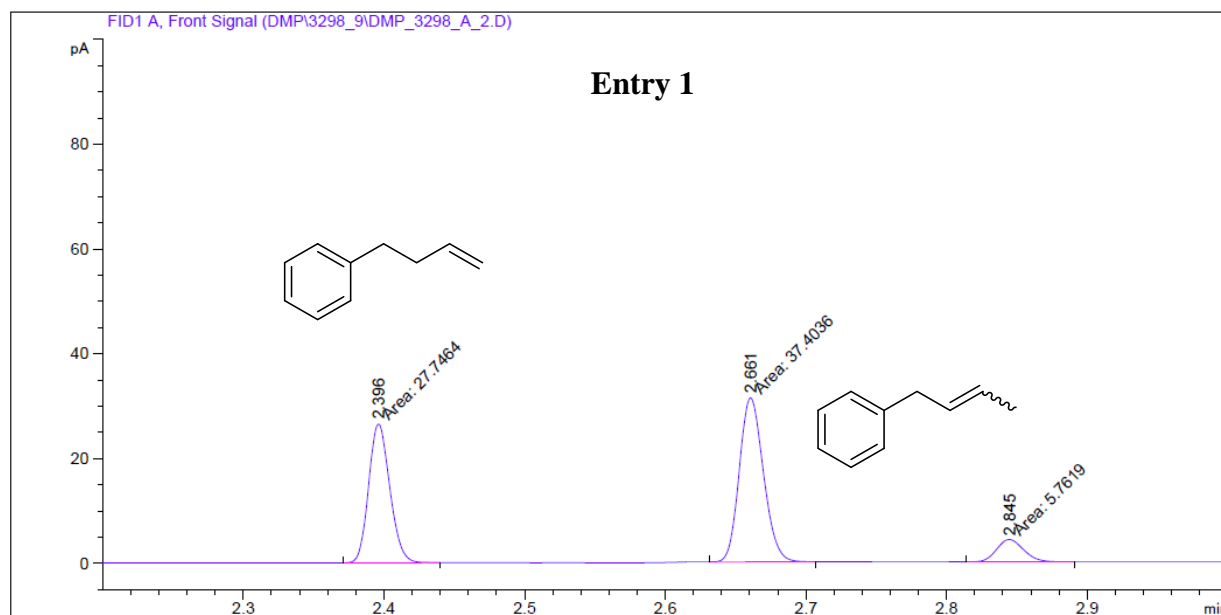


Figure 4.10. GC spectrum of the reaction of 3-bromo-1-phenylbutane with LiOt-Bu and 20 mol% benzophenone imine.

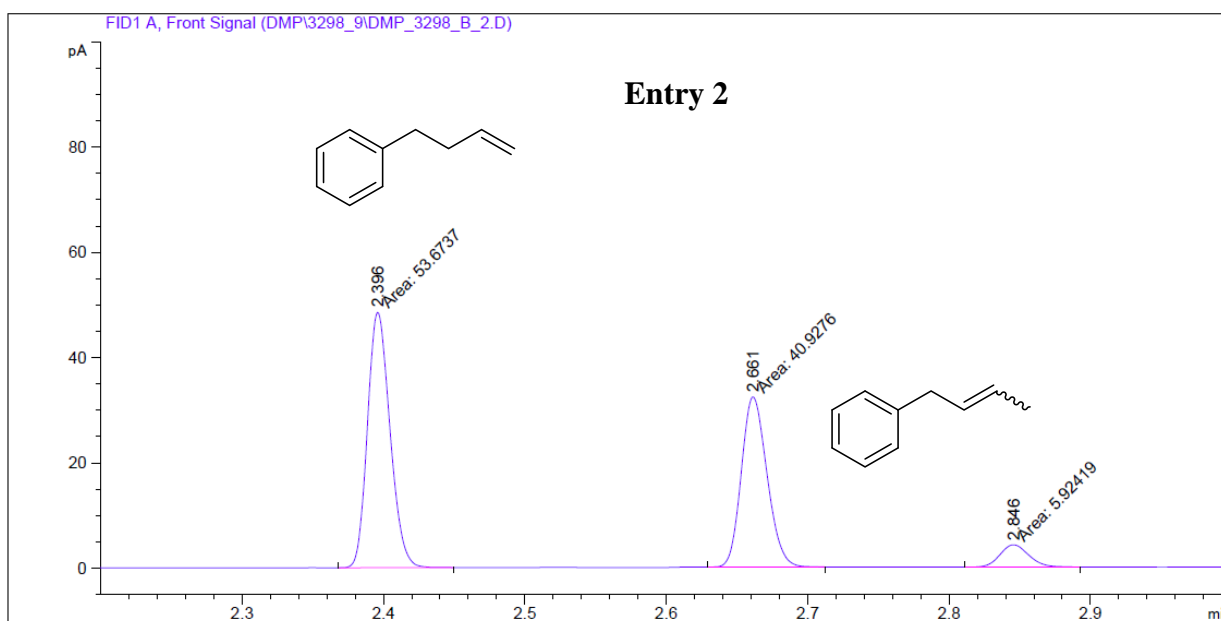


Figure 4.11. GC spectrum of the reaction of 3-bromo-1-phenylbutane with LiOt-Bu, 4 mol% Pd(OAc)₂, and 20 mol% benzophenone imine

4.5 References and notes

1. Jana, R.; Pathak, T. P.; Sigman, M. S., *Chem. Rev.* **2011**, *111* (3), 1417-1492.
2. Frisch, A. C.; Beller, M., *Angew. Chem. Int. Ed.* **2005**, *44* (5), 674-688.
3. Rudolph, A.; Lautens, M., *Angew. Chem. Int. Ed.* **2009**, *48* (15), 2656-2670.
4. Kambe, N.; Iwasaki, T.; Terao, J., *Chem. Soc. Rev.* **2011**, *40* (10), 4937-4947.
5. Netherton, M. R.; Fu, G. C., *Adv. Synth. Catal.* **2004**, *346* (13-15), 1525-1532.
6. Peacock, D. M.; Roos, C. B.; Hartwig, J. F., *ACS Cent. Sci.* **2016**, *2* (9), 647-652.
7. Bissember, A. C.; Lundgren, R. J.; Creutz, S. E.; Peters, J. C.; Fu, G. C., *Angew. Chem. Int. Ed.* **2013**, *52* (19), 5129-5133.
8. Do, H.-Q.; Bachman, S.; Bissember, A. C.; Peters, J. C.; Fu, G. C., *J. Am. Chem. Soc.* **2014**.
9. Ahn, J. M.; Peters, J. C.; Fu, G. C., *J. Am. Chem. Soc.* **2017**.
10. Kainz, Q. M.; Matier, C. D.; Bartoszewicz, A.; Zultanski, S. L.; Peters, J. C.; Fu, G. C., *Science* **2016**, *351* (6274), 681-684.
11. Matier, C. D.; Schwaben, J.; Peters, J. C.; Fu, G. C., *J. Am. Chem. Soc.* **2017**.
12. Hills, I. D.; Netherton, M. R.; Fu, G. C., *Angew. Chem. Int. Ed.* **2003**, *42* (46), 5749-5752.
13. Sobanov, A. A.; Vedernikov, A. N.; Dyker, G.; Solomonov, B. N., *Mendeleev Commun.* **2002**, *12* (1), 14-15.
14. Sehnal, P.; Taylor, R. J. K.; Fairlamb, I. J. S., *Chem. Rev.* **2010**, *110* (2), 824-889.
15. Hanley, P. S.; Marquard, S. L.; Cundari, T. R.; Hartwig, J. F., *J. Am. Chem. Soc.* **2012**, *134* (37), 15281-15284.
16. Marquard, S. L.; Rosenfeld, D. C.; Hartwig, J. F., *Angew. Chem.* **2010**, *122* (4), 805-808.
17. Anselme, J. P.; Fischer, W.; Koga, N., *Tetrahedron* **1969**, *25* (1), 89-94.
18. Bergeron, M.; Guyader, D.; Paquin, J.-F., *Org. Lett.* **2012**, *14* (23), 5888-5891.
19. Böhme, H.; Ingendoh, A., *Justus Liebigs Annalen der Chemie* **1978**, *1978* (3), 381-386.
20. Danner, P.; Bauer, M.; Phukan, P.; Maier, Martin E., *Eur. J. Org. Chem.* **2005**, *2005* (2), 317-325.
21. Janssen R&D Ireland. WO 2014/060411 A1, 2014.
22. Khistiaev, K. A.; Novikov, M. S.; Khlebnikov, A. F.; Magull, J., *Tetrahedron Lett.* **2008**, *49* (7), 1237-1240.
23. Lichtenstein, B. R.; Cerda, J. F.; Koder, R. L.; Dutton, P. L., *Chem. Commun.* **2009**, (2), 168-170.
24. Lin, A.; Mao, H.; Zhu, X.; Ge, H.; Tan, R.; Zhu, C.; Cheng, Y., *Chem. Eur. J.* **2011**, *17* (49), 13676-13679.
25. Meiresonne, T.; Mangelinckx, S.; De Kimpe, N., *Organic & Biomolecular Chemistry* **2011**, *9* (20), 7085-7091.
26. Respondek, T.; Cueny, E.; Kodanko, J. J., *Org. Lett.* **2011**, *14* (1), 150-153.
27. Weidner, R.; Würthwein, E.-U., *Chem. Ber.* **1989**, *122* (6), 1095-1106.
28. Hills, I. D.; Netherton, M. R.; Fu, G. C., *Angew. Chem.* **2003**, *115* (46), 5927-5930.
29. Prema, D.; Wiznycia, A. V.; Scott, B. M. T.; Hilborn, J.; Desper, J.; Levy, C. J., *Dalton Transactions* **2007**, (42), 4788-4796.
30. Minisci, F.; Porta, O.; Recupero, F.; Punta, C.; Gambarotti, C.; Pruna, B.; Pierini, M.; Fontana, F., *Synlett* **2004**, *2004* (05), 0874-0876.

-
31. He, R.; Huang, Z.-T.; Zheng, Q.-Y.; Wang, C., *Angew. Chem. Int. Ed.* **2014**, *53* (19), 4950-4953.
 32. Brown, C.; Grayson, B. T.; Hudson, R. F., *Journal of the Chemical Society, Perkin Transactions 2* **1979**, (4), 427-434.
 33. Eisenberger, P.; Bailey, A. M.; Crudden, C. M., *J. Am. Chem. Soc.* **2012**, *134* (42), 17384-17387.
 34. Molander, G. A.; Argintaru, O. A.; Aron, I.; Dreher, S. D., *Org. Lett.* **2010**, *12* (24), 5783-5785.
 35. Nacsa, E. D.; Lambert, T. H., *Org. Lett.* **2012**, *15* (1), 38-41.
 36. Biorelix, Inc. WO2011126567 A1, 2011.
 37. Szostak, M.; Spain, M.; Procter, D. J., *Org. Lett.* **2014**, *16* (19), 5052-5055.
 38. Campaña, A. G.; Carlone, A.; Chen, K.; Dryden, D. T. F.; Leigh, D. A.; Lewandowska, U.; Mullen, K. M., *Angew. Chem. Int. Ed.* **2012**, *51* (22), 5480-5483.
 39. Bhar, P.; Reed, D. W.; Covello, P. S.; Buist, P. H., *Angew. Chem. Int. Ed.* **2012**, *51* (27), 6686-6690.
 40. Xia, X.; Toy, P. H., *Beilstein Journal of Organic Chemistry* **2014**, *10*, 1397-1405.
 41. Harding, P.; Harding, D. J.; Soponrat, N.; Tinpun, K.; Samuadnuan, S.; Adams, H., *Aust. J. Chem.* **2010**, *63* (1), 75-82.
 42. Gao, X.; Zhang, F.; Deng, G.; Yang, L., *Org. Lett.* **2014**, *16* (14), 3664-3667.
 43. Casarrubios, L.; Esteruelas, M. A.; Larramona, C.; Muntaner, J. G.; Oliván, M.; Oñate, E.; Sierra, M. A., *Organometallics* **2014**, *33* (7), 1820-1833.
 44. Marull, M.; Lefebvre, O.; Schlosser, M., *Eur. J. Org. Chem.* **2004**, *2004* (1), 54-63.
 45. Wang, X.; Ji, X.; Shao, C.; Zhang, Y.; Zhang, Y., *Organic & Biomolecular Chemistry* **2017**, *15* (26), 5616-5624.
 46. Che, J.; Lam, Y., *Adv. Synth. Catal.* **2010**, *352* (10), 1752-1758.
 47. Hoye, T. R.; Jeffrey, C. S.; Shao, F., *Nature Protocols* **2007**, *2*, 2451.

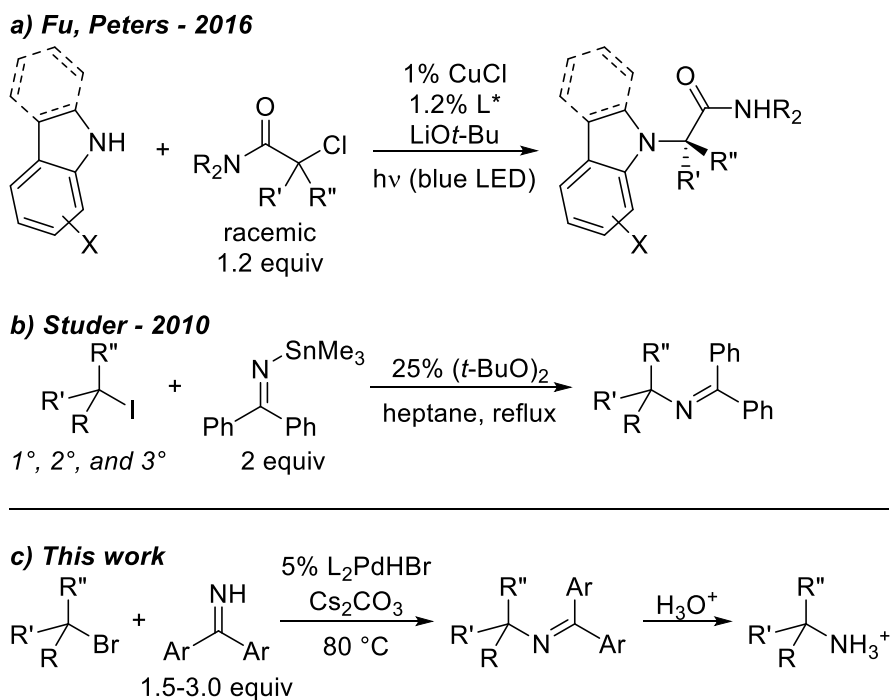
CHAPTER 5

Palladium-catalyzed radical amination of secondary and tertiary alkyl bromides

5.1 Introduction

Cross-coupling reactions catalyzed by transition-metal complexes are now common methods for the construction of carbon–carbon and carbon–heteroatom bonds.^{1–4} Although most work has focused on reactions of aryl and vinyl halides, cross-coupling reactions of alkyl halides have also been developed, and these reactions offer significant advantages over traditional substitution reactions.^{5–7} Most notable is that the scope of alkyl halide often extends to secondary or tertiary alkyl halides, and chiral catalysts can form enantioenriched products from racemic alkyl halides.⁸ However, these reactions have been largely limited to those forming carbon–carbon and carbon–boron bonds. The analogous coupling reactions of alkyl halides with nitrogen nucleophiles are much less developed, despite the prevalence of alkylamines in natural products, agrochemicals, and pharmaceuticals.^{9–12}

Scheme 5.1. Radical-involved *N*-alkylation reactions.



N-alkylation of nitrogen nucleophiles is traditionally achieved through substitution^{13–17} or reductive amination.^{18–21} Although substitution of primary or benzylic alkyl electrophiles is facile, reactions with secondary electrophiles typically require elevated temperatures. Moreover, unactivated²² tertiary alkyl electrophiles often undergo elimination in preference to substitution,²³ and tertiary alcohols are inherently unsuitable for reductive amination or borrowing hydrogen^{24–26} strategies. Transition-metal catalysts typically react with secondary and tertiary alkyl halides by a single-electron reduction event,^{27–28} thereby creating the potential to combine the activity of radical amination reactions^{29–33} with the mild conditions and selectivity of cross-coupling reactions. Fu and Peters have reported photoinduced, copper-catalyzed alkylations of carbazoles,³⁴ amides,^{35–36} heterocycles, and amines³⁷ with alkyl bromides and iodides, including enantioconvergent alkylations of indoles and carbazoles with α -chloro amides (Scheme 5.1a).³⁸ However, no thermal,

transition-metal catalyzed coupling of a nitrogen nucleophile with an alkyl halide has been reported, nor has any catalytic amination of an unactivated tertiary alkyl halide.³⁹

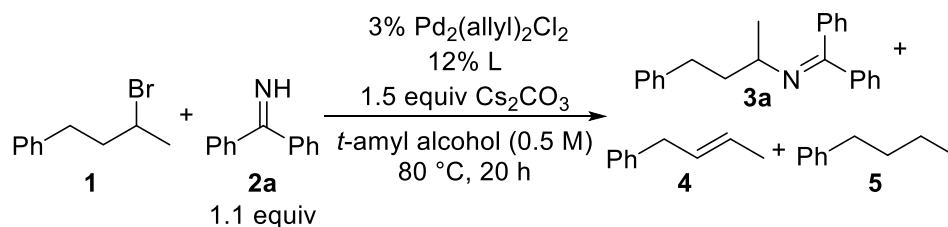
We envisioned that such a reaction could occur in the presence of palladium. A number of palladium-catalyzed reactions of unactivated secondary or tertiary alkyl halides have been reported to occur through alkyl radical intermediates,⁴⁰ including atom-transfer reactions,⁴¹ Heck reactions of alkyl halides,⁴²⁻⁴⁴ and alkylations of arenes.⁴⁵⁻⁴⁷ The formation of this radical is typically proposed to occur by a single-electron-transfer (SET) reaction between the alkyl halide and a palladium(0) complex. The isolation and characterization of cationic (*t*-Bu₃P)₂Pd(I) was reported recently. The identification of this species supports the proposed formation of Pd(I) intermediates from Pd(0)-trialkylphosphine complexes.⁴⁸

Our study to develop this process focused on the reactions of benzophenone imines. We focused on these nucleophiles because benzophenone imines are synthetic equivalents to ammonia and have been used in a variety of amination reactions, including palladium-catalyzed coupling with aryl halides⁴⁹⁻⁵⁰ and catalytic C–H amination reactions.⁵¹ Furthermore, *N*-trimethylstannyl benzophenone imine undergoes radical alkylation reactions with secondary and tertiary alkyl halides (Scheme 5.1b).²⁹ The diarylmethylene protecting group can be removed by hydrolysis or transamination to release primary amines.⁵⁰⁻⁵²

In this chapter, we report the thermal cross-coupling of alkyl halides with benzophenone imines as the nitrogen nucleophiles catalyzed by (Cy₂*t*-BuP)₂Pd⁰, which is generated *in situ* from (Cy₂*t*-BuP)₂PdHBr and base (Scheme 5.1c). This method enables the preparation of protected primary amines from unactivated secondary and tertiary alkyl bromides. Mechanistic experiments confirm that the coupling process occurs through an alkyl radical, and the intermediacy of this radical allows the process to be extended to the intramolecular carboamination of unsaturated alkyl bromides with imines. The radical mechanism also allows the substitution process to occur in the presence of auxiliary electrophilic functional groups.

5.2 Results and Discussion

Initial experiments to identify conditions for the coupling of a secondary alkyl bromide with benzophenone imine showed that a series of palladium complexes catalyzed the reaction between 3-bromo-1-phenylbutane (**1**) and the parent benzophenone imine (**2a**) to produce the *N*-alkyl imine **3a** in alcohol solvents, but olefins (**4**) and an alkane (**5**) formed as side products. Furthermore, in many cases, the combined yield of **3a**, **4**, and **5** was significantly lower than the conversion of **1**, which indicates that other side products also formed. These studies showed that high yields with limiting alkyl bromide would be more difficult to achieve than high yields with limiting imine. However, for most applications, the alkyl bromide would be the more valuable coupling partner because the imine would likely serve as the source of a final NH₂ group.

Table 5.1. Effect of dative ligands.^a

entry	L	% conv 1	% yield 3a	% yield 4 ^b	% yield 5
1	none	28	5	11	1
2	Cy ₂ PhP	86	36	5	11
3	<i>t</i> -Bu ₂ PhP	49	16	9	4
4	Ph ₃ P	46	6	21	2
5	Ph ₂ EtP	67	13	25	5
6	Dcpe (6%)	96	34	13	11
7	Cy ₃ P	96	39	4	13
8	<i>t</i> -Bu ₃ P	77	17	13	5
9	<i>t</i> -Bu ₂ CyP	77	31	8	9
10	<i>t</i> -Bu ₂ MeP	96	41	5	12
11	Ad ₂ MeP	>99	41	7	12
12	Cy ₂ <i>t</i> -BuP	98	44	3	14

^aYields and conversion determined by corrected GC integration against 1,3,5-trimethoxybenzene (TMB).

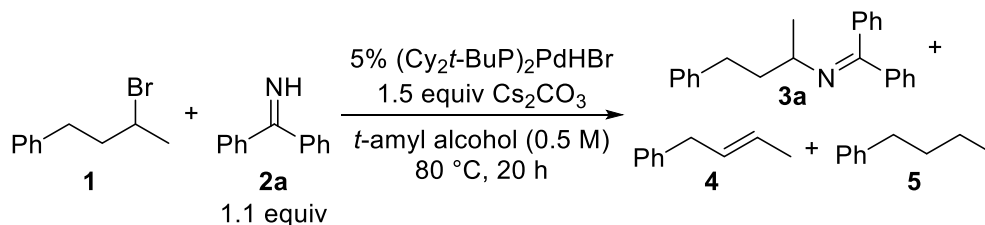
^bCombined signals for four olefin isomers.

To achieve high yields with limiting alkyl halide, we evaluated the effect of the structure of the dative ligand on catalyst activity and product distribution. We studied the reaction of **1** with **2a** and cesium carbonate as base in *tert*-amyl alcohol catalyzed by 3% [Pd(allyl)Cl]₂ alone or 3% [Pd(allyl)Cl]₂ with 12% of a series of phosphines (Table 5.1). The reaction catalyzed by [Pd(allyl)Cl]₂ alone consumed only 28% of the alkyl bromide and formed only 5% of the *N*-alkyl imine product **3a** (entry 1). Reactions conducted with catalysts bearing phosphines occurred in higher yield, and the identity of the phosphine ligand had a large impact on the conversion of the alkyl bromide and on the ratio of product to alkene, while the identity of the phosphine did not significantly affect the ratio of product to alkane (3:1 to 5:1). Reactions catalyzed by complexes of arylphosphines (entries 2-5) consumed less alkyl bromide and were less selective for formation of the *N*-alkyl imine product than were reactions catalyzed by complexes of trialkylphosphines. Reactions catalyzed by complexes bearing bulky trialkylphosphines occurred to high conversion (entries 6-12). Of these, the reaction catalyzed by 3 mol % [Pd(allyl)Cl]₂ and 12 mol % Cy₂(*t*-Bu)P formed the *N*-alkyl imine product in the highest yield and selectivity (entry 12). Similar results were obtained with the single-component precatalyst (Cy₂*t*-BuP)₂PdHBr (Table 5.2, entry 1), which is convenient to use in place of the metal and ligand combination, and this complex was used in all further experiments.

The effects of additional reaction parameters on the yield of coupled product were also investigated (Table 5.2). These studies showed that the substitution reactions did not occur without a catalyst or with nickel in place of palladium (entries 2 and 3). They also showed that reactions

in tertiary alcohols gave more product than those in solvents possessing weak C–H bonds (entry 5) and that reactions with inorganic carbonate bases occurred in higher yield than those with alkoxide or tertiary amine bases (entries 6 and 7).

Table 5.2. Effect of additional reaction parameters.^a



entry	variation	% conv 1	% yield 3a	% yield 4	% yield 5
1	as written	96	46	3	13
2	no cat	19	~1	12	nd
3	6% NiCl ₂ /glyme + 12% Cy ₂ <i>t</i> -BuP as cat	39	~1	23	nd
4	[1] = 0.25 M	81	37	5	11
5	<i>i</i> -PrOH as solvent	>99	36	10	27
6	LiOt-Bu as base	67	32	6	8
7	Cy ₂ MeN as base	21	5	9	1

^aYields and conversion determined by corrected GC integration against TMB.

The identity of the benzophenone imine had a significant effect on selectivity for substitution and yield. The reactions with a variety of symmetrically substituted benzophenone imine derivatives (**2b-d**) (Table 5.3) showed that the electronic properties of the imine had a small effect on the consumption of the alkyl bromide, but they had a large effect on the selectivity for *N*-alkylation. Reactions of the electron-deficient imine **2d** (entries 4-6) produced higher yields of *N*-alkyl imine and lower yields of alkane and olefin than did reactions with electron-rich imines (entries 2 and 3). Reactions conducted with a higher concentration of the imine also occurred with a higher ratio of *N*-alkyl imine to side products. The reaction containing 1.5 equivalents of **2d** produced the corresponding *N*-alkyl imine product **3d** in 83% yield. Moreover, the products containing this trifluoromethyl group were found to be stable to silica gel chromatography (see experimental section). These conditions appeared suitable for the preparation of a variety of *N*-alkyl imines.

Table 5.3. Effect of imine substituents and equivalents.^a

entry	Ar	equiv 2a-d	% conv 1	% yield 3a-d	% 4	% 5
1	Ph (2a)	1.1	88	46	3	14
2	<i>p</i> -Tol (2b)	1.1	96	39	3	25
3	(4-OMe)C ₆ H ₄ (2c)	1.1	93	35	4	20
4	(3-CF ₃)C ₆ H ₄ (2d)	1.1	96	74	2	7
5	“	1.2	99	78	2	6
6	“	1.5	>99	83	1	5

^aYields and conversion determined by corrected GC integration against TMB.

Alkyl bromides and alkyl iodides reacted similarly to form the *N*-alkyl imine products (Table 5.4). However, we focused our studies on alkyl bromides because they are generally less expensive and more readily prepared. The scope of reactions of both secondary and tertiary alkyl bromides to form *N*-alkyl imines is represented in Table 5.5. The acyclic 3-bromo-1-phenylbutane (**1**) reacted to give **3d** in 89% isolated yield. Hydrolysis of **3d** with 1.5 equivalents of HCl in wet MeOH produced the corresponding primary ammonium chloride salt in 90% isolated yield after 1 h at ambient temperature (see experimental section). The coupling reaction also occurred with cyclopentyl, cycloheptyl, and cyclooctyl bromides to give the *N*-alkyl imines **6**, **8**, and **9** in similar yields of 75% to 86%. However, the reaction with cyclohexyl bromide occurred in a lower yield of 40% (**7**). The tolerance of the reaction to electrophilic functionality was demonstrated by the formation of **10**, which contains a methyl ester, and **11**, which contains a nitrile. The product **10** formed as a single constitutional isomer, which eliminates a possible mechanism involving elimination and hydroamination. Both *exo*- and *endo*-2-bromonorbornane reacted to give the *N*-*exo*-norborn-2-yl imine product **12** in 39 and 40% yields, respectively. The formation of the same diastereomer from the two diastereomeric reactants suggests the intermediacy of an alkyl radical intermediate (*vide infra*).

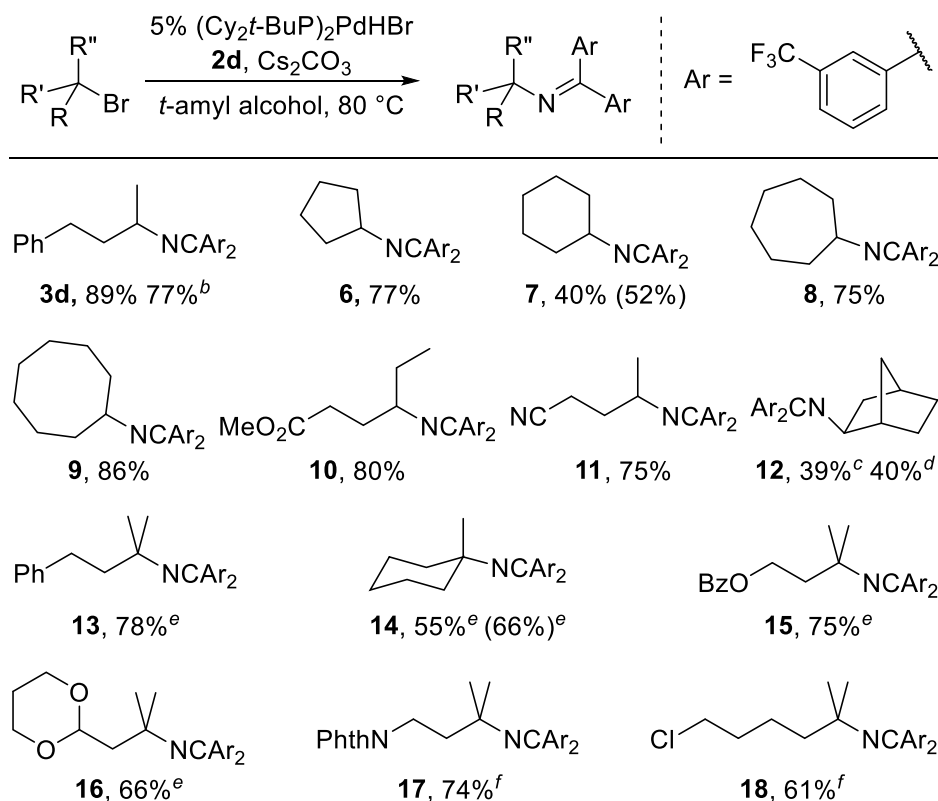
Table 5.4. Cross coupling of an alkyl iodide or alkyl tosylate.^a

entry	X	% yield 3d	% 4	% 5
1	Br (1)	92	1	5
2	I	86	3	6
3	OTs	7	67	<1

^aYields and conversion determined by corrected GC integration against TMB.

Even tertiary alkyl bromides reacted to form the corresponding *N*-alkyl imines. By increasing the equivalents of imine and base, the substitution product **13** from reaction of 2-bromo-2-methyl-4-phenylbutane formed in 78% yield. The reaction of the cyclic 1-bromo-1-methylcyclohexane also occurred, in this case to form the tertiary imine **14** in 55% yield. The reaction tolerated esters and acetals, and products **15** and **16** were isolated in 75 and 66% yields, respectively. The reactions of acyclic, tertiary alkyl bromides were faster than those of secondary alkyl bromides. Thus, **17** and **18** were obtained in good yields after only 3 hours; this short time was necessary to prevent decomposition of the tertiary alkyl imine. Transition metal-catalyzed coupling reactions of unactivated tertiary alkyl electrophiles are typically more challenging to effect than reactions of secondary alkyl halides,⁵³⁻⁶⁴ and no examples of *N*-alkylation of an unactivated tertiary alkyl electrophile have been reported as part of the prior work on photochemical substitution.³⁴⁻³⁸

Table 5.5. Scope of alkyl bromides.^a

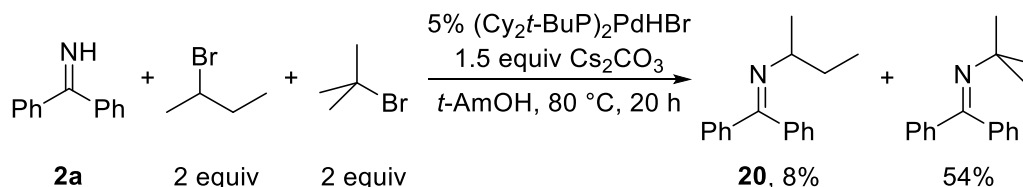


^aConditions unless otherwise noted: alkyl bromide (0.300 mmol), imine **2d** (1.5 equiv), cesium carbonate (1.5 equiv), $(\text{Cy}_2t\text{-BuP})_2\text{PdHBr}$ (5.3 mol %), and *t*-amyl alcohol (0.40 ml) at 80 °C with stirring for 20 h. Reaction mixtures prepared inside an N_2 -filled glovebox. Isolated yields of purified *N*-alkyl imines (yields determined by ^1H NMR spectroscopy). ^bReaction mixture prepared under air; vial flushed with N_2 prior to heating. ^cFrom *exo*-2-bromonorbornane. ^dFrom *endo*-2-bromonorbornane. ^{e,d}The product **12** was >97% *exo*. ^e3 equiv **2d** and 3 equiv Cs_2CO_3 . ^f3 equiv **2d** and 3 h reaction time.

The higher rate observed with tertiary alkyl bromides suggests that the alkylation of an imine could occur selectively with a tertiary alkyl bromide in the presence of a secondary alkyl bromide.

Indeed, the reaction of **2a** with two equivalents each of *tert*-butylbromide and *sec*-butylbromide produced the corresponding *N*-*tert*-butyl and *N*-*sec*-butyl imines in 7.1 : 1 ratio (Scheme 5.2).

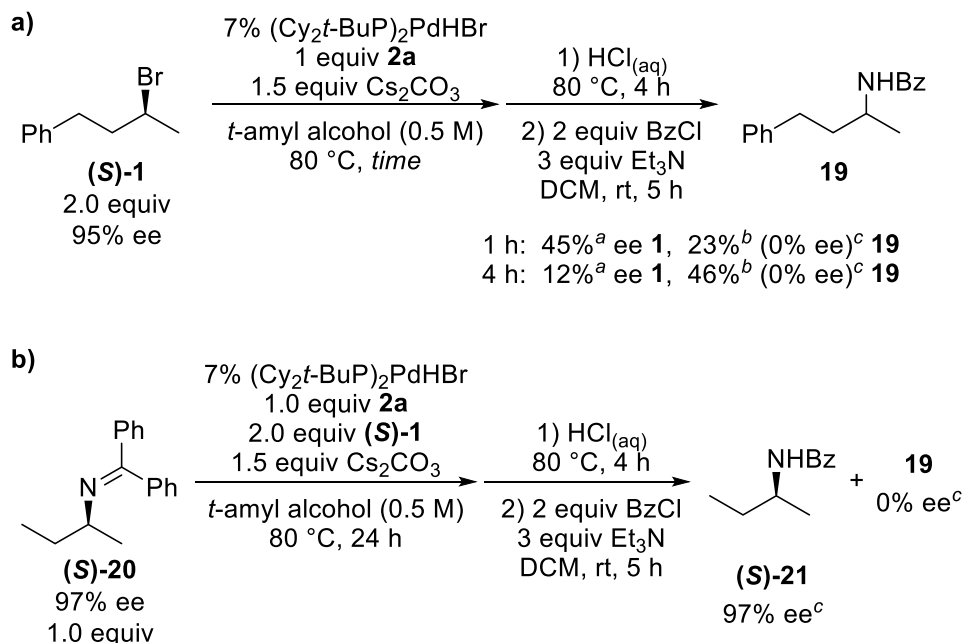
Scheme 5.2. Competitive alkylation of benzophenone imine with a mixture of *s*-BuBr and *t*-BuBr.^a



^aYields determined by corrected GC integration against TMB.

To investigate the stereochemical outcome further, we studied the reaction of enantioenriched 3-bromo-1-phenylbutane ((*S*)-**1**) with benzophenone imine (**2a**) (Scheme 5.3a). The unconverted (*S*)-**1** was enantioenriched, although partially racemized, after 1 h and 4 h at 80 °C, whereas the *N*-alkyl imine product was completely racemic at all reaction times. To assess whether the product racemizes under the reaction conditions, the reaction of (*S*)-**1** was conducted with added authentic (*S*)-*N*-*sec*-butylbenzophenone imine ((*S*)-**20**) (Scheme 5.3b). The enantioenriched *N*-*sec*-butyl imine was recovered from the reaction without any detectable loss of ee. These results indicate that the reaction proceeds through an achiral intermediate or transition state, such as the alkyl radical intermediate in the proposed radical mechanism.

Scheme 5.3. Stereochemical outcome of Pd-catalyzed *N*-alkylation.



^aEnantiomeric excess of unconverted **1** was measured by chiral GC. ^bIsolated yield of the purified *N*-alkyl benzamide **19**. ^cEnantiomeric excess was measured by chiral SFC.

No significant reaction of (*S*)-**1** was observed with cesium carbonate, cesium bromide, or the (Cy₂*t*-BuP)₂PdHBr precatalyst individually. However, when allowed to react with the palladium precatalyst and cesium carbonate at 80 °C for 20 h, the alkyl bromide racemized, and the corresponding alkane byproduct formed (Table 5.6). These experiments indicate that the racemization occurs by reaction of the alkyl bromide with a palladium(0) complex, and this observation is consistent with reversible generation of a free alkyl radical.

Table 5.6. Racemization of (*S*)-**1**.

(*S*)-**1**
95% ee

conditions
t-amyl alcohol (1.0 M)
80 °C, 20 h

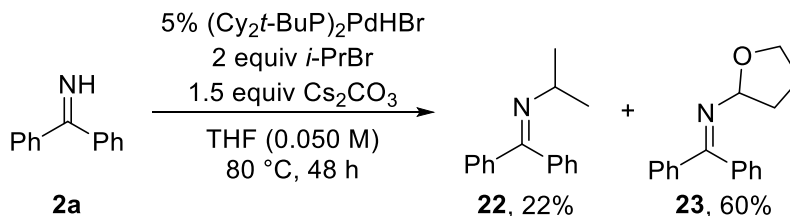
unconverted

entry	conditions	ee unconverted 1 (%)
1	4% [Cy ₂ (<i>t</i> -Bu)P] ₂ PdHBr	93
2	0.5 equiv CsBr	95
3	4% [Cy ₂ (<i>t</i> -Bu)P] ₂ PdHBr + 0.5 equiv CsBr	89
4	0.75 equiv Cs ₂ CO ₃	91
5	4% [Cy ₂ (<i>t</i> -Bu)P] ₂ PdHBr + 0.75 equiv Cs ₂ CO ₃	< 2

^aEnantiomeric excess determined by chiral GC.

Reactions run in THF provided further evidence for the intermediacy of an alkyl radical. These reactions formed an *N*-tetrahydrofuryl imine as side product. At 0.5 M, both the *N*-*iso*-propyl imine **22** and *N*-tetrahydrofuryl imine **23** formed in 75 and 14% yields, respectively. At 0.05 M, the reaction formed **22** and **23** in 22 and 60% yields, respectively (Scheme 5.4). We propose that this product forms by abstraction of a hydrogen atom from the THF solvent by an alkyl radical, and the resulting tetrahydrofuryl radical intermediate generates the observed *N*-tetrahydrofuryl imine product. The effect of concentration on the product distribution is consistent with this proposal because reaction of an alkyl radical with solvent is favored in dilute solutions, and amination is favored in concentrated solutions.

Scheme 5.4. Amination of tetrahydrofuran.^a

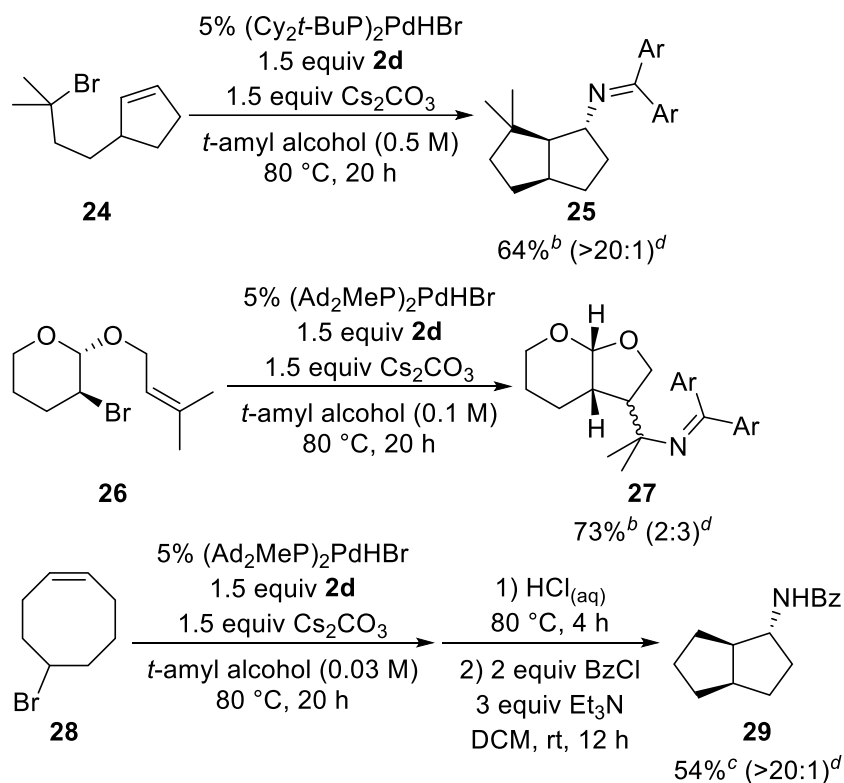


^aYields determined by ¹H NMR spectroscopy.

The intermediacy of an alkyl radical suggested that this method could be extended to the intramolecular carboamination of olefins.^{29-33, 65} Furthermore, these substrates serve as radical clocks to approximate the lifetime of the radical intermediate. Indeed, the reaction of imine **2d** with the unsaturated alkyl bromide **24** produced the corresponding carboamination product **25** in

64% yield and >20:1 dr (Scheme 5.5). Similarly, the bromoacetal **26** underwent a Ueno-Stork type cyclization⁶⁶ and subsequent amination to yield a 3:2 mixture of *endo*- and *exo*-**27** in 73% combined yield. In both cases, the product from direct coupling was not detected by gas chromatography. These results indicate that the amination step is significantly slower than the cyclization of these substrates.

Scheme 5.5. Palladium-catalyzed intramolecular carboamination.^a



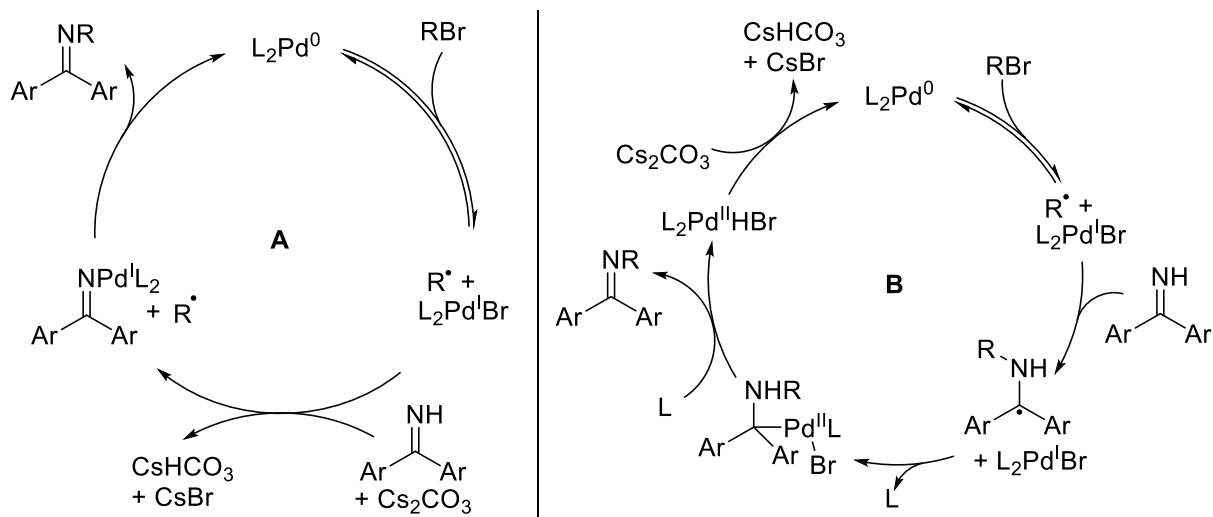
^aCompounds **24–29** are racemic. ^bIsolated yields of purified *N*-alkyl imines. ^cIsolated yield of purified *N*-alkyl benzamide. ^d(*Exo/endo* ratio). See the experimental section for assignments of relative configurations.

However, the reaction of (*Z*)-5-bromocyclooct-1-ene (**28**) produced a 2:1 mixture of products favoring cyclization when run at 0.50 M, and this substrate is thus an appropriate radical clock for the cross-coupling reaction. Renaud and coworkers have measured the rate constant of cyclization for cyclooct-4-enyl radical as $3.3 \times 10^4 \text{ s}^{-1}$ at 80 °C.⁶⁷ Therefore, the formation of a mixture of products indicates that the observed rate constant for the amination of a secondary alkyl radical is on the order of 10^4 s^{-1} . When the reaction was run at 0.03 M, the carboamination product formed predominately and was isolated as the corresponding benzamide **29** in 54% yield. The relatively small rate constant and the dependence of the extent of cyclization on concentration argues against reaction of the radical within a solvent cage.

The stereochemical outcomes of these carboamination reactions are consistent with free radical cyclizations. The reactions of **24** and **28** form structurally similar products *exo*-**25** and *exo*-**29** in high dr. However, the product *exo*-**25** results from addition of the carbon and nitrogen to the opposite faces of the alkene in **24** (*anti*-carboamination), while *exo*-**29** results from addition to the

same face of the alkene in **28** (*syn*-carboamination). These products could also form by reaction of an alkylpalladium complex with an alkene. However, an alkylpalladium(II) complex would be expected to react by *syn*-carbopalladation to form the *syn*-carboamination product after reductive elimination.⁶⁸ The formation of the *anti*-carboamination product **25**, therefore, corroborates the other data supporting a free radical cyclization.

Scheme 5.6. Plausible general mechanisms for Pd-catalyzed cross-coupling of secondary alkyl bromides with benzophenone imines.



A. sp^3 C–N bond formed *via* radical addition to a palladium methyleneamido complex. **B.** sp^3 C–N bond formed *via* radical additions to an unbound imine.

5.3 Conclusions

Although the process we describe constitutes the first thermal, transition metal-catalyzed coupling of unactivated secondary and tertiary alkyl halides with a nitrogen nucleophile, significant additional studies will be needed to make this process into a practical synthetic method. Benzophenone imines are commonly used as ammonia surrogates for palladium-catalyzed coupling of aryl halides,⁴⁹⁻⁵⁰ but these reagents are larger than typical ammonia equivalents. Moreover, a catalyst capable of coupling a wide range of nitrogen nucleophiles to form a variety of *N*-alkyl products would make the process most valuable. A more active catalyst could also expand the scope of alkyl halides by reducing reaction times and temperatures to avoid competitive background reactions, such as elimination. Finally, our results support the intermediacy of a free alkyl radical, but the intimate mechanism by which the C–N bond forms and the Pd(0) species regenerates remains to be revealed by ongoing studies (two plausible general mechanisms are shown above in Scheme 5.6). The significant current scope suggests that these initial findings, in combination with further work, should point the way to valuable new methodology for the synthesis of alkylamines by a catalytic version of a classical transformation.

5.4 Experimental

General experimental details

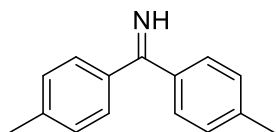
All reactions were performed under a nitrogen atmosphere, unless otherwise specified. Anhydrous *tert*-amyl alcohol was purchased from Sigma Aldrich and used as received. Dry THF, pentane, and diethyl ether were collected from a solvent purification system containing a 0.33 m column of activated alumina under nitrogen prior to use in reactions. Benzophenone imine (97%) purchased from Acros Organics was used in coupling reactions. Benzophenone imine (95%) purchased from Sigma Aldrich was used for the preparation of authentic imines by condensation reactions. All other chemicals were purchased from commercial suppliers and used as received.

Column chromatography was performed with 230-400 mesh silica gel from Fisher Scientific. TLC plates with fluorescent indicators were purchased from Silicycle or EMD and visualized under a 254 nm UV lamp unless otherwise noted. "Prebasified" silica refers to silica gel and TLC plates that have been soaked with 2-5% triethylamine in hexanes prior to use. "Untreated" silica refers to silica gel and TLC plates used as received. Special precautions taken to minimize hydrolysis are noted for relevant compounds.

GC spectra were obtained on an Agilent 7890 GC equipped with an HP-5 column (25 m x 0.20 mm x 0.33 μ m film) and an FID detector. NMR spectra were obtained on 500 MHz or 600 MHz Bruker Avance series instruments at the University of California, Berkeley NMR facility. Chemical shifts are reported relative to the residual solvent signals (CDCl_3 7.26 ppm for ^1H , 77.16 ppm for ^{13}C ; C_6D_6 7.16 ppm for ^1H , 128.06 ppm for ^{13}C). ESI high resolution mass spectrometry (HRMS) was performed by the QB3 Mass Spectrometry Facility or the LBNL Catalysis Center at the University of California, Berkeley. EIMS (positive ionization) was performed on an Agilent 7890A/5975C GC-MS. Elemental analysis was performed by the UC Berkeley Microanalytical Laboratory.

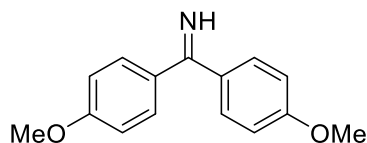
Preparation of benzophenone imine derivatives

Note: The imines prepared below are sensitive to hydrolysis and contain small amounts of the corresponding ketones as impurities. The percent imine was measured by NMR spectroscopy and noted. To prevent further hydrolysis, these compounds were stored in a nitrogen-filled glovebox.



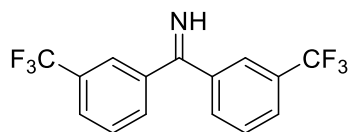
4,4'-Dimethylbenzophenone imine (2b). Dry magnesium turnings (365 mg, 15.0 mmol, 1.50 equiv), dry THF (20 ml), and a magnetic stir bar were placed in a nitrogen-filled flask, and the flask was connected to a reflux condenser. 4-Bromotoluene (1.84 ml, 2.57 g, 15.0 mmol, 1.50 equiv) was dissolved in THF (3 ml), and a small amount of this solution was transferred to the reaction flask. The reaction was initiated with a single iodine crystal. The remaining aryl bromide solution was slowly transferred to the reaction flask, the syringe was rinsed with THF (3 ml), and the mixture was stirred at ambient temperature for 2.5 h at which time the majority of the magnesium was visibly consumed. The reaction mixture was then cooled to 0 $^{\circ}\text{C}$, a solution of *p*-tolunitrile (1.20 ml, 1.17 g, 9.99 mmol) in THF (7 ml) was added to the flask, and the syringe rinsed with THF (3 ml). The reaction mixture was heated at reflux for 20 h, then cooled to 0 $^{\circ}\text{C}$, and then quenched

with dry methanol (3 ml). The reaction mixture was diluted with hexanes (30 ml), filtered through a pad of Celite, and concentrated at reduced pressure. The yellow oil was purified by column chromatography (5 to 10% ethyl acetate gradient and 5% triethylamine in hexanes on prebasified silica) to give the title compound as a pale yellow oil (1.82 g, 8.68 mmol, 87% yield, 97% imine by ^1H NMR spectroscopy). The ^1H NMR spectrum was consistent with the spectrum reported in the literature.⁶⁹ **EIMS** 209.1 (M^+), 194.1 (base peak).



4,4'-Dimethoxybenzophenone imine (2c). A solution of 4-methoxyphenylmagnesium bromide (16 ml, 1.0M, 16 mmol, 1.1 equiv) in THF was transferred to a 100 ml nitrogen-filled flask fitted with a reflux condenser, and the solution was cooled to 0 °C.

A solution of 4-methoxybenzonitrile (2.00 g, 15.0 mmol) in dry THF (9 ml) was added to the flask, and the syringe rinsed with THF (3 ml). The reaction mixture was heated at reflux for 17 h, then cooled to 0 °C, and then quenched with dry methanol (3 ml). The reaction mixture was diluted with hexanes (20 ml), filtered through a pad of Celite, and concentrated at reduced pressure. The yellow solid was purified by column chromatography (0 to 50% ethyl acetate gradient and 5% triethylamine in hexanes on prebasified silica) to give the title compound as an off-white powder (2.48 g, 10.3 mmol, 69% yield, 96% imine by ^1H NMR spectroscopy). The ^1H NMR spectrum was consistent with the spectrum reported in the literature.⁷⁰ **EIMS** 241.1 (M^+), 210.1 (base peak).



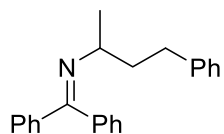
3,3'-Bis(trifluoromethyl)benzophenone imine (2d). Dry magnesium turnings (370 mg, 15.2 mmol, 1.49 equiv), dry THF (10 ml), and a magnetic stir bar were placed in a nitrogen-filled flask, and the flask was connected to a reflux condenser. 3-

Bromobenzotrifluoride (2.10 ml, 3.38 g, 15.0 mmol, 1.47 equiv) was dissolved in THF (3 ml), and a small amount of this solution was transferred to the reaction flask. The reaction was initiated with a single iodine crystal. The remaining aryl bromide solution was slowly transferred to the reaction flask, the syringe was rinsed with THF (3 ml), and the mixture was heated at reflux until the majority of the magnesium was visibly consumed. The reaction mixture was then cooled to 0 °C, a solution of 3-trifluoromethylbenzonitrile (1.37 ml, 1.75 g, 10.2 mmol) in THF (2 ml) was added to the flask, and the syringe rinsed twice with THF (2 ml). The reaction mixture was heated at reflux for 4 h, then cooled to 0 °C, and then quenched with dry methanol (2 ml). The reaction mixture was diluted with hexanes (50 ml), neutralized with sodium bicarbonate, filtered through a pad of Celite, and concentrated at reduced pressure. The red oil was purified by kugelrohr distillation (150 °C, ~0.5 Torr) to give the title compound as a pale yellow oil (2.52 g, 7.94 mmol, 79% yield, >98% imine by ^1H NMR spectroscopy). This procedure has also been run on larger scale with 8.82 g (51.5 mmol) of 3-trifluoromethylbenzonitrile. All masses and volumes were scaled accordingly, and 12.0 g (73% yield) of the title compound was obtained after purification by short path distillation (vapor temp 85-96 °C at approximately 0.20 Torr). **^1H NMR** (500 MHz, CDCl_3) δ 10.05 (s, 1H), 8.05 (s, 1H), 7.85 (d, J = 7.7 Hz, 1H), 7.77 (d, J = 7.5 Hz, 2H), 7.67 (s, 1H), 7.64 – 7.53 (m, 3H). **^{13}C NMR** (151 MHz, CDCl_3) δ 175.7, 140.5, 138.5, 132.5, 131.7 (q, J

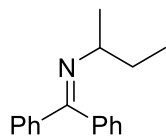
= 32.8 Hz), 131.3 (q, J = 32.8 Hz), 130.8, 129.6, 129.1, 127.8, 127.2, 126.0, 124.4, 124.0 (q, J = 272.1 Hz), 123.8 (q, J = 272.4 Hz). ^{19}F NMR (565 MHz, CDCl_3) δ -63.7. ESI^+ calc'd 318.0712 ($\text{M}+\text{H}^+$), found 318.0709.

Note: when characterized in wet CDCl_3 , the NMR signals were broad. Therefore, this compound was characterized in anhydrous CDCl_3 stored under nitrogen.

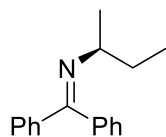
Preparation of authentic products



***N*-(4-phenylbutan-2-yl)benzophenone imine (3a).** Benzophenone imine (181 mg, 1.00 mmol), 1-methyl-3-phenylpropylamine (179 mg, 1.20 mmol, 1.20 equiv), and dry DCM (1 ml) were mixed in a 1 dram vial and stirred for 4 days at ambient temperature. The volatile materials were evaporated at reduced pressure, and the crude product was purified by kugelrohr distillation (0.5 to 1.0 Torr, 180 °C) to give the title compound as a colorless glass (286 mg, 0.912 mmol, 91% yield). ^1H NMR (600 MHz, CDCl_3) δ 7.62 (d, J = 7.4 Hz, 2H), 7.45 - 7.39 (m, 3H), 7.37 (t, J = 7.1 Hz, 1H), 7.33 (t, J = 7.4 Hz, 2H), 7.24 (t, J = 7.5 Hz, 2H), 7.17 - 7.10 (m, 5H), 3.50 - 3.43 (m, 1H), 2.60 (ddd, J = 13.7, 11.2, 5.4 Hz, 1H), 2.44 (ddd, J = 13.8, 11.1, 5.6 Hz, 1H), 2.02 - 1.93 (m, 1H), 1.85 - 1.77 (m, 1H), 1.20 (d, J = 6.2 Hz, 3H). ^{13}C NMR (151 MHz, CDCl_3) δ 166.5, 142.7, 140.4, 137.6, 129.8, 128.5, 128.5, 128.4, 128.4, 128.2, 128.2, 127.9, 125.7, 57.3, 40.2, 33.2, 22.4. ESI^+ calc'd 314.1903 ($\text{M}+\text{H}^+$), found 314.1899.

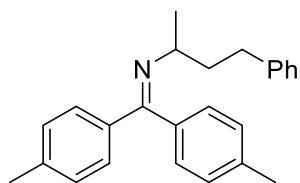


***N*-(*sec*-butyl)benzophenone imine (20).** Benzophenone imine (182 mg, 1.00 mmol), *sec*-butylammonium chloride (115 mg, 1.05 mmol, 1.05 equiv), and dry DCM (2 ml) were mixed in a 1 dram vial and stirred for 14 h at ambient temperature. The reaction mixture was filtered through a plug of Celite, which was rinsed with DCM (2 ml). The volatile materials were evaporated at reduced pressure, and the crude product was purified by column chromatography (2% triethylamine in hexanes on prebasified silica) to give the title compound as a clear and colorless oil (183 mg, 0.771 mmol, 77% yield). The ^1H and ^{13}C NMR spectra matched those of (*S*)-20.



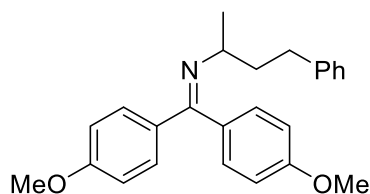
(*S*)-*N*-(*sec*-butyl)benzophenone imine ((*S*)-20). Benzophenone imine (363 mg, 2.00 mmol), (*S*)-*sec*-butylamine (184 mg, 2.51 mmol, 1.25 equiv), and dry DCM (2 ml) were mixed in a 1 dram vial and stirred for 7 days at ambient temperature. The volatile materials were evaporated at reduced pressure, and the crude product was purified by kugelrohr distillation (0.5 to 1.0 Torr, 120 °C) and column chromatography (5% triethylamine in hexanes on prebasified silica; R_f 0.85) to give the title compound as a clear and colorless oil (357 mg, 1.50 mmol, 75% yield). ^1H NMR (500 MHz, CDCl_3) δ 7.62 - 7.57 (m, 2H), 7.47 - 7.38 (m, 3H), 7.38 - 7.29 (m, 3H), 7.15 (dd, J = 7.9, 1.4 Hz, 2H), 3.36 - 3.22 (m, 1H), 1.68 - 1.57 (m, 1H), 1.55 - 1.45 (m, 1H), 1.15 (d, J = 6.2 Hz, 3H), 0.79 (t, J = 7.4 Hz, 3H). ^{13}C NMR (151 MHz, CDCl_3) δ 166.2, 140.5, 137.8, 129.7, 128.5 (2C), 128.1 (2C), 127.9, 59.1, 31.3, 22.1, 11.3. ESI^+ calc'd 238.1590 ($\text{M}+\text{H}^+$), found 238.1588.

(*S*)-*N*-(*sec*-butyl)benzophenone imine ((*S*)-**20**) and (*S*)-*N*-(*sec*-butyl)benzamide ((*S*)-**21**) were prepared from the same sample of (*S*)-*sec*-butylamine. Therefore, the sample of (*S*)-**20** is also presumed to have 97% ee.



***N*-(4-phenylbutan-2-yl)-4,4'-dimethylbenzophenone imine (3b).**

4,4'-Dimethylbenzophenone imine (208 mg, 0.993 mmol), 1-methyl-3-phenylpropylamine (179 mg, 1.20 mmol, 1.20 equiv), and dry DCM (1 ml) were mixed in a 1 dram vial and stirred for 5 days at ambient temperature. The volatile materials were evaporated at reduced pressure, and the crude product was purified by column chromatography (2% triethylamine in hexanes on prebasified silica, *R_f* 0.41) to give the title compound as a clear and colorless oil which solidified into a white solid on standing (259 mg, 0.758 mmol, 76% yield). **¹H NMR** (500 MHz, CDCl₃) δ 7.51 (d, *J* = 8.2 Hz, 2H), 7.25 – 7.20 (m, 4H), 7.17 – 7.10 (m, 5H), 7.01 (d, *J* = 7.9 Hz, 2H), 3.47 (dq, *J* = 8.3, 6.2, 4.3 Hz, 1H), 2.59 (ddd, *J* = 13.7, 11.1, 5.4 Hz, 1H), 2.47 – 2.38 (m, 4H), 2.36 (s, 3H), 1.96 (dddd, *J* = 13.5, 11.0, 8.3, 5.4 Hz, 1H), 1.85 – 1.73 (m, 1H), 1.19 (d, *J* = 6.2 Hz, 3H). **¹³C NMR** (151 MHz, CDCl₃) δ 166.6, 142.8, 139.8, 138.0, 137.8, 134.8, 129.1, 128.8, 128.5, 128.5, 128.3, 127.8, 125.6, 77.4, 77.2, 57.2, 40.3, 33.3, 22.4, 21.5, 21.4. **ESI⁺** calc'd 342.2216 (M+H⁺), found 342.2212.

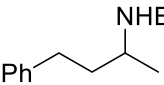


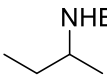
***N*-(4-phenylbutan-2-yl)-4,4'-dimethoxybenzophenone imine (3c).**

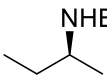
4,4'-Dimethoxybenzophenone imine (241 mg, 0.999 mmol), 1-methyl-3-phenylpropylamine (179 mg, 1.20 mmol, 1.20 equiv), and dry DCM (1 ml) were mixed in a 1 dram vial and stirred for 4 days at ambient temperature. The volatile materials were evaporated at reduced pressure, and the crude product was purified by column chromatography (10% ethylacetate and 5% triethylamine in hexanes on prebasified silica, *R_f* 0.44) to give the title compound as a clear and colorless oil (270 mg, 0.723 mmol, 72% yield). **¹H NMR** (500 MHz, Chloroform-*d*) δ 7.56 (d, *J* = 8.9 Hz, 2H), 7.23 (t, *J* = 7.4 Hz, 2H), 7.16 – 7.10 (m, 3H), 7.04 (d, *J* = 8.7 Hz, 2H), 6.93 (d, *J* = 8.7 Hz, 2H), 6.84 (d, *J* = 8.9 Hz, 2H), 3.87 (s, 3H), 3.82 (s, 3H), 3.47 (dq, *J* = 8.3, 6.2, 4.3 Hz, 1H), 2.58 (ddd, *J* = 13.8, 11.0, 5.5 Hz, 1H), 2.42 (ddd, *J* = 13.8, 10.9, 5.7 Hz, 1H), 1.94 (dddd, *J* = 13.6, 10.9, 8.3, 5.5 Hz, 1H), 1.83 – 1.74 (m, 1H), 1.19 (d, *J* = 6.2 Hz, 3H). **¹³C NMR** (151 MHz, CDCl₃) δ 165.8, 161.1, 159.4, 142.8, 133.7, 130.1, 129.9, 129.3, 128.5, 128.3, 125.6, 113.8, 113.4, 77.4, 77.2, 77.0, 57.0, 55.5, 55.4, 40.3, 33.2, 22.5. **ESI⁺** calc'd 374.2115 (M+H⁺), found 374.2110.

General procedure for the preparation of benzamides: The amine (0.50 mmol), triethylamine (84 μl, 61 mg, 0.60 mmol, 1.2 equiv), and dry DCM (2 ml) were mixed in a 1 dram vial. The reaction mixture was cooled to 0 °C, and the vial was flushed with nitrogen. Benzoyl chloride (70 μl, 85 mg, 0.60 mmol, 1.2 equiv) was slowly added through a septum cap. The reaction mixture was stirred at ambient temperature for 4 h. The reaction was quenched with 0.5 M HCl_(aq) (2 ml). The layers were separated, and the aqueous layer extracted twice more with DCM (2 ml). The

combined organic layers were filtered through a plug of MgSO_4 . The volatile materials were evaporated at reduced pressure. The crude products were purified by column chromatography (25% ethyl acetate in hexanes).

 ***N*-(4-phenylbutan-2-yl)benzamide (19).** Prepared by the general procedure above with 1-methyl-3-phenylpropylamine (74.5 mg, 0.499 mmol) to give the title compound as a white powder (126 mg, 0.497 mmol, 99% yield). The ^1H NMR spectrum was consistent with the spectrum reported in the literature.⁷¹ **Chiral SFC Analysis:** 0% ee, Chiracel OD-H column, 15% *i*-PrOH, 2.5 ml/min flow rate, t_R = 3.76, 5.19 min.

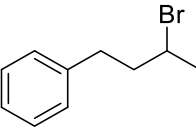
 ***N*-(*sec*-butyl)benzamide (21).** Prepared by the general procedure above with (rac)-*sec*-butylamine (36.6 mg, 0.500 mmol) to give the title compound as a white powder (85.4 mg, 0.482 mmol, 96% yield). The ^1H NMR spectrum was consistent with the spectrum reported in the literature.⁷²

 **(*S*)-*N*-(*sec*-butyl)benzamide ((*S*)-21).** Prepared by the general procedure above with (*S*)-*sec*-butylamine (38.4 mg, 0.525 mmol) to give the title compound as a white powder (84.8 mg, 0.478 mmol, 91% yield, 97% ee by SFC). The ^1H NMR spectrum matched that of the racemic sample. **Chiral SFC Analysis:** 97% ee, Chiracel AS-H column, 15% *i*-PrOH, 2.5 ml/min flow rate, t_R (minor) = 1.16 min, t_R (major) = 1.37 min.

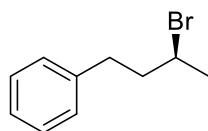
Preparation of alkyl bromides

The following alkyl bromides were prepared according to published procedures: methyl 4-bromohexanoate,⁷³ 3-bromo-3-methyl-1-phenylbutane,⁶¹ 3-bromo-3-methylbutyl benzoate,⁷⁴ 2-(2-bromo-2-methylpropyl)-1,3-dioxane,⁷⁵ 5-bromo-1-chloro-5-methylhexane,⁵³ *trans*-3-bromo-2-((3-methylbut-2-en-1-yl)oxy)tetrahydro-2H-pyran,⁷⁶ and (*Z*)-5-bromocyclooct-1-ene.

The following alkyl bromides were prepared with minor modifications from published procedures: *endo*-2-bromonorbornane⁷⁷ was purified by filtering through silica with hexanes, followed by kugelrohr distillation; the compound was determined to be 98% *endo* by ^1H NMR spectroscopy. *N*-(3-bromo-3-methylbutyl)phthalimide⁷⁸ was purified by column chromatography and recrystallized from hexanes prior to use.

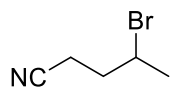
 **3-Bromo-1-phenylbutane (1).** 4-Phenyl-2-butanol (2.98 g, 19.8 mmol) was dissolved in dry DCM (50 ml) in a 100 ml flask. The flask was cooled to 0 °C and flushed with nitrogen. Triphenylphosphine (6.56 g, 25.0 mmol, 1.25 equiv) and carbon tetrabromide (8.30 g, 25.0 mmol, 1.25 equiv) were added slowly in that order. The reaction mixture was stirred at ambient temperature for 2 h. The volume was lowered at reduced pressure. The reaction mixture was diluted with hexanes (50 ml) and filtered

through silica, which was rinsed twice with hexanes (50 ml). The volatile materials were evaporated at reduced pressure. The crude product was purified by kugelrohr distillation (0.5 to 1.0 Torr, 86 °C) to give the title compound as a clear and colorless oil (3.39 g, 15.9 mmol, 80% yield). The ^1H NMR spectrum was consistent with the spectrum reported in the literature.⁷⁹ **EIMS** 214.0 (M^+ , ^{81}Br), 212.0 (M^+ , ^{79}Br), 91.1 (base peak).

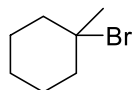


(S)-3-Bromo-1-phenylbutane ((S)-1). (*R*)-4-Phenyl-2-butanol (254 mg, 1.69 mmol) was dissolved in dry DCM (4 ml) in a 25 ml flask. The flask was cooled to 0 °C and flushed with nitrogen. Triphenylphosphine (554 mg, 2.11 mmol, 1.25 equiv) and carbon tetrabromide (700 mg, 2.11 mmol, 1.25 equiv) were slowly added in that order. The reaction mixture was stirred at ambient temperature for 2 h. The reaction mixture was diluted to 10 ml with DCM and washed with 0.5 M HCl (10 ml). The aqueous layer was extracted twice more with DCM (10 ml). The combined organic layers were dried with MgSO_4 . The volatile materials were evaporated at reduced pressure. The crude product was purified by kugelrohr distillation (0.5 to 0.8 Torr, 72 °C) to give the title compound as a clear and colorless oil (337 mg, 1.58 mmol, 94% yield). The ^1H NMR spectrum and EIMS matched that of the racemic sample. **Chiral GC Analysis:** 95% ee, CycloSil-B column (30 m length, 0.25 mm diameter, 0.25 μm film), 85 °C to 93.5 °C ramp at 0.06 °C/min, t_R (minor) = 154 min, t_R (major) = 156 min.

Note: chiral GC retention times for 3-bromo-1-phenylbutane (**1**) varied between 117 and 157 minutes due to variations in column conditions over time.

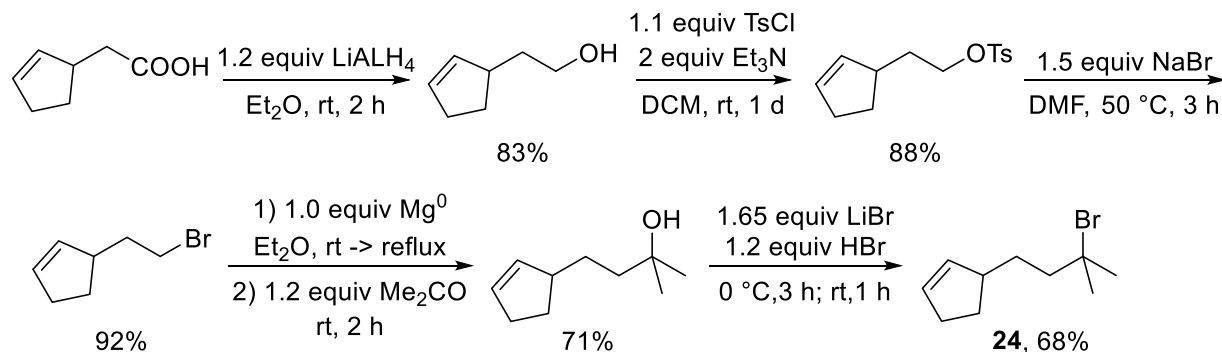


4-Bromopentanenitrile. A 20 dram vial was charged with 1,3-dibromobutane (2.16 g, 10.0 mmol), sodium cyanide (646 mg, 13.2 mmol, 1.32 equiv), ethanol (3 ml), and a magnetic stir bar. The vial was flushed with nitrogen and sealed with a Teflon-lined cap. The reaction mixture was heated at 80 °C for 26 h. The mixture was diluted with ether (approximately 50 ml), washed twice with water (~20 ml) and twice with brine (~20 ml). The organic layers were dried with MgSO_4 , and the volatile materials were evaporated at reduced pressure. The crude product was purified by column chromatography (0 to 25% ethyl acetate gradient in hexanes) followed by kugelrohr distillation (~120 °C, ~28 Torr), followed by column chromatography (0 to 10% ethyl acetate in hexanes gradient) to give the title compound as a clear and colorless oil (639 mg, 3.94 mmol, 39% yield). **^1H NMR** (400 MHz, CDCl_3) δ 4.19 (dq, J = 10.3, 6.7, 3.7 Hz, 1H), 2.65 – 2.53 (m, 2H), 2.22 – 2.11 (m, 1H), 2.11 – 2.00 (m, 1H), 1.77 (d, J = 6.7 Hz, 3H). **EIMS** 162.9 (M^+ , ^{81}Br), 160.9 (M^+ , ^{79}Br), 82.1 (base peak).



1-Bromo-1-methylcyclohexane. 1-methylcyclohexan-1-ol (983 mg, 8.61 mmol) and a magnetic stir bar were placed in a 10 ml flask under air. $\text{HBr}_{(\text{aq})}$ (48%) was added slowly to the flask with stirring, and the mixture was stirred at ambient temperature for 20 h. The mixture was then diluted to approximately 40 ml with water and extracted twice with ether (~40 ml). The combined organic layers were washed twice with $\text{NaHCO}_{3(\text{aq})}$ (~40 ml) and dried with MgSO_4 . The volatile materials were evaporated at reduced pressure. The crude product

was purified by filtering through silica with pentanes, followed by kugelrohr distillation (85 °C, ~40 Torr) to give the title compound as a pale yellow oil (305 mg, 1.72 mmol, 20% yield). The ^1H NMR spectrum was consistent with the spectrum reported in the literature.⁸⁰ EIMS M^+ not observed, 97.0 (base peak), 55.0.



2-(Cyclopent-2-en-1-yl)ethan-1-ol. 2-Cyclopentene-1-acetic acid (3.28 g, 26.0 mmol) was dissolved in dry Et_2O (200 ml) in a 500 ml flask. The reaction mixture was cooled to 0 °C, and the flask flushed with nitrogen. LiAlH_4 (1.18 g, 31.1 mmol, 1.20 equiv) was added slowly. The reaction mixture was stirred at ambient temperature for 2 h. The reaction was then quenched at 0 °C with water (1 ml), 15% $\text{NaOH}_{(\text{aq})}$ (1 ml), and water (3 ml). The mixture was stirred at ambient temperature until white, dried with MgSO_4 , and filtered through Celite. The volatile materials were evaporated at reduced pressure. The crude product was purified by kugelrohr distillation (120 °C, 45 Torr) to give the title compound as a clear and colorless oil (2.43 g, 21.7 mmol, 83% yield). The ^1H NMR spectrum was consistent with the spectrum reported in the literature.⁸¹

2-(Cyclopent-2-en-1-yl)ethyl 4-methylbenzenesulfonate. 2-(Cyclopent-2-en-1-yl)ethan-1-ol (3.38 g, 30.1 mmol) and triethylamine (8.5 ml, 6.2 g, 61 mmol, 2.0 equiv) were mixed in dry DCM (80 ml) in a 250 ml flask. The reaction mixture was cooled to 0 °C, and the flask was flushed with nitrogen. TsCl (6.32 g, 33.1 mmol, 1.10 equiv) was added slowly to the flask, and the reaction mixture was stirred at ambient temperature for 1 d. The reaction mixture was washed with 0.5 M $\text{HCl}_{(\text{aq})}$ (100 ml). The aqueous layer was extracted twice more with DCM (30 ml). The combined organic layers were washed with 5% $\text{NaOH}_{(\text{aq})}$ (100 ml), which was extracted twice more with DCM (30 ml). The organic layers were dried with MgSO_4 . The volatile materials were evaporated at reduced pressure. The crude product was purified by column chromatography (0 to 33% ethyl acetate gradient in hexanes) to give the title compound as a pale yellow oil (7.08 g, 26.6 mmol, 88% yield). The ^1H NMR spectrum was consistent with the spectrum reported in the literature.⁸²

3-(2-Bromoethyl)cyclopent-1-ene. 2-(Cyclopent-2-en-1-yl)ethyl 4-methylbenzenesulfonate (7.08 g, 26.6 mmol) was dissolved in dry DMF (30 ml) in a 50 ml flask. NaBr (4.10 g, 39.8 mmol, 1.50 equiv) was added to flask, and the flask was flushed with nitrogen. The reaction mixture was heated at 50 °C for 3 h. The reaction mixture was diluted with water (100 ml), and the aqueous layer was extracted with pentane (100 ml). The organic layer was washed again with water (100

ml). The combined aqueous layers were extracted with pentane (100 ml), which was washed with water (100 ml) before combining organic layers. The combined organic layers were dried with MgSO_4 . The volatile materials were evaporated at reduced pressure. The crude product was purified by filtering through a plug of silica (60 ml pentane to elute) to give the title compound as a clear and colorless oil (4.28 g, 24.5, 92% yield). **^1H NMR** (500 MHz, CDCl_3) δ 5.79 – 5.74 (m, 1H), 5.69 – 5.63 (m, 1H), 3.49 – 3.35 (m, 2H), 2.90 – 2.79 (m, 1H), 2.40 – 2.23 (m, 2H), 2.08 (dtd, J = 13.0, 8.5, 5.0 Hz, 1H), 1.97 (dtd, J = 14.1, 7.7, 6.7, 6.7 Hz, 1H), 1.84 (dtd, J = 14.0, 7.7, 6.4 Hz, 1H), 1.41 (ddt, J = 12.8, 9.0, 6.4 Hz, 1H). **EIMS** 176.0 (M^+ , ^{81}Br), 174.0 (M^+ , ^{79}Br), 67.1 (base peak).

4-(Cyclopent-2-en-1-yl)-2-methylbutan-2-ol. Dry magnesium turnings (304 mg, 12.5 mmol, 1.04 equiv) and dry Et_2O (4 ml) were placed in a 25 ml flask under nitrogen. 3-(2-Bromoethyl)cyclopent-1-ene (2.11 g, 12.1 mmol) was dissolved in dry Et_2O (6 ml). A few drops of this solution were added to the reaction flask, and the reaction was initiated with a single iodine crystal. The rest of the solution of alkyl bromide was added slowly over 45 min, and the syringe was rinsed with Et_2O (4 ml). The reaction mixture was heated at reflux until the majority of the magnesium was visibly consumed. The reaction mixture was cooled to 0 °C, and acetone (1.0 ml) mixed with Et_2O (6 ml) was slowly added. The reaction mixture was stirred at ambient temperature for 2 h, and then quenched at 0 °C with $\text{NH}_4\text{Cl}_{(\text{aq})}$ (2 ml). The reaction mixture was diluted to approximately 40 ml with ether and washed with $\text{NH}_4\text{Cl}_{(\text{aq})}$ (40 ml). The aqueous layer was extracted twice more with Et_2O (30 ml), and the combined organic layers were dried with MgSO_4 . The volatile materials were evaporated at reduced pressure. The crude product was purified by column chromatography (20 to 33% ether gradient in pentanes; KMnO_4 to visualize) to give the title compound as a clear and colorless oil (1.33 g, 8.62 mmol, 71% yield). **^1H NMR** (500 MHz, CDCl_3) δ 5.74 – 5.70 (m, 1H), 5.69 – 5.66 (m, 1H), 2.67 – 2.55 (m, 1H), 2.41 – 2.21 (m, 2H), 2.04 (dtd, J = 13.0, 8.6, 4.6 Hz, 1H), 1.53 – 1.29 (m, 5H), 1.22 (s, 1H), 1.21 (s, 6H). **^{13}C NMR** (151 MHz, CDCl_3) δ 135.1, 130.6, 71.1, 46.0, 42.2, 32.1, 30.8, 29.9, 29.4, 29.4. **EIMS** 139.0 ($\text{M}^+ - 15$), 80.0 (base peak).

3-(3-Bromo-3-methylbutyl)cyclopent-1-ene (24). 4-(Cyclopent-2-en-1-yl)-2-methylbutan-2-ol (1.13 g, 7.35 mmol) was placed in a 1 dram vial at 0 °C. LiBr (1.05 g, 12.1 mmol, 1.65 equiv) and HBr (47% in H_2O ; 1.5 ml, 8.7 mmol, 1.2 equiv) were added, and the reaction mixture was stirred for 3 h at 0 °C and then at ambient temperature for 1 h. The reaction mixture was diluted with pentane (15 ml) and washed twice with $\text{NaHCO}_{3(\text{aq})}$ (15 ml). The combined aqueous layers were extracted with pentane (15 ml), which was washed again with $\text{NaHCO}_{3(\text{aq})}$ (15 ml) before combining. The combined organic layers were dried with MgSO_4 and filtered through a plug of silica, which was rinsed with pentane (100 ml). The volatile materials were evaporated at reduced pressure. The crude product was purified by kugelrohr distillation (70 °C, approximately 0.5 Torr) to give the title compound as a clear and colorless oil (1.08 g, 4.99 mmol, 68% yield). **^1H NMR** (500 MHz, CDCl_3) δ 5.76 – 5.71 (m, 1H), 5.70 – 5.65 (m, 1H), 2.70 – 2.60 (m, 1H), 2.41 – 2.22 (m, 2H), 2.05 (dtd, J = 12.9, 8.6, 4.6 Hz, 1H), 1.88 – 1.77 (m, 2H), 1.76 (s, 3H), 1.75 (s, 3H), 1.66

– 1.58 (m, 1H), 1.53 – 1.37 (m, 2H). ^{13}C NMR (151 MHz, CDCl_3) δ 134.8, 130.9, 68.7, 45.9, 45.5, 34.4, 34.4, 32.6, 32.2, 29.8. EIMS 217.9 (M^+ , ^{81}Br), 215.9 (M^+ , ^{79}Br), 67.0 (base peak).

Note: This alkyl bromide was stored cold.

Preparation of L_2PdHBr complexes.

The preparations of L_2PdHBr complexes were adapted with minor modifications from a literature procedure for the preparation of $(\text{Cy}_3\text{P})_2\text{PdHBr}$.⁸³

$(t\text{-Bu})\text{Cy}_2\text{P}-\overset{\text{H}}{\underset{\text{Br}}{\text{Pd}}}-\text{PCy}_2(t\text{-Bu})$ (**(Cy α -BuP) $_2$ PdHBr**. (COD)PdBr₂ (749 mg, 2.00 mmol) was suspended in degassed, dry toluene (4 ml) in a 50 ml flask under nitrogen. The reaction mixture was cooled to approximately -5 °C and stirred. NaOH (168 mg, 4.20 mmol, 2.10 equiv) was dissolved in dry methanol (2 ml) and slowly added to the reaction mixture. After the orange color dissipated, Cy α -BuP (1.07 g, 4.20 mmol, 2.10 equiv) dissolved in degassed, dry toluene (7 ml) was added to the reaction mixture. The reaction mixture was stirred at 0 °C for 2 h, then warmed to ambient temperature. Dry MeOH (20 ml) was added to precipitate the product. The mixture was cooled to 0 °C and stirred for 30 min. The crude product was collected by filtration and purified by recrystallization (warm ether layered with pentane, 3 crops) to give the title compound as colorless, blocky crystals (943 mg, 1.35 mmol, 68%). ^1H NMR (600 MHz, C_6D_6) δ 2.45 – 2.32 (m, 8H), 2.02 (d, J = 12.9 Hz, 4H), 1.80 – 1.57 (m, 20H), 1.45 – 1.16 (m, 30H), -13.52 (t, J = 7.0 Hz, 1H). ^{13}C NMR (151 MHz, C_6D_6) δ 35.2 (4C), 33.8 (2C), 32.4 (4C), 30.9 (6C), 29.7 (4C), 27.8 (4C), 27.5 (4C), 26.8 (4C). ^{31}P NMR (243 MHz, C_6D_6) δ 55.5. Analysis calc'd for $\text{C}_{32}\text{H}_{63}\text{BrP}_2\text{Pd}$: C 55.21, H 9.12; found C 55.61, H 8.99.

(1-Ad) $_2$ MeP. (1-Ad) $_2$ CIP (672 mg, 1.99 mmol) was dissolved in dry ether (10 ml) in a 25 ml Schlenk flask under N_2 . The reaction mixture was cooled to -78 °C, and a solution of MeLi (1.5 ml, 1.6 M in Et_2O , 2.4 mmol, 1.2 equiv) was slowly added to the reaction flask with stirring. The reaction mixture was stirred at -78 °C for approximately 10 minutes, then at ambient temperature for one hour. The reaction mixture was put under static vacuum and moved to a nitrogen-filled glovebox. The mixture was carefully filtered through a plug of silica, which was rinsed with ether (approximately 15 ml). The volatile materials were evaporated at reduced pressure to give the title compound as a white powder (586 mg, 1.85 mmol, 93% yield). The ^1H NMR and ^{31}P spectra were consistent with the spectra reported in the literature.⁸⁴

$\text{Ad}_2\text{MeP}-\overset{\text{H}}{\underset{\text{Br}}{\text{Pd}}}-\text{PAd}_2\text{Me}$ [**(1-Ad) $_2$ MeP] $_2$ PdHBr**. (COD)PdBr₂ (240 mg, 0.641 mmol) was suspended in degassed, dry toluene (1 ml) in a 10 ml flask under nitrogen. The reaction mixture was cooled to approximately -5 °C and stirred. NaOH (54 mg, 1.35 mmol, 2.11 equiv) was dissolved in dry methanol (0.5 ml) and slowly added to the reaction mixture. After the orange color dissipated, (1-Ad) $_2$ MeP (426 mg, 1.35 mmol, 2.11 equiv) dissolved in degassed, dry toluene (2.5 ml) was added to the reaction mixture. The reaction mixture was stirred at 0 °C for 3 h, then warmed to ambient temperature.

Dry MeOH (5 ml) was added to precipitate the product. The mixture was cooled to 0 °C and stirred for 15 min. The crude product was collected by filtration and moved to a nitrogen-filled glovebox. The crude product was dissolved in dry toluene (approximately 10 ml) and filtered through a plug of Celite, which was rinsed with toluene (3x2 ml). The solvent was evaporated at reduced pressure. The solid residue was washed twice with cold ether (4 ml) and once with pentane (4 ml). The white powder was dried under vacuum (404 mg, 0.493 mmol, 77% yield). **¹H NMR** (600 MHz, C₆D₆) δ 2.07 (q, J = 12.7 Hz, 24H), 1.94 – 1.85 (m, 12H), 1.72 (t, J = 2.4 Hz, 6H), 1.67 – 1.57 (m, 24H), -12.49 (t, J = 7.3 Hz, 1H). **¹³C NMR** (151 MHz, C₆D₆) δ 40.5 (12C), 37.8 (4C), 37.2 (12C), 29.0 (12C), 3.0 (2C). **³¹P NMR** (243 MHz, C₆D₆) δ 49.6. **Analysis** calc'd for C₄₂H₆₇BrP₂Pd: C 61.50, H 8.23; found C 62.38, H 8.46.

Note: The solid L₂PdHBr complexes are stable to brief handling in air, but solutions of the compounds should not be exposed to air. These compounds were stored cold in a nitrogen-filled glovebox.

Preparation of *N*-alkyl imines by palladium-catalyzed coupling (Table 5.5, Scheme 5.4, and Scheme 5.5)

General notes about product stability and purification: Isolation and purification of most *N*-alkyl imines is complicated due to hydrolysis and streaking during column chromatography. Isolation of the 3,3'-bis(trifluoromethyl)-substituted *N*-alkyl imines is much more straightforward. Stability to silica was determined by two-dimensional TLC (Prebasified: 5% triethylamine + varying % ethyl acetate in hexanes. Untreated: 10 or 25% ethyl acetate in hexanes). The starting 3,3'-bis(trifluoromethyl)benzophenone imine undergoes hydrolysis slowly on prebasified silica and readily on untreated silica. This compound also streaks significantly on untreated columns. However, no hydrolysis of the *N*-alkyl imine products listed below was detected on prebasified silica, and only faint hydrolysis was detected on untreated silica (varies some between compounds). These compounds do not streak significantly on either prebasified or untreated columns. Because the relative R_f values for nitrogen-containing compounds change significantly between prebasified and untreated silica, a combination of these two systems was often used to purify the *N*-alkyl imine products. R_f values on prebasified TLC plates are not well reproduced from trial to trial. With extended exposure, untreated silica gel can induce a selective hydrolysis of 3,3'-bis(trifluoromethyl)benzophenone imine in the presence of the *N*-alkyl imine products.

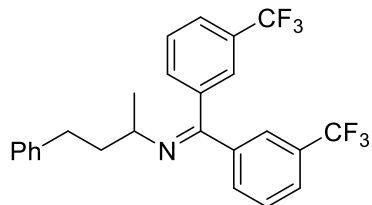
General procedures for Pd-catalyzed cross coupling of alkyl bromides with **2d** (Table 5.5).

In a nitrogen-filled glovebox, a 1 dram vial was charged with the alkyl bromide (0.300 mmol), 3,3'-bis(trifluoromethyl)benzophenone imine (**2d**) (1.5 or 3.0 equiv), (Cy₂t-BuP)₂PdHBr (11 mg, 0.016 mmol, 5.3 mol %), cesium carbonate (1.50 or 3.0 equiv), *tert*-amyl alcohol (0.40 ml; total volume approximately 0.6-0.7 ml), and a magnetic stir bar. The vial was sealed with a Teflon-lined cap and Teflon tape. The reaction mixture was heated at 80 °C with stirring for 3 or 20 h in an aluminum block. The product was isolated by column chromatography. Purification details are noted for each compound. Reaction times, equivalents of **2d**, and equivalents of Cs₂CO₃ are denoted with the letter codes A-C for each compound.

- A) **2d** (143 mg, 0.451 mmol, 1.50 equiv); Cs₂CO₃ (147 mg, 0.451 mmol, 1.50 equiv); 20 h
- B) **2d** (286-288 mg, 0.90 mmol, 3.0 equiv); Cs₂CO₃ (293 mg, 0.899 mmol, 3.00 equiv); 20 h

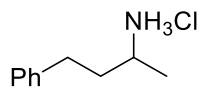
C) **2d** (286 mg, 0.902 mmol, 3.00 equiv); Cs₂CO₃ (147 mg, 0.451 mmol, 1.50 equiv); 3 h

***N*-(4-Phenylbutan-2-yl)- 3,3'-bis(trifluoromethyl)benzophenone imine (3d).**

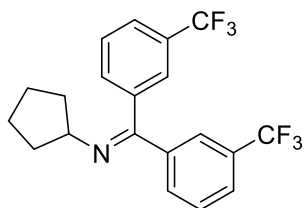


Prepared by general procedure A with 3-phenyl-1-bromobutane (63.9 mg, 0.300 mmol). Purified by column chromatography (2% triethylamine in hexanes on prebasified silica, R_f 0.46; 5% ethyl acetate in hexanes, R_f 0.25) to give the title compound as a colorless oil (trial 1: 122 mg, 0.271 mmol, 90% yield) (trial 2: 120 mg, 0.267 mmol, 89% yield). ¹H NMR (500 MHz, CDCl₃) δ 7.96 (s, 1H), 7.71 (d, *J* = 7.9 Hz, 1H), 7.64 (t, *J* = 8.8 Hz, 2H), 7.58 (t, *J* = 7.7 Hz, 1H), 7.46 (t, *J* = 7.8 Hz, 1H), 7.38 (s, 1H), 7.28 (d, *J* = 7.7 Hz, 1H), 7.23 (t, *J* = 7.5 Hz, 2H), 7.15 (t, *J* = 7.3 Hz, 1H), 7.11 (d, *J* = 7.3 Hz, 2H), 3.36 (m, 1H), 2.58 (ddd, *J* = 13.9, 10.4, 5.8 Hz, 1H), 2.46 (ddd, *J* = 13.8, 10.1, 6.1 Hz, 1H), 2.05 – 1.93 (m, 1H), 1.91 – 1.80 (m, 1H), 1.20 (d, *J* = 6.2 Hz, 3H). ¹³C NMR (151 MHz, CDCl₃) δ 163.3, 142.1, 140.3, 137.3, 131.8, 131.4 (q, *J* = 32.8 Hz), 131.2, 131.0 (q, *J* = 32.5 Hz), 129.5, 128.9, 128.5, 128.4, 126.8, 125.9, 125.6, 124.9, 124.5, 124.1 (q, *J* = 272.3 Hz), 123.9 (q, *J* = 272.6 Hz), 57.6, 39.8, 33.1, 22.1. ¹⁹F NMR (565 MHz, CDCl₃) δ -63.5, -63.6. ESI⁺ calc'd 450.1651 (M+H⁺), found 450.1649.

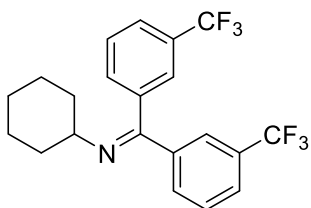
Glovebox-free preparation of **3d**: prepared as described above, with the modification that all components were weighed and mixed under air. The 1 dram vial was then flushed with funnel connected to a nitrogen line prior to sealing and heating. The title compound was isolated as a very pale yellow oil (104 mg, 0.231 mmol, 77% yield).



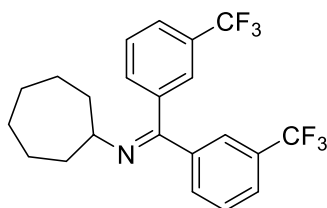
(4-Phenylbutan-2-yl)ammonium chloride. Under air, *N*-(4-Phenylbutan-2-yl)-3,3'-bis(trifluoromethyl)benzophenone imine (**3d**) (104 mg, 0.231 mmol) was dissolved in methanol (3 ml). HCl_(aq) (0.35 ml, 1.0 M, 0.35 mmol, 1.5 equiv) was added dropwise to the reaction mixture with stirring. After 60 min, the reaction mixture was diluted with ether (~5 ml) and filtered through a plug of glass wool, which was rinsed with ether (3x1 ml). The volatile materials were evaporated at reduced pressure. Ether and water (~5 ml each) were added to residue, the organic layer was removed, the aqueous layer was washed again with ether (2 ml), and the combined organic layers were extracted with water (2 ml). The volatile materials were removed from the combined aqueous layers at reduced pressure. The crude ammonium chloride salt was dissolved in DCM (3 ml) and filtered through a plug of Na₂SO₄. Addition of hexanes (~8 ml) at 0 °C caused a precipitate to form, which was collected by filtration, washed with cold hexanes (2x2 ml), and dried under vacuum to give the title compound as a white powder (38.6 mg, 0.208 mmol, 90% yield). The ¹H NMR spectrum was consistent with that reported in the literature.⁸⁵

***N*-Cyclopentyl-3,3'-bis(trifluoromethyl)benzophenone imine (6).**

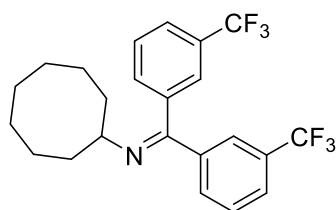
Prepared by general procedure A with bromocyclopentane (44.8 mg, 0.299 mmol). Purified by column chromatography (1 to 3% ethyl acetate gradient in hexanes, Rf 0.24 in 3% EA/Hex; 2% triethylamine in hexanes on prebasified silica, Rf 0.50) to give the title compound as a very pale yellow oil (trial 1: 88.5 mg, 0.230 mmol, 77% yield) (trial 2: 90.0 mg; 0.234 mmol, 78% yield). $^1\text{H NMR}$ (500 MHz, CDCl_3) δ 7.95 (s, 1H), 7.73 (d, $J = 7.9$ Hz, 1H), 7.65 – 7.58 (m, 3H), 7.47 – 7.40 (m, 2H), 7.36 (d, $J = 7.6$ Hz, 1H), 3.62 (p, $J = 6.6$ Hz, 1H), 1.94 – 1.83 (m, 2H), 1.78 – 1.69 (m, 4H), 1.62 – 1.52 (m, 2H). $^{13}\text{C NMR}$ (151 MHz, CDCl_3) δ 162.5, 140.5, 137.5, 131.8, 131.4, 131.4 (q, $J = 32.8$ Hz), 130.93 (q, $J = 32.4$ Hz), 129.4, 128.8, 126.6, 125.7, 124.9, 124.8, 124.2 (q, $J = 272.4$ Hz), 124.0 (q, $J = 272.5$ Hz), 63.8, 35.1, 25.3. $^{19}\text{F NMR}$ (565 MHz, CDCl_3) δ -63.6, -63.7. ESI^+ calc'd 386.1338 ($\text{M}+\text{H}^+$), found 386.1337.

***N*-Cyclohexyl-3,3'-bis(trifluoromethyl)benzophenone imine (7).**

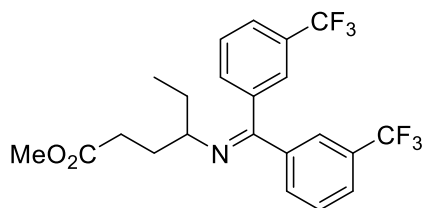
Prepared by general procedure A with bromocyclohexane (49.0 mg, 0.300 mmol). Purified by column chromatography (1 to 3% ethyl acetate gradient in hexanes, Rf 0.17 in 3% EA/Hex; 2% triethylamine in hexanes on prebasified silica, Rf 0.52) to give the title compound as a colorless oil (47.6 mg, 0.119 mmol, 40% yield). $^1\text{H NMR}$ (500 MHz, CDCl_3) δ 7.94 (s, 1H), 7.74 (d, $J = 8.0$ Hz, 1H), 7.66 – 7.61 (m, 2H), 7.60 (d, $J = 7.7$ Hz, 1H), 7.43 (t, $J = 8.1$ Hz, 1H), 7.41 (s, 1H), 7.36 (d, $J = 7.6$ Hz, 1H), 3.13 (tt, $J = 9.5, 4.4$ Hz, 1H), 1.81 – 1.71 (m, 2H), 1.69 – 1.52 (m, 5H), 1.27 (qt, $J = 12.4, 3.4$ Hz, 1H), 1.15 (qt, $J = 12.3, 3.7$ Hz, 2H). $^{13}\text{C NMR}$ (151 MHz, CDCl_3) δ 162.5, 140.5, 137.4, 131.8, 131.4 (q, $J = 32.8$ Hz), 131.2, 130.9 (q, $J = 32.4$ Hz), 129.5, 128.8, 126.7, 125.7, 124.9, 124.5, 124.2 (q, $J = 272.5$ Hz), 124.0 (d, $J = 272.6$ Hz), 62.0, 34.0, 25.7, 24.3. $^{19}\text{F NMR}$ (565 MHz, CDCl_3) δ -63.6, -63.7. ESI^+ calc'd 400.1494 ($\text{M}+\text{H}^+$), found 400.1489.

***N*-Cycloheptyl-3,3'-bis(trifluoromethyl)benzophenone imine (8).**

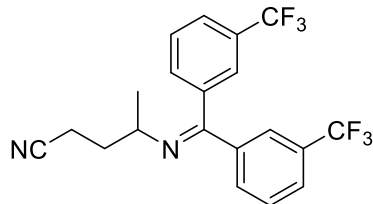
Prepared by general procedure A with bromocycloheptane (53.1 mg, 0.300 mmol). Purified by column chromatography (0 to 3% ethyl acetate gradient in hexanes, Rf 0.21 in 3% EA/Hex; 2% triethylamine in hexanes on prebasified silica, Rf 0.43) to give the title compound as a colorless oil (trial 1: 92.9 mg, 0.225 mmol, 75% yield) (trial 2: 99.4 mg, 0.240 mmol, 80% yield). $^1\text{H NMR}$ (500 MHz, CDCl_3) δ 7.93 (s, 1H), 7.73 (d, $J = 7.9$ Hz, 1H), 7.65 – 7.58 (m, 3H), 7.43 (t, $J = 7.8$ Hz, 1H), 7.40 (s, 1H), 7.35 (d, $J = 7.6$ Hz, 1H), 3.31 (tt, $J = 8.6, 4.4$ Hz, 1H), 1.82 – 1.70 (m, 4H), 1.66 – 1.47 (m, 6H), 1.40 – 1.30 (m, 2H). $^{13}\text{C NMR}$ (151 MHz, CDCl_3) δ 161.2, 140.58, 137.39, 131.83, 131.36 (q, $J = 32.7$ Hz), 131.22, 130.90 (d, $J = 32.4$ Hz), 129.42, 128.78, 126.6, 125.6, 124.9, 124.6, 124.2 (q, $J = 272.4$ Hz), 124.0 (q, $J = 272.5$ Hz), 63.6, 35.9, 28.8, 24.6. $^{19}\text{F NMR}$ (565 MHz, CDCl_3) δ -63.6, -63.7. ESI^+ calc'd 414.1651 ($\text{M}+\text{H}^+$), found 414.1650.

***N*-Cyclooctyl-3,3'-bis(trifluoromethyl)benzophenone imine (9).**

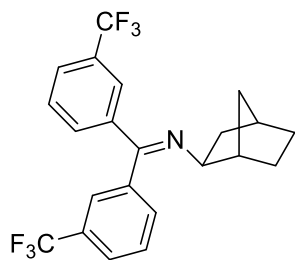
Prepared by general procedure A with bromocyclooctane (57.2 mg, 0.299 mmol). Purified by column chromatography (3% ethyl acetate in hexanes, *R_f* 0.17; 2% triethylamine in hexanes on prebasified silica, *R_f* 0.46) to give the title compound as a colorless oil (111 mg, 0.259 mmol, 86% yield). ¹H NMR (500 MHz, CDCl₃) δ 7.93 (d, *J* = 7.6 Hz, 1H), 7.73 (d, *J* = 7.9 Hz, 1H), 7.66 – 7.60 (m, 3H), 7.46 – 7.40 (m, 2H), 7.35 (d, *J* = 7.6 Hz, 1H), 3.36 (tt, *J* = 8.2, 3.7 Hz, 1H), 1.88 – 1.72 (m, 4H), 1.64 – 1.47 (m, 6H), 1.47 – 1.32 (m, 4H), 1.32 – 1.22 (m, 1H). ¹³C NMR (151 MHz, CDCl₃) δ 161.2, 140.5, 137.5, 131.8, 131.4 (q, *J* = 32.6 Hz), 131.2, 130.9 (q, *J* = 32.3 Hz), 129.4, 128.8, 126.6, 125.6, 124.9, 124.6, 124.2 (q, *J* = 272.5 Hz), 124.0 (q, *J* = 272.4 Hz), 62.5, 33.7, 27.3, 26.1, 24.0. ¹⁹F NMR (565 MHz, CDCl₃) δ -63.6, -63.7. ESI⁺ calc'd 428.1807 (M+H⁺), found 428.1808.

Methyl 4-((bis(3-(trifluoromethyl)phenyl)methylene)amino)hexanoate (10).

Prepared by general procedure A with methyl 4-bromohexanoate (62.7 mg, 0.300 mmol). Purified by column chromatography (1 to 10% ethyl acetate in hexanes, *R_f* 0.30 in 10% EA/Hex; 5% triethylamine in hexanes on prebasified silica, *R_f* 0.28) to give the title compound as a pale yellow oil (trial 1: 109 mg, 0.245 mmol, 82% yield) (trial 2: 105 mg, 0.236 mmol, 79% yield). ¹H NMR (500 MHz, CDCl₃) δ 7.95 (s, 1H), 7.73 (d, *J* = 7.9 Hz, 1H), 7.67 – 7.59 (m, 3H), 7.45 (t, *J* = 7.8 Hz, 1H), 7.41 (s, 1H), 7.36 (d, *J* = 7.6 Hz, 1H), 3.57 (s, 3H), 3.15 (p, *J* = 6.3 Hz, 1H), 2.32 – 2.19 (m, 2H), 1.99 – 1.87 (m, 2H), 1.65 – 1.56 (m, 2H), 0.81 (t, *J* = 7.4 Hz, 3H). ¹³C NMR (151 MHz, CDCl₃) δ 173.9, 164.1, 140.1, 137.3, 131.8, 131.4, 131.4 (q, *J* = 32.7 Hz), 130.9 (q, *J* = 32.5 Hz), 129.4, 128.9, 126.9, 125.6, 124.8 (2C), 124.1 (d, *J* = 272.5 Hz), 123.9 (d, *J* = 272.4 Hz), 63.0, 51.6, 31.0, 31.0, 29.2, 11.0. ¹⁹F NMR (565 MHz, CDCl₃) δ -63.6, -63.7. ESI⁺ calc'd 446.1549 (M+H⁺), found 446.1549.

4-((Bis(3-(trifluoromethyl)phenyl)methylene)amino)pentanenitrile (11).

Prepared by general procedure A with 4-bromopentanenitrile (48.6 mg, 0.300 mmol). Purified by column chromatography (1 to 25% ethyl acetate gradient in hexanes, very slowly to allow all 3,3'-bis(trifluoromethyl)benzophenone imine to hydrolyze, *R_f* 0.50 in 25% EA/Hex) to give the title compound as a pale yellow oil (trial 1: 90.4 mg, 0.227 mmol, 76% yield) (trial 2: 89.2 mg, 0.224 mmol, 75%). ¹H NMR (500 MHz, CDCl₃) δ 7.99 (s, 1H), 7.76 (d, *J* = 7.9 Hz, 1H), 7.70 – 7.65 (m, 2H), 7.61 (d, *J* = 7.9 Hz, 1H), 7.46 (t, *J* = 7.8 Hz, 1H), 7.44 (s, 1H), 7.40 (d, *J* = 7.6 Hz, 1H), 3.47 (dq, *J* = 9.8, 6.3, 3.5 Hz, 1H), 2.41 – 2.27 (m, 2H), 2.08 – 2.00 (m, 1H), 1.91 – 1.81 (m, 1H), 1.16 (d, *J* = 6.3 Hz, 3H). ¹³C NMR (151 MHz, CDCl₃) δ 165.3, 139.7, 136.6, 131.9, 131.7 (q, *J* = 32.8 Hz), 131.1, 131.1 (q, *J* = 32.5 Hz), 129.8, 129.0, 127.2, 126.0, 124.8, 124.3, 124.1 (q, *J* = 272.4 Hz), 123.8 (q, *J* = 272.5 Hz), 119.6, 56.0, 33.6, 21.6, 14.5. ¹⁹F NMR (565 MHz, CDCl₃) δ -63.6, -63.7. ESI⁺ calc'd 399.1290 (M+H⁺), found 399.1289.

Exo-2-((bis(3-(trifluoromethyl)phenyl)methylene)amino)norbornane (12).

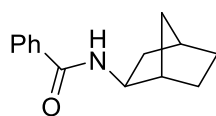
Prepared by general procedure A with *exo*-2-bromonorbornane or *endo*-2-bromonorbornane (52.5 mg, 0.300 mmol). Purified by column chromatography (0 to 3% ethyl acetate gradient in hexanes, R_f 0.21 in 3% EA/Hex; 2% triethylamine in hexanes on prebasified silica, R_f 0.46) to give the title compound as a colorless oil. ¹H NMR (600 MHz, CDCl₃) δ 7.93 (s, 1H), 7.73 (d, *J* = 7.9 Hz, 1H), 7.64 – 7.59 (m, 3H), 7.43 (t, *J* = 7.8 Hz, 1H), 7.40 (s, 1H), 7.34 (d, *J* = 7.6 Hz, 1H), 3.16 (d, *J* = 7.4 Hz, 1H), 2.32 (s, 1H), 2.14 (s, 1H), 2.06 (d, *J* = 9.3 Hz, 1H), 1.52 – 1.44 (m, 3H), 1.40 (dd, *J* = 12.0, 7.6 Hz, 1H), 1.27 (d, *J* = 9.6 Hz, 1H), 1.05 (t, *J* = 8.3 Hz, 1H), 0.97 (t, *J* = 8.4 Hz, 1H). ¹³C NMR (151 MHz, CDCl₃) δ 161.3, 140.5, 137.6, 131.8, 131.6, 131.3 (q, *J* = 32.7 Hz), 130.9 (q, *J* = 32.4 Hz), 129.3, 128.8, 126.6, 125.6, 125.0, 124.9, 124.2 (q, *J* = 272.4 Hz), 124.0 (d, *J* = 272.6 Hz) 65.8, 44.6, 41.0, 36.4, 36.1, 29.1, 26.5. ¹⁹F NMR (565 MHz, CDCl₃) δ -63.6, -63.7. ESI⁺ calc'd 412.1494 (M+H⁺), found 412.1490.

With *exo*-2-bromonorbornane: 48.6 mg, 0.118 mmol, 39% yield.

With *endo*-2-bromonorbornane; trial 1: 56.4 mg, 0.137 mmol, 46% yield; trial 2: 42.1 mg, 0.102 mmol, 34% yield.

Note: The ¹H NMR spectrum obtained from every sample of *exo*-2-((bis(3-(trifluoromethyl)phenyl)methylene)amino)norbornane contains a set of small signals which are presumed to originate from the *endo* isomer of the compound. Integration of the signal at 3.51 ppm (expected to correspond to the C-2 hydrogen of the *endo* isomer) indicates that the samples contain approximately 2% of the *endo* compound (same in every sample).

Exo-stereochemistry of the major isomer of **12** was confirmed by conversion to the corresponding benzamide:

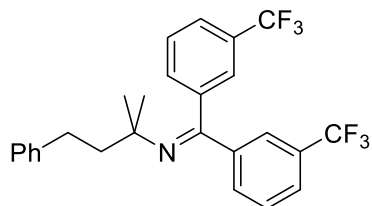
**Exo-2-(benzoylamino)norbornane.**

Exo-2-((bis(3-(trifluoromethyl)phenyl)methylene)amino)norbornane (**12**) (126 mg, 0.306 mmol) and 0.5 M HCl_(aq) (6 ml) were mixed in a 20 ml vial. The vial was flushed with nitrogen and sealed with a Teflon-lined cap. The reaction mixture was heated at 80 °C with stirring for 4 h in an aluminum heating block. The mixture was washed twice with ether (4 ml). The organic layers were extracted with 0.5 M HCl_(aq), and the combined aqueous layers were basified with K₂CO₃ (2.0 g). The mixture was extracted four times with DCM (6 ml). The organic layers were filtered through a plug of Na₂SO₄ into a 20 ml vial. The volatile materials were evaporated at reduced pressure, and the vial flushed with nitrogen.

The crude amine was dissolved in dry DCM (8 ml). Triethylamine (0.13 ml, 93 mg, 0.92 mmol, 3.0 equiv) was added, and the reaction mixture cooled to 0 °C. BzCl (53 μl, 65 mg, 0.46 mmol, 1.5 equiv) was added slowly, and the reaction mixture was stirred at ambient temperature for 13 h. The mixture was diluted to approximately 10 ml with DCM, transferred to a separatory funnel, and washed with 0.5 M HCl_(aq) (approximately 8 ml). The aqueous layer was extracted thrice

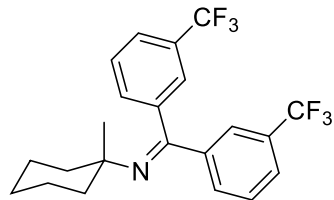
more with DCM (6 ml). The combined organic layers were dried with MgSO_4 . The volatile materials were evaporated at reduced pressure. The crude product was purified by column chromatography (1 to 25% ethyl acetate gradient in hexanes, R_f 0.43 in 25% EA/Hex) to give *exo*-2-(benzoylamino)norbornane as a white solid (50.8 mg, 0.236 mmol, 77% yield, 98% *exo*). The ^1H NMR spectrum was consistent with the spectrum reported in the literature.⁸⁶ The % *exo* was determined by the relative integration of the C-2 ^1H NMR signals at 3.92 and 4.32 ppm for the *exo* and *endo* isomers, respectively.

***N*-(2-methyl-4-phenylbutan-2-yl)-3,3'-bis(trifluoromethyl)benzophenone imine (13).**

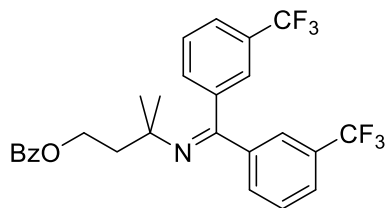


Prepared by general procedure B with 3-bromo-3-methyl-1-phenylbutane (68.1 mg, 0.300 mmol). Purified by column chromatography (1 to 3% ethyl acetate gradient in hexanes, R_f 0.23 in 3% EA/Hex; 2% triethylamine in hexanes on prebasified silica, R_f 0.32) to give the title compound as a pale yellow oil (109 mg, 0.235 mmol, 78% yield). ^1H NMR (500 MHz, CDCl_3) δ 7.98 (s, 1H), 7.72 (d, J = 7.9 Hz, 1H), 7.62 (d, J = 7.8 Hz, 1H), 7.59 (t, J = 7.7 Hz, 1H), 7.55 (d, J = 7.9 Hz, 1H), 7.49 (s, 1H), 7.44 – 7.40 (m, 2H), 7.30 (t, J = 7.5 Hz, 2H), 7.22 (d, J = 7.3 Hz, 2H), 7.19 (t, J = 7.3 Hz, 1H), 2.81 – 2.73 (m, 2H), 1.96 – 1.87 (m, 2H), 1.09 (s, 6H). ^{13}C NMR (151 MHz, CDCl_3) δ 160.6, 143.2, 142.0, 140.0, 131.8, 131.4, 131.0 (q, J = 32.7 Hz), 130.8 (q, J = 32.4 Hz), 128.9, 128.7, 128.5, 128.5, 126.5, 125.8, 125.4, 125.2, 124.6, 124.2 (q, J = 272.4 Hz), 124.0 (q, J = 272.6 Hz), 59.8, 48.6, 3.4, 28.8. ^{19}F NMR (565 MHz, CDCl_3) δ -63.6, -63.7. ESI^+ calc'd 464.1807 ($\text{M}+\text{H}^+$), found 464.1807.

***N*-(1-methylcyclohexyl)-3,3'-bis(trifluoromethyl)benzophenone imine (14).**

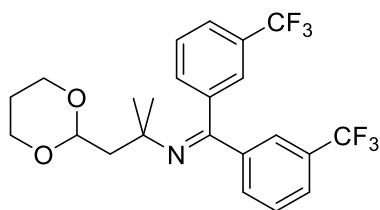


Prepared by general procedure B with 1-bromo-1-methylcyclohexane (53.1 mg, 0.300 mmol). Purified by column chromatography (0 to 3% ethyl acetate gradient in hexanes, R_f 0.24 in 3% EA/Hex; 5% triethylamine in hexanes on prebasified silica, R_f 0.57) to give the title compound as a pale yellow oil (68.4 mg, 0.165 mmol, 55% yield). ^1H NMR (500 MHz, CDCl_3) δ 7.94 (s, 1H), 7.70 (d, J = 7.9 Hz, 1H), 7.63 – 7.53 (m, 3H), 7.47 (s, 1H), 7.44 – 7.37 (m, 2H), 1.73 – 1.64 (m, 2H), 1.64 – 1.49 (m, 3H), 1.49 – 1.38 (m, 2H), 1.36 – 1.23 (m, 3H), 1.01 (s, 3H). ^{13}C NMR (151 MHz, CDCl_3) δ 160.2, 142.0, 140.2, 131.3, 131.2, 130.7 (q, J = 32.5 Hz), 130.6 (q, J = 32.2 Hz), 128.6, 128.4, 126.2, 125.1, 124.7, 124.3, 124.0 (q, J = 272.5 Hz), 123.8 (q, J = 272.5 Hz), 59.2, 40.32, 28.1, 25.8, 22.8. ^{19}F NMR (565 MHz, CDCl_3) δ -63.6, -63.8. ESI^+ calc'd 414.1651 ($\text{M}+\text{H}^+$), found 414.1646.

***N*-(1-(1,3-dioxan-2-yl)-2-methylpropan-2-yl)-3,3'-bis(trifluoromethyl)benzophenone imine (15).**

Prepared by general procedure B with 3-bromo-3-methylbutyl benzoate (81.4 mg, 0.300 mmol). Purified by column chromatography (5% triethylamine in hexanes on prebasified silica, Rf 0.37; 0 to 10% ethyl acetate gradient in hexanes, Rf 0.42 in 10% EA/Hex; 5% DCM in toluene, Rf 0.46) to give the title compound as a clear and colorless oil (115 mg, 0.227 mmol, 76%

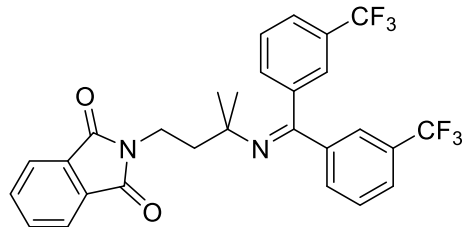
yield). **¹H NMR** (500 MHz, CDCl₃) δ 8.01 (d, *J* = 7.1 Hz, 2H), 7.85 (s, 1H), 7.72 (d, *J* = 7.9 Hz, 1H), 7.62 – 7.56 (m, 3H), 7.53 (t, *J* = 7.4 Hz, 1H), 7.49 (s, 1H), 7.44 – 7.36 (m, 4H), 4.59 (t, *J* = 7.0 Hz, 2H), 2.11 (t, *J* = 7.0 Hz, 2H), 1.12 (s, 6H). **¹³C NMR** (151 MHz, CDCl₃) δ 166.8, 161.1, 141.6, 139.8, 132.9, 131.7, 131.4, 131.0 (q, *J* = 32.8 Hz), 130.8 (q, *J* = 32.3 Hz), 130.6, 129.6, 129.0, 128.7, 128.4, 126.6, 125.5, 125.1, 124.6, 124.1 (q, *J* = 272.5 Hz), 123.9 (q, *J* = 272.8 Hz) 62.59, 59.04, 44.73, 29.18. **¹⁹F NMR** (565 MHz, CDCl₃) δ -63.6, -63.7. **ESI⁺** calc'd 508.1706 (M+H⁺), found 508.1698.

***N*-(1-(1,3-dioxan-2-yl)-2-methylpropan-2-yl)-3,3'-bis(trifluoromethyl)benzophenone imine (16).**

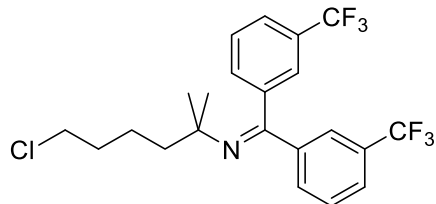
Prepared by general procedure B with 2-(2-bromo-2-methylpropyl)-1,3-dioxane (66.9 mg, 0.300 mmol). Purified by column chromatography (0/5/95 to 20/5/75 EA/TEA/Hex gradient on prebasified silica, Rf 0.62 in 20/5/75 EA/TEA/Hex; 0 to 25% ethyl acetate gradient in hexanes, Rf 0.59 in 25% EA/Hex) to give the title compound as a pale yellow oil (91.4 mg, 0.19 mmol, 66%

yield). **¹H NMR** (600 MHz, CDCl₃) δ 8.00 (s, 1H), 7.71 (d, *J* = 7.7 Hz, 1H), 7.61 (d, *J* = 7.5 Hz, 1H), 7.58 (t, *J* = 7.7 Hz, 1H), 7.48 (s, 2H), 7.41 (q, *J* = 7.5 Hz, 2H), 4.88 (t, *J* = 4.2 Hz, 1H), 4.12 (dd, *J* = 11.5, 4.6 Hz, 2H), 3.81 (t, *J* = 12.1 Hz, 2H), 2.09 (qt, *J* = 12.6, 5.0 Hz, 1H), 1.92 (d, *J* = 3.7 Hz, 2H), 1.35 (d, *J* = 13.4 Hz, 1H), 1.06 (s, 6H). **¹³C NMR** (151 MHz, CDCl₃) δ 160.4, 142.0, 139.9, 131.7, 131.6, 130.9 (q, *J* = 32.8 Hz), 130.8 (q, *J* = 32.4 Hz), 128.9, 128.7, 126.4, 125.4, 125.2 (q, *J* = 3.6 Hz), 124.7, 124.2 (q, *J* = 272.4 Hz), 123.9 (q, *J* = 272.5 Hz), 101.4, 67.1, 58.5, 51.3, 29.6, 25.9. **¹⁹F NMR** (565 MHz, CDCl₃) δ -63.6, -63.7. **ESI⁺** calc'd 460.1706 (M+H⁺), found 460.1696.

Note: this compound hydrolyzed slightly during column chromatography on untreated silica, leading to a 2 mol% ketone impurity detected in the ¹H and ¹⁹F NMR spectra.

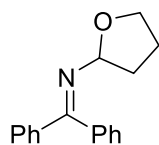
***N*-(3-((bis(3-(trifluoromethyl)phenyl)methylene)amino)-3-methylbutyl)phthalimide (17).**

Prepared by general procedure C with *N*-(3-bromo-3-methylbutyl)phthalimide (88.8 mg, 0.300 mmol). Purified by column chromatography (0/5/95 to 20/5/75 EA/TEA/Hex gradient on prebasified silica, *R_f* 0.48 in 20/5/75 EA/TEA/Hex; 0 to 25% ethyl acetate gradient in hexanes, *R_f* 0.54) to give the title compound as a clear and colorless oil, which solidified into a white solid on standing (119 mg, 0.223 mmol, 74% yield). ¹H NMR (600 MHz, CDCl₃) δ 7.73 (s, 1H), 7.72 – 7.67 (m, 3H), 7.62 – 7.54 (m, 4H), 7.53 – 7.46 (m, 3H), 7.28 (t, *J* = 8.4 Hz, 1H), 3.93 (t, *J* = 7.3 Hz, 2H), 2.04 (t, *J* = 7.3 Hz, 2H), 1.07 (s, 6H). ¹³C NMR (151 MHz, CDCl₃) δ 168.6, 161.1, 141.6, 139.7, 133.8, 132.3, 131.8, 131.3, 130.9 (q, *J* = 32.7 Hz), 130.5 (q, *J* = 32.3 Hz), 128.9, 128.5, 126.4, 125.4, 125.2, 124.5, 124.1 (q, *J* = 272.5 Hz), 123.9 (q, *J* = 272.6 Hz), 123.0, 59.3, 44.4, 34.8, 28.7. ¹⁹F NMR (565 MHz, CDCl₃) δ -63.6, -63.7. ESI⁺ calc'd 533.1658 (M+H⁺), found 533.1646.

***N*-(6-chloro-2-methylhexan-2-yl)-3,3'-bis(trifluoromethyl)benzophenone imine (18).**

Prepared by general procedure C with 5-bromo-1-chloro-5-methylhexane (64.1 mg, 0.300 mmol). Purified by column chromatography (0 to 10% ethyl acetate gradient in hexanes, *R_f* 0.24 in 3% EA/Hex; 2% triethylamine in hexanes on prebasified silica, *R_f* 0.48) to give the title compound as a pale yellow oil (82.3 mg, 0.183 mmol, 61% yield). ¹H NMR (500 MHz, CDCl₃) δ 7.90 (s, 1H), 7.71 (d, *J* = 7.9 Hz, 1H), 7.63 – 7.55 (m, 2H), 7.53 (d, *J* = 7.9 Hz, 1H), 7.48 – 7.45 (m, 1H), 7.43 – 7.37 (m, 2H), 3.57 (t, *J* = 6.6 Hz, 2H), 1.82 – 1.72 (m, 2H), 1.62 – 1.50 (m, 4H), 1.04 (s, 6H). ¹³C NMR (151 MHz, CDCl₃) δ 160.5, 142.0, 140.0, 131.7, 131.4, 130.9 (q, *J* = 32.4 Hz), 130.8 (q, *J* = 32.3 Hz), 128.9, 128.7, 126.5, 125.4, 125.2, 124.6, 124.2 (q, *J* = 272.4 Hz), 123.9 (q, *J* = 272.6 Hz), 59.8, 45.3, 45.2, 33.2, 28.9, 22.1. ¹⁹F NMR (565 MHz, CDCl₃) δ -63.7, -63.7. ESI⁺ calc'd 450.1418 (M+H⁺), found 450.1412.

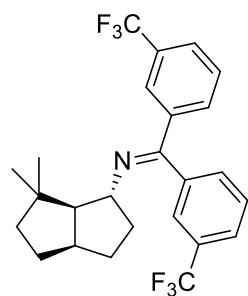
Note: a side product resulting from elimination of the alkyl chloride was also detected in this reaction mixture, but it was removed by column chromatography.



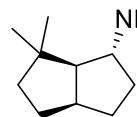
***N*-(tetrahydrofuran-2-yl)benzophenone imine (23).** In a nitrogen-filled glovebox, a 20 ml vial was charged with benzophenone imine (**2a**) (54.4 mg, 0.300 mmol), *i*-PrBr (74 mg, 0.60 mmol, 2.0 equiv), [Cy₂(*t*-Bu)P]₂PdHBr (11 mg, 0.016 mmol, 5.3 mol %), cesium carbonate (147 mg, 0.451 mmol, 1.50 equiv), THF (6.0 ml; total volume approximately 6 ml), and a magnetic stir bar. The vial was sealed with a Teflon-lined cap and Teflon tape. The reaction mixture was heated at 80 °C with stirring for 48 h in an aluminum block. The product was isolated by column chromatography (5% triethylamine in hexanes on prebasified silica, *R_f* 0.43; 0 to 10% ethyl acetate gradient in hexanes, *R_f* 0.22 – some hydrolysis occurs on untreated silica) to give the title compound as a clear and colorless oil (33.0 mg, 0.131 mmol, 44% yield). ¹H NMR (500 MHz, CDCl₃) δ 7.64 (d, *J* = 7.2 Hz, 2H), 7.48 – 7.42 (m, 3H), 7.38 (t, *J* = 7.3 Hz, 1H), 7.32 (t, *J* = 7.4 Hz, 2H), 7.19 (d, *J* = 7.7 Hz, 2H), 5.18 (dd, *J* =

6.3, 3.9 Hz, 1H), 4.22 (q, $J = 7.2$ Hz, 1H), 3.90 (td, $J = 7.8, 7.4, 5.4$ Hz, 1H), 2.22 – 2.10 (m, 1H), 2.01 – 1.94 (m, 1H), 1.89 – 1.78 (m, 2H). ^{13}C NMR (151 MHz, CDCl_3) δ 167.0, 139.5, 136.8, 130.4, 128.9, 128.7, 128.5, 128.1, 128.0, 91.9, 68.0, 34.2, 25.6. ESI^+ calc'd 252.1383 ($\text{M}+\text{H}^+$), found 252.1381.

2-((Bis(3-(trifluoromethyl)phenyl)methylene)amino)-8,8-dimethylbicyclo[3,3,0]octane (25).



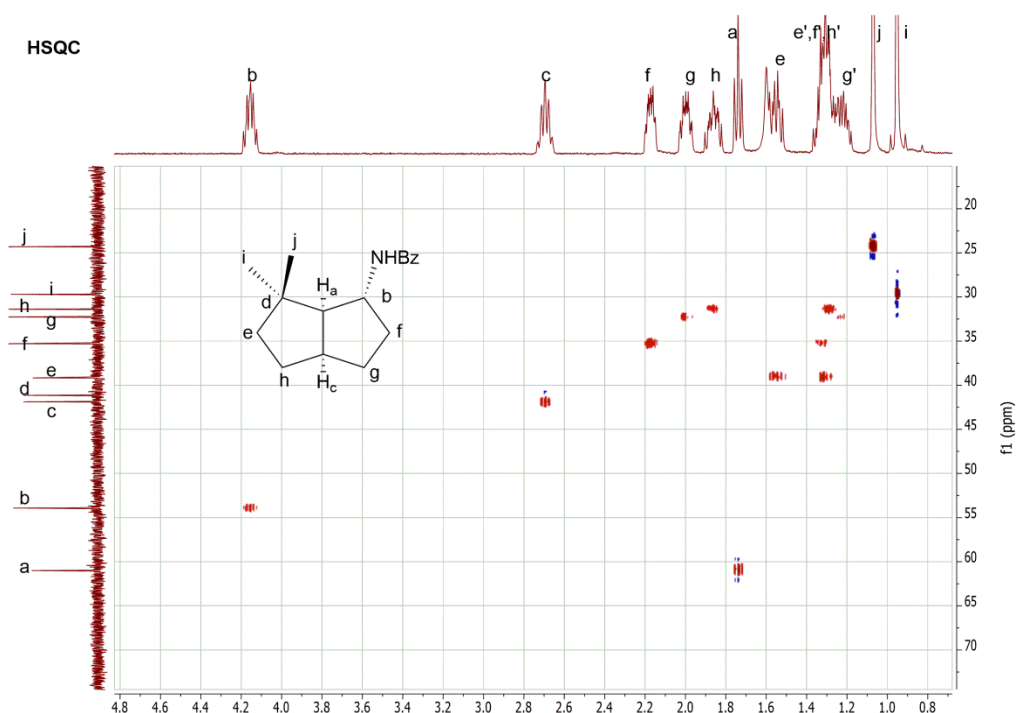
Prepared according to general procedure A for Pd-catalyzed radical amination with 3-(3-bromo-3-methylbutyl)cyclopent-1-ene (**24**) (65.1 mg, 0.300 mmol). The crude product was purified by column chromatography (1 to 3% ethyl acetate gradient in hexanes; R_f 0.30 in 3% EA/Hex) to give the title compound as a pale yellow oil (trial 1: 87.6 mg, 0.193 mmol, 64% yield) (trial 2: 86.5 mg, 0.191 mmol, 64% yield). ^1H NMR (500 MHz, CDCl_3) δ 7.90 (s, 1H), 7.74 (d, $J = 7.9$ Hz, 1H), 7.66 – 7.60 (m, 3H), 7.47 – 7.41 (m, 2H), 7.37 (d, $J = 7.6$ Hz, 1H), 3.33 (dt, $J = 8.5, 6.4$ Hz, 1H), 2.86 – 2.73 (m, 1H), 2.29 (dd, $J = 9.4, 7.0$ Hz, 1H), 2.14 – 2.02 (m, 2H), 1.85 – 1.69 (m, 2H), 1.68 – 1.60 (m, 1H), 1.22 – 1.09 (m, 4H), 0.91 (s, 3H), 0.68 (s, 3H). ^{13}C NMR (151 MHz, CDCl_3) δ 162.6, 140.6, 137.7, 131.7, 131.4, 131.3 (q, $J = 33.1$ Hz), 130.9 (q, $J = 32.4$ Hz), 129.3, 128.8, 126.6, 125.7, 124.9, 124.2 (q, $J = 272.6$ Hz), 124.0 (q, $J = 273.0$ Hz), 77.0, 66.7, 62.7, 43.3, 41.3, 39.9, 36.7, 33.2, 31.3, 29.7, 25.0. ^{19}F NMR (565 MHz, CDCl_3) δ -63.6, -63.8. ESI^+ calc'd 454.1964 ($\text{M}+\text{H}^+$), found 454.1963.



2-Benzamido-8,8-dimethylbicyclo[3,3,0]octane. *N*-(8,8-dimethylbicyclo[3,3,0]octan-2-yl)-3,3'-bis(trifluoromethyl) benzophenone imine (**25**) (130 mg, 0.287 mmol) and 0.5 M $\text{HCl}_{(\text{aq})}$ (6 ml) were mixed in a 20 ml vial. The vial was flushed with nitrogen and sealed with a Teflon-lined cap. The reaction mixture was heated at 80 °C with stirring for 4 h in an aluminum heating block. The mixture was washed twice with ether (4 ml). The organic layers were extracted with 0.5 M $\text{HCl}_{(\text{aq})}$ (4 ml), and the combined aqueous layers were basified with K_2CO_3 (2.0 g). The mixture was extracted four times with DCM (6 ml). The organic layers were filtered through a plug of Na_2SO_4 into a 25 ml flask. The volatile materials were evaporated at reduced pressure, and the flask refilled with nitrogen. The crude amine was dissolved in dry DCM (8 ml). Triethylamine (0.12 ml, 87 mg, 0.86 mmol, 3.0 equiv) was added, and the reaction mixture cooled to 0 °C. BzCl (50 μl , 61 mg, 0.43 mmol, 1.5 equiv) was added slowly, and the reaction mixture was stirred at ambient temperature for 14 h. The mixture was diluted to approximately 10 ml with DCM, transferred to a separatory funnel, and washed with 0.5 M $\text{HCl}_{(\text{aq})}$ (approximately 8 ml). The aqueous layer was extracted thrice more with DCM (6 ml). The combined organic layers were dried with MgSO_4 . The volatile materials were evaporated at reduced pressure. The crude product was purified by column chromatography (1 to 25% ethyl acetate gradient in hexanes, R_f 0.43 in 25% EA/Hex) to give the title compound as a white solid (56.3 mg, 0.219 mmol, 76% yield). ^1H NMR (500 MHz, CDCl_3) δ 7.74 (d, $J = 7.0$ Hz, 2H), 7.49 (t, $J = 7.3$ Hz, 1H), 7.43 (t, $J = 7.4$ Hz, 2H), 5.94 (d, $J = 6.6$ Hz, 1H), 4.16 (qd, $J = 8.6, 6.1$ Hz, 1H), 2.77 – 2.63 (m, 1H), 2.17 (dtd, $J = 11.5, 5.8, 2.2$ Hz, 1H), 2.06 – 1.95 (m, 1H), 1.86 (dddd, $J = 12.9, 11.1, 9.3, 7.2$ Hz, 1H), 1.74 (t, $J = 9.1$ Hz, 1H), 1.55 (td, $J =$

12.2, 7.8 Hz, 1H), 1.40 – 1.16 (m, 4H), 1.07 (s, 3H), 0.95 (s, 3H). ^{13}C NMR (151 MHz, CDCl_3) δ 166.9, 135.3, 131.4, 128.7, 126.9, 61.0, 53.9, 41.9, 41.1, 39.2, 35.3, 32.3, 31.4, 29.7, 24.3. ESI^+ calc'd 258.1852 ($\text{M}+\text{H}^+$), found 258.1856; calc'd ($\text{M}+\text{Na}^+$) 280.1672, found 280.1670.

The relative configurations of this compound were assigned by 2D NMR spectroscopy, as shown below. The carbon skeleton was assigned unambiguously by HSQC and COSY NMR spectra. Strong NOESY correlations of H_a to H_c , H_i , and NH were observed. Only a weak NOESY correlation between H_a and H_b was observed, and no NOESY correlation between H_b and H_c was detected. These spectra are most consistent with the diastereomer drawn.



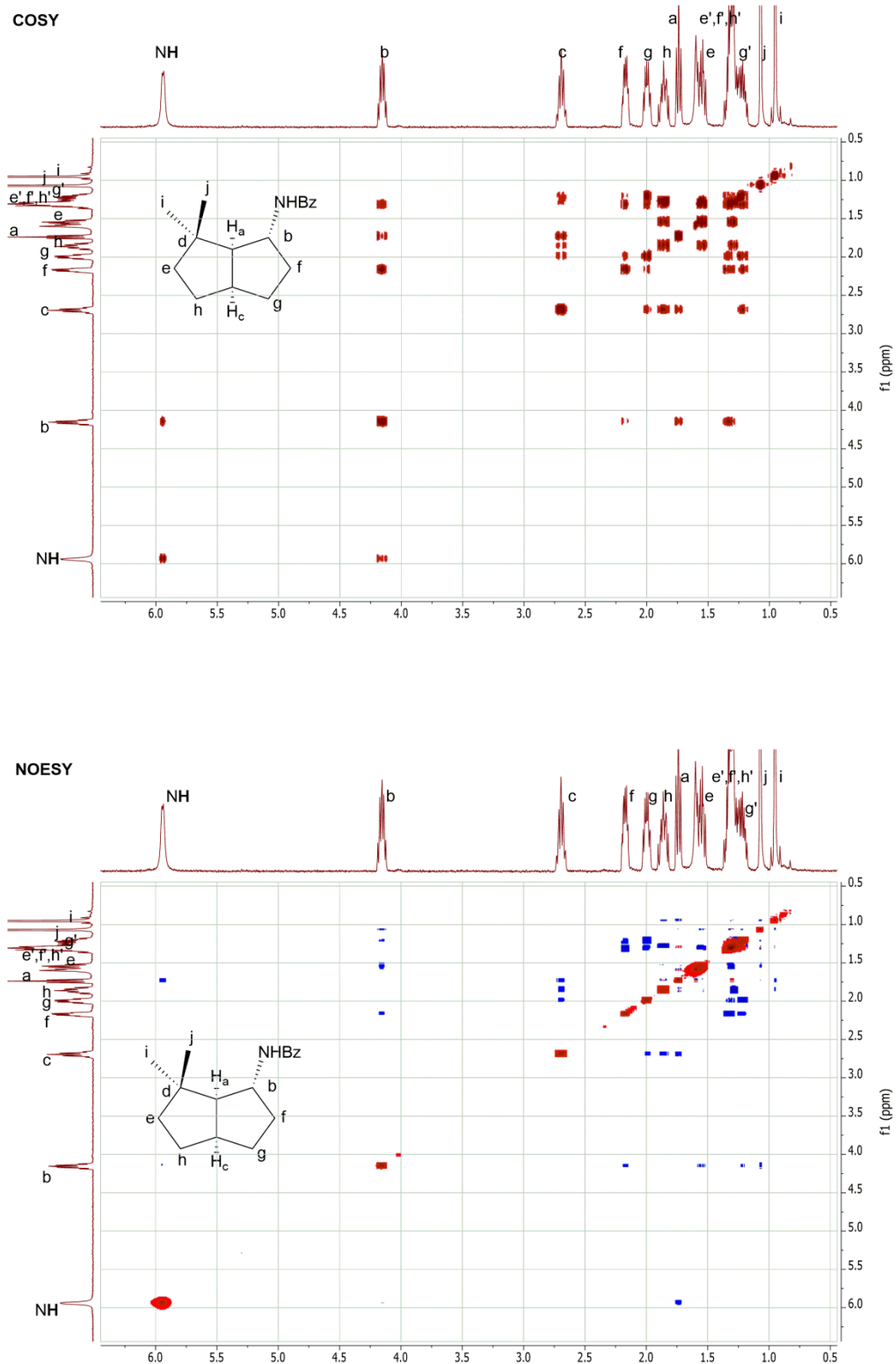
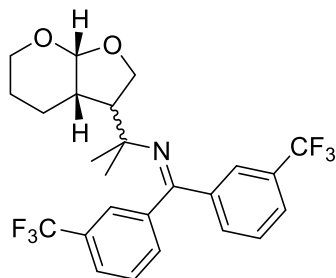


Figure 5.1. 2-Dimensional gradient enhanced ^1H - ^{13}C HSQC, ^1H - ^1H COSY, and ^1H - ^1H NOESY spectra for 2-benzamido-8,8-dimethylbicyclo[3,3,0]octane.

***N*-(2-(hexahydro-4H-furo[2,3-b]pyran-3-yl)propan-2-yl)-3,3'-bis(trifluoromethyl)-benzophenone imine (27).**



In a nitrogen-filled glovebox, a 1 dram vial was charged with *trans*-3-bromo-2-((3-methylbut-2-en-1-yl)oxy)tetrahydro-2H-pyran (**26**) (99.7 mg, 0.400 mmol), 3,3'-bis(trifluoromethyl)benzophenone imine (**2d**) (192 mg, 0.605 mmol, 1.51 equiv), [(1-Ad)₂MeP]₂PdHBr (17 mg, 0.021 mmol, 5.2 mol %), cesium carbonate (195 mg, 0.599 mmol, 1.50 equiv), *tert*-amyl alcohol (3 ml), and a magnetic stir bar. The vial was sealed with a Teflon-lined cap and Teflon tape. The reaction mixture was heated at 80 °C with stirring for 20 h in an aluminum

block. The reaction mixture was diluted to approximately 20 ml with ether, and the mixture was washed with NaHCO_{3(aq)} (~15 ml) and brine (~15 ml). The organic layer was filtered through a plug of Na₂SO₄. The volatile materials were evaporated at reduced pressure. The crude product was purified by column chromatography (0 to 50% ethyl acetate gradient in hexanes, R_f 0.34 in 25% EA/Hex; 0/5/95 to 10/5/85 EA/TEA/Hex gradient on prebasified silica, R_f 0.48 in 10/5/85 EA/TEA/Hex) to give the title compound as a very viscous, clear, and colorless oil (142 mg, 0.293 mmol, 73% yield).

Note: This compound formed as a 2:3 mixture of diastereomers. NMR signals were assigned to either the major or minor isomer by their integrals, and these assignments were confirmed through HSQC and HMBC correlations.

¹H NMR (600 MHz, CDCl₃):

Aryl (major and minor overlap): δ 7.89(major) or 7.80(minor) (s, 1H), 7.73 (d, *J* = 7.8 Hz, 1H), 7.65 – 7.55 (m, 3H), 7.47 – 7.35 (m, 3H).

Aliphatic (major): δ 5.29 (d, *J* = 3.4 Hz, 1H), 4.54 (dd, *J* = 10.9, 7.6 Hz, 1H), 4.07 (t, *J* = 7.8 Hz, 1H), 3.89 – 3.82 (m, 1H), 3.72 – 3.65 (m, 1H), 2.38 – 2.29 (m, 1H), 2.07 (dddd, *J* = 12.2, 8.7, 6.1, 3.3 Hz, 1H), 1.99 – 1.91 (m, 1H), 1.66 – 1.60 (m, 1H), 1.58 – 1.49 (m, 2H), 1.05 (s, 3H), 0.97 (s, 3H).

Aliphatic (minor): δ 5.13 (d, *J* = 3.8 Hz, 1H), 4.26 (t, *J* = 8.7 Hz, 1H), 3.97 (dd, *J* = 8.6, 6.3 Hz, 1H), 3.93 (dtd, *J* = 11.5, 4.0, 1.6 Hz, 1H), 3.50 (td, *J* = 10.7, 2.7 Hz, 1H), 2.43 (td, *J* = 8.6, 6.3 Hz, 1H), 2.38 – 2.29 (m, 1H), 1.99 – 1.82 (m, 2H), 1.80 – 1.69 (m, 1H), 1.43 (dq, *J* = 13.8, 3.9 Hz, 1H), 1.03 (s, 3H), 0.93 (s, 3H).

¹³C NMR (151 MHz, CDCl₃):

CF₃ (only two signals observed; major and minor likely overlap): δ 124.1 (q, *J* = 272.5 Hz), 123.9 (d, *J* = 272.7 Hz).

C-CF₃ (unable to assign major and minor): δ 131.1 (q, *J* = 32.7 Hz), 131.1 (q, *J* = 32.3 Hz), 130.9 (q, *J* = 32.4 Hz), 130.8 (q, *J* = 32.2 Hz).

Other aryl (major): δ 159.8, 141.6, 140.0, 131.5, 131.3, 129.0, 128.9, 126.6, 125.6, 125.0, 124.6.

Aliphatic (major): δ 101.7, 65.7, 61.3, 59.7, 55.1, 37.1, 29.3, 28.3, 23.8, 21.0.

Other aryl (minor): δ 161.6, 141.6, 139.9, 131.7, 131.4, 129.0, 128.8, 126.7, 125.6, 125.1, 124.8.

Aliphatic (minor): δ 102.9, 70.2, 64.3, 61.1, 52.9, 40.0, 27.7, 27.4, 25.3, 21.3.

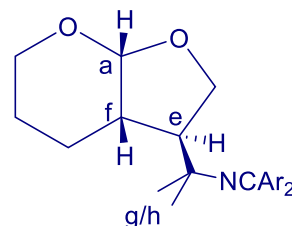
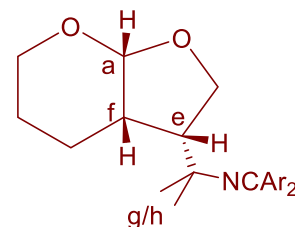
¹⁹F NMR (565 MHz, CDCl₃) δ -63.7(major), -63.7(minor), -63.8(minor), -63.8(major).

ESI⁺ calc'd 486.1862 (M+H⁺), found 486.1857.

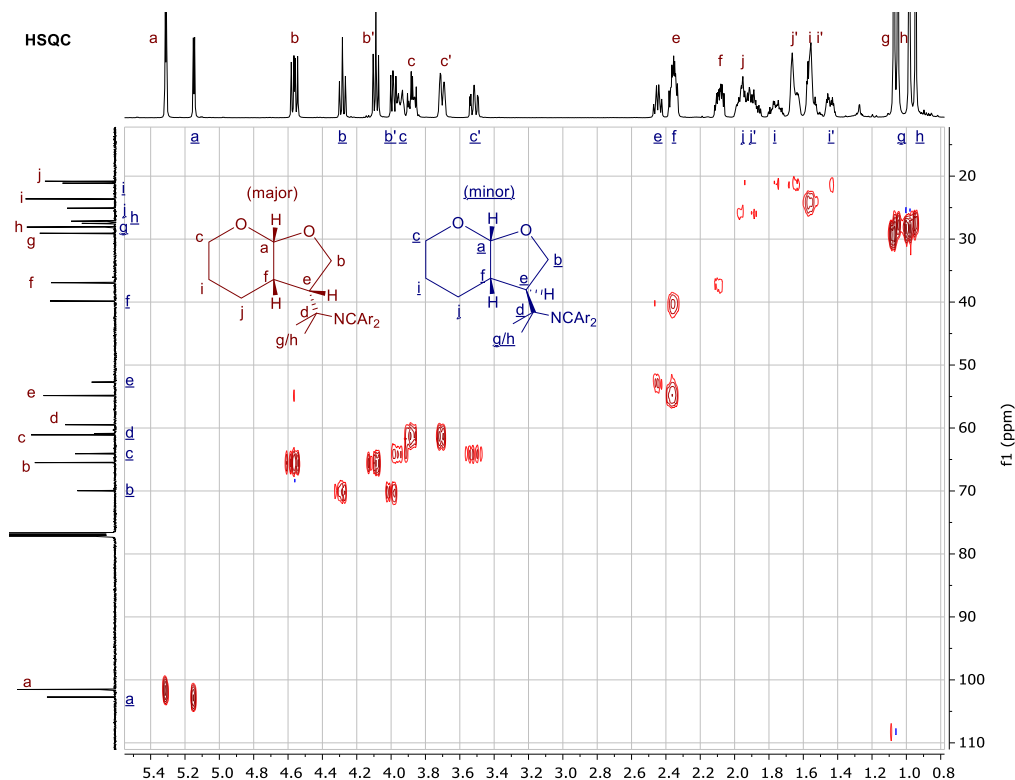
The relative configurations for both isomers of this compound were assigned by 2D NMR spectroscopy as shown below. The aliphatic carbon skeleton was assigned unambiguously by HSQC, HMBC, and COSY NMR spectra. Structurally relevant NOESY correlations are summarized in the following Table 5.7.

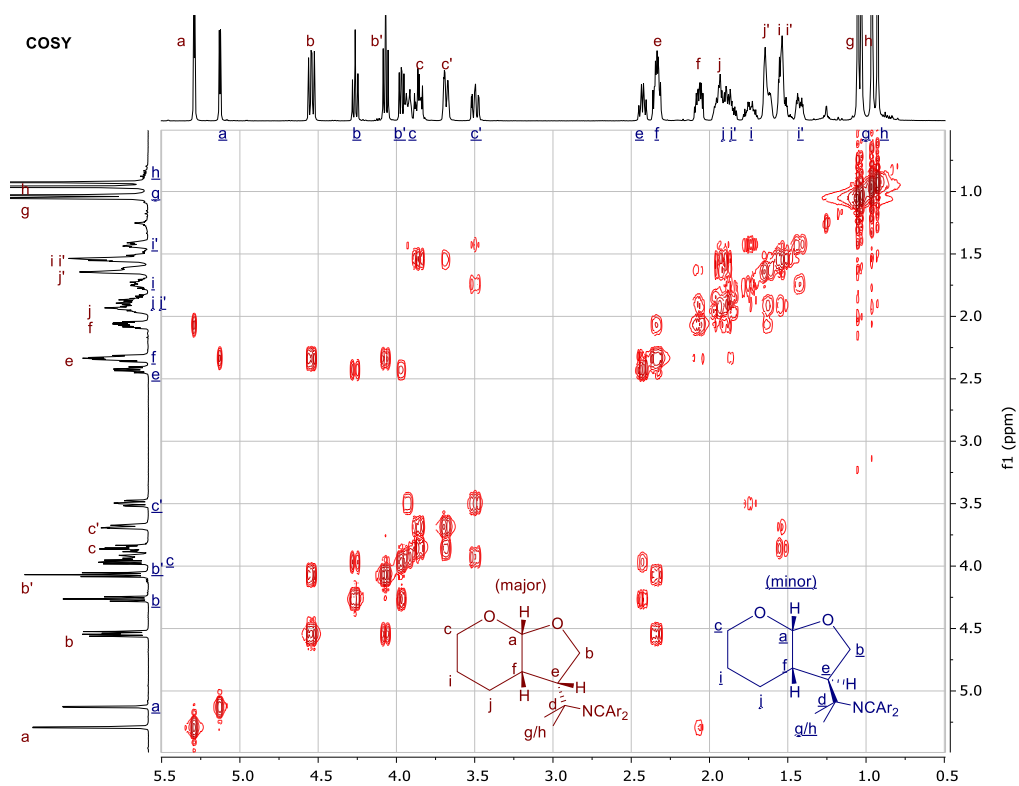
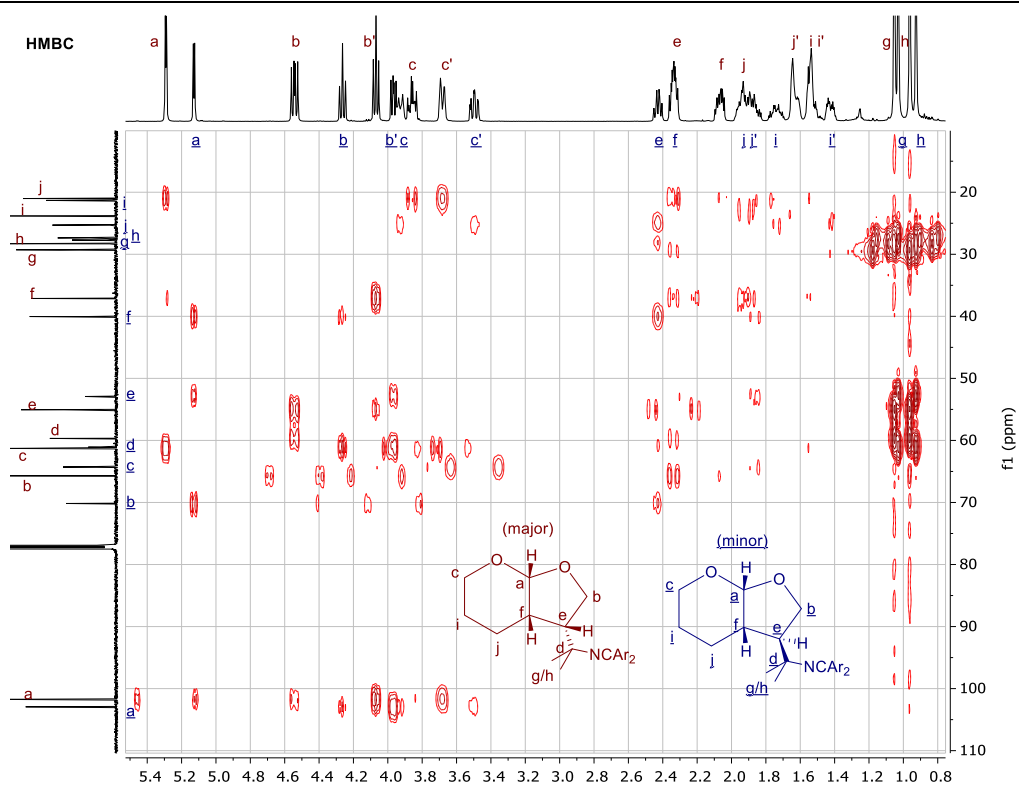
Table 5.7. Qualitative analysis of ^1H - ^1H NOE correlations for **27**.

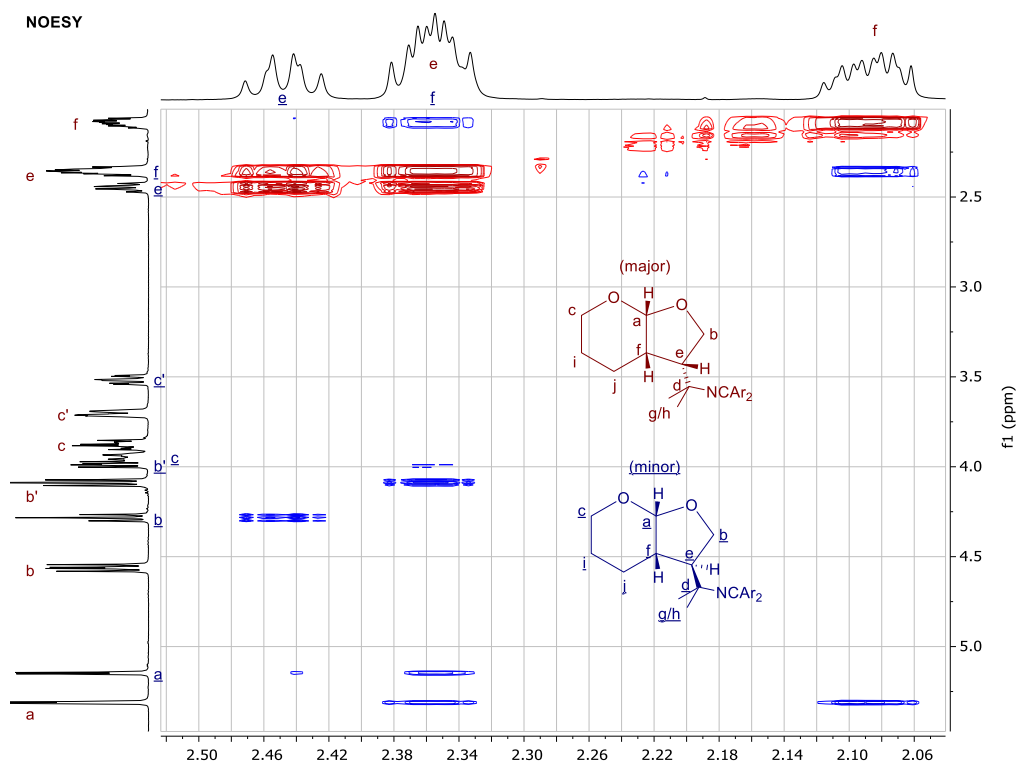
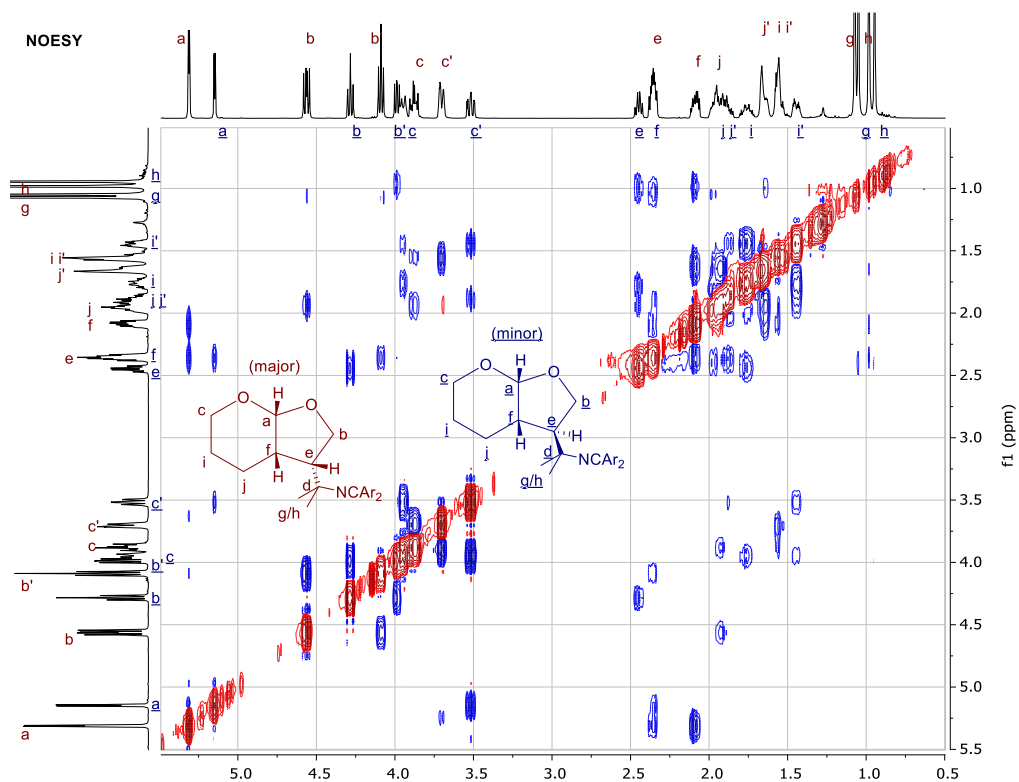
		H_a	H_e	H_f
major	H_e	strong		
	H_f	strong	strong	
	H_g	n.d.	strong	med
	H_h	n.d.	strong	n.d.
minor	H_e	weak		
	H_f	strong	$\Delta\delta$ too small	
	H_g	n.d.	strong	strong
	H_h	n.d.	strong	strong



In the major diastereomer: H_a , H_f , and H_e are all likely on the same face of the 5-ring, such as in the *endo* isomer drawn. In the minor diastereomer: H_a and H_f are likely on the same face, and H_f is close in space to the methyl groups (g) and (h), such as in the *exo* isomer drawn.







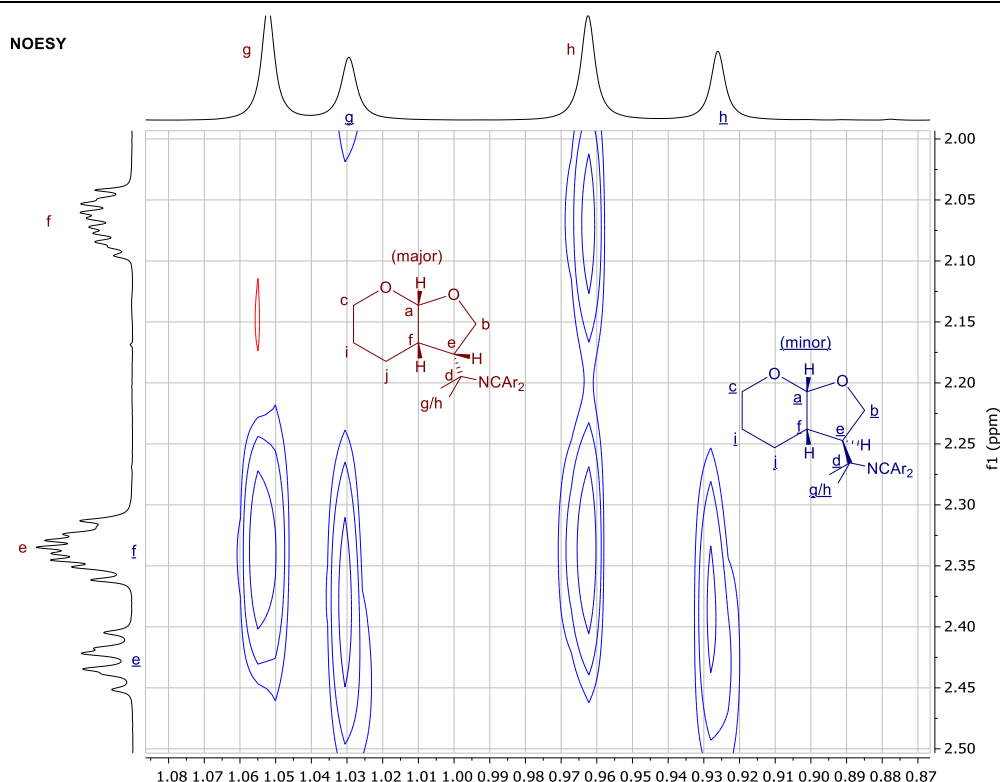
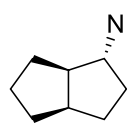


Figure 5.2. 2-Dimensional gradient enhanced ^1H - ^{13}C HSQC, ^1H - ^{13}C HMBC, ^1H - ^1H COSY, and ^1H - ^1H NOESY spectra for **27**.

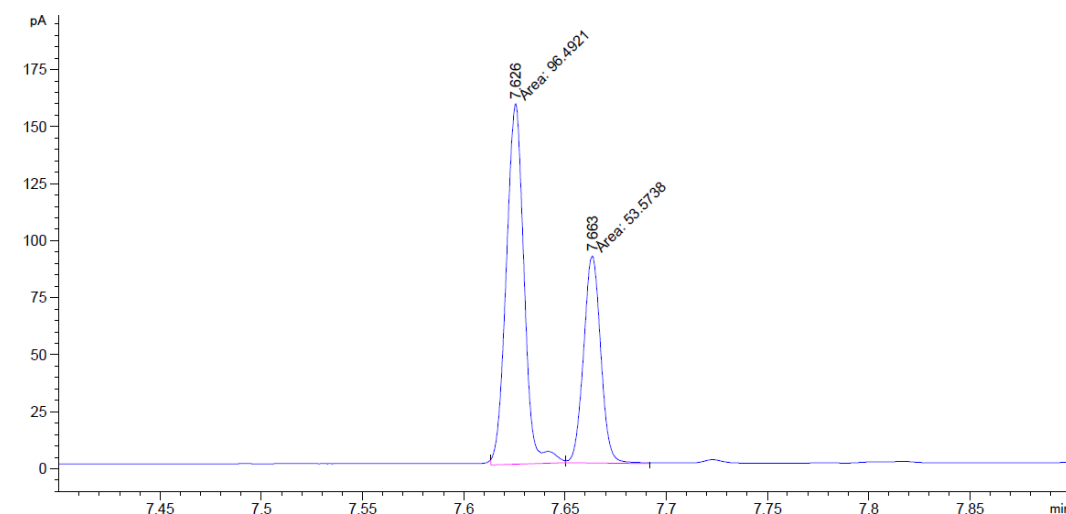


2-Benzamido-bicyclo[3,3,0]octane (29). In a nitrogen-filled glovebox, a 20 ml vial was charged with (Z)-5-bromocyclooct-1-ene (75.6 mg, 0.400 mmol) (**28**), 3,3'-bis(trifluoromethyl)benzophenone imine (**2d**) (190 mg, 0.599 mmol, 1.50 equiv), [(1-Ad)₂MeP]₂PdHBr (16.4 mg, 0.0200 mmol, 5.00 mol %), cesium carbonate (198 mg, 0.608 mmol, 1.52 equiv), *tert*-amyl alcohol (12 ml), and a magnetic stir bar. The vial was sealed with a Teflon-lined cap and Teflon tape. The reaction mixture was heated at 80 °C with stirring for 20 h in an aluminum block. The reaction mixture was diluted to approximately 20 ml with ether and filtered through a pad of Celite, which was rinsed with ether (3 x approximately 10 ml). The volatile materials were evaporated at reduced pressure. The residue was dissolved in approximately 1 ml of 2% triethylamine in hexanes and filtered through a plug of basified silica (2-3 ml), which was rinsed with 2% triethylamine in hexanes (approximately 10 ml). The volatile materials were evaporated at reduced pressure to give the crude *N*-alkyl imine product.

Note: the crude imine product contains both the *endo* isomer and direct coupling product as impurities (tentative assignment). Crude GC traces are shown below of: (a) the reaction run at 0.50 M catalyzed by 5.3% (Cy₂*t*-BuP)₂PdHBr and (b) the reaction run at 0.03 M catalyzed by 5% [(1-Ad)₂MeP]₂PdHBr. The peak at 7.63 minutes is the major product. The small shoulder at 7.64 minutes is presumed to originate from the *endo* isomer (overlap complicates integration, but <5%

in both cases). The peak at 7.66 minutes is presumed to be the direct coupling product, and its formation is greatly suppressed when the reaction is run at dilute concentrations. The change of phosphine ligand does not have a significant effect on either ratio. To remove these impurities, the crude imine product (an oil) was carried on to the corresponding benzamide (**29**), which was recrystallized.

a) **[28]** = 0.50 M, (Cy₂t-BuP)₂PdHBr cat



b) **[28]** = 0.03 M, [(1-Ad)₂MeP]₂PdHBr cat

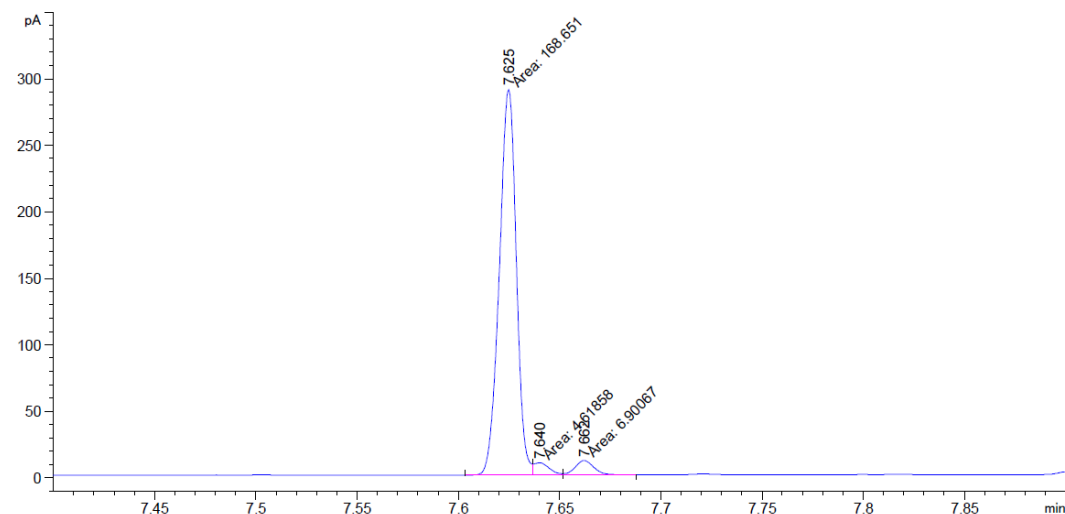


Figure 5.3. Gas chromatograms of crude samples of 2-((bis(3-(trifluoromethyl)phenyl)methylene)amino)bicyclo[3,3,0]octane prior to hydrolysis.

The crude imine and 0.5 M HCl_(aq) (6 ml) were mixed in a 20 ml vial. The vial was flushed with nitrogen and sealed with a Teflon-lined cap. The reaction mixture was heated at 80 °C with stirring for 4 h in an aluminum heating block. The mixture was washed twice with ether (4 ml). The organic

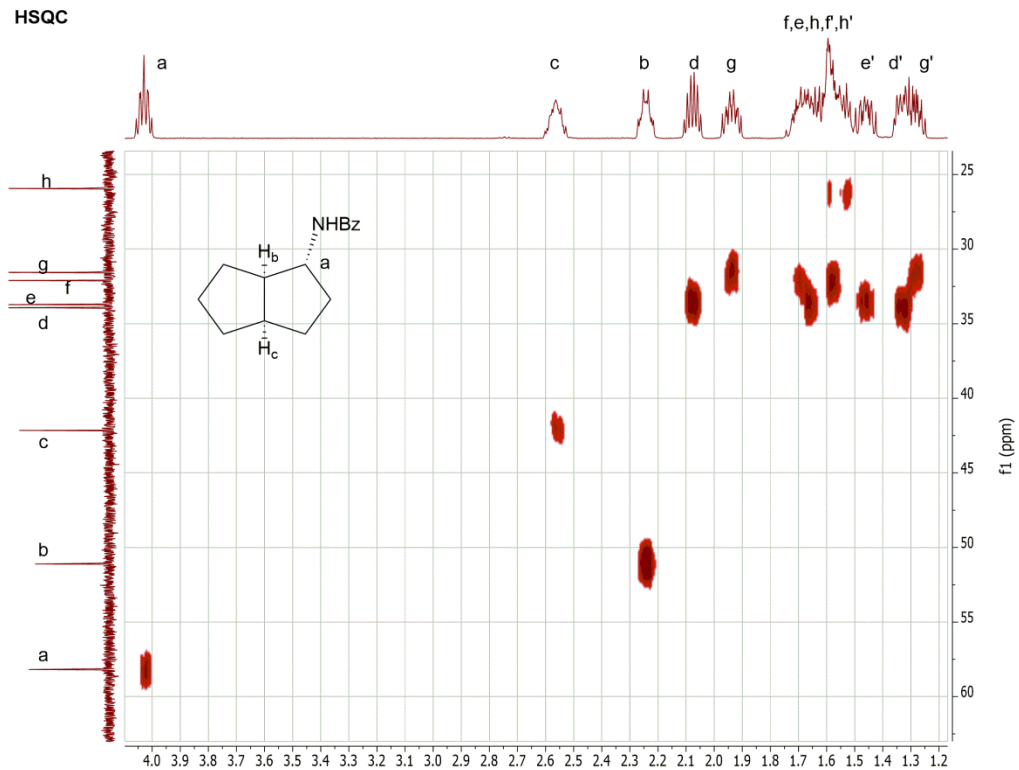
layers were extracted with 0.5 M HCl_(aq) (4 ml), and the combined aqueous layers were basified with K₂CO₃ (1.5 g). The mixture was extracted four times with ether (4 ml). The organic layers were filtered through a plug of Na₂SO₄ into a 25 ml flask. The volatile materials were evaporated at reduced pressure to give the crude primary amine product. The crude amine was dissolved in dry DCM (2 ml) and filtered through a second plug of Na₂SO₄, which was rinsed twice more with DCM (2 ml), into a 25 ml flask under nitrogen.

The solution was cooled to 0 °C, and triethylamine (170 µl, 120 mg, 1.2 mmol, 3.0 equiv) and benzoyl chloride (93 µl, 110 mg, 0.80 mmol, 2.0 equiv) were added with stirring. The reaction mixture was stirred for 12 h at ambient temperature. The mixture was diluted to approximately 10 ml with DCM, and the resulting solution was transferred to a separatory funnel and washed with 0.5 M HCl_(aq) (approximately 15 ml). The aqueous layer was extracted thrice more with DCM (approximately 8 ml), and the combined organic layers were dried with MgSO₄. The volatile materials were evaporated at reduced pressure, and the crude product was purified by column chromatography (0 to 25% ethyl acetate gradient in hexanes, R_f 0.41 in 25% EA/Hex) followed by recrystallization (DCM/Hex, 3 crops) to give the title compound as a fluffy white solid (49.4 mg, 0.215 mmol, 54% yield). ¹H NMR (500 MHz, CDCl₃) δ 7.79 – 7.72 (m, 2H), 7.49 (t, J = 7.3 Hz, 1H), 7.43 (t, J = 7.4 Hz, 2H), 6.05 (broad, NH), 4.03 (ddd, J = 13.7, 7.7, 6.0 Hz, 1H), 2.62 – 2.52 (m, 1H), 2.24 (tdd, J = 9.1, 6.0, 3.3 Hz, 1H), 2.08 (dq, J = 11.8, 5.8 Hz, 1H), 1.94 (dddd, J = 13.4, 8.7, 6.6, 5.0 Hz, 1H), 1.75 – 1.50 (m, 5H), 1.50 – 1.42 (m, 1H), 1.37 – 1.24 (m, 2H). ¹³C NMR (151 MHz, CDCl₃) δ 167.29, 135.19, 131.38, 128.66, 126.97, 58.18, 51.11, 42.15, 33.93, 33.72, 32.11, 31.56, 25.93. ESI⁺ calc'd (M+Na⁺) 252.1359, found 252.1354.

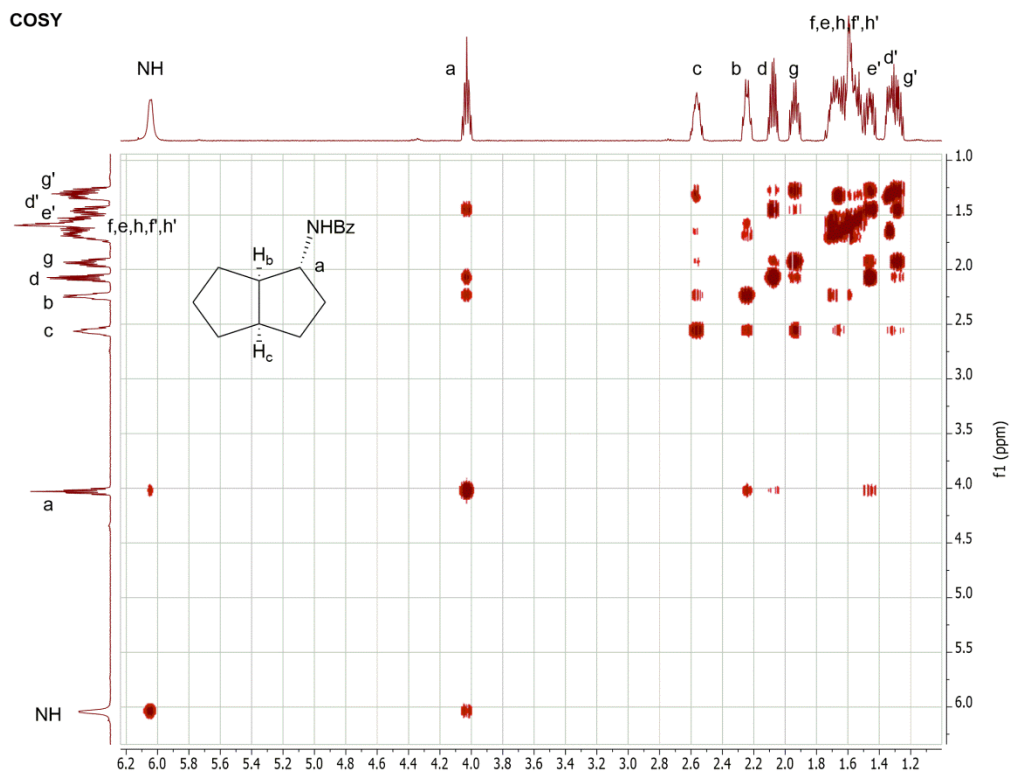
The ¹H NMR spectrum of this compound contains a set of small signals, which integrate to approximately 3% relative to the major compound. These small signals are presumed to originate from an isomer of the product; either the direct coupling product or the *endo* diastereomer of the major compound.

The relative configurations of the major compound were assigned by 2D NMR spectroscopy, as shown below. Many CH₂ ¹H and ¹³C signals were closely spaced or overlapping, and the COSY spectrum was complicated by long-range coupling. Therefore, CH₂ signals were not assigned to the structure drawn below. However, the NH and CH signals were assigned unambiguously. Strong NOESY correlations of H_b to H_c and NH were observed. Only a weak NOESY correlation between H_a and H_b was observed, and no NOESY correlation between H_a and H_c was detected. These spectra are most consistent with the diastereomer drawn.

HSQC



COSY



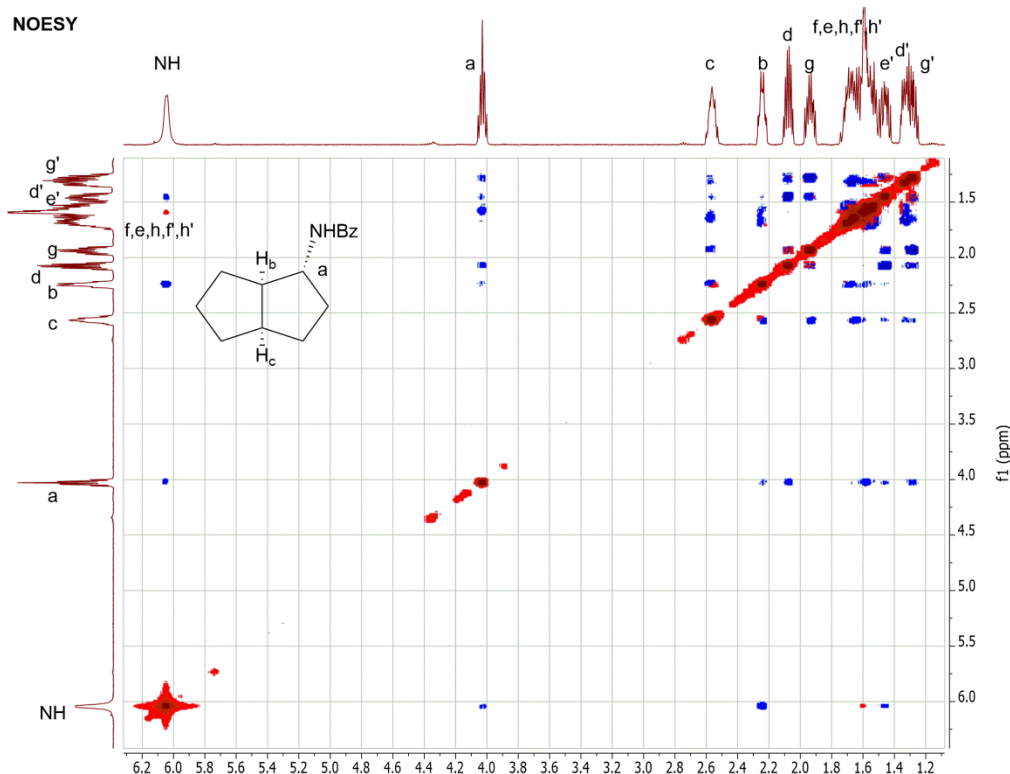


Figure 5.4. 2-Dimensional gradient enhanced ^1H - ^{13}C HSQC, ^1H - ^1H COSY, and ^1H - ^1H NOESY spectra for **29**.

GC response factors

All GC yields (integration relative to a 1.0 equiv 1,3,5-trimethoxybenzene internal standard) were corrected with the following response factors determined with authentic compounds:

3-bromo-1phenylbutane (**1**): 0.685

N-(4-phenylbutan-2-yl)benzophenone imine (**3a**): 0.249

N-(4-phenylbutan-2-yl)-4,4'-dimethylbenzophenone imine (**3b**): 0.246

N-(4-phenylbutan-2-yl)-4,4'-dimethoxybenzophenone imine (**3c**): 0.257

N-(4-phenylbutan-2-yl)-3,3'-bis(trifluoromethyl)benzophenone imine (**3d**): 0.252

4-phenylbutene (**4**): 0.669. *Note*: a mixture of 4 isomers was identified by GC/MS. The response factor was determined with commercially available 4-phenyl-1-butene and assumed to apply equally to the combined mixture of isomers.

1-phenylbutane (**5**): 0.645

N-(*sec*-butyl)benzophenone imine (**20**): 0.362. *Note*: this response factor was assumed to apply equally to a mixture of *N*-(*sec*-butyl)benzophenone imine and *N*-(*tert*-butyl)benzophenone imine.

Experimental details for Table 5.1

General procedure. In a nitrogen-filled glovebox, a 2 ml volumetric flask was charged with 3-bromo-1-phenylbutane (**1**) (426 mg, 2.00 mmol), benzophenone imine (**2a**) (399 mg, 2.20 mmol, 1.10 equiv), palladium allyl chloride dimer (22.0 mg, 0.0601 mmol, 3.01%), and 1,3,5-trimethoxybenzene (336 mg, 2.00 mmol, 1.00 equiv). The mixture was diluted to the mark with *t*-amyl alcohol, then diluted to double volume. A 0.30 ml (0.15 mmol alkyl bromide) sample of this mixture was transferred to a vial with the noted phosphine ligand (0.018 mmol, 12%), cesium carbonate (73 mg, 0.23 mmol, 1.5 equiv), and a magnetic stir bar. The vials were sealed with a Teflon-lined cap and Teflon tape. The reaction mixture was heated at 80 °C with stirring for 20 hours in an aluminum block. The reaction mixture was then diluted with ethyl acetate (~2 ml), and a sample taken for GC analysis after filtration through a plug of silica.

Entry 1: no ligand

Entry 2: Cy₂PhP (4.9 mg)

Entry 3: *t*-Bu₂PhP (4.0 mg)

Entry 4: Ph₃P (4.8 mg)

Entry 5: Ph₂EtP (4.1 mg)

Entry 6: 1,2-(dicyclohexylphosphino)ethane (3.9 mg, 6%)

Entry 7: Cy₃P (5.0 mg)

Entry 8: *t*-Bu₃P (3.7 mg)

Entry 9: *t*-Bu₂CyP (4.2 mg)

Entry 10: *t*-Bu₂MeP (3.1 mg)

Entry 11: Ad₂MeP (5.7 mg)

Entry 12: Cy₂*t*-BuP (4.7 mg)

Experimental details for Table 5.2

General procedure (entries 1-4, 6, and 7). In a nitrogen-filled glovebox, a 2 ml volumetric flask was charged with 3-bromo-1-phenylbutane (**1**) (213 mg, 0.999 mmol), benzophenone imine (**2a**) (200 mg, 1.10 mmol, 1.10 equiv), and 1,3,5-trimethoxybenzene (168 mg, 0.999 mmol, 1.00 equiv). The mixture was diluted to the mark with *t*-amyl alcohol, and 0.30 ml (0.15 mmol alkyl bromide) of this mixture was transferred to a vial with the noted catalyst, cesium carbonate (73 mg, 0.23 mmol, 1.5 equiv), and a magnetic stir bar. The vials were sealed with a Teflon-lined cap and Teflon tape. The reaction mixture was heated at 80 °C with stirring for 20 hours in an aluminum block. The reaction mixture was then diluted with ethyl acetate (~2 ml), and a sample taken for GC analysis after filtration through a plug of silica.

Entry 1: As described above with 5.5 mg (Cy₂*t*-BuP)₂PdHBr

Entry 2: As described above, with no metal catalyst

Entry 3: As described above with 4.1 mg NiCl₂/glyme and 2.0 mg Cy₂*t*-BuP.

Entry 4: As described above with 5.5 mg (Cy₂*t*-BuP)₂PdHBr; an additional 0.30 ml *t*-amyl alcohol was added.

Entry 6: As described above with 5.5 mg (Cy₂*t*-BuP)₂PdHBr and 18.1 mg LiOt-Bu and no Cs₂CO₃.

Entry 7: As described above with 5.5 mg (Cy₂*t*-BuP)₂PdHBr and 44.4 mg Cy₂MeN and no Cs₂CO₃.

Entry 5: In a nitrogen-filled glovebox, a 4 ml vial was charged with 3-bromo-1-phenylbutane (64.3 mg, 0.302 mmol), benzophenone imine (59.5 mg, 0.328 mmol, 1.09 equiv), 1,3,5-trimethoxybenzene (49.5 mg, 0.295 mmol, 0.976 equiv), (Cy₂*t*-BuP)₂PdHBr (11.0 mg, 0.0158 mmol, 5.27%), cesium carbonate (146 mg, 0.448 mmol, 1.48 equiv), *i*-PrOH (0.40 ml), and a magnetic stir bar. The vial was sealed with a Teflon-lined cap and Teflon tape. The reaction mixture was heated at 80 °C with stirring for 20 hours in an aluminum block. The reaction mixture was then diluted with ethyl acetate (~ 2 ml), and a sample taken for GC analysis after filtration through a plug of silica. Data reported for this entry are an average of two experiments.

Experimental details for Table 5.3

General procedure. In a nitrogen-filled glovebox, a 2 ml volumetric flask was charged with 3-bromo-1-phenylbutane (**1**) (213 mg, 0.999 mmol), (Cy₂*t*-BuP)₂PdHBr (37.0 mg, 0.0532 mmol, 5.32%), and 1,3,5-trimethoxybenzene (168 mg, 0.999 mmol, 1.00 equiv). The mixture was diluted to the mark with *t*-amyl alcohol, and 0.30 ml (0.15 mmol alkyl bromide) of this mixture was transferred to a vial with the noted imine (**2a-d**), cesium carbonate (73 mg, 0.23 mmol, 1.5 equiv), and a magnetic stir bar. The vials were sealed with a Teflon-lined cap and Teflon tape. The reaction mixture was heated at 80 °C with stirring for 20 hours in an aluminum block. The reaction mixture was then diluted with ethyl acetate (~2 ml), and a sample taken for GC analysis after filtration through a plug of silica. The reported data are averages of two experiments for each entry.

Entry 1: Benzophenone imine (**2a**) (30.0 mg, 0.166 mmol, 1.11 equiv)

Entry 2: 4,4'-Dimethylbenzophenone imine (**2b**) (34.6 mg, 0.165 mmol, 1.10 equiv)

Entry 3: 4,4'-Dimethoxybenzophenone imine (**2c**) (39.7 mg, 0.165 mmol, 1.10 equiv)

Entry 4: 3,3'-Bis(trifluoromethyl)benzophenone imine (**2d**) (52.4 mg, 0.165 mmol, 1.10 equiv)

Entry 5: 3,3'-Bis(trifluoromethyl)benzophenone imine (**2d**) (57.2 mg, 0.180 mmol, 1.20 equiv)

Entry 6: 3,3'-Bis(trifluoromethyl)benzophenone imine (**2d**) (71.2 mg, 0.224 mmol, 1.49 equiv)

Experimental details for Table 5.4

General procedure. In a nitrogen-filled glovebox, a 2 ml volumetric flask was charged with 3,3'-bis(trifluoromethyl)benzophenone imine (**2d**) (952 mg, 3.00 mmol, 1.50 equiv), (Cy₂*t*-BuP)₂PdHBr (73.8 mg, 0.106 mmol, 5.30%), and 1,3,5-trimethoxybenzene (337 mg, 2.00 mmol, 1.00 equiv). The mixture was diluted to the mark with *t*-amyl alcohol, the resulting solution was then diluted 2x with *t*-amyl alcohol, and 0.30 ml (0.15 mmol TMB) of the final mixture was transferred to a vial with the noted electrophile, cesium carbonate (73 mg, 0.23 mmol, 1.5 equiv), and a magnetic stir bar. The vials were sealed with a Teflon-lined cap and Teflon tape. The reaction mixture was heated at 80 °C with stirring for 20 hours in an aluminum block. The reaction mixture was then diluted with ethyl acetate (~2 ml), and a sample taken for GC analysis after filtration through a plug of silica.

Entry 1: 3-Bromo-1-phenylbutane (**1**) (31.9 mg, 0.150 mmol, 1.00 equiv)

Entry 2: 3-Iodo-1-phenylbutane (39.1 mg, 0.150 mmol, 1.00 equiv)

Entry 3: 4-Phenylbutan-2-yl 4-methylbenzenesulfonate (45.7 mg, 0.150 mmol, 1.00 equiv)

Experimental details for Scheme 5.2

In a nitrogen-filled glovebox, a 1 dram vial was charged with benzophenone imine (**2a**) (33.6 μ l, 36.2 mg, 0.200 mmol), *sec*-butylbromide (43.6 μ l, 54.9 mg, 0.400 mmol, 2.00 equiv), *tert*-butylbromide (45.0 μ l, 54.9 mg, 0.400 mmol, 2.00 equiv), (Cy₂*t*-BuP)₂PdHBr (7.0 mg, 0.010 mmol, 5.0 mol %), cesium carbonate (98 mg, 0.30 mmol, 3.0 equiv), *tert*-amyl alcohol (0.30 ml), and a magnetic stir bar. The vial was sealed with a Teflon-lined cap and Teflon tape. The reaction mixture was heated at 80 °C with stirring for 20 h in an aluminum block. The reaction mixture was then diluted with ether and water (2 ml each). The organic layer was removed, and the aqueous layer was extracted thrice more with ether (2 ml). The organic layers were passed through a plug of silica into a vial containing 1,3,5-trimethoxybenzene (33.6 mg, 0.200 mmol, 1.00 equiv). An aliquot of this solution was then removed for ¹H NMR spectroscopy and GC analysis. Yields were determined by corrected GC integration against TMB and are an average of two trials.

Yield *N*-(*sec*-butyl)benzophenone imine: 8%

Yield *N*-(*tert*-butyl)benzophenone imine: 54%

N-(*tert*-butyl)benzophenone imine to *N*-(*sec*-butyl)benzophenone imine product ratio: 7.1

Experimental details for Scheme 5.3a

General procedure. In a nitrogen-filled glovebox, a 4 ml vial was charged with benzophenone imine (**2a**) (36.1 mg, 0.199 mmol), (*S*)-3-bromo-1-phenylbutane (**(S)-1**) (85.1 mg, 0.399 mmol, 2.01 equiv), [Cy₂(*t*-Bu)P]₂PdHBr (10.0 mg, 0.0144 mmol, 7.22 mol%), cesium carbonate (98.6 mg, 0.303 mmol, 1.52 equiv), *t*-amyl alcohol (0.26 ml), and a magnetic stir bar. The vial was sealed with a Teflon-lined cap and Teflon tape. The reaction mixture was heated at 80 °C with stirring for *x* hours in an aluminum block. The reaction mixture was diluted with ether (2 ml) and filtered through a small plug of Celite into a 20 ml vial. A small aliquot was removed for GC/MS and chiral GC analysis at this stage. The volatile materials were evaporated at reduced pressure.

HCl_(aq) (4 ml, 0.5 M) was added to the vial, and the mixture was heated at 80 °C with stirring for 4 h. The mixture was washed with ether (4 ml, 2x 2 ml). The organic layer was extracted with HCl_(aq) (2 ml, 0.5 M), and the resulting mixture was washed with ether (2x 2 ml). The combined aqueous layers were transferred to a separatory funnel, and the vial was rinsed with H₂O (1 ml). The mixture was basified with K₂CO₃ (1.0 g) and extracted with DCM (3x 4 ml). The combined organic layers were dried with Na₂SO₄ and filtered through cotton. The volatile materials were evaporated at reduced pressure.

The vial was flushed with nitrogen and cooled to 0 °C. Dry DCM (3 ml), triethylamine (42 μ l, 30 mg, 0.30 mmol, 1.5 equiv) then benzoyl chloride (35 μ l, 42 mg, 0.30 mmol, 1.5 equiv) were added to the vial. The reaction mixture was stirred at ambient temperature for 5 h. The mixture was diluted to approximately 10 ml with DCM, transferred to a separatory funnel, and washed with HCl_(aq) (10 ml, 0.5 M). The aqueous layer was extracted further with DCM (2x 10 ml). The combined organic layers were dried with MgSO₄ and the volatile materials were evaporated at reduced pressure. The crude product was purified by column chromatography (25% EA/hexanes) to give (rac)-*N*-(4-phenylbutan-2-yl)benzamide (**19**). The ¹H NMR spectrum matched that of the authentic sample.

Note: To more accurately measure the ee of unconverted alkyl bromide (**(S)**-**1**), the chiral GC data was fit to the following function $y(t)$ by the method of least squares:

$$y(t) = p_1(t) + p_2(t) + b(t)$$

$$p_1(t) = a_1 * (1 / (\sigma_1 * \text{SQRT}(2 * \pi))) * \text{EXP}(-((t - \mu_1)^2 / (2 * \sigma_1^2)))$$

$$p_2(t) = a_2 * (1 / (\sigma_2 * \text{SQRT}(2 * \pi))) * \text{EXP}(-((t - \mu_2)^2 / (2 * \sigma_2^2)))$$

$$b(t) = m * t + c$$

$p_i(t)$ is a Gaussian probability distribution with area a_i , mean μ_i , and standard deviation σ_i to approximate the shape of a GC peak

$b(t)$ is a linear function to correct the GC baseline

Entry 1: Reaction time = 1 h. Unconverted 3-bromo-1-phenylbutane: 45% ee by chiral GC. *N*-(4-phenylbutan-2-yl)benzamide: 11.0 mg, 0.0470 mmol, 23% yield, 0% ee by SFC.

Entry 2: Reaction time = 4 h. Unconverted 3-bromo-1-phenylbutane: 12% ee by chiral GC. *N*-(4-phenylbutan-2-yl)benzamide: 23.5 mg, 0.0928 mmol, 46% yield, 0% ee by SFC.

Experimental details for Scheme 5.3b

In a nitrogen-filled glovebox, a 4 ml vial was charged with benzophenone imine (**2a**) (36.2 mg, 0.200 mmol), (*S*)-3-bromo-1-phenylbutane (**(S)**-**1**) (85.1 mg, 0.399 mmol, 2.00 equiv), $[\text{Cy}_2(t\text{-Bu})\text{P}]_2\text{PdHBr}$ (10.0 mg, 0.0144 mmol, 7.22 mol%), cesium carbonate (97.9 mg, 0.300 mmol, 1.50 equiv), (*S*)-*N*-(*sec*-butyl)benzophenone imine (**20**) (48.1 mg, 0.203 mmol, 1.02 equiv), *t*-amyl alcohol (0.26 ml), and a magnetic stir bar. The vial was sealed with a Teflon-lined cap and Teflon tape. The reaction mixture was heated at 80 °C with stirring for 24 hours in an aluminum block. The reaction mixture was diluted with ether (2 ml) and filtered through a small plug of Celite into a 20 ml vial. A small aliquot was removed for GC/MS and chiral GC analysis at this stage (unconverted alkyl bromide was racemic by chiral GC). The volatile materials were evaporated at reduced pressure.

$\text{HCl}_{(\text{aq})}$ (4 ml, 0.5 M) was added to the vial, and the mixture was heated with stirring at 80 °C for 4 h. The mixture was washed with ether (4 ml, 2x 2 ml). The organic layer was extracted with $\text{HCl}_{(\text{aq})}$ (2 ml, 0.5 M), which was washed with ether (2x 2 ml). The combined aqueous layers were transferred to a separatory funnel, and the vial was rinsed with H_2O (1 ml). DCM (4 ml) was added, and the mixture was basified with K_2CO_3 (1.0 g). The organic layer was transferred to a cold vial, the aqueous layer was extracted with DCM (2x 2ml), and the combined organic layers were dried with Na_2SO_4 and filtered through cotton into another cold vial containing a stir bar.

The vial was flushed with nitrogen. Triethylamine (84 μl , 61 mg, 0.60 mmol, 3.0 equiv), followed by benzoyl chloride (70 μl , 85 mg, 0.60 mmol, 3.0 equiv), were then added to the vial. The reaction mixture was stirred at ambient temperature for 4.5 h. The mixture was washed with $\text{HCl}_{(\text{aq})}$ (8 ml, 0.5 M), and the aqueous layer extracted further with DCM (2x 8 ml). The combined organic layers were dried with MgSO_4 , and the volatile materials were evaporated at reduced pressure. The crude mixture was purified by column chromatography (25% EA/hexanes) to give a mixture of (*S*)-*N*-(*sec*-butyl)benzamide (**21**) (0.062 mmol, 30% yield, 97% ee by SFC: AS-H) and (rac)-*N*-(4-phenylbutan-2-yl)benzamide (**19**) (0.133 mmol, 67% yield, 0% ee by SFC: AS-H).

The combined mass of amides was 44.7 mg. ^1H NMR spectroscopy indicated a molar ratio of 1.0 *N*-(*sec*-butyl)benzamide to 2.15 *N*-(4-phenylbutan-2-yl)benzamide. The yield of each compound was, therefore, determined by solving the equation: $x(2.15 \times 253.35 + 177.25) = 44.7$; in which x = mmol *N*-(*sec*-butyl)benzamide and $2.15 \times x$ = mmol *N*-(4-phenylbutan-2-yl)benzamide.

The low isolated yield of *N*-(*sec*-butyl)benzamide is likely due to the high solubility of *sec*-butylamine in aqueous solutions.

Experimental details for Table 5.6

General procedure. In a nitrogen filled glovebox, a 1.0 M solution of (*S*)-3-bromo-1-phenylbutane ((*S*)-**1**) (95% ee by chiral GC) was prepared. A 200 μl sample (0.20 mmol RBr) of this solution was added to a vial containing the noted compounds and a magnetic stir bar. The vials were sealed with a Teflon-lined cap and Teflon tape. The reaction mixture was heated at 80 $^{\circ}\text{C}$ with stirring for 20 hours in an aluminum block. The reaction mixture was then diluted with ethyl acetate (~ 2 ml), and an aliquot was removed for GC analysis after filtration through a plug of silica. Ee values are averages of two experiments.

Entry 1: ($\text{Cy}_2t\text{-BuP}$) $_2\text{PdHBr}$ (5.0 mg, 0.0072 mmol, 3.6%)

Entry 2: CsBr (21.3 mg, 0.100 mmol, 0.500 equiv)

Entry 3: ($\text{Cy}_2t\text{-BuP}$) $_2\text{PdHBr}$ (5.0 mg, 0.0072 mmol, 3.6%) and CsBr (21.3 mg, 0.100 mmol, 0.500 equiv)

Entry 4: Cs_2CO_3 (48.8 mg, 0.150 mmol, 0.750 equiv)

Entry 5: ($\text{Cy}_2t\text{-BuP}$) $_2\text{PdHBr}$ (5.0 mg, 0.0072 mmol, 3.6%) and Cs_2CO_3 (48.8 mg, 0.150 mmol, 0.750 equiv). Significant formation of *n*-butylbenzene was detected in this reaction mixture.

Experimental details for Scheme 5.4

0.5 M reaction. In a nitrogen-filled glovebox, a 1 dram vial was charged with benzophenone imine (**2a**) (54.4 mg, 0.300 mmol), *i*-PrBr (74 mg, 0.60 mmol, 2.0 equiv), [$\text{Cy}_2(t\text{-Bu})\text{P}$] $_2\text{PdHBr}$ (11 mg, 0.016 mmol, 5.3 mol %), cesium carbonate (147 mg, 0.451 mmol, 1.50 equiv), THF (0.46 ml; total volume approximately 0.6 ml), and a magnetic stir bar. The vial was sealed with a Teflon-lined cap and Teflon tape. The reaction mixture was heated at 80 $^{\circ}\text{C}$ with stirring for 48 h in an aluminum block. The mixture was diluted with ether (2 ml) and filtered through a plug of Celite, which was then rinsed with ether (3 x 2 ml). The volatile materials were evaporated at reduced pressure. The crude product was dissolved in 5% triethylamine in hexanes (approximately 1 ml) and filtered through a plug of basified silica, which was rinsed with 5% triethylamine in hexanes (3 x 2 ml), into a vial containing 1,3,5-trimethoxy benzene (50.5 mg, 0.300 mmol, 1.00 equiv). The volatile materials were removed at reduced pressure. Yields were determined by integrating the ^1H NMR spectroscopy peaks of the product relative to those of trimethoxybenzene ($d_1=12$ s).

N-iso-propylbenzophenone imine (**22**): 75%

N-(tetrahydrofuran-2-yl)benzophenone imine (**23**): 14%

0.05 M reaction. In a nitrogen-filled glovebox, a 20 ml vial was charged with benzophenone imine (**2a**) (54.4 mg, 0.300 mmol), *i*-PrBr (74 mg, 0.60 mmol, 2.0 equiv), [$\text{Cy}_2(t\text{-Bu})\text{P}$] $_2\text{PdHBr}$ (11 mg, 0.016 mmol, 5.3 mol %), cesium carbonate (147 mg, 0.451 mmol, 1.50 equiv), THF (6.0 ml; total

volume approximately 6 ml), and a magnetic stir bar. The vial was sealed with a Teflon-lined cap and Teflon tape. The reaction mixture was heated at 80 °C with stirring for 48 h in an aluminum block. The mixture was filtered through a plug of Celite, which was then rinsed with ether (3 x 2 ml). The volatile materials were evaporated at reduced pressure. The crude product was dissolved in 5% triethylamine in hexanes (approximately 1 ml) and filtered through a plug of basified silica, which was rinsed with 5% triethylamine in hexanes (3 x 2 ml), into a vial containing 1,3,5-trimethoxy benzene (50.5 mg, 0.300 mmol, 1.00 equiv). The volatile materials were removed at reduced pressure. Yields were determined by integrating the ¹H NMR spectroscopy peaks of the product relative to those of trimethoxybenzene (d1=12 s).

N-iso-propylbenzophenone imine (**22**): 22%

N-(tetrahydrofuran-2-yl)benzophenone imine (**23**): 60%

5.5 References and notes

Contributions:

All results were obtained collaboratively by D. Matthew Peacock and Casey B. Roos

Portions of this text were reprinted with permission from:

Peacock, D. M.; Roos, C. B.; Hartwig, J. F., *ACS Cent. Sci.* **2016**, 2 (9), 647-652.

1. de Meijere, A.; Diederich, F., *Metal-Catalyzed Cross-Coupling Reactions*. 2 ed.; Wiley-VCH Verlag GmbH: Weinheim, 2004.
2. Beletskaya, I. P.; Ananikov, V. P., *Chem. Rev.* **2011**, 111 (3), 1596-1636.
3. Hartwig, J. F., Palladium-Catalyzed Amination of Aryl Halides and Sulfonates. In *Modern Amination Methods*, Ricci, A., Ed. Wiley-VCH Verlag GmbH: 2007; pp 195-262.
4. Jana, R.; Pathak, T. P.; Sigman, M. S., *Chem. Rev.* **2011**, 111 (3), 1417-1492.
5. Frisch, A. C.; Beller, M., *Angew. Chem. Int. Ed.* **2005**, 44 (5), 674-688.
6. Kambe, N.; Iwasaki, T.; Terao, J., *Chem. Soc. Rev.* **2011**, 40 (10), 4937-4947.
7. Rudolph, A.; Lautens, M., *Angew. Chem. Int. Ed.* **2009**, 48 (15), 2656-2670.
8. Cherney, A. H.; Kadunce, N. T.; Reisman, S. E., *Chem. Rev.* **2015**, 115 (17), 9587-9652.
9. Dugger, R. W.; Ragan, J. A.; Ripin, D. H. B., *Organic Process Research & Development* **2005**, 9 (3), 253-258.
10. Nugent, T. C., *Chiral Amine Synthesis: Methods, Developments and Applications*. Wiley-VCH Verlag GmbH & Co. KGaA: Weinheim, 2010.
11. Roughley, S. D.; Jordan, A. M., *J. Med. Chem.* **2011**, 54 (10), 3451-3479.
12. Carey, J. S.; Laffan, D.; Thomson, C.; Williams, M. T., *Organic & Biomolecular Chemistry* **2006**, 4 (12), 2337-2347.
13. Lawrence, S. A., In *Science of Synthesis*, Enders, D.; Schaumann, E., Eds. Thieme: Stuttgart, 2009; Vol. 40, pp 523-543.
14. Boyd, G. V., *Advances in the Chemistry of Amino and Nitro Compounds. Patai's Chemistry of Functional Groups*. John Wiley & Sons, Ltd: 2009.
15. Challis, B. C.; Butler, A. R., Substitution at an amino nitrogen. In *The Amino Group (1968)*, Patai, S., Ed. John Wiley & Sons, Ltd.: 2010; pp 277-347.

16. Mitsunobu, O., 1.3 - Synthesis of Amines and Ammonium Salts A2 - Fleming, Barry M. Trostlan. In *Comprehensive Organic Synthesis*, Trost, B. M.; Fleming, I., Eds. Pergamon: Oxford, 1991; Vol. 6, pp 65-101.
17. Scriven, E. F. V.; Turnbull, K., *Chem. Rev.* **1988**, 88 (2), 297-368.
18. Margaretha, P., In *Science of Synthesis Knowledge Updates*, Thieme: Stuttgart, 2010; Vol. 4, pp 405-442.
19. Abdel-Magid, A. F.; Mehrman, S. J., *Organic Process Research & Development* **2006**, 10 (5), 971-1031.
20. Baxter, E. W.; Reitz, A. B., Reductive Aminations of Carbonyl Compounds with Borohydride and Borane Reducing Agents. In *Organic Reactions*, al., L. E. O. e., Ed. John Wiley & Sons, Inc.: 2004; Vol. 59, pp 1-714.
21. Tripathi, R. P.; Verma, S. S.; Pandey, J.; Tiwari, V. K., *Curr. Org. Chem.* **2008**, 12 (13), 1093-1115.
22. By unactivated alkyl halides, we exclude those which possess a functional group (such as aryl, vinyl, or carbonyl) alpha or beta to the halide.
23. Pronin, S. V.; Reiher, C. A.; Shenvi, R. A., *Nature* **2013**, 501 (7466), 195-199.
24. Guillena, G.; J. Ramón, D.; Yus, M., *Chem. Rev.* **2010**, 110 (3), 1611-1641.
25. Hamid, M. H. S. A.; Slatford, P. A.; Williams, J. M. J., *Adv. Synth. Catal.* **2007**, 349 (10), 1555-1575.
26. Leonard, J.; Blacker, A. J.; Marsden, S. P.; Jones, M. F.; Mulholland, K. R.; Newton, R., *Organic Process Research & Development* **2015**, 19 (10), 1400-1410.
27. Studer, A.; Curran, D. P., *Nat Chem* **2014**, 6 (9), 765-773.
28. Studer, A.; Curran, D. P., *Angew. Chem. Int. Ed.* **2016**, 55 (1), 58-102.
29. Lamas, M.-C.; Vaillard, S. E.; Wibbeling, B.; Studer, A., *Org. Lett.* **2010**, 12 (9), 2072-2075.
30. Ollivier, C.; Renaud, P., *J. Am. Chem. Soc.* **2000**, 122 (27), 6496-6497.
31. Ollivier, C.; Renaud, P., *J. Am. Chem. Soc.* **2001**, 123 (20), 4717-4727.
32. Panchaud, P.; Renaud, P., *The Journal of Organic Chemistry* **2004**, 69 (9), 3205-3207.
33. Panchaud, P.; Chabaud, L.; Landais, Y.; Ollivier, C.; Renaud, P.; Zigmantas, S., *Chem. Eur. J.* **2004**, 10 (15), 3606-3614.
34. Bissember, A. C.; Lundgren, R. J.; Creutz, S. E.; Peters, J. C.; Fu, G. C., *Angew. Chem. Int. Ed.* **2013**, 52 (19), 5129-5133.
35. Do, H.-Q.; Bachman, S.; Bissember, A. C.; Peters, J. C.; Fu, G. C., *J. Am. Chem. Soc.* **2014**, 136 (5), 2162-2167.
36. Ahn, J. M.; Peters, J. C.; Fu, G. C., *J. Am. Chem. Soc.* **2017**.
37. Matier, C. D.; Schwaben, J.; Peters, J. C.; Fu, G. C., *J. Am. Chem. Soc.* **2017**.
38. Kainz, Q. M.; Matier, C. D.; Bartoszewicz, A.; Zultanski, S. L.; Peters, J. C.; Fu, G. C., *Science* **2016**, 351 (6274), 681-684.
39. By unactivated alkyl halides, we exclude those which possess a functional group (such as aryl, vinyl, or carbonyl) alpha or beta to the halide.
40. Liu, Q.; Dong, X.; Li, J.; Xiao, J.; Dong, Y.; Liu, H., *ACS Catalysis* **2015**, 5 (10), 6111-6137.
41. Monks, B. M.; Cook, S. P., *Angew. Chem. Int. Ed.* **2013**, 52 (52), 14214-14218.
42. Bloome, K. S.; McMahan, R. L.; Alexanian, E. J., *J. Am. Chem. Soc.* **2011**, 133 (50), 20146-20148.
43. McMahon, C. M.; Alexanian, E. J., *Angew. Chem. Int. Ed.* **2014**, 53 (23), 5974-5977.

44. Zou, Y.; Zhou, J., *Chem. Commun.* **2014**, 50 (28), 3725-3728.
45. Venning, A. R. O.; Bohan, P. T.; Alexanian, E. J., *J. Am. Chem. Soc.* **2015**, 137 (11), 3731-3734.
46. Wu, X.; See, J. W. T.; Xu, K.; Hirao, H.; Roger, J.; Hierso, J.-C.; Zhou, J., *Angew. Chem. Int. Ed.* **2014**, 53 (49), 13573-13577.
47. Xiao, B.; Liu, Z.-J.; Liu, L.; Fu, Y., *J. Am. Chem. Soc.* **2013**, 135 (2), 616-619.
48. Troadec, T.; Tan, S.-y.; Wedge, C. J.; Rourke, J. P.; Unwin, P. R.; Chaplin, A. B., *Angew. Chem. Int. Ed.* **2016**, 55 (11), 3754-3757.
49. Mann, G.; Hartwig, J. F.; Driver, M. S.; Fernández-Rivas, C., *J. Am. Chem. Soc.* **1998**, 120 (4), 827-828.
50. Wolfe, J. P.; Åhman, J.; Sadighi, J. P.; Singer, R. A.; Buchwald, S. L., *Tetrahedron Lett.* **1997**, 38 (36), 6367-6370.
51. Huang, H.; Chen, W.; Xu, Y.; Li, J., *Green Chemistry* **2015**, 17 (10), 4715-4719.
52. Protection for the Amino Group. In *Greene's Protective Groups in Organic Synthesis*, 5 ed.; Wuts, P. G. M., Ed. John Wiley & Sons, Inc.: 2014; pp 895-1193.
53. Dudnik, A. S.; Fu, G. C., *J. Am. Chem. Soc.* **2012**, 134 (25), 10693-10697.
54. Dunsford, J. J.; Clark, E. R.; Ingleson, M. J., *Angew. Chem. Int. Ed.* **2015**, 54 (19), 5688-5692.
55. Mitamura, Y.; Asada, Y.; Murakami, K.; Someya, H.; Yorimitsu, H.; Oshima, K., *Chemistry – An Asian Journal* **2010**, 5 (6), 1487-1493.
56. Mitamura, Y.; Someya, H.; Yorimitsu, H.; Oshima, K., *Synlett* **2010**, 2010 (02), 309-312.
57. Ohmiya, H.; Tsuji, T.; Yorimitsu, H.; Oshima, K., *Chem. Eur. J.* **2004**, 10 (22), 5640-5648.
58. Sai, M.; Someya, H.; Yorimitsu, H.; Oshima, K., *Org. Lett.* **2008**, 10 (12), 2545-2547.
59. Sai, M.; Yorimitsu, H.; Oshima, K., *Bull. Chem. Soc. Jpn.* **2009**, 82 (9), 1194-1196.
60. Someya, H.; Ohmiya, H.; Yorimitsu, H.; Oshima, K., *Org. Lett.* **2008**, 10 (5), 969-971.
61. Someya, H.; Yorimitsu, H.; Oshima, K., *Tetrahedron* **2010**, 66 (32), 5993-5999.
62. Tsuji, T.; Yorimitsu, H.; Oshima, K., *Angew. Chem. Int. Ed.* **2002**, 41 (21), 4137-4139.
63. Yotsuji, K.; Hoshiya, N.; Kobayashi, T.; Fukuda, H.; Abe, H.; Arisawa, M.; Shuto, S., *Adv. Synth. Catal.* **2015**, 357 (5), 1022-1028.
64. Zultanski, S. L.; Fu, G. C., *J. Am. Chem. Soc.* **2013**, 135 (2), 624-627.
65. Renaud, P.; Ollivier, C.; Panchaud, P., *Angew. Chem. Int. Ed.* **2002**, 41 (18), 3460-3462.
66. Salom-Roig, X. J.; Dénès, F.; Renaud, P., *Synthesis* **2004**, 2004 (12), 1903-1928.
67. Villa, G.; Povie, G.; Renaud, P., *J. Am. Chem. Soc.* **2011**, 133 (15), 5913-5920.
68. Hanley, P. S.; Marquard, S. L.; Cundari, T. R.; Hartwig, J. F., *J. Am. Chem. Soc.* **2012**, 134 (37), 15281-15284.
69. Thoman, C. J.; Hunsberger, I. M., *J. Org. Chem.* **1968**, 33 (7), 2852-2857.
70. Keyari, C. M.; Polt, R., *J. Carbohydr. Chem.* **2010**, 29 (4), 181-206.
71. Apsunde, T. D.; Trudell, M. L., *Synthesis* **2014**, 46 (02), 230-234.
72. Roice, M.; Christensen, S. F.; Meldal, M., *Chem. Eur. J.* **2004**, 10 (18), 4407-4415.
73. Schmidt, V. A.; Quinn, R. K.; Brusoe, A. T.; Alexanian, E. J., *J. Am. Chem. Soc.* **2014**, 136 (41), 14389-14392.
74. Wang, X.; Wang, S.; Xue, W.; Gong, H., *J. Am. Chem. Soc.* **2015**, 137 (36), 11562-11565.
75. Singh, S.; Duffy, C. D.; Shah, S. T. A.; Guiry, P. J., *J. Org. Chem.* **2008**, 73 (16), 6429-6432.
76. Miura, K.; Tomita, M.; Yamada, Y.; Hosomi, A., *J. Org. Chem.* **2007**, 72 (3), 787-792.

-
77. Tamao, K.; Yoshida, J.; Murata, M.; Kumada, M., *J. Am. Chem. Soc.* **1980**, *102* (9), 3267-3269.
 78. Larraufie, M.-H.; Malacria, M.; Courillon, C.; Ollivier, C.; Fensterbank, L.; Lacôte, E., *Tetrahedron* **2013**, *69* (36), 7699-7705.
 79. Wang, G.-Z.; Jiang, J.; Bu, X.-S.; Dai, J.-J.; Xu, J.; Fu, Y.; Xu, H.-J., *Org. Lett.* **2015**, *17* (15), 3682-3685.
 80. Hatano, M.; Goto, Y.; Izumiseki, A.; Akakura, M.; Ishihara, K., *J. Am. Chem. Soc.* **2015**, *137* (42), 13472-13475.
 81. Banwell, M. G.; Harvey, J. E.; Hockless, D. C. R.; Wu, A. W., *J. Org. Chem.* **2000**, *65* (14), 4241-4250.
 82. Ambrosini, L. M.; Cernak, T. A.; Lambert, T. H., *Synthesis* **2010**, *2010* (05), 870-881.
 83. Li, H.; Grasa, G. A.; Colacot, T. J., *Org. Lett.* **2010**, *12* (15), 3332-3335.
 84. Tewari, A.; Hein, M.; Zapf, A.; Beller, M., *Synthesis* **2004**, *2004* (06), 935-941.
 85. Waser, J.; Gaspar, B.; Nambu, H.; Carreira, E. M., *J. Am. Chem. Soc.* **2006**, *128* (35), 11693-11712.
 86. Fourneron, J.-D.; Archelas, A.; Vigne, B.; Furstoss, R., *Tetrahedron* **1987**, *43* (10), 2273-2284.